UNCLASSIFIED

AD 426785

DEFENSE DOCUMENTATION CENTER

FOR

SCIENTIFIC AND TECHNICAL INFORMATION

CAMERON STATION, ALEXANDRIA, VIRGINIA



UNCLASSIFIED

NOTICE: When government or other drawings, specifications or other data are used for any purpose other than in connection with a definitely related government procurement operation, the U. S. Government thereby incurs no responsibility, nor any obligation whatsoever; and the fact that the Government may have formulated, furnished, or in any way supplied the said drawings, specifications, or other data is not to be regarded by implication or otherwise as in any manner licensing the holder or any other person or corporation, or conveying any rights or permission to manufacture, use or sell any patented invention that may in any way be related thereto.

64-6

426785

U. S. ARMY
TRANSPORTATION RESEARCH COMMAND
FORT EUSTIS, VIRGINIA

CATALOGED BY DDC
AS AD No.

TRECOM TECHNICAL REPORT 63-21

RESULTS OF WIND TUNNEL TESTS OF A FULL-SCALE, WING-MOUNTED, TIP-TURBINE-DRIVEN LIFT FAN

Task 1D121401D14402
(Formerly Task 9X38-01-020-02)
Contract DA 44-177-TC-584

September 1963

prepared by:

GENERAL ELECTRIC COMPANY
Flight Propulsion Laboratory Department
Cincinnati 15, Ohio

JAN 15 1964
DSIA B



DISCLAIMER NOTICE

When Government drawings, specifications, or other data are used for any purpose other than in connection with a definitely related Government procurement operation, the United States Government thereby incurs no responsibility nor any obligation whatsoever; and the fact that the Government may have formulated, furnished, or in any way supplied the said drawings, specifications, or other data is not to be regarded by implication or otherwise as in any manner licensing the holder or any other person or corporation, or conveying any rights or permission, to manufacture, use, or sell any patented invention that may in any way be related thereto.

* * *

DDC AVAILABILITY NOTICE

Qualified requesters may obtain copies of this report from

Defense Documentation Center
Cameron Station
Alexandria, Virginia 22314

* * *

This report has been released to the Office of Technical Services, U. S. Department of Commerce, Washington 25, D. C., for sale to the general public.

* * *

The information contained herein will not be used for advertising purposes.

* * *

The findings and recommendations contained in this report are those of the contractor and do not necessarily reflect the views of the U. S. Army Mobility Command, the U. S. Army Materiel Command, or the Department of the Army.

HEADQUARTERS
U S ARMY TRANSPORTATION RESEARCH COMMAND
FORT EUSTIS, VIRGINIA

This report concludes the contractor reporting under the Tip-Turbine-Driven Lift Fan project. The report covers the full-scale fan-in-wing model testing conducted in the NASA Ames Research Center 40-foot by 80-foot wind tunnel from October 1961 through February 1962. This series of tests has provided the first large-scale test data with fans installed in wings; prior conclusions based on small-scale tests should be re-evaluated in light of the information presented herein. The lift-fan hardware utilized in the reported tests was subsequently loaned to NASA, and additional testing will be conducted and reported by NASA.

JOHN W. WHITE
Group Leader
Aeronautical Propulsion Group

APPROVED.

FOR THE COMMANDER:

LARRY M. HEWIN
Technical Director

Task 1D121401D14402

(Formerly Task 9X38-01-020-02)

Contract DA 44-177-TC-584

TRECOM TECHNICAL REPORT 63-21

September 1963

RESULTS OF WIND TUNNEL TESTS OF A FULL-SCALE, WING-MOUNTED, TIP-TURBINE-DRIVEN LIFT FAN

Prepared By:

GENERAL ELECTRIC COMPANY

Advanced Engine and Technology Department

Cincinnati 15, Ohio

for

U. S. ARMY TRANSPORTATION RESEARCH COMMAND

FORT EUSTIS, VIRGINIA

TABLE OF CONTENTS

		PAGE
	LIST OF ILLUSTRATIONS	vi
	LIST OF TABLES	xv
I.	SUMMARY	1
	Aerodynamic	3
	Mechanical	5
II.	WIND TUNNEL MODEL	7
	Period I Testing	7
	Period II Testing	11
	Ground Effects Testing	13
III.	TEST INSTRUMENTATION	15
	Fans - Aerodynamic	15
	Fans - Mechanical and Operational	18
	Engine - Operational	18
	Aircraft - Aerodynamic	18
	Miscellaneous	18
IV.	TEST PROCEDURES AND RESULTS	21
	Test Objectives and Limits	21
	Summary of Test Runs	22
	Test Results	29
	Measurement Accuracies	31
V.	ANALYSIS OF RESULTS	33
	A. General Considerations	33
	Gas Generators	33
	B. Basic Aircraft Performance (Power Off)	33
	Lift	35
	Drag	38
	Pitching Moments (Tail Downwash)	39
	Static Stability	40

	PAGE
C. Fan Aerodynamic Performance	41
Performance Model of Basic Fan	43
Performance with Additional Inlet Devices	46
Comparison of Fan Installation in the Right and Left Wings	52
X353-5 Rotor Versus X353-5B Rotor	54
Performance with Inlet Doors and Mid-wing Simulation	57
Performance "Tuning" with the Circular Vane	61
Miscellaneous	61
D. Fan Thermodynamic Performance	62
Comparison of Static Test Results	63
Static Performance Measured in the Wind Tunnel	67
Fan Throttling Characteristics	68
Fan Power Absorption in Transition	69
Flow Direction through Fan in Transition	71
Fan Sound Power Level and Directivity	72
Fan and Engine Inlet Reingestion	72
Ground Temperature Survey	75
E. Fan Powered Aircraft Performance	76
Performance Coefficients	76
General Comparison with Fan-In-Fuselage Results	79
Accuracy of Interaction Analysis	80
Interaction Lift	80
Interaction Pitching Moment	82
Interaction Drag	87
System Lift and Drag and Moment Changes as a Function of Angle of Attack	89
Power-On Tail Downwash and Static Stability	90
Inlet Comparisons	92
Rotor Comparisons in Cross Flow	93
Effects of Fan Inlet Closure Doors	93
Kruger Flap Effects	94
Very High Velocity Ratio Performance	94
Thrust Spoiling for Control	95
Transition Analysis	99
Transition Calculations and Procedure	100
Maximum Level Acceleration	103
Maximum Rate of Climb	104
Level Deceleration at Constant Angle of Attack	104
Conversion	105
STOL	106
Wing Static Pressure Distribution	106
Faired Inlet Door Forces	106

PAGE

F. Fan Mechanical Performance 108

Inlet Configuration Selection and General Considerations 108
X353-5 Versus X353-5B 109
Left Wing Versus Right Wing 109
Rotor Blade Stresses 109
Stator Stresses 114
Blade and Stator Stresses in Ground Effect 114
Circular Inlet Vane Stress 115
Normal Speed Operating Stress 115
Conversion 116
Temperature Measurements 117

VI. HARDWARE INSPECTION RESULTS 119

Lift Fan S/N 001 (Period I) 119
Lift Fan S/N 002 (Period I) 120
Lift Fan S/N 001 (Period II) 121
Lift Fan S/N 002 (Period II) 123
Diverter Valve and Bellows S/N 001 123
Diverter Valve and Bellows S/N 002 124

VII. RECOMMENDATIONS 125

VIII. REFERENCES 127

APPENDIX A 131

Table A-1 Defintions and Symbols 131
Table A-2 Wind Tunnel Test Results 137
Table A-3 Ground Effects Test Results 192

APPENDIX B 193

Figures 1 through 136 193

DISTRIBUTION 379

LIST OF ILLUSTRATIONS

FIGURE		PAGE
1	NASA Fan-in-Wing, Full-Scale Wind Tunnel Model	193
2	Sketch of NASA Full-Scale Aircraft Model	194
3	Schematic of Left and Right Wing Fan Exit Louver Installations	195
4	View of Fan Installed in Wing Showing the Circular Vane Inlet	196
5	Circular Vane with Fixed Side Vanes Inlet Configuration	197
6	Articulated Inlet Louver System Closed Position	198
7	Articulated Inlet Louver System, Open Position	199
8	Articulated Inlet Vane Angle Versus Indicator Reading	200
9	Articulated Inlet Vane Indicator Setting Versus Velocity Ratio	201
10	Fan-in-Wing Test Model with Fuselage Addition for Mid-Wing VZ-11 Simulation and Faired Inlet Closure Doors	202
11	Leading Edge (Kruger) Flap Installation	203
12a	Extra Stator Stiffner Rings (Fan 001)	204
12b	Detail, Stator Stiffner Rings	204
13	Scroll Blocker (Test Equipment)	205
14	Faired Inlet Door Installations	206
15	General Arrangement for Flight Line Testing "Out of Ground Effect"; Right Fan $h/d_F = 1.82$	207
16	General Arrangement for Flight Line Testing "In Ground Effect"; Left Fan $h/d_F = 0.98$	208
17a	Details of Ground Effect Test Setup for Left Wing	209
17b	Details of Ground Effect Test Setup for Left Wing	210
18	Ground Effect Simulation	211
19	Inlet Vane Configuratien (Left Fan Only) for Ground Effect Tests	212
20	Schematic of Instrumentation Planes	213

FIGURE		PAGE
21	Unpowered Aircraft Performance (Run I-1)	214
22	Unpowered Aircraft Performance (Run I-2)	215
23	Unpowered Aircraft Performance (Run I-8)	216
24	Unpowered Aircraft Performance (Run I-9)	217
25	Unpowered Aircraft Performance (Run I-16a)	218
26	Unpowered Aircraft Performance (Run I-16b)	219
27	Unpowered Aircraft Performance (Run I-17)	220
28	Unpowered Aircraft Performance (Run I-20)	221
29	Unpowered Aircraft Performance (Run I-24)	222
30	Unpowered Aircraft Performance (Run I-25a)	223
31	Unpowered Aircraft Performance (Run I-25b)	224
32	Unpowered Aircraft Performance (Run II-1a)	225
33	Unpowered Aircraft Performance (Run II-1b)	226
34	Unpowered Aircraft Performance (Run II-2a)	227
35	Unpowered Aircraft Performance (Run II-2b)	228
36	Unpowered Aircraft Performance (Run II-3a)	229
37	Unpowered Aircraft Performance (Run II-3b)	230
38	Unpowered Aircraft Performance (Run II-22)	231
39	Reynolds Number Based on Wing Mean Aerodynamic Chord Versus Flight Speed	232
40	Change in Pitching Moment Coefficient with Change in Tail Incidence Angle ($\alpha = 0^{\circ}$)	233
41	Tail Downwash Angle Versus Angle of Attack	234
42	Location of Fan Rotor Inlet (10.3) and Exit (10.6) Pressure Measuring Instrumentation	235
43	Pressure Coefficient Versus Percent Annulus Area	236
44a	Pressure Coefficient Versus Percent Annulus Area	237

FIGURE		PAGE
44b	Rotor Discharge Pressure Coefficient Versus Velocity Ratio	238
44c	Rotor Discharge Pressure Coefficient Versus Velocity Ratio	239
45	Pressure Coefficient Versus Percent Annulus Area	240
46	Pressure Coefficient Versus Percent Annulus Area	241
47	Fan Horsepower Parameter and Efficiency Versus Velocity Ratio	242
48	Fan Pressure Rise Coefficient and Effective Area Coefficient Versus Velocity Ratio (Circular Vane Inlet)	243
49a	Pressure Coefficient Versus Percent Annulus Area	244
49b	Pressure Coefficient Versus Percent Annulus Area	245
49c	Pressure Coefficient Versus Percent Annulus Area	246
50	Pressure Coefficient Versus Percent Annulus Area	247
51	Pressure Coefficient Versus Percent Annulus Area	248
52	Pressure Coefficient Versus Percent Annulus Area	249
53	Pressure Coefficient Versus Percent Annulus Area	250
54	Pressure Coefficient Versus Percent Annulus Area	251
55a	Mass averaged Fan Inlet Loss Coefficient Versus Velocity Ratio	252
55b	Fan Inlet Pressure Versus Flight Speed	253
56	Mass Averaged Fan Pressure Rise Coefficient Versus Velocity Ratio	254
57	Effective Area Coefficient Versus Velocity Ratio	255
58	Fan Lift Coefficient Versus Velocity Ratio	256
59	Fan Lift Coefficient Versus Velocity Ratio	257
60	Fan Drag Coefficient Versus Velocity Ratio	258
61	Pressure Coefficient Versus Percent Annulus Area	259
62	Pressure and Flow Coefficients Versus Percent Annulus Area	260

FIGURE		PAGE
63	Pressure Coefficient Versus Percent Annulus Area	261
64	Pressure Coefficient Versus Percent Annulus Area	262
65a	Pressure Coefficient Versus Percent Annulus Area	263
65b	Pressure Coefficient Versus Percent Annulus Area	264
66	Pressure Coefficient Versus Percent Annulus Area	265
67	Pressure and Flow Coefficient Versus Percent Annulus Area	266
68	Pressure and Flow Coefficients Versus Annulus Area for Faired and Unfaired Closure Doors	267
69	Flow at Faired Doors from Tuft Observations	268
70	Pressure Coefficient Versus Percent Annulus Area	269
71	Pressure Coefficient Versus Percent Annulus Area	270
72	Pressure Coefficient Versus Percent Annulus Area	271
73	Inlet Vane Angle of Attack	272
74	Pressure and Flow Coefficient Versus Percent Annulus Area (Static)	273
75	Vertical Lift to Total Thrust Ratio Versus Exit Louver Angle	274
76	Fan Speed Change at Constant Throttle Versus Flight Velocity and Exit Louver Angle for the X353-5 Fan in Left Wing	275
77a	Fan Speed Change at Constant Throttle Versus Flight Velocity and Exit Louver Angle for the X353-5B Fan in the Left Wing	276
77b	Hover Fan Speed Change at Constant Throttle Versus Exit Louver Vector and Stagger Angles for the X353-5B Fan (Evendale Flightworthiness Tests)	277
78	Comparison of X353-5 and X353-5B Rotor Fan Speed as a Function of Flight Speed and Exit Louver Angle	278
79	Fan Stall Characteristics as a Function of Velocity Ratio and Angle of Attack	279
80	Fan Flow Coefficient Ratio Versus Velocity Ratio	280
81	Sound Level Survey Data (Ramp Test)	281

FIGURE		PAGE
82a	Temperature Ratio Versus Height Above Ground	282
82b	Temperature Ratio Versus Height Above Ground	283
82c	Temperature Ratio Versus Height Above Ground	284
83a	Temperature Ratio Versus Height Above Ground	285
83b	Temperature Ratio Versus Height Above Ground	286
83c	Temperature Ratio Versus Height Above Ground	287
84a	Temperature Ratio Versus Height Above Ground	288
84b	Temperature Ratio Versus Height Above Ground	289
84c	Temperature Ratio Versus Height Above Ground	290
85	Fuselage Skin Temperature Ratio in Ground Effect	291
86	Lift, Drag and Moment Coefficient (Slip Stream Notation) Versus Velocity Parameter	292
87	Fan Powered Aircraft Performance (Runs I-3 and 4)	293
88a	Fan Powered Aircraft Performance (Runs I-5, 6 and 7)	294
88b	Fan Powered Aircraft Performance (Runs I-5 and 6)	295
89a	Fan Powered Aircraft Performance (Runs I-10, 11, 12, 13 and 14)	296
89b	Fan Powered Aircraft Performance (Runs I-10, 11, 12, 13 and 14)	297
90a	Fan Powered Aircraft Performance (Run I-15)	298
90b	Fan Powered Aircraft Performance (Run I-15)	299
91a	Fan Powered Aircraft Performance (Runs I-18 and 19)	300
91b	Fan Powered Aircraft Performance (Runs I-18 and 19)	301
92a	Fan Powered Aircraft Performance (Run I-22)	302
92b	Fan Powered Aircraft Performance (Run I-22)	303
93a	Fan Powered Aircraft Performance (Runs I-23, 26 and 27)	304

FIGURE		PAGE
93b	Fan Powered Aircraft Performance (Runs I-23, 26 and 27)	305
94a	Fan Powered Aircraft Performance (Runs II-6, 7 and 8)	306
94b	Fan Powered Aircraft Performance (Runs II-6, 7 and 8)	307
95a	Fan Powered Aircraft Performance (Run II-9)	308
95b	Fan Powered Aircraft Performance (Run II-9)	309
96	Fan Powered Aircraft Performance (Runs II-12 and 14)	310
97a	Fan Powered Aircraft Performance (Run II-16)	311
97b	Fan Powered Aircraft Performance (Run II-16)	312
98	Fan Powered Aircraft Performance (Runs II-17 and 19)	313
99	Interaction Lift Coefficient Versus Velocity Ratio	314
100	Fan Lift Coefficient Versus Velocity Ratio	315
101	Total Fan Thrust Coefficient Versus Fan Speed	316
102	Interaction Moment Coefficient Versus Velocity Ratio	317
103	Fan Drag Coefficient Versus Velocity Ratio	318
104	Lift Center Change Versus Velocity Ratio	319
105	Interaction Drag Coefficient Versus Velocity Ratio	320
106	Lift Coefficient Slope Versus Velocity Ratio	321
107	Drag Curve Slope Versus Velocity Ratio	322
108	Tail Downwash Angle Versus Velocity Ratio	323
109	Lift Coefficient Versus Velocity Ratio	324
110	Static Longitudinal Stability Versus Velocity Ratio Power On and Off	325
111	Moment Coefficient Slope Versus Velocity Ratio	326
112	Pitching Moment Coefficient Versus Velocity Ratio	327
113	Drag Coefficient Versus Velocity Ratio	328

FIGURE		PAGE
114a	Drag Coefficient Versus Velocity Ratio	329
114b	Drag Coefficient Versus Velocity Ratio	330
114c	Drag Coefficient Versus Velocity Ratio	331
115a	Lift Coefficient Versus Velocity Ratio	332
115b	Moment and Drag Coefficients Versus Velocity Ratio	333
116	Comparison of Power-Off and High-Velocity Ratio Polars	334
117a	Total Lift and Drag Variation Versus β_s and V_p/V_{tip} at Constant J85 Engine Power	335
117b	Total Lift and Drag Variation Versus β_s and V_p/V_{tip} at Constant J85 Engine Power	336
117c	Total Lift and Drag Variation Versus β_s and V_p/V_{tip} at Constant J85 Engine Power	337
117d	Total Lift and Drag Variation Versus β_s and V_p/V_{tip} at Constant J85 Engine Power	338
118	Total Fan Thrust Versus Fan Speed (Ref. 19)	339
119	Vector Flow Angle Versus β_s and β_{av} Static Results, (Ref. 19)	340
120a	Fan Speed Change Versus Velocity Ratio and β_s, at Constant J85 Engine Power	341
120b	Fan Speed Change Versus Velocity Ratio and β_s, at Constant J85 Engine Power	342
121a	Total Lift Variation Versus β_{av} and β_s at 1.82 h/d_F and Constant J85 Engine Power	343
121b	Total Lift Variation Versus β_{av} and β_s at 0.98 h/d_F and Constant J85 Engine Power	344
122a	Lift and Drag Coefficients Versus Angle of Attack and Exit Louver Angle	345
122b	Transition Characteristics - Maximum Level Acceleration - L/GW = 1.05, N_F = 100%, X353-5 Rotor, $\delta_f = 30^o$, W/S = 31.5	346
122c	Transition Characteristics - Maximum Level Acceleration - L/GW = 1.20, N_F = 100%, X353-5 Rotor, $\delta_f = 30^o$, W/S = 27.6	347

FIGURE		PAGE
123a	Pitching Moments for Maximum Level Acceleration Transition L/GW = 1.05, N_F = 100%, δ_f = 30°	348
123b	Pitching Moments for Maximum Level Acceleration Transition L/GW = 1.20, N_F = 100%; δ_f = 30°	349
124a	Horizontal Tail Incidence Angle for Trimmed Flight Versus Flight Velocity - Maximum Acceleration Transition L/GW = 1.05, N_F = 100%, δ_f = 30°	350
124b	Horizontal Tail Incidence Angle for Trimmed Flight Versus Flight Velocity - Maximum Acceleration Transition L/GW = 1.20, N_F = 100%, δ_f = 30°	351
125	Maximum Rate of Climb Versus Flight Velocity L/GW = 1.20, N_F = 100%, δ_f = 30°, X353-5 Rotor	352
126	Pitching Moments for Maximum Rate of Climb, L/GW = 1.20, Moment Center No. 2, N_F = 100%, δ_f = 30°	353
127	Transition Characteristics - Level Deceleration L/GW = 1.20, δ_f = 30°, α = 0°	354
128a	Chordwise Pressure Distribution at Station III (V_P/V_{tip} = 0.219)	355
128b	Chordwise Pressure Coefficient Distribution (V_P/V_{tip} = 0.069)	356
128c	Chordwise Pressure Coefficient Distribution (V_P/V_{tip} = 0.146)	357
128d	Chordwise Pressure Coefficient Distribution (V_P/V_{tip} = 0.219)	358
128e	Chordwise Pressure Coefficient Distribution (V_P/V_{tip} = 0.297)	359
128f	Chordwise Pressure Coefficient Distribution (Power Off)	360
129	Diagram of Test Set-Up for Measurement of Fan Closure Door Hinge Moments	361
130	Inlet Doors Hinge Moment Index Versus Flight Velocity - N_F = 100%	362
131a	Cosine 2θ Mode Stress as a Function of Flight Speed and Exit Louver Setting (Five Second Deceleration)	363

FIGURE		PAGE
131b	Cosine 2θ Mode Stress as a Function of Flight Speed and Exit Louver Setting (One Second Deceleration)	364
131c	Cosine 2θ Mode Stress as a Function of Flight Velocity and Exit Louver Setting (Diverter Valve Deceleration)	365
131d	Cosine 2θ Mode Stress as a Function of Flight Speed and Exit Louver Setting	366
131e	Cosine 2θ Mode Stress as a Function of Flight Speed and Yaw Angle (Five Second Deceleration)	367
131f	Cosine 2θ Mode Stress as a Function of Flight Speed, Airplane Configuration and Angle of Attack (Five Second Deceleration)	368
131g	Cosine 2θ Mode Stress as a Function of Flight Speed and Angle of Attack (Five Second Deceleration)	369
131h	Cosine 2θ Mode Stress as a Function of Flight Speed, Airplane Configuration, Yaw Angle and Angle of Attack (Five Second Deceleration)	370
132a	Overall and First Flexural Resonance Stress at 1850 RPM Versus Flight Speed	371
132b	First Flexural Resonance Stress at 1850 RPM Versus Flight Speed	372
133a	Scroll Air Seal Leak (Fan 001)	373
133b	Turbine Rub, Rear Frame Insulation Blanket (Fan 002)	373
134	Front Frame Skin Failure (S/N 002)	374
135	Yielded Convolution in Bellows, S/N 001 (First and Second Convolutions from Bottom)	375
136a	"Straight" Diverter Valve Door, S/N 001, Showing Failed Piece of Heat Shield	376
136b	"Curved" Diverter Valve Door, S/N 001, Showing Separated Heat Shield	377

LIST OF TABLES

TABLE	TITLE	PAGE
I	Instrumentation Summary	16
II	Aerodynamic Instrumentation Breakdown by Instrument Planes	17
III	Location of Pressure Measuring Instrumentation on Left Wing of Model	19
IV	Fan Stress Limits	23
V	Mechanical Checkout Test (on the Ramp - September, 1961)	24
VI	Period I Wind Tunnel Test (October, 1961)	25
VII	Period II Wind Tunnel Test (January, 1961)	26
VIII	Ground Effect Test (on the Ramp - February, 1962)	27
IX	Summary of Lift Fan Operating Time	28
X	Summary of Aircraft Power Off Runs	34
XI	Basic Aircraft - Lift Coefficients Fan Inlets Covered and Exit Louvers Closed	35
XII	Basic Aircraft Lift Coefficient - Conversion Configurations Power-Off, Tail-On, $i_t = 0^o$	36
XIII	X353-5 and X353-5B Static Performance Differences	62
XIV	Comparative Static Thrust Data (Ramp Test)	64
XV	Measured and Calculated Ground Effect Performance (Full Scale and Scale Model Data)	65
XVI	Engine Inlet Reingestion	74
XVII	Conversion Relationships - Aircraft Coefficients	77
XVIII	Conversion Relationships for Slipstream Notation	78

		PAGE
XIX	Transition Equations of Motion	101
XX	Conversion Data ($\delta_f = 30^o$, L/GW = 1.05, Moment Center No. 2, $\beta = 40^o$)	105
XXI	Cosine 2θ Mode Blade Stresses	112

I. SUMMARY

Contract DA-44-177-TC-584 with the U.S. Army Transportation Research Command requires that, in addition to bi-monthly technical progress reports, comprehensive reports of major work phases be prepared and submitted to the contracting officer. Previous reports submitted under this requirement are:

- X353-5 Fan Design Report, May 30, 1960. (Proprietary)

- Fabrication, Test, and Analysis of a Tip Turbine VTOL Propulsion System (Report of Phase I, Static Tests, Fuselage Mounted X353-5) TREC 60-42, August 31, 1960.

- Results of Wind Tunnel Tests of a Full-Scale, Fuselage-Mounted, Tip-Turbine-Driven Lift Fan (Report of Phase II Tests Volumes 1, 2 and 3) TREC 61-15, January 1961, October 1961, and March 1962.

- Results of Static Tests of a Full-Scale, Wind-Mounted, Tip-Turbine-Driven Lift Fan, TREC 62-21, October 1961.

This is the required report for the final portion of Phase II contract work. It includes the results of the full-scale, wing-mounted X353-5 and X353-5B fans obtained during a two-part, 107-fan-hours, wind tunnel test program in the NASA, Ames, 40' x 80' wind tunnel. In addition, this report includes the results of an additional 6 hours of outdoor ground effect testing at Ames, The main sections are:

- Wind Tunnel Model (Section II)

- Test Instrumentation (Section III)

- Test Procedures and Results (Section IV)

- Analysis of Test Results, Conclusions, and Discussions of Any Problems Encountered (Section V)

- Hardware Inspection Results (Section VI)

- Program Recommendations (Section VII)

- References (Section VIII)

- Basic Data (Appendix A)

- Figures, Charts, and Graphs (Appendix B)

The basic test data obtained for every test point are tabulated in Appendix A. A few items of summary:

Tunnel Speed (V_p)	0 to 125 Knots
Angle of Attack (α)	-4° to 20°
Fan Speed (N_F)	0 to 2640 rpm (100%)
Exit Louver Angle:	
Single Actuation	0° to 50° vector
Differential Actuation	0° to 45° vector and -18° to 50° stagger
Wing Flap Angle (δ_f)	0°, 30° and 60°
Tail Position	off and low
Tail Incidence Angle (i_t)	-4° to 20°
Yaw Angle (Ψ)	-12° to 12°
h/d_F (ground proximity testing)[a]	0.98 to 1.82
J85 Engine Speed	0 to 16,500 rpm (100%)
V_p/V_{tip}	0 to 0.6

[a] Where: h is the distance between the lower wing surface and the ground and d_F is the fan blade tip diameter.

Analyses of the results are presented in considerable depth, defining basic aircraft, fan internal system, and fan mechanical performance, in the wind tunnel, as a function of several configuration changes and the variables listed above. In addition, the static fan and system performance is analyzed as a function of ground proximity. A few items of performance conclusions are listed below:

AERODYNAMIC

1. Open fan inlets and exits, simulating the aircraft configuration which may exist during conversion, had the following performance characteristics relative to the basic aircraft: $C_{L\ max.}$ decreased 0.38; C_{D_o} increased 0.01; and longitudinal static stability margin increased 0.11.

2. Static longitudinal stability of the powered aircraft was essentially the same as the power-off case.

3. Tail downwash with the fans operating was a function of velocity ratio (V_p/V_{tip}) and was approximately three times the fan-in-fuselage value.

4. Transition performance with three different inlets tested was nearly identical in spite of vastly different internal fan performance characteristics.

5. The transition characteristics and maximum conversion speed for the fan-in-wing were essentially the same as for the fan-in-fuselage installation.

6. Take-off conversions required $\approx 10^{\circ}$ angle of attack and tail incidence angle changes; however, landing transitions could be demonstrated with practically no trim changes at conversion (low fan speeds).

7. The inlets tested recover little or none of the available ram pressure compared with the near 100% recovery of the fan-in-fuselage installation. The high conversion speeds attained were a result of lower exit louver losses and an increased fan pressure ratio at high transition speeds.

8. Incremental interaction lift improvement offset decreased fan performance for the fan-in-wing installation resulting in system performance similar to the fan-in-fuselage configuration.

9. Interaction drag was insignificant (within data accuracy) and had no sizable effect on fan powered performance.

10. Interaction pitching moments up to conversion speeds were directly proportional to fan ram drag and were equivalent to a ram drag force acting 1.8 fan diameters above the fan inlet (the comparable number for the fan-in-fuselage was 1.6).

11. Moderate angle of attack changes (-4^{o} to $+8^{o}$) and yaw angle changes (-8^{o} to $+8^{o}$) did not affect the fan performance appreciably.

12. The X353-5B (redesigned) rotor produced essentially the same thrust at design horsepower as the X353-5 rotor; the required rotational speed was 3% to 4% lower.

13. Both type rotors tested unload rapidly (overspeed) in cross flow, compared with practically no unloading in the fan-in-fuselage installation.

14. Fan flow and fan lift for the X353-5B rotor at 0.98 h/d_F were 9% and 7 1/2% lower, respecitvely, than at 1.82 h/d_F height. The measured total lift was $\approx$ 9% higher indicating $\approx$ 17% positive aircraft ground effect at 0.98 h/d_F.

15. The fan (X353-5B) did not unload appreciably in ground effect; constant speed was essentially equivalent to constant power performance.

MECHANICAL

1. Cosine 2θ stress in the fan-in-wing installation was a function of cross-flow velocity and exit louver angle setting: it was not significantly affected by inlet doors, mid-wing configuration, angle of attack and yaw angle; it was independent of transient time and not as sensitive to exit louver angle setting as the fan-in-fuselage installation. Maximum measured stress was 58.2% of maximum allowable (X353-5B) and occurred at a fan rpm of 2050, tunnel velocity of 125 knots and exit louver setting of 35^{o}.

2. The first flexural blade stress increased with cross-flow velocity and was a function of exit louver angle setting; running stress limit of 10,000 psi was slightly exceeded above 100 knots and 45^{o} β; X353-5B blade with the single hook dovetail design should permit higher stress operation limited by the tip tang strength (tests to determine tip tang fatigue limit are in process).

3. Conversion transient stresses are no higher than for steady state operation at this (≈ 125 knots) flight condition.

4. Reducing the admission arc by 50% simulating one engine-out operation increased the cosine 2θ mode blade stresses by 52% at 60 knots.

5. A circular vane plus fixed side vane inlet was selected as best tested based on satisfactory mechanical and aerodynamic performance and relative simplicity of design.

6. Addition of inlet closure doors increased first flexural blade stress

from 50% to approximately 80% of running stress limit at 60 knots. Combined blade stress also increased at higher fan speeds because of a larger first flexural component.

7. Blade and stator stresses were not significantly affected by ground proximity (less than 10% stress level increase over the out-of-ground effect values for all critical stress modes).

8. Blade stresses increased with flight velocity. At 125 knots flight speed, combining all stresses present, the blade airfoil and single hook dovetail are within infinite life limits. Without inlet doors installed, the tip tang is near its stress limit (first flexural) as it is currently established.

II. WIND TUNNEL MODEL

The full-scale aircraft model was designed, fabricated and assembled by NASA at the Ames Research Center. The test configuration included an X353-5 lift fan installed in each wing and a YJ85-5 turbojet engine mounted under each wing near the fuselage (see Figure 1).

The wind tunnel fan-in-wing test program required two periods of testing. The details of specific components of the wind tunnel model for Period I testing are described first. For Period II testing, only the modifications to the test model configuration are described.

PERIOD I TESTING

Airplane Model:

The airplane model consisted of structural steel load-carrying members with the aerodynamic shape fabricated of contoured wood and sheet metal. The wing section was an NACA 65-210 series airfoil and was sized to change from fan lift to wing lift at about 100 knots flight speed for a gross weight of 14,100 lbs. (equal to fan hover lift at full power). The fan axis passed through the wing 40% chord line. Plain flaps extended from approximately 17% to 64% of the wing semi-span and were adjustable for a 0°, 30°, or 60° angle. The wing was made with removable tips to permit the testing of two different wing configurations. A sketch of the airplane model with pertinent geometric data for both wing configurations and the tail are presented in Figure 2.

Lift Fans:

Lift fans installed in the aircraft model were X353-5, S/N 001, in the left wing and X353-5, S/N 002, in the right wing. Specific assembly details are presented for each fan.

S/N 001 Assembly:
This fan had been used in development tests (fan-in-fuselage) for 106 hours prior to this testing. There had been four overhauls; 17 hours, 13 minutes of operation[a] were accumulated since the last overhaul and prior to use in this model.

Forward Frame - Cold radial clearance of the air seal in this frame was 0.050 inches. This clearance had been approximately 0.150 inches for fan-in-fuselage testing but was reduced at the last overhaul in preparation for the fan-in-wing installation, which is more sensitive to leakage between the turbine and fan streams.

Rotor - The rotor assembly incorporated a two-piece torque band and rotating seal arrangement corresponding to the configuration designated Design A in reference 18 (see Fan Modification in Section II). These parts were new at the last overhaul and had, therefore, accumulated only 17 hours, 13 minutes of running time.

Rear Frame and Scroll - Scroll mount shims were altered to increase scroll to rear frame radial clearance. This was done to provide additional clearance for rear frame growth with temperature and reduce the possibility of turbine shroud rubs which had been experienced in fan S/N 002 during static fan-in-wing testing.

Exit Louvers - Most fan S/N 002 louvers had to be replaced to accommodate a right wing installation. In as much as they already were modified to provide thrust spoiling as well as vectoring capability (see reference 19, Fan Assembly Details in Section II), they were used wherever possible to replace S/N 001 louvers in the

---

[a] Reference 18

S/N 001 fan. The replacement louvers had an accumulated operating time of ≈ 53 hours (reference 19).

S/N 002 Assembly:
This fan had been used previously for fan-in-wing static testing at Evendale for 53 hours. The fan was overhauled in preparation for this program.

Forward Frame - Minimum cold radial clearance of the air seal in this frame was 0.141 inches. The maximum gap for the combination of minimum rotor runout point and maximum air seal runout point was estimated to have been ≈ 0.266 inches. This estimate was based on the measured minimum clearance plus the design tolerances (± 1/16 inch) of the forward torque band seal lip and honeycomb.

Rotor - The rotor assembly incorporated a tapered single piece torque band-seal corresponding to the configuration designated Design B in reference 18 (see Fan Modification in Section II).

Exit Louvers - Both fans S/N 001 and 002 were designed for installation in a wing with the scroll positioned to the right. In order to locate the scroll next to the fuselage for the right wing installation, Fan 002 had to be rotated 180°. Because of this, the exit louver system also had to be reversed. Figure 3 shows schematics of the louver system for both left and right wing installations. The fundamental change in louver location can be visualized as separating the exit louver system from the frames and rotating the frame 180°. Wherever practical, existing louvers were used, but attached to the opposite side of the rear frame strut. Where noted in Figure 3, new louvers were required to make a satisfactory cascade. The shaded areas in the figure indicate where complete coverage is not provided when the louvers are fully closed. The exit louvers on this fan were also equipped for

staggered louver operation (for thrust spoiling). Since the test linkage system would not permit full closed, $\beta = 90^{o}$, positioning, removal of the staggering attachments was necessary when full closure was required for unpowered aircraft performance investigation.

Inlet Configurations:

As a result of scale model studies and the review of inlet test results with NASA and TRECOM, three inlet configurations were manufactured in full-scale test hardware for the wind-tunnel program. They were:

a. Circular vane (Figure 4)
b. Circular vane with fixed side vanes (Figure 5)
c. Circular vane with articulated spanwise louvers (Figures 6 and 7)

The circular vane inlet consists of a constant section cambered airfoil that extends around the full 360^{o} of the inlet and is flush with the upper wing surface.

The fixed side vanes form a cascade of five parallel spanwise airfoils, equally spaced and variously cambered from moderate camber in front to zero at rear. They are welded, at one end, to a cap that fits over the bulletnose and at the other end, to the circular vane.

The circular vane with articulated spanwise louvers consists of fixed side vanes with hinged movable vanes attached to the leading edge. The movable vanes protrude into the free stream and when fully closed form the wing upper surface. Figure 8 shows the angular displacement of the vanes relative to an indicator reading. A schedule of indicator reading versus cross-flow velocity (Figure 9), determined from previous scale model testing, was used as a guide for choosing vane settings during this testing.

Covered Inlets:

Closed inlets were required for some of the unpowered aircraft performance testing. Inlet covers used for this were made of plywood shaped to conform to the contour of the wings.

YJ85-5 Engines:

Each of the fans was powered by a YJ85-5[a] engine equipped with an electric starter. The idle speed of the -5 model is ≈ 45% rpm compared with ≈ 72% rpm for the -7 model engine used in previous tests. This made it possible to conduct very high velocity ratio tests at lower tunnel speeds.

Diverter Valves:

A second, Air Force owned, X353-5 diverter valve (S/N 002) was borrowed for this test program. The other X353-5 diverter valve used (S/N 001) is also Air Force owned and had been incorporated in previous fan-in-wing static tests at Evendale (reference 19). Effective discharge area for the engines was adjusted by positioning the valve doors for appropriate levels of leakage. The tests described in this report are the first tests of the X353-5 diverter valve in a wind tunnel environment.

PERIOD II TESTING

Airplane Model:

The fuselage was modified by NASA to support a removable cap which was used for some runs to simulate the fan inlet environment of the VZ-11 airplane (see Figure 10). Simulated leading edge (Kruger) flaps were also provided by NASA for attachment to the wings during part of the Period II testing (see Figure 11). Also

---

[a] S/N's 230-155 and -157

for Period II testing, a different mounting system above the wind-tunnel support struts was used. The change in tunnel tares because of this is discussed in the Analysis.

Lift Fans:

In preparation for Period II testing (test points 923 through 1439), Fan 001 was rebuilt using an X353-5B rotor, S/N 009, equipped with a new disc and blades which are different in two major aspects:

1. Dovetail design - 11% longer with a single hook instead of three hooks.

2. Rotor blade reorientation - open 3^{o} uniformly from tip to hub.

This rotor also incorporated the two-piece torque band-seal design and re-used rotor 002 carriers. The forward air seals were re-ground to provide 0.089 inches cold clearance at the torque band-seal lip.

Two additional rear-frame stator stiffening rings were designed and installed in Fan 001 for use in the initial high speed runs in the tunnel (see Figure 12). They were made so that they can be cut into segments and removed and then, if necessary, be reinstalled without requiring a fan disassembly.

Fan 002 was rebuilt using the rotor from Fan 001. This was done so that both fans would utilize the two-piece torque band configuration and compile more operating time on this design; this torque band had an accumulated operating history of 50:05 hours prior to Period II testing. The minimum clearance of the forward torque band-seal lip to honeycomb was 0.140 inches; the maximum gap for the combination of minimum rotor runout point and maximum air seal runout point is

estimated to have been ≈ 0.265 inches. For the previous buildup of Fan 002, these tolerances were 0.141 and 0.266 inches, respectively.

Both fan scrolls were modified to accommodate a scroll blocker (see Figure 13) which, when installed, blocked off half of the scroll to simulate a one engine-out condition for a VZ-11 type ducting arrangement. Each scroll was fitted with a removable spacer at the bellows-scroll joint so that the installation of the scroll blocker was possible during a special run without a mounting disturbance. When the scroll blocker was installed, it was also necessary to make a corresponding discharge nozzle change and a diverter valve position adjustment to discharge half of the J85 gas through the "cruise" nozzle.

Inlet and Inlet Closures:

The circular vane plus fixed side vanes inlet configuration was selected for the Period II testing and was installed in the fans after the fans were mounted in the wings. Simulated inlet closures were designed and fabricated for the Period II testing. The configuration tested was a set of fiberglass "butterfly" doors that attach to the fan front frame with the tips guy-wired to the wings (see Figure 14). Two design variations were tried: one with fairings which streamline the fan bulletnose on closing; the other plain.

GROUND EFFECTS TESTING

To avoid reingestion, special engine inlets were installed for the ground effects testing as shown in Figures 15 and 16. The platform shown in Figure 16 was used to simulate the ground plane for testing at smaller values of h/d_F. Figures 17 and 18 show in more detail the degree of confinement presented the fan. Note that the left wing tip was removed to avoid as much extraneous aircraft ground effect as possible.

As shown in Figure 19, the inlet fixed side vanes tested in the wind tunnel were removed and in their place stub vanes were welded to the circular vane pointing radially toward the hub. The purpose of this configuration was to remove the unrealistic flow disturbances which would be generated by the relatively crude test hardware used to attach the vanes to the hub.[a] The stub vanes retained the primary performance penalty of the side vanes, the junctions at the circular vane.

[a] A bulletnose cover was used to support the fixed side vanes; the fit was poor resulting in fan inlet area blockage of ≈ 1 1/2%.

III. TEST INSTRUMENTATION

The instruments used throughout this test were essentially the same types used for the previous fan-in-fuselage static and wind tunnel tests and the fan-in-wing static test. (For a general description see pages 69-90, reference 15). Table I shows the type and quantity of internal data recorded for the two tunnel tests and the February 1962 outdoor test. During the August 1961 outdoor test only operational instrumentation and temperature instrumentation to measure reingestion were used.

For the tunnel testing, the integral lift-drag-moment force measurement system was used (see reference 16, Figures 5 and 12 for details).

For the February 1962 outdoor test, the contractor provided three, strain-gage type, air-cooled load cells and related readout equipment. These load cells were capable of recording lift only.

FANS - AERODYNAMIC

Extensive pressure instrumentation was installed in the fans to monitor internal performance characteristics such as flow, pressure ratio, distortion, and inlet recovery. In addition, pressure and temperature instrumentation at the diverter valve inlet plane was installed to provide a measurement of total available horsepower supplied to the fans. Figure 20 shows the locations of the instrumentation planes in the fan and engine, and Table II shows the breakdown by instrument planes. All of the pressure signals were displayed on water; alkazine[a] or mercury photo-manometers and photographs were obtained for each data point.[b] Temperature data were recorded on flight recorders and

---

[a] A manometer fluid with specific gravity of 1.75.

[b] All pressure recording equipment were provided by NASA.

TABLE I

INSTRUMENTATION SUMMARY [a]

Sensors	Total Installed and Recorded 1961 October Tunnel Tests		1962 January Tunnel Tests		1962 February Ground Tests	
	Right Fan Engine Wing	Left Fan Engine Wing	Right Fan Engine Wing	Left Fan Engine Wing	Right Fan Engine Wing	Left Fan Engine Wing
Aerodynamic Pressures	73[b]	194[c]	73	73	49	83
Aerodynamic Temperatures	39	15	39	15	39	57
Mechanical Temperature - Nonrotating	6	6	6	6	6	6
Mechanical Temperature - Rotating	11	12	11	8	11	8
Mechanical Pressures	3	3	3	3	3	3
Rotor Strain Gages	30	28	29	27	29	27
Stator Strain Gages	9	11	9	11	9	11
Vibration Pickups (Fan)	3	3	3	3	3	3
Vibration Pickups (Engine)	4	4	4	4	4	4
Speed (Fan)	2	2	2	2	2	2
Speed (Engine)	1	1	1	1	1	1
Total	181	279	180	153	156	205

[a] Includes the two YJ85-5 engines; [b] Increased to 97 beginning with Run 10;

[c] Decreased to 170 beginning with Run 10.

TABLE II

AERODYNAMIC INSTRUMENTATION BREAKDOWN BY INSTRUMENT PLANES

Location	Total Installed and Recorded																	
	1961 October Tunnel Tests						1962 January Tunnel Tests						1962 February Ground Tests					
	Right Fan[a]			Left Fan[a]			Right Fan[a]			Left Fan[a]			Right Fan[a]			Left Fan[a]		
	P_T	P_S	T_T	P_T	P_S	T_T	P_T	P_S	T_T	P_T	P_S	T_T	P_T	P_S	T_T	P_T	P_S	T_T
Plane 5.1 - J85 Turbine Discharge	14		12	14		12	14		12	14		12	14		12	14		12
Plane 10.3 - Fan Rotor Inlet	24		24			24			24		24				24		24	6
Plane 10.6 - Fan Rotor Discharge	24[c]			24[c]			24			24			24			24		
Plane 11.0 - Fan Stator Discharge		2			2			2			2			2			2	
Plane 2.0 - J85 Compressor Inlet		8	3		8	3		8	3		8	3		8	3		8	3
Plane 3.0 - J85 Compressor Discharge		1			1			1			1			1			1	
Wing Statics					145[bd]												10[b]	
Ground Temperature Survey																		27
Fuselage Skin Temperature																		9
Total	62	11	39	38	156	5	62	11	39	38	35	15	38	11	39	38	45	57

[a]Also includes wings and engines; [b]Installed by NASA; [c]Increased to 48 for Runs 10 through 27; [d]Decreased to 97 for Runs 10 through 27.

multi channel potentiometers.

FANS - MECHANICAL AND OPERATIONAL

Fan mechanical and operational instrumentation consisted of fan speed, axial and radial vibration transducers, vibratory strain gages on rotor blades, torque bands and stator vanes, and torque band thermocouples (rotating).

All of the rotating signals were transmitted through a slipring. Strain-gage signals could be visually monitored continously on 24 scopes and could be simultaneously recorded on a 24 channel tape system. Switching circuits were incorporated to allow a choice of up to four different signals to be monitored and recorded on each of the 24 available channels, giving a capability of monitoring and recording a total of 96 strain-gage signals.

ENGINE - OPERATIONAL

Standard engine instrumentation was used during the test including: engine speed, compressor discharge pressure, oil pressure and temperature, fuel pressure, exhaust gas temperature, throttle position and vibration transducers.

AIRCRAFT - AERODYNAMIC

The aircraft left wing was instrumented with five stations of static pressures. See Table III. The right wing was instrumented with static pressures at the same five span stations but extended only to ≈ 5% of the chord. Comparison between peak pressure profiles indicated the wing performance to be symmetrical.

MISCELLANEOUS

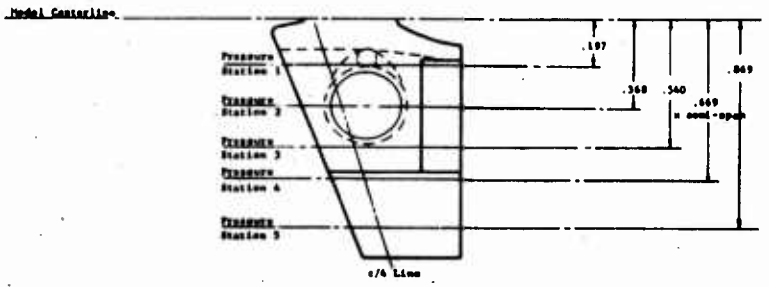
During the outdoor tests in August 1961 and February 1962, temperature data on the fuselage and in the fan discharge vicinity were recorded. Twelve fuselage skin thermocouples and a movable stand with 29 thermo-

TABLE III

LOCATION OF PRESSURE MEASURING INSTRUMENTATION ON LEFT WING OF MODEL

Station 1 (.197 b/2)		Station 2 (.368 b/2)		Station 3 (.540 b/2)		Station 4 (.669 b/2)		Station 5 (.869 b/2)	
Top	Bottom	Top	Bottom	Top	Bottom	Top	Bottom	Top	Bottom
.001c	-	.001c	-	.001c	-	.001c	-	.001c	-
.003c	.003c	.003c	.003c	.003c	.003c	.003c	.003c	.003c	.003c
.0125c	.0125c	.0125c	.0125c	.0125c	.0125c	.0125c	.0125c	.0125c	.0125c
.025c	.025c	.025c	.025c	.025c	.025c	.025c	.025c	.025c	.025c
.05c	.05c	.05c	.05c	.05c	.05c	.05c	.05c	.05c	.05c
-	-	.075c	.075c	-	-	-	-	-	-
.10c	.10c	.10c	.10c	.10c	.10c	.10c	.10c	.10c	.10c
-	-	.125c	.125c	-	-	-	-	-	-
.15c	.15c	Lift Pan		.15c	.15c	.15c	-	.15c	-
.20c	-			.20c	.20c	.20c	.20c	.20c	.20c
.30c	-			.30c	.30c	.30c	-	.30c	-
.40c	-			.40c	.40c	.40c	.40c	.40c	.40c
.50c	-			.50c	.50c	.50c	-	.50c	-
.60c	-			.60c	.60c	.60c	.60c	.60c	.60c
-	-	.65c	.65c	-	-	-	-	-	-
-	-	.675c	.675c	-	-	-	-	-	-
.70c	-	.70c	.70c	.70c	.70c	.70c	-	.70c	-
				.71c	-				
				.7175c	-				
				.725c	-				
		.74c	-						
		.745c	-						
				.75c	-				
		.755c	-						
		.765c	-	-	.765c				
.77c	.77c		Flaps		Flaps				
.78c	-								
.80c	.80c	.80c	.80c	.80c	.80c	.80c	.80c	.80c	.80c
.90c	.90c	.90c	.90c	.90c	.90c	.90c	.90c	.90c	.90c
.95c	.95c	.95c	.95c	.95c	.95c	-	-	-	-

Flaps



couples in a grid were used for this purpose. Sound intensity and directivity measurements were also taken during the outdoor tests to determine sound pressure levels as a function of fan speed.

Forces on the inlet doors (right wing) during transition were measured with ring-type strain-gage load cells installed in four of the six cables which held the doors in place. Cable tension was maintained with "soft" springs to accommodate tunnel temperature changes and wing deflections.

Strain gages were installed on the exit louver actuating rods to measure steady state loads on the louvers as a function of vector angle during both static and cross-flow testing.

The testing required a total of 113 hours and 40 minutes of fan operation (two fans) and was conducted during the periods from September 15, 1961, to October 27, 1961, and from January 9, 1962, to February 8, 1962.

TEST OBJECTIVES AND LIMITS

The formulation of the test objectives and the subsequent development of the detailed test plan were accomplished co-operatively by TRECOM, NASA and contractor personnel.

The program had the following basic objectives:

1. To obtain basic unpowered aircraft performance information with and without the tail installed.

2. To evaluate the effect of various inlet configurations on the mechanical and aerodynamic performance of the fan system.

3. To demonstrate conversion characteristics.

4. To determine the effects of wing area, high and low wing position, inlet "butterfly" doors (faired and unfaired), and Kruger flaps on the aircraft/fan system performance.

5. To test the effectiveness of using vectored and staggered exit louvers for roll, yaw, and altitude control.

6. To evaluate the control effectiveness of the tail for both powered and unpowered conditions.

7. To simulate one engine out-operation.

8. To determine the mechanical and aerodynamic performance characteristics of a lift fan having an X353-5B model rotor (3^{o} open blading).

9. To evaluate ground proximity effects on airplane and fan performance (mechanical and aerodynamic) and on engine and fan reingestion.

Operating limits for testing were established as follows:

Fan Vibration	2 g's; 10 mils
Fan Bearing Temperature	$350^{o}F$
Fan Turbine Inlet Temperature	$1221^{o}F$
Diverter Valve Skin Temperature	$1400^{o}F$
Torque Band Temperature	600 F
Fan Speed	100% (2640 rpm)
J85-5 Speed	104% physical speed (17,160 rpm)
J85-5 Vibration	6 mils compressor (peaking)
	5 mils compressor (steady)
	5 mils turbine (peaking)
	4 mils turbine (steady)
Stresses	See Table IV

SUMMARY OF TEST RUNS

Tables V through VIII summarize the test runs and configurations that were made during this program. Table IX is included to show the total accumulated operating time on both lift fans tested under this contract.

A total of 921 data points were recorded during the Period I testing including power-off and checkout runs. Another 633 data points were recorded during Period II including wind tunnel and ground proximity testing. The following test variables were investigated:

TABLE IV. FAN STRESS LIMITS

Item		Type of Stress	X353-5 Running[a] Stress Limit - SA (psi)	X353-5 Absolute[a] Stress Limit - SA (psi)	X353-5B Running[a] Stress Limit - SA (psi)	X353-5B Absolute[a] Stress Limit - SA (psi)
Rotor Blade:						
	Gage #1 (not installed for this test)	First Flexural Vibratory Stress (1850 rpm Speed Range)	8,000	12,500	10,700	16,700
	Gage #2	First Flexural Vibratory Stress (1850 rpm Speed Range)	3,000	4,700	-	-
	Gage #2	Cosine 2θ Vibratory Stress (2080 rpm)	15,800	22,800	- Not Used -	
	Gage #3	First Flexural Vibratory Stress (1850 rpm Speed Range)	6,500	10,100	8,700	13,600
	Gage #3	Cosine 2θ Vibratory Stress (2080 rpm)	10,800	15,600	20,900	30,100
	Gage #4	First Flexural Vibratory Stress (1850 rpm Speed Range)	5,000	7,800	-	-
	Gage #5	First Flexural Vibratory Stress (1850 rpm Speed Range)	7,400	11,500	10,000	15,600
	Gage #6	Cosine 2θ Vibratory Stress	15,800	22,800	33,000	47,500
Bucket:		First Flexural Vibratory Stress (800 cps)	10,000	15,600	10,000	15,600
		First Torsional Vibratory Stress (1540 cps)	7,500	11,700	7,500	11,700
Disc:		All Vibratory Gages	15,000	23,400	15,000	23,400
Torque Band:		Axial Vibratory Stress	10,000	-	10,000	-
		Tangential Vibratory Stress	10,000	-	10,000	-
Stators[b]:		First Flexural Vibratory Stress	10,000	15,600	10,000	15,600
		Second Flexural Vibratory Stress	8,750	13,600	8,750	13,600
		First Torsional Vibratory Stress	10,000	15,600	10,000	15,600

[a] Strain Gage Factor = 20%
Blade to blade stress variation factor = 30%
Blade to blade stress variation factor (cosine 2θ) = 20%

$\lambda = 1.2 \times 1.3 = 1.56$

λ (cosine 2θ) $= 1.2 \times 1.2 = 1.44$

Running stress limit $= \frac{\text{Absolute Stress Limit}}{\lambda}$

[b] Stator stress limits are not confirmed by bench tests.

TABLE V

MECHANICAL CHECKOUT TEST (ON THE RAMP - SEPTEMBER, 1961)

Run No.	Date	N_F left (RPM)	N_F right (RPM)	β_{left} (Deg.)	β_{right} (Deg.)	h/d_F	Configuration	Purpose of Run
1	9/25/61	-	1100 to 1600	-	0 - 35	1.71	Both fans - circular vane.	Mechanical checkout of right fan and engine combination, ground temperature and fan and engine reingestion data.
2	9/28/61	710 to 1600	-	-	0 - 35	1.71	No fixed side vanes.	Mechanical checkout of left fan and engine combination, and fan and engine reingestion data.
3	9/28/61	1100 to 1660	1100 to 1600	0 - 20	0 - 20	1.71	For all runs.	Compatibility of both fans and engines operating simultaneously, sound measurements, ground temperature and reingestion data.
4	9/28/61		720 to 1600	-	0 - 30	1.71		Additional data same as Run 1.

TABLE VI

PERIOD I WIND TUNNEL TEST (OCTOBER, 1961)

Run No.	Date	V_p (Knots)	α (Deg.)	$N_{F\ right}$ (RPM)	$N_{F\ left}$ (RPM)	δ_f (Deg.)	i_t (Deg.)	β_{right} (Deg.)	β_{left} (Deg.)	ψ (Deg.)	Configuration[1]	Purpose of Run
1	10/11/61	60	-4 to +18	0	0	0	Off	90	90	0	Inlet covered	Power off aircraft polar.
2	10/11/61	80-100	-4 to +16	0	0	0	Off	90	90	0	Inlet covered	Power off aircraft polar.
3	10/11/61	0-40	0	1650 to 1750	1690 to 1750	0	Off	0-40	0-40	0		Powered aircraft performance as a function of exit louver angle - low velocity ratios.
4	10/12/61	60-100	0	1690 to 1740	1690 to 1720	0	Off	0-40	0-40	0		Same as Run 3, but at high velocity ratio.
5	10/12/61	30-60	-4 to +18	1630 to 1770	1630 to 1720	30	Off	0-40	0-40	0		Powered aircraft polars and vectored exit louver performance.
6	10/12/61	0-100	-4 to +18	1590 to 1720	1600 to 1750	30	Off	0-40	0-40	0		Same as Run 5.
7	10/13/61	30-60	-4 to +18	1625 to 1750	1620 to 1690	30	Off	20-35	20-35	0		Powered aircraft polars at 20° and 35° exit louver angles.
8	10/13/61	40-60	-4 to +16	0	0	30	Off	90	90	0	Inlet covered	Power off aircraft polar.
9	10/13/61	20-80	-4 to +18	0	0	30	0	90	90	0	Inlet covered	Power off aircraft polar.
10	10/16/61	60-80	-4 to +16	1670 to 2460	1670 to 2480	30	0	0-45	0-45	0		Powered aircraft polars and vectored exit louver performance.
11	10/17/61	20-80	-4 to +16	1650 to 1760	1650 to 1760	30	0	0-40	0-40	0		Same as Run 10.
12	10/17/61	38-100	-4 to +18	1630 to 1770	1630 to 1705	30	-4 to +12	0-40	0-40	0		Same as Run 10 plus horizontal tail effectiveness.
13	10/18/61	40-100	-4 to +18	1000 to 1725	1000 to 1720	30	0	0-50	0-50	0		Same as Run 10.
14	10/18/61	20-100	-4 to +18	1000 to 1700	1000 to 1700	30	0	0-50	0-50	0		Same as Run 10.
15	10/18/61	20-80	-4 to +18	1105 to 1775	1110 to 1750	60	+4 to +20	0-35	0-35	0		Same as Run 10, but with 60° flap angle.
16	10/19/61	40-60	-4 to +16	0	0	60	0 to +20	90	90	0	Inlet covered	Power off aircraft polar.
17	10/19/61	60	-4 to +20	0	0	30	+4	90	90	0	Short wing span, inlet covered.	Power off aircraft polar.
18	10/19/61	0-60	-4 to +18	1170 to 2450	1190 to 2400	30	+4	0-35	0-35	0	Short wing span.	Same as Run 10, but with short wing span.
19	10/20/61	20-90	-4 to +20	1215 to 2590	1195 to 1760	30	+4	0-35	0-35	0	Short wing span.	Same as Run 18.
20	10/23/61	0-80	-4 to +16	1100 to 1800	1090 to 1790	30	+4 to +12	-18 to +50	-18 to +50	0		Roll and yaw control (staggered exit louvers) as a function of velocity ratio.
21	10/23/61	20-80	-4 to +18	1050 to 2360	1170 to 2400	30	+4 to +16	-10 to +50	-10 to +50	0		Same as Run 20, but with variable α.
22	10/24/61	20-80	-4 to +18	960 to 1800	995 to 1750	30	+4 to +16	0-35	0-35	0	Circular vane only.	Same as Run 10, but with circular vane inlet only.
23	10/26/61	20-80	0	1130 to 1750	1140 to 1775	30	+4	0-40	0-40	0	Circ. vane with articulated inlet louvers.	Powered aircraft polars and vectored exit louver performance.
24	10/26/61	80	-4 to +16	0	0	30	+4	35	35	0	Inlet closed	Power off aircraft polar.
25	10/26/61	20-80	-4 to +18	0	0	30	+4	90	90	0	Inlet closed and opened.	Power off aircraft polar.
26	10/27/61	30-80	-4 to +18	900 to 1850	1100 to 1740	30	+4	0-20	0-20	0		Same as Run 23, but with variable α.
27	10/27/61	60	0	2380 to 2500	2395 to 2460	30	+4	0-35	0-35	0		Same as Run 23, but at high fan speed.

[1] Runs 1 through 21 - circular vane with fixed side vanes; Run 22 - circular vane only; Runs 23 through 27 - circular vane with articulated inlet louvers.

TABLE VII

PERIOD II WIND TUNNEL TEST (JANUARY, 1962)

Run No.	Date	V_P (Knots)	α (Deg.)	$N_{F\ right}$ (RPM)	$N_{F\ left}$ (RPM)	δ_T (Deg.)	i_t (Deg.)	β_{right} (Deg.)	β_{left} (Deg.)	ψ (Deg.)	Configuration[1]	Purpose of Run
1	1/9/62	80	-4 to +18	0	0	30	+4	90	90	0 to +8	No inlet covers	Power off aircraft polar at 0° and 8° yaw angle.
2	1/9/62	80	-4 to +16	0	0	30	+5	90	90	0 to +8	Inlet covers on	Same as Run 1.
3	1/9/62	80	-4 to +16	0	0	30	+5	90	90	0 to +8	Inlet covers on, mid-wing	Same as Run 1.
4	1/10/62	0-125	0	1100-2400	1090-2625	30	Off	0	0-45	0		Fan mechanical checkout, operation up to 125 knots and 100% fan speed on left fan.
5	1/10/62	0	0	1150-1920	1100-1640	30	Off	0	0	0		Hover lift, both fans operating simultaneously.
6	1/11/62	40-80	-4 to +18	1605-1830	1580-1745	30	Off	0-45	0-45	0 to +8		Powered aircraft polars and vectored exit louver performance.
7	1/11/62	0-60	0 to +8	1200-1845	1130-1780	30	Off	0	0	-12 to +12		Powered aircraft yawlers.
8	1/11/62	0-60	-4 to +10	1640-2515	1610-2430	30	Off	-10 to -40	-10 to -40	0 to +8		Powered aircraft polars, roll and yaw control (staggered exit louvers).
9	1/12/62	40-100	-4 to +18	0-1830	1520-1855	0	Off	0-45	0-45	0		Powered aircraft polars and vectored exit louver performance.
10	1/12/62	0	0	1150-2590	0	0	Off	0	0	0	Unfaired inlet doors	Hover lift - right fan
11	1/13/62	0	0	1163-2611	0	0	Off	0	0	0	Faired inlet doors	Same as Run 10.
12	1/15/62	0-80	0	1100-2625	1100-2330	30	Off	0	0	0 to +12	Faired inlet doors, mid-wing	Hover lift - both fans and powered aircraft yawlers.
13	1/15/62	40-60	-4 to +16	1715-1800	1630-1725	30	Off	0-40	0-40	0 to +8	Faired inlet doors, mid-wing	Powered aircraft polars and vectored exit louver performance.
14	1/16/62	40-80	-4 to +16	1680-2350	1600-2350	30	Off	0-45	0-45	-12 to +12	Faired inlet doors, mid-wing	Same as Run 13.
15	1/16/62	60-80	0 to +8	1745-1750	1660-1700	30	Off	0	0	0	Faired inlet doors at 20°, mid-wing	Powered aircraft polars.
16	1/17/62	30-80	-4 to +16	1720-1880	1640-1740	30	Off	0-45	0-45	0	Faired inlet doors at 0°, high wing	Powered aircraft polars and vectored exit louver performance.
17	1/17/62	0-80	-4 to +18	1210-1790	0-2240	30	Off	0-45	0-45	0	Kruger flaps	Same as Run 16.
18	1/18/62	0	0	1700-2630	0	30	Off	0	0	0	Kruger flaps	Hover lift with streamlined (waxed) junctions between fixed side vanes and circular vane on right fan.
19	1/18/62	0-80	-4 to +18	0-2615	0-2310	30	Off	0	0	0	Kruger flaps, lowered circular vane	Powered aircraft polars and vectored exit louver performance, and hover lift.
20	1/18/62	40-80	0	0	1710-1730	30	Off	45	45	0	Split scroll, Kruger flaps	Simulated one engine-out performance - mainly rotor stress data.
21	1/19/62	60	0	0	0-2100	30	Off	0	0-70	0	Split scroll, Kruger flaps	Same as Run 20.
22	1/19/62	40	-4 to +18	0	0	30	Off	90	90	0	Inlets and exits closed, Kruger flaps	Power off aircraft polar.

[1] Runs 4 through 9 and 17 through 22 have no inlet doors installed and are a high wing configuration.

TABLE VIII

GROUND EFFECT TEST (ON THE RAMP - FEBRUARY, 1962)

Run No.	Date	V_P (Knots)	N_F left (RPM)	N_F right (RPM)	β_{left} (Deg.)	β_{right} (Deg.)	h/d_F	Configuration	Purpose of Run
1	2/3/62	Calm	600 to 2130	-	-5 to 20 & Stagger	-	1.82	No inlet doors.	Measure lift of left fan out of ground effect provide thrust spoiling data at hover.
2	2/3/62	Calm	1110 to 2480	1100 to 2350	0	0	1.82	Faired doors on left fan - no doors on right.	Determine influence of faired doors at 1.82 h/d_F measure lift of both fans running simultaneously.
3	2/3/62	Calm	-	-	-	-		-	-
4	2/6/62	Calm	1110 to 2320	-	0	-	0.98	Faired doors.	Determine influence of faired doors at 0.98 h/d_F.
5	2/6/62	7-8 SE	1120 to 2310	-	-5 to 10 & Stagger	-	0.98	No inlet doors.	Measure lift of left fan at 0.98 h/d_F & provide thrust spoiling data in ground effect.
6	2/6/62	5 NW to SE	1120 to 2290	-	-5 to 10 & Stagger	-	1.30	No inlet doors.	Same as 5 at 1.30 h/d_F.
7	2/7/62	8 SSE	1160 to 2370	-	0	-	1.82	No inlet doors, circular vane raised.	Measure performance improvement from raising the circular vane.
8	2/7/62	8 SSE	1710 to 2340	-	0 to 40°	-	1.82	No inlet doors.	Comparison with Run 7.
9	2/8/62	15 to 20 ESE	1130 to 2320	-	0	-	0.98	Unfaired doors.	Determine influence of straight doors at 0.98 h/d_F
10	2/8/62	15 to 20 ESE	1710 to 2265	-	0	-	0.98	No inlet doors.	Comparison with Run 9.
11	2/8/62	5-10 SE	-	1680 to 2345	0	0	1.82	No inlet doors.	Measure right fan performance out of ground effect.

Note: Aircraft nose pointed directly to the south.
h/d_F Calculation based on distance from nearest exit louvers (in the closed position) to the ground and a diameter of 62.5 inches. Right fan inlet configuration was the same as during preceding tunnel tests - Circular vane with fixed side inlet vanes for all ground tests. The left fan inlet consisted of the circular vane with fixed side inlet vanes removed, but with nine 6-inch vane stubs welded to the circular vane pointing radially towards the hub.

TABLE IX

SUMMARY OF LIFT FAN OPERATING TIME

	Fan, S/N 001						Fan, S/N 002					Total Both Fans
	B/U 1 & 2 Evendale	B/U 2, 3 & 4 Ames	B/U 4A Ames	B/U 5[a] Ames W.T.	B/U 5[a] Ames F.L.	Total	B/U 1 Even.	B/U 2 Ames	B/U 3[b] Ames W.T.	B/U 3[b] Ames F.L.	Total	
Speed Range												
0-24	9:10	-	-	-	-	9:10	2:57	-	-	-	2:57	12:07
25-49	10:06	11:21	4:10	1:30	:14	26:57	16:47	4:06	1:29	:05	22:27	49:24
50-74	15:49	42:46	27:14	17:43	3:16	106:51	12:17	27:26	17:24	:27	57:34	164:25
75-89	3:30	5:15	:03	1:18	1:58	12:25	9:38	:03	:20	:18	10:19	22:44
90-100	:10	7:52	1:35	1:12	:06	10:45	11:12	1:26	:27	-	13:05	23:50
TOTAL	38:45	67:14	32:52	21:43	5:34	166:08	52:51	33:01	19:40	:50	106:22	272:30
Temp. Range												
0-599°F	13:29	-	-	-	-	13:29	1:07	-	-	-	1:07	14:36
600-799	3:46	5:58	-	-	-	9:44	1:39	-	-	-	1:39	11:23
800-899	14:54	26:11	3:25	:06	1:10	45:46	15:20	1:00	-	:10	16:30	62:15
900-999	5:39	20:22	26:10	19:07	2:20	73:38	14:06	27:06	18:58	:22	60:32	134:11
1000-1200	:57	14:43	3:17	2:30	2:04	23:31	20:39	4:55	:42	:18	26:34	50:05
TOTAL	38:45	67:14	32:52	21:43	5:34	166:08	52:51	33:01	19:40	:50	106:22	272:30
Data Points	137	1314[c]	761[c]	417[c]	160	2789	554	761[c]	411[c]	17	1743	

[a] Rotor 009

[b] Rotor 001

[c] Not including basic airplane data with fan off

Tunnel Speed (V_p)	0 to 125 knots
Angle of Attack (α)	-4° to 20°
Fan Speed (N_F)	0 to 2640 rpm (100%)
Exit Louver Angle:	
Single Actuation	0° to 50° vector
Differential Actuation	0° to 45° vector and -18° to 50° stagger
Wing Flap Angle (δ_f)	0°, 30° and 60°
Tail Position	off and low
Tail Incidence Angle (i_t)	-4° to 20°
Yaw Angle (Ψ)	-12° to 12°
h/d_F (ground proximity testing)[a]	0.98 to 1.82
J85 Engine Speed	0 to 16,500 rpm (100%)
V_p/V_{tip}	0 to 0.6

TEST RESULTS

Test results are tabulated in Appendix A. Table A-1 contains definitions and symbols. Table A-2 is a compilation of Period I and Period II wind tunnel test results. The results of the February 1962 ground proximity testing is presented in Table A-3.

The following items from the wind tunnel tests (Table A-2) are direct readings (incorporating appropriate calibrations): fan speed (N_F), exit louver angle (β), tail incidence angle (i_t), flap angle (δ_f), barometric pressure, tunnel temperature (T_o), engine speed (N_{J85}), angle of attack (α), and yaw angle (Ψ). The other items in the tables have been converted from direct measurement by means of the formulae listed in the calculation standards (reference 16, Appendix A). These calcu-

[a] Where: h is the distance between the lower wing surface and the ground and d_F is the fan blade tip diameter.

lations were accomplished as follows:

- All the force data (lift, drag and moments) were reduced on the IBM 7090 computer operated by NASA-Ames. The standard 40' x 80' wind-tunnel calculation program was used with the following correction factors applied to account for wind-tunnel wall interference effects. These corrections are applicable only to the unpowered data:

  1. $\alpha_c = \alpha_u + 0.923\ C_{L_u}$ where: u denotes uncorrected, c denotes corrected
  2. $C_{D_c} = C_{D_u} + 0.0161\ C_{L_u}^2$
  3. $C_{M_c} = C_{M_u} + 0.02417\ C_{L_u}$ (tail on tests only)

  Additional corrections were made to the computer-calculated data from the Period II test results (Table A-2) to account for the difference in mounting system above the wind-tunnel support struts. The following corrections were applied to both powered and unpowered data.

  $$C_D = C_{D_{IBM}} - 0.01$$

  $$C_M = C_{M_{IBM}} + 0.02$$

- Both the NASA-Ames and the contractor's Evendale IBM 7090 facility were used for the fan internal aerodynamic data reduction.

- All other fan/aircraft performance calculations were made manually as described in the section on analysis of results, where appropriate.

MEASUREMENT ACCURACIES

The following are the estimated levels of data accuracy:

Power Off:

Drag	± 20 lbs.
Lift	± 40 lbs.
Moment	±200 ft.lbs.

The above values do not apply at or near stall conditions where the flow conditions are unstable.

Power On:

Drag	± 80 lbs.
Lift	±100 lbs.
Moment	±500 ft.lbs.

The above values do not apply at or near stall conditions where the flow conditions are unstable and at very low tunnel velocity (below 20 knots) where some fan and engine reingestion is present.

V. ANALYSIS OF RESULTS

A. GENERAL CONSIDERATIONS

Gas Generators:

Two early model YJ85-5 engines (NASA inventory) were used throughout the test program. These engines are normally operated with an afterburner, and required changes were performed by NASA to prepare them in a dry configuration. The engine cycle was well matched with scroll S/N 002 (large nozzle area)[a] used in the right wing installation. The scroll S/N 001 (smaller nozzle area)[a] resulted in too high engine exhaust temperature requiring the diverter valve for the left wing installation to be slightly opened during the tunnel tests, allowing $\approx$ 6% of the gas to bleed into the cruise nozzle. Thrust from the $\approx$ 6% bleed was negligible and is disregarded in all analyses. During the ground effect tests of the left fan, the diverter valve was fully closed so that the valve losses would be representative in the calculation of fan input horsepower. This necessitated holding the engine speed below 95% for the ramp tests to prevent over-temperature.

B. BASIC AIRCRAFT PERFORMANCE (POWER-OFF)

The basic aircraft polars are presented in detail in Figures 21 through 38, and a summary of the most important parameters is in Table X.

These polars (C_L, C_D and C_M as a function of α) were repeatable and showed very little deviation above 40 knots tunnel speed. This is consistent with results obtained in the 40' x 80' wind tunnel with previously tested models where it was found that Reynolds number effect

---

[a] Reference 17

TABLE X. SUMMARY OF AIRCRAFT POWER OFF RUNS

Run No.	V_p (Knots)	i_t (Deg.)	δ_f (Deg.)	Γ (Deg.)	C_L max.	C_L $\alpha = 0^\circ$	C_H $\alpha = 0^\circ$	C_H @ $C_L = 0$	C_H @ C_L max.	C_{Do}	α @ C_L max. (Deg.)	α @ $C_L = 0$ (Deg.)	β (Deg.)	Inlet	S_w	$\frac{\partial C_H}{\partial C_L}$	$\frac{\partial C_H}{\partial \Gamma}$ $\alpha = 0^\circ$	$\frac{\partial C_H}{\partial \Gamma}$ $\alpha = 8^\circ$
I-1	60	OFF	0	0	1.01	.10	-.017	-.020	.025	.050	15.0	-1.7	90	Covered	426	.0446		
I-2	80	OFF	0	0	1.01	.10	-.008	-.010	.030	.045	15.0	-1.7	90	Covered	426	.0396		
I-8	60	OFF	30	0	1.27	.51	-.145	-.167	-.086	.085	15.0	-8.8	90	Covered	426	.0405		
I-9	60	0	30	0	1.33	.41	.021	.068	-.140	.085	17.0	-6.2	90	Covered	426	-.1163		
I-16a	60	0	60	0	1.34	.49	-.097	-.037	-.200	.120	13.1	-7.2	35	Covered	426	-.1202		
I-16b	60	0	60	0	1.42	.60	-.107	-.030	-.210	.150	13.3	-9.5	90	Covered	426	-.1268		
I-17	60	4	30	0	1.54[4]	.46	-.100	-.070	-.310	.110	21.3	-9.0	90	Covered	305.9	-.267[5]		
I-20	80	4	30	0	1.12[4]	.33	-.105	0	-.410	.100	19.0	-6.5	35	Open	426	-.221[5]		
I-24	80	4	30	0	1.09[4]	.30	-.100	.035	-.335	.113	18.0	-6.6	35	10°	426	-.260[5]		
I-25a	80	4	30	0	1.24	.43	-.127	-.060	-.215	.090	17.2	-7.0	90	Closed	426	-.125[5]		
I-25b	80	4	30	0	1.26[4]	.29	-.139	-.065	-.300	.110	19.0	-5.8	90	10°	426	-.120[5]		
II-1a	80	4	30	0	1.19	.42	-.118	-.067	-.184	.096	15.1	-6.9	90	Open	426	-.1224		
II-1b	80	4	30	6.3	1.17	.42	-.130	-.083	-.184	.100	15.1	-6.9	90	Open	426	-.1102	-.00230	-.00343
II-2a	80	5	30	0	1.395	.50	-.113	-.058	-.185	.090	15.3	-7.9	90	Covered	426	-.112		
II-2b	80	5	30	8	1.32	.495	-.123	-.072	-.209	.098	15.2	-7.6	90	Covered	426	-.104	-.00220	-.00293
II-3a	80	5	30	0	1.39	.50	-.134	-.012	-.229	.110	15.3	-8.2	90	Covered	426	-.126[5]		
II-3b	80	5	30	8	1.36	.49	-.143	-.028	-.227	.116	15.3	-8.0	90	Covered	426	-.112[5]	-.00243	-.00260
II-22	60	OFF	30	0	1.525[4]	.445	-.145	-.160	-.040	.100	19.4	-6.8	90	Covered	426	.085[5]		

Notes: (1) Runs I-24 and I-25 - circular vane with articulated inlet louvers; all other runs - circular vane with fixed side vanes.

(2) Run II-3 - mid-wing configuration simulating VZ-11 airplane.

(3) Run II-22 - Kruger flaps installed.

(4) Read as highest value corresponding to largest angle of attack tested.

(5) Average value recorded since C_H versus C_L relationship was not linear.

with a Reynolds number above three million (based on mean aerodynamic wing chord) was practically nonexistent. For this model, a tunnel speed of approximately 25 knots on a standard day is equivalent to three million Reynolds number (see Figure 39).

Many aircraft configurations were investigated during this series of wind tunnel tests. For ease of comparison in Table X, data are tabulated for only the higher tunnel speeds (60 and 80 knots) where Reynolds number effects are insignificant.

Lift:

A summary of the changes in $C_{L\ max}$ and C_L because of installing the tail, and because of flap and tail incidence angle changes is presented in Table XI.

TABLE XI

BASIC AIRCRAFT - LIFT COEFFICIENTS

FAN INLETS COVERED AND EXIT LOUVERS CLOSED

Aircraft Configuration	$C_{L\ max.}$	C_L ($\alpha=0^o$)	$\Delta C_{L\ max.}$	ΔC_L ($\alpha=0^o$)
No Tail, $\delta_f = 0^o$	1.01	0.10	-	-
No Tail, $\delta_f = 30^o$	1.27	0.51	0.26	0.41
Tail On, $i_t = 0^o$, $\delta_f = 30^o$	1.33	0.41	0.06	-0.10
Tail On, $i_t = 5^o$, $\delta_f = 30^o$	1.395	0.50	0.065	0.09

Aircraft configurations simulating various fan inlet and exit conditions which may exist during conversion were investigated;

Table XII shows a summary of the results.

TABLE XII

BASIC AIRCRAFT LIFT AND DRAG COEFFICIENTS - CONVERSION CONFIGURATIONS

POWER-OFF, TAIL-ON, $i_t = 0^\circ$

	δ_f	$C_{L\ max.}$	$C_{L(\alpha=0^\circ)}$	$\Delta C_{L\ max.}$	$\Delta C_{L(\alpha=0^\circ)}$	$C_{D(\alpha=0^\circ)}$
Circular Vane + Fixed Side Vane Inlet:						
Inlet Covered Exit Closed	30	1.33	0.41	-	-	.085
Inlet Open Exit Closed	30	1.14	0.35	-0.19	-0.06	.092
Inlet Open Exit Open ($\beta = 35^\circ$)	30	1.07*	0.26	-0.26	-0.15	.096
Inlet Covered Exit Closed	60	1.42	0.60	+0.09	+0.19	.150
Inlet Covered Exit Open ($\beta = 35^\circ$)	60	1.34	0.49	+0.01	+0.08	.120
Articulated Inlet:						
Inlet Closed Exit Closed	30	1.19	0.36	-0.14	-0.05	.086
Inlet Open ($\theta = 10^\circ$) Exit Closed	30	1.21*	0.22	-0.12	-0.19	.106
Inlet Open ($\theta = 10^\circ$) Exit Open ($\beta = 35^\circ$)	30	1.04*	0.23	-0.29	-0.18	.109

*Values correspond to largest angle of attack tested

With the inlet and exit closed, the poorer aircraft performance for the articulated inlet system is attributed to two factors:

1. The articulated inlet louvers did not cover the inlet completely.

2. In the closed position, the test hardware did not provide a smooth wing surface and was not representative of flight type hardware in this regard.

When the fan inlet and exit were open, the aircraft performance characteristics at $\alpha = 18^{\circ}$ was about the same for both inlet systems. As expected, the articulated inlet produced higher drag at lower angles of attack. See Figures 28 and 29.

Period II testing included investigation of the effects of yaw angle, simulated mid-wing VZ-11 configuration, and Kruger flaps on aircraft performance. (See Figures 32 through 38.) The following statements describe the results as related to aircraft lift characteristics:

1. Increasing yaw angle decreased $C_{L\ max.}$ as follows:

Configuration	$\Delta\Psi$	$\Delta C_{L\ max.}$
Inlet Open Exit Closed	6.3	-0.02
Inlet Covered Exit Closed	8	-0.075
Inlet Covered Exit Closed Mid-Wing Configuration	8	-0.03

2. The mid-wing configuration was not as sensitive as the top-wing configuration to change in yaw angle.

3. Changing to the mid-wing configuration made no significant change in basic aircraft lift characteristics.

4. The addition of Kruger flaps produced an expected increase in maximum lift coefficient. They also caused a forward shift in the center of lift at higher angles of attack as indicated by the more positive moment coefficients.

Drag:

The aircraft mounting system above the wind tunnel support strut used during Period II testing was larger and contributed more drag than the mounting system used during Period I testing:

	Period I	Period II
Basic Aircraft, $\alpha = 0^{\circ}$, $\delta_f = 0^{\circ}$ Total Measured C_{Do}	0.05	0.06
Estimated Drag Contribution of Mounting System	0.02	0.03
Net Aircraft Drag $\alpha = 0^{\circ}$, $\delta_f = 0^{\circ}$	0.03	0.03

Consequently, Period II drag coefficients tabulated in Appendix A must be reduced by 0.01 to be on a comparable basis with Period I data. This was done for the preparation of Table X and the aircraft polar curves, Figures 21 through 38.

Referring to Table X, the following observations concerning aircraft drag characteristics can be made:

1. Addition of the tail caused no measurable change in C_{Do}.

2. Changing flap angle produced large changes in C_{Do}:
   from 0° to 30° δ_f, $\Delta C_{Do} = + 0.04$
   from 30° to 60° δ_f, $\Delta C_{Do} = + 0.075$

3. Opening the inlet and exit ($\beta = 35^{\circ}$) changed C_{Do} by 0.01 (circular vane plus fixed side vane inlet configuration).

4. With the articulated inlet configuration, opening the louvers to an indicated reading of 10° increased C_{Do} by 0.02. Opening the exit louvers to $\beta = 35^{\circ}$ increased C_{Do} by an additional 0.003.

5. Increasing yaw angle from 0° to 8°, increased C_{Do} by 0.008.

6. Adding the fuselage cap to simulate the mid-wing VZ-11, increased C_{Do} by 0.01.

7. The Kruger flap installation increased C_{Do} by 0.015.

8. Opening exit louvers to $\beta = 35^{\circ}$ with $\delta_f = 60^{\circ}$ reduced C_{Do} by 0.03. The open exit louvers apparently change the flow pattern in front of the flaps at this very large flap angle setting resulting in lower drag.

9. The short wing span configuration (Period I, Run 17) had a higher C_{Do} compared to the full wing span model.

Pitching Moments (Tail Downwash):

At zero angle of attack, the change in pitching moment between tail-on and tail-off test configurations is the moment contribution from tail downwash. Comparing Period I Runs 8 and 9, Table X,

$\Delta C_M\ (\alpha = 0^o) = 0.166.$

The change in moment coefficient (ΔC_M) with tail incidence angle at zero wing angle of attack is shown in Figure 40. The tail incidence angle that will produce a ΔC_M of 0.166 is 6.23° which is the downwash angle, ϵ, for the uncambered airfoil tail used in this testing.

From Figure 41, downwash angle as a function of angle of attack, the value of $\partial\epsilon/\partial\alpha$ was determined to be 0.605.

Static Stability:

Longitudinal - For the basic aircraft with the tail off, $\partial C_M/\partial C_L$ was positive and approximately equal to 0.042 indicating a small amount of static instability. With the horizontal tail installed, there was adequate static margin, the value of $\partial C_M/\partial C_L$ being approximately equal to -0.12 at all flap settings.

Larger negative values of $\partial C_M/\partial C_L$ (-0.22 to -0.26) resulted for test configurations with both fan inlet and exit open (Period I Runs 20 and 24). The open fan passage spoils the leading edge lift of the wing and the center of lift moves aft of the wing quarter chord as angle of attack is increased.

The aircraft model with wing tips removed exhibited static longitudinal instability for angles of attack up to about 10°. At higher angles of attack, this configuration becomes very stable accompanied by an excessively high drag.

Directional - The static directional stability derivative for the aircraft, $\partial C_N/\partial \Psi$,[a] was negative and approximately equal to

[a] Absolute values of yaw angle and side slip angle are equal in the wind tunnel.

-0.0022 with the tail installed. Values of $\partial C_N/\partial \Psi$ are inclused in Table X for angles of attack of 0° and 8° (Period II, Runs 1, 2 and 3).

The unpowered aircraft with no tail was tested at 0° side slip angle only. Therefore, the contribution of the vertical tail to the directional stability can not be established directly from the wind-tunnel test results. The methods outlined in reference 12, pages 322-326, were used to estimate $(\partial C_N/\partial \Psi)_{tail} = -0.00337$. This indicates that the aircraft with no vertical tail is unstable and has a value of $\partial C_N/\partial \Psi = -0.0022 - (-0.00337) = +0.0017$. As a further check on the accuracy of this result, a value of $\partial C_N/\partial \Psi = +0.00127$ was calculated for this aircraft model with no tail, using the methods of reference 12, pages 317-322.

This information is used in analyzing the directional stability of the fan-powered aircraft tested with the tail off (see Part E of this Section).

C. FAN AERODYNAMIC PERFORMANCE

The fan internal performance is deduced primarily from a survey of rotor discharge total pressures given by four fixed rakes of six Kiel-head total pressure elements located on centers of equal area. These were installed in both fans for most of the tests. When inlet modifications were tested, (Period I, Runs 10 through 27) the discharge total pressure was measured by eight fixed rakes of six Kiel-head total pressure elements located on centers of equal areas. For some of the static testing, a survey of rotor inlet static pressures was given by four fixed rakes of six static pressure elements located on centers of equal areas. (For location of pressure elements, see Figure 42.)

It should be noted that a direct measurement of flow is not available in most of the testing. There is no measurement plane in which velocities

and densities are known over the flow area to afford a flow integration. The test configurations for which flow is best known are the static test points where inlet static pressures are measured and where the total pressure locally can be assumed ambient because of the minimum inlet hardware.

It should also be noted that no total or static pressures downstream of the stator are ever measured. Thus, the losses of the stator or the exit deflecting vanes are not known, nor is the static pressure field at the stator or exit vane discharge known from any measurement. Assumptions leading to a level of total and static pressure downstream from the exit louvers are made and justified later in the analysis.

A basic configuration consists of the fan installed in the wing without any inlet or closure device ahead of the fan except the circular bellmouth vane. This configuration is referred to as the "circular vane inlet". The bellmouth vane is known to be necessary for static operation of the fan to prevent separation because of the small radius bellmouth ($r/d_F = 0.061$). A model of the internal performance of this configuration in cross-flow will be discussed first; this model of operation in cross-flow is necessary to explain the unexpectedly good performance of this configuration. The comparative performance of two inlet flow control devices will then be presented. One device consists of fixed side vanes arranged for minimum static loss, and located in the inboard and outboard portions of the fan annulus with the intent of turning the flow axially in these regions where most of the rotor loading and unloading occurs in cross-flow (similar to the helicopter effect of cross-flow on the advancing and retreating blades of the rotor). The second device has articulated louvers hinged to fixed, spanwise vanes which were scheduled as a function of flight speed to turn all the flow axially. With some additional hardware, the movable louvers could also be used to close the fan annulus for cruise. These additional inlet configurations are referred to as the "fixed inlet" and "articulated inlet", respectively.

A comparison of the operation of the right and left fan is also necessary because of the difference in operation which became apparent as a result of the tests. The comparison will be made from tests for which both fans consisted of the X353-5 rotor with the same inlet on each fan.

The -5 rotor was modified for Period II testing by reorienting the rotor blading 3^{o} in the direction to increase the power consumption. The performance of this opened-up rotor, designated X353-5B, is compared to the -5 rotor statically in- and out-of-ground effect, and in cross-flow.

A final part of this analysis will present the effects of closure doors statically in- and out-of-ground effect and in cross-flow. The presence of the fuselage close to the fan inlet, as in a mid-wing installation, is also discussed.

Performance Model of Basic Fan:

A model of the internal operation of the basic fan without any inlet or closure is first described qualitatively and then substantiated with the necessary qualifications.

Without any inlet, there is a strong cross-flow component imposed on the fan in flight. This cross-flow component causes the advancing blades to load up and the retreating blades to unload. As the cross-flow velocity is increased, the retreating blades eventually stall-out while the advancing blades continue to pick up load. The net result of this process is a gradual, moderate reduction in power absorbed at constant speed. As flight speed is increased, there is a portion of the annulus which is stalled and which handles no flow. This dead area increases with flight speed. In the balance of the annulus, the flow is being pumped with energy input continually higher than the energy input at

static conditions, up to and beyond the conversion flight speed.

If the power lost in the dead region is not great, and if the efficiency in the active region remains high, the internal efficiency will be moderately good. Moreover, this process will result in an effectively smaller fan absorbing nearly the same power at higher pressure ratio with increasing flight speed. As a result of this, there is net thrust available to higher flight speeds than would occur if the same power were absorbed uniformly in the entire annulus at a lower pressure ratio. In summary, the fan acts to provide an increasing mass-averaged pressure ratio with increasing flight speed and thus provides net thrust up to a higher flight speed than would be predicted. The efficiency in the region where the loading is increased can be reasonably good. A one-dimensional analysis would predict only a small change in stator incidence angles because of the high axial velocity of the flow. Thus, if the rotor can handle the loading, the efficiency can be good. System efficiency deduced would indicate that the system efficiency at 120 knots with the jet deflected 35° is nearly as high as static system efficiency.

Figures 43 and 44a show rotor discharge total pressures for the left and right fans, respectively. Each fan has the nominal rotor with the circular vane inlet. The ordinate is total pressure coefficient roughly proportional to the difference between local rotor discharge total and ambient static pressure. In both figures, rakes B and F are most nearly measuring advancing and retreating blade performance. The numbers on the curves denote flight velocity ratio (V_p/V_{tip}). In both figures, the advancing blades (rake B) pump an increasingly higher pressure rise. The retreating blades (rake F) unload up to a flight velocity ratio of 0.15; beyond this, the tip region stalls out. Also the leading edge portion of the fan (rake H) stalls at flight velocity ratios

above 0.15. A similar process occurs at $\beta = 35^{\circ}$ as shown in Figures 45 and 46 for the left and right fan, respectively.

The extreme distortion of the flow field in flight is apparent. An attempt is made to assign a local flow to each measurement point in the fan annulus. If the local flow is correct, it can afford a basis for a flow integration. The following assumptions lead to a level of total and static pressure at an area downstream from the exit louvers. The static pressure is assumed to be tunnel ambient over the entire fan annulus. The total pressure is taken to be the local rotor discharge total pressure reduced by a loss determined at static conditions as a function of exit louver angle.[a] It is implied that this loss does not change greatly in cross-flow which is fairly consistent with the small change in stator incidence angle with loading. If the local flow level calculated from this total and static pressure is assumed to exist from inlet to discharge, it becomes possible to mass average the rotor inlet total pressure, the rotor discharge total pressure, and the calculated stage discharge total pressure. From these, a mass averaged inlet total pressure loss and mass averaged stage total pressure rise can be obtained. Also, it becomes possible to integrate the thrust and discharge kinetic energy.

The net thrust obtained in this manner can be compared to the thrust measured on the model system. For this purpose, the drag of the aircraft is deducted from the system measurement. The remaining drag or thrust will then consist of fan thrust and any induced drag.

For the case of expansion down to ambient static pressure, the kinetic energy at the discharge is higher than the kinetic energy due to the approach velocity by an amount equal to the useful power

[a] Reference 16

output integrated from the calculated discharge velocity field and is shown in Figure 47, for $\beta = 0^{\circ}$ and $\beta = 35^{\circ}$. The ordinate represents useful delivered power at 100% fan speed. It is known that the fan tends to overspeed at constant throttle setting as the flight velocity is increased: the available power from the gas generator increases slightly with increasing flight velocity; and flight speed and exit throttling tend to unload the fan. The apparent required power for constant fan speed can be estimated by scaling down the available power by the cube of the overspeed. This required power for 100% fan speed is also shown in Figure 47 for both $\beta = 0^{\circ}$ and $\beta = 35^{\circ}$. The ratio of useful output to required input is the system efficiency. This is also shown in Figure 47. The system efficiency at low louver angles and low flight speed, and the system efficiency at high louver angles and high flight speeds near transition (120 knots, $V_p/V_{tip} = 0.28$) are approximately the same and reasonably high.

The increase in mass-averaged pressure rise at constant speed as flight velocity is increased is shown in Figure 48. If the entire fan annulus were to pump at this increased pressure rise, the flow would also increase and the power would increase on both accounts. The fraction of the annulus required to satisfy the actual flow and power gets smaller as flight velocity is increased. This effective flow area is also shown in Figure 48.

In summary, the fan effective flow area decreases and the fan pressure rise increases with flight velocity (Figure 48) with fairly uniform fan efficiency (Figure 47) up to the conversion range.

Performance with Additional Inlet Devices:

The "fixed vane" inlet, consists of fixed cascades of straight vanes running span-wise with the wing located in the inboard and outboard portions of the fan annulus within the confines of the

wing profile. A separate closure for the fan would be required. The "articulated inlet", has roughly similar fixed spanwise blades located within the wing confines. A movable vane is hinged to the leading edge of each of these fixed vanes such that, when closed, they close the fan aperture, and, when open, they extend out into the airstream. They must be scheduled primarily as a function of flight speed.

Total pressure elements were located immediately behind the inlets, positioned as indicated in Figure 42.

In general, despite the great difference in internal operation with each of the inlets, the result is only a small difference in maximum attainable forward flight speed.

The field of rotor discharge pressures for the circular vane inlets has already been presented in Figures 43 to 46. Similar data are presented for the fixed vane inlet in Figures 49 and 50, and for the articulated inlet in Figures 51 to 54. Where available, data for both fans are shown. Exit louver angles of 0° and 35° are chosen for representing unthrottled and throttled operation, respectively. Three or four levels of velocity ratio are chosen with 0.29 being near conversion. There are four circumferential locations where total pressure rakes of six elements are located: two in the advancing arc, two in the retreating arc. These are, also, either in the active arc of the partial admission tip turbine or the inactive arc and are so labeled.

With the circular vane inlet, the loading on the advancing side increases greatly (Figures 43 and 44a - rake B) with increasing flight speed. Where the advancing side is outboard (right fan, Figure 44a - rake B), the increase is much greater than when inboard (left fan, Figure 43 - rake B). This comparison is shown in Figure 44b. From wing static pressure data, the chordwise velocity distribution on the upper surface of the wing in the region of the advancing blade is higher ($\approx$ 15%) when the advancing blade is outboard; therefore

the fan appears to be operating at a higher velocity ratio (V_p/V_{tip}). This higher velocity results from the difference in wing area (due to wing leading edge sweep) upstream of the fan at the outboard panel as compared to the inboard panel. Similarly, the unloading of the retreating side is apparent. At low velocity ratios, the unloading is greater when the retreating side is outboard (left fan, Figure 43 - rake F) than when the inboard (right fan, Figure 44a - rake F), but in either case gets very poor at even moderate velocity ratios. This is illustrated in Figure 44c. At a given flight velocity, as the retreating side unloads, the ratio of cross-flow to local through-flow velocity becomes adversely high and eventually local through-flow virtually ceases. This is even more pronounced when the retreating blades are in the active arc of the turbine (right fan, Figure 44a - rakes F and H).

The effect of fixed vanes in reducing the peak pressure rise and loading is apparent (right fan, Figures 49a and 50 - rake B). The comparison with circular vane inlet at $\beta = 0^{o}$ and 35^{o} is shown in Figures 49b and 49c. This may as likely be a result of fixed vane separation as flow straightening, judging from these data. No left-wing fan data are presented from this run as it was not instrumented at the time.

The articulated inlet data are shown in Figures 51 to 54. A predicted schedule of louver angles versus flight velocity was tested and other schedules selected $\pm 5^{o}$ from this setting. At least two of these settings would produce nearly equal thrust with only small loss in thrust for the other setting; apparently, a fairly loose schedule is permissable. Their effect on equalizing the loading is apparent.

The method of calculating local flow for the circular vane inlet was applied to the fixed vane and articulated inlets. As previously noted, by assuming this calculated local flow to persist through the fan, it becomes possible to form a mass-averaged inlet total pressure loss and stage total pressure rise.

The inlet total pressure loss expressed in coefficient form is shown in Figure 55a. A comparison of fan-in-fuselage[a] and fan-in-wing inlet performance is shown in Figure 55b. The fan-in-wing circular vane inlet had a significant static loss and negligible recovery in transition. As reported previously the fan-in-fuselage circular vane inlet had insignificant static loss and recovered essentially 100% of the flight dynamic head.

The loss data for circular vane and articulated inlet relate to one another realistically. Both have increasing loss with flight velocity ratio. The articulated inlet, with its additional hardware, is poorer at low flight velocities, but improves with flight speed because of its variable geometry, greater solidity, and consequently, better ram recovery. The calculated loss for the fixed inlet looks low and was expected to be somewhat worse than the circular vane inlet at all flight conditions.

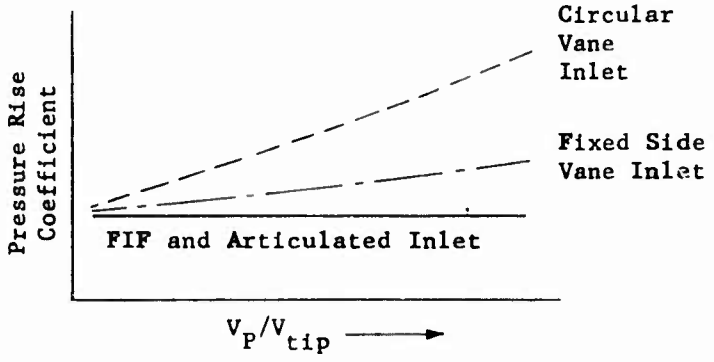
The stage total pressure rise coefficient for each of the inlets is shown in Figure 56. This is the same type of data as presented for the circular vane configuration in Figure 48. The internal operation of the fan is seen to be very different among the three inlet configurations.

It was the intention of this analysis to deduce the change in mass-averaged pressure rise at a constant fan speed as a function of flight velocity ratio for each of the three inlets. The discharge velocity from this, with a distortion coefficient would determine both flow and thrust for the distorted flow that actually occurs. It was anticipated that the rise in mass-averaged total pressure rise would be primarily a function of how little

---

[a] Reference 17, Figure 23

flow straightening would occur upstream. Thus, a fan-in-fuselage configuration with its uniform axial flow pattern, should have as nearly a constant pressure ratio as a function of flight speed (for a given fan speed) as could be expected.[a] The circular vane inlet should have a map with pressure ratio rising the most (similar to "Performance Model of Basic Fan" described near the beginning of this section). The articulated louver inlet might be close to a constant map with the fixed inlet intermediate between it and the circular vane inlet as illustrated below.



The results depicted in Figure 56 show the rise in characteristic of the circular vane inlet, with cross-flow. The right fan has a greater rise than the left. This is probably because the advancing arc of the right fan is outboard and local wing upper surface velocities are higher there than inboard; thus, the left fan pressure rise is lower. The level for a 35^{o} louver setting is higher at all flight speeds.

The articulated louver inlet has what appears to be a constant pressure rise (excepting one high flight speed data point). Again the right fan is higher. The drop measured at low flight speed may not be real.

---

[a] See Reference 18, Figure 33

The fixed vane results do not look intermediate at all. At $\beta = 0^{\circ}$, they decrease and at $\beta = 35^{\circ}$, they appear reasonably constant.

For the fixed inlet, then, it would appear that not much error would be incurred if a constant map were used with the pressure rise interpreted as a mass-averaged pressure rise. However, the effective area coefficient should be used as shown in Figure 57.

The effective area coefficients for each of the three inlets are shown in Figure 57 as a function of flight velocity ratio. The right and left fan data points are intermixed and the area coefficients do not appear to be a function of exit louver setting. The single curves for each of the three inlets are superimposed in the upper right-hand figure and they relate to one another sensibly.

The mass-averaged inlet total pressure loss, the mass-averaged total pressure rise, and effective flow area are consistent with a calculated thrust (drag) and lift. Lift and drag data are presented in Figures 58, 59, and 60. The measured drag (thrust) shown by the lines in Figure 60 is the total measured drag with the measured unpowered aircraft drag and engine ram drag deleted (includes intereaction drag). The data points are calculated drags based on the mass-averaged data.

The agreement of the calculated thrust (drag) at $\beta = 0^{\circ}$ with the measured thrust (drag) is good. At exit louver angles other than zero (35° and 40°), agreement is good except for the articulated louver inlet system. This comparison of calculated versus measured thrust (drag) affords a check on the integrated flow and is in encouraging agreement.

The corresponding fan lift based on these calculations is presented in Figures 58 and 59. In Figure 58, three sets of curves appear; one set for each inlet. Where available, the contribution of each fan is shown separately. In Figure 59 each set of curves compares the inlets at the same exit louver angle. It would appear, in general, that the articulated louver system was poorest at low velocity ratios and the fixed vane inlet best at high velocity ratios. At low velocity ratios, the circular vane is probably best, but the test data do not extend low enough in velocity ratio with sufficient accuracy for valid comparison.

Comparison of Fan Installations in the Right and Left Wings: Several installation differences exist between the right and left fans. Many of these can be seen in the sketch of Figure 42. The location of the four rotor discharge rakes is of particular importance. The angular locations of the rakes were 22 1/2° off from the wing chordwise and spanwise axes. Other aspects of geometric difference are tabulated as follows:

	Loading Position	Turbine Arc	Wing Thickness	Spanwise Location	Wing L.E.
Left Fan					
Rake B	Advancing	Active	Thick	Inboard	-
D	Weak Advancing	Active	Thin	-	-
F	Retreating	Inactive	Thick	Outboard	-
H	Weak Retreating	Inactive	Thin	-	Closest
Right Fan					
Rake B	Advancing	Inactive	Thick	Outboard	-
D	Weak Advancing	Inactive	Thin	-	-
F	Retreating	Active	Thick	Inboard	-
H	Weak Retreating	Active	Thin	-	-

	Left Fan	Right Fan
Period I (October 1961)	X353-5 Rotor S/N 001	X353-5 Rotor S/N 002
Period II (January 1962)	X353-5B Rotor S/N 009	X353-5 Rotor S/N 001

The difference of most concern between the left and right installations is the lower stall envelope of the right fan. This is an envelope of decreasing angle of attack with increasing flight velocity as shown in Figure 79. This envelope was relatively independent of inlet configuration but was increased by wind modifications such as the addition of Kruger flaps on the leading edge of the wing and the removal of the wing tip section. Both wing modifications are such as to reduce the local wing lift coefficient and hence average cross-flow velocity in the outboard region, especially at angle of attack.

In an earlier section it was noted that the advancing blades of the right fan, which were outboard, picked up loading more rapidly with flight speed than the advancing blades of the left fan, which were inboard (see rake B of Figures 43 and 44). Similarly, the retreating blades of the left fan, which were outboard, unloaded faster than the retreating blades of the right fan, which were inboard. This differential rate would occur if the average cross-flow velocity in the outboard region were approximately 15% higher than the inboard region. This would cause the rotor blading of the right fan to load up and stall earlier than the left fan. Also, the stall might be more severe because the advancing blades of the right fan were operating in the inactive arc. If the advancing blades operated in the active arc with turbine air leakage present, the performance should deteriorate more gradually and the stall might not occur so suddenly. Figures 56 and 58 show the generally more rapid increase

in pressure rise and lift of the right fan as compared to the left fan as flight speed is increased.

X353-5 Rotor Versus X353-5B Rotor:

Static Performance Out of Ground Effect - The X353-5 rotor was found to absorb 5 to 6% less than design power at design speed.[a] Low speed scale-model tests in a wing configuration had been run with simulated X353-5 rotor blading and with blading twisted open just at the tip to increase the tip loading. Both of these rotor blades were run at blade orientations for increasing the power consumption to determine the effect on fan efficiency. The better characteristics were obtained with the -5 rotor blade reoriented 3^{o} open (X353-5B). These scale model tests showed that the power consumption increased 10 to 11% with no change in static unthrottled efficiency, although there was more rapid unloading under throttled and cross-flow conditions. These characteristics were generally verified in the full scale tests as discussed in Part D of this Section of the report.

The rotor discharge total pressure rise coefficients for the two rotor configurations (full scale) are compared in Figure 61 showing a substantial ($\approx$ 6%) increase in pressure coefficient for the -5B rotor. The -5 rotor was tested at a ground height of $h/d_F = 2.3$ as set by the lift fan facility arrangement in Evendale. The X353-5B rotor was tested at a ground height of 1.82 which was the highest ground height obtainable for the Ames outdoor ramp test.

Static Performance in Ground Effect - The X353-5B rotor was also tested at a ground height of $h/d_F = 0.98$. The problems anticipated for this test configuration were:

[a] Reference 15

1. Hub stall due to heavy throttling of the hub region in proximity to the ground.

2. Reduction in power consumption and efficiency under throttling imposed by the ground plane.

The rotor discharge total pressure profile and radial variation of inflow velocity (local flow coefficient) are shown in Figure 62. The hub does not stall at $h/d_F = 0.98$. In going from an h/d_F of 1.82 to h/d_F of 0.98, the flow is reduced 9% at constant speed.

A momentum and static pressure integral can be made to deduce the fan internal thrust if the static pressure distribution across the discharge annulus is known. During these tests, static pressure was measured underneath the fan in the dead region beneath the hub. The only information available from which a reasonable estimate could be made of the static pressure distribution across the annulus was data from a scale-model of the fan tested in ground effect. Using this with the measured hub static pressure, the evaluation showed a 10% reduction in fan lift at $h/d_F = 0.98$. The corresponding reduction in measured power consumed, at constant fan speed, was 2.1% which, together with the lower lift, implies a reduction in system efficiency $(F^{3/2}/HP)$ of 13%. This is a much larger reduction in efficiency than occurs with normal throttling via exit louvers and can be attributed to the concentration of throttling at the hub evidenced by the very large drop-off in flow in that region (see Figure 62). On the average, the hub flow is reduced 16% versus 4 1/2% at the tip.

There is a plug thrust from the static pressure under the hub equivalent to about 2 1/2% of the out-of-ground effect thrust. Thus, the net thrust loss at constant speed is about 7 1/2% for the X353-5B rotor at $h/d_F = 0.98$ based on fan internal performance measurements.

Performance in Cross-Flow - The internal performance of the -5B rotor

was compared to the -5 rotor on the basis of the rotor discharge pressure rise coefficients. The performance of the -5 rotor with the fixed vane inlet in the right wing installation was shown previously as a function of flight speed in Figures 49a and 50 for $\beta = 0^{\circ}$ and $\beta = 35^{\circ}$. Similar curves for the X353-5B rotor with a fixed vane inlet but in the left wing installation are shown in Figures 63 and 64 for $\beta = 0^{\circ}$ and $\beta = 35^{\circ}$ (30° flap angle). Comparison of the two installations shows the -5B to exhibit a more rapid unloading of the retreating side (rakes F and H) and a less pronounced increase in loading on the advancing side (rakes B and D). Also the tip performance on the advancing side is poorer. These differences are certainly, in part, because of the higher outboard wing upper surface velocities on the right fan;[a] the poorer tip performance of the left fan (opened-up rotor) results from the advancing blades being in the active arc. They must also be partly the result of the inherently higher -5B rotor loading which would break down more rapidly under adverse conditions.

The effect of 30° flap angle is shown in Figures 65a and 65b. Some small circumferential redistribution of loading can be seen with the advancing blades loading up and the retreating blades unloading. The effect of angle of attack is illustrated in Figure 65a for $V_p/V_{tip} = 0.22$. At $V_p/V_{tip} = 0.22$ with $+16^{\circ}$ α and at $V_p/V_{tip} = 0.31$ with $+10^{\circ}$ α, there was still throttling margin since loading increased with the addition of 35° of exit throttling. Consequently, backpressuring resulting from underwing pressure at these angles of attack and velocity ratios is not severe. At $V_p/V_{tip} = 0.38$, the highly loaded side collapsed in stall (Figure 65b - rake B).

The effects of yaw angle are shown for $\Psi = \mp 12^{\circ}$ at $V_p/V_{tip} = 0.22$ (Figure 66). The effect of the combination shown is fairly small. There is some indication of circumferential redistribution of loading consistent with the changes in on-coming wind direction.

---

[a] This was discussed earlier in this section on pages 47 and 48.

In summary, the major variable on fan performance is flight speed with which the opened-up-rotor unloads slightly more rapidly than the -5 rotor. Of the variables of angle of attack, flap angle and yaw angle, only extreme angles of attack (above 14^{o}) have any serious effect causing rotor unloading.

Performance with Inlet Doors and Mid-Wing Simulation:

Static Performance Out of Ground Effect - Two closure door configurations were tested. Both of these doors were basically "butterfly" doors hinged along the fore and aft centerline. The hinge line was along the top of the major strut and the leading edge of the major strut was raised so that the axial location of the hinge line was well above the wing surface. Thus, when the doors were open, the trailing edges of the doors were well above the bellmouth and in a lower velocity region. Two types of doors were tested: 1) unfaired doors and 2) faired doors. The upper surface of the unfaired doors in the closed position corresponded to the upper surface of the wing contour everywhere except where the bulletnose protrudes through the wing surface. The unfaired doors were cut out to butt up against the bulletnose. The outer half of the faired doors in the closed position was identical to the unfaired doors. The fairing refers to a change in door contour which was in the direction to fair out most of the protruding bulletnose for improved wing performance in cruise. The fairing starts around a line which is roughly the mid-annulus of the fan and intersects the bulletnose near its top. Except for the effect of the wing spanwise contour, the fairing is roughly axisymmetrical.

In the open position, the unfaired doors showed no separation under static conditions. The faired doors, because of the reversed curvature, showed some separation near the hub. Static tests were

run on both configurations in the wind tunnel throat with the overhead tunnel doors open. Rotor discharge pressures are shown in Figure 67. There is a slight distortion near the hub because of the door fairing but no change in average pressure.

Static Performance in Ground Effect - Both closure doors were tested during the static ramp tests. The faired doors were tested at $h/d_F = 1.82$ and 0.98. The unfaired doors were tested at $h/d_F = 0.98$ only. The internal performance with the faired doors in ground effect is shown in Figure 67 in terms of flow and rotor discharge pressure rise coefficients; the effect is similar to that shown for the fan without doors in ground effect in Figure 62. A comparison of the faired and unfaired doors at $h/d_F = 0.98$ is shown in Figure 68. To satisfy continuity, the following relationship must hold: $\Delta\Phi \propto (\Delta\Psi)^{1/2}$. Since this was not the case, as shown in Figure 68, there is an indication that one or both of these measurements are in error. Using the relationship $F \propto \Psi^{1/2}\,\Phi$, the thrust difference between faired and unfaired doors is 2.2% at constant fan speed. (Using the same relationship, the thrust difference between no doors and faired doors is $\approx$ 1.6%.) There is an indication that the pressure instrumentation did not measure all of the loss because high loss areas are concentrated around the fore and aft struts. For comparison the measured thrust penalty between no door and faired door installation at 0.98 h/d_F and constant fan speed was 9.2% (see Table XIV, part D of this Section). In general, internal measurements are not satisfactory for identifying fan performance changes which affect the fan primarily in isolated, local areas.

The ground effect on the entire aircraft system was positive at $h/d_F = 0.98$; i.e., there was more thrust at constant fan speed or at constant fan power at $h/d_F = 0.98$ than at $h/d_F = 1.82$. Wind

conditions apparently had a considerable effect on system measurements, and consequently, only test points at similar wind conditions are comparable. A discussion of system measurements is presented in part D of this Section of the report.

Performance in Cross-Flow - Wind tunnel tests were made of the wing configuration with the faired closure doors. In addition, a series of tests was made with a simulation of a mid-wing installation by adding a superstructure to the topside of the fuselage. Its lateral cross-section at the fan centerline was roughly box-shaped such that the vertical sides were close to the fan inlet bellmouth at the wing surface. This body was added to the basic top-wing model and faired fore and aft. Most of the data discussed here compare the mid-wing configuration with faired closure doors installed to the top-wing configuration without closure doors installed. Some data for the top-wing configuration with closure doors are also given.

The flow over the closure doors was apparent from tufts applied to the door surfaces. The left fan doors could only be viewed when the mid-wing fuselage body was not on the model. A view from the right side of the aircraft model would show the outboard side of the outboard "butterfly" door of the right fan, and the inboard side of the inboard "butterfly" door of the left fan. A sketch of some of the tuft patterns is shown in Figure 69. Small regions of separated flow at static conditions are shown and these occurred within the light semi-circular line which circumscribes the bulletnose fairing. In normal level flight, the aft region cleared up and looked like the lower right figure shown for 80 knots. At high angle of attack, as shown in the upper right figure for 16^{o}, the inboard side of the left fan was badly separated at the leading edge. The effect was similar and more severe than that shown for the right fan in positive yaw. This implies a strong spanwise

flow component in the inboard direction at high angle of attack.

The comparison of the effect of the mid-wing installation with closure doors, to the top wing installation without closure doors is made on the basis of the measured rotor discharge total pressure field. Comparison is first made at zero angle of attack and zero yaw. Then a comparison is made at an angle of attack and in yaw. All of the data are from the left wing fan installation (X353-5B rotor and fixed vane inlet).

The combined effect of the mid-wing installation and doors is to increase the loading of rakes D and F in the back half of the fan. This effect noted at a flight velocity ratio $V_p/V_{tip} = 0.22$ is more pronounced at $V_p/V_{tip} = 0.31$. At this latter condition, rake B indicates poorer performance, especially in the tip region. This is shown in Figure 70.

Comparing the curve for the top-wing, no-doors configuration in Figure 70 with the same configuration in Figure 71 shows the loading effect of an angle of attack change of 10°. This is similar to the loading effect from increasing velocity ratio. Figure 71 indicates that the addition of doors alone is the big factor in increasing fan loading and that the mid-wing configuration of itself probably has little influence.

The effect of the mid-wing installation with the doors in yaw is shown in Figure 72. The positive yaw (clockwise) of these comparisons is in the direction to cause the flow to approach from the left and thus be similar to angle of attack variations, which seem to cause a strong spanwise inboard flow component (left fan). Indeed the effects are in the same direction and more pronounced.

The pronounced effect of the modifications of either the doors

alone or the combination of mid-wing simulation and doors is the increase in loading of rakes D and F in the aft portion of the fan. The change in peak total pressure attained by rake D is roughly that which would be attained with full ram recovery and normal work input. The aft portion of the fan annulus could be expected to have local full ram recovery. Normal work input would imply no circumferential velocity component in this region.

It is possible that the doors and fuselage prevent a strong inboard velocity component in the vicinity of rake D; this would imply a strong inboard velocity in this region with the top-wing installation without doors which would cause the region of the fan near rakes D and F to unload.

Performance "Tuning" with the Circular Vane:

An investigation was made during the outdoor testing to show the effect of increased inlet vane loading. Because of fabrication, welding and rewelding, and installation changes to accommodate the various test configurations, the vane shape became distorted in a direction to unload it in the middle of both the active and inactive arcs of the fan. The vane was raised at both locations to increase its loading. Geometric angles before and after this change, which reflect this loading, are shown in Figure 73. The effects of improved tip performance appear on rakes B and F in Figure 74. The 3.3% increase in average pressure coefficient was reflected in a measured 2 to 3% increase in thrust with practically no change in power requirements, indicating a fan efficiency improvement. The vane was raised only for one test run at 1.82 h/d_F and was in its normal position for all other runs.

Miscellaneous:

In order to identify effects related to use of test equipment (see

Figure 5) instead of flight type hardware, wax was applied to the side vane to circular vane attachment joints to provide a smoother aerodynamic flow path. This investigation was accomplished on the right fan in the wind tunnel for a hover condition with the tunnel throat opened to atmosphere. Fan efficiency was markedly increased (2 to 3% lift increase) indicating the significance of the junction points to good performance.

D. FAN THERMODYNAMIC PERFORMANCE

The preceding part of this Section evaluated the fan performance based on internal measurements. A corresponding evaluation can be made based on system performance measurements; primarily, system input horsepower and fan thrust. For convenience, the fan speed-thrust relationship is also used as a means of comparing performance, loading and basic differences in fan operation.

As noted in Section II, part of the testing involved simultaneous testing of fans with different rotors. Their primary design difference was to obtain an increase in power absorption with essentially equivalent efficiency so that for a given power input each fan type would produce the same thrust with the -5B operating at approximately 3% lower speed (favorable from mechanical performance aspect). Table XIII shows the basic X353-5 and -5B measured characteristics:

TABLE XIII

X353-5 AND X353-5B STATIC PERFORMANCE DIFFERENCES

	Thrust at Design HP[a] (lbs.)	Thrust at 100% N_F (lbs.)	Speed at Design HP (%)	Efficiency Parameter $\frac{F^{3/2}}{HP}$
X353-5[b]:				
Maximum Power	7020	7050	99.8	138.5
Minimum Power	7155	7050	100.8	141.6
X353-5B	7130	7620	96.8	141.0

[a]4270 Horsepower; [b]Reference 19, page 29.

The actual performance data indicate an increase of 9 to 12 1/2% in power absorption with the -5B rotor which was accompanied by an increase of 0 to 2% in fan efficiency depending upon the level of power which is actually associated with X353-5 performance (this power discrepancy is discussed in detail in reference 19). There were other slight differences in configuration between these two fans in Table XIII: The -5 fan was installed in a test wing at Evendale (NACA 65-210 series with no taper) and located at an $h/d_F = 2.3$; the -5B data were obtained with the fan installed in the left wing (NACA 65-210 series, 0.5 taper ratio) of the wind tunnel airplane model and located at an $h/d_F = 1.82$[a]; the -5 fan had only a circular vane installed in the inlet, while the -5B had the circular vane and the radial stub vanes (see Section II). The stub vanes were welded in place and this provided smooth junctions at the circular vane. Because of these variations in configuration the static performance differences in Table XIII must be considered approximate.

Comparison of Static Test Results:

Tables XIV and XV gives a comparison of static test results to identify the magnitude of performance effects resulting from the many configuration and test variables. The following conclusions can be inferred from the tables (it should be noted that the measurements of wind velocity at the ramp were not precise[b] and that only one fan was operated for the comparative tests):

1. The X353-5B fan will operate at ≈ 3-4% lower speed than the -5 for a given power level and has the same efficiency.

2. The maximum test height on the ramp ($h/d_F = 1.82$) is con-

---

[a] The X353-5B will be tested at $h/d_F = 2.3$ at Evendale under contract DA 44-177-TC-715 and will provide another comparison. The inlet for this proposed testing will be the circular vane with fixed side vanes.

[b] Phoned from Moffett Field tower.

TABLE XIV

COMPARATIVE STATIC THRUST DATA (RAMP TEST)

Configuration	$\left(F_{Test}/F_{Evendale}\right)_{HP = C}$	$\left(F_{Test}/F_{Evendale}\right)_{NF = C}$	N_F at Design HP[a] %	Efficiency Parameter $F^{3/2}/HP$
X353-5 w/circular vane inlet (at Evendale):[b]				
$h/d_F = 2.30$: Max. Power	1.000	1.000	99.8	138.5
Min. Power	1.024	1.000	100.8	141.6
X353-5B w/circular vane + stub side vane inlet (at Ames):				
$h/d_F = 1.82$:				
No Inlet Doors	1.015	1.080	96.9	141.0
No Doors + 8 Knot Wind	0.988	1.038	96.9	135.2
No Doors + 8 Knot Wind - + Raised Inlet Vane	1.005	1.065	96.9	138.7
Faired Inlet Doors	1.015	1.080	96.9	141.0
$h/d_F = 1.30$:				
No Doors + 5 Knot Wind	0.927	0.974	97.3	122.8
$h/d_F = 0.98$:[c]				
No Doors + 8 Knot Wind	1.084	1.131	97.6	155.5
No Doors + 15 Knot Wind	1.085	1.092	99.5	155.6
Unfaired Doors + 15 Knot Wind	1.092	1.107	99.3	157.2
Faired Doors	1.062	1.080	98.9	150.5

[a] 4270 Horsepower

[b] Reference 19, page 29

[c] VZ-11 Equivalent

TABLE XV

MEASURED AND CALCULATED GROUND EFFECT PERFORMANCE

(FULL-SCALE AND SCALE-MODEL DATA)

Configuration	Constant Power				Constant Speed			
	ΔF Measured		ΔF *Calculated		ΔF Measured		ΔF *Calculated	
	Full Scale (%)	Scale Model (%)	Full Scale (%)	Scale Model (%)	Full Scale (%)	Scale Model (%)	Full Scale (%)	Scale Model (%)
X353-5B with Circular Vane								
$h/d_F = 1.82$:	Reference Configuration							
$h/d_F = 0.98$:								
No Inlet Doors	+9.9	-	-6.4	0	+9.2	-11.0	-7.7	-4.0
Faired Doors	+4.7	-	-	-	0	-	-9.3	-

* Calculated valves refers to values determined from fan internal pressure measurements similar to the method used in Part C of this Section (see page 55).

sidered out of ground effect based on the -5B thrust at constant power falling within the accuracy of -5 data at h/d_F = 2.30 for similar configurations.

3. The unfaired doors have no effect on fan performance out of ground effect (from hover wind tunnel tests) or in ground effect; the slight increase in fan efficiency at 0.98 h/d_F is considered negligible relative to test accuracy.

4. The faired doors have no effect on fan performance out of ground effect but cause approximately 5% lift loss in ground effect at a given power level with over 9% lift loss at a given speed. The door effect comes from both unloading and a decrease in fan efficiency. The unloading ($\approx$ 2% in fan speed) accounts for $\approx$ 4% of the constant speed lift loss. The 5.2% lift loss at constant power (Table XV) measures the decrease in fan efficiency.

5. Increased loading on the fan inlet circular vane increased fan efficiency by 2 to 3%.

6. Wind had an erratic effect on fan performance: out of ground effect an 8 knot wind resulted in an apparent 4% decrease in fan efficiency; in ground effect a change from an 8 to a 15-knot wind did not affect fan efficiency but unloaded the fan ($\approx$ 2% in speed). There are insufficient wind data, accuracy and control of test conditions to understand fully wind effects; however, both on the ramp and during Evendale testing, light crosswinds have adversely affected fan hover performance.

7. Ground effects were significant and were dependent on the test arrangement. The change relative to h/d_F = 1.82 in-

dicates a large positive ground effect at $h/d_F = 0.98$ but a large negative ground effect at $h/d_F = 1.30$. Figure 18 graphically illustrates the basic configuration difference: at $h/d_F = 0.98$, the fuselage and ground plane simulate two-fan operation by presenting an effective image plane to the discharge flow; at $h/d_F = 1.30$, there is a gap between the fuselage wind ground plane allowing fan discharge air to flow out under the fuselage.

8. Internal measurements (Table XV) indicate that the fan performance is reduced in proximity to the ground. The positive system ground effect because of the aircraft configuration must account for the difference and is, therefore, a very large effect, say 15 to 17% in lift.

9. The fan did not unload appreciably in ground effect (less than 1% in speed change for comparable conditions). This was a very different result than was obtained in scale model work which indicated a power reduction of 10 to 11% to maintain a constant speed. This is equivalent to $\approx$ 3.5% increase in speed for the same power input.

Static Performance Measured in the Wind Tunnel:

Static performance is considered approximate whenever measured inside the wind tunnel but is obtained for comparative purposes. In general, with the fan-in-wing configuration, static results measured in the tunnel with the throat opened to the atmosphere indicated fan lift to be 200 to 300 pounds lower than measured outdoors during ramp testing or at Evendale.

A primary difference between static tests in the wind tunnel and elsewhere was the fixed side vane installation; these were not involved during Evendale tests, and on the ramp radial stub vanes discussed above were substituted. A simple test was made on one

of the fans to determine the penalty of the crude vane attachments (refer to Figure 5) at the circular vane: a run was made with wax filler applied to the junctions to smooth out the aerodynamic flow path. This resulted in a 270 pound increase in the static lift performance and would fully account for the difference noted between tunnel and other static test results. This "calculated" close agreement between the various static data was also obtained for the fan-in-fuselage program (see reference 17, Table V).

One as yet unexplained difference in static performance was obtained both in the tunnel and during ramp tests: the right fan performed markedly worse than the left fan. This was of no significance to the ground effect program which involved comparison tests on one fan only, but, during the wind tunnel program, fan lift is taken as the average of two "identical" fans, and worse performance of the right fan would reflect in the presented data's indicated lower fan contribution to the total performance than would be realized with two actually identical fans. This difference is over and above the difference in the fan loading characteristics between the left and right wing fans discussed in Part C of this Section, which has to do with inlet environment and not basic fan capability. Although measured forward air seal clearances are indicated to be very similar for the the two fans (Section II), it is believed that, with different rotor to frame dimensional runouts and possibly different thermal growths in the two fans, the right fan was adversely affected by higher forward air seal leakage.

The significance of both the junction loss and the right fan deficiency is that the wind tunnel results presented are slightly pessimistic in terms of lift and net thrust capability in transition.

Fan Throttling Characteristics:

Figure 75 compares the X353-5 and -5B constant power static throttling characteristics. During these tests, the -5B data were obtained at lower fan speed and are, therefore, less reliable. Much more data is now available from the flightworthiness test of the X353-5B propulsion system in the Contractor's Evendale static test facility. These results

have been added to Figure 75 for comparison. In addition, the fan speed variation as a function of exit louver vector and stagger angles is shown in Figure 77b. At the static condition, the increase in fan speed with louver setting is not as severe as indicated in Figure 77a.

Fan Power Absorption in Transition:

The fan-in-wing unloads[a] rapidly as cross-flow velocity is increased. This is in marked contrast to the fan-in-fuselage installation where the fan operated at practically constant speed throughout the transition range (see reference 17, Figure 34). The fan-in-wing unloading characteristics are shown in Figures 76 and 77a for the left wing installation of X353-5 and X353-5B rotors; the X353-5B unloaded more both as a function of exit louver angle and forward speed. This characteristic is a function of its blade loading (see Part C of this Section). Figure 78 shows the predicted fan speed attainable as a function of forward speed and exit louver angle for a J85-5 power setting equivalent to $HP_{5.4} = 4180$ at hover. The X353-5B rotor is more highly loaded at its static design point and, therefore, runs at a lower speed at hover conditions and $\beta = 0^{\circ}$. At high forward velocities and high louver settings the two rotors approach the same speed. This is why system performance in cross-flow based on the same fan speed does not appear to differ for the two fan types.

All of the transition aircraft performance analyses are based on a 100% fan speed limit. It is possible to improve this performance appreciably if all available energy from the J85 engine were utilized. This kind of operation would have to be based on mechanical considerations, since an increase of $\approx$ 7% above the design fan speed would result.

---

[a] Fan speed increases as power supplied to the turbine remains constant.

Unloading characteristics shown in Figure 77 are applicable for the left fan installation with either the circular vane with fixed side vanes or the circular vane only inlet configuration. The articulated inlet did not unload as rapidly as a function of cross-flow. This is not based on the power absorption measurement but on the fan internal performance and higher aircraft pitching moments for the articulated inlet at velocity ratios above 0.2 which indicate higher fan flow. Based on internal fan performance it also appears that the right fan at velocity ratios below 0.3 unloaded less as a function of velocity ratio than the left fan. (See Figure 58.) This difference is probably too small to identify in power measurements.

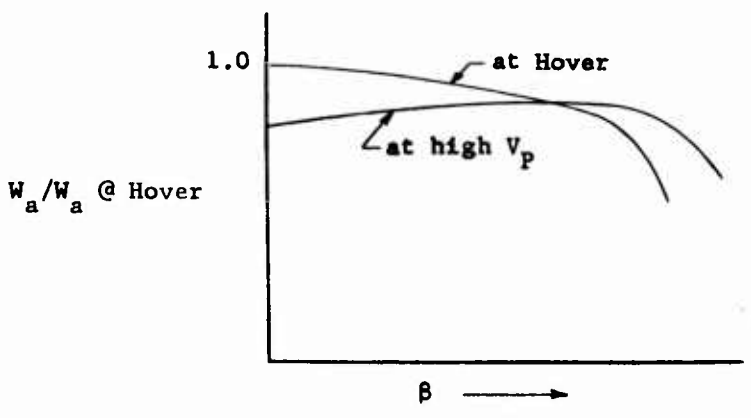
The internal measurements provide insight to the marked dissimilarity in performance between the right and left installation at high velocity ratios. The right fan experienced an instantaneous unloading (stall) of $\approx$ 10% speed change (equivalent to $\approx$ 30% power absorption change at constant speed); the locus of these stall points is shown in Figure 79. In general, increase in exit louver angle allowed an increase in velocity ratio before this stall occurred. As velocity ratio is increased, the fan does not remove all of the cross-flow component and the discharge flow angle becomes positive. This results in additional louver losses and throttling and less stall margin at $\beta = 0^{\circ}$, and a decrease in louver losses and throttling at high exit louver angles (see Figure 80).

This phenomenon contributes to the good conversion capability of the fan-in-wing compared to the fan-in-fuselage in spite of the much poorer inlet ram recovery. The other contributor, the variable pressure ratio phenomenon, is described in Part C of this Section.

The left fan did not experience this rapid unloading, except at very high velocity ratios. It did, however, unload slowly as a function of angle of attack at velocity ratios around 0.4. This characteristic is shown in Figure 79 for the X353-5 and -5B rotors in the left wing. The X353-5 rotor tolerated ≈ 10% higher velocity ratio before becoming sensitive to angle of attack changes. Installation of fan inlet doors and changing to a mid-wing configuration reduced this velocity ratio threshold by ≈ 20%; angle of yaw of 8° reduced it by another 10%. Left fan unloading above this velocity ratio-angle of attack envelope was ≈ 0.5% fan speed per degree of angle of attack; within the envelope, fan speed was not affected by angle of attack.

Flow Direction Through Fan in Transition:

With the fan mounted below a deep duct as in the fan-in-fuselage installation, the flow is turned 90° into the fan. In the thin wing installation the fan flow is axial only at hover and, as flight speed increases, the flow angles through the fan without being fully turned into the inlet. At the higher flight speeds with β set at low angles, the louvers are at negative incidence to the flow. At high β settings the louvers line up with the flow angle through the fan, resulting in less throttling effect at high β angles in cross-flow than at low β angles. The sketch below illustrates the general characteristic believed to exist, although this is not directly measurable in transition:



This effect is best indicated in the data by the increase in net thrust beyond β settings which at hover indicate excessive throttling losses without an increase in horizontal thrust. The maximum useful β setting around conversion velocity ratios for the fan-in-wing configuration was ≈ 50°; for the fan-in-fuselage, 37° was optimum.

Fan Sound Power Levels and Directivity:

A far field noise measurement of the lift fan installed in the NASA airplane was made during the ground effect testing. A sound pressure survey was made around one side of the aircraft model at a radial distance of 65 feet and in the plane of the fan, which was about 10 feet above the pavement.

Fan speeds ranged from 600 to 2300 rpm and the measured sound pressure levels (average for each survey) are shown in Figure 81. For each survey a maximum sound pressure was recorded in a direction normal to the aircraft fuselage, probably the result of sound reflection. The range of sound pressure levels for any one survey (one fan speed) was ± 4 db, which is not significant. Fan exit louvers were actuated from 0° to 20° at 1400 and 1725 fan rpm, and no significant change in fan noise was detected.

It is assumed (based on propeller noise experience) that the maximum noise is radiated in the plane of the fan. The sound power level measured for the blade passing frequency at Evendale previously was 151 db compared with 158 db indicated by these results and considering directivity was 3 to 7 db lower than measured at Ames.

Fan and Engine Inlet Reingestion:

The most severe case of engine reingestion occurred during the ground checkout test conducted on the ramp in September 1961.

Severe engine reingestion was encountered for all cases of two-fan operation and, as shown in Table XVI exit louver angles up to 20^{o} were not effective in clearing the engine inlet condition. No fan reingestion was noted under any conditions. The fan discharge was 8 feet 11 inches above ground equivalent to 1.71 h/d_F and the engine nacelles terminated 6 feet 10 inches forward of the fan centerline and 2 feet 9 inches below the fan discharge. Operation was unsteady because of random variations in engine inlet temperature of $\approx \pm 20^{o}F$. With one fan operating, there was again no fan reingestion; however, the engine inlets operated $\approx 12^{o}F$ above ambient without the speed variation problem.

With two-fan operation the hot air from the fan turbines is pinched between the cold, denser, fan discharge air, and it issues in a narrow stream fore and aft. The stream was so narrow that sometimes only one engine was influenced (refer to Table XVI). As far forward as the nose of the aircraft, the stream was only 4 to 5 feet wide.

For the February 1962 ground effect tests, engine inlets were modified to prevent reingestion simulating a high inlet configuration (see Figure 15).

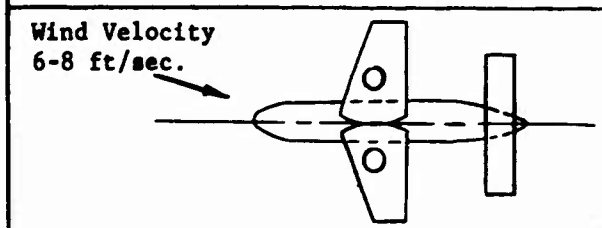
There was no inlet temperature rise noted during these tests with both fans operating ($h/d_F = 1.82$). A few of the runs with only one fan operating indicated a fan and engine inlet temperature rise of up to $10^{o}F$. The maximum value was observed for a few data readings and did not appear to be a function of h/d_F value or any other variable in the testing. Fan speed stability was generally within $\pm$ 1/2%; with $10^{o}F$ reingestion the fan speed varied $\pm$ 1%.

In wind tunnel tests, engine and fan reingestion was present be-

TABLE XVI

ENGINE INLET REINGESTION

Left Wing Fan (001)							Right Wing Fan (002)					
Amb. Temp. (°F)	Fan Speed (rpm)	EGT (°F)	CIT (°F)	Δ CIT (°F)	CIT Spread (°F)	β (deg.)	Fan Speed (rpm)	EGT (°F)	CIT (°F)	Δ CIT (°F)	CIT Spread (°F)	β (deg.)
68	-	-					1100	840	77	9	1	0
68	-	-					1400	840	79	11	10	0
68	-	-					1600	840	80	12	17	0
68	-	-					1600	840	73	5	0	35
70	1100	850	84	14	5	0	-	-				
70	1400	850	82	12	5	0	-	-				
70	1600	850	81	11	4	0	-	-				
70	1600	850	80	10	5	10	-	-				
71	1600	850	80	9	5	20	-	-				
71	1600	850	83	12	4	30	-	-				
73	1100	860	74	1	1	0	1100	980	181	108	24	0
73	1400	930	153	80	13	0	1400	1010	150	77	37	0
74	1600	930	90	16	10	20	1600	1020	110	36	38	20
75	1600	850	84	9	4	0	1600	1050	160	85	24	0
75	1600	850	81	6	2	0	1600	1080	168	93	20	0
75	1600	850	82	7	12	0	1600	1050	154	79	28	0
75	1600	1020	142	67	12	0	1600	880	78	3	5	0
75	1600	850	86	11	11	0	1600	1110	178	103	16	0



low velocity ratios of 0.08 when both fans were operating. This caused unsteady fan operation and prevented obtaining reliable data. The maximum level or reingestion was about 20°F.

During static tests in the tunnel (overhead doors opened), with only one fan running, the fan and engine inlet temperatures increased gradually up to 20°F above the temperature at the start of the test run. This was normal tunnel heating because of engine operation. The fan operation showed ± 1% speed fluctuation and permitted valid data recording.

Ground Temperature Survey:

During the ramp tests, temperature surveys were taken in the fan discharge and vicinity and on the fuselage skin near the fan turbine. Results of the air temperature measurements are shown in Figures 82a to 83c with the fan discharge at an h/d_F value of 1.30. The data were taken at two vertical planes, and measurements were recorded at eight values of h/d_F. The results also indicate that the hot fan turbine discharge air is confined by the cold, denser, fan discharge air to the vicinity of aircraft fuselage and that the hot air leaves in a thin sheet fore and aft (this is also substantiated by observation while walking around the model).

Air temperature data at 0.98 h/d_F is not as extensive and consistent as that obtained at 1.30 h/d_F but it generally shows higher temperature and more penetration of the hot gasses into the cold fan shown in Figures 84a, b, and c. General temperature surveys around the fans are difficult to obtain because of the large volume to be covered and the steep temperature gradients in the mixing regions. Fan height above ground, fuselage geometry and the adequacy of single fan tests (simulated image plane of symmetry) also would cause difficulty in applying these results directly to

other configurations. The levels of temperature encountered should, however, be a good indication of possible problems.

For a case with the fans located about one diameter above ground which is realistic for an actual fan-in-wing aircraft (viz. the VZ-11), the maximum temperature profile under the turbine stream reaches approximately 450°F above ambient 5 to 15 inches above ground. The maximum occurs near the interface with the fan stream, and sharp gradients are encountered within a few inches. This local high temperature mixes after turning by the ground and the temperature drops rapidly to 50 to 100°F above ambient within a few fan diameters distance.

Fuselage skin temperatures for the two values of h/d_F are shown in Figure 85. These values were very consistent between runs, and can be safely used for design values after making corrections for heat transfer characteristics of the fuselage wall (test fuselage was made of 1/8 inch thick sheets of mild steel). The maximum temperature reached within 77% of the gas generator T_5 level which is close to fan turbine discharge temperature.

E. FAN POWERED AIRCRAFT PERFORMANCE

Performance Coefficients:

Non-dimensionalized coefficients used throughout this report were described in references 16, 17, and 18. Changes were made for this report to make the moment coefficient more meaningful. Previously the moment coefficient, H_M, was non-dimensionalized with the tail moment arm, ℓ_t. For this report, except as specifically marked otherwise, it is non-dimensionalized with the wing mean aerodynamic chord, C_{mac}. In search of the most appropriate basis for comparison of fan powered aircraft configurations, fan diameter is used in place of wing chord in the moment coefficient definition in some cases. Where this is done, the change is noted accordingly.

Other than these changes the coefficients are as described in references 16, 17, and 18. Table XVII gives the conversion relationships for a general fan-in-wing case and for the specific model tested.

TABLE XVII

CONVERSION RELATIONSHIPS - AIRCRAFT COEFFICIENTS

To Convert		Multiply By:	
From	To	For General Case	For Specific Model Tested
C_L	H_L	$(V_P/V_{tip})^2 S_W/2A_F$	$5.98 (V_P/V_{tip})^2$
C_D	H_D	Ditto	Ditto
C_M	$H_M(C_{mac})$	Ditto	Ditto
C_M	$H_M(d_F)$	$(V_P/V_{tip})^2 S_W C_{mac}/2 A_F d_F$	$13.14 (V_P/V_{tip})^2$
H_L	C_L	$2A_F/(V_P/V_{tip})^2 S_W$	$0.167/(V_P/V_{tip})^2$
H_D	C_D	Ditto	Ditto
$H_M(C_{mac})$	C_M	Ditto	Ditto
$H_M(d_F)$	C_M	$2A_F d_F/(V_P/V_{tip})^2 S_W C_{mac}$	$0.0761/(V_P/V_{tip})^2$

Notes: 1) A_F in the general conversion relationship is the area of both fans.

2) $H_M(C_{mac})$ is used to identify the moment coefficient non-dimensionalized with mean aerodynamic chord.

3) $H_M(d_F)$ is used to identify the moment coefficient non-dimensionalized with fan diameter.

A third set of non-dimensionalized coefficients is commonly used for VTOL devices. This system uses the slip stream notation. For

example: $C_L^S = L/q_S A_F$ where $q_S = F_{oooo}/2 A_F + q_0$. F_{oooo} is defined as the hover thrust at any given fan speed, out of ground effect with β_{av} and $\beta_S = 0^\circ$. The conversion between these coefficients and fan coefficients (H_L, H_D, H_M) is shown in Table XVIII and for comparison, data from Runs I-5, -6 and -7 are shown in this form in Figure 86. These type data are included only for the convenience of readers more used to this method of presentation.

TABLE XVIII

CONVERSION RELATIONSHIPS FOR SLIPSTREAM NOTATION

To Convert		Multiply By:	
From	To	For General Case	For Specific Model Tested
C_L^S	H_L	$\left(\Phi^2 + (V_P/V_{tip})^2\right)/2$	$0.161 + (V_P/V_{tip})^2/2$
C_D^S	H_D	Ditto	Ditto
C_M^S	H_M	$d_F/2C_{mac}\left(\Phi^2 + (V_P/V_{tip})^2\right)$	$0.073 + (V_P/V_{tip})^2/2$
H_L	C_L^S	$\frac{2}{\Phi^2 + (V_P/V_{tip})^2}$	$2/\left[0.321 + (V_P/V_{tip})^2\right]$
H_D	C_D^S	Ditto	Ditto
H_M	C_M^S	$2C_{mac}/d_F \left[\Phi^2 + (V_P/V_{tip})^2\right]$	$4.4/\left[0.321 + (V_P/V_{tip})^2\right]$

To convert the velocity parameters, the following relationships apply:

	General	Specific
T_C^S =	$1/\left[1 + (V_P/V_{tip})^2 \frac{1}{\Phi^2}\right]$ =	$1/\left[1 + 3.12\ (V_P/V_{tip})^2\right]$
V_P/V_{tip} =	$\Phi\left(1/T_C^S - 1\right)^{1/2}$ =	$0.567\left(1/T_C^S - 1\right)^{1/2}$

Where:

Φ is the ratio of jet velocity to fan tip speed at hover.

General Comparison With Fan-In-Fuselage Results:

The total lift, drag and moment data for all of the fan powered tests are shown in Figures 87 to 98. In general, the lift data are very similar to the fan-in-fuselage results (references 16 and 17); a large lift increase is measured as velocity ratio is increased. At velocity ratios about 0.36 with β set at 0°, the right fan experiences a rapid unloading resulting in a lift decrease and a discontinuity in the lift coefficient characteristic.

Drag data at $\beta = 0^{\circ}$ are quite different from fan-in-fuselage results as a function of velocity ratio. The fan-in-fuselage drag increased at an increasing rate because of fan flow increase (favorable inlet ram recovery) while fan-in-wing drag increased at a decreasing rate because of both fan flow reduction (poorer inlet ram recovery) and high exit louver losses with the $\beta = 0^{\circ}$ setting. At velocity ratios about 0.36 the drag became nearly constant because there was a large flow reduction when the right fan stalled.

For β settings of 20° and greater, the drag characteristics appeared similar to the fan-in-fuselage results (both gross thrust and ram drag were relatively lower but the net drag was essentially unchanged).

Pitching moments, which are a function of moment center selection, appeared to be quite dissimilar from the fan-in-fuselage results, however, are actually similar when proper correction for installation thickness is made. Pitching moment is found to be a function of fan flow and therefore the number and performance of the fans in the configuration. There was a marked difference in fan-in-wing flow versus flight speed compared with fan-in-fuselage flow because of the different inlet environments and this significantly influenced the results presented in the following discussions.

Accuracy of Interaction Analysis:

The accuracy of interaction lift, drag, and moments discussed next is mainly dependent on two factors: force and moment measurement accuracy and accuracy of calculated fan performance based on internal aerodynamic pressure measurements. (See Section V, Part C.)

The measurement accuracy discussed in Section IV was estimated directly based on normal periodic force balance calibrations and repeatability of force data. The limitations of the fan performance calculations are discussed in Section V, Part C. In view of these limitations, it is estimated that fan momentum thrust based on calculated fan flow and used in interaction calculations could be in error by $\pm$ 10%. In addition, the flow angle at the exit louver cascade (because of incomplete turning by the inlet) could be up to 20° higher than the indicated angle, affecting the moment contribution from the exit louvers. The overall accuracies estimated for the interaction analyses are:
$H_L \pm 0.035$, $H_D \pm 0.02$, and $H_M \pm 0.05$ units.

Interaction Lift:

Interaction lift is shown in Figure 99 for several configurations tested. For comparison, fan-in-fuselage results are also shown. In estimating the interaction lift, the following analysis was used. The total measured power-on lift was assumed to consist of:

1. Power-off aircraft lift
2. Fan momentum lift (including contribution from fan turbine)
3. Lift change from tail downwash
4. Interaction lift (induced lift plus interference effects)

The power-off aircraft lift can be calculated for each configuration in units of H_L using the conversion from C_L to H_L.

Fan momentum lift was calculated from internal fan pressure measurements and is shown in Figure 100 (with fan turbine contribution included) as a function of velocity ratio. For details of fan performance calculations, see Part C of this Section. Lift change from tail downwash was considered for the tail-on configurations tested using the previously determined tail downwash angle as a function of velocity ratio and tail lift vs. angle of incidence relationship based on power-off tests.

Subtracting items 1, 2, and 3 from the total measured lift gives the interaction lift caused by fan operation.[a]

The results for the three major configuration changes shown in Figure 99 indicate that interaction lift increased with an increase of velocity ratio and was considerably larger for the $\beta = 0^{o}$ case. The interaction lift for a configuration with $\delta_f = 0^{o}$ is indicated to be larger than one with $\delta_f = 30^{o}$ at velocity ratios above 0.2, but this is probably because of the calculation assumptions: the flap effectiveness was assumed to be the same for both power-on and power-off operation. Actually, the position of the extended flap area directly behind the fan is affected by the fan stream and its effectiveness should be significantly decreased as velocity ratio is increased.

The interaction lift appears to be a function of fan jet angle relative to the cross-flow. Based on internal measurements, fan flow was higher for $\beta = 35^{o}$ than $\beta = 0^{o}$ at velocity ratios above 0.2; however, the interaction lift calculated for $\beta = 0^{o}$ is considerably larger. This characteristic was even more pronounced for the fan-in-fuselage configuration where at $\beta = 35^{o}$ there was essentially no interaction lift indicated. This is not unexpected

[a] No correction has been attempted for any effect of the tunnel floor (or other walls) on these results.

since a jet flap exhibits similar characteristics. It is also indicated from the data that the fan mounted in a wing causes a higher level of interaction lift per unit of fan flow than the fan mounted in a fuselage. The fan-in-fuselage flow was higher for all β settings, but the absolute value of interaction lift was as large or larger for the fan-in-wing at all β settings.

It was not possible to obtain good lift measurements in the wind tunnel at velocity ratios below ≈ 0.08 because of fan and engine reingestion. Any performance indicated in this range must be considered questionable wherever the wind tunnel results are presented as a ratio or percentage of fan static lift; the static fan performance level used is that obtained during Evendale static tests (X353-5) which is repeated in Figure 101 (from reference 19).

Interaction Pitching Moment:

Interaction moments are shown in Figure 102 for the several configurations tested. For comparison, fan-in-fuselage results are shown corrected for the difference in installation thickness.

In estimating the interaction moments, the following analysis was used. The total measured power-on moment was assumed to consist of:

1. Power-off aircraft moment
2. Moment from displacement of the fan lift and thrust vectors from the moment center[a]
3. Moment caused by the J85 ram drag
4. Moment contribution from the tail
5. Interaction moment (from induced and interference effects)

---

[a] For moment center No. 2: $M_\beta = + 0.85\ F_X - 1.38\ F_Y$.

Power-off aircraft moment can be calculated for each configuration in units of H_M using the conversion from C_M to H_M.

Moments caused by the displacement of fan lift and thrust vectors from the moment center are calculated using internal fan performance results.

Moments caused by the J85 ram drag are obtained using the relationship of engine flow to fan speed and the moment arm from the moment centers to the engine centerline. This is approximately -

$$\frac{H_{D\ ram}\ (2.95)\ V_P/V_{tip}}{c_{mac}} = \frac{-0.0446\ (2.95)\ V_P/V_{tip}}{11.44} = 0.0115\ V_P/V_{tip}.$$

The reason this is only an approximate relationship is that the fan speed to engine flow is not an exactly constant ratio for all fan speeds. This error, however, is less than 1% of the total moment and is, therefore, insignificant.

Moment contribution from the tail installation is calculated from the previously obtained relationships of tail downwash, and velocity ratio and tail lift-angle of incidence slope.

Subtracting items 1 through 4 from the total measured moment gives the interaction moment caused by fan operation.

Comparing Figures 102 and 103, it can be seen that the interaction moment at $\beta = 0^\circ$ and $\delta_f = 0^\circ$ follow about the same pattern as the fan drag at $\beta = 0^\circ$. Assuming the relationship $H_{M\ int} \times d_F = a$ constant $\times H_{DR}$, the constant can be evaluated and is found to be approximately equal 9.5 for the velocity ratio range from 0 to 0.30 ($\beta = 0^\circ$ and $\delta_f = 0^\circ$). It is therefore possible to account for all fan caused moments by considering the fan ram drag force to act at a distance of 9.5 ft. above the moment center (No.2) or $\approx$ 9.0 ft.

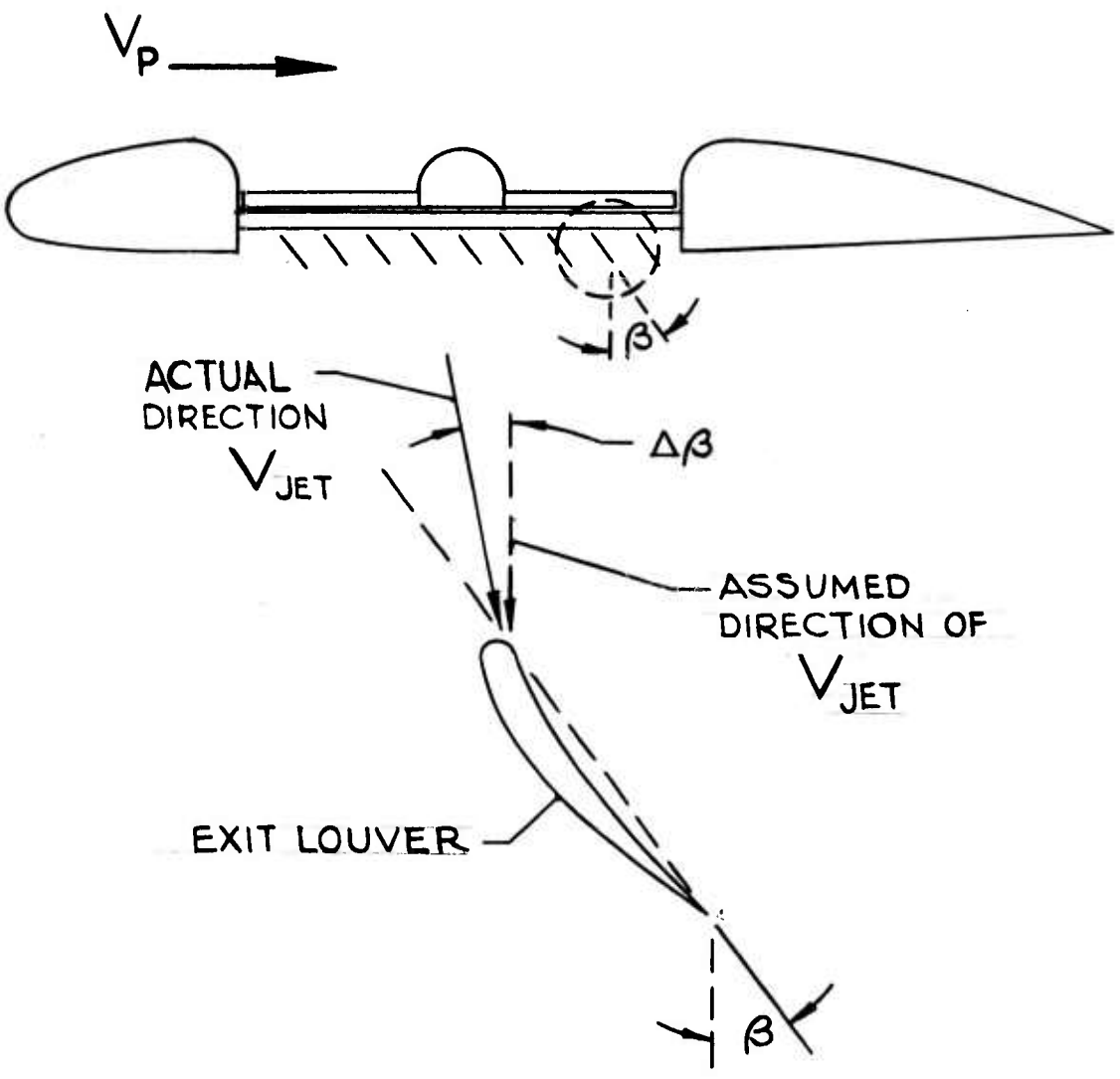
above the top surface of the fan (wing). This is comparable with a value of ≈ 8.4 ft. above the wing for the fan-in-fuselage model.[a]

Other studies indicate the interaction moment should be directly proportional to chord and inversely proportional to the effective aspect ratio. The fan-in-wing model had both a larger mean aerodynamic chord (11.44 vs. 7.33 ft.) and smaller effective aspect ratio than the fan-in-fuselage model. The 7% difference in interaction moment between these two relatively dissimilar models is, therefore, considered reasonable.

At $\beta = 35^{\circ}$ the interaction moment was less than at $\beta = 0^{\circ}$, even though fan flow was larger at $\beta = 35^{\circ}$ at velocity ratios above 0.2. This is partially the same phenomenon as described in reference 17, page 48; pre-turning the discharge flow by the exit louvers reduces the interference of the issuing jet with the cross-flow. An additional factor not present in the fan-in-fuselage installation tested is that of the flow not being axial through the wing installed fan at high velocity ratios, as evidenced by the more severe throttling of the fan at $\beta = 0^{\circ}$ than at $\beta = 35^{\circ}$ above 0.2 V_P/V_{tip}. In calculating interaction moments, it was assumed that there was a force on exit louvers equal to F_X and a resulting nose-up pitching moment of 0.85 F_X. The flow angle leaving the exit louver cascade is approximately β when there is no separation in the cascade. (Refer to Sketch.) If inflow is axial, the horizontal force (neglecting friction) on the louver cascade is F sin β or F_X and the pitching moment caused by the exit louvers relative to moment center No. 2 is 0.85 F_X. If the inflow is not axial, the horizontal force on the cascade is F (sin β - sin $\Delta\beta$) or less than F_X, and the resulting pitching moment is less than 0.85 F_X. The actual flow angle entering the exit louver cascade is between

---

[a] Reference 16, Table 9


V_P
β
ACTUAL
DIRECTION
V_{JET}
$\Delta\beta$
ASSUMED
DIRECTION OF
V_{JET}
EXIT LOUVER
β

0 and $\text{Tan}^{-1} V_P/V_{jet}$. At $V_P/V_{tip} = 0.3$, the $\text{Tan}^{-1} V_P/V_{jet}$ is $\approx 24^o$. Assuming this flow condition, the interaction pitching moment for $\beta = 35^o$ (Figure 102) would increase by 0.017; at this same velocity ratio but for $\beta = 0^o$ it would decrease by 0.016 bringing the results for the two exit louver settings closer together.

The interaction pitching moment calculated for runs with $\beta = 35^o$ and $\delta_f = 30^o$ does not follow the constant relationship with ram drag. The 30^o plain flap used in this test contributed ≈ 0.13 nose-down C_M. Review of the various data shows changes in lift, drag and moment that strongly indicate the flap to be separated directly behind the fan. This separation could be caused by the large cut-out in the flap which was necessary to accommodate the test exit louver actuation system (see Figure 1). This implies reduced basic aircraft moment and lift contributions (see Figure 99 for change in interaction lift with flap setting). In the analysis of interaction pitching moments it was assumed that the basic aircraft moment contribution remained constant, and this would result in evaluating the interaction moment at too high a level for operation with the flaps extended. If a flap effectiveness of $\approx 80\%$ is assumed, both the interaction moment and lift results become independent of flap setting.

It is not possible to exactly account for the non-axial flow and flap effectiveness influences on the results, so results are presented for assumed axial flow and 100% flap effectiveness. The reader is, however, cautioned to consider such influences in applying these results to specific applications.

The center of lift change as a function of velocity ratio is shown in Figure 104. The maximum forward shift of the center of lift is $\approx$ 25% of C_{mac} or 55% of fan diameter. This is another way of presenting the system moment characteristic.

Within the accuracy of the data there is no indication that configura-

tion changes such as addition of Kruger flaps, a short span wing, or a mid-wing installation affect the moment to any appreciable degree. There was, however, a larger decrease in interaction moment at $\approx 0.35\ V_p/V_{tip}$ where the right fan stalled and its mass flow decreased considerably.

Interaction Drag:

Interaction drag is shown in Figure 105 for several configurations tested. For comparison, fan-in-fuselage results are also shown. In estimating the interaction drag the total measured power-on drag is assumed to consist of:

1. Power-off aircraft drag
2. J85 ram drag
3. Fan ram drag
4. Fan gross thrust (including fan turbine thrust contribution)
5. Interaction drag (induced drag plus interference effects)

The power-off aircraft drag can be calculated for each configuration in units of H_D using the conversion from C_D to H_D. J85 ram drag was $\approx 0,0446\ V_p/V_{tip}$ based on the engine flow-fan speed relationship. Fan ram drag and gross thrust were obtained from internal fan pressure measurements, Figure 103.

Subtracting items 1 through 4 from the total measured drag gives the interaction drag caused by fan operation. The interaction drag increased with velocity ratio and is higher at $\beta = 35^o$ than $\beta = 0^o$. The $\delta_f = 0^o$ data has a larger interaction drag component which is consistent with the flap effectiveness reduction discussed in evaluating interaction lift and moment. The fan-in-fuselage results indicate a much higher level of interaction drag at $\beta = 0^o$. This could be partly caused by the higher fan flow in the fuselage installation; however,

the large part of the difference is suspected to be the result of flow separations along the fuselage behind the fan with that relatively unstreamlined model.

For the evaluation of interaction effects (lift, drag and moment), fan flow, gross thrust and ram drag are calculated from fan internal performance discussed in Part C of this Section. Based on the non-uniform flow conditions described there, it should be considered that the calculations of fan performance are not exact and that the interaction effects are subject to the same inaccuracies involved in determining internal fan performance.

The fan lift and drag coefficient determined from fan internal performance measurements shown in Figures 58, 59 and 60 do not include the lift or drag (thrust) contribution from the fan turbine exhaust gases. This was added in preparing Figures 100 and 103 of the interaction analysis.

System Lift and Drag and Moment Changes as a Function of Angle of Attack:

The lift changes as a function of angle of attack were reasonably unaffected by fan operation at $\beta = 0^{\circ}$. To obtain preliminary estimates of total system lift at any angle of attack between -4° and $+10^{\circ}$, it is possible to add the fan lift, Figure 100, to the interaction lift, Figure 99, and the power-off aircraft lift at the desired angle of attack. Figure 106 shows the slope of the lift coefficient vs. angle of attack for power-on and power-off conditions. The $\beta = 0^{\circ}$ value was always slightly lower than the power-off value mainly because of fan performance deterioration as angle of attack was increased. At $\beta = 35^{\circ}$ the geometry effects are in a direction to increase fan lift $\left(F_Y = F \left\lfloor \text{Cos } (\beta - \alpha) \right\rfloor\right)$ and apparently overcome the fan total thrust decrease caused by angle of attack increase. At velocity ratios above 0.25 the fan performance deterioration with α was more pronounced and the power-on value of $\Delta C_L/\Delta\alpha$ was less than the power-off value.

Total drag changes as a function of angle of attack were mainly a function of fan jet discharge angle especially at low velocity ratios. At any condition the drag changes can be expressed (for an α range from -4° to $+10^{\circ}$) as a $\Delta H_D/\Delta\alpha = k_1 \alpha + k_2 \alpha^2$. The squared term is usually less than 10% of the total change and as an approximation a linear relationship can be used. Figure 107 shows the variation of $\Delta H_D/\Delta\alpha$ vs. velocity ratio. This ratio did not vary much with velocity ratio (except at low β settings in the high velocity ratio ranges where increases in angle of attack caused the right fan to stall; this was usually accompanied by a decrease in drag from reduced fan flow).

The change in pitching moment with α was essentially a constant $\Delta C_M/\Delta\alpha$ phenomenon, again, except when fan stall was present.

In general, it can be said that, as a function of angle of attack:

1. Lift changes were similar to the power-off case. There were some small influences of fan jet exit geometry at high β settings and low velocity ratios, and of fan performance deterioration at high velocity ratios.

2. Drag (thrust) changes were primarily a function of geometry. Some small influence of the basic aircraft drag changes which may be obscured by fan performance changes is also present.

3. Pitching moment changes are similar to the power-off case with little fan influence.

Power-On Tail Downwash and Static Stability:

Tail downwash variation as a function of velocity ratio is shown in Figure 108. As expected the downwash angle was higher than for the power-off condition and decreased with velocity ratio. Tail downwash values below a velocity ratio of 0.075 (equivalent to $\approx$ 30 knots at 100% fan speed) are difficult to determine because of the small values of the moment forces used for calculations. Also the tunnel effects at these conditions are large, affecting the applicability of these data.

The downwash angle at the aerodynamic center is a function of C_L and aspect ratio; tangent $\epsilon = C_L/\pi AR$, which for small angles reduces to $\epsilon = 57.3\ C_L/\pi AR$. Theoretically the downwash angle at infinity approaches a value equal to twice the value at aerodynamic center. In practice the downwash angle approaches zero some distance behind the wing because of viscous effects and is a finite value at the tail plane. This value depends primarily on the lift coefficient, aspect ratio, and taper ratio of the wing, and the distance of the

tail behind and above the wing chord. For the same configuration, the tail downwash should be a function of C_L only. Figure 109 shows the variation of C_L with velocity ratio for $\beta = 0^\circ$ and 35°. Based on this it would be expected that downwash angle be some 10 to 50% higher for the $\beta = 0^\circ$ compared to $\beta = 35^\circ$ case over the velocity ratio range tested. This is not the case, probably because of tunnel effects and/or data scatter.

The fan-in-fuselage installation had an aspect ratio of 1.43 times the fan-in-wing value; it also had a slightly longer distance to the tail plane, a higher tail position, and $\approx$ 20% lower C_L at a given velocity ratio ($\beta = 0^\circ$ and $\delta_f = 0^\circ$). All these factors would indicate approximately three times as much downwash for the fan-in-wing compared to fan-in-fuselage configuration. Figure 108 shows the downwash angle of both configurations. The ratio of fan-in-wing to the fan-in-fuselage downwash angle varies from $\approx$ 2 at the lowest velocity ratio to $\approx$ 4.5 at 0.3 V_p/V_{tip} indicating a reasonably good agreement with the estimated ratio of 3.

The change of tail downwash angle with angle of attack was the same with the fans running as the power-off value ($\partial\epsilon/\partial\alpha = 0.6$), and was independent of velocity ratio or exit louver angle setting.

The longitudinal static stability[a] power-on and power-off is shown in Figure 110. The value of static stability power-on is generally higher than power-off. This phenomenon is caused by rearward shift of the aerodynamic center (when the fan is operating) of $\approx$ 2% chord as can be seen in Figure 111.

The above results are for the high-wing configuration with 30° flap

[a] Moment center No. 2 shown on Figure 2 was used for the longitudinal static stability calculations.

deflection (no fan inlet doors). Sufficient data are not available to evaluate tail downwash and static longitudinal stability for all of the configurations tested; however, it seems likely that the fan contribution would be of constant magnitude and only the power-off base point would change.

Inlet Comparisons:

Three fan inlets were used during Period I testing (see Section II for detail description).

Inlet No. 1 - Fixed side vanes plus circular vane

Inlet No. 2 - Circular vane only

Inlet No. 3 - Articulated louvers plus circular vane

The drag lift and moments obtained with inlets No. 1 and 2 were practically the same for all ranges of variables tested indicating the fan gross performance to be unaffected by the presence of the side vanes. The side vanes did not influence system performance; however, they did reduce inlet distortion and, therefore, reduced blade stresses (see Parts C and F of this Section, fan internal and fan mechanical performance).

Using inlet No. 3 resulted in slightly lower lift (0 to 10%) at low velocity ratios up to $V_p/V_{tip} = 0.18$, because of the higher inlet losses under these conditions. At velocity ratios from 0.18 to 0.30 inlet No. 3 resulted in slightly higher lift (0 to 10%); above 0.30 V_p/V_{tip} up to 20% higher lift. This increase was caused by an effectively higher fan flow area present with the articulated louvers rather than an increase in ram recovery (see Figure 55a and 57).

As would be expected from the higher fan flow, the drag moment tended to be higher for inlet No. 3 at higher velocity ratios. The moment comparison in Figure 112 is based on tail-on moment data corrected for tail downwash. Some error is probably present since the downwash was assumed to be the same for all inlet configurations. Data are not available for a direct tail downwash evaluation for all of the inlet configurations.

The maximum conversion speed was nearly the same for all inlets (see Figure 113). This phenomenon can be best explained from the internal fan performance (Part C). Inlet distortion reduces effective flow area but increases fan effective pressure ratio for inlets No. 1 and 2 relative to inlet No. 3. This results in decreased flow but higher thrust per unit of flow for inlets No. 1 and 2, and the net thrust output is essentially the same for all three inlets.

Rotor Comparisons in Cross Flow:

The installation of the X353-5B rotor in the left wing for the Period II tests did not affect the total aircraft performance to any measurable degree. It would be expected that at low velocity ratios and $\beta = 0^{o}$ there should be a difference in total lift of about 4% at the same fan speed because of the higher loading of the -5B fan. The inherent scatter of low velocity ratio data obscures any such trend. At high velocity ratios and/or high exit louver angles the -5B rotor unloads faster than the -5 rotor and the performance of each rotor at constant speed should become nearly the same; this indeed was the case with some indication that the -5B rotor may provide less lift.

Effects of Fan Inlet Closure Doors:

Addition of "butterfly"-style, faired, inlet doors caused an increase

in aircraft drag coefficient (C_D) of ≈ 0.02 to 0.03 for the velocity ratio range of 0.15 to 0.30 at all exit louver angle settings (Figures 114a to 114c). Since the ΔC_D caused by door installation is reasonably constant for all louver settings and changes only slightly with velocity ratio, it is reasonable to assume that it is mainly an increase in form drag and not a change in fan performance (in the latter case ΔC_D would vary as $\frac{1}{(V_P/V_{tip})^2}$). Additional support for this conclusion is the lift coefficient not being affected by door presence.

The doors were installed using external cables and turnbuckles. Estimating $\approx$ 2 square feet projected area for the above, it is possible to account for $\approx$ 20% of the additional drag caused by door installation. Converting the remaining drag to D/q units, it appears that the faired doors used in test cause an additional drag equivalent to $\approx$ 10 D/q (in the open position) for a two-fan installation.

Kruger Flap Effects:

Addition of Kruger flaps had practically no effect on drag other than the power-off difference of 0.01 C_D (see Table X). Interaction pitching moment comparisons are shown in Figure 112 with no appreciable difference except that Kruger flaps improved the fan performance slightly, resulting in higher moments at velocity ratios above 0.3. This improvement is probably caused by a reduction in cross-flow velocity in the vicinity of the fan inlet because of the increase in wing chord ahead of the fan inlet. The total lift at $\alpha = -4^\circ$ to $+4^\circ$ was not affected; however, at higher angles of attack, the lift with Kruger flaps was increased and $C_{L\ max}$ was approximately 10% higher.

Very High Velocity Ratio Performance:

Normal take-off transitions should be completed at velocity ratios

below 0.3. It is possible that landing transitions can be performed that involve very high velocity ratios (0.4 to 0.6) because of the reduced fan speed requirement; also advanced lift fan systems using flow division[a] between the cruise nozzles and the fans would tend to be operated at higher velocity ratios. Data for the high velocity ratio ranges, 0.4 to 0.6, are shown in Figures 115a and b. Fan performance is poor and the total performance approaches the power-off aircraft case. A complete polar at $\beta = 45^{\circ}$ and $V_p/V_{tip} = 0.57$ is shown in Figure 116, indicating the similarity of power-on to the power-off results. This similarity of high velocity ratio to the basic aircraft results suggests that low fan speed landing conversions can be accomplished smoothly without trim changes; also, take-off conversions using sequential diverter valve switching can be accomplished with considerably less trim changes than required during simultaneous switching.

Thrust Spoiling for Control:

The exit louver system was designed to provide lift modulation at constant engine power. Initial lift spoiling tests at static conditions were performed at Evendale (reference 19). During this wind tunnel phase of fan test the lift spoiling characteristics were evaluated further as a function of cross-flow and angle of attack. The four important results are the lift reduction, thrust reduction, pitching moment reduction and fan speed change as a function of exit louver stagger angle ($\beta_s = \frac{\beta_2 - \beta_1}{2}$).

The combined lift spoiling results of the Evendale and Ames tests are shown in Figures 117a to 117d showing the variation of

[a] Reference 20

vertical lift and horizontal thrust as a function of velocity ratio, average exit louver angle ($\beta_{av} = \frac{\beta_1 + \beta_2}{2}$) and stagger angle ($\beta_s$).

Lift and thrust reductions at a given fan speed are expressed as a percentage of the fan lift at hover with $\beta_{av} = 0^o$, $\beta_s = 0^o$, and at the same fan speed. (See Figure 118c for fan lift vs. speed at these conditions.) Data presented include the total effect due to stagger; that is, both fan momentum lift and thrust changes as well as changes in induced lift and drag. Figure 117a shows the lift and thrust variation as a function of velocity ratio and stagger angle for $\beta_{av} = 0^o$. There is no appreciable effect on thrust for all β_s values and no effect on lift for β_s up to 10^o. The maximum amount of lift spoiling possible at hover ($\beta_{av} = 0^o$), with the X353-5 louver geometry, is 25% of hover lift with the exit louver setting of $\beta_s = 40^o$.

Figure 117b shows the same variables for $\beta_{av} = 10^o$. The main differences from the $\beta_{av} = 0^o$ results are the increase in thrust variation with β_s and the change in both lift and thrust variation with velocity ratio. The reduction in thrust with increase in stagger angle is caused by the reduction in effective turning angle relative to the vector angle (see Figure 119). The increase in lift spoiling effectiveness as velocity ratio is increased up to $V_p/V_{tip} \approx 0.15$ is apparently caused by reduction in induced lift effects in addition to fan momentum lift reduction when staggering. The reduction in thrust spoiling with increasing velocity ratio is caused by the decrease of fan flow and the resulting decrease in ram drag; the gross thrust changes are reasonably independent of velocity ratio changes; however, the ram drag changes are proportional to velocity ratio, and, therefore, the net thrust changes, through staggering, decrease with velocity ratio increases.

Figures 117c and 117d give the lift and thrust variation for $\beta_{av} = 20^{\circ}$ and 35°. An additional phenomenon present is that, for velocity ratios above 0.15, the lift spoiling effectiveness decreases apparently because of the relatively lower fan contribution to total lift at higher velocity ratios (Figure 100).

In addition to altitude control, staggering can provide roll control by spoiling one fan more than the other. Some asymmetrical staggering data were obtained which show the lift and thrust losses to be only about half of the value obtained with equal staggering, indicating that there is no cross-coupling between the two fans.

The roll and yaw results show considerable scatter throughout the test, but can be used as a rough check on the point of action of the forces produced by staggering. The yaw moment was approximately equal to $\Delta D \times 8$ ft. and the roll moment was approximately equal to $\Delta L \times 6$ ft. Based on this, it can be assumed that the lift and drag changes produced by staggering act at about the fan center which is 7.12 ft. from the aircraft centerline. More accurate roll and yaw moment measurements would be necessary to establish the exact position; at hover these forces act slightly inboard from fan center because of the turbine location. As cross-flow velocity is increased, the point of action of drag and lift forces moves inboard of the fans (for counter-rotating fans: left wing fan, counter-clockwise; right wing fan, clockwise rotation, looking from the top) because of increased loading on the advancing blades relative to the retreating blades. Changes in induced effects may modify this to some extent depending on aircraft configuration.

Pitching moment changes (moment center No. 2) were insignificant as a function of staggering: fan lift decreased reducing nose-down moment, while fan flow also decreased reducing ram drag and its attendant nose-up moment. If the center of gravity is located on

a chord station corresponding to the fan centerline, then staggering would decrease pitch-up moment.

It is apparent that symmetrical staggering (altitude control) reduces horizontal thrust and, without automatic control adjustment, descents will be accompanied by a reduction in horizontal acceleration rate. In a coordinated control system, staggering could be accompanied by simultaneous increase in vector angle to preserve the horizontal force balance with a resulting larger vertical force change than attributable to staggering alone (vectoring decreases lift).

During asymmetrical staggering (roll control) an adverse yaw is developed. In a coordinated control system the adverse yaw could be eliminated by a simultaneous increase in vector angle on the staggered side resulting in decreased lift and a larger roll moment than possible with staggering alone. If a yaw force is desired, vectoring exit louvers further produces an adverse roll which has to be compensated by unstaggering; this in turn yields more horizontal thrust and increases the yaw input.

From the above discussion it is evident that a given altitude, roll or yaw control input is increased by the additional inputs necessary to prevent change in acceleration or prevent adverse yaw-roll or roll-yaw coupling. An automatic control system which would completely compensate for these cross-couplings is, therefore, a function of several variables such as β_{av}, β_s and V_p.

Figures 117a to 117d are for a constant engine power input. During fast transient changes in β_{av} and β_s, the fan speed may never reach equilibrium and the resulting thrust and lift changes will be instantly greater than the steady state (constant power) values in Figures 117a to 117d. The changes are greater during fast

transients because the fan characteristic is such that increased staggering unloads the fan resulting in fan speed increase. Constant speed thrust changes are therefore greater than constant power changes and very fast relative to fan rotor time constant) β_s changes approximate a constant speed change. These control responses would depend on the rate of change of β_{av} and β_s and the exact fan acceleration and deceleration characteristics.[a] These data in conjunction with the steady state speed change shown in Figures 120a and b enable the complete definition of transient control response. The speed change figures are for the X353-5 rotor with the solid data points indicating the X353-5B rotor.

All of the cross-flow thrust and lift spoiling data are based on the tests with the X353-5 rotor since these data are more complete.

Figures 121a and b show the lift spoiling characteristics of the X353-5B rotor in- and out-of-ground effects. The significant point is that at the lowest position, spoiling up to 20° β_s has no appreciable influence on lift. The X353-5B rotor indicated less lift spoiling capability at $\beta_s = 30^\circ$ than the X353-5 rotor but this may be partially the result of exit louver wear at this later point in the program resulting in a lesser actual louver angle than indicated.

Transition Analyses:

The aerodynamic characteristics of the fan powered aircraft are shown in Figures 87 through 98. Aerodynamic differences for the various configurations tested are relatively small and the transition characteristics would be generally the same, the one exception being the

---

[a] Time constant $= \frac{I \omega_o^2}{T_o} \left(\frac{1}{2\omega} \pm \Delta\omega\right) = \frac{302 \times 276}{12800} = 0.65$ seconds at $\approx 100\%$ N_F (for small unbalanced torque)

short-wing span configuration which would require larger angles of attack throughout transition to maintain the same levels of lift.

The transition analysis presented here is based on the high-wing aircraft configuration as shown in Figure 1 with the flap angle, δ_f, set at 30^o but without the tail installed. This aircraft model has a wing area of 426 square feet, an aspect ratio of 3.5, a wing taper ratio of 0.5, and a mean aerodynamic chord of 11.44 feet. The X353-5 fans installed in each wing are equipped with the fixed side vane inlet and have no inlet closure doors installed.

Two levels of total installed lift to gross weight were used; L/GW = 1.05 and 1.20 equivalent to 13,400 and 11,750 lbs., respectively. These correspond to test requirements of the VZ-11 specification.

Transition Calculations and Procedure:
Transition equations of motion are summarized in Table XIX.

The aerodynamic characteristics of the fan powered aircraft are taken from Figures 87 through 98 and plotted as illustrated in Figure 122a. In this way, the coefficients H_L and H_D are available as a function of angle of attack (α) and exit louver setting (β) for any desired number of velocity ratio values required to define the transition flight schedule.

Using the maximum level acceleration schedule as an example, the equations of motion (Table XIX) are as follows:

$$-\rho A_F (V_{tip})^2 \quad H_D = \frac{G.W.}{g} a$$

$$\rho A_F (V_{tip})^2 \quad H_L = G.W.$$

Assuming fan speed is constant at 2640 rpm, ρ is sea level standard density and L/G.W. is 1.20 (G.W. = 11,750 lbs.), the following

TABLE XIX

TRANSITION EQUATIONS OF MOTION

Flight Condition	Equations of Motion
1. Level unaccelerated flight.	$-\rho A_F (V_{tip})^2 H_D = \frac{G.W.}{g} \frac{dV_P}{dt} = 0$ $\rho A_F (V_{tip})^2 H_L = G.W.$
2. Level accelerated flight and level decelerated flight.	$-\rho A_F (V_{tip})^2 H_D = \frac{G.W.}{g} \frac{dV_P}{dt}$ $\rho A_F (V_{tip})^2 H_L = G.W.$
3. Constant speed climb.	$-\rho A_F (V_{tip})^2 H_D - G.W. \sin \theta = \frac{G.W.}{g} \frac{dV_P}{dt} = 0$ and $\rho A_F (V_{tip})^2 H_L = G.W. \cos \theta$
4. Accelerated climb and decelerated descent.	$-\rho A_F (V_{tip})^2 H_D - G.W. \sin \theta = \frac{G.W.}{g} \frac{dV_P}{dt}$ $\rho A_F (V_{tip})^2 H_L = G.W. \cos \theta$
5. S.T.O.L.	
a. Ground run	$-\rho A_F (V_{tip})^2 H_D - \mu (G.W. - \rho A_F (V_{tip})^2 H_L) = \frac{G.W.}{g} \frac{dV_P}{dt}$ or $-H_D - \mu H_{\dot{G.W.}} + \mu H_L = \frac{H_{G.W.}}{g} V_P \frac{dV_P}{dx}$
b. Distance for rotation.	$X_2 = V_P \left(\frac{\tan^{-1} H_D/H_L}{\omega} \right)$ where $\omega = \frac{\Delta G.W.}{G.W.} \frac{g}{V_P}$
c. Distance to climb out	$X_3 = \frac{50 - X_2 \sin 1/2 (\tan^{-1} H_D/H_L)}{\tan H_D/H_L}$

relationships are calculated.

$$a = -120.6\ H_D$$

$$H_L = 0.2667$$

Then, at each V_P/V_{tip}, for which the fan powered aircraft performance coefficients are plotted as illustrated by Figure 122a, read values of α and β that correspond to the maximum negative value of H_D and satisfy the requirement that $H_L = 0.2667$. The following data illustrates the typical results.

V_P/V_{tip}	V_P ft/sec.	V_P knots	α deg.	β deg.	H_D	a ft/sec.[a]
0	0	0	-8	17	-.155	18.70
.05	36	21.33	-8	19.5	-.140	16.89
.10	72	42.66	-8	23.5	-.123	14.84
.15	108	63.99	-6	31	-.096	11.58
.20	144	85.32	-6	33	-.062	7.48
.25	180	106.65	-6	37.5	-.030	3.62
.30	216	127.98	-6	40	0	0

V_P/V_{tip}	$\bar{a}$ ft/sec.[a]	a g	Δt sec.	t sec.	Δs ft.	s ft.
0	-	.581	0	0	0	0
.05	17.80	.525	2.02	2.02	36	36
.10	15.87	.461	2.27	4.29	123	159
.15	13.21	.360	2.73	7.02	245	404
.20	9.53	.232	3.77	10.79	476	880
.25	5.55	.113	6.49	17.28	1051	1931
.30	1.81	0	19.89	37.17	3938	5869

In this case, changes in time and distance are based on average acceleration and velocity values.

$$\Delta t = \frac{\Delta V}{\bar{a}} \; ; \quad \text{where } \bar{a} = \text{average acceleration}$$

$$\Delta s = (\Delta t)\ (\bar{V}_p); \quad \text{where } \bar{V}_p = \text{average velocity}$$

Similar procedures are followed to determine the other transition schedules. For more detailed description of the methods used for computing transitions, see reference 17, pages 52 to 57.

Maximum Level Acceleration:

A maximum level acceleration transition schedule is shown in Figures 122b and c. From Figure 122b it can be seen that some decrease in total distance covered and time required can be obtained by choosing an α and β schedule which reverses as flight speed is increased. This improvement is small and it appears that the relative simplicity of unidirectional changes in these variables is more advantageous. As the gross weight is decreased to 11,750 lbs. in Figure 122c the time and distance requirements to complete transition are reduced by $\approx$ 50%. The additional pitching moment requirements for these transitions and the horizontal tail incidence angle schedules are shown in Figures 123b to 124c. Two levels are shown. One uses the c.g. location at moment center No. 2 (see Figure 2); this location results in higher nose-up trim requirements at hover but large pitch control margin at intermediate velocities, $\approx$ 40 knots. The other level is based on an aft c.g. shift to a point where there is just enough nose-down trim available from the horizontal tail at $\approx$ 40 knots. This c.g. location is the same vertically as moment center No. 2 but only $\approx$ 0.9 ft. ahead of the fan centerline. The tail volume coefficient is assumed to be 0.45 and a maximum C_L tail used is 0.6. A pitch fan mounted in the nose of the aircraft is assumed to provide the nose-up moment required at hover

and very low air speeds. None of the trim forces from the tail or pitch fan is included in the transition analysis shown in Figures 122b and 122c. If the trim forces were included, the transition performance would be slightly improved. Points indicating the trimmed angle of attack and tail position are shown in Table XX for the aircraft after the fans are shut down with inlets and exits open and also closed to identify major steps in the conversion. Moment caused by engine thrust was not considered. In order to reduce the angle of attack and tail incidence changes required at conversion, higher exit louver angles ($\beta = 50^{o}$) and higher angles of attack can be used. This approach would not improve the transition performance but it would be in the direction to make the conversions smoother.

Maximum Rate of Climb:

The locus of maximum rate of climb and climb angle points is shown as a function of flight speed, α and β in Figure 125. The maximum angle of climb occurs at lowest flight velocities while the maximum rate of climb is possible at velocities from 50 to 70 knots. The large increase in rate of climb and climb angle capability over the results in reference 17 is caused by the greater margin of L/GW. The additional pitching moments requirements are shown in Figure 126. The reduction in trim required relative to the maximum level acceleration case results from the high β angle setting at and near hover which affects the negative moment from the fan lift vector.

Level Deceleration at Constant Angle of Attack:

While the previous transitions used maximum constant fan speed, this landing sequence uses variable fan speed. Total time and distance to complete this transition is similar to the maximum level acceleration schedule. Higher deceleration rates than shown in Figure 127 are possible but require reversals in the β or angle of attack

schedules. The additional trim moment requirements in this, as in any other, landing sequence is lower than for take-off transitions because of the lower fan speed required.

Conversion:

The conversion from fan mode to turbojet mode can be accomplished as soon as the flight velocity is sufficient to provide the necessary lift from the wings alone. Two velocities are arbitrarily chosen: 110 and 120 knots. The angles of attack required for trim lift, fan-off, are shown in Table XX. The higher angle of attack is necessary for the condition where the inlets and exits are still opened. The lower value of α is for the cruise configuration. Angle of attack for the condition where inlets are opened but exit louvers closed falls between these two values.

Tail incidence angles for trim pitching moment, fan-off, are also shown in Table XX.

TABLE XX

CONVERSION DATA ($\delta_f = 30^\circ$, L/GW = 1.05, MOMENT CENTER NO. 2, $\beta = 40^\circ$)

		Wing Supported Flight		
	Fan Supported Flight	Closed Exit & Inlet	Opened Exit & Inlet	Closed Exit Opened Inlet
Stall Speed (Knots)	-	85	93	89
Acceleration (% of g) at 110 Knots	9	23	21	22
Acceleration (% of g) at 120 Knots	3	22	19	20
Angle of Attack - α at 110 Knots	-6	+6	+9	+7
Angle of Attack - α at 120 Knots	-6	+4	+7	+5
Tail Incidence Angle - i_t at 110 Knots	+9	-1	-4	-2
Tail Incidence Angle - i_t at 120 Knots	+8	-1	-3	-2

STOL:

The STOL performance of this configuration will not differ significantly from the fan-in-fuselage STOL performance described in reference 17. This is based on the total aerodynamic forces being very similar for the two configurations as well as the similarity of the maximum acceleration transition schedule shown in Figure 122b and Figure 67, reference 17.

Wing Static Pressure Distribution:

Wing pressure coefficients are shown in Figures 128a to 128f for several velocity ratios. The pressure data substantiates some of the system results. Comparing $\beta = 35^{\circ}$ with $\beta = 0^{\circ}$ results from Figure 128a, it is apparent that the lift is less for $\beta = 35^{\circ}$. The $\delta_f = 30^{\circ}$ pressure distribution from the same figure is similar to $\delta_f = 0^{\circ}$ except for the flap contribution. All of the data indicate a high velocity region on the lower surface along the side of fan discharge (station No. III which is located $\approx$ 5 inches from the fan edge). This is similar to the velocity distribution around a circular cylinder where the surface velocity at the maximum thickness point is $\approx$ 2.2 times the free stream velocity. This local velocity increase could be responsible for some lift loss. At the lowest velocity ratio ($V_P/V_{tip} = 0.069$) there is no loading of the leading edge. As the velocity ratio is increased to 0.146, the leading edge loading increases rapidly and then remains reasonably constant as velocity ratio is increased further.

Faired Inlet Door Forces:

The system described and shown in Figure 129 was used to measure some of the door forces during the testing. These data provide the basis for an estimate of the door aerodynamic hinge moments with a reasonable accuracy for design purposes. Figure 130 is a compilation of some of the results to illustrate the relative change in hinge moment as a function of test variables.

The forces plotted in Figure 130 are for the outboard door on the right wing. The hover hinge moment was observed to vary approximately at the square of the fan speed, and at 100% speed was about 3500 inch-pounds, maximum, tending to close the doors. This number represents a hinge moment index of 1.0 in Figure 130; however, the absolute value must be evaluated for design by appropriate consideration of factors of safety and other allowances.

F. FAN MECHANICAL PERFORMANCE

Inlet Configuration Selection and General Considerations: Rotor blade stresses were verified to be one of the primary considerations in selecting a satisfactory fan inlet configuration. Mechanical evaluation of the three configurations tested showed the following results:

1. The circular vane plus fixed side vane inlet produced the lowest rotor blade stresses with a moderate hover thrust penalty ($\approx$ 1%).

2. The articulated vane inlet produced approximately the same stress levels as the circular vane plus fixed side vane inlet with a large hover thrust penalty ($\approx$ 3 1/2%).

3. The circular vane inlet has the lowest potential weight and simplest design and the best hover performance, but resulted in the highest rotor blade stresses during transition.

With the circular vane inlet, the first flexural blade stress of the X353-5 rotor was 25% over running limits at V_p = 60 knots and part fan speed (N_F = 1650). Increased flight speed and combinations of higher fan speed with higher flight speeds would both increase the blade stress level.

It was shown in Parts C and D of this Section that system performance in transition was nearly identical with each of the three inlet configurations. The circular vane only was not satisfactory from mechanical considerations and the articulated inlet system indicates a severe hover penalty. The choice of the circular vane with fixed side vane configuration as best thus follows:

Mechanical performance presented in this part pertains to the selected inlet, which is also planned for the VZ-11 application.

X353-5 Versus X353-5B:
Reorientation of the blade did not of itself have any significant influence on fan mechanical performance. Data obtained with either type rotor is interchangeable. A significant difference was associated with different torque band designs as described in later paragraphs.

Left Wing Versus Right Wing:
The left wing fan was used to investigate the high speed characteristics and was identical to VZ-11 hardware with respect to blade dovetail, blade orientation angle, torque band design (two-piece), and fan rotation direction. The rotor stress characteristics for the VZ-11 counter-rotating right wing fan are expected to be similar to these data.

Rotor Blade Stresses:

Cosine 2θ Mode - Blade stress data obtained during Period II testing was analyzed to determine the cosine 2θ mode characteristic for the new rotor design as a function of tunnel speed, exit louver angle, wing angle of attack, yaw, fan acceleration time, wing-fuselage relationship, and fan inlet configuration including inlet doors. To evaluate these parameters, approximately 150 accelerations and decelerations were performed.

The cosine 2θ mode blade stresses in this testing appeared to be independent of acceleration or deceleration time through the resonance speed. See Figures 131a through d. This was also true of the Period I test series for similar tests with the original rotor design. Earlier fan-in-wing static testing at Evendale

(reference 19), during which a single piece torque band was used, indicated that stress level was a function of acceleration and deceleration time, but this was not conclusive because of data scatter; it is believed that a larger number of test points at each set of conditions would show the same characteristic as measured at Ames. On the other hand, both one and two-piece torque band designs have been tested in the fuselage configuration and show the blade stress to be sensitive to the acceleration and deceleration rate. The conclusion is that transient rate (via J85 throttle or the diverter valve) is an important variable in determining cosine 2θ stress level in the fuselage but not in the wing installation.

Predicted values of cosine 2θ stress based on previous wind tunnel results are included in Figure 131a indicating a marked reduction in this mode stress attributable to the two-piece torque band design.

Another important result of the fan-in-wing tests has been to identify that the change in cosine 2θ blade stress with exit louver setting was much lower than predicted from fan-in-fuselage data. All fan-in-wing data show this same result. One factor that may cause the reduced sensitivity of the cosine 2θ stress to exit louver angle setting for the fan-in-wing installation is the characteristic of the exit louver angle for minimum throttling versus cross-flow (V_p/V_{tip}). For the fan-in-fuselage installation, an exit louver angle setting of $\beta = 0^o$ produced minimum throttling (maximum flow) and increasing β increased throttling (and stress). As shown in Figure 80, the β setting for minimum throttling increased with cross-flow for the fan-in-wing installation. Based on this characteristic, it would be expected that β setting corresponding to minimum throttling should represent minimum stress, and changing exit louver angle from this setting should increase

stress. As shown in Figure 131a, the variation of stress with β setting at high tunnel velocities did not produce the expected characteristic. Another factor to be considered is that the fan circumferential loading was not uniform at high cross-flows which changed the back pressure patterns transmitted to the rotor. The net result of these two effects apparently reduced blade sensitivity in the cosine 2θ mode to exit louver angle changes.

The effect of inlet doors, the mid-wing configuration, angle of attack and yaw on cosine 2θ mode stress was insignificant within the range tested for these variables (see Figures 131e through h); in some cases the stress was lowered.

In addition to the above transient data, the fan was operated at the cosine 2θ mode speed of 2050 rpm for six minutes at 125 knots tunnel speed with the following results:

Conditions	Blade No.	Measured Stress psi (SA)	Predicted Stress psi (SA)	Test Limit Stress psi (SA)
125 knots $\beta = 35^{\circ}$ $\alpha = 0^{\circ}$ $\Psi = 0^{\circ}$ $N_F = 2050$ rpm	3	15,500	-	-
	7	19,500	20,250	33,500
	10	16,000		

The data indicate the measured levels would probably not be more than 2000 psi higher at $\beta = 45^{\circ}$.

Since the cosine 2θ mode stress magnitude is influenced by excitation from partial arc admission,[a] it was believed that the cosine 2θ mode

[a] Cosine 2θ mode stress magnitude for a fan-in-wing is the result of excitations from partial arc admission; exit louver throttling, inlet distortion from cross-flow, and loading of advancing and retreating blades (relative to the air stream).

stresses would increase if the admission arc were reduced 50% to simulate one-engine-out operation. A blocker (refer to Figure 13) was put into the scroll to simulate the engine-out condition and the fan was operated through the cosine 2θ mode resonance, 2050 rpm, at 20, 40, and 60 knots. The stresses were as shown in the following table:

TABLE XXI

COSINE 2θ MODE BLADE STRESSES

Tunnel Velocity (knots)	Stress with one engine-out simulated (psi - SA)	Stress during slow deceleration normal operation (psi - SA)	Percent Increase
20	21,500	11,000	95.0
40	19,500	12,500	56.0
60	20,500	13,500	52.0

Extrapolating the "engine-out" stress data to higher tunnel velocities would give an approximate stress of 20,500 - 22,500 psi.[a] If the 52% increase found at 60 knots were applied at 125 knots, the "engine-out" stress would be 30,500 psi versus a 33,500 psi calculated stress limit. From this extrapolation it appears that the cosine 2θ mode stress would be within the stress limit with one engine-out at all transition speeds.

Rotor Blade First Flexural Stress - The stress limit for the first flexural mode is based primarily on the tip tang and dovetail strength. The airfoil itself is strong enough to permit a higher stress limit. For the X353-5B fan, because of the stronger single hook dovetail design, it is expected that the stress limit will be higher and

[a] All stress levels are single amplitude.

will be limited by the tip tang strength. Based on laboratory tests, 10,000 psi was selected for the tip tang as a safe running limit. This was obtained from a 20,000 psi run-out point (no failure) and then reduced for temperature effects and allowance for blade-to-blade stress variation. The actual fatigue limit has not as yet been determined; however, more tests to determine this limit are in process.

Stress data in the 1850 rpm speed region where the first flexural mode is in resonance with an 8/rev excitation, are shown in Figures 132a and b. Figure 132a shows the stress as a function of tunnel velocity and exit louver angle for the basic airplane configuration with no fan inlet doors installed. Note that the running stress limit of 10,000 psi is slightly exceeded above 100 knots at $\beta = 45^{\circ}$. The overall blade stress levels for these same conditions are included in Figure 132a.

Figure 132b shows that there is no significant change in stress level with angle of attack.

At 60 knots and above, the first flexural stress was significantly higher for the mid-wing aircraft configuration with fan inlet doors installed than for the basic aircraft with no doors (see Figure 132b). Changing from the mid-wing to the basic (high) wing caused only a slight reduction in stress level. It is concluded that the addition of the faired doors to the inlets of the wing-mounted fans was the primary cause of the higher first flexural blade stress. The blade stress not only increased at the flexural resonance which is excited by 8/rev inputs at 1850 rpm but also at speeds above 2200 rpm where there are no per rev resonances. Here, the blades apparently were responding simply to separated

flow distortions from the fan inlet doors.

Stator Stresses:

During static fan-in-wing testing (reference 19), the stator stresses were increased compared with fan-in-fuselage levels. This resulted from a combined effect of separated flow and resonance. This deficiency was basic in the design and is being changed for the VZ-11 program. The single large stiffener ring dividing the fan stator into two annuli is being replaced by two thinner rings. This corrects both sensitivities by changing the natural resonance frequency with increased stiffness, and the increased stiffness, in turn, reduces the influence of separated flow conditions. New full-scale hardware for the VZ-11 has been bench tested to verify the resonance frequencies. Actual test experience will be obtained during the VZ-11 program. Scale model testing indicates no aerodynamic performance penalty because of the additional stiffener ring. This was achieved by reducing the maximum thickness to chord length (tm/c) ratio of the stiffener.

Most of the wind-tunnel testing was conducted by selecting the variables so that the stator stresses remained within limits. For high speed and extreme variable ranges, test stiffener rings were added (refer to Figure 12); they were not used continuously to avoid any performance penalty because of this test hardware.

Blade and Stator Stresses in Ground Effect:

Blade and stator stresses were not significantly affected by ground proximity (less than 10% stress level increase above the out-of-ground effect values for all critical stress modes). This is in

marked contrast to the fan-in-fuselage results (stator stress more than doubled at low h/d_F values) but these two configurations are basically different in terms of the in-flow velocity profiles which give a higher hub loading even out-of-ground effect for the fan-in-fuselage. For that case the fan flow is obtained from a column of air directly above the fan requiring the air in the center to accelerate over the bulletnose to get into the fan hub. For the fan-in-wing case the air is obtained from essentially a hemispherical source and the hub velocity is much lower (the tip velocities are higher and require good inlet design to control bellmouth separation).

The fan is throttled by the ground just as by vectoring with the exit louvers except that the flow is turned by static pressure gradients which cause high hub loading. The initially higher fan-in-fuselage hub loading causes the hub to stall in proximity to the ground whereas the fan-in-wing hub performance deteriorates short of stall.

Increasing β in proximity to the ground has a similar effect as increasing ground height and tends to relieve hub loading and reduce stress levels approaching out-of-ground effect results.

Circular Inlet Vane Stress:

The test inlet vane was not representative of flight type hardware (over 100 pounds weight). Strain gages on the supports gave no indication of vibration.

Normal Speed Operating Stress:

In the operating range above the cosine 2θ resonant speed, 78%, the rotor blade stress derives from a torsional resonance at 2350 rpm, first flexural and first torsional mode stresses excited by separated flow, and off resonance cosine 2θ mode stress. At

low tunnel velocities, these stresses are low. As tunnel velocity increases these stresses increase with the maximum stress occurring at 125 knots tunnel velocity. At 125 knots the first flexural mode varied from 4,500 psi to 9,000 psi and was independent of β setting (0° to 45°), angle of attack ($\pm 4^{\circ}$) and fan speed (78% to 100%).

The torsional resonance at 2350 rpm and the off resonance cosine 2θ stress were not significant in themselves but they added to the total stress level.

Combining all the stresses present shows that the blade airfoil and single hook dovetail to be within infinite life limits and the tip tang to be near the stress limit set for the testing.

When the faired inlet doors were tested, the rotor blade first flexural stress above 78% N increased significantly at 80 knots tunnel velocity. It appears probable that at higher tunnel velocities the first flexural stress will be over the stress limit presently chosen. The limiting stress in the first flexural mode is in the tip tang. As described above, tests are being made to determine more accurately the true safe value for this limit. To help alleviate the first flexural stress an attempt to reduce the excitation from the doors should be made. These tests should be made in the wind tunnel at high velocities since the type of data is difficult to extrapolate reliably.

Conversion:

With both the wing and fuselage installations the first flexural and torsional modes were not a significant function of diverter valve door actuation rates and, for very short actuation times, these mode responses did not change.

As noted earlier, the cosine 2θ mode response in the fuselage, was

a function of diverter valve door closure time, whereas in the wing, it was almost independent of closure time. Steady state operation at the resonance speed was a higher stress indication than transient operation through the resonance range for the wing installation. Conversion for that configuration is, therefore, not a special problem. The fuselage installation was never operated steady state at the cosine 2θ resonance[a] so it is not known if this would also be true for that configuration; the tendency toward higher stress with faster transients indicates that conversion stresses may be higher than steady state and should be investigated.

Temperature Measurements:

Bearing Temperatures - Bearing temperatures were well within limits for all test operation.

Wing Temperatures - Temperatures were recorded inside the wing in the vicinity of the fan installation. Normal operating temperature was approximately 150°F; however, under conditions of high exit louver settings, this temperature was recorded as high as 400°F. The sealing arrangement between the lower wing surfaces and the fan installation was not effective in preventing the hot turbine exhaust gases from leaking into the wing. These high wing temperatures will be eliminated by an improved seal design that will be incorporated in the VZ-11 installation.

During Period I testing, the high wing temperatures caused some of the instrumentation leads to be burned off. These were replaced with high temperature Teflon leads for Period II testing and were no longer a problem.

---

[a] Required X353-5B rotor dovetail design.

VI. HARDWARE INSPECTION RESULTS

Both lift fans used during Period I testing were disassembled and inspected at Ames with the following results:

LIFT FAN S/N 001 (PERIOD I)

Forward Frame and Scroll (not disassembled):

1. Ball and roller bearings showed no sign of wear.

2. The frame and scroll were dirty but no signs of wear or fatigue were observed.

3. The frame insulation was not removed.

4. The scroll air seals had shifted on the inner band causing a gap of approximately 1/4 inch at one point. See Figure 133a.

5. The forward air seals were rubbed by the torque band causing a groove, the maximum depth of which was 1/16 inch.

Rotor:

1. The rotor was completely disassembled and the following parts showed no discrepancies after being zygloed or magnafluxed:
   a. Blades
   b. Carriers
   c. Torque bands
   d. Tabs
   e. Covers
   f. Retainer rings

2. The pins were hardness checked, and all fell within limits.

3. Five carrier pins were bowed and were rejected.

Rear Frame:

1. No teardown was accomplished on the rear frame.

2. All β_2 exit louvers were loose at the lever arms.

3. Three exit louvers were failed at the riveted joint on one end of the louvers.

LIFT FAN S/N 002 (PERIOD I)

Forward Frame and Scroll - No Discrepancies Noted:

Rotor:

1. Two axial cracks about 1/8 inch long were noted from zyglo inspection of the forward torque band (single piece, design B - reference 18, Figure 3a).

2. Eleven carrier pins were found sheared approximately 0.10 inch. Subsequent analysis indicated lack of proper heat treatment.

3. Four carriers were damaged in the process of disassembling the partially sheared carrier pins.

Rear Frame:

1. The rear frame insulation blanket had seven tears caused by turbine shroud rubs. See Figure 133b.

2. The turbine shroud was slightly damaged from the rub.

3. All β_2 exit louvers were loose at the lever arms.

4. Two exit louvers failed at the riveted joint at one end of the louver.

Diverter valves S/N 001 and 002 were inspected visually and no discrepancies were noted.

The J85 engines were sent to the Aircraft Service Shop of General Electric, Ontario, California for inspection and minor overhaul.

Both fans were overhauled, damaged parts were repaired or replaced, modifications were made as outlined in Section II, and all fan instrumentation was repaired prior to reinstallation in the wind tunnel model in preparation for Period II testing at Ames.

At the end of Period II testing, both fans were completely disassembled and inspected with the following results:

LIFT FAN S/N 001 (PERIOD II)

Forward Frame and Scroll:

1. No signs of wear or fatigue were discovered.

2. A small piece of diverter valve heat shield (see Diverter Valve and Bellows S/N 001 paragraph) was found lodged at the nozzle inlet to the scroll. The scroll was not damaged.

3. Ball and roller bearings showed no sign of wear.

Rotor:

1. The blades were magnafluxed and showed no indications of failure.

2. The buckets and carriers were zygloed and were in good condition.

3. Zyglo inspection of the torque band showed no indication.

4. A dye penetrant check of the disc and dovetail slots was made and no indications were noted.

5. A visual inspection of the covers, platforms and pins was made. They were in satisfactory condition.

6. One platform failed early in the test and was removed. The aluminum sheet was improperly welded to the platform structure. Vehicle operation with this part removed was satisfactory with no noticeable effect on rotor residual unbalance.

Rear Frame:

All parts were in good condition except the exit louvers. The pins were again worn badly giving a poor fit at the actuation lever arms. Also, the hot end of the aluminum louvers were nearly failed as experienced during previous testing.

LIFT FAN S/N 002 (PERIOD II)

Forward Frame and Scroll:

The only discrepancy noted was a skin failure in the bellmouth near the 3 o'clock strut shown in Figure 134. The skin pictured is the original skin; the covering over the bellmouth, added at manufacture for this frame only, was previously removed locally at this section during baffle installation.[a]

Rotor:

1. Blades were magnafluxed and the buckets, carriers, and torque bands were zygloed. All were in satisfactory condition.

2. All other parts were inspected visually and no discrepancies were noted.

Rear Frame:

1. Previous turbine rubbing into the insulation blanket was not repeated. All parts were in good condition except the exit louvers.

2. This set of exit louvers was also in poor condition: pins were worn badly giving poor fit at the actuation lever arms; and the hot ends of the aluminum louvers were nearly failed.

DIVERTER VALVE AND BELLOWS S/N 001

1. One convolution of the bellows yielded but did not fail (see Figure 135). The length of the bellows is nominally 0.200" longer

[a] Reference 19

than print. Indications are that at some time during the test history this bellows had been improperly installed. It was retired from use with an accumulated operating time of 164 hours.

2. A 2" x 2" x 0.015" piece of the heat shield was missing from the straight door of the diverter valve (see Figure 136a). The piece was recovered in the scroll. Visual inspection indicates failure of several "puddle" welds. These welds were good at points where thin sections were joined but did not hold where the heat shield was attached to the much thicker trunnion mount. Imminent failure of another piece on the curved door is also apparent from visual inspection (see Figure 136b). A complete zyglo check was performed.

DIVERTER VALVE AND BELLOWS S/N 002

This diverter valve and the bellows were inspected and found to be in good condition.

In addition, the J85 engines used were visually inspected and all parts appeared to be normal.

VII. RECOMMENDATIONS

The nature of the work under contract DA 44-177-TC-584 is such that specific individual recommendations are made in the regular and continuing working relationships between the contractor, USA TRECOM, and NASA-Ames. Such recommendations are usually presented in correspondence and in the bi-monthly technical progress reports and are not restated here. Also, in the body of this report, individual technical recommendations are incorporated in the technical discussions of which they are appropriately an inseparable part.

The intent of this section of the report is to summarize the major program recommendations relating to the continuation of the work and related programs. These are:

A. Provide NASA-Ames with the government-owned lift fan hardware obtained for this contract work. The other available lift fan owned by General Electric has been loaned to NASA-Ames, and together these fans can be used in NASA-sponsored, full-scale, wind-tunnel tests of a simulated VZ-11 airplane by mid 1962. The NASA-Ames program will provide advance data on this configuration available for the VZ-11 detailed design.

B. Undertake scale-model and full-scale tests to investigate fan loading and stall characteristics of the fan mounted in an outboard wing panel, as would be required in a four fan-in-wing airplane. Consideration should be given to the effects of: wing pressure and velocity fields; active and inactive fan arc orientation; direction of rotor rotation; fan seal clearances (leakage); and inlet design.

C. Undertake ground effect tests of scale model or full-scale fan powered aircraft to more precisely identify the aircraft ground

effects and important configuration influences including fan spacing and location; fuselage shape; wing shape; fan-to-wing area ratio; h/d_F; etc. Fan contributions per se are now reasonably well understood. (Some scale model work has been started within NASA and reported.)

D. Conduct full-scale tests of an aircraft model with various engine inlet locations in proximity to the ground to identify specific re-ingestion patterns and identify possible alternate locations to the high, VZ-11 type inlet arrangement. Investigation of mixing devices may also be appropriate to such a study.

E. Complete, as planned for contract DA 44-177-TC-715, full-scale wind tunnel evaluation of one actual VZ-11 airplane with particular attention to control effectiveness, stability, ground effect, re-ingestion and systems evaluation.

F. Conduct full-scale wind-tunnel tests of a nose mounted pitch control fan (X376) for mechanical and aero-thermodynamic evaluation prior to VZ-11 testing. Influence of the pitch fan on reingestion and aircraft ground effect should also be investigated.

G. Extend contract DA 44-177-TC-584 to include the provision of a General Electric prepared summary report of NASA-Ames, full-scale simulated VZ-11 tests (A. above). Correlation of these data with TCREC 62-21, reference 19, and this report would be of value in refining the analyses and possibly identifying accurate scaling parameters for the different aircraft configurations.

H. Investigate the low forward speed range effect on full-scale fan loading and efficiency. Scale-model tests of fan-in-wing aircraft in the 0-to 50-knot flight speed range with a very large tunnel to model size relationship to minimize tunnel effects should complement this investigation.

VIII. REFERENCES

1. Aoyagi, K., Hickey, D.H., and deSavigny, R.A., Aerodynamic Characteristics of a Large-Scale Model with a High Disk-Loading Lifting Fan Mounted in the Fuselage, NASA Technical Note D-775.

2. Corning, Gerald, Supersonic and Subsonic Airplane Design, Second Edition, Edwards Brothers, Inc., Ann Arbor, Michigan, 1953.

3. Hickey, D.H., and Ellis, D.R., Wind-Tunnel Tests of a semispan Wing with a Fan Rotating in the Plane of the Wing, NASA Technical Note D-88, October 1959.

4. Hoerner, S.F., Dr., Fluid-Dynamic Drag, Published by the Author, 1958, Library of Congress Catalog Card Number 57-13009.

5. *Kelly, M.W., Large-Scale Wind-Tunnel Studies of Several VTOL Types, Ames Research Center.

6. Kuhn, R.E., and Naeseth, R.L., Tunnel-Wall Effects Associated with VTOL-STOL Model Testing, NASA, Langley Research Center, Langley Field, Va., March 1959.

7. *Maki, R.L., and Hickey, D.H., Aerodynamics of Fan-in-Fuselage Model, Ames Research Center.

8. Pope, Alan, Wind-Tunnel Testing, Second Edition, John Wiley and Sons, Inc., New York, 1954.

9. *Spreemann, K.P., Induced Interference Effects on Jet and Burried Fan VTOL Configurations in Transition, Langley Research Center.

---

* From NASA Conference on V/STOL Aircraft (a compilation of papers presented), Langley Research Center, Langley Field, Virginia, November 17-18, 1960.

10. Heyson, Harry, H., Linearized Theory of Wind Tunnel Jet-Boundary Corrections and Ground Effect for VTOL-STOL Aircraft, NASA Technical Note R-124, Langley Research Center, Langley Air Force Base, Va., 1962.

11. Davenport, Edwin E., and Spreemann, Kenneth P., Thrust Characteristics of Multiple Lifting Jets in Ground Proximity, NASA Technical Note D-513, September 1960.

12. Perkins, Courtland D., and Hage, Robert E., Airplane Performance Stability and Control, John Wiley & Sons, Inc., New York, 1958.

13. Switzer, J.R., VTOL Wing-Fan Model Tests, General Electric Company, Flight Propulsion Laboratory Department, Cincinnati 15, Ohio, 1958, unclassified. Report No. R58AGT953.

14. Theodorsen, Th., Dr., Theoretical Investigation of Ducted Propeller Aerodynamics, Volume 1, USA TRECOM Contract No. DA 44-177-TC-606, Project No. 9R 38-01-017-24, Republic Aviation Corporation, Farmingdale, New York, August 10, 1960, unclassified.

15. Joyce, J., Fabrication, Test and Analysis of a Tip-Turbine Lift-Fan VTOL Propulsion System, USA TRECOM Contract No. DA 44-177-TC-584, Project No. 9R 38-01-017-04, Technical Report TREC 60-42, General Electric Company, Flight Propulsion Laboratory Department, Cincinnati 15, Ohio, August 1960, unclassified.

16. Przedpelski, Z.J., Results of Wind Tunnel Tests of a Full Scale Fuselage Mounted, Tip Turbine Driven Lift Fan, USA TRECOM Contract No. DA 44-177-TC-584, Project No. 9R 38-01-020-02, Technical Report TREC 61-15, Volume 1, General Electric Company, Flight Propulsion Laboratory Department, Cincinnati 15, Ohio, January 1961, unclassified.

17. Przedpelski, Z.J., Results of Wind Tunnel Tests of a Full Scale Fuselage Mounted, Tip Turbine Driven Lift Fan, USA TRECOM Contract No. DA 44-177-TC-584, Task No. 9R 38-01-020-02, Technical Report TCREC 61-15, Volume 2, General Electric Company, Flight Propulsion Laboratory Department, Cincinnati 15, Ohio, April 1961, unclassified.

18. Przedpelski, Z.J., Results of Wind Tunnel Tests of a Full Scale Fuselage Mounted, Tip Turbine Driven Lift Fan, USA TRECOM Contract No. DA 44-177-TC-584, Task No. 9R 38-01-020-02, Technical Report TCREC 61-15, Volume 3, General Electric Company, Flight Propulsion Laboratory Department, Cincinnati 15, Ohio, March 1962, unclassified.

19. Heikkinen, A.H., Results of Static Tests of a Full Scale Wing Mounted, Tip Turbine Driven Lift Fan, USA TRECOM Contract No. DA 44-177-TC-584, Task No. 9R 38-01-020-02, Technical Report TCREC 62-21, General Electric Company, Flight Propulsion Laboratory Department, Cincinnati 15, Ohio, October 1961, unclassified.

20. Oliva, J.J., Progress Report on VTO Transition Analysis, General Electric Company, Flight Propulsion Laboratory Department, Cincinnati 15, Ohio, DM #61-336, December 5, 1961, unclassified.

APPENDIX A

TABLE A-1 LIST OF SYMBOLS

a	Velocity of sound at fan inlet, ft/sec.
A_{ef}	Effective flow area
A_F	Fan exit area = 17.8 sq. ft.
AR	Wing aspect ratio, b^2/S_w = 3.5
b	Wing span = 38.62 ft.
c	Local wing chord, ft.
$\bar{c}$	Mean wing chord S_w/b = 11.03 ft.
C_D	Drag coefficient $D/q\ S_w$ (based on tunnel q)
C_{Di}	Induced drag coefficient, C_L^2/π AR e
C_{Do}	Drag coefficient at zero lift
C_{Dw}	Drag coefficient based on wetted area
C_F	A_{ef}/A_F
c.g.	Center of gravity
C_L	Lift coefficient, $L/q\ S_w$ (based on tunnel q)
$\bar{C}_L$	Lift coefficient calculated from wing static pressure distribution

$$\frac{1}{2} \int_{-1}^{1} \frac{c_\ell\, c}{c}\, d\left(\frac{y}{b/2}\right)$$

$C_{L\ max}$	Maximum lift coefficient at $\Delta C_L/\Delta a = 0$
C_{Lt}	Horizontal tail lift coefficient

TABLE A-1 (Cont'd)

C_ℓ	Rolling moment coefficient, Roll Force/q b S_w (based on tunnel q)
C_M	Pitching moment coefficient, M/q S_w c_{mac} (based on tunnel q)
c_ℓ	Wing section lift coefficient
$\bar{C}_M$	Pitching moment coefficient calculated from wing static pressure distribution
ΔC_M	Change in moment coefficient due to change in tail incidence
c_{mac}	Mean aerodynamic chord $\int_{-b/2}^{b/2} \frac{c^2\, dy}{S_w}$ = 11.44 ft.
C_Z	Fan average axial (or through flow) velocity, ft/sec.
d	Diameter, ft.
D	Basic aircraft drag (fan off-holes covered), lbs.
D_{int}	Interaction drag, lbs.
D_R	Ram drag, lbs.
D_T	Total measured drag (fan on), lbs.
e	Oswald efficiency = 0.8 (assumed)
F	Total fan thrust, lbs.
F_{J85}	Thrust from J85 bleed gas
F_x	Horizontal component of fan thrust, F [sin (α - β_v)] lbs.

TABLE A-1 (Cont'd)

F_y	Vertical component of fan thrust, $F [\cos (\beta_v - \alpha)]$ lbs.
g	Acceleration due to gravity = 32.2 ft/sec.^{2}
G.W.	Aircraft gross weight, lbs.
H_D	Drag coefficient, $D_T/\rho A_F (V_{tip})^2$ (based on fan q)
H_{DF}	Drag coefficient, $F_x/\rho A_F (V_{tip})^2$
H_{DN}	Drag coefficient, $H_{DF} - H_{DR}$
H_{DR}	Drag coefficient, $D_R/\rho A_F (V_{tip})^2$
$H_{G.W.}$	Coefficient, $G.W./\rho A_F (V_{tip})^2$
H_L	Lift coefficient, $L_T/\rho A_F (V_{tip})^2$ (based on fan q)
H_{LF}	Lift coefficient, $F_y/\rho A_F (V_{tip})^2$
H_M	Moment coefficient, $M_T/\rho A_F (V_{tip})^2 c_{mac}$ (based on fan q)
HP	Horsepower
H_T	Thrust coefficient, $F/\rho A_F (V_{tip})^2$
h	Height of the bottom of the fan above the ground, ft.
i_t	Tail incidence angle, degrees
L	Basic aircraft lift (fan off - holes covered), lbs.
L_{int}	Interaction lift, lbs.
L_T	Total measured lift (fan on), lbs.
l_t	Tail moment arm = 22.14 ft.

TABLE A-1 (Cont'd)

M	Basic aircraft pitching moment (tail off, power off), ft. lbs.
M_{β}	Pitching moment due to exit louver vectoring, ft. lbs.
$M_{D_{RJ85}}$	Pitching moment due to J85 ram drag
M_{int}	Interaction pitching moment, ft. lbs.
M_{J85}	Pitching moment due to J85 bleed thrust, ft. lbs.
M_T	Total measured pitching moment (fan on), ft. lbs.
M_t	Pitching moment due to tail, ft. lbs.
N_F	Fan speed, RPM or % of design = 2640 RPM at 100%
N_{J85}	Engine speed, RPM or % of design = 16,500 RPM at 100%
P	Pressure, lbs/sq. in.
P/P	Fan rotor or fan stage pressure ratio
$P_{s\ell}$	Local static pressure, lbs/sq. in.
P_{to}	Tunnel total pressure, lbs/sq. in.
P_{so}	Tunnel static pressure, lbs/sq. in.
q	Tunnel dynamic pressure, lbs/sq. ft.
r/r_{fan}	Radius ratio, number of fan radii from fan centerline
S_t	Horizontal tail gross area = 100 sq. ft.
S_w	Wing gross area = 426 sq. ft.
T	Temperature, ^{o}R or ^{o}F

TABLE A-1 (Cont'd)

V_p	Tunnel or airplane velocity, Knots
V_{tip}	Fan blade tip speed = 720 ft/sec. or 426.6 knots at 2640 RPM
V_p/V_{tip}	Velocity ratio parameter (non-dimensional)
V_{stall}	Airplane stall speed (fan off), Knots
W	Weight flow, lbs/sec.
y	Spanwise location from center line of the aircraft, ft.
ϕ	Flow coefficient - C_Z/V_{tip} (non-dimensional)
α	Angle of attack, degrees
β	Indicated exit louver angle, degrees
β_1	Indicated exit louver angle for every other louver beginning with the first forward louver, degrees
β_2	Indicated exit louver angle for every other louver beginning with the second forward louver, degrees
β_{av}	Average exit louver angle = $(\beta_1 + \beta_2)/2$, degrees
β_s	Exit louver stagger angle = $\beta_2 - \beta_1$, degrees
β_v	Effective exit louver turning angle, degrees
δ	Pressure correction parameter, $P_{ambient}/14.696$
δ_f	Wing flap angle, degrees
ϵ	Tail downwash angle, degrees
η_R	Fraction of tunnel velocity head recovered by fan inlet (includes static loss)

TABLE A-1 (Cont'd)

θ	Temperature correction parameter, $T_{ambient}/518.7$
ρ	Mass density, slugs/cu. ft.
$\bar{\omega}$	Loss coefficient in per cent of fan inlet velocity head at the face of the rotor
Ψ	Aircraft yaw angle, or pressure coefficient = $\frac{2}{\gamma-1}\frac{(P/P)^{\gamma-1/\gamma} - 1}{(V_{tip}/a)^2}$

SUBSCRIPTS

c	Corrected
F	Denotes fan
f	Denotes flap or frontal area
P	Denotes airplane
s	Denotes static
t	Denotes total or tail
u	Uncorrected
w	Denotes wing or wetted area
10.1; 5.3; etc.	Denotes measurement plane identification
oooo	Denotes $\beta_s = 0^o$, $\beta_{av} = 0^o$, $V_P = 0$ and $h/d_F > 1.8$ (equivalent to zero ground effect)

TABLE A-2

WIND TUNNEL TEST RESULTS

Data Description:

Each page of data includes two sets of column headings. The column headings at the top of each page are self-explanatory and the symbols are consistent with the definitions and symbols presented in Table A-1.

Near the middle of each page of data, the second set of column headings are made in two lines and correspond to the two lines of data presented for each test point. An explanation of the meaning of the column titles beginning with the first double-lined column heading is as follows:

PT	- Point of run
AVG	- Number of readings used for average
ALPHA	- Corrected Angle of Attack, α, Degrees
BETA	- Sideslip Angle, Degrees = Negative of Yaw Angle, Ψ, Degrees
Q	- Tunnel Dynamic Pressure, q, Lbs/Sq. Ft.
V, NOM	- Equivalent Nominal Velocity, Ft/Sec.
LIFT, U	- Total Measured Lift, Lbs.
CL*QS	- Total Measured Lift, Lbs.
DRAG, U	- Total Measured Drag, Uncorrected, Lbs.
CD*QS	- Corrected Drag = C_D q S_W, Lbs.

M,U - Total Measured Pitching Moment, Uncorrected, Ft-Lbs.

CM*QSC - Corrected Pitching Moment = C_M q S_W c_{mac}

CL - Lift Coefficient, C_L

CY - Side Force Coefficient, Uncorrected

CD - Corrected Drag Coefficient, C_D

CN - Yawing Moment Coefficient, Uncorrected

CM - Corrected Pitching Moment Coefficient, C_M

CROLL - Rolling Moment Coefficient, Uncorrected

SIDE F,U - Total Measured Side Force, Uncorrected, Lbs.

CY*QS - Total Measured Side Force, Uncorrected, Lbs.

YAW,U - Total Measured Yawing Moment, Uncorrected, Ft-Lbs.

CN*QSB - Total Measured Yawing Moment, Uncorrected, Ft/Lbs.

ROLL, U - Total Measured Rolling Moment, Uncorrected, Ft-Lbs.

CL*QSB - Total Measured Rolling Moment, Uncorrected, Ft-Lbs.

Data Corrections:

Data includes tunnel corrections as described in Section IV.

Period II data (test runs numbered II-1 through II-22) corrections as described in Section IV should be applied to account for the different mounting system above the wind tunnel support struts.

Period I data (test runs numbered I-1 through I-27) corrections for tunnel dynamic pressure must be applied to the following tabulated parameters: CL, CD, CM, CY, CN, CROLL and V, NOM. The correction factors (q/qc) are listed in the last column at the top of each

page for those runs to be corrected. The tabulated coefficients are corrected as follows:

C_L = tabulated CL (q/qc)

C_D = tabulated CD (q/qc) etc., for CM, CY, CN and CROLL

The velocity can be corrected as follows:

V, NOM = tabulated V, NOM/$\sqrt{q/qc}$

Test Point No.	Run No.	Point of Run	Left N_p RPM	Right N_p RPM	Left β_1 Deg.	Left β_0 Deg.	Right β_1 Deg.	Right β_0 Deg.	Tail i_t Deg.	δ_f Deg.	Baro. in. Hg	To °F	Left N_{JBS} % RPM	Right N_{JBS} % RPM	Average V_p/V_{tip}	q/qc
1	I-1	1	0	0	90	90	90	90	OFF	0	30.24	78	0	0	N/A	N/A
2		2														
3		3														
4		4														
5		5														
6		6														
7		7														
8		8														
9		9														
10	I-2	1	0	0	90	90	90	90	OFF	0	30.24	82	0	0	N/A	N/A
11		2														
12		3														
13		4														
14		5														
15		6														
16		7														
17		8														
18		9														
19		10														
20		11														
21		12														
22		13														
23		14														
24	I-3	1	1700	1700	0	0	0	0	OFF	0	29.8	73	86	89	0.020	N/A
15		2	1750	1750	0	0	0	0				73	86	89	0.035	
26		3	1695	1695	0	0	0	0				73	85	88	0.0687	
27		4	1690	1700	20	20	20	20				91	85	88	0.0687	
28		5	1700	1700	35	35	35	35				93	85	88	0.0710	

Test Point No.	Run No.	PT AVG	ALPHA	BETA	Q V,NOM	LIFT,U CL*QS	DRAG,U CD*QS	M,U CM*QSC	CL CY	CD CN	CM CROLL	SIDE F,U CY*QS	YAW,U CN*QSB	ROLL,U CL*QSB
1	I-1	1	-4.13	-0.	11.80	-726.	262.	-1317.	-0.1444	0.0524	-0.0229	0.	-3.	-9.
		1			99.62	-726.	263.	-1317.	0.	-0.0090	-0.0000	0.	-3.	-9.
2		2	0.10	-0.	11.80	522.	218.	-482.	0.1038	0.0436	-0.0084	0.	-3.	7.
		1			99.62	522.	219.	-482.	0.	-0.0000	0.0000	0.	-3.	7.
3		3	4.32	-0.	11.61	1722.	245.	-367.	0.3482	0.0515	-0.0065	0.	-3.	22.
		1			98.81	1722.	254.	-367.	0.	-0.0000	0.0001	0.	-3.	22.
4		4	8.34	-0.	11.80	1830.	338.	-14279.	0.3641	0.0695	-0.2483	0.	-4.	24.
		1			99.62	1830.	349.	-14279.	0.	-0.0000	0.0001	0.	-4.	24.
5		5	10.68	-0.	11.61	5642.	415.	999.	0.7365	0.0927	0.0177	0.	-5.	47.
		1			98.81	5642.	458.	999.	0.	-0.0000	0.0002	0.	-5.	47.
6		6	12.82	-0.	11.80	4446.	528.	942.	0.8845	0.1176	0.0164	0.	-7.	58.
		1			99.62	4446.	591.	942.	0.	-0.0000	0.0003	0.	-7.	58.
7		7	14.93	-0.	11.80	5082.	658.	1411.	1.0110	0.1473	0.0245	0.	-9.	66.
		1			99.62	5082.	740.	1411.	0.	-0.0000	0.0003	0.	-9.	66.
8		8	16.89	-0.	11.61	4770.	955.	549.	0.9846	0.2081	0.0097	0.	-12.	62.
		1			98.81	4770.	1029.	549.	0.	-0.0001	0.0003	0.	-12.	62.
9		9	18.92	-0.	11.61	4938.	1359.	213.	0.9986	0.2909	0.0038	0.	-18.	64.
		1			98.81	4938.	1439.	213.	0.	-0.0001	0.0003	0.	-18.	64.
10	I-2	1	-4.13	-0.	20.62	-1218.	473.	-2613.	-0.1380	0.0541	-0.0260	0.	-6.	-16.
		1			131.69	-1218.	475.	-2613.	0.	-0.0000	-0.0000	0.	-6.	-16.
11		2	0.10	-0.	20.81	984.	396.	-750.	0.1110	0.0449	-0.0076	0.	-5.	13.
		1			132.30	984.	398.	-750.	0.	-0.0000	0.0000	0.	-5.	13.
12		3	4.33	-0.	20.81	3132.	442.	469.	0.3533	0.0578	0.0048	0.	-6.	41.
		1			132.30	3132.	459.	469.	0.	-0.0000	0.0001	0.	-6.	41.
13		4	8.57	-0.	20.62	5460.	612.	2121.	0.6216	0.0759	0.0211	0.	-8.	71.
		1			131.69	5460.	667.	2121.	0.	-0.0000	0.0002	0.	-8.	71.
14		5	10.69	-0.	20.62	6576.	781.	2389.	0.7486	0.0945	0.0238	0.	-10.	85.
		1			131.69	6576.	830.	2389.	0.	-0.0000	0.0003	0.	-10.	85.
15		6	12.83	-0.	20.62	7840.	941.	2292.	0.8948	0.1200	0.0228	0.	-12.	102.
		1			131.69	7840.	1054.	2292.	0.	-0.0000	0.0003	0.	-12.	102.
16		7	14.94	-0.	20.81	8988.	1179.	2792.	1.0138	0.1494	0.0275	0.	-15.	117.
		1			132.30	8988.	1326.	2792.	0.	-0.0000	0.0003	0.	-15.	117.
17		8	16.93	-0.	20.62	8832.	1808.	1612.	1.0055	0.2221	0.0140	0.	-24.	115.
		1			131.69	8832.	1951.	1612.	0.	-0.0001	0.0003	0.	-24.	115.
18		9	-4.13	-0.	32.66	-2004.	765.	-5484.	-0.1440	0.0552	-0.0219	0.	-10.	-26.
		1			165.73	-2004.	768.	-5484.	0.	-0.0000	-0.0000	0.	-10.	-26.
19		10	0.10	-0.	32.66	1512.	641.	-1616.	0.1087	0.0463	-0.0102	0.	-8.	20.
		1			165.73	1512.	643.	-1616.	0.	-0.0000	0.0000	0.	-8.	20.
20		11	4.33	-0.	32.66	4980.	708.	757.	0.3580	0.0530	0.0048	0.	-9.	65.
		1			165.73	4980.	737.	757.	0.	-0.0000	0.0001	0.	-9.	65.
21		12	8.57	-0.	32.66	8616.	979.	3408.	0.6193	0.0766	0.0216	0.	-13.	113.
		1			165.73	8616.	1065.	3408.	0.	-0.0000	0.0002	0.	-13.	113.
22		13	10.70	-0.	32.66	10512.	1203.	3676.	0.7556	0.0957	0.0231	0.	-16.	137.
		1			165.73	10512.	1331.	3676.	0.	-0.0000	0.0003	0.	-16.	137.
23		14	12.83	-0.	32.66	12504.	1494.	3591.	0.8988	0.1204	0.0226	0.	-19.	163.
		1			165.73	12504.	1675.	3591.	0.	-0.0000	0.0003	0.	-19.	163.
24	I-3	1	0.	-0.	1.00	5328.	-316.	-4898.	12.5070	-0.7414	-1.0051	12.	780.	170.
		5			0.	5328.	-316.	-4898.	0.0270	0.0474	0.0104	12.	780.	170.
25		2	0.	-0.	1.00	5578.	-156.	-5995.	13.0930	-0.3662	-1.2301	-10.	120.	-1084.
		5			0.	5578.	-156.	-5995.	-0.0225	0.0073	-0.0659	-10.	120.	-1084.
26		3	0.	-0.	1.16	5306.	601.	-380.	10.7124	1.2142	-0.0671	-60.	736.	101.
		5			31.47	5306.	601.	-380.	-0.1221	0.0385	0.0053	-60.	736.	101.
27		4	0.	-0.	1.12	4812.	-1549.	2587.	10.0491	-3.2355	0.4723	-52.	-256.	-124.
		5			30.75	4812.	-1549.	2587.	-0.1003	-0.0138	-0.0067	-52.	-256.	-124.
28		5	0.	-0.	1.20	3571.	-2420.	-775.	6.9768	-4.7288	-0.1323	76.	-696.	384.
		5			31.79	3571.	-2420.	-775.	0.1491	-0.0352	0.0194	76.	-696.	384.

TABLE A-2 (Continued)

Test Point No.	Run No.	Point of Run	Left N_p RPM	Right N_p RPM	Left β_t Deg.	Left β_0 Deg.	Right β_t Deg.	Right β_0 Deg.	Tail i_t Deg.	δ_f Deg.	Baro. in. Hg	To ^oF	Left $N_{.785}$ % RPM	Right $N_{.785}$ % RPM	Average V_p/V_{tip}	q/qc
29	I-3	6	1700	1700	0	0	0	0	OFF	0	29.8	98	86	89	0.1109	N/A
30		7			20	20	20	20				98	86	89	0.1109	
31		8			35	35	35	35				100	85	88	0.1112	
32		9			0	0	0	0				100	86	89	0.1463	
33		10			20	20	20	20				102	86	89	0.1494	
34		11			35	35	35	35				103	85	88	0.1467	
35		12		1660	40	40	40	40				103	84		0.1513	
36	I-4	1	1700	1700	0	0	0	0	OFF	0	30.28	90	85		0.2193	N/A
37		2	1680	1700	20	20	20	20				92			0.2210	
38		3	1700	1710	35	35	35	35				93			0.2193	
39		4	1714	1740	40	40	40	40				94			0.2149	
40		5	1708	1650	0	0	0	0				97			0.2971	
41		6	1690	1693	20	20	20	20				100		89	0.3040	
42		7	1710	1730	35	35	35	35				101	84.5	89	0.3015	
43		8	1730	1730	40	40	40	40				101	84.5	88.5	0.2908	
44		9	1700	1700	0	0	0	0				103	85	89	0.3756	
45		10	1705	1690	20	20	20	20				105	85	89	0.3809	
46		11	1700	1695	35	35	35	35				105	85	89	0.3693	
47		12	1705	1720	40	40	40	40				106	84.5	88.5	0.3738	
48	I-5	1	1700	1680	0	0	0	0	OFF	30	30.22	98	86	89	0.1489	1.004
49		2	1700	1680	0	0	0	0				100			0.1496	1.038
50		3	1700	1670	20	20	20	20				101			0.1497	1.004
51		4	1730	1710	35	35	35	35				102			0.1468	1.004
52		5	1710	1660	0	0	0	0				104			0.1508	1.032
53		6	1708	1711								104		90	0.1474	0.975
54		7	1707	1705								104		90	0.1483	1.042
55		8	1705	1705								104		90	0.1484	1.004
56		9	1690	1700								105		90	0.1501	1.032

Test Point No.	Run No.	PT AVG	ALPHA	BETA	Q V,NOM	LIFT,U CL*QS	DRAG,U CD*QS	M,U CM*QSC	CL CY	CD CN	CM CROLL	SIDE F,U CY*QS	YAW,U CN*QSB	ROLL,U CL*QSB
29	I-3	6	0.	-0.	2.91	6139.	996.	2305.	4.9574	0.8043	0.1627	-161.	187.	-119.
		5			49.45	6139.	996.	2305.	-0.1302	0.0039	-0.0025	-161.	187.	-119.
30		7	0.	-0.	2.91	5107.	-1129.	4580.	4.1241	-0.9115	0.3233	-88.	-431.	-758.
		5			49.45	5107.	-1129.	4580.	-0.0709	-0.0099	-0.0159	-88.	-431.	-758.
31		8	0.	-0.	2.91	3293.	-1976.	5392.	2.6590	-1.5956	0.3806	-8.	-460.	1727.
		5			49.45	3293.	-1976.	5392.	-0.0062	-0.0096	0.0361	-8.	-460.	1727.
32		9	0.	-0.	5.04	6338.	1402.	5949.	2.9529	0.8531	0.2423	-129.	527.	491.
		5			65.10	6338.	1402.	5949.	-0.0599	0.0084	0.0059	-129.	527.	491.
33		10	0.	-0.	5.23	5347.	-629.	6098.	2.5984	-0.2821	0.2391	-75.	-610.	-2729.
		5			66.34	5347.	-629.	6098.	-0.0336	-0.0071	-0.0317	-75.	-610.	-2729.
34		11	0.	-0.	5.04	3624.	-1572.	7783.	1.6883	-0.7323	0.3170	-11.	-349.	-1302.
		5			65.10	3624.	-1572.	7783.	-0.0049	-0.0042	-0.0157	-11.	-349.	-1302.
35		12	0.	-0.	5.23	3019.	-1523.	7270.	1.3545	-0.6832	0.2851	-72.	858.	-471.
		5			66.34	3019.	-1523.	7270.	-0.0321	0.0100	-0.0055	-72.	858.	-471.
36	I-4	1	0.	-0.	11.61	7097.	2239.	8246.	1.4351	0.4528	0.1458	-239.	2255.	-3605.
		5			98.81	7097.	2239.	8246.	-0.0481	0.0118	-0.0189	-239.	2255.	-3605.
37		2	0.	-0.	11.61	5954.	514.	9303.	1.2041	0.1040	0.1645	-245.	856.	-2265.
		5			98.81	5954.	514.	9303.	-0.0496	0.0045	-0.0119	-245.	856.	-2265.
38		3	0.	-0.	11.61	4714.	-587.	9011.	0.9532	-0.1187	0.1593	-134.	-221.	-1924.
		5			98.81	4714.	-587.	9011.	-0.0272	-0.0012	-0.0101	-134.	-221.	-1924.
39		4	0.	-0.	11.42	4092.	-797.	8231.	0.8414	-0.1639	0.1479	-181.	1316.	-2306.
		5			97.99	4092.	-797.	8231.	-0.0373	0.0070	-0.0123	-181.	1316.	-2306.
40		5	0.	-0.	20.43	8362.	2696.	10682.	0.9604	0.3097	0.1073	-183.	2378.	-2961.
		5			131.08	8362.	2696.	10682.	-0.0211	0.0071	-0.0088	-183.	2378.	-2961.
41		6	0.	-0.	21.58	7382.	1395.	10685.	0.8032	0.1518	0.1016	-355.	1551.	-1351.
		5			134.71	7382.	1395.	10685.	-0.0386	0.0044	-0.0038	-355.	1551.	-1351.
42		7	0.	-0.	21.77	6106.	584.	9349.	0.6584	0.0614	0.0881	-348.	1527.	-4485.
		5			135.31	6106.	584.	9349.	-0.0375	0.0043	-0.0012	-348.	1527.	-4485.
43		8	0.	-0.	20.62	5410.	69.	8106.	0.6158	0.0079	0.0867	-285.	2228.	-2708.
		5			131.69	5410.	69.	8106.	-0.0324	0.0066	-0.0080	-285.	2228.	-2708.
44		9	0.	-0.	32.85	10660.	3134.	9655.	0.7614	0.2239	0.0603	-291.	4577.	-4475.
		5			166.21	10660.	3134.	9655.	-0.0208	0.0085	-0.0083	-291.	4577.	-4475.
45		10	-0.	-0.	33.61	-5494.	2078.	-161531.	-0.3837	0.1452	-0.9862	-386.	3714.	-2578.
		5			168.13	-5494.	2078.	-161531.	-0.0270	0.0067	-0.0047	-386.	3714.	-2578.
46		11	0.	-0.	31.40	7567.	1048.	8097.	0.5657	0.0784	0.0529	-486.	3668.	-403.
		5			162.51	7567.	1048.	8097.	-0.0363	0.0071	-0.0008	-486.	3668.	-403.
47		12	0.	-0.	32.85	7154.	911.	6659.	0.5113	0.0651	0.0416	-295.	2900.	-341.
		5			166.21	7154.	911.	6659.	-0.0211	0.0054	-0.0006	-295.	2900.	-341.
48	I-5	1	-4.00	-0.	5.23	6614.	1180.	891.	2.9673	0.5294	0.0349	-24.	-290.	-3288.
		5			66.34	6614.	1180.	891.	-0.0138	-0.0034	-0.0382	-24.	-290.	-3288.
49		2	0.	-0.	5.43	7267.	1559.	453.	3.1437	0.6746	0.0171	-66.	183.	-2897.
		5			67.56	7267.	1559.	453.	-0.0287	0.0021	-0.0324	-66.	183.	-2897.
50		3	0.	-0.	5.23	6031.	-501.	3003.	2.7057	-0.2248	0.1178	-74.	-736.	-2065.
		5			66.34	6031.	-501.	3003.	-0.0334	-0.0085	-0.0240	-74.	-736.	-2065.
51		4	0.	-0.	5.23	4644.	-1561.	3536.	2.0834	-0.7002	0.1387	-88.	-67.	732.
		5			66.34	4644.	-1561.	3536.	-0.0396	-0.0008	0.0085	-88.	-67.	732.
52		5	4.00	-0.	5.43	7750.	1942.	416.	3.3524	0.8403	0.0157	-133.	762.	-1971.
		5			67.56	7750.	1942.	416.	-0.0575	0.0085	-0.0221	-133.	762.	-1971.
53		6	8.00	-0.	5.04	8321.	2357.	-160.	3.8764	1.0979	-0.0065	-236.	1968.	-2116.
		5			65.10	8321.	2357.	-160.	-0.1100	0.0237	-0.0255	-236.	1968.	-2116.
54		7	10.00	-0.	5.43	8633.	2613.	-94.	3.7345	1.1303	-0.0035	-243.	2103.	-2478.
		5			67.56	8633.	2613.	-94.	-0.1053	0.0236	-0.0278	-243.	2103.	-2478.
55		8	12.00	-0.	5.23	8797.	2834.	293.	3.9665	1.2713	0.0115	-210.	1789.	-3907.
		10			66.34	8797.	2834.	293.	-0.0962	0.0208	-0.0454	-210.	1789.	-3907.
56		9	14.00	-0.	5.43	9041.	3079.	1166.	3.9110	1.3519	0.0441	-113.	1562.	-3684.
		10			67.56	9041.	3079.	1166.	-0.0489	0.0175	-0.0413	-113.	1562.	-3684.

TABLE A-2 (Continued)

Test Point No.	Run No.	Point of Run	Left N_p RPM	Right N_p RPM	Left β_1 Deg.	Left β_0 Deg.	Right β_1 Deg.	Right β_0 Deg.	Tail i_t Deg.	δ_f Deg.	Bare. Lo. Rg	To α_p	Left N_{J85} % RPM	Right N_{J85} % RPM	Average V_p/V_{tip}	q/qc
57	I-5	10	1700	1720	0	0	0	0	OFF	30	30.22	106	86.5	90.5	0.1118	1.064
58		11	1700	1730	0							106		90.5	0.1110	0.990
59		12	1700	1710	20	20	20	20				108		90	0.1118	1.054
60		13	1730	1740	35	35	35	35				109			0.1105	1.084
61		14	1700	1700	0	0	0	0				110			0.1129	1.044
62		15	1700	1690								110	86		0.1132	1.017
63		16	1710	1690								110			0.1137	1.030
64		17	1706	1694								111			0.1131	1.044
65		18	1700	1700								111			0.1153	1.003
66		19	1700	1700								111			0.1130	1.044
67		20	1690	1690								112			0.1134	0.932
68		21	1730	1715								113	86.5		0.2215	1.032
69		22	1740	1720								113	86.5		0.2206	1.015
70		23	1725	1703	20	20	20	20				113	86.5		0.2230	1.027
71		24	1670	1640	35	35	35	35				112	84	88	0.2304	1.032
72		25	1690	1660	40	40	40	40				112		88	0.2277	1.015
73		26	1650	1610	0	0	0	0				112		88.5	0.2334	1.013
74		27	1650	1658								112		88.5	0.2303	1.017
75		28	1650	1670								112		88.5	0.2298	1.015
76		29	1640	1700								112		88.5	0.2283	1.032
77		30	1540	1550								111	86	90	0.0506	1.405
78	I-6	1	1680	1680	0	0	0	0	OFF	30	30.26	87	84	87	0.295	1.009
79		2	1680	1670	0	0	0	0				88		87.5	0.297	1.024
80		3	1675	1675	20	20	20	20				88		87.5	0.297	1.024
81		4	1700	1700	35	35	35	35				91		87.5	0.293	1.015
82		5	1710	1710	40	40	40	40				91		87.5	0.291	1.015
83		6	1692	1694	0	0	0	0				93	85	88	0.293	1.015
84		7	1700	1700								93	85.5	88	0.293	1.015

Test Point No.	Run No.	PT AVG	ALPHA	BETA	Q V,NOM	LIFT,U CL*QS	DRAG,U CD*QS	M,U CM*QSC	CL CY	CD CN	CM CROLL	SIDE F,U CY*QS	YAW,U CN*QSB	ROLL,U CL*QSB
57	I-5	10	-4.00	-0.	3.16	6395.	786.	-980.	4.7520	0.5844	-0.0637	-150.	1416.	10.
		10			51.54	6395.	786.	-980.	-0.1116	0.0272	0.0002	-150.	1416.	10.
58		11	0.	-0.	2.91	6497.	1138.	-668.	5.2462	0.9192	-0.0671	-158.	1288.	699.
		10			49.45	6497.	1138.	-668.	-0.1277	0.0269	0.0146	-158.	1288.	699.
59		12	0.	-0.	3.10	5556.	-1029.	1977.	4.2661	-0.7789	0.1508	-102.	614.	310.
		10			51.07	5556.	-1029.	1977.	-0.0776	0.0120	0.0061	-102.	614.	310.
60		13	0.	-0.	3.22	4159.	-2004.	5128.	3.0349	-1.4621	0.1995	-81.	1087.	4048.
		10			52.02	4159.	-2004.	5128.	-0.0592	0.0205	0.0765	-81.	1087.	4048.
61		14	4.00	-0.	3.10	6672.	1545.	-454.	5.0509	1.1698	-0.0300	-550.	8321.	10955.
		10			51.07	6672.	1545.	-454.	-0.4161	0.1631	0.2147	-550.	8321.	10955.
62		15	8.00	-0.	3.02	6872.	1962.	-371.	5.3361	1.5233	-0.0252	-773.	11525.	18921.
		10			50.43	6872.	1962.	-371.	-0.6600	0.2317	0.3804	-773.	11525.	18921.
63		16	10.00	-0.	3.10	7156.	2223.	-296.	5.4173	1.6829	-0.0196	-766.	11280.	17639.
		10			51.07	7156.	2223.	-296.	-0.5796	0.2211	0.3458	-766.	11280.	17639.
64		17	12.00	-0.	3.10	7218.	2424.	-103.	5.4644	1.8349	-0.0068	-765.	11113.	20000.
		10			51.07	7218.	2424.	-103.	-0.5778	0.2178	0.3920	-765.	11113.	20000.
65		18	14.00	-0.	3.10	7544.	2702.	-83.	5.7114	2.0457	-0.0055	-427.	5893.	7569.
		10			51.07	7544.	2702.	-83.	-0.3236	0.1155	0.1484	-427.	5893.	7569.
66		19	16.00	-0.	3.10	7481.	2899.	8.	5.6632	2.1965	0.0065	-416.	5339.	7257.
		10			51.07	7481.	2899.	8.	-0.3152	0.1046	0.1423	-416.	5339.	7257.
67		20	18.00	-0.	2.75	7466.	3097.	549.	6.3688	2.6418	0.0409	-393.	5553.	9367.
		10			48.11	7466.	3097.	549.	-0.3355	0.1224	0.2069	-393.	5553.	9367.
68		21	-4.00	-0.	11.99	7741.	2060.	1259.	1.5154	0.4033	0.0215	-481.	6264.	4158.
		10			100.43	7741.	2060.	1259.	-0.0942	0.0318	0.0211	-481.	6264.	4158.
69		22	0.	-0.	11.80	8768.	2250.	2319.	1.7444	0.4476	0.0403	-486.	6640.	5745.
		10			99.62	8768.	2250.	2319.	-0.0986	0.0342	0.0296	-486.	6640.	5745.
70		23	0.	-0.	11.99	8210.	610.	1694.	1.6072	0.1195	0.0290	-374.	3834.	7282.
		10			100.43	8210.	610.	1694.	-0.0752	0.0194	0.0369	-374.	3834.	7282.
71		24	0.	-0.	11.99	6571.	-251.	696.	1.2863	-0.0492	0.0119	-454.	4950.	7973.
		10			100.43	6571.	-251.	696.	-0.0888	0.0250	0.0404	-454.	4950.	7973.
72		25	0.	-0.	11.80	6132.	-428.	-130.	1.2199	-0.0852	-0.0023	-444.	5725.	7407.
		10			99.62	6132.	-428.	-130.	-0.0884	0.0295	0.0382	-444.	5725.	7407.
73		26	4.00	-0.	11.72	9158.	2339.	2380.	1.8349	0.4684	0.0417	-484.	6641.	8151.
		10			99.30	9158.	2339.	2380.	-0.0969	0.0344	0.0425	-484.	6641.	8151.
74		27	8.00	-0.	11.80	10510.	2716.	2579.	2.0907	0.5403	0.0448	-401.	5819.	8062.
		10			99.62	10510.	2716.	2579.	-0.0797	0.0300	0.0415	-401.	5819.	8062.
75		28	10.00	-0.	11.80	11005.	2957.	3054.	2.1893	0.5885	0.0531	-408.	6025.	7564.
		10			99.62	11005.	2957.	3054.	-0.0812	0.0310	0.0390	-408.	6025.	7564.
76		29	12.00	-0.	11.99	11440.	3165.	3842.	2.2394	0.6195	0.0657	-360.	4948.	7554.
		10			100.43	11440.	3165.	3842.	-0.0704	0.0251	0.0383	-360.	4948.	7554.
77		30	0.	-0.	0.52	4340.	-808.	-3011.	19.4717	-5.6262	-1.1807	-333.	5619.	8760.
		10			20.98	4340.	-808.	-3011.	-1.4933	0.6527	1.0176	-333.	5619.	8760.
78	I-6	1	-4.00	-0.	20.70	9038.	2900.	1068.	1.0252	0.3290	0.0106	-244.	3441.	-2488.
		5			131.93	9038.	2900.	1068.	-0.0277	0.0101	-0.0073	-244.	3441.	-2488.
79		2	0.	-0.	21.00	10988.	3049.	200.	1.2277	0.3408	0.0020	-172.	2388.	-472.
		5			138.91	10988.	3049.	200.	-0.0192	0.0049	-0.0016	-172.	2388.	-472.
80		3	0.	-0.	21.00	10241.	1623.	-828.	1.1486	0.1814	-0.0081	-280.	388.	1139.
		5			132.91	10241.	1623.	-828.	-0.0313	0.0011	0.0033	-280.	388.	1139.
81		4	0.	-0.	20.81	9245.	683.	-3502.	1.0428	0.0726	-0.0345	-263.	1248.	963.
		5			132.30	9245.	683.	-3502.	-0.0296	0.0036	0.0028	-265.	1248.	963.
82		5	0.	-0.	20.81	8654.	426.	-4920.	0.9762	0.0480	-0.0485	-232.	1380.	508.
		5			132.30	8654.	426.	-4920.	-0.0262	0.0040	0.0015	-232.	1380.	508.
83		6	4.00	-0.	20.81	12815.	3286.	1166.	1.4455	0.3707	0.0115	-168.	2270.	-845.
		5			132.30	12815.	3286.	1166.	-0.0190	0.0066	-0.0025	-168.	2270.	-845.
84		7	8.00	-0.	20.81	14687.	3531.	4402.	1.6567	0.3983	0.0434	-204.	1458.	2248.
		5			132.30	14687.	3531.	4402.	-0.0231	0.0043	0.0066	-204.	1458.	2248.

TABLE A-2 (Continued)

Test Point No.	Run No.	Point of Run	Left N_p RPM	Right N_p RPM	Left β_i Deg.	Left β_0 Deg.	Right β_i Deg.	Right β_0 Deg.	Tail i_t Deg.	δ_f Deg.	Baro. in. Hg	To $^\circ_F$	Left N_{J85} % RPM	Right N_{J85} % RPM	Average V_p/V_{tip}	q/qc
85	I-6	8	1695	1695	0	0	0	0	OFF	30	30.26	95	85	83	0.294	1.026
86		9	1610	1610								95	82.5	81	0.391	1.021
87		10	1600	1600	20	20	20	20				95	82.5	81	0.394	1.022
88		11	1600	1620	35	35	35	35				98	82	81	0.391	1.021
89		12	1700	1690	20	20	20	20				98	85	88.5	0.295	1.024
90		13	1700	1700								99			0.294	1.015
91		14	1690	1700								99			0.295	1.015
92		15	1680	1700								99			0.296	1.024
93		16	1680	1700								100			0.295	1.015
94		17	1660	1680	20	20	20	20				101		88	0.299	1.015
95		18	1700	1723	0	0	0	0				101	86	89.5	0.063	0.764
96		19	1705	1730								101	86	89.5	0.063	0.776
97		20	1710	1730								103	86	89.5	0.069	0.913
98		21	1715	1730	20	20	20	20				106	86.5	89.5	0.069	0.913
99		22	1700	1720	35	35	35	35				106	86	88	0.088	0.989
100		23	1750	1720	0	0	0	0				107	87	90	0.074	1.023
101		24	1700	1725								108	86.5	89.5	0.070	0.959
102		25	1690	1700								110			0.065	0.764
103		26	1690	1710								111			0.071	0.913
104		27	1660	1680								111			0.072	0.913
105		28	1680	1690								111			0.071	0.913
106		29	1680	1690								111			0.071	0.913
107		30	1680	1700								111			0.070	0.882
108		31	1680	1690								111			0.071	0.913
109		32	1680	1690								110		89	0	3.030
110		33	1630	1660								109		90	0	16.667

Test Point No.	Run No.	PT AVG	ALPHA	BETA	Q V,NOM	LIFT,U CL*QS	DRAG,U CD*QS	M,U CM*QSC	CL CY	CD CN	CM CROLL	SIDE F,U CY*QS	YAW,U CN*QSB	ROLL,U CL*QSB
85	I-6	8	10.00	-0.	21.00	13326.	3015.	-1210.	1.4895	0.5370	-0.0118	-455.	-2246.	11531.
		5			132.91	13326.	3015.	-1210.	-0.0509	-0.0065	0.0334	-455.	-2246.	11531.
86		9	0.	-0.	33.04	11545.	2842.	-13704.	0.8201	0.2020	-0.0851	-480.	877.	9981.
		5			166.69	11545.	2842.	-13704.	-0.0341	0.0016	0.0184	-480.	877.	9981.
87		10	0.	-0.	35.23	11239.	2190.	-13974.	0.7940	0.1547	-0.0863	-458.	3009.	6634.
		5			167.17	11239.	2190.	-13974.	-0.0324	0.0055	0.0121	-458.	3009.	6634.
88		11	0.	-0.	35.04	10483.	1645.	-15056.	0.7448	0.1169	-0.0935	-305.	3898.	4835.
		5			166.69	10483.	1645.	-15056.	-0.0217	0.0072	0.0089	-305.	3898.	4835.
89		12	-4.00	-0.	21.00	8167.	1357.	-816.	0.9124	0.1517	-0.0080	-264.	1216.	-234.
		5			132.91	8167.	1357.	-816.	-0.0296	0.0035	-0.0007	-264.	1216.	-234.
90		13	0.	-0.	20.81	10260.	1612.	-639.	1.1577	0.1818	-0.0063	-318.	989.	410.
		5			132.30	10260.	1612.	-639.	-0.0359	0.0029	0.0012	-318.	989.	410.
91		14	4.00	-0.	20.81	12278.	1954.	-1527.	1.3850	0.2204	-0.0151	-525.	1149.	2831.
		5			132.30	12278.	1954.	-1527.	-0.0367	0.0034	0.0083	-525.	1149.	2831.
92		15	8.00	-0.	21.00	13506.	2172.	-1799.	1.5096	0.2427	-0.0176	-315.	1833.	1750.
		5			132.91	13506.	2172.	-1799.	-0.0352	0.0053	0.0051	-315.	1833.	1750.
93		16	8.00	-0.	20.81	14378.	2364.	-655.	1.6217	0.2667	-0.0065	-388.	1847.	2237.
		5			132.30	14378.	2364.	-655.	-0.0437	0.0059	0.0065	-388.	1847.	2237.
94		17	10.00	-0.	20.81	15165.	2609.	-462.	1.7105	0.2943	-0.0046	-444.	2753.	4068.
		5			132.30	15165.	2609.	-462.	-0.0501	0.0080	0.0119	-444.	2753.	4068.
95		18	-4.00	-0.	0.97	5227.	180.	-2903.	12.6637	0.4372	-0.6147	-68.	2141.	3964.
		5			28.55	5227.	180.	-2903.	-0.1651	0.1343	0.2486	-68.	2141.	3964.
96		19	-2.00	-0.	0.97	5230.	388.	-3143.	12.6688	0.9395	-0.6655	-53.	2072.	3344.
		5			28.55	5230.	388.	-3145.	-0.1291	0.1300	0.2098	-53.	2072.	3344.
97		20	0.	-0.	1.16	5378.	615.	-3134.	10.8577	1.2423	-0.5531	-63.	2057.	2973.
		5			31.27	5378.	615.	-3134.	-0.1279	0.1075	0.1554	-63.	2057.	2973.
98		21	0.	-0.	1.16	5110.	-1389.	-565.	10.5151	-2.8050	-0.0994	-135.	1515.	3935.
		5			31.27	5110.	-1389.	-565.	-0.2735	0.0791	0.2057	-135.	1515.	3935.
99		22	0.	-0.	1.86	3998.	-2227.	1815.	5.0449	-2.8099	0.2000	-93.	886.	2971.
		5			39.56	3998.	-2227.	1815.	-0.1169	0.0290	0.0971	-93.	886.	2971.
100		23	2.00	-0.	1.36	5933.	985.	-3199.	10.2659	1.7043	-0.4858	-105.	2364.	2983.
		5			34.78	5933.	985.	-3199.	-0.1811	0.1059	0.1537	-105.	2364.	2983.
101		24	4.00	-0.	1.16	5424.	1088.	-3482.	10.9498	2.1976	-0.6145	-113.	2444.	3829.
		5			31.27	5424.	1088.	-3482.	-0.2287	0.1277	0.2002	-113.	2444.	3829.
102		25	6.00	-0.	0.97	5318.	1236.	-3240.	12.8839	2.9950	-0.6861	-66.	2320.	3600.
		5			28.55	5318.	1236.	-3240.	-0.1594	0.1455	0.2258	-66.	2326.	3600.
103		26	8.00	-0.	1.16	5515.	1541.	-3082.	11.1339	3.1102	-0.5439	-120.	2219.	3879.
		5			31.27	5515.	1541.	-3082.	-0.2423	0.1160	0.2028	-120.	2219.	3879.
104		27	10.00	-0.	1.16	5378.	1688.	-3401.	10.8577	3.4077	-0.6002	-90.	2068.	3203.
		5			31.27	5378.	1688.	-3401.	-0.1812	0.1081	0.1674	-90.	2068.	3203.
105		28	12.00	-0.	1.16	5455.	1911.	-3332.	11.0128	3.8573	-0.5880	-121.	2176.	4208.
		5			31.27	5455.	1911.	-3332.	-0.2442	0.1138	0.2200	-121.	2176.	4208.
106		29	14.00	-0.	1.16	5688.	2156.	-3385.	11.4827	4.3534	-0.5974	-90.	2075.	3913.
		5			31.27	5688.	2156.	-3385.	-0.1822	0.1084	0.2045	-90.	2075.	3913.
107		30	16.00	-0.	1.12	5594.	2372.	-4342.	11.6852	4.9546	-0.7926	-73.	2234.	4112.
		5			30.75	5594.	2372.	-4342.	-0.1554	0.1208	0.2223	-73.	2234.	4112.
108		31	18.00	-0.	1.16	5806.	2662.	-4708.	11.7201	5.5748	-0.8307	-113.	2114.	5212.
		5			31.27	5806.	2662.	-4708.	-0.2287	0.1105	0.2725	-113.	2114.	5212.
109		32	0.	-0.	1.00	4949.	-71.	-7484.	11.6169	-0.1656	-1.5356	-72.	2789.	1983.
		5			0.	4949.	-71.	-7484.	-0.1693	0.1695	0.1205	-72.	2789.	1983.
110		33	0.	-0.	1.00	4579.	-247.	-5428.	10.7491	-0.5803	-1.0933	-84.	3470.	1867.
		5			0.	4579.	-247.	-5428.	-0.1983	0.2109	0.1135	-84.	3470.	1867.

TABLE A-2 (Continued)

Test Point No.	Run No.	Point of Run	Left N_p RPM	Right N_p RPM	Left β_1 Deg.	Left β_0 Deg.	Right β_1 Deg.	Right β_0 Deg.	Tail i_t Deg.	δ_f Deg.	Baro. in. Hg	T_0 °F	Left N_{305} % RPM	Right N_{305} % RPM	Average V_p/V_{tip}	q/qc
111	I-7	1	1700	1715	20	20	20	20	OFF	30	30.24	85	85	88	0.1087	1.069
112		2	1700	1710								88		88	0.1089	1.003
113		3	1690	1710								89		88	0.1079	1.032
114		4	1680	1700								90		88	0.1122	0.967
115		5	1670	1690								93		88.5	0.1131	1.030
116		6										94			0.1108	1.010
117		7										96			0.1171	1.038
118		8										97			0.1183	1.080
119		9										98			0.1159	1.072
120		10										98		88	0.1173	1.038
121		11	1660	1700								99			0.1168	1.101
122		12	1650	1720								100			0.1155	1.058
123		13	1650	1665								104			0.1539	1.025
124		14	1660	1660								105			0.1510	1.023
125		15										106			0.1553	1.025
126		16										107			0.1519	1.067
127		17										107			0.1507	1.044
128		18		1700								108			0.1507	1.067
129		19	1640	1700								108			0.1516	1.046
130		20	1640	1740								109			0.1519	1.064
131		21	1630	1750								109			0.1485	1.016
132		22	1630	1750	35	35	35	35				112			0.1478	1.032
133		23	1680	1670								112			0.1542	1.013
134		24	1690	1670								113			0.1539	1.049
135		25	1700	1670								114			0.1521	1.032
136		26	1700	1670								115			0.1523	1.032
137		27	1700	1680								115			0.1524	1.060
138		28	1700	1680								116			0.1513	1.042

Test Point No.	Run No.	PT AVG	ALPHA	BETA	Q V,NOM	LIFT,U CL*QS	DRAG,U CD*QS	M,U CM*QSC	CL CY	CD CN	CM CROLL	SIDE F,U CY*QS	YAW,U CN*QSB	ROLL,U CL*QSB
111	I-7	1	-4.00	-0.	3.10	5350.	-1399.	1936.	4.0498	-1.0591	0.1281	-2.	-118.	-1497.
		5			51.07	5350.	-1399.	1936.	-0.0018	-0.0023	-0.0294	-2.	-116.	-1497.
112		2	-2.00	-0.	2.91	5544.	-1229.	1782.	4.4768	-0.9925	0.1258	-5.	-156.	-1140.
		5			49.45	5544.	-1229.	1782.	-0.0043	-0.0033	-0.0238	-5.	-156.	-1140.
113		3	0.	-0.	2.91	5726.	-1041.	2002.	4.6241	-0.8407	0.1415	-15.	-240.	-1016.
		5			49.45	5726.	-1041.	2002.	-0.0120	-0.0050	-0.0212	-15.	-240.	-1016.
114		4	2.00	-0.	2.91	5875.	-836.	1920.	4.7443	-0.6752	0.1355	-16.	-352.	-1477.
		5			49.45	5875.	-836.	1920.	-0.0132	-0.0074	-0.0309	-16.	-352.	-1477.
115		5	4.00	-0.	3.10	6098.	-614.	1909.	4.6167	-0.4651	0.1263	-8.	-169.	-1002.
		5			51.07	6098.	-614.	1909.	-0.0062	-0.0033	-0.0196	-8.	-169.	-1002.
116		6	6.00	-0.	2.91	6209.	-411.	2321.	5.0196	-0.3822	0.1638	-13.	-92.	-1525.
		5			49.45	6209.	-411.	2321.	-0.0139	-0.0019	-0.0319	-13.	-92.	-1525.
117		7	8.00	-0.	3.29	6578.	-127.	2481.	4.6871	-0.0906	0.1545	-30.	77.	-994.
		5			52.64	6578.	-127.	2481.	-0.0215	0.0014	-0.0185	-30.	77.	-994.
118		8	10.00	-0.	3.49	6871.	121.	2387.	4.6238	0.0817	0.1404	12.	-19.	-1625.
		5			54.17	6871.	121.	2387.	0.0081	-0.0003	-0.0283	12.	-19.	-1625.
119		9	12.00	-0.	3.29	6938.	274.	2241.	4.9436	0.1949	0.1396	-33.	163.	-1413.
		5			52.64	6938.	274.	2241.	-0.0236	0.0030	-0.0241	-33.	163.	-1413.
120		10	14.00	-0.	3.29	7075.	534.	2491.	5.0411	0.3803	0.1551	51.	43.	-1532.
		5			52.64	7075.	534.	2491.	0.0219	0.0008	-0.0283	51.	43.	-1532.
121		11	16.00	-0.	3.49	7334.	806.	2573.	4.9355	0.5623	0.1514	29.	101.	-1684.
		5			54.17	7334.	806.	2573.	0.0197	0.0018	-0.0293	29.	101.	-1684.
122		12	18.00	-0.	3.29	7301.	992.	2256.	5.2019	0.7071	0.1405	64.	189.	-2482.
		5			52.64	7301.	992.	2256.	0.0455	0.0035	-0.0458	64.	189.	-2482.
123		13	-4.00	-0.	3.43	5194.	-705.	3255.	2.2847	-0.3048	0.1231	-92.	-107.	-3809.
		5			67.56	5194.	-705.	3255.	-0.0397	-0.0012	-0.0427	-92.	-107.	-3809.
124		14	0.	-0.	3.23	5880.	-444.	3213.	2.6879	-0.1994	0.1260	-87.	-19.	-1392.
		5			66.34	5880.	-444.	3213.	-0.0392	-0.0002	-0.0162	-87.	-19.	-1392.
125		15	4.00	-0.	3.43	6658.	-98.	3080.	2.8779	-0.0249	0.1146	-57.	-204.	-1960.
		5			67.86	6658.	-98.	3080.	-0.0245	-0.0023	-0.0220	-57.	-204.	-1960.
126		16	8.00	-0.	3.43	7258.	293.	2897.	3.1396	0.1267	0.1098	-49.	-53.	-2102.
		5			67.56	7258.	293.	2897.	-0.0212	-0.0006	-0.0235	-49.	-53.	-2102.
127		17	10.00	-0.	3.23	7502.	476.	3251.	3.3657	0.2136	0.1275	-32.	-195.	-1528.
		5			66.34	7502.	476.	3251.	-0.0142	-0.0023	-0.0177	-32.	-195.	-1528.
128		18	12.00	-0.	3.54	7889.	737.	3435.	3.4610	0.3123	0.1272	-5.	-305.	-1802.
		5			68.28	7889.	737.	3435.	-0.0022	-0.0033	-0.0198	-5.	-305.	-1802.
129		19	14.00	-0.	3.43	8172.	965.	3321.	3.5351	0.4175	0.1256	47.	-570.	-1726.
		5			67.56	8172.	965.	3321.	0.0201	-0.0064	-0.0193	47.	-570.	-1726.
130		20	16.00	-0.	3.66	8525.	1252.	3464.	3.5362	0.5194	0.1256	76.	-579.	-1035.
		5			68.99	8525.	1252.	3465.	0.0317	-0.0062	-0.0111	76.	-579.	-1035.
131		21	18.00	-0.	5.23	8657.	1414.	3398.	5.8836	0.6345	0.1333	99.	-691.	-984.
		5			66.34	8657.	1414.	3398.	0.0446	-0.0080	-0.0114	99.	-691.	-984.
132		22	-16.00	-0.	5.23	3737.	-1636.	32523.	1.6764	-0.7340	1.2754	-14.	-393.	-154.
		5			66.34	3737.	-1636.	32523.	-0.0062	-0.0046	-0.0018	-14.	-393.	-154.
133		23	-4.00	-0.	5.43	5948.	-1539.	3612.	1.7079	-0.6656	0.1366	-9.	-100.	-449.
		5			67.56	5948.	-1539.	3612.	-0.0039	-0.0011	-0.0050	-9.	-100.	-449.
134		24	0.	-0.	5.62	6682.	-1278.	4137.	1.9557	-0.5336	0.1510	-26.	-428.	6.
		5			68.75	6682.	-1278.	4137.	-0.0110	-0.0046	0.0001	-26.	-428.	6.
135		25	4.00	-0.	5.43	5340.	-1028.	3735.	2.3100	-0.4448	0.1412	-66.	-65.	-132.
		5			67.56	5340.	-1028.	3735.	-0.0287	-0.0007	-0.0015	-66.	-65.	-132.
136		26	8.00	-0.	5.43	6022.	-677.	3511.	2.6049	-0.2930	0.1328	-100.	310.	570.
		5			67.56	6022.	-677.	3511.	-0.0434	0.0035	0.0064	-100.	310.	570.
137		27	10.00	-0.	5.62	6436.	-498.	3782.	2.6875	-0.2079	0.1381	-108.	-8.	110.
		5			68.75	6436.	-498.	3782.	-0.0455	-0.0001	0.0012	-108.	-8.	110.
138		28	12.00	-0.	5.43	6727.	-308.	3868.	2.9101	-0.1331	0.1463	-100.	-29.	-65.
		5			67.56	6727.	-308.	3868.	-0.0432	-0.0003	-0.0007	-100.	-29.	-65.

TABLE A-2 (Continued)

Test Point No.	Run No.	Point of Run	Left N_p RPM	Right N_p RPM	Left β_1 Deg.	Left β_0 Deg.	Right β_1 Deg.	Right β_0 Deg.	Tail i_t Deg.	δ_f Deg.	Baro. in. Hg	To $^\circ_F$	Left N_{JBS} % RPM	Right N_{JBS} % RPM	Average V_p/V_{tip}	q/qc
139	I-7	29	1690	1720	35	35	35	35	OFF	30	30.24	116	85	88	0.1450	1.042
140		30	1680	1730											0.1488	1.019
141		31	1680	1750											0.1462	1.084
142		32	1670	1630	20	20	20	20				117			0.2328	1.025
143		33	1680	1680								117		89	0.2294	1.034
144		34	1680	1680								118			0.2273	1.038
145		35	1680	1690											0.2294	1.030
146		36	1680	1700											0.2287	1.030
147		37	1680	1720											0.2268	1.020
148		38	1650	1760											0.2256	1.023
149		39	1660	1890								120	84.5	88.5	0.2171	1.023
150		40	1660	1660	35	35	35	35				120	84	88	0.2324	1.021
151		41	1670	1660								121			0.2315	1.025
152		42	1670	1670											0.2304	1.028
153		43	1670	1650											0.2313	1.032
154		44	1660	1660											0.2315	1.035
155		45	1670	1650										87.5	0.2315	1.032
156		46	1670	1640										82	0.2314	1.022
157		47	1670	1630										32.5	0.2260	1.031
158	I-8	1	0	0	90	90	90	90	OFF	30	30.14	91	0	0	N/A	0.951
159		2														1.002
160		3														1.009
161		4														1.009
162		5														1.009
163		6														0.998
164		7														0.998
165		8														0.926
166		9														1.028

Test Point No.	Run No.	Pt AVG	ALPHA	BETA	Q V,NOM	LIFT,U CL*QS	DRAG,U CD*QS	M,U CM*QSC	CL CY	CD CN	CM CROLL	SIDE F,U CY*QS	YAW,U CN*QSB	ROLL,U CL*QSB
139	I-7	29	14.00	-0.	5.43	7075.	-48.	3505.	3.0807	-0.0206	0.1325	-77.	314.	-585.
		5			67.56	7075.	-48.	3505.	-0.0332	0.0035	-0.0066	-77.	314.	-585.
140		30	16.00	-0.	5.23	7368.	165.	3126.	3.3054	0.0739	0.1226	-84.	315.	105.
		5			66.34	7368.	165.	3126.	-0.0375	0.0037	0.0012	-84.	315.	105.
141		31	18.00	-0.	5.43	7752.	408.	3176.	3.3535	0.1765	0.1201	-60.	537.	475.
		5			67.56	7752.	408.	3176.	-0.0257	0.0060	0.0053	-60.	537.	475.
142		32	-4.00	-0.	11.99	6334.	492.	2144.	1.2398	0.0963	0.0367	-139.	553.	-1464.
		5			100.43	6334.	492.	2144.	-0.0272	0.0028	-0.0074	-139.	553.	-1464.
143		33	0.	-0.	12.18	7728.	753.	2198.	1.4490	0.1451	0.0370	-97.	193.	-760.
		5			101.23	7728.	753.	2198.	-0.0187	0.0010	-0.0038	-97.	193.	-760.
144		34	4.00	-0.	11.99	9082.	1054.	646.	1.7778	0.2063	0.0111	-58.	-229.	-1789.
		5			100.43	9082.	1054.	646.	-0.0074	-0.0012	-0.0091	-58.	-229.	-1789.
145		35	8.00	-0.	12.18	10603.	1472.	1216.	2.0435	0.2837	0.0205	-76.	-72.	-956.
		5			101.23	10603.	1472.	1216.	-0.0147	-0.0004	-0.0048	-76.	-72.	-956.
146		36	10.00	-0.	12.18	11191.	1689.	1356.	2.1562	0.3255	0.0228	-91.	359.	-348.
		5			101.23	11191.	1689.	1356.	-0.0176	0.0018	-0.0017	-91.	359.	-348.
147		37	12.00	-0.	11.80	11621.	1962.	1863.	2.3118	0.3903	0.0324	-71.	109.	-169.
		5			99.62	11621.	1962.	1863.	-0.0141	0.0006	-0.0009	-71.	109.	-169.
148		38	14.00	-0.	11.99	12067.	2274.	1057.	2.3622	0.4452	0.0181	32.	-796.	-863.
		5			100.43	12067.	2274.	1057.	0.0063	-0.0040	-0.0044	32.	-796.	-863.
149		39	16.00	-0.	11.99	12789.	2771.	-1502.	2.5035	0.5425	-0.0257	28.	-660.	-1502.
		5			100.43	12789.	2771.	-1502.	0.0055	-0.0033	-0.0076	28.	-660.	-1502.
150		40	-4.00	-0.	11.99	4973.	-474.	1255.	0.9735	-0.0927	0.0214	-149.	281.	-516.
		5			100.43	4973.	-474.	1255.	-0.0292	0.0014	-0.0026	-149.	281.	-516.
151		41	0.	-0.	11.99	6485.	-225.	1267.	1.2694	-0.0440	0.0217	-131.	-11.	-1115.
		5			100.43	6485.	-225.	1267.	-0.0257	-0.0001	-0.0057	-131.	-11.	-1115.
152		42	4.00	-0.	11.99	7939.	113.	-148.	1.5541	0.0221	-0.0025	-90.	-150.	-1593.
		5			100.43	7939.	113.	-148.	-0.0177	-0.0008	-0.0081	-90.	-150.	-1593.
153		43	8.00	-0.	11.99	9322.	487.	210.	1.8248	0.0954	0.0036	-53.	-83.	-1290.
		5			100.43	9322.	487.	210.	-0.0164	-0.0004	-0.0065	-53.	-83.	-1290.
154		44	10.00	-0.	12.03	10005.	701.	755.	1.9519	0.1368	0.0129	-66.	100.	-2180.
		5			100.59	10005.	701.	755.	-0.0129	0.0005	-0.0110	-66.	100.	-2180.
155		45	12.00	-0.	11.99	10356.	1064.	386.	2.0272	0.2084	0.0066	-40.	-75.	-1220.
		5			100.43	10356.	1064.	386.	-0.0078	-0.0004	-0.0062	-40.	-75.	-1220.
156		46	14.00	-0.	11.80	10154.	1440.	-2414.	2.0201	0.2864	-0.0420	-61.	1203.	2650.
		5			99.62	10154.	1440.	-2414.	-0.0122	0.0062	0.0137	-61.	1203.	2650.
157		47	16.00	-0.	11.42	10498.	1818.	-3832.	2.1565	0.3737	-0.0689	-224.	2871.	5677.
		5			97.99	10498.	1818.	-3832.	-0.0461	0.0153	0.0302	-224.	2871.	5677.
158	I-8	1	-3.75	-0.	5.04	593.	173.	-3892.	0.2762	0.0820	-0.1585	-1.	-49.	196.
		5			65.10	593.	176.	-3892.	-0.0007	-0.0006	0.0024	-1.	-49.	196.
159		2	0.48	-0.	5.43	1212.	218.	-3604.	0.5243	0.0989	-0.1363	0.	-46.	1.
		5			67.56	1212.	229.	-3604.	0.0002	-0.0005	0.0000	0.	-46.	1.
160		3	4.69	-0.	5.43	1716.	265.	-3658.	0.7425	0.1237	-0.1376	-0.	-54.	403.
		5			67.56	1716.	286.	-3638.	-0.0002	-0.0006	0.0045	-0.	-54.	403.
161		4	8.91	-0.	5.43	2278.	349.	-3145.	0.9853	0.1666	-0.1189	-0.	-79.	369.
		5			67.56	2278.	385.	-3145.	-0.0002	-0.0009	0.0041	-0.	-79.	369.
162		5	11.01	-0.	5.43	2527.	399.	-2967.	1.0932	0.1918	-0.1122	2.	-30.	526.
		5			67.56	2527.	443.	-2967.	0.0011	-0.0003	0.0059	2.	-30.	526.
163		6	13.15	-0.	5.43	2878.	468.	-2964.	1.2448	0.2276	-0.1121	5.	-51.	537.
		5			67.56	2878.	526.	-2964.	0.0021	-0.0003	0.0060	5.	-51.	537.
164		7	15.11	-0.	5.43	2772.	588.	-2424.	1.1991	0.2775	-0.0917	44.	-698.	-2316.
		5			67.56	2772.	642.	-2424.	0.0189	-0.0078	-0.0259	44.	-698.	-2316.
165		8	17.06	-0.	5.04	2474.	762.	-2962.	1.1527	0.3765	-0.1268	18.	-159.	198.
		5			65.10	2474.	808.	-2962.	0.0085	-0.0019	0.0024	18.	-159.	198.
165		9	-3.75	-0.	11.95	1404.	427.	-9298.	0.2757	0.0850	-0.1596	-1.	-177.	231.
		5			100.27	1404.	435.	-9298.	-0.0002	-0.0009	0.0012	-1.	-177.	231.

TABLE A-2 (Continued)

Test Point No.	Run No.	Point of Run	Left N_p RPM	Right N_p RPM	Left β_1 Deg.	Left β_2 Deg.	Right β_1 Deg.	Right β_2 Deg.	Tail i_t Deg.	δ_f Deg.	Baro. in. Hg	To °F	Left N_{J85} % RPM	Right N_{J85} % RPM	Average V_p/V_{tip}	q/qc
167	I-8	10	0	0	90	90	90	90	OFF	30	30.14	91	0	0	N/A	1.032
168		11														1.032
169		12														1.015
170		13														1.032
171		14														1.015
172		15														1.015
173		16														1.015
174	I-9	1	0	0	90	90	90	90	0	30	30.15	91	0	0	N/A	N/A
175		2														
176		3														
177		4														
178		5														
179		6														
180		7														
181		8														
182		9														
183		10														
184		11														
185		12														
186		13														
187		14														
188		15														
189		16														
190		17														
191		18														
192		19														
193		20														
194		21														

Test Point No.	Run No.	MT AVG	ALPHA	BETA	Q V,NOM	LIFT,U CL*QS	DRAG,U CD*QS	M,U CM*QSC	CL CY	CD CN	CM CROLL	SIDE F,U CY*QS	YAW,U CN*QSB	ROLL,U CL*QSB
167	I-8	10	0.49	-0.	11.99	2693.	488.	-8388.	0.5271	0.0999	-0.1435	-1.	-73.	268.
		5			100.43	2693.	511.	-8388.	-0.0062	-0.0004	0.0014	-1.	-73.	268.
168		11	4.70	-0.	11.99	3859.	600.	-7709.	0.7555	0.1265	-0.1319	7.	-132.	594.
		5			100.43	3859.	646.	-7709.	0.0014	-0.0007	0.0030	7.	-132.	594.
169		12	8.93	-0.	11.80	5057.	786.	-6770.	1.0060	0.1726	-0.1177	6.	-98.	514.
		5			99.62	5057.	868.	-6770.	0.0011	-0.0005	0.0026	6.	-98.	514.
170		13	11.04	-0.	11.99	5746.	906.	-6918.	1.1247	0.1977	-0.1184	-4.	-75.	819.
		5			100.43	5746.	1010.	-6918.	-0.0006	-0.0004	0.0041	-4.	-75.	819.
171		14	13.16	-0.	11.80	6300.	1039.	-6494.	1.2533	0.2320	-0.1129	-12.	-146.	644.
		5			99.62	6300.	1166.	-6494.	-0.0023	-0.0008	0.0033	-12.	-146.	644.
172		15	15.16	-0.	11.80	6343.	1320.	-4406.	1.2619	0.2883	-0.0855	73.	-854.	-3600.
		5			99.62	6343.	1449.	-4906.	0.0146	-0.0044	-0.0185	73.	-854.	-3600.
173		16	17.13	-0.	11.80	6127.	1635.	-5145.	1.2189	0.3491	-0.0895	35.	-92.	-5831.
		5			99.62	6127.	1755.	-5145.	0.0069	-0.0005	-0.0197	35.	-92.	-5831.
174	I-9	1	-5.63	-0.	1.16	36.	43.	246.	0.0727	0.0873	0.0652	-7.	139.	468.
		5			31.27	36.	43.	256.	-0.0136	0.0072	0.0245	-7.	139.	468.
175		2	-1.80	-0.	1.16	108.	40.	152.	0.2187	0.0822	0.0321	-3.	71.	159.
		5			31.27	108.	41.	182.	-0.0068	0.0037	0.0083	-3.	71.	159.
176		3	0.49	-0.	0.97	219.	42.	60.	0.5291	0.1057	0.0255	-1.	9.	348.
		5			28.55	218.	44.	120.	-0.0023	0.0006	0.0218	-1.	9.	348.
177		4	2.55	-0.	0.97	245.	50.	-13.	0.5930	0.1266	0.0116	-6.	69.	355.
		5			28.55	245.	52.	55.	-0.0151	0.0043	0.0221	-6.	69.	355.
178		5	4.68	-0.	1.16	362.	58.	-110.	0.7314	0.1249	-0.0017	0.	-37.	205.
		5			31.27	362.	62.	-10.	0.0010	-0.0020	0.0106	0.	-37.	205.
179		6	6.84	-0.	1.16	451.	66.	306.	0.9109	0.1461	0.0760	-1.	-8.	406.
		5			31.27	451.	72.	431.	-0.0029	-0.0004	0.0212	-1.	-8.	406.
180		7	9.01	-0.	1.16	540.	82.	-55.	1.0901	0.1839	0.0166	4.	-65.	242.
		5			31.27	540.	91.	94.	0.0078	-0.0034	0.0126	4.	-65.	242.
181		8	11.13	-0.	1.16	605.	100.	189.	1.2209	0.2256	0.0629	3.	-62.	171.
		5			31.27	605.	112.	357.	0.0058	-0.0033	0.0090	3.	-62.	171.
182		9	13.23	-0.	1.16	658.	132.	-491.	1.3275	0.2939	-0.0545	1.	-6.	319.
		5			31.27	658.	146.	-309.	0.0029	-0.0003	0.0167	1.	-6.	319.
183		10	15.08	-0.	1.16	581.	178.	-585.	1.1725	0.3807	-0.0749	-4.	13.	380.
		5			31.27	581.	189.	-424.	-0.0079	0.0007	0.0199	-4.	13.	380.
184		11	17.06	-0.	1.16	569.	207.	-840.	1.1483	0.4398	-0.1205	1.	-53.	541.
		5			31.27	569.	218.	-683.	0.0029	-0.0028	0.0283	1.	-53.	541.
185		12	19.09	-0.	1.16	586.	239.	-1350.	1.1822	0.5061	-0.2097	2.	-90.	370.
		5			31.27	586.	250.	-1189.	0.0048	-0.0047	0.0193	2.	-90.	370.
186		13	-3.87	-0.	4.84	300.	187.	948.	0.1454	0.0908	0.0436	1.	-67.	191.
		5			63.83	300.	187.	1029.	0.0007	-0.0008	0.0024	1.	-67.	191.
187		14	0.44	-0.	5.23	1066.	219.	287.	0.4780	0.1019	0.0228	-3.	33.	374.
		5			66.34	1066.	227.	582.	-0.0015	0.0004	0.0043	-3.	33.	374.
188		15	4.68	-0.	5.04	1574.	261.	-909.	0.7355	0.1301	-0.0193	-0.	2.	518.
		5			65.10	1574.	279.	-473.	-0.0000	0.0000	0.0062	-0.	2.	518.
189		16	8.95	-0.	5.04	2210.	340.	-1767.	1.0298	0.1754	-0.0471	7.	-136.	477.
		5			65.10	2210.	376.	-1156.	0.0031	-0.0016	0.0058	7.	-136.	477.
190		17	11.08	-0.	5.04	2520.	387.	-2060.	1.1742	0.2026	-0.0555	7.	-84.	670.
		5			65.10	2520.	435.	-1363.	0.0034	-0.0010	0.0081	7.	-84.	670.
191		18	13.20	-0.	5.04	2784.	455.	-2815.	1.2972	0.2388	-0.0833	5.	-114.	531.
		5			65.10	2784.	513.	-2045.	0.0025	-0.0014	0.0064	5.	-114.	531.
192		19	15.20	-0.	5.23	2902.	608.	-2524.	1.3017	0.3001	-0.0675	56.	-853.	-1413.
		5			66.34	2902.	669.	-1721.	0.0252	-0.0099	-0.0164	56.	-853.	-1413.
193		20	17.16	-0.	4.84	2593.	775.	-3248.	1.2564	0.4011	-0.1072	31.	-126.	-1551.
		10			63.83	2593.	826.	-2530.	0.0151	-0.0016	-0.0195	31.	-126.	-1551.
194		21	-3.85	-0.	11.42	769.	445.	2609.	0.1582	0.0918	0.0507	-1.	-257.	-56.
		10			97.99	769.	447.	2822.	-0.0003	-0.0014	-0.0003	-1.	-257.	-56.

TABLE A-2 (Continued)

Test Point No.	Run No.	Point of Run	Left N_p RPM	Right N_p RPM	Left β_L Deg.	Left β_M Deg.	Right β_R Deg.	Right β_O Deg.	Tail i_t Deg.	δ_f Deg.	Baro. in. Hg	To °F	Left N_{J85} % RPM	Right N_{J85} % RPM	Average V_p/V_{tip}	q/qc
195	I-9	22	0	0	90	90	90	90	0	30	30.15	91	0	0	N/A	N/A
196		23														
197		24														
198		25														
199		26														
200		27														
201		28														
202		29														
203		30														
204		31														
205		32														
206		33														
207		34														
208		35														
209	I-10	1	2450	2440	20	20	20	20	0	30	30.02	104	99.5	100.0	0.1572	N/A
210		2	2450	2460	20							104		100.5	0.1558	
211		3	2450	2450	0	0	0	0				108		100.0	0.1584	
212		4	2450	2430	35	35	35	35				112	99.0	99.5	0.1574	
213		5	2400	2400	20	20	20	20				114		99.5	0.1603	
214		6	2450	2460								94		100.0	0.1576	
215		7	2460	2460								97			0.1557	
216		8	2450	2480								98			0.1525	
217		9	2460	2440								101		98.5	0.1551	
218		10	2450	2440								104		100.0	0.2078	
219		11	2450	2440								106			0.2095	
220		12	2470	2440	0	0	0	0				108			0.2097	
221		13	2470	2440	35	35	35	35				108			0.2094	

Test Point No.	Run No.	PT AVG	ALPHA	BETA	Q V,NOM	LIFT,U CL*QS	DRAG,U CD*QS	M,U CM*QSC	CL CY	LD CN	CM CROLL	SIDE F,U CY*QS	YAW,U CN*QSB	ROLL,U CL*QSB
195	I-9	22	0.42	-0.	11.44	2228.	492.	497.	0.4574	0.1043	0.0200	-4.	139.	427.
		10			98.07	2228.	508.	1113.	-0.0007	0.0007	0.0023	-4.	139.	427.
196		23	4.68	-0.	11.42	3562.	591.	-1843.	0.7323	0.1301	-0.0154	-4.	-36.	614.
		10			97.99	3562.	633.	-859.	-0.0008	-0.0002	0.0023	-4.	-36.	614.
197		24	8.93	-0.	11.42	4894.	766.	-3864.	1.0062	0.1738	-0.0451	-4.	-203.	861.
		5			97.99	4894.	845.	-2511.	-0.0008	-0.0011	0.0035	-4.	-203.	861.
198		25	11.05	-0.	11.41	5633.	897.	-5103.	1.1391	0.2022	-0.0627	-4.	-46.	868.
		5			98.01	5633.	1000.	-3545.	-0.0009	-0.0022	0.0045	-4.	-46.	868.
199		26	13.20	-0.	11.42	6305.	1040.	-6238.	1.2964	0.2408	-0.0808	-4.	-114.	861.
		5			97.99	6305.	1171.	-4494.	-0.0008	-0.0026	0.0046	-4.	-114.	861.
200		27	15.21	-0.	11.42	6350.	1356.	-7054.	1.3058	0.3062	-0.0952	85.	-1272.	-4206.
		5			97.99	6350.	1489.	-5298.	0.0176	-0.0068	-0.0224	85.	-1272.	-4206.
201		28	17.21	-0.	11.42	6396.	1683.	-9473.	1.3152	0.3739	-0.1385	38.	-277.	-2988.
		5			97.99	6396.	1818.	-7704.	0.0078	-0.0035	-0.0159	58.	-277.	-2988.
202		29	-3.86	-0.	20.43	1279.	799.	5437.	0.147	0.0921	0.0582	12.	-727.	-802.
		5			131.08	1279.	802.	5790.	0.0014	-0.0022	-0.0024	12.	-727.	-802.
203		30	0.42	-0.	20.43	3948.	871.	936.	0.4557	0.1034	0.0204	-9.	-59.	675.
		5			131.08	3948.	900.	2428.	-0.001	-0.0002	0.0020	-9.	-59.	675.
204		31	4.68	-0.	20.43	6403.	1050.	-1649.	0.7358	0.1294	-0.1171	-9.	29.	1233.
		5			131.08	6403.	1126.	-1698.	-0.001	0.0001	0.0037	-9.	29.	1233.
205		32	8.94	-0.	20.70	8945.	1390.	-7056.	1.0145	0.1745	-0.0454	5.	-504.	1193.
		5			131.93	8945.	1537.	-4583.	0.0009	-0.0009	0.0035	5.	-504.	1193.
206		33	11.06	-0.	20.62	10044.	1601.	-9291.	1.1434	0.2035	-0.0648	-5.	65.	1117.
		5			131.69	10044.	1786.	-6514.	-0.0006	0.0002	0.0033	-5.	65.	1117.
207		34	13.19	-0.	20.43	11210.	1855.	-11126.	1.2842	0.2376	-0.0796	-15.	-117.	554.
		5			131.08	11210.	2067.	-7926.	-0.0018	-0.0003	0.0016	-15.	-117.	554.
208		35	15.24	-0.	20.24	11573.	2264.	-11254.	1.3424	0.2916	-0.0815	41.	210.	-2766.
		5			130.46	11573.	2514.	-8034.	0.0048	0.0006	-0.0083	41.	210.	-2766.
209	I-10	1	-4.00	-0.	11.90	10859.	-1551.	24132.	2.1428	-0.3061	0.4163	-266.	-232.	-4079.
		5			100.02	10859.	-1551.	24132.	-0.0525	-0.0012	-0.0208	-266.	-232.	-4079.
210		2	0.	-0.	11.78	12445.	-948.	22716.	2.4798	-0.1889	0.3957	-236.	-717.	-4808.
		5			99.54	12445.	-948.	22716.	-0.0471	-0.0037	-0.0248	-236.	-717.	-4808.
211		3	0.	-0.	12.05	13755.	3220.	20671.	2.6797	0.6273	0.3520	-278.	32.	-3999.
		5			100.67	13755.	3220.	20671.	-0.0541	0.0002	-0.0262	-278.	32.	-3999.
212		4	0.	-0.	11.70	8920.	-2833.	25265.	1.7895	-0.5681	0.4429	-228.	-168.	527.
		5			99.21	8920.	-2833.	25265.	-0.0456	-0.0009	0.0027	-228.	-168.	527.
213		5	4.00	-0.	11.70	15237.	114.	21789.	2.6549	0.0229	0.3820	-103.	-130.	-5441.
		5			99.21	15237.	114.	21789.	-0.0206	-0.0007	-0.0283	-103.	-130.	-5441.
214		6	8.00	-0.	12.28	15704.	573.	21481.	3.0021	0.1095	0.3590	21.	-4780.	-3375.
		5			101.62	15704.	573.	21481.	0.0039	-0.0237	-0.0167	21.	-4780.	-3375.
215		7	10.00	-0.	11.97	16174.	947.	20322.	3.1712	0.1856	0.3483	47.	-5004.	-1941.
		5			100.35	16174.	947.	20322.	0.0092	-0.0254	-0.0099	47.	-5004.	-1941.
216		8	12.00	-0.	11.51	16628.	1330.	18553.	3.3905	0.2711	0.3307	5.	-4488.	-735.
		5			98.40	16628.	1330.	18553.	0.0011	-0.0237	-0.0039	5.	-4488.	-735.
217		9	14.00	-0.	11.70	17021.	1862.	18432.	3.4119	0.3735	0.3302	265.	-6804.	-1059.
		5			99.21	17021.	1862.	18432.	0.0552	-0.0353	-0.0055	265.	-6804.	-1059.
218		10	-4.00	-0.	20.72	11108.	-25.	40223.	1.2588	-0.0028	0.3984	-144.	-4050.	-3075.
		5			131.99	11108.	-25.	40225.	-0.0164	-0.0119	-0.0090	-144.	-4050.	-3075.
219		11	0.	-0.	20.72	13431.	532.	37137.	1.5219	0.0602	0.3679	-107.	-4393.	-2445.
		5			131.99	13431.	532.	37137.	-0.0121	-0.0129	-0.0072	-107.	-4393.	-2445.
220		12	0.	-0.	21.10	15346.	4347.	34194.	1.7074	0.4836	0.3326	-566.	1769.	-3672.
		5			133.21	15346.	4347.	34194.	-0.0655	0.0051	-0.0106	-566.	1769.	-3672.
221		13	0.	-0.	21.29	11192.	-1403.	36113.	1.2341	-0.1547	0.3481	-463.	-502.	-584.
		5			133.81	11192.	-1403.	36113.	-0.0513	-0.0014	-0.0017	-463.	-502.	-584.

TABLE A-2 (Continued)

Test Point No.	Run No.	Point of Run	Left N_p RPM	Right N_p RPM	Left β_1 Deg.	Left β_0 Deg.	Right β_1 Deg.	Right β_0 Deg.	Tail i_t Deg.	δ_e Deg.	Baro. in. Hg	To °F	Left N_{JBS} % RPM	Right N_{JBS} % RPM	Average V_p/V_{tip}	q/qc
222	I-10	14	1680	1680	0	0	0	0	0	30	30.02	98	87.0	88.0	0.2275	N/A
223		15	1690	1670	0	0	0	0				100	87.5		0.2279	
224		16	1680	1670	20	20	20	20				101	87.5		0.2288	
225		17	1700	1700	35	35	35	35				102	87.0		0.2257	
226		18	1720	1720	40	40	40	40				102			0.2212	
227		19	1750	1750	45	45	45	45				102			0.2157	
228		20	1680	1670	0	0	0	0				102			0.2272	
229		21	1670	1680								104	87.5	88.5	0.2276	
230		22	1690	1690								104			0.2256	
231		23	1690	1720								106			0.2257	
232		24	1690	1707								106			0.2266	
233		25	1700	1740								106		86.5	0.2238	
234	I-11	1	1750	1750	0	0	0	0	0	30	30.09	78	88.0	88.0	0.0713	1.165
235		2	1640	1750	0	0	0	0				78		88.5	0.0726	1.054
236		3	1730	1720	20	20	20	20				86			0.0724	1.183
237		4	1750	1750	35	35	35	35				87			0.0782	0.987
238		5	1785	1785	40	40	40	40				90			0.0734	1.217
239		6	1700	1690	0	0	0	0				93			0.0730	1.102
240		7	1690	1690								94			0.0710	1.202
241		8	1690	1680								95			0.0753	1.165
242		9	1680	1680								96			0.0754	1.165
243		10	1670	1660								97			0.0746	1.071
244		11	1670	1670								97			0.0756	1.183
245		12	1715	1705								104	88.5	89.0	0.1477	1.064
246		13	1720	1700								104			0.1486	1.036
247		14	1715	1700	20	20	20	20				105			0.1487	1.077
248		15	1750	1750	35	35	35	35				105			0.1456	1.032

Test Point No.	Run No.	PT AVG	ALPHA	BETA	Q V,NOM	LIFT,U CL*QS	DRAG,U CD*QS	M,U CM*QSC	CL CY	CD CN	CM CROLL	SIDE F,U CY*QS	YAW,U CN*QSB	ROLL,U CL*QSB
222	I-10	14	-4.00	-0.	11.90	6664.	2168.	21117.	1.5150	0.4278	0.3643	-154.	716.	-3491.
		5			100.02	6664.	2168.	21117.	-0.0303	0.0037	-0.0178	-154.	716.	-3491.
223		15	0.	-0.	11.90	7820.	2301.	18518.	1.5432	0.4541	0.3194	-244.	2144.	-1992.
		5			100.02	7820.	2301.	18518.	-0.0481	0.0110	-0.0102	-240.	2144.	-1992.
224		16	0.	-0.	11.90	7009.	625.	20732.	1.3831	0.1233	0.3576	-78.	-1551.	-2261.
		5			100.02	7009.	625.	20732.	-0.0155	-0.0079	-0.0116	-78.	-1551.	-2261.
225		17	0.	-0.	11.90	5790.	-455.	18316.	1.1426	-0.0897	0.3159	-208.	-454.	1242.
		5			100.02	5790.	-455.	18316.	-0.0410	-0.0023	0.0063	-208.	-454.	1242.
226		18	0.	-0.	11.70	5488.	-630.	16921.	1.1006	-0.1265	0.2967	-170.	1470.	-1649.
		5			99.21	5488.	-630.	16921.	-0.0341	0.0076	-0.0086	-170.	1470.	-1649.
227		19	0.	-0.	11.51	4775.	-736.	15602.	0.9736	-0.1501	0.2781	-150.	2116.	-2222.
		5			98.40	4775.	-736.	15602.	-0.0306	0.0112	-0.0117	-150.	2116.	-2222.
228		20	4.00	-0.	11.70	8968.	2402.	16127.	1.7986	0.4819	0.2827	-236.	2905.	-4185.
		5			99.21	8968.	2402.	16127.	-0.0474	0.0151	-0.0217	-236.	2905.	-4185.
229		21	8.00	-0.	11.70	10217.	2761.	15148.	2.0492	0.5538	0.2656	-219.	3115.	-2704.
		5			99.21	10217.	2761.	15148.	-0.0439	0.0162	-0.0140	-219.	3115.	-2704.
230		22	10.00	-0.	11.70	10594.	3043.	15589.	2.1248	0.6103	0.2733	-187.	3181.	-2495.
		5			99.21	10594.	3043.	15589.	-0.0375	0.0165	-0.0130	-187.	3181.	-2495.
231		23	12.00	-0.	11.90	11362.	3237.	15457.	2.2421	0.6387	0.2666	-151.	1994.	-234.
		5			100.02	11362.	3237.	15457.	-0.0297	0.0102	-0.0012	-151.	1994.	-234.
232		24	14.00	-0.	11.90	12044.	3345.	16588.	2.3766	0.6601	0.2861	-66.	72.	-2842.
		5			100.02	12044.	3345.	16588.	-0.0135	0.0004	-0.0145	-66.	72.	-2842.
233		25	16.00	-0.	11.90	11931.	3567.	6988.	2.3543	0.7038	0.1205	-141.	-2722.	3890.
		5			100.02	11931.	3567.	6988.	-0.0278	-0.0139	0.0199	-141.	-2722.	3890.
234	I-11	1	-4.00	-0.	1.55	5928.	415.	1626.	8.9754	0.6286	0.2152	-67.	1502.	-521.
		1			36.11	5928.	415.	1626.	-0.1017	0.0589	-0.0204	-67.	1502.	-521.
235		2	0.	-0.	1.36	5916.	797.	426.	10.2369	1.3788	0.0644	-84.	1097.	-1417.
		1			33.78	5916.	797.	426.	-0.1454	0.0492	-0.0635	-84.	1097.	-1417.
236		3	0.	-0.	1.55	5256.	-1383.	2844.	7.9587	-2.0935	0.3764	11.	200.	-551.
		5			36.11	5256.	-1383.	2844.	0.0160	0.0079	-0.0216	11.	200.	-551.
237		4	0.	-0.	1.55	4032.	-2521.	4088.	6.1047	-3.8174	0.5411	60.	-576.	832.
		5			36.11	4032.	-2521.	4088.	0.0916	-0.0224	0.0326	60.	-576.	832.
238		5	0.	-0.	1.74	3120.	-2599.	5010.	4.1990	-3.4973	0.5894	53.	10.	1125.
		5			38.30	3120.	-2599.	5010.	0.0711	0.0003	0.0392	53.	10.	1125.
239		6	4.00	-0.	1.40	5657.	1199.	1329.	9.5165	2.0169	0.1954	-12.	612.	183.
		5			34.26	5657.	1199.	1329.	-0.0210	0.0267	0.0080	-12.	612.	183.
240		7	8.00	-0.	1.43	5719.	1591.	483.	9.3614	2.6035	0.0691	-59.	692.	-284.
		5			34.73	5719.	1591.	483.	-0.0966	0.0293	-0.0120	-59.	692.	-284.
241		8	10.00	-0.	1.55	5839.	1850.	202.	8.8410	2.8014	0.0267	14.	855.	-2038.
		5			36.11	5839.	1850.	202.	0.0218	0.0327	-0.0799	14.	855.	-2038.
242		9	12.00	-0.	1.55	5818.	2058.	923.	8.8089	3.1154	0.1222	-34.	493.	1443.
		5			36.11	5818.	2058.	923.	-0.0516	0.0193	0.0566	-34.	493.	1443.
243		10	14.00	-0.	1.36	5671.	2232.	-695.	9.8133	3.8627	-0.1052	-36.	818.	-369.
		5			33.78	5671.	2232.	-695.	-0.0625	0.0366	-0.0157	-36.	818.	-369.
244		11	16.00	-0.	1.55	5962.	2510.	-1634.	9.0265	3.8000	-0.2162	-33.	1227.	-1103.
		5			36.11	5962.	2510.	-1634.	-0.0494	0.0481	-0.0432	-33.	1227.	-1103.
245		12	-4.00	-0.	5.50	6115.	1279.	10560.	2.6081	0.5453	0.3937	-27.	-400.	-530.
		5			68.04	6115.	1279.	10560.	-0.0117	-0.0044	-0.0059	-27.	-400.	-530.
246		13	0.	-0.	5.43	6797.	1596.	10574.	2.9402	0.6903	0.3999	-34.	-97.	-454.
		5			67.56	6797.	1596.	10574.	-0.0147	-0.0011	-0.0051	-34.	-97.	-454.
247		14	0.	-0.	5.62	5880.	-464.	11364.	2.8559	-0.1939	0.4149	-73.	-272.	-1367.
		5			68.75	5880.	-464.	11364.	-0.0307	-0.0029	-0.0148	-73.	-272.	-1367.
248		15	0.	-0.	5.43	4450.	-1597.	12726.	1.9249	-0.6910	0.4812	-111.	-326.	1344.
		5			67.56	4450.	-1597.	12726.	-0.0480	-0.0037	0.0151	-111.	-326.	1344.

TABLE A-2 (Continued)

Test Point No.	Run No.	Point of Run	Left N_p RPM	Right N_p RPM	Left β_t Deg.	Left β_o Deg.	Right β_t Deg.	Right β_o Deg.	Tail i_t Deg.	δ_f Deg.	Baro. in. Hg	To °F	Left $N_{.85}$ % RPM	Right $N_{.85}$ % RPM	Average V_F/V_{tip}	q/qc
249	I-11	16	1785	1785	40	40	40	40	0	30	30.09	106	88.5	89.0	0.1426	1.040
250		17	1730	1710	0	0	0	0				106			0.1473	1.008
251		18	1730	1710								106	89.0		0.1471	1.019
252		19	1730	1710								106			0.1463	1.039
253		20	1730	1710								107			0.1472	1.050
254		21	1730	1720								107			0.1468	1.050
255		22	1720	1780								107			0.1450	1.046
256		23	1700	1670								109	87.5	88.5	0.3005	1.018
257		24	1700	1700								109	88.0		0.2984	1.024
258		25	1710	1700	20	20	20	20				110	88.0		0.2981	1.031
259		26	1715	1725	35	35	35	35				110	87.5		0.2952	1.024
260		27	1725	1725	40	40	40	40				110	87.5	88.0	0.2947	1.030
261		28	1690	1690	0	0	0	0				110	88.0	88.5	0.3005	1.024
262		29	1680	1700								111		88.5	0.3006	1.025
263		30	1670	1680								111		88.5	0.3042	1.032
264		31	1670	1690								111			0.3026	1.023
265		32	1660	1700								111			0.3026	1.031
266		33	1700	1710								112			0.2979	1.027
267	I-12	1	1650	1630	0	0	0	0	0	30	29.88	83	85.5	85.0	0.3822	1.022
268		2	1640	1640	20	20	20	20				84	85.5	85.0	0.3823	1.021
269		3	1650	1640	35	35	35	35				84	85.5	86.5	0.3809	1.019
270		4	1650	1640	40	40	40	40				86	85.0	86.5	0.3827	1.010
271		5	1700	1690	0	0	0	0				91	88.0	89.0	0.1142	0.971
272		6	1700	1685								92			0.1122	1.010
273		7	1695	1685								93			0.1119	0.956
274		8	1690	1680	20	20	20	20				95			0.1105	0.989
275		9	1720	1720	35	35	35	35				96			0.1099	0.897
276		10	1690	1670	0	0	0	0	-4			98			0.1115	0.983

Test Point No.	Run No.	PT AVG	ALPHA	BETA	Q V,NOM	LIFT,U CL*QS	DRAG,U CD*QS	M,U CM*QSC	CL CY	CD CN	CM CROLL	SIDE F,U CY*QS	YAW,U CN*QSB	ROLL,U CL*QSB
249	I-11	16	0.	-0.	5.43	4010.	-1689.	11163.	1.7349	-0.7308	0.4221	-149.	1470.	-1015.
		5			67.56	4010.	-1689.	11163.	-0.0646	0.0165	-0.0114	-149.	1470.	-1015.
250		17	4.00	-0.	5.23	7267.	1908.	9668.	3.2602	0.8561	0.3791	-94.	285.	-1480.
		5			66.34	7267.	1908.	9668.	-0.0422	0.0033	-0.0172	-94.	285.	-1480.
251		18	8.00	-0.	5.27	7915.	2306.	8635.	3.5248	1.0270	0.3361	-135.	700.	-456.
		5			66.58	7915.	2306.	8635.	-0.0603	0.0081	-0.0053	-135.	700.	-456.
252		19	10.00	-0.	5.31	8210.	2524.	7784.	3.6295	1.1156	0.3008	-127.	715.	-1208.
		5			66.83	8210.	2524.	7784.	-0.0562	0.0082	-0.0138	-127.	715.	-1208.
253		20	12.00	-0.	5.43	8501.	2759.	7423.	3.6774	1.1937	0.2958	-66.	462.	-3910.
		5			67.56	8501.	2759.	7423.	-0.0287	0.0045	-0.0438	-66.	462.	-3910.
254		21	14.00	-0.	5.43	8676.	3007.	7515.	3.7532	1.3008	0.2842	-29.	198.	-2624.
		5			67.56	8676.	3007.	7515.	-0.0125	0.0022	-0.0294	-29.	198.	-2624.
255		22	16.00	-0.	5.43	8964.	3193.	6808.	3.8778	1.3811	0.2574	26.	229.	-3825.
		5			67.56	8964.	3193.	6808.	0.0114	0.0026	-0.0428	26.	229.	-3825.
256		23	-4.00	-0.	20.81	7327.	2888.	31592.	0.8265	0.3258	0.3115	-106.	1408.	-1147.
		5			132.30	7327.	2888.	31592.	-0.0119	0.0041	-0.0033	-106.	1408.	-1147.
257		24	0.	-0.	21.00	9509.	2944.	27812.	1.0628	0.3290	0.2717	-92.	1117.	-868.
		5			132.91	9509.	2944.	27812.	-0.0103	0.0032	-0.0025	-92.	1117.	-868.
258		25	0.	-0.	21.19	8882.	1552.	27059.	0.9838	0.1719	0.2620	-256.	-34.	1897.
		5			133.51	8882.	1552.	27059.	-0.0284	-0.0031	0.0054	-256.	-34.	1897.
259		26	0.	-0.	21.00	7771.	580.	24235.	0.8866	0.0649	0.2568	-248.	157.	1608.
		5			132.91	7771.	580.	24235.	-0.0277	0.0005	0.0047	-248.	157.	1608.
260		27	0.	-0.	21.19	7320.	389.	21981.	0.8104	0.0431	0.2128	-183.	809.	-1164.
		5			133.51	7320.	389.	21981.	-0.0203	0.0023	-0.0033	-183.	809.	-1164.
261		28	4.00	-0.	21.00	11522.	3119.	22654.	1.2877	0.3486	0.2215	-138.	1262.	-802.
		5			132.91	11522.	3119.	22654.	-0.0155	0.0037	-0.0023	-138.	1262.	-802.
262		29	8.00	-0.	21.00	13658.	3337.	20774.	1.5265	0.3729	0.2030	-178.	1303.	493.
		5			132.91	13658.	3337.	20774.	-0.0199	0.0038	0.0014	-178.	1303.	493.
263		30	10.00	-0.	21.27	12827.	2894.	8014.	1.4156	0.3194	0.0773	-687.	2382.	12322.
		5			133.75	12827.	2894.	8014.	-0.0759	0.0068	0.0352	-687.	2382.	12322.
264		31	12.00	-0.	21.00	13629.	3198.	4918.	1.5233	0.3574	0.0481	-572.	1480.	12705.
		5			132.91	13629.	3198.	4918.	-0.0659	0.0043	0.0368	-572.	1480.	12705.
265		32	14.00	-0.	21.16	14210.	3982.	1878.	1.5767	0.4418	0.0182	-519.	1475.	13809.
		5			133.39	14210.	3982.	1878.	-0.0576	0.0042	0.0397	-519.	1475.	13809.
266		33	16.00	-0.	21.00	14457.	4632.	-5124.	1.6158	0.5177	-0.0501	-326.	-1454.	17901.
		5			132.91	14457.	4632.	-5124.	-0.0565	-0.0042	0.0518	-326.	-1454.	17901.
267	I-12	1	0.	-0.	33.13	10084.	2812.	24659.	0.7144	0.1992	0.1527	-635.	2037.	12091.
		5			166.93	10084.	2812.	24659.	-0.0450	0.0037	0.0222	-635.	2037.	12091.
268		2	0.	-0.	33.06	9662.	2159.	23014.	0.6861	0.1533	0.1428	-504.	3931.	7360.
		5			166.74	9662.	2159.	23014.	-0.0358	0.0072	0.0135	-504.	3931.	7360.
269		3	0.	-0.	32.94	9862.	1632.	26635.	0.7027	0.1163	0.1659	-315.	3733.	1723.
		5			166.45	9862.	1632.	26635.	-0.0225	0.0069	0.0032	-315.	3733.	1723.
270		4	0.	-0.	32.83	9218.	1335.	24351.	0.6591	0.0955	0.1522	-216.	2740.	2767.
		5			166.16	9218.	1335.	24351.	-0.0154	0.0051	0.0051	-216.	2740.	2767.
271		5	-4.00	-0.	3.00	5851.	730.	4995.	4.5725	0.5702	0.3412	-84.	386.	895.
		5			50.26	5851.	730.	4995.	-0.0656	0.0078	0.0181	-84.	386.	895.
272		6	-2.00	-0.	3.00	6014.	917.	5018.	4.7000	0.7168	0.3428	-87.	586.	1973.
		5			50.26	6014.	917.	5018.	-0.0683	0.0119	0.0399	-87.	586.	1973.
273		7	0.	-0.	2.81	6079.	1099.	4752.	5.0783	0.9181	0.3470	-95.	796.	2110.
		5			48.61	6079.	1099.	4752.	-0.0794	0.0172	0.0456	-95.	796.	2110.
274		8	0.	-0.	2.81	5275.	-1000.	5182.	4.4066	-0.8556	0.3784	-19.	-2.	931.
		5			48.61	5275.	-1000.	5182.	-0.0160	-0.0000	0.0201	-19.	-2.	931.
275		9	0.	-0.	2.62	3895.	-2073.	6686.	3.4949	-1.8603	0.5244	48.	-1171.	1962.
		5			46.91	3895.	-2073.	6686.	0.0426	-0.0272	0.0456	48.	-1171.	1962.
276		10	0.	-0.	2.81	5861.	1124.	5172.	4.8958	0.9393	0.3776	-94.	255.	3314.
		5			48.61	5861.	1124.	5172.	-0.0786	0.0055	0.0717	-94.	255.	3314.

TABLE A-2 (Continued)

Test Point No.	Run No.	Point of Run	Left n_p RPM	Right n_p RPM	Left β_L Deg.	Left β_0 Deg.	Right β_L Deg.	Right β_0 Deg.	Tail i_t Deg.	δ_f Deg.	Baro. in. Hg	To °F	Left n_{J85} % RPM	Right n_{J85} % RPM	Average V_p/V_{clp}	q/qc
277	I-12	11	1685	1665	0	0	0	0	4	30	29.88	98	88.0	89.0	0.1139	1.010
278		12	1680	1660					8			99	88.0	89.0	0.1149	1.003
279		13	1670	1660					12			99	87.5	88.5	0.1152	1.003
280		14	1670	1660					0			99			0.1148	1.010
281		15	1715	1661								100			0.1124	0.962
282		16	1675	1660								101			0.1153	1.003
283		17	1675	1660								101			0.1153	1.003
284		18	1700	1700								77	87.0	87.0	0.1093	1.027
285		19	1695	1695								79			0.1098	1.027
286		20	1690	1690								80			0.1111	1.000
287		21	1690	1690								82		87.5	0.1125	0.990
288		22	1685	1690								83			0.1124	0.997
289		23	1675	1680								64			0.1118	0.956
290		24	1710	1700	20	20	20	20				86	88.0	88.0	0.1112	1.003
291		25	1710	1700								87			0.1109	1.010
292		26	1710	1720								89			0.1108	1.003
293		27	1710	1720								90			0.1113	0.997
294		28	1710	1710								92			0.1110	1.010
295		29	1710	1715								92			0.1109	0.946
296		30	1710	1715								93			0.1125	0.984
297		31	1710	1715								94			0.1106	1.020
298		32	1710	1715								94			0.1145	0.952
299		33	1705	1710								95			0.1115	1.010
300		34	1705	1710								95			0.1115	1.010
301		35	1700	1715								96			0.1116	1.010
302		36	1705	1705								99		88.5	0.1477	0.998

Test Point No.	Run No.	PT AVG	ALPHA	BETA	Q V_s,NOM	LIFT,U CL*QS	DRAG,U CD*QS	M,U CM*QSC	CL CY	CD CN	CM CROLL	SIDE F,U CY*QS	YAW,U CN*QSB	ROLL,U CL*QSB
277	I-12	11	0.	-0.	5.00	6053.	1105.	3864.	4.7300	0.8637	0.2639	-123.	713.	1370.
		5			50.26	6053.	1105.	3864.	-0.0940	0.0144	0.0277	-123.	713.	1370.
278		12	0.	-0.	5.00	6017.	1102.	2001.	4.7019	0.8615	0.1367	-103.	474.	3246.
		5			50.26	6017.	1102.	2001.	-0.0803	0.0096	0.0657	-103.	474.	3246.
279		13	0.	-0.	5.00	6127.	1102.	441.	4.7861	0.8615	0.0302	-114.	669.	2273.
		5			50.24	6127.	1102.	441.	-0.0893	0.0135	0.0460	-114.	669.	2273.
280		14	0.	-0.	5.00	5861.	1082.	4837.	4.5800	0.8453	0.3304	-122.	542.	2468.
		5			50.26	5861.	1082.	4837.	-0.0957	0.0110	0.0499	-122.	542.	2468.
281		15	2.00	-0.	2.81	5962.	1254.	4188.	4.9800	1.0472	0.3058	-106.	674.	1645.
		5			48.61	5962.	1254.	4188.	-0.0882	0.0146	0.0356	-106.	674.	1645.
282		16	4.00	-0.	5.00	6175.	1470.	4440.	4.8238	1.1488	0.3033	-120.	670.	536.
		5			50.26	6175.	1470.	4440.	-0.0954	0.0136	0.0109	-120.	670.	536.
283		17	6.00	-0.	5.00	6317.	1702.	4467.	4.9363	1.3304	0.3052	-87.	547.	-180.
		5			50.26	6317.	1702.	4467.	-0.0683	0.0111	-0.0036	-87.	547.	-180.
284		18	8.00	-0.	5.00	6830.	2003.	3972.	5.3377	1.5652	0.2713	-42.	102.	-3926.
		5			50.26	6830.	2003.	3972.	-0.0328	0.0021	-0.0794	-42.	102.	-3926.
285		19	10.00	-0.	5.00	6876.	2183.	4026.	5.3733	1.7058	0.2750	-72.	548.	-1401.
		5			50.26	6876.	2183.	4026.	-0.0543	0.0111	-0.0283	-72.	548.	-1401.
286		20	12.00	-0.	2.97	6982.	2406.	3541.	5.5271	1.9048	0.2451	-37.	76.	-2546.
		5			49.94	6982.	2406.	3541.	-0.0296	0.0016	-0.0326	-37.	76.	-2546.
287		21	14.00	-0.	5.00	7286.	2678.	3550.	5.6940	2.0926	0.2425	-89.	555.	-2532.
		5			50.26	7286.	2678.	3550.	-0.0694	0.0112	-0.0512	-89.	555.	-2532.
288		22	16.00	-0.	5.00	7402.	2913.	3535.	5.7840	2.2764	0.2278	-116.	901.	-3033.
		5			50.26	7402.	2913.	3535.	-0.0908	0.0182	-0.0614	-116.	901.	-3033.
289		23	18.00	-0.	2.81	7272.	3154.	1350.	6.0747	2.6349	0.0986	-132.	973.	-2312.
		5			48.61	7272.	3154.	1350.	-0.1099	0.0210	-0.0500	-132.	973.	-2312.
290		24	-4.00	-0.	5.00	5095.	-1349.	4481.	3.9817	-1.0539	0.3061	-2.	289.	-3149.
		5			50.26	5095.	-1349.	4481.	-0.0015	0.0058	-0.3637	-2.	289.	-3149.
291		25	-2.00	-0.	5.00	5304.	-1176.	4491.	4.1448	-0.9189	0.3204	-2.	-18.	-3431.
		5			50.26	5304.	-1176.	4491.	-0.0015	-0.0006	-0.0694	-2.	-18.	-3431.
292		26	0.	-0.	5.00	5510.	-1025.	4769.	4.3061	-0.8007	0.3257	-15.	140.	-3382.
		5			50.26	5510.	-1025.	4769.	-0.0116	0.0028	-0.0684	-15.	140.	-3382.
293		27	2.00	-0.	5.00	5700.	-796.	4911.	4.4543	-0.6219	0.3355	-25.	281.	-3125.
		5			50.26	5700.	-796.	4911.	-0.0195	0.0057	-0.0632	-25.	281.	-3125.
294		28	4.00	-0.	5.00	5777.	-621.	5273.	4.5143	-0.4854	0.3602	-30.	591.	-3018.
		5			50.26	5777.	-621.	5273.	-0.0236	0.0120	-0.0611	-30.	591.	-3018.
295		29	6.00	-0.	2.81	6017.	-417.	5095.	5.0261	-0.3480	0.3721	-3.	430.	-3392.
		5			48.61	6017.	-417.	5095.	-0.0024	0.0093	-0.0734	-3.	430.	-3392.
296		30	8.00	-0.	5.00	6300.	-177.	5727.	4.9232	-0.1384	0.3912	-14.	396.	-3488.
		5			50.26	6300.	-177.	5727.	-0.0109	0.0080	-0.0706	-14.	396.	-3488.
297		31	10.00	-0.	5.00	6434.	-21.	4955.	5.0282	-0.0165	0.3885	-6.	369.	-3522.
		5			50.26	6434.	-21.	4955.	-0.0049	0.0075	-0.0672	-6.	369.	-3522.
298		32	12.00	-0.	5.00	6749.	252.	4486.	5.2739	0.1969	0.3044	-12.	57.	-2992.
		5			50.26	6749.	252.	4486.	-0.0090	0.0012	-0.0605	-12.	57.	-2992.
299		33	14.00	-0.	5.00	6852.	453.	3991.	5.3545	0.3537	0.2726	-40.	66.	-3315.
		5			50.26	6852.	453.	3991.	0.0311	0.0014	-0.0670	-40.	66.	-3310.
300		34	16.00	-0.	5.00	7051.	664.	2902.	5.5102	0.5188	0.1983	-8.	569.	-3133.
		5			50.24	7051.	664.	2902.	0.0064	0.0115	-0.0634	-8.	569.	-3133.
301		35	18.00	-0.	5.00	7250.	929.	1788.	5.6659	0.7262	0.1221	-15.	859.	-3540.
		5			50.24	7250.	929.	1788.	-0.0120	0.0174	-0.0716	-15.	859.	-3540.
302		36	-4.00	-0.	5.14	5076.	-819.	10047.	2.3201	-0.5743	0.4014	-119.	593.	-4552.
		5			65.72	5076.	-819.	10047.	-0.0544	0.0070	-0.0539	-119.	593.	-4552.

TABLE A-2 (Continued)

Test Point No.	Run No.	Point of Run	Left N_p RPM	Right N_p RPM	Left β_1 Deg.	Left β_0 Deg.	Right β_1 Deg.	Right β_0 Deg.	Tail i_t Deg.	δ_f Deg.	Baro. in. Hg	To °F	Left $N_{.785}$ % RPM	Right $N_{.785}$ % RPM	Average V_p/V_{tip}	q/qc
303	I-12	37	1705	1705	20	20	20	20	0	30	29.88	99	88.0	88.0	0.1483	0.990
304		38	1710	1710								100			0.1499	1.002
305		39	1710	1710								100			0.1480	1.027
306		40	1710	1710								100			0.1499	0.994
307		41	1710	1720								100			0.1489	1.038
308		42	1700	1760								101		88.5	0.1448	1.014
309		43	1680	1780								101		88.5	0.1471	1.017
310		44	1680	1710								101		86.5	0.1483	1.035
311	I-13	1	1720	1725	35	35	35	35	0	30	30.01	68	86.0	86.0	0.1400	N/A
312		2	1727	1727								69	86.0		0.1398	
313		3	1730	1735								71	86.5		0.1396	
314		4	1740	1740								72			0.1418	
315		5	1740	1745								74			0.1419	
316		6	1730	1750								75		86.5	0.1396	
317		7	1715	1730								76		85.5	0.1433	
318		8	1705	1720								77		85.0	0.1448	
319		9	1700	1710								77		84.5	0.1462	
320		10	1685	1690	20	20	20	20				82	87.0	86.5	0.2202	
321		11	1695	1695								82		87.0	0.2202	
322		12	1700	1700								84		86.5	0.2190	
323		13	1695	1718								84		87.0	0.2182	
324		14	1695	1705								84		87.0	0.2190	
325		15	1690	1700								86		86.5	0.2196	
326		16	1690	1780								86		86.5	0.2146	
327		17	1685	1700								87		87.5	0.2224	
328		18	1685	1685								89	86.5	87.0	0.2220	
329		19	1685	1685	35	35	35	35				90	86.5	87.0	0.2224	
330		20	1685	1695								91	86.5	87.0	0.2218	

Test Point No.	Run No.	PT AVG	ALPHA	BETA	Q V_∞NOM	LIFT,U CL*QS	DRAG,U CD*QS	M,U CM*QSC	CL CY	CD CN	CM CROLL	SIDE F,U CY*QS	YAW,U CN*QSB	ROLL,U CL*QSB
303	I-12	37	0.	-0.	5.14	5731.	-503.	10201.	2.6196	-0.2297	0.4076	-100.	366.	-4032.
		5			65.72	5731.	-503.	10201.	-0.0456	0.0043	-0.0477	-100.	366.	-4032.
304		38	4.00	-0.	5.33	6444.	-136.	9543.	2.8383	-0.0598	0.3674	-93.	423.	-3839.
		5			66.95	6444.	-136.	9543.	-0.0408	0.0048	-0.0438	-93.	423.	-3839.
305		39	8.00	-0.	5.33	7222.	229.	8862.	3.1808	0.1011	0.3412	-42.	296.	-3703.
		5			66.95	7222.	229.	8862.	-0.0188	0.0034	-0.0422	-42.	296.	-3703.
306		40	10.00	-0.	5.29	7560.	425.	8442.	3.3543	0.1887	0.3274	3.	-336.	-4100.
		5			66.71	7560.	425.	8442.	0.0013	-0.0039	-0.0471	3.	-336.	-4100.
307		41	12.00	-0.	5.48	7908.	673.	8953.	3.3847	0.2882	0.3350	123.	-1046.	-4749.
		5			67.92	7908.	673.	8953.	0.0528	-0.0116	-0.0526	123.	-1046.	-4749.
308		42	14.00	-0.	5.14	7987.	900.	8489.	3.6528	0.4136	0.3392	167.	-1498.	-4651.
		5			65.72	7987.	900.	8489.	0.0704	-0.0177	-0.0550	167.	-1498.	-4651.
309		43	16.00	-0.	5.33	8405.	1164.	7400.	3.7020	0.5126	0.2849	134.	-1986.	-2870.
		5			66.95	8405.	1164.	7400.	0.0590	-0.0226	-0.0327	134.	-1986.	-2870.
310		44	18.00	-0.	5.29	8436.	1375.	6558.	3.7429	0.6101	0.2543	121.	-2073.	-993.
		5			66.71	8436.	1375.	6558.	0.0537	-0.0268	-0.0114	121.	-2073.	-993.
311	I-13	1	-4.00	-0.	5.04	3756.	-1916.	12685.	1.7498	-0.8926	0.5166	-17.	787.	-212.
		5			65.10	3756.	-1916.	12685.	-0.0081	0.0095	-0.0026	-17.	787.	-212.
312		2	0.	-0.	5.04	4452.	-1711.	11832.	2.0740	-0.7971	0.4818	14.	81.	-59.
		5			65.10	4452.	-1711.	11832.	0.0065	0.0010	-0.0007	14.	81.	-59.
313		3	4.00	-0.	5.04	5237.	-1444.	11616.	2.4397	-0.6728	0.4730	-4.	-312.	83.
		5			65.10	5237.	-1444.	11616.	-0.0021	-0.0038	0.0010	-4.	-312.	83.
314		4	8.00	-0.	5.23	5959.	-1114.	11860.	2.6734	-0.4999	0.4651	-93.	-340.	1687.
		5			66.34	5959.	-1114.	11860.	-0.0041	-0.0039	0.0196	-93.	-340.	1687.
315		5	10.00	-0.	5.23	6377.	-940.	11686.	2.8607	-0.4218	0.4583	-111.	-17.	1052.
		5			66.34	6377.	-940.	11686.	-0.0505	-0.0002	0.0122	-111.	-17.	1052.
316		6	12.00	-0.	5.04	6646.	-757.	11643.	3.0967	-0.3526	0.4741	-91.	-451.	501.
		5			65.10	6646.	-757.	11643.	-0.0423	-0.0054	0.0060	-91.	-451.	501.
317		7	14.00	-0.	5.19	6979.	-387.	10954.	3.1543	-0.1751	0.4328	-64.	-165.	594.
		5			66.09	6979.	-387.	10954.	-0.0289	-0.0019	0.0069	-64.	-165.	594.
318		8	16.00	-0.	5.23	7255.	-106.	9922.	3.2546	-0.0476	0.3891	-57.	32.	1300.
		5			66.34	7255.	-106.	9922.	-0.0254	0.0004	0.0151	-57.	32.	1300.
319		9	18.00	-0.	5.04	7526.	163.	8898.	3.5065	0.0758	0.3624	-64.	404.	1580.
		5			65.10	7526.	163.	8898.	-0.0297	0.0049	0.0191	-64.	404.	1580.
320		10	-4.00	-0.	11.61	5707.	369.	21517.	1.1541	0.0745	0.3804	-98.	-386.	-1235.
		5			98.81	5707.	369.	21517.	-0.0199	-0.0020	-0.0065	-98.	-386.	-1235.
321		11	0.	-0.	11.61	6970.	624.	20602.	1.4094	0.1262	0.3642	-26.	-1431.	-2171.
		5			98.81	6970.	624.	20602.	-0.0052	-0.0075	-0.0114	-26.	-1431.	-2171.
322		12	4.00	-0.	11.61	8381.	915.	18198.	1.6940	0.1850	0.3217	6.	-1829.	-818.
		5			98.81	8381.	915.	18198.	0.0013	-0.0096	-0.0043	6.	-1829.	-818.
323		13	8.00	-0.	11.61	9754.	1296.	16624.	1.9724	0.2621	0.2939	40.	-1825.	-1910.
		5			98.81	9754.	1296.	16624.	0.0082	-0.0096	-0.0100	40.	-1825.	-1910.
324		14	10.00	-0.	11.61	10423.	1505.	16027.	2.1078	0.3044	0.2833	-45.	-907.	-1050.
		5			98.81	10423.	1505.	16027.	-0.0091	-0.0047	-0.0055	-45.	-907.	-1050.
325		15	12.00	-0.	11.61	11111.	1809.	15237.	2.2471	0.3659	0.2693	-101.	-748.	-207.
		5			98.81	11111.	1809.	15237.	-0.0205	-0.0039	-0.0011	-101.	-748.	-207.
326		16	14.00	-0.	11.61	11634.	2131.	13656.	2.3528	0.4309	0.2414	82.	-2139.	-1608.
		5			98.81	11634.	2131.	13656.	0.0166	-0.0112	-0.0084	82.	-2139.	-1608.
327		17	14.00	-0.	11.80	11411.	2226.	12292.	2.2761	0.4428	0.2137	25.	-1796.	494.
		5			99.62	11411.	2226.	12292.	0.0051	-0.0093	0.0025	25.	-1796.	494.
328		18	16.00	-0.	11.61	11382.	2534.	5331.	2.3018	0.5125	0.0942	-180.	610.	5240.
		5			98.81	11382.	2534.	5331.	-0.0365	0.0032	0.0275	-180.	610.	5240.
329		19	-4.00	-0.	11.80	4190.	-658.	20123.	0.8336	-0.1309	0.3499	-159.	402.	-855.
		5			99.62	4190.	-658.	20123.	-0.0317	0.0021	-0.0044	-159.	402.	-855.
330		20	0.	-0.	11.61	5707.	-436.	18534.	1.1541	-0.0882	0.3276	-126.	-377.	-324.
		5			98.81	5707.	-436.	18534.	-0.0255	-0.0020	-0.0017	-126.	-377.	-324.

TABLE A-2 (Continued)

Test Point No.	Run No.	Point of Run	Left N_y RPM	Right N_y RPM	Left β_L Deg.	Left β_0 Deg.	Right β_L Deg.	Right β_0 Deg.	Tail i_t Deg.	δ_f Deg.	Baro. in. Hg	To $^\circ_F$	Left N_{J85} % RPM	Right N_{J85} % RPM	Average V_p/V_{tip}	q/qc
331	I-13	21	1700	1700	35	35	35	35	0	30	30.01	91	86.5	87.0	0.2205	N/A
332		22	1695	1705								92		86.0	0.2207	
333		23	1685	1685								92		86.0	0.2226	
334		24	1685	1685								92		83.0	0.2226	
335		25	1690	1680								93			0.2228	
336		26	1690	1720								93			0.2221	
337		27	1640	1645	20	20	20	20				95	86.0	86.5	0.3087	
338		28	1640	1650								95		86.5	0.3083	
339		29	1630	1630								96		86.0	0.3100	
340		30	1640	1620								97	86.5		0.3086	
341		31	1635	1625								97			0.3086	
342		32	1640	1640								98		80.5	0.3087	
343		33	1645	1655	35	35	35	35				99	86.0	86.5	0.3071	
344		34	1635	1665										87.0	0.2926	
345		35	1620	1660										86.5	0.2944	
346		36	1670	1660									86.5		0.2900	
347		37	1670	1660											0.2900	
348		38	1680	1635								100		80.5	0.3063	
349		39	1640	1650								100	83.5	80.5	0.3083	
350		40	1660	1645								102	86.0	86.5	0.3076	
351		41	1650	1645								102	86.0	86.5	0.3088	
352		42	1645	1645								103	85.0	81.0	0.3909	
353		43	1655	1645										80.5	0.3892	
354		44	1670	1645										80.0	0.3857	
355		45	1660	1640									84.0	80.0	0.3886	
356		46	965	985	0	0	0	0					64.5	65.0	0.3253	
357		47	980	970								104	65.0	65.0	0.3295	

Test Point No.	Run No.	PT AVG	ALPHA	BETA	Q V,NOM	LIFT,U CL*QS	DRAG,U CD*QS	M,U CM*QSC	CL CY	CD CN	CM CROLL	SIDE F,U CY*QS	YAW,U CN*QSB	ROLL,U CL*QSB
331	I-13	21	4.00	-0.	11.61	7126.	-126.	16353.	1.4413	-0.0254	0.2891	-70.	-808.	-1220.
		5			98.81	7126.	-126.	16353.	-0.0141	-0.0042	-0.0066	-70.	-808.	-1220.
332		22	8.00	-0.	11.61	8798.	238.	19945.	1.7792	0.0481	0.2642	-31.	-1266.	-950.
		5			98.81	8798.	238.	19945.	-0.0062	-0.0046	-0.0050	-31.	-1266.	-950.
333		23	10.00	-0.	11.61	9446.	471.	14502.	1.9109	0.0953	0.2563	-40.	-861.	-1233.
		5			98.81	9446.	471.	14502.	-0.0082	-0.0065	-0.0065	-40.	-861.	-1233.
334		24	12.00	-0.	11.61	9977.	826.	13417.	2.0175	0.1670	0.2372	-35.	-1063.	-476.
		5			98.81	9977.	826.	13417.	-0.0078	-0.0056	-0.0025	-35.	-1063.	-476.
335		25	14.00	-0.	11.61	10219.	1277.	8583.	2.0666	0.2583	0.1517	-75.	2257.	634.
		5			98.81	10219.	1277.	8583.	-0.0151	0.0118	0.0033	-75.	2257.	634.
336		26	16.00	-0.	11.80	11016.	1882.	1549.	2.1915	0.3745	0.0269	-203.	3854.	2539.
		5			99.62	11016.	1882.	1549.	-0.0401	0.0199	0.0131	-203.	3854.	2539.
337		27	-4.00	-0.	21.00	6307.	1453.	30115.	0.7049	0.1624	0.2942	-168.	-494.	-374.
		5			132.91	6307.	1453.	30115.	-0.0188	-0.0014	-0.0011	-168.	-494.	-374.
338		28	0.	-0.	21.00	8518.	1643.	25766.	0.9520	0.1836	0.2517	-229.	359.	395.
		5			132.91	8518.	1643.	25766.	-0.0256	0.0010	0.0011	-229.	359.	395.
339		29	4.00	-0.	20.81	10858.	1849.	21260.	1.2247	0.2086	0.2076	-262.	1304.	1943.
		5			132.30	10858.	1849.	21260.	-0.0296	0.0038	0.0057	-262.	1304.	1943.
340		30	8.00	-0.	20.62	12984.	2196.	18692.	1.4759	0.2500	0.1860	-298.	1335.	862.
		5			131.69	12984.	2196.	18692.	-0.0339	0.0039	0.0025	-298.	1335.	862.
341		31	10.00	-0.	20.62	13960.	2442.	17114.	1.5892	0.2780	0.1703	-322.	1424.	2576.
		5			131.69	13960.	2442.	17114.	-0.0366	0.0042	0.0076	-322.	1424.	2576.
342		32	12.00	-0.	20.81	13422.	2432.	4900.	1.5140	0.2744	0.0483	-699.	6468.	12130.
		5			132.30	13422.	2432.	4900.	-0.0788	0.0189	0.0354	-699.	6468.	12130.
343		33	-4.00	-0.	20.81	5150.	458.	26454.	0.5809	0.0517	0.2608	-275.	558.	1037.
		5			132.30	5150.	458.	26454.	-0.0310	0.0016	0.0030	-275.	558.	1037.
344		34	0.	-0.	20.62	7507.	673.	22221.	0.8546	0.0766	0.2211	-231.	390.	504.
		5			131.69	7507.	673.	22221.	-0.0263	0.0012	0.0015	-231.	390.	504.
345		35	4.00	-0.	20.84	9737.	984.	18345.	1.1085	0.1121	0.1826	-163.	-832.	-72.
		5			131.69	9737.	984.	18345.	-0.0185	-0.0025	-0.0002	-163.	-832.	-72.
346		36	8.00	-0.	20.62	12113.	1375.	14543.	1.3790	0.1565	0.1447	-218.	-193.	3082.
		5			131.69	12113.	1375.	14543.	-0.0248	-0.0006	0.0091	-218.	-193.	3082.
347		37	10.00	-0.	20.62	13305.	1660.	12821.	1.5147	0.1889	0.1276	-210.	761.	3140.
		5			131.69	13305.	1660.	12821.	-0.0239	0.0022	0.0093	-210.	761.	3140.
348		38	12.00	-0.	20.85	13434.	1921.	1258.	1.5126	0.2163	0.0124	-514.	8669.	7808.
		5			132.42	13434.	1921.	1258.	-0.0579	0.0253	0.0228	-514.	8669.	7808.
349		39	14.00	-0.	20.81	13180.	2480.	-5775.	1.4866	0.2798	-0.0569	-163.	4496.	4295.
		5			132.30	13180.	2480.	-5775.	-0.0184	0.0131	0.0125	-163.	4496.	4295.
350		40	-4.00	-0.	32.85	6173.	1438.	31997.	0.4411	0.1028	0.1999	-422.	2956.	-500.
		5			166.21	6173.	1438.	31997.	-0.0392	0.0055	-0.0009	-422.	2956.	-500.
351		41	0.	-0.	32.85	9614.	1616.	25595.	0.6871	0.1155	0.1599	-262.	2620.	608.
		5			166.21	9614.	1616.	25595.	-0.0187	0.0048	0.0011	-262.	2620.	608.
352		42	4.00	-0.	33.04	11578.	1760.	7452.	0.8226	0.1251	0.0463	-345.	7784.	1713.
		5			166.49	11578.	1760.	7452.	-0.0245	0.0143	0.0032	-345.	7784.	1713.
353		43	8.00	-0.	32.96	14752.	2226.	-2829.	1.0506	0.1585	-0.0176	-342.	8459.	4752.
		5			166.50	14752.	2226.	-2829.	-0.0245	0.0156	0.0088	-342.	8459.	4752.
354		44	10.00	-0.	32.66	16110.	2536.	-7551.	1.1585	0.1823	-0.0474	-263.	6523.	4246.
		5			165.73	16110.	2536.	-7551.	-0.0189	0.0121	0.0079	-263.	6523.	4246.
355		45	12.00	-0.	32.85	17375.	3058.	-10524.	1.2417	0.2186	-0.0657	-130.	4162.	7149.
		5			166.21	17375.	3058.	-10524.	-0.0093	0.0077	0.0132	-130.	4162.	7149.
356		46	-4.00	-0.	8.14	2683.	1035.	11160.	0.7738	0.2985	0.2813	-25.	277.	-1889.
		5			82.74	2683.	1035.	11160.	-0.0072	0.0021	-0.0161	-25.	277.	-1889.
357		47	0.	-0.	8.33	3564.	1024.	9743.	1.0039	0.2885	0.2399	-70.	782.	-1012.
		5			83.72	3564.	1024.	9743.	-0.0196	0.0057	-0.0074	-70.	782.	-1012.

TABLE A-2 (Continued)

Test Point No.	Run No.	Point of Run	Left N_p RPM	Right N_p RPM	Left β_1 Deg.	Left β_0 Deg.	Right β_1 Deg.	Right β_0 Deg.	Tail i_t Deg.	δ_f Deg.	Baro. In. Hg	To $^\circ_F$	Left $N_{.85}$ % RPM	Right $N_{.85}$ % RPM	Average V_p/V_{tip}	q/qc
358	I-13	48	980	980	20	20	20	20	0	30	30.01	104	65.0	65.0	0.3239	N/A
359		49	980	990	35	35	35	35					65.0	65.0	0.3262	
360		50	995	990	40	40	40	40					64.0	64.5	0.3236	
361		51	1000	1000	45	45	45	45					64.5	65.0	0.3213	
362		52	1000	1010	50	50	50	50					64.0	64.5	0.3196	
363		53	990	980	0	0	0	0					65.5	65.0	0.3262	
364		54	980	1100									65.5	64.5	-	
365		55	1110	1110									71.0		0.3184	
366		56	1105	1105								103			0.3225	
367		57	1105	1105											0.3254	
368		58	1110	1120											0.3196	
369		59	1130	1120											0.3187	
370		60	1130	1140									64.5		0.3315	
371	I-14	1	1700	1690	10	10	10	10	0	30	30.00	86	87.5	87.0	0.0175	0.945
372		2	1705	1690								90	87.5	87.0	0.1825	1.046
373		3	975	940	0	0	0	0				93	65.0	65.0	0.1971	1.053
374		4	980	990								93		65.5	0.1977	1.051
375		5	950	990	20	20	20	20				93			0.1922	1.046
376		6	1005	1015	35	35	35	35				94			0.1885	1.038
377		7	1030	1030	40	40	40	40				95			0.1836	1.053
378		8	990	995	0	0	0	0				95		66.0	0.1911	1.046
379		9	990	1000								96			0.1902	1.053
380		10	995	995											0.1924	1.031
381		11	1000	1000											0.1898	1.046
382		12	995	1025											0.1874	1.053
383		13	1000	1060								97	66.0		0.1845	1.046

Test Point No.	Run No.	PT AVG	ALPHA	BETA	Q V,NOM	LIFT,U CL*QS	DRAG,U CD*QS	M,U CM*QSC	CL CY	CD CN	CM CROLL	SIDE F,U CY*QS	YAW,U CN*QSB	ROLL,U CL*QSB
358	I-13	48	0.	-0.	8.14	3257.	578.	9032.	0.9392	0.1668	0.2277	-93.	-194.	318.
		5			82.74	3257.	578.	9032.	-0.0269	-0.0014	0.6024	-93.	-194.	318.
359		49	0.	-0.	8.33	3043.	313.	7753.	0.8572	0.0882	0.1909	-91.	731.	-187.
		5			83.72	3043.	313.	7753.	-0.0256	0.0053	-0.0014	-91.	731.	-187.
360		50	0.	-0.	8.33	2861.	239.	7211.	0.8059	0.0673	0.1776	-76.	642.	-1133.
		5			83.72	2861.	239.	7211.	-0.0215	0.0047	-0.0083	-76.	642.	-1133.
361		51	0.	-0.	8.33	2760.	186.	6410.	0.7775	0.0525	0.1578	-51.	1216.	-952.
		5			83.72	2760.	186.	6410.	-0.0145	0.0029	-0.0049	-51.	1216.	-952.
362		52	0.	-0.	8.33	2582.	142.	5520.	0.7159	0.0399	0.1359	-6.	765.	-1509.
		5			83.72	2582.	142.	5520.	-0.0016	0.0034	-0.0110	-6.	765.	-1509.
363		53	4.00	-0.	8.33	4474.	1032.	7614.	1.2602	0.2908	0.1875	-25.	559.	-2162.
		5			83.72	4474.	1032.	7614.	-0.0072	0.0041	-0.0158	-25.	559.	-2162.
364		54	8.00	-0.	8.33	4819.	962.	3514.	1.3575	0.2709	0.0865	-188.	603.	2830.
		5			83.72	4819.	962.	3514.	-0.0529	0.0044	0.0206	-188.	603.	2830.
365		55	8.00	-0.	10.07	5566.	1221.	3954.	1.2969	0.2846	0.0806	-369.	1499.	6187.
		5			92.05	5566.	1221.	3954.	-0.0859	0.0090	0.0373	-369.	1499.	6187.
366		56	10.00	-0.	10.27	5988.	1357.	3142.	1.3695	0.3103	0.0628	-343.	1066.	6379.
		5			92.92	5988.	1357.	3142.	-0.0784	0.0083	0.0378	-343.	1066.	6379.
367		57	12.00	-0.	10.46	6420.	1499.	1791.	1.4417	0.3365	0.0351	-345.	872.	7687.
		5			93.78	6420.	1499.	1791.	-0.0774	0.0051	0.0447	-345.	872.	7687.
368		58	14.00	-0.	10.27	6703.	1801.	222.	1.5328	0.4119	0.0044	-248.	1347.	5857.
		5			92.92	6703.	1801.	222.	-0.0566	0.0080	0.0347	-248.	1347.	5857.
369		59	16.00	-0.	10.07	6763.	2101.	-2068.	1.5760	0.4897	-0.0421	-172.	122.	8547.
		5			92.05	6763.	2101.	-2068.	-0.0402	0.0007	0.0516	-172.	122.	8547.
370		60	18.00	-0.	10.46	6566.	2254.	-5029.	1.4746	0.5061	-0.0987	3.	-768.	3918.
		5			93.78	6566.	2254.	-5029.	0.0008	-0.0045	0.0228	3.	-768.	3918.
371	I-14	1	0.	-0.	1.16	5318.	-445.	546.	10.7366	-0.8983	0.0963	-66.	1064.	-2536.
		5			31.27	5318.	-445.	546.	-0.1337	0.0556	-0.1326	-66.	1064.	-2536.
372		2	0.	-0.	3.10	5844.	18.	6102.	4.4241	0.0134	0.4038	-71.	1134.	-551.
		5			51.07	5844.	18.	6102.	-0.0538	0.0222	-0.0108	-71.	1134.	-551.
373		3	-4.00	-0.	3.10	2114.	592.	4671.	1.6007	0.4480	0.3091	-26.	416.	-1886.
		5			51.07	2114.	592.	4671.	-0.0196	0.0082	-0.0370	-26.	416.	-1886.
374		4	0.	-0.	3.29	2477.	677.	4900.	1.7647	0.4826	0.3052	11.	-177.	-1561.
		5			52.64	2477.	677.	4900.	0.0075	0.0033	-0.0288	11.	-177.	-1561.
375		5	0.	-0.	3.10	2170.	80.	5069.	1.6425	0.0607	0.3354	26.	-415.	-1565.
		5			51.07	2170.	80.	5069.	0.0196	-0.0081	-0.0307	26.	-415.	-1565.
376		6	0.	-0.	3.10	1752.	-284.	4465.	1.3263	-0.2148	0.2955	-8.	126.	-1742.
		5			51.07	1752.	-284.	4465.	-0.0058	0.0025	-0.0341	-8.	126.	-1742.
377		7	0.	-0.	3.10	1529.	-332.	4562.	1.1574	-0.2515	0.3019	-43.	694.	-1288.
		5			51.07	1529.	-332.	4562.	-0.0327	0.0136	-0.0252	-43.	694.	-1288.
378		8	4.00	-0.	3.10	2690.	755.	4318.	2.0367	0.5712	0.2857	-11.	155.	-849.
		5			51.07	2690.	755.	4318.	-0.0080	0.0030	-0.0166	-11.	155.	-849.
379		9	8.00	-0.	3.10	2986.	853.	4191.	2.2602	0.6461	0.2773	-21.	311.	-272.
		5			51.07	2986.	853.	4191.	-0.0160	0.0061	-0.0053	-21.	311.	-272.
380		10	10.00	-0.	3.10	3132.	952.	4197.	2.3715	0.7209	0.2777	-15.	212.	-752.
		5			51.07	3132.	952.	4197.	-0.0113	0.0042	-0.0147	-15.	212.	-752.
381		11	12.00	-0.	3.10	3262.	1040.	3935.	2.4691	0.7877	0.2604	-36.	516.	-1853.
		5			51.07	3262.	1040.	3935.	-0.0269	0.0101	-0.0363	-36.	516.	-1853.
382		12	14.00	-0.	3.10	3358.	1092.	3685.	2.5418	0.8269	0.2412	-30.	432.	-741.
		5			51.07	3358.	1092.	3685.	-0.0229	0.0085	-0.0185	-30.	432.	-741.
383		13	16.00	-0.	3.10	3643.	1191.	3137.	2.7580	0.9018	0.2076	-22.	300.	-116.
		5			51.07	3643.	1191.	3137.	-0.0164	0.0059	-0.0023	-22.	300.	-116.

TABLE A-2 (Continued)

Test Point No.	Run No.	Point of Run	Left n_p RPM	Right n_p RPM	Left i_h Deg.	Left i_b Deg.	Right i_h Deg.	Right i_b Deg.	Tail i_t Deg.	δ_f Deg.	Bore. in. Hg	To σ_T	Left $n_{.385}$ % RPM	Right $n_{.385}$ % RPM	Average V_p/V_{tip}	q/qo
384	I-14	14	995	1075	0	0	0	0	0	30	30.00	97	65.5	65.5	0.1852	1.031
385		15	1120	1110								98	70.0	68.0	0.4511	1.024
386		16	1110	1100										66.0	0.4546	1.026
387		17	1120	1120	20	20	20	20						66.0	0.4486	1.017
388		18	1125	1090	35	35	35	35						69.0	0.4542	1.026
389		19	1140	1100	40	40	40	40							0.4490	
390		20	1145	1100	45	45	45	45				99			0.4485	
391		21	1150	1120	50	50	50	50						68.5	0.4436	
392		22	1056	1140	0	0	0	0					67.0	65.0	0.4385	
393		23	1100	1130									67.0		0.4515	
394		24	1145	1125									69.0		0.4436	
395		25	1150	1115											0.4445	
396		26	1105	1105											0.4555	
397		27	-	-									62.0		-	N.G.
398		28	1130	1390								100	69.0	69.0	0.4165	1.024
399		29	1075	1075										63.0	0.5905	1.027
400		30	1075	1070											0.5919	
401		31	1085	1085	20	20	20	20							0.5851	
402		32	1100	1080	35	35	35	35							0.5823	
403		33	1100	1075	40	40	40	40					68.5		0.5837	
404		34	1120	1090	45	45	45	45					68.5		0.5737	1.029
405		35	1125	1075	50	50	50	50					68.0		0.5771	1.027
406		36	1100	1060	0	0	0	0				101	68.5		0.5884	
407		37	1075	1055	0	0	0	0					69.0		0.5965	
408		38	1090	1130	45	45	45	45					68.0	69.5	0.5725	
409		39	1100	1130									67.5	65.5	0.5698	1.028
410		40	1140	1130									67.5	64.0	0.5599	1.027
411		41	1120	1140									63.0	64.0	0.5623	1.027

Test Point No.	Run No.	PT AVG	ALPHA	BETA	Q V,NOM	LIFT,U CL*QS	DRAG,U CD*QS	M,U CM*QSC	CL CY	CD CN	CM CROLL	SIDE F,U CY*QS	YAW,U CN*QSB	ROLL,U CL*QSB
384	I-14	14	18.00	-0.	3.10	3782.	1266.	2200.	2.8634	0.9581	0.1456	-12.	150.	262.
		5			51.07	3782.	1266.	2200.	-0.0087	0.0029	0.0051	-12.	150.	262.
385		15	-4.00	-0.	21.00	3926.	1781.	19735.	0.4388	0.1990	0.1928	-58.	926.	-1345.
		5			132.91	3926.	1781.	19735.	-0.0665	0.0627	-0.0039	-58.	926.	-1345.
386		16	0.	-0.	21.19	5482.	1543.	10537.	0.6071	0.1709	0.1061	-299.	4747.	1509.
		5			133.51	5482.	1543.	10537.	-0.0331	0.0116	0.0043	-299.	4747.	1509.
387		17	0.	-0.	20.81	5306.	1234.	9338.	0.5965	0.1392	0.0921	-258.	4106.	1754.
		5			132.30	5306.	1234.	9338.	-0.0291	0.0120	0.0051	-258.	4106.	1754.
388		18	0.	-0.	21.00	5196.	1001.	11540.	0.5827	0.1119	0.1127	-83.	1313.	653.
		5			132.91	5196.	1001.	11540.	-0.0093	0.0038	0.0019	-83.	1313.	653.
389		19	0.	-0.	21.00	4882.	918.	11229.	0.5456	0.1026	0.1097	-87.	1375.	1115.
		5			132.91	4882.	918.	11229.	-0.0097	0.0040	0.0032	-87.	1375.	1115.
390		20	0.	-0.	21.00	4805.	842.	9963.	0.5570	0.0941	0.0973	-55.	518.	1519.
		5			132.91	4805.	842.	9963.	-0.0037	0.0015	0.0044	-33.	518.	1519.
391		21	0.	-0.	21.00	4646.	808.	8892.	0.5193	0.0903	0.0869	9.	-148.	-234.
		5			132.91	4646.	808.	8892.	0.0011	-0.0006	-0.0007	9.	-148.	-234.
392		22	4.00	-0.	21.00	6686.	1467.	2520.	0.7473	0.1639	0.0246	-240.	3726.	2876.
		5			132.91	6686.	1467.	2520.	-0.0264	0.0108	0.0083	-240.	3726.	2876.
393		23	8.00	-0.	21.00	8266.	1677.	-3554.	0.9231	0.1875	-0.0347	-163.	2467.	4094.
		5			132.91	8266.	1677.	-3554.	-0.0162	0.0071	0.0118	-163.	2467.	4094.
394		24	10.00	-0.	21.00	9103.	1903.	-7172.	1.0174	0.2127	-0.0701	-135.	2016.	5450.
		5			132.91	9103.	1903.	-7172.	-0.0151	0.0058	0.0158	-135.	2016.	5450.
395		25	12.00	-0.	21.00	9718.	2160.	-7302.	1.0861	0.2415	-0.0713	-75.	1088.	6053.
		5			132.91	9718.	2160.	-7302.	-0.0084	0.0031	0.0175	-75.	1088.	6053.
396		26	14.00	-0.	21.00	10241.	2650.	-8548.	1.1446	0.2962	-0.0835	-5.	43.	5045.
		5			132.91	10241.	2650.	-8548.	-0.0006	0.0001	0.0146	-5.	43.	5045.
397		27	16.00	-0.	21.00	9770.	2965.	-16441.	1.0920	0.3292	-0.1606	35.	-549.	-877.
		5			132.91	9770.	2965.	-16441.	0.0039	-0.0016	-0.0025	35.	-549.	-877.
398		28	16.00	-0.	21.00	9763.	2968.	-17018.	1.0912	0.3317	-0.1663	41.	-634.	-1015.
		5			132.91	9763.	2968.	-17018.	0.0046	-0.0018	-0.0029	41.	-634.	-1015.
399		29	-4.00	-0.	33.23	4714.	2414.	27092.	0.3337	0.1707	0.1673	-134.	2165.	-344.
		5			167.17	4714.	2414.	27092.	-0.0095	0.0040	-0.0006	-134.	2165.	-344.
400		30	0.	-0.	33.23	7106.	2011.	10076.	0.5020	0.1420	0.0622	-375.	5960.	6609.
		5			167.17	7106.	2011.	10076.	-0.0265	0.0109	0.0121	-375.	5960.	6609.
401		31	0.	-0.	33.23	6871.	1739.	8590.	0.4854	0.1228	0.0530	-237.	3756.	3579.
		5			167.17	6871.	1739.	8590.	-0.0167	0.0069	0.0065	-237.	3756.	3579.
402		32	0.	-0.	33.23	6684.	1568.	7766.	0.4722	0.1108	0.0480	-160.	2540.	2617.
		5			167.17	6684.	1568.	7766.	-0.0113	0.0046	0.0048	-160.	2540.	2617.
403		33	0.	-0.	33.23	6468.	1510.	8083.	0.4569	0.1067	0.0499	-60.	938.	-488.
		5			167.17	6468.	1510.	8083.	-0.0042	0.0017	-0.0009	-60.	938.	-488.
404		34	0.	-0.	33.23	6420.	1466.	6418.	0.4535	0.1022	0.0396	-48.	740.	1368.
		5			167.17	6420.	1466.	6418.	-0.0034	0.0014	0.0025	-48.	740.	1368.
405		35	0.	-0.	33.23	6163.	1414.	6068.	0.4354	0.0999	0.0375	11.	-187.	678.
		5			167.17	6163.	1414.	6068.	0.0007	-0.0003	0.0012	11.	-187.	678.
406		36	0.	-0.	33.23	9677.	2060.	4938.	0.6836	0.1456	0.0305	-319.	5070.	10881.
		5			167.17	9677.	2060.	4938.	-0.0225	0.0093	0.0199	-319.	5070.	10881.
407		37	8.00	-0.	33.23	11294.	2545.	-10105.	0.7979	0.1798	-0.0624	-234.	3532.	7282.
		5			167.17	11294.	2545.	-10105.	-0.0165	0.0065	0.0133	-234.	3532.	7282.
408		38	-4.00	-0.	33.23	3024.	1441.	20784.	0.2136	0.1018	0.1283	8.	-144.	-1240.
		5			167.17	3024.	1441.	20784.	0.0005	-0.0003	-0.0023	8.	-144.	-1240.
409		39	0.	-0.	33.27	6420.	1452.	7157.	0.4535	0.1024	0.0441	22.	-384.	-703.
		5			167.27	6420.	1452.	7157.	0.0015	-0.0007	-0.0013	22.	-384.	-703.
410		40	4.00	-0.	33.23	9401.	1710.	-4578.	0.6641	0.1208	-0.0283	3.	-75.	3120.
		5			167.17	9401.	1710.	-4578.	0.0002	-0.0001	0.0057	3.	-75.	3120.
411		41	8.00	-0.	33.23	12026.	2224.	-15865.	0.8496	0.1571	-0.0980	39.	-629.	1660.
		5			167.17	12026.	2224.	-15865.	0.0028	-0.0012	0.0030	39.	-629.	1660.

TABLE A-2 (Continued)

Test Point No.	Run No.	Point of Run	Left N_p RPM	Right N_p RPM	Left β_1 Deg.	Left β_0 Deg.	Right β_1 Deg.	Right β_0 Deg.	Tail i_t Deg.	δ_f Deg.	Baro. in. Hg	To °F	Left $N_{.385}$ % RPM	Right $N_{.385}$ % RPM	Average V_p/V_{tip}	q/qc
412	I-14	42	1100	1130	45	45	45	45	0	30	30.00	102	83.0	84.0	0.5703	1.026
413		43	1080	1125											0.5768	1.030
414	I-15	1	1735	1735	0	0	0	0	4	60	30.02	67	87.0	88.0	0.0665	N/A
415		2	1690	1710	20	20	20	20				72			0.0749	
416		3	1740	1780	35	35	35	35				74			0.0764	
417		4	1700	1715	0	0	0	0				80	87.5	88.5	0.1120	
418		5	1695	1710								82			0.1090	
419		6	1695	1705								83			0.1093	
420		7	1735	1735								85		89.0	0.2253	
421		8	1740	1735								86		89.0	0.2236	
422		9	1695	1695								87	86.5	88.5	0.2997	
423		10	1685	1685								87			0.3015	
424		11	1685	1690	20	20	20	20				87			0.2956	
425		12	1700	1715	35	35	35	35				88			0.2938	
426		13	1675	1675	0	0	0	0				90			0.2989	
427		14	1660	1690											0.2982	
428		15	1705	1795									87.0	82.5	0.2937	
429		16	1380	1410									79.5	81.0	0.3569	
430		17	1380	1390										80.5	0.3662	
431		18	1380	1405	20	20	20	20							0.3609	
432		19	1380	1405	35	35	35	35					79.0		0.3625	
433		20	1400	1410	0	0	0	0				91	80.0	75.5	0.3546	
434		21	1415	1405										75.0	0.3551	
435		22	1435	1400											0.3548	
436		23	1375	1400									77.0		0.3557	
437		24	1410	1410									80.0	81.0	0.2636	
438		25	1405	1415	20	20	20	20							0.2659	
439		26	1450	1440	35	35	35	35							0.2612	

Test Point No.	Run No.	PT AVG	ALPHA	BETA	Q V,NOM	LIFT,U CL*QS	DRAG,U CD*QS	M,U CM*QSC	CL CY	CD CN	CM CROLL	SIDE F,U CY*QS	YAW,U CN*QSB	ROLL,U CL*QSB
412	I-14	42	10.00	-0.	33.19	13202.	2584.	-19610.	0.8337	0.1827	-0.1212	48.	-765.	2124.
		5			167.08	13202.	2584.	-19610.	0.0034	-0.0014	0.0039	48.	-765.	2124.
413		43	12.00	-0.	33.31	14471.	3019.	-21896.	1.0208	0.2128	-0.1349	56.	-877.	1663.
		5			167.37	14471.	3019.	-21896.	0.0040	-0.0016	0.0030	56.	-877.	1663.
414	I-15	1	0.	-0.	1.16	5855.	801.	-991.	11.8195	1.6168	-0.1748	-134.	2132.	1614.
		5			31.27	5855.	801.	-991.	-0.2708	0.1114	0.0843	-134.	2132.	1614.
415		2	0.	-0.	1.40	5490.	-1380.	1354.	9.2358	-2.3209	0.1991	-32.	535.	-1538.
		5			34.26	5490.	-1380.	1354.	-0.0545	0.0233	-0.0670	-32.	535.	-1538.
416		3	0.	-0.	1.55	4376.	-2467.	2866.	6.6267	-3.7349	0.3793	22.	-324.	-327.
		5			36.11	4376.	-2467.	2866.	0.0338	-0.0127	-0.0128	22.	-324.	-327.
417		4	-4.00	-0.	3.10	5507.	819.	19792.	4.1688	0.6197	1.3097	-67.	1084.	602.
		5			51.07	5507.	819.	19792.	-0.0557	0.0212	0.0118	-67.	1084.	602.
418		5	-2.00	-0.	2.91	6445.	1033.	1976.	5.2045	0.8338	0.1395	-41.	650.	151.
		5			49.45	6445.	1033.	1976.	-0.0331	0.0136	0.0032	-41.	650.	151.
419		6	0.	-0.	2.91	6568.	1237.	1423.	5.3634	0.9989	0.1287	-19.	287.	768.
		5			49.45	6568.	1237.	1423.	-0.0155	0.0060	0.0161	-19.	287.	768.
420		7	-4.00	-0.	12.76	7952.	2502.	12480.	1.4631	0.4603	0.2007	40.	-680.	-3674.
		5			103.59	7952.	2502.	12480.	0.0075	-0.0042	-0.0175	40.	-680.	-3674.
421		8	0.	-0.	12.57	9025.	2690.	10956.	1.6854	0.5026	0.1789	35.	-598.	-2605.
		5			102.81	9025.	2690.	10956.	0.0066	-0.0029	-0.0126	35.	-598.	-2605.
422		9	-4.00	-0.	21.39	8703.	3235.	17142.	0.9553	0.3551	0.1645	-60.	942.	-1417.
		5			134.11	8703.	3235.	17142.	-0.0066	0.0027	-0.0040	-60.	942.	-1417.
423		10	0.	-0.	21.39	10776.	3310.	13974.	1.1829	0.3633	0.1341	-110.	1716.	-159.
		5			134.11	10776.	3310.	13974.	-0.0121	0.0049	-0.0005	-110.	1716.	-159.
424		11	0.	-0.	20.62	10163.	1817.	13035.	1.1575	0.2069	0.1297	-40.	609.	-3501.
		5			131.69	10163.	1817.	13035.	-0.0045	0.0018	-0.0103	-40.	609.	-3501.
425		12	0.	-0.	20.81	9532.	1078.	8802.	1.0751	0.1216	0.0868	-131.	2075.	-1955.
		5			132.30	9532.	1078.	8802.	-0.0148	0.0061	-0.0057	-131.	2075.	-1955.
426		13	4.00	-0.	20.66	12557.	3437.	9008.	1.4269	0.3905	0.0895	-128.	1951.	-363.
		5			131.81	12557.	3437.	9008.	-0.0145	0.0057	-0.0011	-128.	1951.	-363.
427		14	8.00	-0.	21.19	14768.	3633.	7089.	1.6356	0.4023	0.0686	-164.	2460.	970.
		5			133.51	14768.	3633.	7089.	-0.0182	0.0071	0.0028	-164.	2460.	970.
428		15	10.00	-0.	21.77	14400.	3442.	-7078.	1.5529	0.3711	-0.0667	-555.	5307.	3423.
		5			135.31	14400.	3442.	-7078.	-0.0383	0.0148	0.0096	-355.	5307.	3423.
429		16	-4.00	-0.	20.45	6450.	2633.	14307.	0.7412	0.3025	0.1437	-61.	966.	-1781.
		5			131.08	6450.	2633.	14307.	-0.0077	0.0029	-0.0053	-61.	966.	-1781.
430		17	0.	-0.	21.19	8452.	2505.	9754.	0.9361	0.2774	0.0944	-97.	1512.	1332.
		5			133.51	8452.	2505.	9754.	-0.0107	0.0043	0.0038	-97.	1512.	1332.
431		18	0.	-0.	20.81	8051.	1488.	7654.	0.8681	0.1904	0.0755	-112.	1760.	500.
		5			132.30	8051.	1488.	7654.	-0.0126	0.0051	0.0015	-112.	1760.	500.
432		19	0.	-0.	21.00	7650.	1226.	4300.	0.8550	0.1370	0.0420	-43.	670.	-993.
		5			132.91	7650.	1226.	4300.	-0.0048	0.0019	-0.0029	-43.	670.	-993.
433		20	4.00	-0.	20.62	9443.	2308.	-3418.	1.0750	0.2627	-0.0340	-342.	5299.	2992.
		5			131.69	9443.	2308.	-3418.	-0.0589	0.0156	0.0088	-342.	5299.	2992.
434		21	8.00	-0.	20.81	11320.	2646.	-2767.	1.2768	0.2984	-0.0766	-375.	5686.	3848.
		5			132.30	11320.	2646.	-2767.	-0.0423	0.0166	0.0112	-375.	5686.	3848.
435		22	10.00	-0.	21.00	12022.	2826.	-9261.	1.3437	0.3158	-0.0905	-311.	4656.	4642.
		5			132.91	12022.	2826.	-9261.	-0.0348	0.0135	0.0134	-311.	4656.	4642.
436		23	12.00	-0.	21.00	12250.	3047.	-13340.	1.3692	0.3406	-0.1303	-170.	2490.	5289.
		5			132.91	12250.	3047.	-13340.	-0.0196	0.0072	0.0153	-170.	2490.	5289.
437		24	0.	-0.	11.42	6749.	2084.	9407.	1.3819	0.4285	0.1511	-70.	1096.	-420.
		5			97.99	6749.	2084.	9407.	-0.0145	0.0058	-0.0022	-70.	1096.	-420.
438		25	0.	-0.	11.41	6515.	1074.	8445.	1.5174	0.2173	0.1493	4.	-79.	-2479.
		5			98.81	6515.	1074.	8445.	0.0008	-0.0004	-0.0130	4.	-79.	-2479.
439		26	0.	-0.	11.41	5910.	410.	6593.	1.1951	0.0829	0.1165	2.	-32.	-1762.
		5			98.81	5910.	410.	6593.	0.0003	-0.0002	-0.0092	2.	-32.	-1762.

TABLE A-2 (Continued)

Test Point No.	Run No.	Points of Run	Left N_p RPM	Right N_p RPM	Left β_t Deg.	Left β_0 Deg.	Right β_t Deg.	Right β_0 Deg.	Tail i_t Deg.	δ_f Deg.	Baro in. Hg	To °F	Left N_{305} % RPM	Right N_{305} % RPM	Average V_p/V_{tip}	q/qc
440	I-15	27	1395	1400	0	0	0	0	0	60	30.02	92	80.0	81.0	0.2246	N/A
441		28	1395	1395	0	0	0	0				92	80.5		0.2249	
442		29	1400	1410	20	20	20	20				93			0.2365	
443		30	1425	1435	35	35	35	35							0.2324	
444		31	1400	1405	0	0	0	0							0.2208	
445		32	1395	1415											0.2289	
446		33	1395	1425											0.2281	
447		34	1390	1450									80.0		0.2238	
448		35	1187	1187									74.0	74.0	0.1631	
449		36	1190	1190								94			0.1679	
450		37	1190	1190	20	20	20	20	4						0.1679	
451		38	1215	1225	35	35	35	35							0.1638	
452		39	1180	1180	0	0	0	0				95			0.1682	
453		40	1190	1190											0.1557	
454		41	1190	1190											0.1681	
455		42	1185	1195										74.5	0.1681	
456		43	1180	1190									73.5	74.0	0.1637	
457		44	1175	1195											0.1637	
458		45	1170	1210											0.1579	
459		46	1160	1240											0.1565	
460		47	1165	1185									73.0	70.0	0.1651	
461		48	1100	1100									71.5	70.1	0.1097	
462		49	1100	1100									71.5	70.1	0.1166	
463		50	1110	1100									72.0	71.0	0.1166	
464		51	1110	1110	20	20	20	20					72.0		0.1235	
465		52	1135	1135	35	35	35	35					71.5		0.1281	
466		53	1120	1110	0	0	0	0				96	72.0		0.0754	
467		54	1130	1110	0	0	0	0				96	72.0	71.5	0.0866	

Test Point No.	Run No.	PT AVG	ALPHA	BETA	Q V,NOM	LIFT,U CL*QS	DRAG,U CD*QS	M,U CM*QSC	CL CY	CD CN	CM CROLL	SIDE F,U CY*QS	YAW,U CN*QSB	ROLL,U CL*QSB
440	I-15	27	-4.00	-0.	8.14	5104.	1602.	7747.	1.4719	0.4620	0.1953	-2.	14.	-2462.
		5			82.74	5104.	1602.	7747.	-0.0016	0.0001	-0.0184	-2.	14.	-2462.
441		28	0.	-0.	8.14	5969.	1801.	6324.	1.6926	0.5193	0.1594	13.	-227.	-490.
		5			82.74	5869.	1861.	6324.	0.0037	-0.0017	-0.0037	13.	-227.	-490.
442		29	0.	-0.	9.11	5922.	804.	7824.	1.5262	0.2673	0.1763	21.	-344.	-2371.
		5			87.53	5922.	804.	7824.	0.0054	-0.0023	-0.0158	21.	-344.	-2371.
443		30	0.	-0.	9.11	5322.	154.	6206.	1.3716	0.0396	0.1398	-10.	163.	-3255.
		5			87.53	5322.	154.	6206.	-0.0027	0.0011	-0.0217	-10.	163.	-3255.
444		31	4.00	-0.	7.91	6666.	1920.	5204.	1.9799	0.5708	0.1351	37.	-598.	-2554.
		5			81.55	6666.	1920.	5204.	0.0169	-0.0046	-0.0196	37.	-598.	-2554.
445		32	8.00	-0.	8.53	7950.	2248.	3945.	2.1885	0.6188	0.0949	1.	-40.	-1055.
		5			84.69	7950.	2248.	3945.	0.0002	-0.0003	-0.0075	1.	-40.	-1055.
446		33	10.00	-0.	8.53	8348.	2398.	3584.	2.2982	0.6600	0.0862	-11.	132.	-832.
		5			84.69	8348.	2398.	3584.	-0.0021	0.0009	-0.0059	-11.	132.	-832.
447		34	12.00	-0.	8.33	8617.	2555.	3111.	2.4274	0.7197	0.0766	1.	-44.	-1006.
		5			83.72	8617.	2555.	3111.	0.0002	-0.0005	-0.0073	1.	-44.	-1006.
448		35	-4.00	-0.	3.10	3361.	833.	2991.	2.5446	0.6303	0.1979	-6.	87.	397.
		5			51.07	3361.	833.	2991.	-0.0049	0.0017	0.0078	-6.	87.	397.
449		36	0.	-0.	3.29	3788.	987.	2975.	2.6993	0.7032	0.1853	41.	-668.	-340.
		5			52.64	3788.	987.	2975.	0.0292	-0.0123	-0.0043	41.	-668.	-340.
450		37	0.	-0.	3.29	3421.	110.	3409.	2.8376	0.0785	0.2123	6.	-105.	-1257.
		5			52.64	3421.	110.	3409.	0.0046	-0.0019	-0.0232	6.	-105.	-1257.
451		38	0.	-0.	3.29	2879.	-387.	3592.	2.0512	-0.2758	0.2237	-26.	453.	-1446.
		5			52.64	2879.	-387.	3592.	-0.020	0.0084	-0.0267	-26.	453.	-1446.
452		39	2.00	-0.	2.52	3533.	907.	1858.	3.5166	0.8455	0.1516	1.	-23.	-301.
		5			44.03	3533.	907.	1858.	0.0007	-0.0006	-0.0073	1.	-23.	-301.
453		40	4.00	-0.	2.83	3870.	1067.	2241.	3.2107	0.8854	0.1625	-5.	-12.	-612.
		5			48.78	3870.	1067.	2241.	-0.0002	-0.0002	-0.0131	-5.	-12.	-612.
454		41	6.00	-0.	3.29	4153.	1247.	2801.	2.9592	0.8882	0.1745	31.	-501.	241.
		5			52.64	4153.	1247.	2801.	0.0224	-0.0092	0.0044	31.	-501.	241.
455		42	8.00	-0.	3.29	4304.	1320.	1868.	3.0669	0.9402	0.1164	15.	-248.	-195.
		5			52.64	4304.	1320.	1868.	0.0108	-0.0046	-0.0036	15.	-248.	-195.
456		43	10.00	-0.	3.10	4396.	1421.	1766.	3.3276	1.0757	0.1169	-7.	86.	-374.
		5			51.07	4396.	1421.	1766.	-0.0059	0.0017	-0.0073	-7.	86.	-374.
457		44	12.00	-0.	3.10	4506.	1536.	1539.	3.4112	1.1625	0.1019	-17.	227.	-358.
		5			51.07	4506.	1536.	1539.	-0.0125	0.0044	-0.0070	-17.	227.	-358.
458		45	14.00	-0.	2.91	4573.	1680.	1793.	3.6929	1.3567	0.1266	-45.	642.	-7.
		5			49.45	4573.	1680.	1793.	-0.0362	0.0134	-0.0061	-45.	642.	-7.
459		46	16.00	-0.	2.91	4784.	1766.	-31.	3.8654	1.4264	-0.0022	-23.	317.	-49.
		5			49.45	4784.	1766.	-31.	-0.0164	0.0066	-0.0010	-23.	317.	-49.
460		47	18.00	-0.	3.10	4753.	1808.	-787.	3.5981	1.3685	-0.0521	35.	-532.	1003.
		5			51.07	4753.	1808.	-787.	0.0267	-0.0104	0.0197	35.	-532.	1003.
461		48	-4.00	-0.	1.20	2555.	360.	370.	4.9912	0.7038	0.0632	-13.	203.	1473.
		5			31.79	2555.	360.	370.	-0.0249	0.0103	0.0745	-13.	203.	1473.
462		49	-2.00	-0.	1.36	2728.	492.	1091.	4.7198	0.8518	0.1650	-14.	222.	60.
		5			33.78	2728.	492.	1091.	-0.0245	0.0100	0.0027	-14.	222.	60.
463		50	0.	-0.	1.36	2783.	580.	686.	4.8153	1.0029	0.1037	-21.	326.	49.
		5			33.78	2783.	580.	686.	-0.0361	0.0146	0.0022	-21.	326.	49.
464		51	0.	-0.	1.55	2560.	-266.	1331.	3.8754	-0.4023	0.1762	-10.	161.	-1014.
		5			36.11	2560.	-266.	1331.	-0.0149	0.0063	-0.0397	-10.	161.	-1014.
465		52	0.	-0.	1.74	2123.	-600.	2110.	2.857	-0.8078	0.2482	-1.	27.	-117.
		5			38.30	2123.	-600.	2110.	-0.0016	0.0039	-0.0041	-1.	27.	-117.
466		53	2.00	-0.	0.58	2473.	458.	-1027.	9.9856	1.8479	-0.3624	-18.	286.	292.
		5			22.11	2473.	458.	-1027.	-0.0746	0.0299	0.0306	-18.	286.	292.
467		54	4.00	-0.	0.78	2617.	591.	-961.	7.9253	1.7900	-0.2544	-18.	281.	29.
		5			25.53	2617.	591.	-961.	-0.0560	0.0220	0.0023	-18.	281.	29.

TABLE A-2 (Continued)

Test Point No.	Run No.	Point of Run	Left N_p RPM	Right N_p RPM	Left β_1 Deg.	Left β_0 Deg.	Right β_1 Deg.	Right β_0 Deg.	Tail i_t Deg.	δ_f Deg.	Baro. in. Hg	To °F	Left N_{J85} % RPM	Right N_{J85} % RPM	Average V_p/V_{tip}	q/qc
468	I-15	55	1100	1115	0	0	0	0	4	60	30.02	96	71.0	71.5	0.1159	N/A
469		56	1110	1115											0.1234	
470		57	1110	1115											0.1218	
471		58	1112	1112											0.1154	
472		59	1114	1114											0.1152	
473		60	1110	1110									71.5		0.1071	
474		61	1210	1190					4			97	74.5	74.0	0.1853	
475		62	1200	1180					8						0.1631	
476		63	1200	1180					12						0.1526	
477		64	1200	1180					16						0.1631	
478		65	1205	1180					20						0.1634	
479	I-16	1	0	0	35	35	35	35	0	60	30.12	74	0	0	N/A	N/A
480		2														
481		3														
482		4														
483		5														
484		6														
485		7														
486		8														
487		9														
488		10														
489		11														
490		12														
491		13			90	90	90	90								
492		14														
493		15														
494		16														
495		17							4							

Test Point No.	Run No.	PT AVG	ALPHA	BETA	Q V,NOM	LIFT,U CL*QS	DRAG,U CD*QS	M,U CM*QSC	CL CY	CD CN	CM CROLL	SIDE F,U CY*QS	YAW,U CN*QSB	ROLL,U CL*QSB
468	I-15	55	6.00	-0.	1.36	2944.	785.	645.	5.0935	1.3576	3.3976	0.	-14.	-111.
		5			33.78	2944.	785.	645.	0.0004	-0.0006	-0.0050	0.	-14.	-111.
469		56	8.00	-0.	1.55	3088.	904.	441.	4.6740	1.3688	0.0584	-35.	519.	-491.
		5			36.11	3088.	904.	441.	-0.0527	0.0205	-0.0192	-35.	519.	-491.
470		57	10.00	-0.	1.61	3150.	1003.	495.	4.8916	1.4575	0.3672	-0.	-9.	-1250.
		5			35.66	3150.	1003.	495.	-0.0004	-0.0004	-0.0503	-0.	-9.	-1250.
471		58	12.00	-0.	1.36	3150.	1095.	154.	5.4837	1.8955	0.0283	-5.	54.	143.
		5			33.78	3150.	1095.	154.	-0.0077	0.0024	0.0044	-5.	54.	143.
472		59	14.00	-0.	1.36	3172.	1190.	-66.	5.488	2.0662	-0.0099	-18.	257.	352.
		5			33.78	3172.	1190.	-66.	-0.0324	0.0115	0.0158	-18.	257.	352.
473		60	16.00	-0.	1.16	3179.	1285.	-391.	6.4172	2.5942	-0.0690	-17.	232.	751.
		5			31.27	3179.	1285.	-391.	-0.0344	0.0121	0.0393	-17.	232.	751.
474		61	0.	-0.	4.07	3976.	1092.	3197.	2.2031	0.8299	0.1612	52.	-846.	-789.
		5			58.51	3976.	1092.	3197.	0.0301	-0.0126	-0.0118	52.	-846.	-789.
475		62	0.	-0.	3.10	3697.	1010.	1722.	2.7989	0.7646	0.1140	38.	-615.	-1330.
		5			51.07	3697.	1010.	1722.	0.0285	-0.0121	-0.0261	38.	-615.	-1330.
476		63	0.	-0.	2.71	3685.	923.	-192.	3.1884	0.7987	-0.0145	4.	-69.	-147.
		5			47.77	3685.	923.	-192.	0.0031	-0.0016	-0.0033	4.	-69.	-147.
477		64	0.	0.	3.10	3863.	988.	-1798.	2.9243	0.7479	-0.1190	17.	-285.	-754.
		5			51.07	3863.	988.	-1798.	0.0129	-0.0056	-0.0168	17.	-285.	-754.
478		65	0.	-0.	3.10	3947.	1014.	-3778.	2.9876	0.7758	-0.2500	22.	-376.	276.
		5			51.07	3947.	1014.	-3778.	0.0164	-0.0072	0.0056	22.	-376.	276.
479	I-16	1	-3.81	-0.	5.23	448.	274.	-1629.	0.2008	0.1246	-0.0590	6.	-166.	78.
		5			66.34	448.	278.	-1505.	0.0027	-0.0019	0.0009	6.	-166.	78.
480		2	0.47	-0.	5.23	1139.	316.	-2930.	0.5109	0.1458	-0.1625	-4.	-110.	210.
		5			66.34	1139.	325.	-2615.	-0.0016	-0.0015	0.0024	-4.	-110.	210.
481		3	4.75	-0.	5.23	1816.	383.	-4195.	0.8145	0.1826	-0.1448	-2.	91.	340.
		5			66.34	1816.	407.	-3693.	-0.0008	0.0011	0.0040	-2.	91.	340.
482		4	9.02	-0.	5.16	2435.	472.	-4902.	1.1087	0.2345	-0.1683	4.	49.	269.
		5			65.85	2435.	515.	-4228.	0.0019	0.0006	0.0032	4.	49.	269.
483		5	11.18	-0.	5.04	2744.	530.	-5627.	1.2785	0.2731	-0.1982	5.	5.	161.
		5			65.10	2744.	586.	-4868.	0.0015	0.0001	0.0019	5.	5.	161.
484		6	13.28	-0.	5.04	2965.	606.	-5779.	1.3814	0.3130	-0.2019	10.	49.	-121.
		5			65.10	2965.	672.	-4959.	0.0041	0.0006	-0.0015	10.	49.	-121.
485		7	15.22	-0.	5.04	2838.	838.	-5563.	1.3221	0.4165	-0.1946	42.	-436.	-1355.
		5			65.10	2838.	898.	-4778.	0.0193	-0.0053	-0.0163	42.	-436.	-1355.
486		8	17.15	-0.	5.04	2665.	1005.	-5974.	1.2416	0.4932	-0.2133	24.	183.	-838.
		5			65.10	2665.	1059.	-5237.	0.0113	0.0022	-0.0101	24.	183.	-838.
487		9	-3.80	-0.	11.61	1050.	623.	-3071.	0.2123	0.1268	-0.0492	12.	-376.	-949.
		5			98.81	1050.	627.	-2781.	0.0024	-0.0020	-0.0050	12.	-376.	-949.
488		10	0.47	-0.	11.80	2543.	703.	-6515.	0.5059	0.1440	-0.1011	23.	-432.	-751.
		5			99.62	2543.	724.	-5811.	0.0045	-0.0022	-0.0039	23.	-432.	-751.
489		11	4.75	-0.	11.61	4021.	839.	-9048.	0.8132	0.1803	-0.1403	18.	-343.	-14.
		5			98.81	4021.	891.	-7937.	0.0035	-0.0018	-0.0021	18.	-343.	-14.
490		12	9.02	-0.	11.61	5480.	1065.	-11659.	1.1083	0.2351	-0.1758	18.	-199.	-540.
		5			98.81	5480.	1163.	-9943.	0.0035	-0.0010	-0.0028	18.	-199.	-540.
491		13	11.15	-0.	11.42	6068.	1195.	-12687.	1.2476	0.2708	-0.1979	43.	-436.	-428.
		5			97.99	6068.	1317.	-11009.	0.0089	-0.0023	-0.0023	43.	-436.	-428.
492		14	13.23	-0.	11.61	6613.	1385.	-12787.	1.3373	0.3089	-0.1937	39.	-414.	-1520.
		5			98.81	6613.	1527.	-10959.	0.0079	-0.0022	-0.0080	39.	-414.	-1520.
493		15	15.22	-0.	11.42	6407.	1779.	-13335.	1.3174	0.3937	-0.2078	22.	104.	-6636.
		5			97.99	6407.	1915.	-11564.	0.0046	0.0006	-0.0353	22.	104.	-6636.
494		16	17.19	-0.	11.42	6270.	2173.	-13926.	1.2892	0.4736	-0.2191	-13.	988.	-5794.
		5			97.99	6270.	2303.	-12193.	-0.0026	0.0053	-0.0338	-13.	988.	-5794.
495		17	0.59	-0.	11.80	5198.	786.	-7207.	0.6362	0.1628	-0.1100	-9.	-551.	805.
		5			99.62	5198.	818.	-6323.	-0.0019	-0.0028	0.0041	-9.	-551.	805.

TABLE A-2 (Continued)

Test Point No.	Run No.	Point of Run	Left N_p RPM	Right N_p RPM	Left β_1 Deg.	Left β_2 Deg.	Right β_1 Deg.	Right β_2 Deg.	Tail i_t Deg.	δ_f Deg.	Baro. in. Hg	To $^\circ_F$	Left N_{J85} % RPM	Right N_{J85} % RPM	Average V_p/V_{tip}	q/qc
496	I-16	18	0	0	90	90	90	90	8	60	30.12	74	0	0	N/A	N/A
497		19							12							
498		20							16							
499		21							20							
500		22							0							
501		23														
502		24														
503		25														
504		26														
505		27														
506		28														
507		29														
508	I-17	1	0	0	90	90	90	90	4	30	30.08	77	0	0	N/A	N/A
509		2														
510		3														
511		4														
512		5														
513		6														
514		7														
515		8														
516		9														
517		10														
518	I-18	1	2400	2450	35	35	35	35	4	30	30.08	83	99.0	100.0	0.0306	N/A
519		2			20	20	20	20							0.0362	
520		3			10	10	10	10							0.0324	
521		4			0	0	0	0				84			-	
522		5	1690	1690	0	0	0	0				72	87.0	87.0	0.1503	
523		6	1675	1695	0	0	0	0				75	87.0	87.5	0.1453	

Test Point No.	Run No.	Pt AVG	ALPHA	BETA	Q V,NOM	LIFT,U CL*QS	DRAG,U CD*QS	M,U CM*QSC	CL CY	CD CN	CM CROLL	SIDE F,U CY*QS	YAW,U CN*QSB	ROLL,U CL*QSB
496	I-16	18	0.84	-0.	11.61	3433.	800.	-11706.	0.6943	0.1696	-0.1901	5.	-797.	392.
		5			98.81	3433.	839.	-10756.	0.0506	-0.0042	0.0021	5.	-797.	392.
497		19	0.70	-0.	11.61	3731.	838.	-18131.	0.7545	0.1787	-0.3023	14.	-569.	101.
		5			98.81	3731.	884.	-17399.	0.0028	-0.0030	0.0005	14.	-569.	101.
498		20	0.76	-0.	11.61	4076.	911.	-25494.	0.8243	0.1952	-0.4307	2.	-366.	182.
		5			98.81	4076.	965.	-24367.	0.0003	-0.0019	0.0010	2.	-366.	182.
499		21	0.80	-0.	11.61	4273.	1001.	-30111.	0.8641	0.2144	-0.5114	-10.	-628.	1159.
		5			98.81	4273.	1060.	-28929.	-0.0020	-0.0035	0.0061	-10.	-628.	1159.
500		22	-3.66	-0.	11.62	1792.	717.	-4860.	0.3684	0.1496	-0.0785	-1.	-622.	548.
		5			97.99	1792.	728.	-4365.	-0.0032	-0.0035	0.0029	-1.	-622.	548.
501		23	0.59	-0.	11.61	3179.	783.	-7108.	0.6428	0.1649	-0.1101	-4.	-701.	582.
		5			98.81	3179.	816.	-6229.	-0.0007	-0.0037	0.0030	-4.	-701.	582.
502		24	4.84	-0.	11.61	4487.	918.	-9365.	0.9073	0.1990	-0.1436	15.	-697.	976.
		5			98.81	4487.	984.	-8125.	0.0051	-0.0036	0.0051	15.	-697.	976.
503		25	9.10	-0.	11.62	5778.	1112.	-11564.	1.1891	0.2513	-0.1791	9.	-267.	283.
		5			97.99	5778.	1222.	-9986.	0.0018	-0.0014	0.0015	9.	-267.	283.
504		26	11.20	-0.	11.61	6455.	1241.	-13276.	1.3054	0.2823	-0.2051	2.	-182.	31.
		5			98.81	6455.	1396.	-11492.	0.0003	-0.0010	0.0002	2.	-182.	31.
505		27	13.31	-0.	11.61	7031.	1432.	-13815.	1.4216	0.3222	-0.2098	16.	-48.	-471.
		5			98.81	7031.	1593.	-11871.	0.0033	-0.0003	-0.0025	16.	-48.	-471.
506		28	15.28	-0.	11.61	6865.	1884.	-12545.	1.3883	0.4119	-0.1882	73.	-851.	-4808.
		5			98.81	6865.	2057.	-10646.	0.0147	-0.0045	-0.0252	73.	-851.	-4808.
507		29	17.20	-0.	11.62	6330.	2245.	-15514.	1.3016	0.4888	-0.2474	12.	1215.	-5760.
		5			97.99	6330.	2377.	-13764.	0.0024	0.0065	-0.0307	12.	1215.	-5760.
508	I-17	1	-3.75	-0.	11.54	965.	441.	-4121.	0.2734	0.1262	-0.0868	7.	-186.	333.
		5			98.53	965.	446.	-3829.	0.0019	-0.0021	0.0038	7.	-186.	333.
509		2	0.45	-0.	11.54	1721.	532.	-5170.	0.4876	0.1544	-0.1054	12.	-183.	100.
		5			98.53	1721.	545.	-4650.	0.0035	-0.0021	0.0011	12.	-183.	100.
510		3	4.65	-0.	11.35	2431.	642.	-6340.	0.7006	0.1929	-0.0831	4.	-10.	404.
		5			97.71	2431.	669.	-5605.	0.0011	-0.0001	0.0047	4.	-10.	404.
511		4	8.78	-0.	11.54	2998.	790.	-762.	0.8494	0.2355	0.0033	-1.	39.	563.
		5			98.53	2998.	831.	143.	-0.0006	0.0005	0.0064	-1.	39.	563.
512		5	10.88	-0.	11.62	3391.	892.	-715.	0.9546	0.2659	0.0070	-11.	113.	584.
		5			98.86	3391.	945.	311.	-0.0030	0.0013	0.0066	-11.	113.	584.
513		6	12.99	-0.	11.74	3852.	1039.	-3252.	1.0737	0.3081	-0.0466	-1.	-121.	751.
		5			99.35	3852.	1105.	-2088.	-0.0004	-0.0014	0.0085	-1.	-121.	751.
514		7	15.14	-0.	11.39	4313.	1224.	-7155.	1.2386	0.3763	-0.1344	1.	-2.	201.
		5			97.88	4313.	1310.	-5852.	0.0004	-0.0030	0.0023	1.	-2.	201.
515		8	17.25	-0.	11.54	4798.	1460.	-10813.	1.3595	0.4434	-0.2123	20.	-130.	434.
		5			98.53	4798.	1565.	-9163.	0.0056	-0.0015	0.0050	20.	-130.	434.
516		9	19.36	-0.	11.35	5119.	1714.	-12968.	1.4751	0.5288	-0.2633	48.	-137.	39.
		5			97.71	5119.	1835.	-11422.	0.0141	-0.0016	0.0005	48.	-137.	39.
517		10	21.43	-0.	11.35	5383.	2043.	-15134.	1.5512	0.6275	-0.3114	67.	-523.	503.
		5			97.71	5383.	2178.	-13508.	0.0192	-0.0061	0.0059	67.	-523.	503.
518	I-18	1	0.	-0.	0.48	7338.	-5887.	-1185.	49.5437	-39.7484	-0.6400	-118.	1184.	-2955.
		10			20.19	7338.	-5887.	-1185.	-0.7972	0.5228	-0.8056	-118.	1184.	-2955.
519		2	0.	-0.	0.68	9590.	-3544.	-2312.	46.2508	-17.0925	-0.8922	-303.	-398.	1694.
		10			25.88	9590.	-3544.	-2312.	-1.4631	-0.0775	0.3298	-303.	-398.	1694.
520		3	0.	-0.	0.54	10331.	-1972.	-8265.	62.2769	-11.8873	-5.9861	-197.	-819.	-2963.
		10			21.36	10331.	-1972.	-8265.	-1.1849	-0.1994	-0.7211	-197.	-819.	-2963.
521		4	0.	-0.	1.00	11010.	-532.	-11679.	36.0157	-1.7413	-3.0562	-144.	-182.	-485.
		10			0.	11010.	-532.	-11679.	-0.4718	-0.0240	-0.0640	-144.	-182.	-485.
522		5	-4.00	-0.	5.56	6114.	1296.	7416.	3.5958	0.7620	0.3489	13.	-2307.	-1797.
		10			68.40	6114.	1296.	7416.	0.0075	-0.0548	-0.0627	13.	-2307.	-1797.
523		6	0.	-0.	5.14	6460.	1562.	6418.	4.1144	0.9951	0.3270	-82.	-1194.	-2138.
		5			65.72	6460.	1562.	6418.	-0.0521	-0.0307	-0.0550	-82.	-1194.	-2138.

TABLE A-2 (Continued)

Test Point No.	Run No.	Point of Run	Left N_y RPM	Right N_y RPM	Left β_t Deg.	Left β_b Deg.	Right β_t Deg.	Right β_b Deg.	Tail i_t Deg.	δ_f Deg.	Baro. in. Hg	To °F	Left N_{J85} % RPM	Right N_{J85} % RPM	Average V_p/V_{tip}	q/qc
524	I-18	7	1675	1690	20	20	20	20	4	30	30.08	76	86.5	87.5	0.1633	N/A
525		8	1690	1680	35	35	35	35				77	86.5	86.5	0.1600	
526		9	1695	1690	0	0	0	0				78	87.0	87.5	0.1623	
527		10	1695	1685								79		87.5	0.1656	
528		11	1695	1685								80		88.0	0.1628	
529		12	1695	1685								80			0.1628	
530		13	1705	1695								82			0.2160	
531		14	1710	1700								83			0.2185	
532		15	1700	1700	20	20	20	20							0.2265	
533		16	1735	1725	35	35	35	35							0.2209	
534		17	1720	1700	0	0	0	0				84			0.2254	
535		18	1725	1710								85	87.5		0.2176	
536		19	1715	1700									87.0		0.2153	
537		20	1720	1705									87.5		0.2187	
538		21	1725	1700								86			0.2203	
539		22	1720	1700								86			0.2188	
540		23	1195	1190								85	73.5	73.0	0.3138	
541		24	1195	1185									73.5	73.0	0.3167	
542		25	1195	1170	20	20	20	20					73.0	72.5	0.3109	
543		26	1188	1210	35	35	35	35					73.0	72.5	0.3066	
544		27	1200	1170	0	0	0	0					73.5	73.0	0.3256	
545		28	1190	1175										72.5	0.3263	
546		29	1185	1165											0.3258	
547		30	1180	1165								86			0.3253	
548		31	1178	1162											0.3224	
549		32	1182	1165											0.3215	
550	I-19	1	1450	1450	0	0	0	0	4	30	30.11	72	Not Recorded		0.3809	1.013
551		2	1450	1460	0	0	0	0				73			0.3800	1.013
552		3	1460	1470	20	20	20	20				74			0.3803	1.020

Test Point No.	Run No.	PT AVG	ALPHA	BETA	Q V,NOM	LIFT,U CL*QS	DRAG,U CD*QS	M,U CM*QSC	CL CY	CD CN	CM CROLL	SIDE F,U CY*QS	YAW,U CN*QSB	ROLL,U CL*QSB
524	I-18	7	0.	-0.	4.45	5602.	-258.	9171.	2.8850	-0.1309	0.3719	-30.	-1514.	-1353.
		5			73.67	5692.	-258.	9171.	-0.0150	-0.0310	-0.0277	-30.	-1514.	-1353.
525		8	-.	-0.	4.75	3726.	-1630.	9351.	2.5670	-1.1229	0.5154	-132.	784.	2002.
		5			63.19	3726.	-1630.	9351.	-0.0911	0.0212	0.0557	-132.	784.	2002.
526		9	4.00	-0.	4.94	6791.	1916.	5423.	4.4950	1.2686	0.2872	-214.	102.	-1474.
		5			64.47	6791.	1916.	5423.	-0.1419	0.0027	-0.0394	-214.	102.	-1474.
527		10	8.00	-0.	5.14	6995.	2364.	5195.	4.4553	1.5060	0.2647	-150.	-766.	-389.
		5			65.72	6995.	2364.	5195.	-0.0938	-0.0197	-0.0100	-150.	-766.	-389.
528		11	10.00	-0.	4.94	7091.	2519.	5336.	4.6936	1.6673	0.2826	-233.	163.	-2298.
		5			64.47	7091.	2519.	5336.	-0.1539	0.0043	-0.0614	-233.	163.	-2298.
529		12	12.00	-0.	4.94	7170.	2727.	5190.	4.7460	1.8052	0.2748	-290.	745.	-383.
		5			64.47	7170.	2727.	5190.	-0.1921	0.0199	-0.0102	-290.	745.	-383.
530		13	-4.00	-0.	11.36	6587.	2161.	12651.	1.8969	0.6224	0.2915	-179.	-374.	-2329.
		5			97.74	6587.	2161.	12651.	-0.0516	-0.0043	-0.0271	-179.	-374.	-2329.
531		14	0.	-0.	11.67	7144.	2479.	11866.	2.0032	0.6950	0.2662	-141.	-1164.	-1595.
		5			99.05	7144.	2479.	11866.	-0.0395	-0.0132	-0.0181	-141.	-1164.	-1595.
532		15	0.	-0.	12.47	6450.	759.	14958.	1.6918	0.1992	0.3139	-169.	-1095.	1186.
		5			102.41	6450.	759.	14958.	-0.0443	-0.0116	0.0126	-169.	-1095.	1186.
533		16	0.	-0.	12.28	5099.	-395.	14229.	1.3383	-0.1052	0.3032	-232.	353.	967.
		5			101.62	5099.	-395.	14229.	-0.0618	0.0038	0.0104	-232.	353.	967.
534		17	4.00	-0.	12.47	7789.	2831.	12248.	2.0431	0.7425	0.2570	-232.	874.	-1626.
		5			102.41	7789.	2831.	12248.	-0.0607	0.0093	-0.0172	-232.	874.	-1626.
535		18	8.00	-0.	11.10	8235.	3109.	12561.	2.3016	0.8688	0.2809	-207.	766.	-1294.
		5			99.21	8235.	3109.	12561.	-0.0579	0.0086	-0.0146	-207.	766.	-1294.
536		19	12.00	-0.	11.32	8782.	3483.	13353.	2.5377	1.0063	0.3087	-195.	786.	-927.
		6			97.57	8782.	3483.	13353.	-0.0562	0.0092	-0.0108	-195.	786.	-927.
537		20	14.00	-0.	11.74	9113.	3685.	15333.	2.5388	1.0259	0.3417	-155.	-98.	-1903.
		5			99.38	9113.	3685.	15333.	-0.0433	-0.0011	-0.0214	-155.	-98.	-1903.
538		21	16.00	-0.	11.90	9116.	3849.	17008.	2.5073	1.0584	0.3741	-522.	1468.	227.
		5			100.02	9118.	3849.	17005.	-0.0886	0.0163	0.0025	-522.	1468.	227.
539		22	18.00	-0.	11.70	9365.	4059.	18334.	2.6175	1.1345	0.4099	-241.	841.	1930.
		5			98.31	9368.	4059.	18334.	-0.0678	0.0095	0.0218	-241.	841.	1930.
540		23	-4.00	-0.	11.70	3601.	1611.	10532.	1.0065	0.4502	0.2355	-112.	635.	-1420.
		5			99.21	3601.	1611.	10532.	-0.0312	0.0071	-0.0160	-112.	635.	-1420.
541		24	0.	-0.	11.90	4276.	1731.	9143.	1.1764	0.4759	0.2011	-163.	1382.	-1404.
		5			100.02	4278.	1731.	9143.	-0.0449	0.0153	-0.0156	-163.	1382.	-1404.
542		25	0.	-0.	11.32	3786.	975.	9579.	1.0943	0.2818	0.2214	-174.	855.	218.
		5			97.57	3786.	975.	9579.	-0.0504	0.0100	0.0025	-174.	855.	218.
543		26	0.	-0.	11.52	3239.	478.	8857.	0.9359	0.1381	0.2047	-84.	-108.	214.
		5			97.57	3239.	478.	8857.	-0.0242	-0.0013	0.0025	-84.	-108.	214.
544		27	4.00	-0.	12.47	487	1870.	9355.	1.2789	0.4906	0.1963	-207.	1726.	-220.
		5			102.41	487	1870.	9355.	-0.0542	0.0183	-0.0023	-207.	1726.	-220.
545		28	8.00	-0.	12.47	526	1993.	11318.	1.3821	0.5227	0.2375	-280.	2127.	2155.
		5			102.41	526.	1993.	11318.	-0.0735	0.0225	0.0228	-280.	2127.	2155.
546		29	12.00	-0.	12.28	5759.	2121.	13189.	1.5361	0.5650	0.2815	-261.	703.	2155.
		5			101.62	5759.	2121.	13190.	-0.0695	0.0076	0.0232	-261.	703.	2155.
547		30	14.00	-0.	12.28	5968.	2281.	13982.	1.5898	0.6076	0.2980	-276.	1071.	2444.
		5			101.62	5968.	2281.	13982.	-0.0736	0.0115	0.0263	-276.	1071.	2444.
548		31	16.00	-0.	11.90	6172.	2373.	14870.	1.6971	0.6525	0.3271	-315.	966.	3035.
		5			100.02	6172.	2373.	14870.	-0.0865	0.0107	0.0537	-315.	966.	3035.
549		32	18.00	-0.	11.90	6436.	2519.	13847.	1.7697	0.6927	0.3046	-376.	1279.	2770.
		5			100.02	6436.	2519.	13847.	-0.1033	0.0142	0.0308	-376.	1279.	2770.
550	I-19	1	-4.00	-0.	26.56	6120.	3044.	18366.	0.7594	0.3802	0.1823	-247.	3220.	-806.
		6			148.90	6120.	3044.	18366.	-0.0306	0.0161	-0.0040	-247.	3220.	-806.
551		2	0.	-0.	26.36	7498.	3150.	14878.	0.9304	0.3909	0.1477	-355.	4816.	91.
		5			148.90	7498.	3150.	14878.	-0.0440	0.0241	0.0005	-355.	4816.	91.
552		3	0	-0.	26.55	7037.	2222.	14871.	0.8669	0.2737	0.1426	-370.	4422.	780.
		5			149.44	7037.	2222.	14871.	-0.0455	0.0220	0.0039	-370.	4422.	780.

TABLE A-2 (Continued)

Test Point No.	Run No.	Point of Run	Left N_p RPM	Right N_p RPM	Left β_1 Deg.	Left β_2 Deg.	Right β_1 Deg.	Right β_2 Deg.	Tail i_t Deg.	δ_f Deg.	Baro. in. Hg	To °F	Left N_{305} % RPM	Right N_{305} % RPM	Average V_p/V_{tip}	q/qc
553	I-19	4	1450	1460	35	35	35	35	4	30	30.11	75	Not Recorded		0.3808	1.013
554		5	1440	1460	0	0	0	0				76			0.3825	1.010
555		6	1440	1470								77			0.3815	1.013
556		7	1470	1465								79			0.3790	1.013
557		8	1470	1460								80			0.3797	1.021
558		9	1465	1465								81			0.3803	1 011
559		10	1200	1250								82			0.1003	1.063
560		11	1195	1215											0.1020	0.906
561		12	1195	1220	20	20	20	20							0.1030	0.885
562		13	1220	1250	35	35	35	35				84			0.0997	1.063
563		14	1200	1225	0	0	0	0				85			0.1016	0.906
564		15		1230								86			0.1015	
565		16		1225								87			0.1018	
566		17										88			0.1019	
567		18													0.1019	0.969
568		19		1230											0.1017	0.906
569		20	1210	1230											0.1026	1.038
570		21	1710	1725								89			0.0720	0.906
571		22	1675	1665	20	20	20	20				90			0.0741	
572		23	1760	1765	35	35	35	35				92			0.0738	
573		24	1650	1660	20	20	20	20				93			0.0657	0.990
574		25	-	2590	35	35	35	35							-	0.614
575	I-20	1	1350	1420	0	0	0	0	4	30	30.14	72	Not Recorded		0	N/A
576		2	1390	1400	-5	5	-5	5				73				
577		3	1410	1420	-10	10	-10	10				75				
578		4	1430	1440	-18	18	-18	18				76				
579		5	1740	1650	0	0	0	0				76				
580		6	1660	1630	0	0	0	0				76				

Test Point No.	Run No.	PT AVG	ALPHA	BETA	Q V,MOM	LIFT,U CL*QS	DRAG,U CD*QS	M,U CM*QSC	CL CY	CD CN	CM CROLL	SIDE F,U CY*QS	YAW,U CN*QSB	ROLL,U CL*QSB
553	I-19	4	0.	-0.	26.36	6242.	1464.	13161.	0.7746	0.1816	0.1307	-290.	2610.	1204.
		5			148.98	6242.	1464.	13161.	-0.0366	0.0131	0.0060	-290.	2610.	1204.
554		5	4.00	-0.	26.29	7375.	2664.	11486.	0.9178	0.3315	0.1144	-506.	250.	916%.
		5			148.68	7375.	2664.	11486.	-0.0636	0.0015	0.0060	-506.	250.	916%.
555		6	8.00	-0.	26.36	8321.	2849.	12951.	1.0325	0.3535	0.1286	-610.	2609.	9257.
		5			148.90	8321.	2849.	12951.	-0.0757	0.0131	0.0064	-610.	2609.	9257.
556		7	12.00	-0.	26.36	9413.	3166.	8326.	1.1685	0.3929	0.0827	-660.	4026.	8446.
		5			148.90	9413.	3166.	8326.	-0.0820	0.0202	0.0423	-660.	4026.	8446.
557		8	14.00	-0.	26.55	10322.	3480.	7651.	1.2716	0.4287	0.0754	-606.	4658.	7024.
		5			149.44	10322.	3480.	7651.	-0.0747	0.0232	0.0349	-606.	4658.	7024.
558		9	16.00	-0.	26.32	10924.	3814.	1692.	1.3575	0.4740	0.0168	-516.	4122.	5857.
		5			148.79	10924.	3814.	1692.	-0.0641	0.0207	0.0294	-516.	4122.	5857.
559		10	-4.00	-0.	1.36	2930.	311.	1383.	7.0661	0.7590	0.2668	-12.	204.	542.
		5			33.78	2930.	311.	1383.	-0.0289	0.0198	0.0528	-12.	204.	542.
560		11	0.	-0.	1.16	2918.	489.	1037.	8.2100	1.3746	0.2335	-34.	11.	-118.
		5			31.27	2918.	489.	1037.	-0.0959	0.0013	-0.0135	-34.	11.	-118.
561		12	0.	-0.	1.16	2638.	-557.	1466.	7.4201	-1.5677	0.3298	-84.	262.	-400.
		5			31.27	2638.	-557.	1466.	-0.1809	0.0298	-0.0455	-84.	262.	-400.
562		13	0.	-0.	1.36	1802.	-1087.	3339.	4.3461	-2.6204	0.6440	29.	-574.	591.
		5			33.78	1802.	-1087.	3339.	0.0694	-0.0559	0.0575	29.	-574.	591.
563		14	4.00	-0.	1.16	3096.	694.	135.	8.7096	1.9526	0.0303	-36.	-60.	-66.
		5			31.27	3096.	694.	135.	-0.1026	-0.0068	-0.0075	-36.	-60.	-66.
564		15	8.00	-0.	1.16	3168.	945.	779.	8.9122	2.6588	0.1752	-60.	79.	-109.
		5			31.27	3168.	945.	779.	-0.1701	0.0090	-0.0124	-60.	79.	-109.
565		16	12.00	-0.	1.16	3096.	1142.	757.	8.7096	3.2133	0.1705	-27.	35.	-745.
		5			31.27	3096.	1142.	757.	-0.0756	0.0040	-0.0846	-27.	35.	-745.
566		17	14.00	-0.	1.16	3094.	1238.	741.	8.7029	3.4821	0.1668	-57.	-82.	685.
		5			31.27	3094.	1238.	741.	-0.1595	-0.0093	0.0777	-57.	-82.	685.
567		18	16.00	-0.	1.24	3190.	1382.	249.	8.4122	3.6455	0.0526	-45.	-22.	186.
		5			32.50	3190.	1382.	249.	-0.1177	-0.0026	0.0198	-45.	-22.	186.
568		19	18.00	-0.	1.16	3017.	1451.	-1207.	8.4868	4.0850	-0.2715	-71.	519.	635.
		5			31.27	3017.	1451.	-1207.	-0.1985	0.0590	0.0719	-71.	519.	635.
569		20	20.00	-0.	1.24	3221.	1443.	-279.	7.7664	3.9615	-0.0539	-48.	868.	-162.
		5			33.78	3221.	1443.	-279.	-0.1146	0.0845	-0.0158	-48.	868.	-162.
570		21	0.	-0.	1.16	5616.	715.	-1239.	15.7989	2.0052	-0.2788	-154.	1831.	-1592.
		5			31.27	5616.	715.	-1239.	-0.4335	0.2080	-0.1808	-154.	1831.	-1592.
571		22	0.	-0.	1.16	5006.	-1412.	1319.	14.0840	-5.9709	0.2970	-102.	469.	1138.
		5			31.27	5006.	-1412.	1319.	-0.2876	0.0533	0.1292	-102.	469.	1138.
572		23	0.	-0.	1.16	4744.	-2608.	1740.	10.5938	-7.3224	0.3915	-18.	618.	567.
		5			31.27	3766.	-2603.	1740.	-0.0513	0.0701	0.0644	-18.	618.	567.
573		24	0.	-0.	0.97	4867.	-1397.	705.	14.4508	-4.7166	0.1904	-119.	1381.	-1050.
		5			28.58	4867.	-1397.	705.	-0.4019	0.1882	-0.1431	-119.	1381.	-1050.
574		25	0.	-0.	0.78	3830.	-3821.	6744.	16.1635	-16.1257	2.2765	-153.	-11717.	-24039.
		5			29.53	3830.	-3821.	6744.	-0.6441	-1.9961	-4.0954	-153.	-11717.	-24039.
575	I-20	1	0.	-0.	1.00	3619.	-240.	-3281.	8.4958	-0.5623	-0.6733	-68.	-857.	-702.
		10			0.	3619.	-240.	-3281.	-0.1660	-0.0521	-0.0627	-68.	-857.	-702.
576		2	0.	-0.	1.00	3607.	-185.	-3567.	8.4676	-0.4349	-0.7320	-74.	-169.	-63.
		10			0.	3607.	-185.	-3567.	-0.1735	-0.0102	-0.0038	-74.	-169.	-63.
577		3	0.	-0.	1.00	3146.	-369.	-2851.	7.3859	-0.8186	-0.5850	-40.	175.	103.
		10			0.	3146.	-369.	-2851.	-0.0946	0.0106	0.0062	-40.	175.	103.
578		4	0.	-0.	1.00	2389.	-377.	-2506.	5.6085	-0.8839	-0.5143	-37.	-52.	182.
		10			0.	2389.	-377.	-2506.	-0.0862	-0.0032	0.0110	-37.	-52.	182.
579		5	0.	-0.	1.00	5058.	-524.	-5196.	11.8732	-1.2297	-1.0662	-214.	2329.	-1613.
		10			0.	5058.	-524.	-5196.	-0.5031	0.1416	-0.0859	-214.	2329.	-1613.
580		6	0.	-0.	1.00	4732.	-499.	-5279.	11.1070	-1.1718	-1.0831	-59.	758.	-234.
		10			0.	4732.	-499.	-5279.	-0.1380	0.0461	-0.0142	-59.	758.	-234.

TABLE A-2 (Continued)

Test Point No.	Run No.	Point of Run	Left N_p RPM	Right N_p RPM	Left β_1 Deg.	Left β_0 Deg.	Right β_1 Deg.	Right β_0 Deg.	Tail i_t Deg.	ϵ_t Deg.	Baro. In. Hg	T_0 °F	Left N_{J85} % RPM	Right N_{J85} % RPM	Average V_p/V_{tip}	q/qc
581	I-20	7	1680	1630	-5	5	-5	5	4	30	30.14	78	Not Recorded		0	N/A
582		8	1720	1680	-10	10	-10	10				80				
583		9	1680	1640	-18	18	-18	18				80				
584		10	1705	1735	0	0	0	0				86			0.0654	
585		11	1700	1725	10	10	10	10				89			0.0659	
586		12	1700	1735	5	15	5	15				91			0.0659	
587		13	1700	1705	0	20	0	20				92			0.0664	
588		14	1730	1750	-5	25	-5	25				92			0.0650	
589		15	1740	1800	-10	30	-10	30				93			0.0639	
590		16	1685	1715	20	20	0	0				95			0.0723	
591		17	1650	1615	30	30	-10	-10				95			0.0691	
592		18	1725	1725	10	10	0	20				96			0.0679	
593		19	1725	1730	10	10	-5	25				97			0.0655	
594		20	1725	1775	10	10	-10	30				98			0.0646	
595		21	1695	1695	0	0	0	0				99			0.1128	
596		22	1695	1685	10	10	10	10				99			0.1131	
597		23	1690	1685	5	15	5	15				100			0.1027	
598		24	1690	1700	0	20	0	20				100			0.1054	
599		25	1700	1715	-5	25	-5	25				101			0.1084	
600		26	1740	1760	-10	30	-10	30				102			0.1021	
601		27	1685	1685	20	20	0	0							0.1136	
602		28	1700	1685	30	30	-10	-10							0.1133	
603		29	1685	1690	10	10	0	20							0.1083	
604		30	1680	1705	10	10	-5	25				103			0.1134	
605		31	1680	1750	10	10	-10	30				103			0.1118	
606		32	1690	1690	0	0	0	0				104			0.1514	
607		33	1685	1685	10	10	10	10							0.1518	
608		34	1685	1685	20	20	20	20							0.1551	

Test Point No.	Run No.	PT AVG	ALPHA	BETA	Q V_t,NOM	LIFT,U CL*QS	DRAG,U CD*QS	M,U CM*QSC	CL CY	CD CN	CM CROLL	SIDE F,U CY*QS	YAW,U CN*QSB	ROLL,U CL*QSB
581	I-20	7	0.	-0.	1.00	4819.	-507.	-5654.	11.3127	-1.1910	-1.1601	-16.	61.	1630.
		10			0.	4819.	-507.	-5654.	-0.0372	0.0037	0.0991	-16.	61.	1630.
582		8	0.	-0.	1.00	4560.	-480.	-4770.	10.7042	-1.1264	-0.9788	-26.	-299.	2281.
		10			0.	4560.	-480.	-4770.	-0.0608	-0.0182	0.1387	-26.	-299.	2281.
583		9	0.	-0.	1.00	3510.	-518.	-4589.	8.2394	-1.2158	-0.8390	-17.	-490.	1162.
		10			0.	3510.	-518.	-4589.	-0.0436	-0.0298	0.0706	-17.	-490.	1162.
584		10	11.26	-0.	1.07	5539.	597.	-296.	12.1969	3.7104	0.2378	-79.	1575.	-1389.
		5			29.94	5539.	1685.	1235.	-0.1739	0.6898	-0.0792	-79.	1575.	-1389.
585		11	10.93	-0.	1.07	5376.	-458.	773.	11.8395	1.2489	0.4350	-43.	710.	-1560.
		5			29.94	5376.	567.	2260.	-0.0944	0.0405	-0.0889	-43.	710.	-1560.
586		12	10.91	-0.	1.07	5369.	-373.	314.	11.8236	1.4289	0.5462	-178.	1080.	-1851.
		5			29.94	5369.	649.	1798.	-0.3927	0.0616	-0.1055	-178.	1080.	-1851.
587		13	9.87	-0.	1.07	4858.	-183.	1172.	10.6978	1.4303	0.4842	-178.	773.	-397.
		5			29.94	4858.	654.	2535.	-0.3927	0.0441	-0.0226	-178.	773.	-397.
588		14	8.72	-0.	1.07	4289.	99.	1141.	9.4457	1.6535	0.4470	-165.	1116.	427.
		5			29.94	4289.	751.	2326.	-0.3631	0.0637	0.0244	-165.	1116.	427.
589		15	7.64	-0.	1.07	3761.	397.	1296.	8.2824	1.9781	0.4496	-162.	1246.	-132.
		5			29.94	3761.	898.	2436.	-0.3557	0.0711	-0.0076	-162.	1246.	-132.
590		16	8.90	-0.	1.26	5172.	-362.	1134.	9.6379	0.8206	0.4176	12.	7568.	-1817.
		5			32.55	5172.	440.	2564.	0.0219	0.3652	-0.0877	12.	7568.	-1817.
591		17	9.42	-0.	1.07	4632.	-421.	1881.	10.2010	0.7478	0.6086	10.	12588.	-3767.
		5			29.94	4632.	340.	3161.	0.0227	0.7178	-0.2148	10.	12588.	-3767.
592		18	9.79	-0.	1.14	5165.	-301.	1098.	10.6032	1.1927	0.4533	-141.	1659.	362.
		5			31.01	5165.	581.	2526.	-0.2902	0.0882	0.0192	-141.	1659.	362.
593		19	9.84	-0.	1.07	4838.	-176.	1197.	10.6555	1.4395	0.4879	-188.	3227.	2215.
		5			29.94	4838.	654.	2534.	-0.4149	0.1840	0.1263	-188.	3227.	2215.
594		20	9.14	-0.	1.07	4498.	-36.	917.	9.9052	1.5008	0.4160	-221.	4554.	3855.
		5			29.94	4498.	681.	2161.	-0.4868	0.2597	0.2198	-221.	4554.	3855.
595		21	4.51	-0.	3.00	6247.	1052.	4171.	4.8819	1.2056	0.4029	-136.	200.	-136.
		5			50.26	6247.	1543.	5899.	-0.1063	0.0040	-0.0028	-136.	200.	-136.
596		22	4.27	-0.	3.00	5914.	58.	4622.	4.6212	0.3894	0.4276	-74.	187.	-1045.
		5			50.26	5914.	498.	6761.	-0.0576	-0.0058	-0.0211	-74.	187.	-1045.
597		23	4.91	-0.	2.44	5573.	62.	4693.	5.3156	0.5136	0.4697	-100.	866.	-9.
		5			45.50	5573.	539.	5634.	-0.0955	0.0214	-0.0002	-100.	866.	-9.
598		24	4.37	-0.	2.62	5280.	209.	4956.	4.7374	0.5437	0.5032	-90.	122.	-693.
		5			46.91	5280.	606.	6416.	-0.0803	0.0628	-0.0161	-90.	122.	-693.
599		25	3.66	-0.	2.81	4750.	491.	4865.	3.9676	0.6658	0.4512	-141.	354.	707.
		5			48.61	4750.	795.	6179.	-0.1177	0.0077	0.0153	-141.	354.	707.
600		26	3.48	-0.	2.62	4205.	751.	4339.	3.7727	0.9034	0.4315	-126.	479.	-315.
		5			46.91	4205.	1007.	5501.	-0.1126	0.0111	-0.0073	-126.	479.	-315.
601		27	4.00	-0.	3.00	5549.	62.	4414.	4.3361	0.3513	0.4065	-174.	7351.	-2366.
		5			50.26	5549.	450.	5948.	-0.1356	0.1487	-0.0479	-174.	7351.	-2366.
602		28	3.65	-0.	3.00	5066.	111.	5552.	3.9592	0.3392	0.4750	-166.	13120.	-5628.
		5			50.26	5066.	434.	6953.	-0.1300	0.2655	-0.1138	-166.	13120.	-5628.
603		29	4.26	-0.	2.77	5453.	67.	4836.	4.6187	0.4902	0.4697	-125.	1491.	-5.
		5			48.28	5453.	472.	6344.	-0.1055	0.0327	-0.0001	-125.	1491.	-5.
604		30	3.72	-0.	3.00	5160.	256.	4498.	4.0323	0.4619	0.4047	-153.	2685.	2285.
		5			50.26	5160.	591.	5925.	-0.1198	0.0543	0.0462	-153.	2685.	2285.
605		31	3.57	-0.	3.00	4949.	363.	4041.	3.8673	0.5242	0.3695	-99.	3280.	1839.
		5			50.26	4949.	671.	5409.	-0.0775	0.0664	0.0372	-99.	3280.	1839.
606		32	2.74	-0.	5.33	6746.	1487.	6679.	2.9715	0.7972	0.5290	-56.	-704.	305.
		5			66.95	6746.	1810.	8545.	-0.0248	-0.0080	0.0035	-56.	-704.	305.
607		33	2.58	-0.	5.33	6336.	514.	7061.	2.7907	0.3517	0.3393	-85.	346.	-1785.
		5			66.95	6336.	799.	8813.	-0.0374	0.0039	-0.0204	-85.	346.	-1785.
608		34	2.31	-0.	5.56	5923.	-414.	8600.	2.4998	-0.0743	0.3777	-138.	764.	-2636.
		5			68.40	5925.	-176.	10238.	-0.0582	0.0084	-0.0288	-138.	764.	-2636.

TABLE A-2 (Continued)

Test Point No.	Run No.	Point of Run	Left N_p RPM	Right N_p RPM	Left β_1 Deg.	Left β_2 Deg.	Right β_1 Deg.	Right β_2 Deg.	Tail i_t Deg.	δ_f Deg.	Baro. in. Hg	To °F	Left $N_{.85}$ % RPM	Right $N_{.85}$ % RPM	Average V_p/V_{tip}	q/qc
609	I-20	35	1690	1690	15	25	15	25	4	30	30.14	104	Not Recorded		0.1554	N/A
610		36	1695	1695	10	30	10	30				104			0.1453	
611		37	1725	1735	5	35	5	35				105			0.1424	
612		38	1785	1775	0	40	0	40							0.1384	
613		39	1710	1685	30	30	10	10							0.1587	
614		40	1770	1680	38	38	0	0							0.1433	
615		41	1690	1695	20	20	10	30				106			0.1516	
616		42	1685	1675	20	20	0	40							0.1499	
617		43	1690	1690	15	15	20	30							0.1518	
618		44	1685	1705	15	15	15	35							0.1561	
619		45	1685	1750	15	15	10	40							0.1496	
620		46	1685	1685	10	10	10	10				107			0.2251	
621		47	1690	1695	20	20	20	20				107			0.2277	
622		48	1695	1695	15	25	15	25				106			0.2246	
623		49	1700	1700	10	30	10	30							0.2221	
624		50	1735	1720	5	35	5	35							0.2189	
625		51	1775	1750	0	40	0	40							0.2142	
626		52	1720	1690	30	30	10	10							0.2251	
627		53	1745	1690	38	38	0	0							0.2199	
628		54	1700	1700	20	20	10	30							0.2280	
629		55	1695	1750	20	20	0	40							0.2192	
630		56	1695	1700	15	15	20	30							0.2279	
631		57	1695	1710	15	15	15	35							0.2254	
632		58	1690	1725	15	15	10	40							0.2229	
633		59	1695	1695	10	10	10	10							0.3009	
634		60	1725	1725	35	35	35	35							0.2956	
635		61	1725	1725	30	40	30	40				105			0.2954	
636		62	1738	1738	25	45	25	45				105			0.2921	

Test Point No.	Run No.	PT AVG	ALPHA	BETA	Q V,NOM	LIFT,U CL*QS	DRAG,U CD*QS	M,U CM*QSC	CL CY	CD CN	CM CROLL	SIDE F,U CY*QS	YAW,U CN*QSB	ROLL,U CL*QSB
609	I-20	35	2.32	-0.	5.33	5710.	-368.	8459.	2.5148	-0.0602	0.3903	-31.	-774.	-1576.
		5			66.95	5710.	-137.	10138.	-0.0138	-0.0088	-0.0180	-31.	-774.	-1576.
610		36	2.31	-0.	4.94	5273.	-114.	8625.	2.5046	0.0471	0.4186	-89.	-298.	-1758.
		5			66.47	5273.	99.	10083.	-0.0421	-0.0037	-0.0216	-89.	-298.	-1758.
611		37	2.04	-0.	4.94	4651.	299.	8431.	2.2093	0.2207	0.4035	-83.	-207.	-2370.
		5			66.47	4651.	465.	9717.	-0.0300	-0.0025	-0.0292	-83.	-207.	-2370.
612		38	1.80	-0.	4.94	4109.	702.	7479.	1.9517	0.3946	0.3743	-126.	940.	-1686.
		5			66.47	4109.	831.	9016.	-0.0601	0.0116	-0.0207	-126.	940.	-1686.
613		39	2.11	-0.	5.01	5746.	-261.	8653.	2.2818	-0.0198	0.3555	-215.	7441.	-6435.
		5			70.51	5746.	-50.	10242.	-0.0847	0.0765	-0.0662	-213.	7441.	-6435.
614		40	2.29	-0.	4.98	5266.	-80.	7721.	2.4817	0.0613	0.3781	-296.	13320.	-10579.
		5			66.72	5266.	150.	9177.	-0.1395	0.1626	-0.1291	-296.	13320.	-10579.
615		41	2.24	-0.	5.33	5498.	-278.	8696.	2.4218	-0.0279	0.3933	-44.	687.	-757.
		5			66.95	5498.	-63.	10216.	-0.0193	0.0078	-0.0086	-44.	687.	-757.
616		42	2.15	-0.	5.14	5093.	63.	7535.	2.3278	0.1161	0.3573	-53.	4857.	1176.
		5			65.72	5093.	254.	8943.	-0.0240	0.0575	0.0139	-53.	4857.	1176.
617		43	2.32	-0.	5.33	5705.	-378.	8116.	2.5127	-0.0646	0.3732	-38.	-3346.	-105.
		5			66.95	5705.	-147.	9694.	-0.0168	-0.0382	-0.0012	-38.	-3346.	-105.
618		44	2.18	-0.	5.52	5558.	-182.	8805.	2.3623	0.0126	0.3842	-31.	-2426.	816.
		5			68.16	5558.	30.	10342.	-0.0154	-0.0247	0.0090	-31.	-2426.	816.
619		45	2.10	-0.	5.35	5162.	35.	8243.	2.2758	0.0986	0.3723	55.	-1071.	2696.
		5			66.95	5162.	224.	9671.	0.0242	-0.0122	0.0307	55.	-1071.	2696.
620		46	1.41	-0.	11.70	7601.	1487.	12532.	1.5245	0.3357	0.2566	-123.	775.	-1377.
		5			99.21	7601.	1674.	14634.	-0.0246	0.0040	-0.0072	-123.	775.	-1377.
621		47	1.52	-0.	12.09	7346.	617.	13679.	1.4267	0.1526	0.2667	-29.	-1165.	-2686.
		5			100.83	7346.	786.	15711.	-0.0056	-0.0059	-0.0135	-29.	-1165.	-2686.
622		48	1.33	-0.	11.70	7205.	676.	13618.	1.4450	0.1692	0.2737	-18.	-1981.	-963.
		5			99.21	7205.	844.	15610.	-0.0035	-0.0103	-0.0050	-18.	-1981.	-963.
623		49	1.33	-0.	11.51	7056.	839.	13471.	1.4388	0.2045	0.2749	-154.	-193.	-2403.
		5			98.40	7056.	1003.	15422.	-0.0314	-0.0010	-0.0127	-154.	-193.	-2403.
624		50	1.26	-0.	11.55	6722.	1145.	12345.	1.3662	0.2627	0.2523	-247.	1099.	-1101.
		5			98.56	6722.	1293.	14202.	-0.0503	0.0058	-0.0058	-247.	1099.	-1101.
625		51	1.19	-0.	11.51	6319.	1393.	11077.	1.2885	0.3108	0.2286	-306.	2819.	-278.
		5			98.40	6319.	1524.	12824.	-0.0623	0.0149	-0.0015	-306.	2819.	-278.
626		52	1.31	-0.	11.90	7212.	655.	12590.	1.4232	0.1619	0.2516	-198.	6809.	-5727.
		5			100.02	7212.	821.	14584.	-0.0391	0.0348	-0.0293	-198.	6809.	-5727.
627		53	1.31	-0.	11.51	6958.	907.	11333.	1.4187	0.2173	0.2363	-176.	10896.	-8607.
		5			98.40	6958.	1066.	13256.	-0.0360	0.0575	-0.0454	-176.	10896.	-8607.
628		54	1.29	-0.	12.13	7229.	725.	13203.	1.3994	0.1718	0.2573	-111.	484.	-794.
		5			100.99	7229.	887.	15202.	-0.0215	0.0024	-0.0040	-111.	484.	-794.
629		55	1.27	-0.	11.51	6756.	958.	11371.	1.3776	0.2259	0.2360	-44.	2731.	132.
		5			98.40	6756.	1108.	13239.	-0.0097	0.0144	0.0007	-44.	2731.	132.
630		56	1.31	-0.	12.09	7296.	653.	13350.	1.4169	0.1591	0.2609	-55.	-3879.	-713.
		5			100.83	7296.	819.	15367.	-0.0108	-0.0195	-0.0036	-55.	-3879.	-713.
631		57	1.30	-0.	11.90	7116.	760.	13470.	1.4042	0.1816	0.2663	19.	-3559.	1368.
		5			100.02	7116.	920.	15437.	0.0037	-0.0182	0.0070	19.	-3559.	1368.
632		58	1.28	-0.	11.70	6895.	915.	12207.	1.3830	0.2142	0.2474	50.	-2238.	1932.
		5			99.21	6895.	1068.	14114.	0.0100	-0.0116	0.0100	50.	-2238.	1932.
633		59	1.03	-0.	20.91	9931.	2289.	14937.	1.1151	0.2770	0.1736	-36.	-721.	-517.
		5			132.60	9931.	2667.	17683.	-0.0041	-0.0021	-0.0015	-36.	-721.	-517.
634		60	0.88	-0.	20.71	8965.	598.	14888.	0.9208	0.0817	0.1475	-263.	1673.	-1089.
		5			132.60	8465.	727.	15027.	-0.0272	0.0049	-0.0032	-263.	1673.	-1089.
635		61	0.87	-0.	20.87	8393.	675.	12946.	0.9441	0.0902	0.1501	-302.	2353.	-338.
		5			132.48	8393.	802.	15267.	-0.0346	0.0049	-0.0010	-302.	2353.	-338.
636		62	0.87	-0.	20.72	8328.	878.	11420.	0.9437	0.1138	0.1359	-305.	3852.	-1013.
		5			131.99	8328.	1005.	13723.	-0.0345	0.0113	-0.0030	-305.	3852.	-1013.

TABLE A-2 (Continued)

Test Point No.	Run No.	Point of Run	Left N_p RPM	Right N_p RPM	Left β_1 Deg.	Left β_0 Deg.	Right β_1 Deg.	Right β_0 Deg.	Tail i_t Deg.	δ_f Deg.	Baro. in. Hg	To °F	Left $N_{.85}$ % RPM	Right $N_{.85}$ % RPM	Average V_p/V_{tip}	q/qc
637	I-20	63	1750	1750	20	50	20	50	4	30	32.14	105	Not Recorded		0.2887	N/A
638		64	1730	1730	35	35	25	45							0.2948	
639		65	1730	1760	35	35	20	55							0.2945	
640		66	1715	1720	30	30	20	40							0.2987	
641		67	1715	1740	30	30	25	45							0.2955	
642		68	1720	1750	30	30	20	50							0.2940	
643		69	1700	1700	0	0	0	0							0.2903	
644		70	1690	1700	0	0	0	0							0.2853	
645		71	1642	1642	20	50	20	50							0.3078	
646		72	1640	1640											0.3081	
647		73	1640	1630											0.3162	
648		74	1770	1760	0	40	0	40							0.2195	
649		75	1765	1750											0.2184	
650		76	1765	1750								106			0.2170	
651		77	1700	1700	0	0	0	0	12						0.1481	
652		78	1700	1700											0.1481	
653		79	1700	1775											0.1476	
654		80	1700	1710											0.1499	
655		81	1705	1715											0.1500	
656		82	1705	1720											0.1498	
657		83	1705	1740											0.1462	
658		84	1700	1780											0.1474	
659		85	1080	1080					4			104			0.4745	
660		86	30	18	35	35	35	35				100			N/A	
661		87	22	17								98				
662		88	73	60								97				
663		89	105	80								96				
664		90	145	90								95				

Test Point No.	Run No.	PT AVG	ALPHA	BETA	Q V,NOM	LIFT,U CL*QS	DRAG,U CD*QS	M,U CM*QSC	CL CY	CD CN	CM CROLL	SIDE F,U FY*QS	YAW,U CN*QSB	ROLL,U CL*QSB
637	I-20	63	0.83	-0.	20.52	7870.	1125.	9472.	0.9061	0.1417	0.1165	-301.	4380.	518.
		5			151.38	7870.	1239.	11648.	-0.0344	0.0130	0.0015	-301.	4380.	518.
638		64	0.90	-0.	20.91	8645.	881.	11706.	0.9766	0.1141	0.1384	-166.	2539.	-2103.
		5			132.60	8645.	1016.	14696.	-0.0188	0.0074	-0.0061	-166.	2539.	-2103.
639		65	0.82	-0.	20.98	7894.	914.	9856.	0.8631	0.1148	0.1177	-233.	5026.	2941.
		5			132.85	7894.	1026.	12039.	-0.0261	0.0146	0.0085	-233.	5026.	2941.
640		66	0.94	-0.	20.91	9070.	1036.	12581.	1.0183	0.1330	0.1481	-241.	2534.	-1411.
		5			132.60	9070.	1184.	15089.	-0.0271	0.0074	-0.0041	-241.	2534.	-1411.
641		67	0.89	-0.	20.95	8580.	912.	11807.	0.9616	0.1171	0.1389	-206.	1063.	48.
		5			132.72	8580.	1045.	14179.	-0.0251	0.0051	0.0001	-206.	1063.	48.
642		68	0.86	-0.	20.91	8514.	1029.	11064.	0.9334	0.1296	0.1312	-212.	2686.	2702.
		5			132.60	8514.	1154.	13363.	-0.0238	0.0078	0.0079	-212.	2686.	2702.
643		69	1.09	-0.	19.57	9823.	2904.	14559.	1.1785	0.3708	0.1791	-108.	1334.	-1095.
		5			124.26	9823.	3090.	17075.	-0.0139	0.0041	-0.0034	-108.	1334.	-1095.
644		70	1.12	-0.	18.80	9686.	2802.	14324.	1.2094	0.3734	0.1856	-85.	1154.	-265.
		5			125.75	9686.	2990.	17003.	-0.0106	0.0037	-0.0009	-85.	1154.	-265.
645		71	-3.46	-0.	21.29	5326.	1112.	12667.	0.5872	0.1281	0.1305	-245.	3606.	-246.
		5			133.81	5326.	1162.	13539.	-0.0268	0.0103	-0.0007	-245.	3606.	-246.
646		72	0.79	-0.	20.52	7512.	1193.	7933.	0.8592	0.1483	0.1001	-227.	3093.	-797.
		5			131.38	7512.	1297.	10010.	-0.0260	0.0092	-0.0024	-227.	3093.	-797.
647		73	5.01	-0.	21.48	10022.	1534.	5031.	1.0952	0.1870	0.0554	-118.	2195.	82.
		5			134.41	10022.	1711.	5802.	-0.0129	0.0062	0.0002	-118.	2195.	82.
648		74	-3.11	-0.	12.13	4994.	1316.	13059.	0.9669	0.2698	0.2444	-304.	2775.	-2468.
		5			100.99	4994.	1394.	14440.	-0.0588	0.0139	-0.0124	-304.	2775.	-2468.
649		75	1.18	-0.	11.90	6485.	1372.	11120.	1.2797	0.2972	0.2228	-284.	2509.	-2422.
		5			100.02	6485.	1506.	12914.	-0.0566	0.0128	-0.0124	-284.	2509.	-2422.
650		76	5.41	-0.	11.74	7646.	1560.	9091.	1.5286	0.3494	0.1958	-260.	2247.	-860.
		5			99.38	7646.	1748.	11206.	-0.0521	0.0116	-0.0045	-260.	2247.	-860.
651		77	-1.28	-0.	5.14	6437.	1178.	1956.	2.9421	0.6776	0.1492	-78.	392.	-1271.
		5			65.72	6437.	1482.	3735.	-0.0354	0.0046	-0.0150	-78.	392.	-1271.
652		78	2.96	-0.	5.14	7020.	1506.	1891.	3.2087	0.8540	0.1531	-100.	87.	-1796.
		5			65.72	7020.	1868.	3852.	-0.0457	0.0010	-0.0213	-100.	87.	-1796.
653		79	7.12	-0.	5.33	7678.	1896.	1008.	3.3817	1.0190	0.1206	-173.	727.	-1528.
		5			66.95	7678.	2314.	3131.	-0.0762	0.0083	-0.0174	-173.	727.	-1528.
654		80	11.39	-0.	5.29	8270.	2319.	237.	3.6694	1.2459	0.0979	-137.	392.	-1099.
		5			66.71	8270.	2808.	2524.	-0.0668	0.0045	-0.0126	-137.	392.	-1099.
655		81	13.48	-0.	5.33	8566.	2571.	-620.	3.7728	1.3610	0.0673	-148.	665.	-2827.
		5			66.95	8566.	3091.	1749.	-0.0654	0.0076	-0.0322	-148.	665.	-2827.
656		82	15.61	-0.	5.33	8890.	2793.	-1207.	3.9155	1.4771	0.0482	-141.	713.	-1405.
		5			66.95	8890.	3354.	1251.	-0.0621	0.0081	-0.0160	-141.	713.	-1405.
657		83	17.77	-0.	5.14	8947.	3027.	-1372.	4.0896	1.6528	0.0440	-42.	66.	-2002.
		5			65.72	8947.	3616.	1102.	-0.0194	0.0008	-0.0237	-42.	66.	-2002.
658		84	19.75	-0.	5.33	9221.	3263.	-2015.	4.0614	1.7028	0.0206	7.	159.	-1825.
		5			66.95	9221.	3866.	535.	0.0033	0.0018	-0.0208	7.	159.	-1825.
659		85	0.43	-0.	21.10	4210.	1572.	-6510.	0.4684	0.1784	-0.0520	-168.	1085.	2506.
		5			133.21	4210.	1604.	-5346.	-0.0187	0.0031	0.0072	-168.	1085.	2506.
660		86	-3.88	-0.	20.91	1142.	861.	-5008.	0.1283	0.0970	-0.0461	44.	-384.	-502.
		5			132.60	1142.	864.	-4692.	0.0049	-0.0011	-0.0015	44.	-384.	-502.
661		87	0.33	-0.	21.10	3259.	890.	-12811.	0.3626	0.1012	-0.1158	58.	-894.	-1093.
		5			133.21	3259.	909.	-11910.	0.0064	-0.0026	-0.0031	58.	-894.	-1093.
662		88	4.53	-0.	21.10	5134.	1139.	-18643.	0.5712	0.1320	-0.1675	20.	-39.	-674.
		5			133.21	5134.	1186.	-17224.	0.0022	-0.0001	-0.0019	20.	-39.	-674.
663		89	8.68	-0.	20.91	6576.	1491.	-21398.	0.7384	0.1762	-0.1922	44.	-597.	-710.
		5			132.60	6576.	1570.	-19578.	0.0050	-0.0017	-0.0021	44.	-597.	-710.
664		90	10.77	-0.	20.91	7399.	1740.	-22984.	0.8308	0.2064	-0.2055	62.	-474.	-1311.
		5			32.60	7399.	1839.	-20938.	0.0076	-0.0018	-0.0038	62.	-474.	-1311.

TABLE A-2 (Continued)

Test Point No.	Run No.	Point of Run	Left N_y RPM	Right N_y RPM	Left δ_h Deg.	Left δ_a Deg.	Right δ_h Deg.	Right δ_a Deg.	Tail i_t Deg.	δ_f Deg.	Baro. in. Hg	To ^oF	Left N_{JBS} % RPM	Right N_{JBS} % RPM	Average V_p/V_{tip}	q/qc
665	I-20	91	150	115	35	35	35	35	4	30	30.14	94	Not Recorded		N/A	N/A
666		92	200	160								92				
667		93	220	170								91				
668		94	230	186								90				
669	I-21	1	1700	1700	0	0	0	0	16	30	30.15	70	87.0	86.5	0.1077	N/A
670		2	1695	1700								71			0.1115	
671		3		1695								71			0.1081	
672		4		1695								74		87.0	0.1047	
673		5		1700								76			0.1120	
674		6		1695								76			0.1121	
675		7		1695								78			0.1124	
676		8		1690								79			0.1126	
677		9		1690								79	87.5	87.5	0.1126	
678		10	1735	1725	-10	30	-10	30				82	87.0	86.5	0.1139	
679		11	1740	1720								82			0.1105	
680		12	1745									83			0.1105	
681		13										83		87.0	0.1033	
682		14										84			0.1033	
683		15		1730								85			0.1069	
684		16	1730	1745											0.1104	
685		17	1730	1770											0.1096	
686		18	1720	1770								86			0.1100	
687		19	1695	1685	0	0	0	0				87	88.0	88.0	0.0752	
688		20	1700	1690								88			0.0717	
689		21	1700	1690								88			0.0739	
690		22	1695	1685								89			0.0753	
691		23	1695	1685								89			0.0753	
692		24	1695	1685								90			0.0754	

Test Point No.	Run No.	PT AVG	ALPHA	BETA	Q V,NOM	LIFT,U CL*QS	DRAG,U CD*QS	M,U CM*QSC	CL CY	CD CN	CM CROLL	SIDE F,U CY*QS	YAW,U CN*QSB	ROLL,U CL*QSB
665	I-20	91	12.84	-0.	21.10	8134.	2011.	-23882.	0.9056	0.2370	-0.2104	24.	-77.	-1086.
		5			133.21	8134.	2130.	-21633.	0.0027	-0.0002	-0.0031	24.	-77.	-1086.
666		92	14.91	-0.	20.91	8827.	2510.	-25575.	0.9911	0.2977	-0.2271	75.	-187.	-2514.
		5			132.60	8827.	2651.	-23134.	0.0084	-0.0005	-0.0073	75.	-187.	-2514.
667		93	16.96	-0.	20.72	9204.	2985.	-29341.	1.0415	0.3558	-0.2654	18.	395.	-3004.
		5			131.99	9204.	3140.	-26796.	0.0022	-0.0012	-0.0088	18.	395.	-3004.
668		94	19.05	-0.	20.91	10116.	4169.	-44488.	1.1358	0.4889	-0.4492	74.	-421.	-4565.
		5			132.60	10116.	4354.	-41691.	0.0063	-0.0012	-0.0133	74.	-421.	-4565.
669	I-21	1	-4.00	-0.	2.81	6440.	672.	-1380.	5.2067	0.5428	-0.0946	-168.	2246.	-710.
		5			49.45	6440.	672.	-1380.	-0.1355	0.0470	-0.0148	-168.	2246.	-710.
670		2	-2.00	-0.	3.10	6572.	895.	-1620.	4.9755	0.6779	-0.1072	-115.	651.	195.
		5			51.07	6572.	895.	-1620.	-0.0874	0.0124	0.0038	-115.	651.	195.
671		3	0.	-0.	2.91	6714.	1063.	-1740.	5.4216	0.8582	-0.1228	-107.	781.	-1368.
		5			49.45	6714.	1063.	-1740.	-0.0866	0.0163	-0.0286	-107.	781.	-1368.
672		4	2.00	-0.	2.71	6760.	1249.	-2342.	5.8483	1.0806	-0.1771	-94.	722.	-482.
		5			47.77	6760.	1249.	-2342.	-0.0812	0.0162	-0.0108	-94.	722.	-482.
673		5	4.00	-0.	3.10	7004.	1525.	-2577.	5.3026	1.1545	-0.1706	-104.	496.	-453.
		5			51.07	7004.	1525.	-2577.	-0.0787	0.0097	-0.0089	-104.	496.	-453.
674		6	6.00	-0.	3.10	7177.	1779.	-2804.	5.4334	1.3467	-0.1855	-90.	152.	-355.
		5			51.07	7177.	1779.	-2804.	-0.0685	0.0029	-0.0070	-90.	152.	-355.
675		7	8.00	-0.	3.10	7249.	1996.	-3048.	5.4879	1.5110	-0.2017	-111.	633.	-1013.
		5			51.07	7249.	1996.	-3048.	-0.0841	0.0124	-0.0199	-111.	633.	-1013.
676		8	10.00	-0.	3.10	7429.	2227.	-3447.	5.6242	1.6858	-0.2281	-85.	424.	-1706.
		5			51.07	7429.	2227.	-3447.	-0.0641	0.0083	-0.0334	-85.	424.	-1706.
677		9	12.00	-0.	3.10	7655.	2501.	-3670.	5.7950	1.8933	-0.2429	-87.	60.	-942.
		5			51.07	7655.	2501.	-3670.	-0.0656	0.0012	-0.0185	-87.	60.	-942.
678		10	-4.00	-0.	3.29	4021.	655.	821.	2.8651	0.4667	0.0511	-95.	455.	237.
		5			52.64	4021.	655.	821.	-0.0679	0.0084	0.0044	-95.	455.	237.
679		11	0.	-0.	3.10	4379.	868.	447.	3.3149	0.6568	0.0296	-91.	776.	574.
		5			51.07	4379.	868.	447.	-0.0692	0.0152	0.0112	-91.	776.	574.
680		12	4.00	-0.	3.10	4727.	1076.	-550.	3.5784	0.8144	-0.0364	-107.	367.	821.
		5			51.07	4727.	1076.	-550.	-0.0812	0.0072	0.0161	-107.	367.	821.
681		13	8.00	-0.	2.71	5017.	1305.	-662.	4.3408	1.1288	-0.0501	-80.	84.	616.
		5			47.77	5017.	1305.	-662.	-0.0691	0.0019	0.0138	-80.	84.	616.
682		14	10.00	-0.	2.71	5192.	1456.	-1308.	4.4924	1.2596	-0.0989	-57.	-236.	351.
		5			47.77	5192.	1456.	-1308.	-0.0496	-0.0053	0.0079	-57.	-236.	351.
683		15	12.00	-0.	2.91	5459.	1623.	-1220.	4.4080	1.3109	-0.0861	-83.	-91.	493.
		5			49.45	5459.	1623.	-1220.	-0.0669	-0.0019	0.0103	-83.	-91.	493.
684		16	14.00	-0.	3.10	5696.	1826.	-1569.	4.3124	1.3623	-0.1038	-24.	-990.	-415.
		5			51.07	5696.	1826.	-1569.	-0.0810	-0.0194	-0.0081	-24.	-990.	-415.
685		17	16.00	-0.	3.10	5963.	1953.	-2358.	4.5141	1.5012	-0.1560	0.	-842.	973.
		5			51.07	5963.	1953.	-2358.	0.0002	-0.0165	0.0191	0.	-842.	973.
686		18	18.00	-0.	3.10	5996.	2111.	-2949.	4.5395	1.5978	-0.1951	29.	-1112.	932.
		5			51.07	5996.	2111.	-2949.	0.0216	-0.0218	0.0183	29.	-1112.	932.
687		19	-4.00	-0.	1.36	5413.	319.	-1801.	9.3668	0.5527	-0.2724	-106.	2336.	-570.
		5			33.78	5413.	319.	-1801.	-0.1840	0.1047	-0.0256	-106.	2336.	-570.
688		20	-2.00	-0.	1.24	5418.	475.	-1844.	10.2541	0.8998	-0.3050	-117.	1814.	139.
		5			32.30	5418.	475.	-1844.	-0.2221	0.0889	0.0068	-117.	1814.	139.
689		21	0.	-0.	1.32	5459.	702.	-1892.	9.7236	1.2513	-0.2946	-80.	1519.	202.
		5			33.29	5459.	702.	-1892.	-0.1424	0.0700	0.0093	-80.	1519.	202.
690		22	2.00	-0.	1.36	5646.	962.	-2786.	9.7697	1.6646	-0.4214	-82.	1566.	57.
		5			33.78	5646.	962.	-2786.	-0.1416	0.0702	0.0025	-82.	1566.	57.
691		23	4.00	-0.	1.36	5759.	1182.	-2994.	9.9648	2.0458	-0.4528	-65.	1185.	115.
		5			33.78	5759.	1182.	-2994.	-0.1117	0.0531	0.0051	-65.	1185.	115.
692		24	6.00	-0.	1.36	5653.	1399.	-3082.	9.7821	2.4213	-0.4662	-49.	934.	415.
		5			33.78	5653.	1399.	-3082.	-0.0851	0.0418	0.0186	-49.	934.	415.

TABLE A-2 (Continued)

Test Point No.	Run No.	Point of Run	Left N_p RPM	Right N_p RPM	Left β_1 Deg.	Left β_0 Deg.	Right β_1 Deg.	Right β_0 Deg.	Tail i_t Deg.	δ_f Deg.	Baro. in. Hg	To ^oF	Left $N_{.785}$ % RPM	Right $N_{.785}$ % RPM	Average V_p/V_{tip}	q/qc
693	I-21	25	1690	1680	0	0	0	0	16	30	30.15	90	88.0	88.0	0.0756	N/A
694		26	1685	1680								91	88.0	88.0	0.0758	
695		27	2370	2330								91	99.0	100.0	0.0502	
696		28	2380	2340	-5	5	-5	5				92			0.0461	
697		29	2400	2330	-10	10	-10	10				93			0.0455	
698		30	2380	2310	-5	5	-5	5							0.0417	
699		31	1700	1700	0	40	0	40	12				86.5	87.0	0.1504	
700		32	1705	1705											0.1472	
701		33	1710	1710								98			0.1475	
702		34	1730	1730								97			0.1510	
703		35	1735	1740											0.1529	
704		36	1730	1765											0.1469	
705		37	1730	1780											0.1462	
706		38	1715	1780											0.1442	
707		39	1715	1815											0.1428	
708		40	0	0	35	35	35	35	4			89	0	0	N/A	
709		41										87				
710		42										86				
711		43										85				
712		44										84				
713		45										84				
714		46										83				
715		47										83				
716		48										83				
717		49	1615	1670	20	50	20	50				82	85.5	86.5	0.3015	
718		50	1555	1660								84	85.0		0.3008	
719		51		1680								86			0.2985	
720		52		1645								86		80.0	0.3039	

Test Point No.	Run No.	PT AVG	ALPHA	BETA	Q V,NOM	LIFT,U CL*QS	DRAG,U CD*QS	M,U CM*QSC	CL CY	CD CN	CM CROLL	SIDE F,U CY*QS	YAW,U CN*QSB	ROLL,U CL*QSB
693	I-21	25	8.00	-0.	1.36	5730.	1585.	-3804.	9.915[illegible]	2.7419	-0.5753	-33.	1001.	569.
		5			33.78	5730.	1585.	-3804.	-0.0569	0.0449	0.0255	-33.	1001.	569.
694		26	10.00	-0.	1.36	5785.	1815.	-4407.	10.0644	3.1414	-0.6665	-6.	571.	876.
		5			33.78	5785.	1815.	-4407.	-0.0112	0.0256	0.0393	-6.	571.	876.
695		27	0.	-0.	1.16	9664.	534.	-7561.	19.5085	1.0771	-1.3343	-128.	3403.	-3214.
		10			31.27	9664.	534.	-7561.	-0.2587	0.1779	-0.1660	-128.	3403.	-3214.
696		28	0.	-0.	0.99	9619.	393.	-7961.	22.8429	0.9325	-1.6527	-192.	1169.	-1435.
		10			28.83	9618.	393.	-7961.	-0.4566	0.0719	-0.0883	-192.	1169.	-1435.
697		29	0.	-0.	0.97	9162.	690.	-8244.	22.1951	1.6710	-1.7458	-323.	5147.	-3353.
		10			28.55	9162.	690.	-8244.	-0.7814	0.1974	-0.2103	-323.	5147.	-3353.
698		10	0.	-0.	0.79	9580.	617.	-8329.	28.3009	1.8215	-2.1510	-134.	2811.	-1364.
		10			25.85	9580.	617.	-8329.	-0.5971	0.2150	-0.1043	-134.	2811.	-1364.
699		51	-4.00	-0.	5.43	3762.	653.	3345.	1.6274	0.2825	0.1265	-140.	1075.	-2590.
		5			67.56	3762.	653.	3345.	-0.0607	0.0120	-0.0290	-140.	1075.	-2590.
700		52	0.	-0.	5.23	4192.	800.	4567.	1.8804	0.3589	0.1791	-143.	1418.	-1152.
		5			66.34	4192.	800.	4567.	-0.0647	0.0165	-0.0134	-143.	1418.	-1152.
701		53	4.00	-0.	5.23	4871.	973.	2493.	2.1851	0.4366	0.0978	-111.	1013.	-2038.
		5			66.34	4871.	974.	2493.	-0.0498	0.0118	-0.0237	-111.	1013.	-2038.
702		54	8.00	-0.	5.62	5946.	1275.	1206.	2.4835	0.5325	0.0440	-152.	1412.	-404.
		5			68.75	5946.	1275.	1206.	-0.0637	0.0153	-0.0044	-152.	1412.	-404.
703		55	10.00	-0.	5.81	6251.	1436.	1254.	2.5238	0.5799	0.0443	-125.	1112.	-1230.
		5			69.93	6251.	1436.	1254.	-0.0505	0.0116	-0.0129	-125.	1112.	-1230.
704		56	12.00	-0.	5.43	6325.	1521.	1199.	2.7362	0.6581	0.0453	-29.	290.	-2167.
		5			67.58	6325.	1521.	1199.	-0.0126	0.0033	-0.0243	-29.	290.	-2167.
705		57	14.00	-0.	5.43	6692.	1699.	949.	2.8951	0.7351	0.0359	-29.	323.	-111.
		5			67.58	6692.	1699.	949.	-0.0124	0.0036	-0.0012	-29.	324.	-111.
706		58	16.00	-0.	5.23	6964.	1851.	-314.	3.1247	0.8304	-0.0125	21.	-276.	-627.
		5			66.34	6964.	1851.	-314.	0.0094	-0.0032	-0.0073	21.	-276.	-627.
707		59	18.00	-0.	5.23	7184.	2005.	-1405.	3.223[illegible]	0.8993	-0.0551	34.	-52.	-839.
		5			66.34	7184.	2005.	-1405.	0.0152	-0.0036	-0.0097	34.	-52.	-839.
708		60	-4.00	-0.	20.62	1098.	851.	-3573.	0.1257	0.0969	-0.0356	21.	-148.	-336.
		5			131.69	1098.	851.	-3573.	0.0024	-0.0004	-0.0010	21.	-148.	-336.
709		61	0.	-0.	21.00	3157.	886.	-11324.	0.3529	0.0993	-0.1106	27.	-591.	-667.
		5			132.91	3157.	886.	-11324.	0.0056	-0.0017	-0.0019	27.	-591.	-667.
710		62	4.00	-0.	20.81	4988.	1125.	-17470.	0.5627	0.1269	-0.1723	9.	-225.	-221.
		5			132.30	4988.	1125.	-17470.	0.0011	-0.0007	-0.0006	9.	-225.	-221.
711		63	8.00	-0.	20.62	6474.	1447.	-19948.	0.7377	0.1647	-0.1985	19.	-279.	27.
		5			131.69	6474.	1447.	-19948.	0.0022	-0.0008	0.0001	19.	-279.	27.
712		64	10.00	-0.	20.62	7283.	1693.	-22123.	0.8291	0.1927	-0.2202	33.	-44.	-681.
		5			131.69	7283.	1693.	-22123.	0.0037	-0.0001	-0.0020	33.	-44.	-681.
713		65	12.00	-0.	20.81	8070.	1995.	-23426.	0.9103	0.2251	-0.2310	55.	-437.	-1756.
		5			132.30	8070.	1995.	-23426.	0.0063	-0.0013	-0.0051	55.	-437.	-1756.
714		66	14.00	-0.	20.43	8740.	2496.	-25700.	1.0044	0.2868	-0.2581	36.	-350.	-1672.
		5			131.08	8740.	2496.	-25700.	0.0042	-0.0010	-0.0050	36.	-350.	-1672.
715		67	16.00	-0.	21.00	9479.	3047.	-29605.	1.0594	0.3406	-0.2892	1.	557.	-1588.
		5			132.91	9479.	3047.	-29605.	0.0001	0.0016	-0.0046	1.	557.	-1588.
716		68	18.00	-0.	20.62	9846.	3716.	-36755.	1.1209	0.4230	-0.3658	35.	642.	-2877.
		5			131.69	9846.	3716.	-36755.	0.0044	0.0019	-0.0085	35.	642.	-2877.
717		49	4.00	-0.	20.62	10110.	1469.	6280.	1.1510	0.1673	0.0625	-167.	2975.	-70.
		5			131.69	10110.	1469.	6280.	-0.0194	0.0088	-0.0002	-167.	2975.	-70.
718		50	8.00	-0.	20.81	12587.	1864.	1327.	1.4197	0.2103	0.0131	-54.	1339.	-1261.
		5			132.30	12587.	1864.	1327.	-0.0061	0.0039	-0.0037	-54.	1339.	-1261.
719		51	10.00	-0.	20.81	13172.	1962.	-3214.	1.4857	0.2191	-0.0317	-255.	4709.	2834.
		5			132.30	13172.	1962.	-3214.	-0.0287	0.0138	0.0083	-255.	4709.	2834.
720		52	12.00	-0.	21.00	13376.	2260.	-11047.	1.4950	0.2526	-0.1079	-404.	7[illegible]0.	7932.
		5			132.91	13376.	2260.	-11047.	-0.0451	0.0210	0.0230	-404.	7[illegible]0.	7932.

TABLE A-2 (Continued)

Test Point No.	Run No.	Point of Run	Left N_p RPM	Right N_p RPM	Left β_1 Deg.	Left β_2 Deg.	Right β_1 Deg.	Right β_2 Deg.	Tail i_t Deg.	δ_f Deg.	Baro. in. Hg	To °F	Left N_{JBS} % RPM	Right N_{JBS} % RPM	Average V_p/V_{tip}	q/qc
721	I-21	53	1175	1200	0	0	0	0	4	30	30.15	87	72.5	71.0	0.5824	N/A
722		54	1165	1165	0	0	0	0						66.0	0.4329	
723		55	1160	1150	20	20	20	20							0.4306	
724		56	1220	1140	35	35	35	35							0.4235	
725		57	1180	1155	0	0	0	0							0.4280	
726		58	1210	1150											0.4242	
727		59	1230	1150											0.4199	
728		60	1240	1140										65.5	0.4199	
729		61	1240	1130										66.0	0.4197	
730		62	1240	1140											0.4138	
731		63	1695	1700	0	40	0	40				89	86.0	87.0	0.2216	
732		64	1695	1720								90			0.2205	
733		65	1690	1725								90			0.2205	
734		66	1695	1740								91			0.2195	
735		67	1695	1800								91		85.0	0.2167	
736	I-22	1	1725	1715	0	0	0	0	16	30	30.04	80	87.5	88.0	0.0809	1.049
737		2	1685	1715	20	20	20	20				82			0.0792	1.203
738		3	1715	1735	35	35	35	35				83			0.0861	0.887
739		4	1705	1690	0	0	0	0				87			0.1125	0.984
740		5	1700	1690	20	20	20	20				88			0.1185	0.950
741		6	1740	1725	35	35	35	35				90			0.1091	1.077
742		7	1695	1695	0	0	0	0	12			91			0.1495	0.966
743		8	1700	1690	0	0	0	0				92			0.1461	1.014
744		9	1695	1690	20	20	20	20				92			0.1471	1.115
745		10	1735	1730	35	35	35	35				93		88.5	0.1390	1.031
746		11	1700	1690	0	0	0	0				93			0.1453	0.986
747		12	1710	1695	0	0	0	0				94			0.1509	0.958
748		13	1705	1695	0	0	0	0				94			0.1486	1.049

Test Point No.	Run No.	PT AVG	ALPHA	BETA	Q V,NOM	LIFT,U CL*QS	DRAG,U CD*QS	M,U CM*QSC	CL CY	CD CN	CM CROLL	SIDE F,U CY*QS	YAW,U CN*QSB	ROLL,U CL*QSH
721	I-21	53	-4.00	-0.	20.62	5130.	1921.	10986.	0.5846	0.2186	0.1093	-92.	2111.	768.
		5			131.69	5130.	1921.	10986.	-0.0105	0.0062	0.0023	-92.	2111.	768.
722		54	0.	-0.	21.19	6452.	1652.	-898.	0.7147	0.1830	-0.0087	-385.	4120.	4001.
		5			133.51	6452.	1652.	-898.	-0.0424	0.0118	0.0115	-385.	4120.	4001.
723		55	0.	-0.	20.62	6145.	1295.	-894.	0.6996	0.1474	-0.0089	-332.	4595.	2337.
		4			131.69	6145.	1295.	-894.	-0.0378	0.0135	0.0069	-332.	4595.	2337.
724		56	0.	-0.	20.81	5732.	1020.	-2800.	0.6466	0.1151	-0.0276	-172.	3411.	1430.
		5			132.30	5732.	1020.	-2800.	-0.0194	0.0100	0.0042	-172.	3411.	1430.
725		57	4.00	-0.	20.81	7873.	1738.	-6577.	0.8881	0.1961	-0.0649	-426.	5476.	5715.
		5			132.30	7873.	1738.	-6577.	-0.0480	0.0160	0.0167	-426.	5476.	5715.
726		58	8.00	-0.	20.49	9260.	1967.	-12036.	1.0437	0.2210	-0.1182	-508.	4952.	6890.
		5			132.54	9260.	1967.	-12036.	-0.0347	0.0144	0.0200	-508.	4952.	6890.
727		59	10.00	-0.	20.81	10016.	2129.	-13571.	1.1298	0.2401	-0.1338	-175.	3594.	6624.
		5			132.30	10016.	2129.	-13571.	-0.0198	0.0105	0.0193	-175.	3594.	6624.
728		60	12.00	-0.	20.81	10583.	2383.	-13719.	1.1937	0.2688	-0.1353	-112.	2317.	5819.
		5			132.30	10583.	2383.	-13719.	-0.0126	0.0068	0.0170	-112.	2317.	5819.
729		61	14.00	-0.	20.62	11051.	2799.	-13456.	1.2581	0.3187	-0.1339	-4.	977.	6793.
		5			131.69	11051.	2799.	-13456.	-0.0005	0.0029	0.0200	-4.	977.	6793.
730		62	16.00	-0.	20.54	11069.	3440.	-18322.	1.2648	0.3930	-0.1830	162.	-162.	-129.
		5			131.44	11069.	3440.	-18322.	0.0186	-0.0005	-0.0004	162.	-162.	-129.
731		63	4.00	-0.	11.80	7420.	1618.	8918.	1.4766	0.3218	0.1551	-281.	2849.	-759.
		5			99.62	7420.	1618.	8918.	-0.0559	0.0147	-0.0039	-281.	2849.	-759.
732		64	8.00	-0.	11.80	8848.	1844.	7911.	1.7601	0.3669	0.1376	-237.	2127.	-205.
		5			99.62	8848.	1844.	7911.	-0.0411	0.0110	-0.0011	-237.	2127.	-205.
733		65	10.00	-0.	11.80	9469.	2010.	6965.	1.8838	0.3998	0.1211	-127.	1052.	-1007.
		5			99.62	9469.	2010.	6965.	-0.0255	0.0054	-0.0052	-127.	1052.	-1007.
734		66	12.00	-0.	11.80	9896.	2269.	6703.	1.9688	0.4514	0.1166	-20.	-639.	-153.
		5			99.62	9896.	2269.	6703.	-0.0043	-0.0033	-0.0008	-20.	-639.	-153.
735		67	14.00	-0.	11.91	10753.	2510.	4237.	2.1185	0.4945	0.0730	-111.	512.	32.
		5			100.10	10753.	2510.	4237.	-0.0219	0.0026	0.0002	-111.	512.	32.
736	I-22	1	0.	-0.	1.72	6031.	813.	-2510.	8.2082	1.1063	-0.2986	-35.	1682.	-780.
		5			38.09	6031.	813.	-2510.	-0.0487	0.0593	-0.0275	-35.	1682.	-780.
737		2	0.	-0.	1.84	5335.	-1322.	-428.	6.8024	-1.6849	-0.0366	-16.	1232.	-1982.
		5			39.35	5335.	-1322.	-428.	-0.0199	0.0407	-0.0654	-16.	1232.	-1982.
738		3	0.	-0.	1.65	3962.	-2394.	1264.	5.6466	-3.4119	0.2321	-110.	1297.	-2322.
		5			37.22	3962.	-2394.	1263.	-0.1563	0.0479	-0.0857	-110.	1297.	-2322.
739		4	0.	-0.	5.30	6497.	1124.	-2131.	5.0775	0.8783	-0.1456	-54.	1095.	-2356.
		5			50.26	6497.	1124.	-2131.	-0.0426	0.0222	-0.0477	-54.	1095.	-2356.
740		5	0.	-0.	5.20	5779.	-885.	-114.	4.2425	-0.6496	-0.0073	-9.	-32.	-1403.
		5			51.86	5779.	-885.	-114.	-0.0069	-0.0096	-0.0267	-9.	-32.	-1403.
741		6	0.	-0.	5.20	4289.	-2046.	5139.	3.1484	-1.5022	0.2014	-101.	1369.	-2323.
		5			51.86	4289.	-2046.	5139.	-0.0736	0.0260	-0.0442	-101.	1369.	-2323.
742		7	-4.00	-0.	5.14	6401.	1135.	1445.	2.9257	0.5189	0.0577	-68.	1074.	-2658.
		5			65.72	6401.	1135.	1445.	-0.0313	0.0127	-0.0315	-68.	1074.	-2658.
743		8	0.	-0.	5.14	6948.	1447.	470.	3.1758	0.6613	0.0188	-90.	1069.	-3481.
		5			65.72	6948.	1447.	470.	-0.0414	0.0127	-0.0412	-90.	1069.	-3481.
744		9	0.	-0.	5.72	6130.	-480.	3238.	2.5168	-0.1970	0.1162	-69.	515.	-2432.
		5			69.34	6130.	-480.	3238.	-0.0283	0.0055	-0.0259	-69.	515.	-2432.
745		10	0.	-0.	4.94	4522.	-1646.	5186.	2.1478	-0.7816	0.2153	-173.	1702.	-2374.
		5			64.47	4522.	-1646.	5186.	-0.0822	0.0209	-0.0292	-173.	1702.	-2374.
746		11	4.00	-0.	4.94	7406.	1797.	-635.	3.5181	0.8537	-0.0265	-89.	756.	-2454.
		5			64.47	7406.	1797.	-635.	-0.0421	0.0093	-0.0302	-89.	756.	-2454.
747		12	8.00	-0.	5.21	8081.	2260.	-1223.	3.6386	1.0178	-0.0481	-75.	1056.	-2715.
		5			66.22	8081.	2260.	-1223.	-0.0336	0.0125	-0.0317	-75.	1056.	-2715.
748		13	10.00	-0.	5.52	8525.	2487.	-1924.	3.6231	1.0572	-0.0715	-70.	706.	-2791.
		5			68.16	8525.	2487.	-1924.	-0.0294	0.0078	-0.0307	-70.	706.	-2791.

TABLE A-2 (Continued)

Test Point No.	Run No.	Point of Run	Left N_p RPM	Right N_p RPM	Left β_1 Deg.	Left β_2 Deg.	Right β_1 Deg.	Right β_2 Deg.	Tail i_t Deg.	δ_f Deg.	Baro. in. Hg	To °F	Left N_{J85} - RPM	Right N_{J85} % RPM	Average V_p/V_{tip}	q/qo
749	I-22	14	1700	1700	0	0	0	0	12	30	30.04	94	87.5	88.5	0.1448	1.030
750		15	1695	1705								95			0.1493	1.006
751		16	1670	1770											0.1498	1.011
752		17	1650	1800											0.1488	1.055
753		18	1710	1700					4						0.2239	0.995
754		19	1710	1700											0.2201	1.013
755		20	1710	1710	20	20	20	20						89.0	0.2243	1.033
756		21	1750	1740	35	35	35	35				96			0.2200	1.033
757		22	1715	1700	0	0	0	0				96			0.2207	1.007
758		23	1705	1705								97			0.2212	1.024
759		24	1710	1710											0.2220	1.026
760		25	1705	1735											0.2187	1.029
761		26	1030	1030								95	65.5	67.5	0.3658	1.022
762		27	1000	960								94			0.3856	1.030
763		28	1003	970	20	20	20	20							0.3797	1.047
764		29	1040	980	35	35	35	35							0.3675	1.033
765		30	995	960	0	0	0	0							0.3850	1.055
766		31	1020	970								93			0.3765	1.029
767		32	1040	990											0.3716	1.015
768		33	1040	1190											0.3375	1.027
769		34	1690	1685	10	10	10	10	16				88.0	88.0	0.1123	1.010
770		35		1685											0.1123	1.064
771		36		1695											0.1139	0.977
772		37		1685								94		88.5	0.1165	1.003
773		38										95			0.1128	1.134
774		39	1695												0.1131	0.997
775		40	1695												0.1150	1.028
776		41	1695	1680								99			0.1163	1.076

Test Point No.	Run No.	PT AVG	ALPHA	BETA	Q V_iNOM	LIFT $_i$U CL*QS	DRAG $_i$U CD*QS	M_iU CM*QSC	CL CY	CD CN	CM ιROLL	SIDE F_iU CY*QS	YAW $_i$U ιN*QSb	ROLL $_i$U CL*QSB
749	I-22	14	12.00	-0.	5.14	8465.	2679.	-2095.	5.8691	1.2247	-0.0837	-78.	755.	-1875.
		5			65.72	8465.	2679.	-2095.	-0.0339	0.0089	-0.0222	-78.	755.	-1875.
750		15	14.00	-0.	5.33	8844.	2955.	-2971.	5.8954	1.3017	-0.1144	-6.	295.	-3152.
		5			66.95	8844.	2955.	-2971.	-0.0024	0.0034	-0.0360	-6.	295.	-3152.
751		16	16.00	-0.	5.52	9034.	3146.	-3265.	5.8393	1.3372	-0.1213	70.	133.	-2516.
		5			68.16	9034.	3146.	-3265.	0.0299	0.0015	-0.0277	70.	133.	-2516.
752		17	18.00	-0.	5.72	9454.	3383.	-4312.	5.8816	1.3490	-0.1548	36.	375.	-2121.
		5			69.34	9454.	3383.	-4312.	0.0149	0.0040	-0.0225	36.	375.	-2121.
753		18	-4.00	-0.	11.90	6948.	2031.	12320.	1.3711	0.4008	0.2125	-75.	634.	-4750.
		5			100.02	6948.	2031.	12320.	-0.0144	0.0032	-0.0243	-75.	634.	-4750.
754		19	0.	-0.	11.70	8102.	2172.	9915.	1.6251	0.4356	0.1738	-34.	444.	-4821.
		5			99.21	8102.	2172.	9915.	-0.0069	0.0025	-0.0250	-34.	444.	-4821.
755		20	0.	-0.	12.47	7356.	589.	12524.	1.3844	0.1109	0.2061	100.	-2645.	-1938.
		5			102.41	7356.	589.	12524.	0.0187	-0.0129	-0.0095	100.	-2645.	-1938.
756		21	0.	-0.	12.47	6235.	-479.	12575.	1.1736	-0.0901	0.2069	-110.	-214.	-872.
		5			102.41	6235.	-479.	12575.	-0.0206	-0.0010	-0.0045	-110.	-214.	-872.
757		22	4.00	-0.	11.70	9266.	2451.	8674.	1.8585	0.4917	0.1521	-157.	3176.	-2758.
		5			99.21	9266.	2451.	8674.	-0.0315	0.0165	-0.0145	-157.	3176.	-2758.
758		23	8.00	-0.	11.90	10632.	2744.	5763.	2.0981	0.5415	0.0994	-121.	3035.	-2560.
		5			100.02	10632.	2744.	5763.	-0.0239	0.0155	-0.0131	-121.	3035.	-2560.
759		24	10.00	-0.	12.09	11342.	2998.	5461.	2.2026	0.5819	0.0995	-78.	2750.	-4002.
		5			100.85	11342.	2998.	5461.	-0.0151	0.0138	-0.0206	-78.	2750.	-4002.
760		25	12.00	-0.	11.90	11721.	3303.	5895.	2.3129	0.6518	0.1016	-100.	2501.	-2757.
		5			100.02	11721.	3303.	5895.	-0.0197	0.0128	-0.0141	-100.	2501.	-2757.
761		26	-4.00	-0.	11.90	3444.	1206.	7034.	0.6796	0.2340	0.1217	-34.	490.	-1872.
		5			100.02	3444.	1206.	7034.	-0.0106	0.0025	-0.0096	-34.	490.	-1872.
762		27	0.	-0.	12.09	4546.	1229.	3749.	0.8828	0.2387	0.0656	-92.	1044.	-1767.
		5			100.85	4546.	1229.	3749.	-0.0179	0.0053	-0.0089	-92.	1044.	-1767.
763		28	0.	-0.	12.09	4402.	823.	3209.	0.8548	0.1598	0.0545	-92.	710.	-1444.
		5			100.85	4402.	823.	3209.	-0.0179	0.0036	-0.0075	-92.	710.	-1444.
764		29	0.	-0.	11.70	3881.	489.	2147.	0.7784	0.0981	0.0376	-86.	1071.	14.
		5			99.21	3881.	489.	2147.	-0.0173	0.0056	0.0001	-86.	1071.	14.
765		30	4.00	-0.	12.28	5674.	1289.	937.	1.0846	0.2465	0.0157	-78.	1358.	-1248.
		5			101.62	5674.	1289.	937.	-0.0149	0.0067	-0.0062	-78.	1358.	-1248.
766		31	8.00	-0.	11.90	6662.	1361.	-2461.	1.3147	0.2685	-0.0425	-80.	2143.	-580.
		5			100.02	6662.	1361.	-2461.	-0.0158	0.0109	-0.0030	-80.	2143.	-580.
767		32	10.00	-0.	11.90	7126.	1546.	-3547.	1.4061	0.3050	-0.0612	-43.	1167.	-1341.
		5			100.02	7126.	1546.	-3547.	-0.0086	0.0060	-0.0079	-43.	1167.	-1341.
768		33	12.00	-0.	11.97	7015.	1530.	-7133.	1.3755	0.3000	-0.1222	-124.	1443.	1373.
		5			100.35	7015.	1530.	-7133.	-0.0247	0.0073	0.0070	-124.	1443.	1373.
769		34	-4.00	-0.	3.00	5623.	-506.	122.	4.5943	-0.2388	0.0085	-61.	1338.	-2005.
		5			50.26	5623.	-506.	122.	-0.0878	0.0271	-0.0406	-61.	1338.	-2005.
770		35	-2.00	-0.	3.16	5803.	-102.	39.	4.3124	-0.0758	0.0025	-60.	1342.	-2686.
		5			51.54	5803.	-102.	39.	-0.0448	0.0297	-0.0517	-60.	1342.	-2686.
771		36	0.	-0.	3.00	5950.	90.	-32.	4.6494	0.0703	-0.0022	-72.	1334.	-1841.
		5			50.26	5950.	90.	-32.	-0.0565	0.0270	-0.0372	-72.	1334.	-1841.
772		37	2.00	-0.	3.20	6274.	330.	-743.	4.8054	0.2423	-0.0477	-33.	1398.	-2601.
		5			51.86	6274.	330.	-743.	-0.0241	0.0266	-0.0494	-33.	1398.	-2601.
773		38	4.00	-0.	3.39	6685.	488.	-1369.	4.9884	0.3377	-0.0828	-40.	1401.	-1881.
		5			53.41	6685.	488.	-1369.	-0.0274	0.0251	-0.0337	-40.	1401.	-1881.
774		39	6.00	-0.	3.00	6703.	693.	-1861.	5.2384	0.5418	-0.1271	-62.	1463.	-2100.
		5			50.26	6703.	693.	-1861.	-0.0482	0.0296	-0.0425	-62.	1463.	-2100.
775		40	8.00	-0.	3.20	6967.	953.	-2473.	5.1146	0.6993	-0.1587	-58.	1047.	-2390.
		5			51.86	6967.	953.	-2473.	-0.0428	0.0199	-0.0454	-58.	1047.	-2390.
776		41	10.00	-0.	3.39	7279.	1190.	-2861.	5.0383	0.8237	-0.1731	-93.	1585.	-2107.
		5			53.41	7279.	1190.	-2861.	-0.0646	0.0284	-0.0378	-93.	1585.	-2107.

TABLE A-2 (Continued)

Test Point No.	Run No.	Point of Run	Left N_p RPM	Right N_p RPM	Left β_t Deg.	Left β_0 Deg.	Right β_t Deg.	Right β_0 Deg.	Tail i_t Deg.	δ_f Deg.	Baro. In. Hg	To ^oF	Left $N_{.785}$ % RPM	Right $N_{.785}$ % RPM	Average V_p/V_{tip}	q/qc
777	I-22	42	1715	1690	35	35	35	35	4	30	30.04	99	86.0	88.5	0.2962	0.940
778		43	1720	0									86.0	0	0.2897	0.961
779		44	1685										86.5		0.2263	1.024
780		45	1655										86.5		0.1526	1.023
781		46	1630										86.0		0.0777	0.962
782	I-23	1	1710	1700	0	0	0	0	4	30	30.12	76	87.5	84.0	0.0763	N/A
783		2	1710	1700								76		84.5	0.0753	
784		3	1705	1695								78		84.5	0.0714	
785		4	1700	1700	20	20	20	20				80		85.0	0.0658	
786		5	1690	1710								80			0.0525	
787		6	1660	1690								82			0.0451	
788		7	1740	1740	35	35	35	35				83			0.0793	
789		8	1740	1735								86			0.0977	
790		9	1735	1710								88			0.0947	
791		10	1710	1680	0	0	0	0				88			0.1187	
792		11	1695	1675								92			0.1128	
793		12	1700	1670								92			0.1091	
794		13	1700	1670	20	20	20	20				93	88.0	85.5	0.1348	
795		14	1700	1670								94			0.1201	
796		15	1695	1665											0.1094	
797		16	1730	1690	35	35	35	35							0.1039	
798		17	1735	1675											0.0869	
799		18	1735	1690								95			0.0999	
800		19	1690	1690	0	0	0	0				97			0.1506	
801		20	1695	1695											0.1502	
802		21	1685	1680											0.1513	
803		22	1690	1690	20	20	20	20							0.1560	
804		23	1690	1690	20	20	20	20				98			0.1458	

Test Point No.	Run No.	PT AVG	ALPHA	BETA	Q V,NOM	LEFT,U CL*QS	DRAG,U CD*US	M,U CM*USC	CL CY	CD CM	CM CROLL	SIDE F,U CY*QS	YAW,U CM*QSB	ROLL,U CL*QSB
777	I-22	42	0.	-0.	19.58	8131.	527.	11065.	0.9851	0.0638	0.1172	-83.	-1023.	-2720.
		5			127.65	8131.	527.	11065.	-0.0101	-0.0052	-0.0085	-83.	-1023.	-2720.
778		43	0.	-0.	19.34	5510.	731.	-1500.	0.6689	0.0887	-0.0159	-558.	11395.	9724.
		5			127.53	5510.	731.	-1500.	-0.0678	0.0358	0.0306	-558.	11395.	9724.
779		44	0.	-0.	11.90	3811.	106.	357.	0.7521	0.0209	0.0062	-502.	11091.	8367.
		5			100.02	3811.	106.	357.	-0.0991	0.0567	0.0428	-502.	11091.	8367.
780		45	0.	-0.	5.33	2450.	-532.	1856.	1.0795	-0.2341	0.0715	-845.	10629.	7103.
		5			66.95	2450.	-532.	1856.	-0.1521	0.1212	0.0810	-345.	10629.	7103.
781		46	0.	-0.	1.26	1646.	-1067.	1217.	3.0885	-1.9888	0.1983	-121.	9658.	8122.
		5			52.55	1646.	-1067.	1217.	-0.2259	0.4660	0.3919	-121.	9658.	8122.
782	I-23	1	0.	-0.	1.45	5434.	764.	-110.	8.7753	1.2341	-0.0155	-83.	1209.	1394.
		5			34.96	5434.	764.	-110.	-0.1345	0.0505	0.0583	-83.	1209.	1394.
783		2	0.	-0.	1.41	5388.	734.	535.	8.9801	1.2186	0.0776	-97.	1552.	-270.
		5			34.49	5388.	734.	535.	-0.1605	0.0667	-0.0116	-97.	1552.	-270.
784		3	0.	-0.	1.26	5242.	682.	-489.	9.7678	1.2701	-0.0796	-102.	1864.	2.
		5			32.55	5242.	682.	-489.	-0.1892	0.0899	0.0001	-102.	1864.	2.
785		4	0.	-0.	1.07	4877.	-1376.	1260.	10.7401	-3.0303	0.2426	6.	1660.	-310.
		5			29.94	4877.	-1376.	1260.	0.0132	0.0946	-0.0177	6.	1660.	-310.
786		5	0.	-0.	0.68	4670.	-1479.	-167.	16.1630	-5.1101	-0.0505	-6.	1451.	165.
		5			23.88	4670.	-1479.	-167.	-0.0224	0.1300	-0.0148	-6.	1451.	165.
787		6	0.	-0.	0.48	4378.	-1430.	-743.	21.2096	-6.9296	-0.3149	8.	1197.	-357.
		5			20.19	4378.	-1430.	-743.	0.0384	0.1501	-0.0447	8.	1197.	-357.
788		7	0.	-0.	1.61	3888.	-2304.	2699.	5.6739	-3.3621	0.3442	-139.	1588.	-1688.
		5			36.78	3888.	-2304.	2699.	-0.2028	0.0600	-0.0638	-139.	1588.	-1688.
789		8	0.	-0.	2.42	4044.	-2117.	5100.	3.9187	-2.0510	0.4320	-158.	1646.	-1605.
		5			45.14	4044.	-2117.	5100.	-0.1533	0.0413	-0.0403	-158.	1646.	-1605.
790		9	0.	-0.	2.23	3871.	-2088.	4959.	4.0774	-2.1996	0.4566	-166.	2085.	-1161.
		5			43.29	3871.	-2088.	4959.	-0.1747	0.0569	-0.0317	-166.	2085.	-1161.
791		10	0.	-0.	3.39	6130.	1189.	4871.	4.2426	0.8228	0.2947	-52.	167.	738.
		5			53.41	6130.	1189.	4871.	-0.0360	0.0030	0.0132	-52.	167.	738.
792		11	0.	-0.	3.00	6050.	1107.	3483.	4.7281	0.8449	0.2379	-18.	412.	-1658.
		5			50.26	6050.	1107.	3483.	-0.0137	0.0083	-0.0336	-18.	412.	-1658.
793		12	0.	-0.	2.81	6046.	1046.	2750.	5.0502	0.8736	0.2008	-30.	612.	-1607.
		5			48.61	6046.	1046.	2750.	-0.0251	0.0132	-0.0348	-30.	612.	-1607.
794		13	0.	-0.	4.28	5561.	-541.	6599.	3.0478	-0.2965	0.3161	-70.	738.	-1065.
		5			60.02	5561.	-541.	6599.	-0.0385	0.0105	-0.0151	-70.	738.	-1065.
795		14	0.	-0.	3.39	5292.	-687.	5648.	3.6628	-0.4754	0.3417	-107.	1201.	-78.
		5			53.41	5292.	-687.	5648.	-0.0743	0.0215	-0.0014	-107.	1201.	-78.
796		15	0.	-0.	2.85	5234.	-848.	3491.	4.3131	-0.6989	0.2514	-6.	924.	608.
		5			48.95	5234.	-848.	3491.	-0.0045	0.0197	0.0130	-6.	924.	608.
797		16	0.	-0.	2.62	3979.	-2037.	9515.	3.5702	-1.8280	0.7462	-166.	2723.	-1753.
		5			46.91	3979.	-2037.	9515.	-0.1892	0.0633	-0.0407	-166.	2723.	-1753.
798		17	0.	-0.	1.84	3809.	-2062.	4011.	4.8563	-2.6290	0.4471	-151.	2240.	-1801.
		5			39.35	3809.	-2062.	4011.	-0.1931	0.0740	-0.0595	-151.	2240.	-1801.
799		18	0.	-0.	2.42	3854.	-2040.	9140.	3.7349	-1.9766	0.7742	-142.	2262.	-1192.
		5			45.14	3854.	-2040.	9140.	-0.1374	0.0568	-0.0299	-142.	2262.	-1192.
800		19	0.	-0.	5.33	6518.	1562.	6924.	2.8711	0.6879	0.2666	99.	-977.	-1213.
		5			66.95	6518.	1562.	6924.	0.0437	-0.0111	-0.0138	99.	-977.	-1213.
801		20	0.	-0.	5.33	6485.	1597.	7404.	2.8563	0.7035	0.2851	155.	-1406.	-1149.
		5			66.95	6485.	1597.	7404.	0.0684	-0.0160	-0.0131	155.	-1406.	-1149.
802		21	0.	-0.	5.33	6593.	1581.	6626.	2.9038	0.6966	0.2551	206.	-1778.	-799.
		5			66.95	6593.	1581.	6626.	0.0906	-0.0203	-0.0091	206.	-1778.	-799.
803		22	0.	-0.	5.72	5894.	-272.	9073.	2.4202	-0.1116	0.3256	-135.	1430.	-2352.
		5			69.34	5894.	-272.	9073.	-0.0555	0.0152	-0.0250	-135.	1430.	-2352.
804		23	0.	-0.	4.98	5717.	-394.	8205.	2.6944	-0.1857	0.3380	-147.	2025.	-2172.
		5			64.72	5717.	-394.	8205.	-0.0691	0.0247	-0.0265	-147.	2025.	-2172.

TABLE A-2 (Continued)

Test Point No.	Run No.	Point of Run	Left N_p RPM	Right N_p RPM	Left B_i Deg.	Left B_o Deg.	Right B_i Deg.	Right B_o Deg.	Tail i_t Deg.	δ_f Deg.	Baro. In. Hg	To °F	Left $N_{.385}$ % RPM	Right $N_{.385}$ % RPM	Average V_p/V_{tip}	q/qc
805	I-23	24	1690	1680	20	20	20	20	4	30	30.12	98	88.0	85.5	0.1490	N/A
806		25	1730	1710	35	35	35	35				98			0.1540	
807		26	1735	1725								99			0.1527	
808		27	1725	1710								99			0.1538	
809		28	1695	1690	0	0	0	0				100		86.0	0.2220	
810		29	1705	1705											0.2240	
811		30	1700	1695											0.2250	
812		31	1695	1695	20	20	20	20							0.2289	
813		32	1695	1710											0.2226	
814		33	1695	1695											0.2253	
815		34	1735	1720	35	35	35	35							0.2211	
816		35	1740	1735											0.2180	
817		36	1735	1720											0.2211	
818		37	1775	1750	40	40	40	40							0.2150	
819		38	1775	1760	40	40	40	40							0.2191	
820		39	1695	1700	0	0	0	0					87.5	85.5	0.2976	
821		40	1690	1670											0.3021	
822		41	1685	1670											0.3040	
823		42	1685	1705	20	20	20	20							0.2981	
824		43	1685	1680											0.3028	
825		44	1680	1675											0.3015	
826		45	1725	1725	35	35	35	35							0.2929	
827		46	1715	1700											0.2973	
828		47	1715	1690											0.2981	
829		48	1745	1725	40	40	40	40							0.2899	
830		49	1745	1710	40	40	40	40							0.2938	
831		50	1200	1180	0	0	0	0				98	70.0	67.0	0.4305	

Test Point No.	Run No.	Pt AVG	ALPHA	BETA	Q V,NOM	LIFT,U CL*QS	DRAG,U CD*QS	M,U CM*QSC	CL CY	CD CN	CM CMROLL	SIDE F,U CY*QS	YAW,U CN*QSB	ROLL,U CL*QSB
805	I-23	24	0.	-0.	5.17	5717.	-354.	8693.	2.5935	-0.1607	0.3209	-119.	1400.	-1275.
		5			65.97	5717.	-354.	8693.	-0.0541	0.0164	-0.0150	-119.	1400.	-1275.
806		25	0.	-0.	5.76	6812.	-1310.	10786.	1.9625	-0.5344	0.5845	-254.	3715.	-2394.
		5			69.58	6812.	-1310.	10786.	-0.1034	0.0392	-0.0253	-255.	3715.	-2394.
807		26	0.	-0.	5.72	6711.	-1280.	10653.	1.9344	-0.5256	0.5823	-247.	5833.	-1949.
		5			69.34	6711.	-1280.	10653.	-0.1018	0.0408	-0.0267	-247.	5833.	-1949.
808		27	0.	-0.	5.72	6666.	-1347.	10796.	1.9157	-0.5552	0.5875	-215.	5395.	-956.
		5			69.34	6666.	-1347.	10796.	-0.0882	0.0361	-0.0102	-215.	5395.	-956.
809		28	0.	-0.	11.51	8484.	2474.	13493.	1.7350	-0.5044	0.2405	-6.	276.	-3945.
		5			98.40	8484.	2474.	13493.	-0.0611	0.0015	-0.0208	-6.	276.	-3945.
810		29	0.	-0.	11.90	8532.	2501.	14181.	1.6856	-0.4936	0.2446	-69.	722.	-3527.
		5			100.02	8532.	2501.	14181.	-0.0136	0.0047	-0.0180	-69.	722.	-3527.
811		40	0.	-0.	11.90	8674.	2495.	13814.	1.7117	-0.4924	0.2245	-113.	-618.	-62.
		5			100.02	8674.	2495.	13814.	-0.0015	-0.0042	-0.0003	-12.	-618.	-62.
812		51	0.	-0.	12.28	7730.	750.	15964.	1.4779	0.1458	0.2668	-171.	1570.	-1957.
		5			101.62	7730.	750.	15964.	-0.0527	0.0078	-0.0097	-171.	1570.	-1957.
813		12	0.	-0.	11.70	7344.	715.	15721.	1.4735	0.1434	0.2756	-159.	1395.	-1750.
		5			99.21	7344.	715.	15721.	-0.0318	0.0072	-0.0091	-159.	1395.	-1750.
814		53	0.	-0.	11.90	7536.	712.	15524.	1.4671	0.1405	0.2678	-116.	958.	-2250.
		5			100.02	7536.	712.	15524.	-0.0229	0.0049	-0.0115	-116.	950.	-2250.
815		14	0.	-0.	11.90	6485.	-412.	14693.	1.2797	-0.0813	0.2535	-196.	3451.	-3834.
		5			100.02	6485.	-412.	14693.	-0.0586	0.0178	-0.0156	-196.	3451.	-3834.
816		35	0.	-0.	11.70	6475.	-399.	14247.	1.2987	-0.0800	0.2498	-240.	3789.	-2013.
		5			99.21	6475.	-399.	14247.	-0.0482	0.0197	-0.0105	-240.	3789.	-2013.
817		36	0.	-0.	11.90	6525.	-442.	14240.	1.2872	-0.0871	0.2456	-123.	2551.	-2907.
		5			100.02	6525.	-442.	14240.	-0.0241	0.0130	-0.0149	-123.	2551.	-2907.
818		57	0.	-0.	11.70	5995.	-649.	13214.	1.2624	-0.1303	0.2317	-199.	3917.	-3673.
		5			99.21	5995.	-649.	13214.	-0.0399	0.0203	-0.0191	-199.	3917.	-3673.
819		58	0.	-0.	12.09	6098.	-646.	12766.	1.1845	-0.1254	0.2157	-156.	3059.	-2856.
		5			100.83	6098.	-646.	12766.	-0.0357	0.0154	-0.0144	-156.	3059.	-2856.
820		59	-0.	-0.	20.72	-1222.	5398.	-122642.	-0.1384	0.3851	-1.2148	-140.	5073.	-1704.
		5			131.99	-1222.	5398.	-122642.	-0.0159	0.0090	-0.0050	-140.	5073.	-1704.
821		40	-0.	-0.	20.91	-1248.	5442.	-123586.	-0.1401	0.3864	-1.2128	-59.	2394.	-2721.
		5			132.60	-1248.	5442.	-123586.	-0.0067	0.0070	-0.0079	-59.	2394.	-2721.
822		41	0.	-0.	21.10	11087.	5307.	17529.	1.2536	0.3679	0.1705	-64.	1002.	559.
		5			133.21	11087.	5307.	17529.	-0.0171	0.0029	0.0016	-64.	1002.	559.
823		42	0.	-0.	20.72	10193.	1846.	20142.	1.1556	0.2092	0.1995	-152.	1753.	-850.
		5			131.99	10193.	1846.	20142.	-0.0172	0.0051	-0.0025	-152.	1753.	-850.
824		43	0.	-0.	21.06	10332.	1862.	19259.	1.1516	0.2076	0.1876	-99.	313.	175.
		5			133.09	10332.	1862.	19259.	-0.011	0.0009	0.0005	-99.	313.	175.
825		44	0.	-0.	20.75	10080.	1784.	18123.	1.1401	0.2018	0.1792	-68.	-399.	-357.
		5			132.12	10080.	1784.	18123.	-0.0077	-0.0012	-0.0010	-68.	-399.	-357.
826		45	0.	-0.	20.72	9002.	709.	16426.	1.0201	0.0804	0.1627	-164.	2176.	-2331.
		5			131.99	9002.	709.	16426.	-0.0186	0.0064	-0.0068	-164.	2176.	-2331.
827		46	0.	-0.	20.91	9046.	713.	17652.	1.0156	0.0800	0.1674	-121.	1534.	-2408.
		5			132.60	9046.	713.	17652.	-0.0136	0.0045	-0.0070	-121.	1534.	-2408.
828		47	0.	-0.	20.91	9053.	663.	15724.	1.0164	0.0744	0.1543	-62.	194.	-2171.
		5			132.60	9053.	663.	15724.	-0.0072	0.0006	-0.0063	-62.	194.	-2171.
829		48	0.	-0.	20.52	8258.	417.	14463.	0.9445	0.0477	0.1446	-225.	3388.	-2035.
		5			131.38	8258.	417.	14463.	-0.0258	0.0100	-0.0060	-225.	3388.	-2035.
830		49	0.	-0.	20.91	8417.	396.	14208.	0.9455	0.0444	0.1394	-166.	2306.	-1999.
		5			132.60	8417.	396.	14208.	-0.0187	0.0067	-0.0058	-166.	2306.	-1999.
831		50	0.	-0.	21.29	7786.	2113.	5851.	0.8584	0.2330	0.0564	-55.	1804.	-2193.
		5			135.81	7786.	2113.	5851.	-0.0061	0.0051	-0.0063	-55.	1804.	-2193.

TABLE A-2 (Continued)

Test Point No.	Run No.	Point of Run	Left N_p RPM	Right N_p RPM	Left β_1 Deg.	Left β_2 Deg.	Right β_1 Deg.	Right β_2 Deg.	Tail i_t Deg.	δ_f Deg.	Baro. in. Hg	To °y	Left $N_{.385}$ % RPM	Right $N_{.385}$ % RPM	Average V_p/V_{tip}	q/qc
832	I-23	51	1185	1165	0	0	0	0	4	30	30.12	98	70.0	67.0	0.4315	N/A
833		52	1170	1170	0	0	0	0							0.4330	
834		53	1160	1150	20	20	20	20							0.4366	
835		54	1140	1160											0.4406	
836		55	1150	1150								97			0.4422	
837		56	1160	1130	35	35	35	35				96			0.4416	
838		57	1170	1150											0.4358	
839		58	1190	1160											0.4307	
840		59	1220	1175	40	40	40	40							0.4197	
841		60	1195	1160										66.5	0.4275	
842		61	1185	1140									69.5	66.5	0.4350	
843		62	1682	-	35	35	35	35				95	87.0	-	0.3031	
844	I-24	1	100	125	35	35	35	35	4	30	30.23	74	0	0	N/A	N/A
845		2	70	93												
846		3	45	52												
847		4	7	20												
848		5	0	0												
849		6	-50	-36												
850		7	-80	-90												
851		8	-144	-134												
852		9	-160	-160												
853		10	-190	-190												
854	I-25	1	0	0	90	90	90	90	4	30	30.24	77	0	0	N/A	N/A
855		2														
856		3														
857		4														
858		5														
859		6														

Test Point No	Run No.	PT AVG	ALPHA	BETA	Q V,NOM	LIFT,U CL*QS	DRAG,U CD*QS	M,U CM*USC	CL CY	CD CN	CM CROLL	SIDE F,U CY*QS	YAW,U CN*QSB	ROLL,U CL*QSB
832	I-23	51	0.	-0.	20.91	7786.	2215.	7461.	0.8742	0.2486	0.0732	-4.	1329.	-1514.
		5			132.60	7786.	2215.	7461.	-0.0065	0.0039	-0.0044	-4.	1329.	-1514.
833		52	0.	-0.	20.91	7774.	2171.	7770.	0.8728	0.2438	0.0763	62.	385.	-3276.
		5			132.60	7774.	2171.	7770.	0.0069	0.0011	-0.0095	62.	385.	-3276.
834		53	0.	-0.	20.72	7698.	1704.	5941.	0.8496	0.1931	0.0588	27.	569.	-2690.
		5			131.99	7698.	1704.	5941.	0.0031	0.0017	-0.0079	27.	569.	-2690.
835		54	0.	-0.	20.91	7582.	1681.	5820.	0.8513	0.1887	0.0571	-38.	703.	-2581.
		5			132.60	7582.	1681.	5820.	-0.0042	0.0020	-0.0075	-38.	703.	-2581.
836		55	0.	-0.	21.10	7433.	1659.	5406.	0.8277	0.1846	0.0526	-67.	749.	-660.
		5			133.21	7433.	1659.	5406.	-0.0075	0.0022	-0.0019	-67.	749.	-660.
837		56	0.	-0.	20.91	6773.	1212.	2993.	0.7604	0.1361	0.0294	-70.	1164.	-1713.
		5			132.60	6775.	1212.	2993.	-0.0078	0.0034	-0.0050	-70.	1164.	-1713.
838		57	0.	-0.	20.91	6804.	1255.	3229.	0.7446	0.1409	0.0317	-28.	992.	-132.
		5			132.60	6804.	1255.	3229.	-0.0031	0.0029	-0.0004	-28.	992.	-132.
839		58	0.	-0.	20.91	6766.	1272.	2634.	0.7596	0.1428	0.0259	74.	-885.	-2412.
		5			132.60	6766.	1272.	2634.	0.0081	-0.0026	-0.0070	74.	-885.	-2412.
840		59	0.	-0.	20.60	6317.	1122.	1036.	0.7198	0.1278	0.0103	90.	-1079.	154.
		5			131.63	6317.	1122.	1036.	0.0103	-0.0032	0.0005	90.	-1079.	154.
841		60	0.	-0.	20.72	6456.	1116.	2605.	0.7316	0.1264	0.0258	-7.	40.	219.
		5			131.99	6456.	1116.	2605.	-0.0001	0.0001	0.0006	-7.	40.	219.
842		61	0.	-0.	20.91	6497.	1070.	1577.	0.7295	0.1202	0.0135	14.	35.	-608.
		5			132.60	6497.	1070.	1577.	0.0016	0.0001	-0.0018	14.	35.	-608.
843		62	0.	-0.	21.29	5976.	629.	1867.	0.6589	0.0694	0.0180	-602.	11263.	14048.
		5			133.81	5976.	629.	1867.	-0.0064	0.0322	0.0401	-602.	11263.	14048.
844	I-24	1	-3.89	-0.	20.81	1078.	1092.	-3194.	0.1215	0.1234	-0.0286	49.	-834.	-1642.
		5			132.30	1078.	1094.	-2896.	0.0056	-0.0024	-0.0048	49.	-834.	-1642.
845		2	0.27	-0.	21.00	2652.	1124.	-10847.	0.2964	0.1270	-0.0988	62.	-789.	-565.
		5			132.91	2652.	1137.	-10115.	0.0073	-0.0023	-0.0016	62.	-789.	-565.
846		3	4.43	-0.	21.00	4176.	1305.	-15802.	0.4667	0.1494	-0.1431	24.	-263.	514.
		5			132.91	4176.	1337.	-14647.	0.0027	-0.0008	0.0015	24.	-263.	514.
847		4	6.53	-0.	21.00	5122.	1462.	-17498.	0.5724	0.1687	-0.1571	22.	-161.	-142.
		5			132.91	5122.	1509.	-16081.	0.0025	-0.0005	-0.0004	22.	-161.	-142.
848		5	8.61	-0.	21.00	5904.	1639.	-18649.	0.6599	0.1901	-0.1604	5.	-176.	-135.
		5			132.91	5904.	1701.	-16417.	0.0005	-0.0005	-0.0004	5.	-176.	-135.
849		6	10.69	-0.	20.85	6602.	1819.	-19036.	0.7434	0.2136	-0.1694	12.	-286.	-959.
		5			132.42	6602.	1898.	-17211.	0.0014	-0.0008	-0.0028	12.	-286.	-959.
850		7	12.78	-0.	21.04	7603.	2130.	-21925.	0.8482	0.2492	-0.1933	32.	-332.	-1066.
		5			133.05	7603.	2234.	-19825.	0.0036	-0.0010	-0.0031	32.	-332.	-1066.
851		8	14.88	-0.	20.81	8422.	2580.	-26004.	0.9499	0.3056	-0.2334	17.	297.	-1827.
		5			132.30	8422.	2709.	-23675.	0.0019	0.0009	-0.0053	17.	297.	-1827.
852		9	16.93	-0.	20.62	8890.	3014.	-29774.	1.0120	0.3596	-0.2718	13.	1227.	-1619.
		5			131.69	8890.	3158.	-27316.	0.0015	0.0036	-0.0048	13.	1227.	-1619.
853		10	19.01	-0.	21.27	9871.	3828.	-37550.	1.0894	0.4815	-0.3359	19.	874.	-3776.
		5			135.75	9871.	4001.	-34821.	0.0021	0.0025	-0.0108	19.	874.	-3776.
854	I-25	1	0.47	-0.	1.36	293.	65.	-1343.	0.5067	0.1163	-0.1909	-1.	-13.	-153.
		5			33.78	293.	67.	-1262.	-0.0025	-0.0006	-0.0069	-1.	-13.	-153.
855		2	0.45	-0.	5.39	1116.	217.	-3920.	0.4862	0.0985	-0.1376	-6.	120.	659.
		5			67.31	1116.	226.	-3612.	-0.0027	0.0014	0.0074	-6.	120.	659.
856		3	0.43	-0.	11.99	2400.	492.	-8454.	0.4698	0.0998	-0.1333	5.	-126.	452.
		5			100.43	2400.	510.	-7791.	0.0010	-0.0006	0.0023	5.	-126.	452.
857		4	-3.83	-0.	21.00	1610.	797.	-9542.	0.1800	0.0896	-0.0889	44.	-572.	172.
		5			132.91	1610.	802.	-9397.	0.0049	-0.0017	0.0005	44.	-572.	172.
858		5	0.43	-0.	21.19	4202.	886.	-14691.	0.4655	0.1016	-0.1310	16.	-393.	59.
		5			133.51	4202.	917.	-13529.	0.0018	-0.0011	0.0002	16.	-393.	59.
859		6	4.68	-0.	21.19	4658.	1100.	-19427.	0.7994	0.1316	-0.1703	-9.	-8.	664.
		5			133.51	6658.	1188.	-17586.	-0.0010	0.0000	0.0019	-9.	-8.	664.

TABLE A-2 (Continued)

Test Point No.	Run No.	Point of Run	Left N_p RPM	Right N_p RPM	Left β_1 Deg.	Left β_0 Deg.	Right β_1 Deg.	Right β_0 Deg.	Tail i_t Deg.	δ_f Deg.	Baro. in. Hg	T_0 - $^\circ_F$	Left N_{J85} % RPM	Right N_{J85} % RPM	Average V_p/V_{tip}	q/qc
860	I-25	7	0	0	90	90	90	90	4	30	30.24	77	0	0	N/A	N/A
861		8														
862		9														
863		10														
864		11														
865		12														
866		13														
867		14														
868		15														
869		16														
870		17														
871		18														
872		19														
873		20														
874		21														
875	I-26	1	Not Recorded		0	0	0	0	4	30	30.24	63	—— Not Recorded ——			0.724
876		2										64				1.134
877		3										67				1.380
878		4										67				1.380
879		5	1710	1690								70	87.0	85.0	0.1109	1.003
880		6	1710	1690								71			0.1092	1.037
881		7										74			0.1082	1.062
882		8										75	87.5	85.5	0.1083	1.062
883		9										76			0.1097	1.037
884		10	1720	1685								77			0.1096	1.037
885		11	1715	1685								78			0.1113	1.010
886		12	1715	1680								80			0.1098	1.044
887		13	1715	1680								80			0.1121	1.003

Test Point No.	Run No.	PT AVG	ALPHA	BETA	Q V,NOM	LIFT,U CL*QS	DRAG,U CD*QS	M,U CM*QSC	CL CY	CD CN	CM CROLL	SIDE F,U CY*QS	YAW,U CN*QSB	ROLL,U CL*QSB
860	I-25	7	8.91	-0.	20.81	8707.	1446.	-22591.	0.9821	0.1786	-0.1990	-10.	-106.	295.
		5			132.30	8707.	1584.	-20184.	-0.0011	-0.0003	0.0009	-10.	-106.	295.
861		8	11.00	-0.	21.00	9722.	1669.	-24407.	1.0867	0.2055	-0.2122	-9.	116.	67.
		5			132.91	9722.	1859.	-21719.	-0.0010	0.0003	0.0002	-9.	116.	67.
862		9	13.08	-0.	21.00	10459.	1925.	-25110.	1.1690	0.2369	-0.2171	12.	-468.	-1227.
		5			132.91	10459.	2120.	-22218.	-0.0014	-0.0036	0.0036	12.	-468.	-1227.
863		10	15.13	-0.	20.81	10855.	2390.	-24103.	1.2244	0.2937	-0.2061	53.	388.	-2448.
		5			132.30	10855.	2604.	-21102.	0.0066	0.0011	-0.0071	53.	388.	-2448.
864		11	17.14	-0.	20.62	10812.	3065.	-26726.	1.2309	0.4735	-0.2362	-36.	1165.	-2290.
		5			131.69	10812.	3279.	-23736.	-0.0060	0.0034	-0.0068	-36.	1164.	-2290.
865		12	-5.91	-0.	20.81	854.	990.	-9573.	0.0964	0.1118	-0.0921	29.	-858.	-399.
		5			132.30	854.	991.	-9336.	0.0092	-0.0025	-0.0012	29.	-858.	-399.
866		13	0.30	-0.	21.16	2902.	1151.	-15789.	0.5229	0.1294	-0.1454	38.	-609.	-1064.
		5			133.39	2902.	1166.	-14987.	0.0042	-0.0017	-0.0031	38.	-609.	-1064.
867		14	4.49	-0.	21.04	4750.	1377.	-20020.	0.5299	0.1581	-0.1824	19.	-310.	-752.
		5			133.03	4750.	1417.	-18707.	0.0021	-0.0009	-0.0022	19.	-310.	-752.
868		15	6.60	-0.	21.00	5834.	1571.	-20402.	0.6521	0.1824	-0.1836	13.	112.	-104.
		5			132.91	5834.	1632.	-18789.	0.0015	0.0003	-0.0003	13.	112.	-104.
869		16	8.69	-0.	21.00	6679.	1726.	-21997.	0.7465	0.2019	-0.1969	30.	-78.	-726.
		5			132.91	6679.	1807.	-20150.	0.0033	-0.0002	-0.0021	30.	-78.	-726.
870		17	10.77	-0.	21.19	7488.	1930.	-22582.	0.8294	0.2248	-0.1986	39.	95.	-18.
		5			133.51	7488.	2030.	-20511.	0.0044	0.0005	-0.0001	39.	95.	-18.
871		18	12.87	-0.	21.00	8446.	2146.	-23278.	0.9439	0.2542	-0.2046	-0.	101.	-1736.
		5			132.91	8446.	2275.	-20942.	-0.0000	0.0005	-0.0050	-0.	101.	-1736.
872		19	14.99	-0.	20.81	9475.	2468.	-24961.	1.0688	0.2968	-0.2205	12.	60.	-1832.
		5			132.30	9475.	2651.	-22341.	0.0014	0.0002	-0.0054	12.	60.	-1832.
873		20	17.06	-0.	20.81	10207.	2973.	-27741.	1.1513	0.3567	-0.2457	8.	750.	-2195.
		5			132.30	10207.	3162.	-24919.	0.0009	0.0022	-0.0064	8.	750.	-2195.
874		21	19.15	-0.	20.62	10924.	3745.	-32981.	1.2456	0.4513	-0.2981	-6.	900.	-1608.
		5			131.69	10924.	3964.	-29960.	-0.0007	0.0027	-0.0047	-6.	900.	-1608.
875	I-26	1	0.	-0.	1.86	4094.	-2847.	5092.	5.1660	-3.5924	0.5616	-162.	-16104.	-23873.
		5			59.56	4094.	-2847.	5092.	-0.2047	-0.5261	-0.7759	-162.	-16104.	-23873.
876		2	0.	-0.	2.71	5618.	-1297.	426.	4.8616	-1.1224	0.0322	155.	-10817.	-32017.
		5			47.77	5618.	-1297.	426.	0.1337	-0.2423	-0.7173	155.	-10817.	-32017.
877		3	0.	-0.	1.78	5431.	-3198.	115907.	7.1506	-4.2099	13.3393	224.	3213.	-36053.
		5			38.72	5431.	-3198.	115907.	0.2951	0.1095	-1.2291	224.	3213.	-36053.
878		4	0	-0.	1.16	5453.	315.	-5947.	11.0078	0.6357	-1.0495	284.	2525.	-37084.
		5			31.27	5453.	315.	-5947.	0.5737	0.1320	-1.9385	284.	2525.	-37084.
879		5	-4.00	-0.	3.10	5947.	808.	4150.	4.5022	0.6116	0.2746	-48.	353.	-321.
		5			51.07	5947.	808.	4150.	-0.0363	0.0069	-0.0063	-48.	353.	-321.
880		6	-2.00	-0.	3.10	6240.	928.	3500.	4.7239	0.7024	0.2316	-55.	14.	-761.
		5			51.07	6240.	928.	3500.	-0.0418	0.0003	-0.0149	-55.	14.	-761.
881		7	0.	-0.	3.10	6307.	1131.	3116.	4.7748	0.8564	0.2062	-36.	-442.	-394.
		5			51.07	6307.	1131.	3116.	-0.0269	-0.0087	-0.0077	-36.	-442.	-394.
882		8	2.00	-0.	3.10	6466.	1528.	2687.	4.8947	1.0057	0.1778	-83.	-169.	-230.
		5			51.07	6466.	1528.	2687.	-0.0629	-0.0033	-0.0045	-83.	-169.	-230.
883		9	4.00	-0.	3.10	6626.	1546.	2490.	5.0164	1.1703	0.1912	-63.	-98.	-655.
		5			51.07	6626.	1546.	2490.	-0.0480	-0.0019	-0.0128	-63.	-98.	-655.
884		10	6.00	-0.	3.10	6790.	1765.	2755.	5.1400	1.3366	0.1823	-45.	-610.	-433.
		5			51.07	6790.	1765.	2755.	-0.0338	-0.0120	-0.0085	-45.	-610.	-433.
885		11	8.00	-0.	3.10	6941.	1997.	2545.	5.2544	1.5115	0.1684	-11.	-805.	-415.
		5			51.07	6941.	1997.	2545.	-0.0084	-0.0158	-0.0061	-11.	-805.	-415.
886		12	10.00	-0.	3.10	7063.	2188.	2133.	5.3671	1.6562	0.1412	5.	-1325.	292.
		5			51.07	7063.	2188.	2133.	0.0040	-0.0260	0.0057	5.	-1325.	292.
887		13	12.00	-0.	3.10	7241.	2434.	2391.	5.4815	1.8429	0.1582	58.	-1444.	-1073.
		5			51.07	7241.	2434.	2391.	0.0436	-0.0287	-0.0210	58.	-1444.	-1075.

TABLE A-2 (Continued)

Test Point No.	Run No.	Point of Run	Left N_p RPM	Right N_p RPM	Left β_1 Deg.	Left β_2 Deg.	Right β_1 Deg.	Right β_2 Deg.	Tail i_t Deg.	δ_f Deg.	Baro. in. Hg	To $^\circ_y$	Left N_{JBS} % RPM	Right N_{JBS} % RPM	Average V_p/V_{tip}	q/qc
888	I-26	14	1710	1680	0	0	0	0	4	30	30.24	81	87.5	85.5	0.1109	1.030
889		15	1710	1680								82			0.1114	1.023
890		16	1710	1680								82			0.1121	1.010
891		17	1710	1710								84	88.0	86.5	0.1472	1.013
892		18	1712	1712								85			0.1455	0.998
893		19	1710	1715								86			0.1441	0.982
894		20	1710	1715								86			0.1438	0.986
895		21	1710	1720								88			0.1415	1.018
896		22	1710	1720								88			0.1421	1.010
897		23	1715	1750								89			0.1443	0.998
898		24	1730	1700								90			0.1464	0.991
899		25	1705	1700								92			0.2202	1.027
900		26	1705	1705								92			0.2196	1.014
901		27	1715	1700								93			0.2204	1.020
902		28	1725	1720								93			0.2176	1.012
903		29	1725	1725								94			0.2175	0.996
904		30	1730	1744								95			0.2163	1.012
905		31	1740	1780								95			0.2132	1.030
906		32	1700	1700	20	20	20	20				97		87.0	0.2943	1.024
907		33	1720	1705								98			0.2923	1.024
908		34	1725	1705											0.2918	1.015
909		35	1740	1740											0.2876	1.015
910		36	1730	1780											0.2852	1.015
911		37	1730	1850								99			0.2803	1.021
912		38	1110	1100	0	0	0	0				99	71.0	67.0	0.3981	1.023
913		39	1160	1100								99	70.0		0.3893	
914		40	1150	1160								98	68.0		0.3806	
915		41	1160	1292								98	68.0		0.3585	

Test Point No.	Run No.	PT AVG	ALPHA	BETA	Q V,NOM	LIFT,U CL*QS	DRAG,U CD*QS	M,U CM*QSC	CL CY	CD CM	CM CROLL	SIDE F,U CY*QS	YAW,U CN*QSB	ROLL,U CL*QSB
888	I-26	14	14.00	-0.	3.10	7315.	2660.	2227.	5.5361	2.0134	0.1474	72.	-1634.	-2568.
		5			51.07	7315.	2660.	2227.	0.0545	-0.0320	-0.0503	72.	-1634.	-2568.
889		15	16.00	-0.	3.10	7529.	2897.	1546.	5.6996	2.1929	0.1023	57.	-1683.	-905.
		5			51.07	7529.	2897.	1546.	0.0429	-0.0330	-0.0177	57.	-1682.	-905.
890		16	18.00	-0.	3.10	7668.	3164.	615.	5.8050	2.3955	0.0407	67.	-1542.	-2120.
		5			51.07	7668.	3164.	615.	0.0505	-0.0302	-0.0416	67.	-1542.	-2120.
891		17	-4.00	-0.	5.43	6278.	1312.	7491.	2.7167	0.5674	0.2833	108.	-2016.	-944.
		5			67.56	6278.	1312.	7491.	0.0467	-0.0226	-0.0106	108.	-2016.	-944.
892		18	0.	-0.	5.23	6931.	1595.	6621.	3.1094	0.7157	0.2596	94.	-1897.	1062.
		5			66.34	6931.	1595.	6621.	0.0422	-0.0220	0.0123	94.	-1897.	1062.
893		19	4.00	-0.	5.04	7565.	1953.	5890.	3.5242	0.9098	0.2398	56.	-1159.	-1614.
		5			65.10	7565.	1953.	5890.	0.0262	-0.0140	-0.0195	56.	-1159.	-1614.
894		20	8.00	-0.	5.04	8153.	2372.	5557.	3.7981	1.1050	0.2263	36.	-388.	-3109.
		5			65.10	8153.	2372.	5557.	0.0170	-0.0047	-0.0375	36.	-388.	-3109.
895		21	10.00	-0.	5.04	8374.	2590.	5166.	3.9016	1.2066	0.2104	92.	-604.	-4784.
		5			65.10	8374.	2590.	5166.	0.0429	-0.0073	-0.0577	92.	-604.	-4784.
896		22	12.00	-0.	5.04	8659.	2826.	4174.	4.0345	1.3164	0.1700	34.	-409.	-2213.
		5			65.10	8659.	2826.	4174.	0.0157	-0.0049	-0.0267	34.	-439.	-2213.
897		23	14.00	-0.	5.23	9137.	3144.	3611.	4.0989	1.4103	0.1416	68.	-653.	-2593.
		5			66.34	9137.	3144.	3611.	0.0304	-0.0076	-0.0601	68.	-653.	-2593.
898		24	16.00	-0.	5.23	9431.	3415.	3382.	4.2310	1.5322	0.1326	166.	-1044.	-5816.
		5			66.34	9431.	3415.	3382.	0.0743	-0.0121	-0.0676	166.	-1044.	-5816.
899		25	-4.00	-0.	11.99	7380.	2306.	15918.	1.4447	0.4515	0.2724	-145.	222.	-2408.
		5			100.43	7380.	2306.	15918.	-0.0284	0.0011	-0.0122	-145.	222.	-2408.
900		26	0.	-0.	11.80	8626.	2512.	14281.	1.7160	0.4997	0.2483	-132.	515.	-412.
		5			99.62	8626.	2512.	14281.	-0.0264	0.0027	-0.0021	-132.	515.	-412.
901		27	4.00	-0.	11.99	9984.	2866.	12793.	1.9548	0.5611	0.2189	-108.	646.	-1386.
		5			100.43	9984.	2866.	12793.	-0.0210	0.0033	-0.0070	-108.	646.	-1386.
902		28	8.00	-0.	11.80	11476.	3250.	10006.	2.2835	0.6465	0.1740	-33.	503.	-1910.
		5			99.62	11476.	3250.	10006.	-0.0065	0.0016	-0.0098	-33.	503.	-1910.
903		29	10.00	-0.	11.61	11903.	3490.	9076.	2.4071	0.7058	0.1604	-15.	-418.	-2950.
		5			98.81	11903.	3490.	9076.	-0.0035	-0.0022	-0.0154	-15.	-418.	-2950.
904		30	12.00	-0.	11.80	12198.	3777.	8768.	2.4267	0.7513	0.1525	26.	-571.	-4073.
		5			99.62	12198.	3777.	8768.	0.0053	-0.0029	-0.0210	26.	-571.	-4073.
905		31	14.00	-0.	11.99	12978.	3965.	5369.	2.5408	0.7762	0.0919	-9.	134.	-1652.
		5			100.43	12978.	3965.	5369.	-0.0017	0.0007	-0.0084	-9.	134.	-1652.
906		32	4.00	-0.	21.00	7838.	1484.	4557.	0.8761	0.1658	0.0445	-51.	-1390.	-118.
		5			132.91	7838.	1484.	4557.	-0.0057	-0.0040	-0.0003	-51.	-1390.	-118.
907		33	0.	-0.	21.00	10354.	1750.	20332.	1.1572	0.1956	0.1986	-99.	-480.	309.
		5			132.91	10354.	1750.	20332.	-0.0111	-0.0014	0.0009	-99.	-480.	309.
908		34	4.00	-0.	20.81	12652.	2124.	16650.	1.4271	0.2396	0.1642	-97.	-668.	-650.
		5			132.30	12652.	2124.	16650.	-0.0109	-0.0019	-0.0019	-97.	-668.	-650.
909		35	8.00	-0.	20.81	14949.	2580.	13964.	1.6862	0.2910	0.1377	-108.	-278.	19.
		5			132.30	14949.	2580.	13964.	-0.0121	-0.0008	0.0001	-108.	-278.	19.
910		36	10.00	-0.	20.81	16002.	2875.	11407.	1.8050	0.3242	0.1125	-166.	-131.	1144.
		5			132.30	16002.	2875.	11407.	-0.0187	-0.0004	0.0033	-166.	-131.	1144.
911		37	12.00	-0.	21.00	16660.	3175.	4275.	1.8621	0.3546	0.0418	-847.	-5366.	22870.
		5			132.91	16660.	3175.	4275.	-0.0946	-0.0155	0.0662	-847.	-5366.	22870.
912		38	-4.00	-0.	16.21	5225.	2004.	12847.	0.7566	0.2902	0.1626	-55.	1921.	-2044.
		5			116.77	5225.	2004.	12847.	-0.0079	0.0072	-0.0077	-55.	1921.	-2044.
913		39	0.	-0.	16.21	6842.	1960.	8225.	0.9908	0.2838	0.1061	-18.	937.	-3426.
		5			116.77	6842.	1960.	8225.	-0.0026	0.0035	-0.0128	-18.	937.	-3426.
914		40	4.00	-0.	16.21	8045.	1961.	3033.	1.1649	0.2811	0.0384	46.	702.	-2268.
		5			116.77	8045.	1961.	3033.	0.0066	0.0026	-0.0085	46.	702.	-2268.
915		41	8.00	-0.	16.21	8875.	1889.	-4075.	1.2851	0.2735	-0.0516	-6.	-147.	-8.
		5			116.77	8875.	1889.	-4075.	-0.0008	-0.0006	-0.0000	-6.	-147.	-8.

TABLE A-2 (Continued)

Test Point No.	Run No.	Point of Run	Left N_p RPM	Right N_p RPM	Left β_1 Deg.	Left β_2 Deg.	Right β_1 Deg.	Right β_2 Deg.	Tail i_t Deg.	δ_f Deg.	Baro. in. Hg	To °F	Left N_{JBS} % RPM	Right N_{JBS} % RPM	Average V_p/V_{tip}	q/qc
916	I-26	42	1140	1065	0	0	0	0	4	30	30.24	98	68.5	68.5	0.3841	1.011
917		43	1100	900	0	0	0	0	4	30	30.24	98	69.0	69.0	0.4235	1.011
918	I-27	1	2400	2400	0	0	0	0	4	30	30.19	86	99.0	95.0	0.1541	0.985
919		2	2415	2500	20	20	20	20				92		95.0	0.1560	1.075
920		3	2460	2430	35	35	35	35				92		95.5	0.1584	1.042
921		4	2395	2380	20	20	20	20				98		96.0	0.1610	1.054
922		5	2395	2385	20	20	20	20				98		96.0	0.1596	1.022
923	II-1	1	0	0	90	90	90	90	4	30	30.19	80	0	0	N/A	N/A
924		2														
925		3														
926		4														
927		5														
928		6														
929		7														
930		8														
931		9														
932		10														
933		11														
934		12														
935		13														
936		14														
937	II-2	1	0	0	90	90	90	90	5	30	30.21	82	0	0	N/A	N/A
938		2														
939		3														
940		4														
941		5														
942		6														
943		7														

Test Point No.	Run No.	MT AVG	ALPHA	BETA	Q V,NOM	LIFT,U CL*QS	DRAG,U CD*QS	M,U CM*QSC	CL CY	CD CN	CM CROLL	SIDE F,U CY*QS	YAW,U CN*QSB	ROLL,U CL*QSB
916	I-26	42	10.00	-0.	16.02	8914.	1999.	-6532.	1.3062	0.2929	-0.0837	-252.	2330.	3857.
		5			116.07	8914.	1999.	-6532.	-0.0370	0.0088	0.0146	-252.	2330.	3857.
917		43	12.00	-0.	16.02	8566.	2161.	-10461.	1.2260	0.3167	-0.1340	-129.	633.	3202.
		5			116.07	8566.	2161.	-10461.	-0.0189	0.0024	0.0122	-129.	633.	3202.
918	I-27	1	0.	-0.	11.30	13768.	3223.	15890.	2.8598	0.6694	0.2522	93.	-2781.	-1172.
		5			97.49	13768.	3223.	15890.	0.0193	-0.0150	-0.0063	93.	-2781.	-1172.
919		2	0.	-0.	13.10	12502.	-405.	19658.	2.2395	-0.0726	0.3078	-244.	787.	-4234.
		5			104.98	12502.	-405.	19658.	-0.0437	0.0046	-0.0196	-244.	787.	-4234.
920		3	0.	-0.	12.95	10080.	-2644.	22997.	1.8271	-0.4792	0.3644	-619.	6892.	-1062.
		5			104.56	10080.	-2644.	22997.	-0.1122	0.0323	-0.0050	-619.	6892.	-1062.
921		4	0.	-0.	12.76	12098.	-428.	19531.	2.2259	-0.0787	0.3141	-225.	-362.	-3124.
		5			103.59	12098.	-428.	19531.	-0.0413	-0.0017	-0.0149	-225.	-362.	-3124.
922		5	0.	-0.	12.18	12038.	-516.	18564.	2.5195	-0.0994	0.3127	-277.	945.	-3271.
		5			101.23	12038.	-516.	18564.	-0.0534	0.0067	-0.0163	-277.	945.	-3271.
923	II-1	1	-3.84	-0.	21.12	1548.	929.	-11373.	0.1726	0.1037	-0.1063	74.	-2222.	57.
		4			133.28	1548.	933.	-10940.	0.0065	-0.0044	0.0002	74.	-2222.	57.
924		2	0.43	-0.	21.19	4184.	984.	-15973.	0.4612	0.1124	-0.1433	70.	-1533.	-394.
		4			133.51	4184.	1015.	-14806.	0.0078	-0.0044	-0.0011	70.	-1533.	-394.
925		3	4.68	-0.	21.19	6603.	1194.	-19967.	0.7313	0.1409	-0.1754	52.	-1420.	1624.
		4			133.51	6603.	1272.	-18117.	0.0057	-0.0041	0.0047	52.	-1420.	1624.
926		4	6.80	-0.	21.00	7797.	1334.	-22281.	0.8715	0.1613	-0.1963	36.	-1225.	1708.
		4			132.91	7797.	1443.	-20695.	0.004	-0.0035	0.0049	36.	-1225.	1708.
927		5	8.91	-0.	21.22	8937.	1551.	-25924.	0.9887	0.1874	-0.2071	30.	-1013.	2599.
		4			133.59	8937.	1693.	-21419.	0.0037	-0.0029	0.0074	32.	-1013.	2599.
928		6	11.01	-0.	20.98	9768.	1738.	-24636.	1.093	0.2138	-0.2142	41.	-1173.	2941.
		4			132.83	9768.	1910.	-21898.	0.0046	-0.0034	0.0085	41.	-1173.	2941.
929		7	13.08	-0.	20.84	10344.	1934.	-25005.	1.1654	0.2398	-0.2177	54.	-1133.	3268.
		4			132.38	10344.	2128.	-22103.	0.0061	-0.0033	0.0095	54.	-1133.	3268.
930		8	15.10	-0.	20.98	10638.	2485.	-23873.	1.1905	0.3066	-0.2043	104.	-2261.	-5381.
		4			132.83	10638.	2687.	-20891.	0.0116	-0.0066	-0.0156	104.	-2261.	-5381.
931		9	-5.85	-6.3	21.00	1486.	969.	-11971.	0.166	0.1087	-0.1129	45.	-6304.	5455.
		5			132.91	1486.	973.	-11557.	0.0505	-0.0182	0.0159	45.	-6304.	5499.
932		10	0.42	-6.3	21.12	4054.	1039.	-17121.	0.4506	0.1187	-0.1554	459.	-6566.	6581.
		5			133.27	4054.	1068.	-15992.	0.0511	-0.0189	0.0193	459.	-6566.	6706.
933		11	4.66	-6.3	20.95	6410.	1240.	-20762.	0.7184	0.1472	-0.1859	473.	-7223.	7542.
		5			132.72	6410.	1314.	-18977.	0.053	-0.0210	0.0225	473.	-7223.	7739.
934		12	6.78	-6.3	20.96	7531.	1371.	-22240.	0.8431	0.1669	-0.1971	473.	-7693.	8313.
		5			132.78	7531.	1473.	-20142.	0.0529	-0.0223	0.0248	473.	-7693.	8544.
935		13	8.90	-6.3	20.95	8664.	1567.	-24130.	0.971	0.1897	-0.2128	478.	-8432.	9641.
		5			132.72	8664.	1695.	-21717.	0.0533	-0.0245	0.0282	478.	-8432.	9707.
936		14	10.99	-6.3	21.04	9631.	1764.	-25234.	1.0745	0.2154	-0.2199	439.	-8700.	9849.
		5			133.03	9631.	1931.	-22551.	0.0490	-0.0251	0.0293	439.	-8700.	10146.
937	II-2	1	-3.78	-0.	21.00	2177.	896.	-10596.	0.2433	0.1011	-0.0976	39.	-1193.	293.
		5			132.91	2177.	904.	-9986.	0.0043	-0.0035	0.0008	39.	-1193.	293.
938		2	0.49	-0.	20.79	4742.	969.	-15656.	0.5354	0.1160	-0.1414	41.	-841.	1043.
		5			132.24	4742.	1010.	-14327.	0.0046	-0.0025	0.0030	41.	-841.	1043.
939		3	4.76	-0.	20.75	7262.	1206.	-19682.	0.8214	0.1673	-0.1745	26.	-994.	2022.
		5			132.12	7262.	1302.	-17647.	0.0035	-0.0029	0.0059	26.	-994.	2022.
940		4	6.88	-0.	20.73	8446.	1376.	-21901.	0.9561	0.1705	-0.1933	34.	-1146.	1315.
		5			132.06	8446.	1506.	-19534.	0.0039	-0.0034	0.0039	34.	-1146.	1315.
941		5	9.02	-0.	20.83	9821.	1568.	-23130.	1.1067	0.1964	-0.2007	46.	-1024.	2095.
		5			132.36	9821.	1743.	-20378.	0.0052	-0.0030	0.0061	46.	-1024.	2095.
942		6	11.14	-0.	20.75	10934.	1792.	-25060.	1.2368	0.2273	-0.2175	50.	-1265.	1979.
		5			132.12	10934.	2009.	-21995.	0.0057	-0.0037	0.0058	50.	-1265.	1979.
943		7	13.24	-0.	20.77	11846.	2036.	-26659.	1.3387	0.2590	-0.2305	57.	-1242.	1871.
		5			132.18	11846.	2292.	-23339.	0.0064	-0.0036	0.0055	57.	-1242.	1871.

TABLE A-2 (Continued)

Test Point No.	Run No.	Point of Run	Left N_p RPM	Right N_p RPM	Left β_L Deg.	Left β_R Deg.	Right β_L Deg.	Right β_R Deg.	Tail i_t Deg.	δ_f Deg.	Baro. in. Hg	To α_y	Left N_{JBS} % RPM	Right N_{JBS} % RPM	Average V_p/V_{tip}	q/qc
944	II-2	8	0	0	90	90	90	90	5	30	30.21	82	0	0	N/A	N/A
945		9														
946		10														
947		11														
948		12														
949		13														
950		14														
951		15														
952		16														
953		17														
954		18														
955	II-3	1	0	0	90	90	90	90	5	30	30.24	82	0	0	N/A	N/A
956		2														
957		3														
958		4														
959		5														
960		6														
961		7														
962		8														
963		9														
964		10														
965		11														
966		12														
967		13														
968		14														
969		15														
970		16														
971		17														

Test Point No.	Run No.	PT AVG	ALPHA	BETA	Q V,NOM	LIFT,U CL*QS	DRAG,U CD*QS	M,U CM*QSC	CL CY	CD CN	CM CROLL	SIDE F,U CY*QS	YAW,U CN*QSB	ROLL,U CL*QSB
944	II-2	8	15.29	-0.	20.66	12276.	2422.	-24047.	1.3949	0.3065	-0.2047	97.	-819.	-2803.
		5			131.81	12276.	2698.	-20606.	0.0111	-0.0024	-0.0082	97.	-819.	-2803.
945		9	17.23	-0.	20.28	11486.	3157.	-23929.	1.3298	0.3960	-0.2098	22.	-459.	-2951.
		5			130.58	11486.	3403.	-20710.	0.0026	-0.0014	-0.0088	22.	-459.	-2951.
946		10	-3.79	-8.0	20.70	1982.	954.	-11780.	0.2248	0.1090	-0.1113	513.	-6644.	5028.
		5			131.93	1982.	961.	-11230.	0.0582	-0.0196	0.0150	513.	-6644.	5105.
947		11	0.48	-8.0	20.81	4654.	1033.	-16368.	0.5249	0.1210	-0.1487	539.	-6828.	6048.
		5			132.30	4654.	1073.	-15077.	0.0607	-0.0199	0.0182	539.	-6828.	6230.
948		12	4.73	-8.0	20.79	7037.	1268.	-19993.	0.7945	0.1553	-0.1780	553.	-8132.	7010.
		5			132.24	7037.	1358.	-18640.	0.0624	-0.0238	0.0213	553.	-8132.	7285.
949		13	6.86	-8.0	20.72	8203.	1410.	-21540.	0.9296	0.1736	-0.1908	544.	-8546.	8307.
		5			131.99	8203.	1532.	-19263.	0.0617	-0.0251	0.0253	544.	-8546.	8627.
950		14	8.99	-8.0	20.72	9446.	1614.	-23472.	1.0704	0.2013	-0.2065	539.	-8989.	8376.
		5			131.99	9446.	1776.	-20850.	0.061	-0.0264	0.0257	539.	-8989.	8744.
951		15	11.11	-8.0	20.77	10680.	1857.	-25404.	1.2049	0.2333	-0.2217	577.	-9994.	8858.
		5			132.18	10680.	2045.	-22440.	0.0652	-0.0292	0.0271	577.	-9994.	9274.
952		16	13.20	-8.0	20.75	11527.	2084.	-26158.	1.3050	0.2634	-0.2272	529.	-9410.	9924.
		5			132.06	11527.	2326.	-22959.	0.0599	-0.0276	0.0304	529.	-9410.	10373.
953		17	15.22	-8.0	20.66	11599.	2449.	-26235.	1.3181	0.3062	-0.2286	389.	-7578.	4759.
		5			131.81	11599.	2695.	-23016.	0.0442	-0.0223	0.0153	389.	-7578.	5211.
954		18	17.18	-8.0	20.33	11062.	3256.	-28321.	1.2771	0.4022	-0.2548	47.	-1613.	2755.
		5			130.77	11062.	3484.	-25251.	0.0654	-0.0048	0.0095	47.	-1613.	3187.
955	II-3	1	-3.76	-0.	20.66	2297.	1060.	-10989.	0.2611	0.1215	-0.1028	13.	-859.	-1145.
		5			131.81	2297.	1069.	-10345.	0.0015	-0.0025	-0.0004	13.	-859.	-1145.
956		2	0.48	-0.	21.08	4649.	1172.	-17118.	0.5177	0.1346	-0.1540	-10.	-930.	1134.
		5			133.15	4649.	1210.	-15815.	-0.0011	-0.0027	0.0033	-10.	-930.	1134.
957		3	4.73	-0.	21.06	7068.	1360.	-21679.	0.7878	0.1638	-0.1919	38.	-986.	844.
		5			133.09	7068.	1470.	-19698.	0.0043	-0.0028	0.0024	38.	-986.	844.
958		4	6.86	-0.	20.98	8285.	1546.	-23908.	0.9268	0.1856	-0.2111	27.	-1185.	1981.
		5			132.85	8285.	1670.	-21586.	0.0031	-0.0034	0.0057	27.	-1185.	1981.
959		5	8.98	-0.	20.72	9382.	1704.	-25056.	1.0631	0.2113	-0.2221	34.	-1435.	1734.
		5			131.99	9382.	1865.	-22427.	0.0045	-0.0042	0.0051	34.	-1435.	1734.
960		6	11.09	-0.	20.62	10336.	1907.	-26411.	1.1790	0.2395	-0.2339	36.	-1426.	1724.
		5			131.69	10336.	2103.	-23508.	0.0042	-0.0042	0.0051	36.	-1426.	1724.
961		7	13.20	-0.	20.45	11345.	2151.	-28053.	1.3024	0.2743	-0.2496	38.	-1801.	2472.
		5			131.14	11345.	2389.	-24874.	0.0044	-0.0054	0.0073	38.	-1801.	2472.
962		8	15.25	-0.	20.14	11938.	2424.	-27803.	1.3915	0.3137	-0.2492	61.	-1302.	684.
		5			130.15	11938.	2692.	-24457.	0.0072	-0.0039	0.0021	61.	-1302.	684.
963		9	17.24	-0.	19.76	11311.	3112.	-26358.	1.3438	0.3988	-0.2408	54.	1067.	-4830.
		5			128.91	11311.	3357.	-23188.	0.0064	0.0033	-0.0149	54.	1067.	-4830.
964		10	-3.76	-8.0	21.02	2311.	1119.	-12866.	0.2581	0.1260	-0.1193	730.	-8340.	2924.
		5			132.07	2311.	1129.	-12225.	0.0815	-0.0261	0.0087	730.	-8340.	3014.
965		11	0.49	-8.0	21.04	4711.	1218.	-18626.	0.5256	0.1403	-0.1689	610.	-7660.	6674.
		5			133.03	4711.	1257.	-17318.	0.0681	-0.0221	0.0198	610.	-7660.	6858.
966		12	4.71	-8.0	20.91	6869.	1396.	-22218.	0.7712	0.1663	-0.1994	551.	-7179.	6855.
		5			132.60	6869.	1481.	-20312.	0.0618	-0.0209	0.0207	551.	-7179.	7123.
967		13	6.83	-8.0	20.85	8014.	1558.	-24232.	0.9022	0.1885	-0.2166	545.	-8133.	7858.
		5			132.42	8014.	1674.	-22068.	0.0614	-0.0237	0.0238	545.	-8133.	8150.
968		14	8.95	-8.0	20.72	9065.	1748.	-25306.	1.0272	0.2151	-0.2257	502.	-8508.	8804.
		5			131.99	9065.	1898.	-22790.	0.0569	-0.0250	0.0269	502.	-8508.	9157.
969		15	11.07	-8.0	20.89	10334.	1981.	-26502.	1.1614	0.2444	-0.2350	474.	-8140.	9396.
		5			132.54	10334.	2175.	-23714.	0.0533	-0.0237	0.0285	474.	-8140.	9799.
970		16	13.19	-8.0	20.73	11347.	2190.	-27761.	1.2866	0.2765	-0.2436	457.	-7677.	8699.
		5			132.06	11347.	2425.	-24611.	0.0518	-0.0225	0.0260	457.	-7677.	9142.
971		17	15.26	-8.0	20.39	11813.	2478.	-27861.	1.3600	0.3150	-0.2472	344.	-6593.	8403.
		5			130.95	11813.	2736.	-24562.	0.0396	-0.0197	0.0264	344.	-6593.	8864.

TABLE A-2 (Continued)

Test Point No.	Run No.	Point of Run	Left N_p RPM	Right N_p RPM	Left β_t Deg.	Left β_s Deg.	Right β_t Deg.	Right β_s Deg.	Tail i_t Deg.	δ_f Deg.	Sens. in. Hg	To °F	Left $N_{.785}$ % RPM	Right $N_{.785}$ % RPM	Average V_p/V_{tip}	q/qc
972	II-3	18	0	0	90	90	90	90	5	30	30.24	82	0	0	N/A	N/A
973	II-4	1	1090	0	0	0	0	0	OFF	30	30.30	72	72.5	0	0	N/A
974		2	1400									72	83.0		0	
975		3	1600									72	87.0		0	
976		4	1800									74	90.0		0.0318	
977		5	2050									74	94.5		0.0293	
978		6	2300									75	98.0		0.0303	
979		7	2380									75	99.5		0.0303	
980		8	0	1100	0	0	0	0				77	0	65.0	0	
981		9		1400								76		75.5	0	
982		10		1600								77		81.0	0	
983		11		1800								77		85.5	0	
984		12		2300								77		92.0	0.0286	
985		13		2400								77		94.0	0.0234	
986	II-5	1	1100	1150	0	0	0	0	OFF	30	30.41	Not Read	73.5	68.0	0	N/A
987		2	1440	1570	0	0	0	0					78.0	91.0	0	
988		3	1640	1420	0	0	0	0					88.0	87.5	0.0393	
989	II-6	1	1650	1725	0	0	0	0	OFF	30	30.40	71	87.0	84.0	0.1453	N/A
990		2	1660	1730	0	0	0	0				73			0.1427	
991		3	1660	1720	20	20	20	20				74			0.1510	
992		4	1745	1745	35	35	35	35				76			0.1474	
993		5	1650	1720	0	0	0	0				77	87.5		0.1481	
994		6	1660	1720								78			0.1487	
995		7	1660	1720								79			0.1482	
996		8	1665	1720								80			0.1450	
997		9	1680	1725								80			0.1446	
998		10	1680	1740								81			0.1441	
999		11	1680	1775								82			0.1428	

Test Point No.	Run No.	PT AVG	ALPHA	BETA	Q V,NOM	LIFT,U CL*QS	DRAG,U CD*QS	M,U CM*QSC	CL CY	CD CN	CM CROLL	SIDE F,U CY*QS	YAW,U CN*QSB	ROLL,U CL*QSB
972	II-3	18	17.21	-8.0	20.81	11645.	3379.	-29167.	1.3135	0.4089	-0.2557	143.	-1762.	5749.
		5			132.30	11645.	3625.	-25935.	0.0161	-0.0051	0.0181	143.	-1762.	6204.
973	II-4	1	0.	-0.	1.00	1178.	-100.	-584.	2.7662	-0.2344	-0.1198	-23.	848.	8189.
		10			0.	1178.	-100.	-584.	-0.0535	0.0515	0.4978	-23.	848.	8189.
974		2	0.	-0.	1.00	1920.	-205.	-1383.	4.5070	-0.4817	-0.2839	-33.	1748.	13845.
		10			0.	1920.	-205.	-1383.	-0.0777	0.1062	0.8415	-33.	1748.	13845.
975		3	0.	-0.	1.00	2531.	-276.	-2120.	5.9408	-0.6468	-0.4350	-79.	2131.	18245.
		10			0.	2531.	-276.	-2120.	-0.1859	0.1295	1.1090	-79.	2131.	18245.
976		4	0.	-0.	0.28	3194.	-317.	-2697.	26.6845	-2.6504	-1.9695	-83.	2151.	22838.
		10			15.37	3194.	-317.	-2697.	-0.6917	0.4652	4.9398	-83.	2151.	22838.
977		5	0.	-0.	0.31	4146.	-452.	-3475.	31.3868	-3.4230	-2.2994	-140.	2816.	29748.
		10			16.15	4146.	-452.	-3475.	-1.0592	0.5519	5.8313	-140.	2816.	29748.
978		6	0.	-0.	0.42	5128.	-590.	-4237.	28.8877	-3.3235	-2.0866	-200.	3498.	36195.
		10			18.72	5128.	-590.	-4237.	-1.1263	0.5102	5.2800	-200.	3498.	36195.
979		7	0.	-0.	0.45	5614.	-573.	-5004.	29.5631	-3.0182	-2.3034	-272.	3893.	38850.
		10			19.36	5614.	-573.	-5004.	-1.4346	0.5309	5.2976	-272.	3893.	38850.
980		8	0.	-0.	1.00	1010.	-148.	72.	2.5352	-0.3465	0.0147	-2.	-1261.	-7244.
		10			0.	1080.	-148.	72.	-0.0045	-0.0767	-0.4403	-2.	-1261.	-7244.
981		9	0.	-0.	1.00	1700.	-231.	-840.	3.9915	-0.5414	-0.1724	7.	-1904.	-11804.
		10			0.	1700.	-231.	-840.	0.0169	-0.1157	-0.7175	7.	-1904.	-11804.
982		10	0.	-0.	1.00	2234.	-317.	-1681.	5.2451	-0.7442	-0.3450	5.	-2352.	-15645.
		10			0.	2234.	-317.	-1681.	0.0124	-0.1429	-0.9509	5.	-2352.	-15645.
983		11	0.	-0.	1.00	2771.	-359.	-2151.	6.5042	-0.8423	-0.4414	31.	-2727.	-19791.
		10			0.	2771.	-359.	-2151.	0.0738	-0.1658	-1.2030	31.	-2727.	-19791.
984		12	0.	-0.	0.37	4469.	-466.	-4685.	28.4888	-2.9682	-2.2764	100.	-3098.	-31631.
		10			17.60	4469.	-466.	-4685.	0.6356	-0.5114	-5.2214	100.	-3098.	-31631.
985		13	0.	-0.	0.27	4854.	-589.	-4958.	41.9961	-5.0935	-3.6741	87.	-4071.	-34775.
		10			15.11	4854.	-589.	-4858.	0.7517	-0.9121	-7.7904	87.	-4071.	-34775.
986	II-5	1	0.	-0.	1.00	2404.	-195.	-2970.	5.6423	-0.4575	-0.6093	-33.	19.	-626.
		10			0.	2404.	-195.	-2970.	-0.0766	0.0012	-0.0381	-33.	19.	-626.
987		2	0.	-0.	1.00	3994.	-420.	-4760.	9.3746	-0.9859	-0.9767	-0.	-911.	-10111.
		10			0.	3994.	-420.	-4760.	-0.0011	-0.0554	-0.0615	-0.	-911.	-10111.
988		3	0.	-0.	0.31	5459.	-657.	-7499.	41.3251	-4.9728	-4.9627	-61.	-1264.	-5848.
		10			16.15	5459.	-657.	-7499.	-0.4597	-0.2478	-1.1463	-61.	-1264.	-5848.
989	II-6	1	-4.00	-0.	5.39	6480.	1223.	1594.	2.8234	0.5330	0.0607	-13.	158.	-3243.
		5			67.31	6480.	1223.	1594.	-0.0056	0.0018	-0.0366	-13.	158.	-3243.
990		2	0.	-0.	5.14	6972.	1508.	1583.	3.1868	0.6891	0.0632	-47.	329.	-5118.
		5			65.72	6972.	1508.	1583.	-0.0213	0.0039	-0.0606	-47.	329.	-5118.
991		3	0.	-0.	5.81	6190.	-327.	3931.	2.4991	-0.1320	0.1387	-119.	1883.	-4593.
		5			69.93	6190.	-327.	3931.	-0.0479	0.0197	-0.0480	-119.	1883.	-4593.
992		4	0.	-0.	5.81	6783.	-1311.	3945.	1.9312	-0.5294	0.1392	-238.	2959.	-4330.
		5			69.93	6783.	-1311.	3945.	-0.0961	0.0309	-0.0453	-238.	2959.	-4330.
993		5	4.00	-0.	5.37	7498.	1858.	1087.	3.2785	0.8124	0.0415	-92.	1279.	-4077.
		5			67.19	7498.	1858.	1087.	-0.0403	0.0145	-0.0462	-92.	1279.	-4077.
994		6	6.00	-0.	5.33	7610.	2039.	900.	3.3521	0.8983	0.0346	-7.	613.	-4106.
		5			66.95	7610.	2039.	900.	-0.0035	0.0070	-0.0468	-7.	613.	-4106.
995		7	8.00	-0.	5.50	8059.	2263.	559.	3.4372	0.9650	0.0208	24.	992.	-3279.
		5			68.04	8059.	2263.	559.	0.0104	0.0110	-0.0362	24.	992.	-3279.
996		8	10.00	-0.	5.23	8189.	2450.	-12.	3.6736	1.0990	-0.0005	-0.	1294.	-3559.
		5			66.34	8189.	2450.	-12.	-0.0000	0.0150	-0.0413	-0.	1294.	-3559.
997		9	12.00	-0.	5.23	8477.	2662.	449.	3.8028	1.1942	0.0176	-37.	1901.	-4688.
		5			66.34	8477.	2662.	449.	-0.0166	0.0221	-0.0545	-37.	1901.	-4688.
998		10	14.00	-0.	5.21	8731.	2893.	471.	3.9315	1.3026	0.0185	-22.	1987.	-3137.
		5			66.22	8731.	2893.	471.	-0.0097	0.0232	-0.0346	-22.	1987.	-3137.
999		11	16.00	-0.	5.33	8846.	3145.	83.	3.8965	1.3851	0.0032	16.	1435.	-4008.
		5			66.95	8846.	3145.	83.	0.0070	0.0164	-0.0457	16.	1435.	-4008.

TABLE A-2 (Continued)

Test Point No.	Run No.	Point of Run	Left n_p RPM	Right n_p RPM	Left δ_h Deg.	Left δ_b Deg.	Right δ_h Deg.	Right δ_b Deg.	Tail δ_t Deg.	δ_f Deg.	Baro. In. Hg	To t_y	Left n_{JBS} % RPM	Right n_{JBS} % RPM	Average V_p/V_{tip}	q/qc
1000	II-6	12	1675	1800	0	0	0	0	077	30	30.40	83	87.5	84.0	0.1643	N/A
1001		13	1630	1690								84			0.1516	
1002		14	1640	1690								86			0.1507	
1003		15	1645	1695								86			0.1483	
1004		16	1650	1695								87			0.1491	
1005		17	1655	1700								87			0.1496	
1006		18	1660	1700								88			0.1509	
1007		19	1660	1700											0.1492	
1008		20	1660	1705											0.1456	
1009		21	1665	1720								89			0.1472	
1010		22	1670	1780								90			0.1462	
1011		23	1660	1730								93			0.2221	
1012		24	1660	1735										85.0	0.2205	
1013		25	1660	1735											0.2218	
1014		26	1665	1735											0.2206	
1015		27	1675	1740											0.2212	
1016		28	1654	1742											0.2205	
1017		29	1660	1760											0.2212	
1018		30	1660	1790											0.2118	
1019		31	1660	1830								94			0.2157	
1020		32	1655	1720								96			0.2223	
1021		33	1655	1720											0.222.	
1022		34	1655	1725	20	20	20	20							0.2241	
1023		35	1710	1735	35	35	35	35							0.2187	
1024		36	1735	1785	40	40	40	40							0.2158	
1025		37	1660	1720	0	0	0	0				97			0.2252	
1026		38	1660	1725	0	0	0	0				98			0.2247	
1027		39	1655	1720	0	0	0	0				98			0.2241	

Test Point No.	Run No.	PT AVG	ALPHA	BETA	Q V,NOM	LIFT,U CL*QS	DRAG,U CD*QS	M,U CM*QSC	CL CY	CD CN	CM CROLL	SIDE F,U CY*QS	YAW,U CN*QSB	ROLL,U CL*QSB
1000	II-6	12	18.00	-0.	5.33	9079.	3321.	1354.	3.9990	1.4627	0.0521	1.	1375.	-4098.
		5			66.95	9079.	3321.	1354.	0.0006	0.0157	-0.0467	1.	1375.	-4098.
1001		13	-4.00	-8.0	5.23	6091.	1146.	1133.	2.7326	0.5139	0.0444	79.	1009.	-713.
		5			66.34	6091.	1146.	1133.	0.0355	0.0117	-0.0083	79.	1009.	-713.
1002		14	0.	-8.0	5.35	6674.	1474.	351.	2.9390	0.6492	0.0135	20.	1334.	-1341.
		5			66.95	6674.	1474.	351.	0.0089	0.0152	-0.0153	20.	1334.	-1341.
1003		15	4.00	-8.0	5.25	7291.	1787.	510.	3.2589	0.7989	0.0199	-84.	1040.	-881.
		5			66.46	7291.	1787.	510.	-0.0373	0.0120	-0.0102	-84.	1040.	-881.
1004		16	8.00	-8.0	5.38	7543.	1982.	607.	3.3225	0.8729	0.0234	-188.	1642.	-1126.
		5			66.95	7544.	1982.	607.	-0.0829	0.0187	-0.0128	-188.	1642.	-1126.
1005		17	8.00	-8.0	5.33	7788.	2189.	253.	3.4503	0.9640	0.0098	-168.	1744.	-1048.
		5			66.95	7788.	2189.	253.	-0.0742	0.0201	-0.0119	-168.	1744.	-1048.
1006		18	10.00	-8.0	5.45	8083.	2424.	460.	3.4841	1.0450	0.0173	-226.	1985.	861.
		5			67.48	8083.	2424.	460.	-0.097	0.0222	0.0096	-226.	1985.	861.
1007		19	12.00	-8.0	5.33	8263.	2612.	559.	3.6396	1.1505	0.0215	-211.	1873.	180.
		5			66.95	8263.	2612.	559.	-0.0928	0.0214	0.0021	-211.	1873.	180.
1008		20	14.00	-8.0	5.14	8350.	2819.	467.	3.8164	1.2884	0.0187	-238.	1990.	-1004.
		5			65.72	8350.	2819.	467.	-0.1088	0.0236	-0.0119	-238.	1990.	-1004.
1009		21	16.00	-8.0	5.21	8554.	3084.	669.	3.8515	1.3887	0.0265	-226.	2005.	670.
		5			66.22	8554.	3084.	669.	-0.1016	0.0234	0.0078	-226.	2005.	670.
1010		22	18.00	-8.0	5.35	8935.	3346.	1914.	3.9356	1.4759	0.0737	-293.	1950.	691.
		5			66.95	8935.	3346.	1914.	-0.1292	0.0222	0.0079	-293.	1950.	691.
1011		23	-4.00	-8.0	11.74	6953.	2053.	1480.	1.3899	0.4104	0.0259	-85.	3432.	-7.
		5			99.38	6953.	2053.	1480.	-0.0171	0.0178	-0.0000	-85.	3432.	-7.
1012		24	0.	-8.0	11.72	7874.	2266.	2586.	1.5768	0.4537	0.0453	-79.	3573.	-711.
		5			99.30	7874.	2266.	2586.	-0.0158	0.0185	-0.0037	-79.	3573.	-711.
1013		25	4.00	-8.0	11.90	9132.	2525.	2030.	1.8026	0.4982	0.0350	-138.	3645.	645.
		5			100.02	9132.	2525.	2030.	-0.0273	0.0186	0.0033	-138.	3645.	645.
1014		26	6.00	-8.0	11.76	9749.	2690.	3267.	1.9457	0.5369	0.0570	-126.	3540.	-153.
		5			99.46	9749.	2690.	3267.	-0.0252	0.0184	-0.0008	-126.	3540.	-153.
1015		27	8.00	-8.0	11.91	10349.	2916.	4012.	2.0389	0.5765	0.0691	-163.	2736.	2199.
		5			100.10	10349.	2916.	4012.	-0.0321	0.0180	0.0112	-163.	2736.	2199.
1016		28	10.00	-8.0	11.78	10866.	3143.	3757.	2.1652	0.6263	0.0654	-195.	3338.	-732.
		5			99.54	10866.	3143.	3757.	-0.0389	0.0172	-0.0038	-195.	3338.	-732.
1017		29	12.00	-8.0	11.90	11474.	3470.	2585.	2.2641	0.6848	0.0446	-329.	4001.	2740.
		5			100.02	11474.	3470.	2585.	-0.0449	0.0204	0.0190	-329.	4001.	2740.
1018		30	14.00	-8.0	11.91	11901.	3691.	3048.	2.3846	0.7273	0.0525	-330.	3384.	3050.
		5			100.10	11901.	3691.	3048.	-0.065.	0.0173	0.0156	-330.	3384.	3050.
1019		31	16.00	-8.0	11.76	12342.	3994.	3433.	2.4634	0.7972	0.0599	-327.	2401.	2634.
		5			99.46	12342.	3994.	3433.	-0.0652	0.0124	0.0136	-327.	2401.	2634.
1020		32	-4.00	-0.	11.98	7260.	2058.	342.	1.4326	0.4061	0.0059	-164.	2235.	-2658.
		5			100.02	7260.	2058.	342.	-0.0324	0.0114	-0.0136	-164.	2235.	-2658.
1021		33	0.	-0.	11.70	8342.	2228.	652.	1.6732	0.4469	0.0114	-189.	2748.	-5366.
		5			99.21	8342.	2228.	652.	-0.0378	0.0143	-0.0279	-189.	2748.	-5366.
1022		34	0.	-0.	12.18	7579.	753.	2918.	1.4603	0.1450	0.0491	-49.	637.	-2683.
		5			101.23	7579.	753.	2918.	-0.0095	0.0032	-0.0136	-49.	637.	-2683.
1023		35	0.	-0.	11.86	6377.	-256.	1830.	1.2626	-0.0586	0.0317	-94.	1278.	-3161.
		5			99.86	6377.	-256.	1830.	-0.0185	0.0066	-0.0162	-94.	1278.	-3161.
1024		36	0.	-0.	11.95	6144.	-401.	922.	1.2066	-0.0787	0.0158	-143.	2181.	-4197.
		5			100.27	6144.	-401.	922.	-0.0280	0.0111	-0.0213	-143.	2181.	-4197.
1025		37	4.00	-0.	12.09	9590.	2539.	1208.	1.8625	0.4931	0.0205	-198.	2850.	-4735.
		5			100.83	9590.	2539.	1208.	-0.0385	0.0145	-0.0238	-198.	2850	-4735.
1026		38	6.00	-0.	11.91	10046.	2711.	1805.	1.9793	0.5361	0.0311	-176.	2744.	-3699.
		5			100.10	10046.	2711.	1805.	-0.0336	0.0140	-0.0178	-170.	2744.	-3699.
1027		39	8.00	-0.	11.86	10622.	2924.	1720.	2.1029	0.5793	0.0208	-171	2442.	-3791.
		5			99.86	10622.	2924.	1720.	-0.0339	0.0125	-0.0194	-171.	2442.	-3791.

TABLE A-2 (Continued)

Test Point No.	Run No.	Point of Run	Left N_T RPM	Right N_T RPM	Left β_1 Deg.	Left β_2 Deg.	Right β_1 Deg.	Right β_2 Deg.	Tail i_t Deg.	δ_f Deg.	Baro. in. Hg	To °F	Left $N_{.385}$ % RPM	Right $N_{.385}$ % RPM	Average V_p/V_{tip}	q/qc
1028	II-6	40	1655	1720	0	0	0	0	OFF	30	30.40	98	87.5	85.0	0.2230	N/A
1029		41	1655	1745											0.2227	
1030		42	1650	1800											0.2205	
1031		43	1655	1740								99		81.0	0.2238	
1032		44	1680	1780								99		80.5	0.2169	
1033		45	1580	1650								100	86.0	83.0	0.3139	
1034		46	1585	1685											0.3110	
1035		47	1585	1685	20	20	20	20							0.3101	
1036		48	1600	1695	35	35	35	35							0.3094	
1037		49	1625	1710	40	40	40	40							0.3033	
1038		50	1645	1705	45	45	45	45							0.3064	
1039		51	1575	1645	0	0	0	0							0.3138	
1040		52	1575	1645											0.3138	
1041		53	1580	1660											0.3118	
1042		54	1580	1680										78.0	0.3100	
1043		55	1580	1680											0.3089	
1044		56	1575	1690											0.3078	
1045		57		1660										83.0	0.3122	
1046		58		1665								101			0.3139	
1047		59		1665											0.3139	
1048		60													0.3139	
1049		61	1580												0.3134	
1050		62	1620	1680											0.3069	
1051		63	1620	1605										76.5	0.3083	
1052		64	1625	1635										76.5	0.3027	
1053	II-7	1	1185	0	0	0	0	0	OFF	30	30.00	70	Not Recorded	0	0.0221	N/A
1054		2	1515	0	0	0	0	0				72		0	0.0174	
1055		3	1780	0	0	0	0	0				74	90.0	0	0.0148	

Test Point No.	Run No.	PT AVG	ALPHA	BETA	Q V,NOM	LIFT,U CL*QS	DRAG,U CD*QS	M,U CM*QSC	CL CY	CD CN	CM CROLL	SIDE F,U CY*QS	YAW,U CN*QSB	ROLL,U CL*QSB
1028	II-6	40	10.00	-0.	11.80	11032.	3142.	1526.	2.1947	0.6250	0.0265	-147.	2224.	-4243.
		5			99.62	11052.	3142.	1526.	-0.0292	0.0115	-0.0219	-147.	2224.	-4243.
1029		41	12.00	-0.	11.90	11457.	3341.	1381.	2.2608	0.6593	0.0238	-10.	1551.	-4615.
		5			100.02	11457.	3341.	1381.	-0.0019	0.0079	-0.0236	-10.	1551.	-4615.
1030		42	14.00	-0.	12.07	11903.	3622.	1653.	2.3153	0.7046	0.0281	102.	46.	-4402.
		5			100.75	11903.	3622.	1653.	0.0190	0.0002	-0.0222	102.	46.	-4402.
1031		43	16.00	-0.	11.93	12167.	3792.	1067.	2.3935	0.7658	0.0183	57.	-2261.	-1769.
		5			100.18	12167.	3792.	1067.	0.0111	-0.0115	-0.0090	57.	-2261.	-1769.
1032		44	18.00	-0.	11.68	12246.	3940.	-1365.	2.4603	0.7914	-0.0240	-86.	-3568.	2724.
		5			99.13	12246.	3940.	-1365.	-0.0173	-0.0186	0.0182	-86.	-3568.	2724.
1033		45	-4.00	-0.	21.23	8489.	2803.	-1916.	0.9385	0.3098	-0.0185	103.	761.	-4092.
		5			133.65	8489.	2803.	-1916.	0.0114	0.0022	-0.0117	103.	761.	-4092.
1034		46	0.	-0.	21.27	10306.	2901.	-1911.	1.1373	0.3201	-0.0186	36.	1443.	-3591.
		5			133.75	10306.	2901.	-1911.	0.0040	0.0041	-0.0103	36.	1443.	-3591.
1035		47	0.	-0.	21.10	9463.	1755.	-3535.	1.0529	0.1950	-0.0344	-6.	555.	-1869.
		5			133.21	9463.	1755.	-3535.	-0.0006	0.0016	-0.0054	-6.	555.	-1869.
1036		48	0.	-0.	21.27	8806.	921.	-4751.	0.9718	0.1017	-0.0458	-122.	1377.	-3091.
		5			133.75	8806.	921.	-4751.	-0.0135	0.0039	-0.0088	-122.	1377.	-3091.
1037		49	0.	-0.	20.85	8172.	725.	-4886.	0.9159	0.0813	-0.0479	-72.	1126.	-4172.
		5			132.72	8172.	725.	-4886.	-0.0081	0.0053	-0.0121	-72.	1126.	-4172.
1038		50	0.	-0.	20.72	7562.	553.	-6120.	0.8569	0.0627	-0.0606	-20.	679.	-2577.
		5			131.99	7562.	553.	-6120.	-0.0022	0.0020	-0.0076	-20.	679.	-2577.
1039		51	4.00	-0.	21.04	11915.	3095.	-1182.	1.3295	0.3453	-0.0115	93.	318.	-4380.
		5			133.03	11915.	3095.	-1182.	0.0104	0.0009	-0.0127	93.	318.	-4380.
1040		52	6.00	-0.	21.14	12921.	3160.	-1005.	1.4350	0.3510	-0.0098	75.	705.	-3161.
		5			133.53	12921.	3160.	-1005.	0.0083	0.0020	-0.0091	75.	705.	-3161.
1041		53	8.00	-0.	21.17	13816.	3318.	914.	1.5319	0.3679	0.0089	20.	538.	-2685.
		5			133.45	13816.	3318.	914.	0.0022	0.0015	-0.0077	20.	538.	-2685.
1042		54	10.00	-0.	21.17	12618.	2787.	-2862.	1.3989	0.3089	-0.0277	-369.	-2163.	10418.
		5			133.45	12618.	2787.	-2862.	-0.0409	-0.0062	0.0299	-369.	-2163.	10418.
1043		55	12.00	-0.	20.79	13466.	3075.	-2411.	1.5203	0.3672	-0.0238	-254.	-3867.	11421.
		5			132.24	13466.	3075.	-2411.	-0.0287	-0.0113	0.0334	-254.	-3867.	11421.
1044		56	14.00	-0.	20.75	14152.	3832.	-5132.	1.4007	0.4335	-0.0507	-154.	-3575.	9511.
		5			132.12	14152.	3832.	-5132.	-0.0174	-0.0105	0.0279	-154.	-3575.	9511.
1045		57	-4.00	-8.0	20.98	8172.	2828.	143.	0.9142	0.3164	0.0014	-36.	5800.	1480.
		5			132.85	8172.	2828.	143.	-0.0040	0.0168	0.0048	-36.	5800.	1480.
1046		58	0.	-8.0	21.33	10018.	2951.	472.	1.1026	0.3248	0.0045	94.	4847.	2464.
		5			133.93	10018.	2951.	472.	0.0104	0.0138	0.0070	94.	4847.	2464.
1047		59	4.00	-8.0	21.39	11673.	3090.	2744.	1.2813	0.3392	0.0263	-21.	4853.	7200.
		5			134.11	11673.	3090.	2744.	-0.0023	0.0138	0.0205	-21.	4853.	7200.
1048		60	6.00	-8.0	21.35	12630.	3216.	1627.	1.3897	0.3536	0.0156	-3.	4011.	6497.
		5			133.99	12630.	3216.	1627.	-0.0009	0.0116	0.0185	-3.	4011.	6497.
1049		61	8.00	-8.0	21.19	13658.	3328.	2623.	1.5122	0.3686	0.0234	-47.	3038.	9663.
		5			133.51	13658.	3328.	2623.	-0.0052	0.0087	0.0277	-47.	3038.	9663.
1050		62	10.00	-8.0	21.06	14399.	3560.	5055.	1.6050	0.3968	0.0493	34.	2074.	7285.
		5			133.09	14399.	3560.	5055.	0.0040	0.0060	0.0209	34.	2074.	7255.
1051		63	12.00	-8.0	20.35	12890.	2879.	374.	1.4867	0.3821	0.0038	-345.	-1306.	19050.
		5			130.83	12890.	2879.	374.	-0.0398	-0.0850	0.0549	-345.	-1306.	19050.
1052		64	14.00	-8.0	20.95	13696.	3450.	640.	1.5350	0.3867	0.0063	-378.	-208.	18705.
		5			132.72	13696.	3450.	640.	-0.0423	-0.0906	0.0583	-378.	-208.	18705.
1053	II-7	1	0.	-0.	1.00	1436.	-159.	-1671.	3.3718	-0.3735	-0.3429	-1243.	-8813.	49236.
		10			0.	1436.	-159.	-1671.	-2.9189	-0.5357	2.9927	-1243.	-8813.	49236.
1054		2	0.	-0.	1.00	2237.	-268.	-2208.	5.2507	-0.6299	-0.4530	-1271.	-8368.	55705.
		10			0.	2237.	-268.	-2208.	-2.9825	-0.5087	3.3859	-1271.	-8368.	55705.
1055		3	0.	-0.	1.00	3136.	-387.	-3408.	7.3606	-0.9093	-0.6993	-1332.	-7369.	62449.
		10			0.	3136.	-387.	-3408.	-3.1273	-0.4679	3.8077	-1332.	-7369.	62449.

TABLE A-2 (Continued)

Test Point No.	Run No.	Point of Run	Left N_p RPM	Right N_p RPM	Left δ_h Deg.	Left δ_a Deg.	Right δ_h Deg.	Right δ_a Deg.	Tail i_t Deg.	δ_f Deg.	Baro. in. Hg	T_0 °F	Left N_{305} % RPM	Right N_{305} % RPM	Average V_p/V_{tip}	q/qc
1056	II-7	4	1100	1210	0	0	0	0	OFF	30	30.00	92	Not Recorded		0.0426	N/A
1057		5	1520	1550								92	86.0	81.0	0.0320	
1058		6	N.G.	N.G.								92	-	-	-	
1059		7	0	1200								80	0	69.0	0.0404	
1060		8	0	1550								80	0	79.0	0.0313	
1061		9	0	1845								80	0	86.0	-	
1062		10	1665	1720								72	86.0	83.0	0.2171	
1063		11	1665	1710								72	86.5		0.2175	
1064		12	1665	1700								74			0.2184	
1065		13	1660	1690								75			0.2192	
1066		14	1665	1685								77			0.2209	
1067		15		1690								78			0.2203	
1068		16		1690								78			0.2201	
1069		17		1770								80		85.0	0.2158	
1070		18		1765								80			0.2163	
1071		19	1655	1775								81			0.2164	
1072		20	1655	1765								82	87.0		0.2174	
1073		21	1650									83			0.2182	
1074		22										83			0.2182	
1075		23										84			0.2203	
1076	II-8	1	1650	1670	0	0	0	0	OFF	30	29.92	69	86.0	81.5	0.347	N/A
1077		2	1645	1685	0	0	0	0				71		86.5	0.366	
1078		3	1645	1665	20	20	20	20				73		86.5	0.367	
1079		4	1695	1705	35	35	35	35				73		83.0	0.358	
1080		5	1695	1705	40	40	40	40				74			0.359	
1081		6	1710	1715	45	45	45	45				75			0.358	
1082		7	1610	1720	0	0	0	0				76	85.0	78.0	0.356	
1083		8	1630	1690	0	0	0	0				77	85.0	77.0	0.364	

Test Point No.	Run No.	PT AVG	ALPHA	BETA	Q V,NOM	LIFT,U CL*QS	DRAG,U CD*QS	M,U CM*QSC	CL CY	CD CN	CM CROLL	SIDE F,U CY*QS	YAW,U CN*QSB	ROLL,U CL*QSB
1056	II-7	4	0.	-0.	1.00	2298.	-98.	-2439.	5.3944	-0.2299	-0.5004	-985.	-7177.	29403.
		10			0.	2298.	-98.	-2439.	-2.3127	-0.4362	1.7872	-985.	-7177.	29403.
1057		5	0.	-0.	1.00	4246.	-245.	-4525.	9.9662	-0.5741	-0.9285	-1307.	-7851.	40789.
		10			0.	4246.	-245.	-4525.	-3.0670	-0.4772	2.4792	-1307.	-7851.	40789.
1058		6	0.	-0.	1.00	5423.	-268.	-6687.	12.7296	-0.6282	-1.3721	-824.	-5202.	23142.
		10			0.	5423.	-268.	-6687.	-1.9346	-0.3162	1.4066	-824.	-5202.	23142.
1059		7	0.	-0.	1.00	1246.	-58.	-1977.	2.9718	-0.0885	-0.4056	-106.	-1157.	-5525.
		10			0.	1246.	-58.	-1977.	-0.2496	-0.0703	-0.3358	-106.	-1157.	-5525.
1060		8	0.	-0.	1.00	1997.	-30.	-2816.	4.4873	-0.0704	-0.5779	294.	2121.	-23409.
		10			0.	1997.	-30.	-2816.	0.6913	0.1289	-1.4228	294.	2121.	-23409.
1061		9	0.	-0.	1.00	2881.	-36.	-4167.	6.7634	-0.0851	-0.8551	-802.	-7424.	6666.
		10			0.	2881.	-36.	-4167.	-1.8828	-2.4512	0.4051	-802.	-7424.	6666.
1062		10	0.	-0.	10.94	8478.	2254.	822.	1.8197	0.4837	0.0154	161.	5168.	-11521.
		10			95.91	8478.	2254.	822.	0.0345	0.0287	-0.0640	161.	5168.	-11521.
1063		11	0.	-0.	11.02	8576.	2334.	824.	1.6883	0.4594	0.0142	133.	4947.	3969.
		10			100.14	8576.	2334.	824.	0.0263	0.0252	0.0202	133.	4947.	3969.
1064		12	0.	-0.	11.62	8068.	2322.	2518.	1.6301	0.4491	0.0445	199.	3659.	21765.
		10			98.85	8068.	2322.	2518.	0.0402	0.0191	0.1139	199.	3659.	21765.
1065		13	0.	-0.	11.61	7754.	2317.	3014.	1.5681	0.4686	0.0533	226.	3962.	-62105.
		10			98.81	7754.	2317.	3014.	0.0462	0.0206	-0.3252	226.	3962.	-62105.
1066		14	0.	-0.	11.80	8258.	2243.	1639.	1.6429	0.4502	0.0285	132.	6125.	-30662.
		10			99.62	8258.	2243.	1639.	0.0243	0.0316	-0.1579	132.	6125.	-30662.
1067		15	0.	-0.	11.70	7956.	2232.	1587.	1.5957	0.4477	0.0278	238.	5022.	-48198.
		10			99.21	7956.	2232.	1587.	0.0478	0.0261	-0.2503	238.	5022.	-48198.
1068		16	0.	-0.	11.67	7765.	2255.	-841.	1.5626	0.4538	-0.0148	294.	4908.	-67661.
		10			99.05	7765.	2255.	-841.	0.0591	0.0256	-0.3525	294.	4908.	-67661.
1069		17	0.00	-0.	11.62	10860.	3052.	1000.	2.1944	0.4166	0.0177	180.	5757.	-14569.
		10			98.85	10860.	3052.	1000.	0.0363	0.0301	-0.0762	180.	5757.	-14569.
1070		18	0.00	-0.	11.77	10956.	3080.	332.	2.1850	0.4142	0.0058	251.	6982.	1794.
		10			99.50	10956.	3080.	332.	0.0301	0.0361	0.0093	251.	6982.	1794.
1071		19	0.00	-0.	11.71	10760.	3013.	2640.	2.1579	0.4038	0.0463	340.	7049.	19357.
		10			99.25	10760.	3013.	2640.	0.0722	0.0366	0.1004	340.	7049.	19357.
1072		20	0.00	-0.	11.75	10445.	2960.	3659.	2.0844	0.5912	0.0639	526.	6092.	36133.
		10			99.42	10445.	2960.	3659.	0.1051	0.0315	0.1849	526.	6092.	36133.
1073		21	0.00	-0.	11.84	10796.	3002.	1811.	2.1407	0.5952	0.0245	199.	4248.	-61953.
		10			99.78	10796.	3002.	1811.	0.0595	0.0218	-0.3181	199.	4248.	-61953.
1074		22	0.00	-0.	11.76	10533.	2955.	2424.	2.1022	0.5807	0.0423	185.	6495.	-49728.
		10			99.46	10533.	2955.	2424.	0.0369	0.0283	-0.2570	185.	6495.	-49728.
1075		23	0.00	-0.	11.74	10227.	2931.	1121.	2.0445	0.5859	0.0196	124.	4265.	-66909.
		10			99.38	10227.	2931.	1121.	0.0248	0.0221	-0.3463	124.	4265.	-66909.
1076	II-8	1	-4.00	-0.	32.47	10968.	3686.	-4489.	0.7930	0.2665	-0.0281	89.	454.	-2773.
		1			165.25	10968.	3686.	-4489.	0.0064	0.0009	-0.0052	89.	454.	-2773.
1077		2	0.	-0.	33.51	11544.	2964.	-12576.	0.8086	0.2064	-0.0770	-302.	-1944.	8366.
		1			167.89	11544.	2964.	-12576.	-0.0212	-0.0035	0.0152	-302.	-1944.	8366.
1078		3	0.	-0.	32.75	11172.	2266.	-13267.	0.8007	0.1624	-0.0830	-170.	30.	4839.
		1			165.97	11172.	2266.	-13267.	-0.0122	0.0001	0.0090	-170.	30.	4839.
1079		4	0.	-0.	32.56	11400.	1714.	-11076.	0.8218	0.1236	-0.0698	-77.	1909.	-1777.
		1			165.49	11400.	1714.	-11076.	-0.0055	0.0036	-0.0033	-77.	1909.	-1777.
1080		5	0.	-0.	32.85	10920.	1491.	-11036.	0.7804	0.1066	-0.0489	-22.	983.	-329.
		1			166.21	10920.	1491.	-11036.	-0.0015	0.0010	-0.0006	-22.	983.	-329.
1081		6	0.	-0.	32.94	10368.	1299.	-11669.	0.7368	0.0926	-0.0727	41.	348.	-1857.
		1			166.45	10368.	1299.	-11669.	0.0029	0.0006	-0.0034	41.	348.	-1857.
1082		7	4.00	-0.	32.75	13108.	2847.	-9572.	0.9304	0.2491	-0.0600	-331.	276.	7481.
		1			165.97	13108.	2847.	-9572.	-0.0237	0.0005	0.0137	-331.	276.	7481.
1083		8	4.00	-0.	32.75	14044.	2878.	-9075.	1.0065	0.2063	-0.0549	-317.	460.	7134.
		1			165.97	14044.	2878.	-9075.	-0.0227	0.0009	0.0132	-317.	460.	7134.

TABLE A-2 (Continued)

Test Point No.	Run No.	Point of Run	Left N_p RPM	Right N_p RPM	Left β_t Deg.	Left β_0 Deg.	Right β_t Deg.	Right β_0 Deg.	Tail i_t Deg.	δ_f Deg.	Baro. in. Hg	To Φ_p	Left N_{JBS} % RPM	Right N_{JBS} % RPM	Average V_p/V_{tip}	q/qc
1084	II-8	9	1665	1675	0	0	0	0	OFF	30	29.92	78	85.0	76.5	0.367	N/A
1085		10	1655	1640								78		76.0	0.375	
1086		11	1655	1700								80	87.0	84.0	0.355	
1087		12	1665	1715								80		83.5	0.352	
1088		13	1675	1710								81		78.0	0.360	
1089		14	1710	1710								81			0.361	
1090		15	1725	1715								82			0.360	
1091		16	1760	1715								82			0.360	
1092		17	1640	1760	10	10	10	10				84	88.5	86.0	0.109	
1093		18	1640	1770	10	10	0	20				85			0.112	
1094		19	1635	1830	10	10	-10	30				86			0.103	
1095		20	1640	1820	0	0	-10	30				86			0.099	
1096		21	1645	1760	0	20	10	10				87			0.114	
1097		22	1710	1760	-10	30	10	10				88			0.107	
1098		23	1650	1760	20	20	20	20				89			0.147	
1099		24	1650	1775	20	20	10	30				89			0.141	
1100		25	1640	1845	20	20	0	40				89			0.133	
1101		26	1640	1845	10	10	0	40				90			0.134	
1102		27	1640	1845	0	0	0	40							0.134	
1103		28	1665	1770	10	30	20	20							0.149	
1104		29	1750	1760	0	40	20	20					88.0		0.142	
1105		30	2400	2500	10	10	10	10				91	100.0	96.0	0.101	
1106		31	2400	2500	5	15	5	15				94			0.101	
1107		32	2405	2505	0	20	0	20				95			0.100	
1108		33	2430	2515	-5	25	-5	25				96			0.101	
1109		34	1650	1735	20	20	20	20				98	89.0	86.0	0.149	
1110		35	1640	1750	20	20	10	30				98	88.5	86.0	0.145	
1111		36	1640	1825	20	20	0	40				98	88.5	86.0	0.136	

Test Point No.	Run No.	HT AVG	ALPHA	BETA	Q V_s,NOM	LIFT,U CL*QS	DRAG,U CD*QS	M,U CM*QSC	CL CY	CD CN	CM CROLL	SIDE F,U CY*QS	YAW,U CN*QSB	ROLL,U CL*QSB
1084	II-8	6	8.00	-0.	32.66	14848.	2970.	-5335.	1.0677	0.2135	-0.0325	-439.	-504.	9935.
		1			165.73	14848.	2970.	-5435.	-0.0164	-0.0009	0.0185	-234.	-504.	9935.
1085		10	10.00	-0.	32.75	15808.	3299.	-5.78.	1.133	..2365	-0.0331	-45.	-125E.	11461.
		1			164.97	15808.	3299.	-5.78.	-0.0	-0.0023	0.0213	-43.	-125E.	11461.
1086		11	-4.00	-8.0	32.56	10588.	3712.	-4594.	0.7685	..2676	-0.0269	-5.	8635.	6770.
		1			165.49	10588.	3712.	-4594.	-0.00	0.0165	0.0126	-5.	8635.	6770.
1087		12	0.	-8.0	32.94	13072.	3611.	-2404.	0.9315	0.2573	-0.0150	-2.	8534.	9721.
		1			166.45	13072.	3611.	-2404.	-0.00	0.1157	0.0179	-2.	8534.	9721.
1088		13	4.00	-8.0	32.75	13180.	2903.	-5669.	0.9446	0.2281	-0.0355	-30.	4393.	21487.
		1			165.97	13180.	2903.	-5669.	-0.021	0.0082	0.0199	-30.	4393.	21487.
1089		14	6.00	-8.0	32.66	14248.	2992.	-2128.	1.0241	0.2151	-0.0134	-211.	1736.	20351.
		1			165.73	14248.	2992.	-2128.	-0.0152	0.0032	0.0379	-211.	1736.	20351.
1090		15	8.00	-8.0	32.75	14992.	3023.	-96.	1.0744	0.2167	-0.0006	-86.	1395.	22055.
		1			165.97	14992.	3023.	-96.	-0.0062	0.0026	0.0409	-86.	1395.	22055.
1091		16	10.00	-8.0	32.56	15916.	3302.	-58.	1.1474	0.2368	-0.0004	2.	-60.	21948.
		1			165.49	15916.	3302.	-58.	0.0012	0.0012	0.0430	2.	-60.	21948.
1092		17	0.	-8.0	5.10	6096.	163.	1 48.	4.6146	0.1235	0.0694	72.	2729.	-86.
		1			51.07	6096.	163.	1 48.	0.6545	0.0535	-0.0017	72.	2729.	-86.
1093		18	0.	-8.0	5.29	5748.	223.	1592.	4.6955	0.1590	0.0991	11..	2611.	324.
		1			52.64	5748.	223.	1592.	0.0787	0.0482	0.0598	11..	2611.	324.
1094		19	0.	-8.0	5.10	4932.	331.	1853.	3.7334	0.2907	0.1226	41.	4079.	5844.
		1			51.07	4932.	331.	1853.	0.0559	0.0800	0.1146	41.	4079.	5844.
1095		20	0.	-8.0	2.71	4032.	775.	-10.57.	3.4884	0.6727	-0.7606	41.	744.	5669.
		1			47.77	4032.	775.	-10.57.	0.6354	0.0166	0.1270	41.	744.	5669.
1096		21	0.	-8.0	3.29	5892.	307.	1709.	4.1981	0.2189	0.1064	2..	2091.	-2179.
		1			52.64	5892.	307.	1709.	0.	0.0386	-0.0402	2.	2091.	-2179.
1097		22	0.	-8.0	3.29	5316.	559.	1 66.	3.7877	5.3944	0.0664	7.	-58.	-3529.
		1			52.64	5316.	559.	1 66.	0.0351	-0.0011	-0.0651	7.	-58.	-3529.
1098		23	0.	-8.0	5.52	6216.	-372.	3452.	2.6418	-0.1581	0.1283	247.	1678.	-634.
		1			88.16	6216.	-372.	3452.	0.1651	0.0185	-0.0070	247.	1678.	-634.
1099		24	0.	-8.0	5.33	5712.	-202.	3681.	2.5159	-0.0888	0.1417	180.	3723.	2645.
		1			66.95	5712.	-202.	3681.	0.0791	0.0425	0.0302	180.	3726.	2645.
1100		25	0.	-8.0	4.75	5004.	130.	3927.	2.4759	0.0641	0.1697	197.	5793.	4561.
		1			63.19	5004.	130.	3927.	0.0974	0.0742	0.0584	197.	5793.	4561.
1101		26	0.	-8.0	5.04	5328.	626.	2870.	2.4821	0.2918	0.1169	23..	2177.	5107.
		1			65.10	5328.	626.	2870.	0.1079	0.0265	0.0616	23..	2177.	5107.
1102		27	0.	-8.0	5.04	5496.	1068.	2338.	2.5604	0.4975	0.0952	25..	-1236.	7194.
		1			65.10	5496.	1068.	2338.	0.1165	-0.0149	0.0868	25..	-1236.	7194.
1103		28	0.	-8.0	6.01	6132.	-108.	3919.	2.3959	-0.0422	0.1338	161.	1042.	-2354.
		1			71.08	6132.	-108.	3919.	0.0628	0.0105	-0.0238	161.	1042.	-2354.
1104		29	0.	-8.0	5.23	5448.	180.	2891.	2.444	0.0868	0.1134	89.	-1335.	-4329.
		1			66.34	5448.	180.	2891.	0.0398	-0.0155	-0.0503	89.	-1335.	-4329.
1105		30	0.	-0.	5.43	12096.	29.	742.	5.2326	0.0125	0.0280	-115.	4654.	-3031.
		1			67.56	12096.	29.	742.	-0.0498	0.0521	-0.0340	-115.	4654.	-3031.
1106		31	0.	-0.	5.23	11808.	235.	1595.	5.2972	0.1055	0.0625	-122.	3875.	-1000.
		1			66.34	11808.	235.	1595.	-0.0544	0.0456	-0.0116	-122.	3875.	-1000.
1107		32	0.	-0.	5.23	11004.	473.	2799.	4.9365	0.2121	0.1058	-96.	2905.	1541.
		1			66.34	11004.	473.	2799.	-0.0431	0.0337	0.0179	-96.	2905.	1541.
1108		33	0.	-0.	5.43	10416.	965.	2996.	4.5059	0.4174	0.1133	-156.	2189.	868.
		1			67.56	10416.	965.	2996.	-0.0675	0.0245	0.0097	-156.	2189.	868.
1109		34	0.	-0.	5.43	5940.	-312.	3190.	2.5696	-0.1350	0.1206	-132.	2027.	-3009.
		1			67.56	5940.	-312.	3190.	-0.0571	0.0227	-0.0337	-132.	2027.	-3009.
1110		35	0.	-0.	5.23	5508.	-166.	3526.	2.4715	-0.0743	0.1383	-75.	2593.	-570.
		1			66.34	5508.	-166.	3526.	-0.0312	0.0301	-0.0066	-75.	2593.	-570.
1111		36	0.	-0.	4.94	4860.	146.	3006.	2.3085	0.0695	0.1248	2.	4922.	1850.
		1			64.47	4860.	146.	3006.	0.0011	0.0605	0.0228	2.	4922.	1850.

TABLE A-2 (Continued)

Test Point No.	Run No.	Point of Run	Left N_p RPM	Right N_p RPM	Left β_t Deg.	Left β_0 Deg.	Right β_t Deg.	Right β_0 Deg.	Tail i_t Deg.	ϕ_f Deg.	Baro. in. Hg	To °F	Left $N_{.85}$ % RPM	Right $N_{.85}$ % RPM	Average V_p/V_{tip}	q/qc
1112	II-8	37	1630	1825	10	10	0	40	OFF	30	29.92	98	88.5	86.0	0.139	N/A
1113		38	1635	1825	0	0	0	40							0.137	
1114		39	1650	1750	10	30	20	20				97			0.146	
1115		40	1740	1735	0	40	20	20					88.0		0.146	
1116		41	1685	1760	20	20	20	20					88.5		0.215	
1117		42	1685	1770	20	20	10	30							0.213	
1118		43	1685	1820	20	20	0	40							0.208	
1119		44	1675	1820	10	10	0	40				96			0.207	
1120		45	1685	1765	10	30	20	20							0.214	
1121		46	1750	1765	0	40	20	20					88.0		0.214	
1122	II-9	1	1660	1760	0	0	0	0	OFF	0	30.03	60	87.0	84.0	0.1385	N/A
1123		2	1670	1720	0	0	0	0				63	87.5	83.5	0.1440	
1124		3	1670	1680	20	20	20	20				66		83.0	0.1465	
1125		4	1755	1695	35	35	35	35				67		83.0	0.1415	
1126		5	1680	1750	0	0	0	0				71		85.0	0.1470	
1127		6	1675	1750								73	87.8	85.0	0.1440	
1128		7	1670	1740								74			0.1425	
1129		8	1685	1740								75			0.1465	
1130		9	1685	1800								75		84.5	0.1430	
1131		10	1690	1830								76	88.0	84.7	0.1425	
1132		11	1650	1740								79	87.5	84.8	0.2200	
1133		12	1665	1740								79		85.0	0.2190	
1134		13	1665	1740	20	20	20	20				80	87.3		0.2195	
1135		14	1710	1740	35	35	35	35				81			0.2135	
1136		15	1735	1760	40	40	40	40				81			0.2105	
1137		16	1760	1770	45	45	45	45				91		84.8	0.2085	
1138		17	1660	1740	0	0	0	0				82	87.5	84.9	0.2220	
1139		18	1660	1735	0	0	0	0				82	87.5	84.9	0.2225	

Test Point No.	Run No.	PT AVG	ALPHA	BETA	Q V,NOM	LIFT,U CL*QS	DRAG,U CD*QS	M,U CM*QSC	CL CY	CD CN	CM CROLL	SIDE F,U CY*QS	YAW,U CN*QSB	ROLL,U CL*QSB
1112	II-8	17	0.	-0.	5.04	5244.	674.	2131.	2.4453	0.3142	0.0868	60.	1555.	2887.
		1			65.10	5244.	674.	2131.	0.028	0.0108	0.0348	60.	1555.	2887.
1113		58	0.	-0.	5.43	5340.	1128.	1973.	2.5100	0.4880	0.0406	151.	-2521.	4452.
		1			67.56	5340.	1128.	1973.	0.0654	-0.0282	0.0469	151.	-2521.	4452.
1114		59	0.	-0.	5.81	5676.	-65.	3120.	2.2917	-0.0262	0.1066	-209.	665.	-4337.
		1			69.93	5676.	-65.	3020.	-0.0843	0.0070	-0.0453	-209.	665.	-4337.
1115		40	0.	-0.	5.14	5340.	254.	2413.	2.4408	0.1163	0.0984	-194.	-1406.	-7055.
		1			65.72	5340.	254.	2413.	-0.0889	-0.0166	-0.0835	-194.	-1406.	-7055.
1116		41	0.	-8.0	11.99	7464.	730.	2195.	1.4611	0.1379	0.0376	242.	1857.	2066.
		1			100.43	7464.	720.	2195.	0.0475	0.0094	0.0105	242.	1857.	2066.
1117		42	0.	-8.0	11.80	7356.	862.	1690.	1.4634	0.1714	0.0294	250.	2108.	2947.
		1			99.62	7356.	862.	1690.	0.0497	0.0109	0.0152	250.	2108.	2947.
1118		43	0.	-8.0	11.61	6924.	1104.	1824.	1.4002	0.2233	0.0323	221.	4511.	4633.
		1			98.81	6924.	1104.	1824.	0.0447	0.0236	0.0243	221.	4511.	4633.
1119		44	0.	-8.0	11.80	7188.	1482.	2254.	1.4300	0.2947	0.0392	144.	2376.	5898.
		1			99.62	7188.	1482.	2254.	0.0286	0.0122	0.0304	144.	2376.	5898.
1120		45	0.	-8.0	12.28	7512.	908.	3731.	1.4361	0.1736	0.0623	74.	2494.	1721.
		1			101.62	7512.	908.	3731.	0.0142	0.0123	0.0085	74.	2494.	1721.
1121		46	0.	-8.0	11.80	7044.	1172.	3277.	1.4013	0.2332	0.0570	-70.	2317.	-326.
		1			99.62	7044.	1172.	3277.	-0.0138	-0.0119	-0.0017	-70.	2317.	-326.
1122	II-9	1	-4.00	-0.	4.84	5813.	1142.	3757.	2.8168	0.5534	0.1591	-182.	2006.	-828.
		5			63.83	5813.	1142.	3757.	-0.0881	0.0252	-0.0104	-182.	2006.	-828.
1123		2	0.	-0.	5.17	6262.	1467.	4827.	2.8436	0.6658	0.1914	-279.	2493.	-1000.
		5			65.97	6262.	1467.	4827.	-0.1265	0.0293	-0.0117	-279.	2493.	-1000.
1124		3	0.	-0.	5.33	5294.	-423.	5420.	2.332	-0.1863	0.2087	-69.	2081.	-3849.
		5			66.95	5294.	-423.	5420.	-0.0304	0.0237	-0.0439	-69.	2081.	-3849.
1125		4	0.	-0.	5.14	3991.	-1463.	6939.	1.8243	-0.6687	0.2772	-240.	2936.	-5243.
		5			65.72	3991.	-1463.	6939.	-0.1095	0.0348	-0.0621	-240.	2936.	-5243.
1126		5	4.00	-0.	5.43	6888.	1818.	3857.	2.9797	0.7863	0.1459	-288.	2605.	-511.
		5			67.56	6888.	1818.	3857.	-0.1248	0.0292	-0.0057	-288.	2605.	-511.
1127		6	8.00	-0.	5.25	7282.	2128.	4659.	3.2666	0.9547	0.1592	-166.	1773.	-2916.
		5			66.34	7282.	2128.	4659.	-0.0745	0.0206	-0.0339	-166.	1773.	-2916.
1128		7	12.00	-0.	4.94	7649.	2503.	3709.	3.6332	1.1887	0.1540	-122.	2296.	-763.
		5			64.47	7649.	2503.	3709.	-0.0581	0.0202	-0.0094	-122.	2296.	-763.
1129		8	14.00	-0.	5.43	8114.	2740.	3446.	3.5102	1.1654	0.1303	-134.	2089.	-1531.
		5			67.56	8114.	2740.	3446.	-0.0579	0.0234	-0.0171	-134.	2089.	-1531.
1130		9	16.00	-0.	5.33	8285.	3040.	3723.	3.6491	1.3390	0.1433	-153.	2695.	488.
		5			66.95	8285.	3040.	3723.	-0.0672	0.0307	0.0056	-153.	2695.	488.
1131		10	18.00	-0.	5.43	8434.	3190.	3527.	3.6483	1.3799	0.1334	-35.	753.	-3529.
		5			67.56	8434.	3190.	3526.	-0.035	0.0084	-0.0395	-35.	753.	-3529.
1132		11	-4.00	-0.	11.80	5822.	1971.	10310.	1.1583	0.3921	0.1793	-346.	3622.	-3821.
		5			99.62	5822.	1971.	10310.	-0.0688	0.0187	-0.0197	-346.	3622.	-3821.
1133		12	0.	-0.	11.80	6797.	2155.	8037.	1.5521	0.4287	0.1398	-403.	4213.	-3035.
		5			99.62	6797.	2155.	8036.	-0.0801	0.0217	-0.0156	-403.	4213.	-3035.
1134		13	0.	-0.	11.97	5938.	600.	8293.	1.1642	0.1175	0.1421	-217.	2246.	-1849.
		5			100.35	5938.	600.	8293.	-0.0426	0.0114	-0.0094	-217.	2246.	-1849.
1135		14	0.	-0.	11.42	4608.	-515.	10025.	0.9475	-0.1058	0.1802	-103.	1102.	-2151.
		5			97.99	4608.	-515.	10025.	-0.0212	0.0059	-0.0115	-103.	1102.	-2151.
1136		15	0.	-0.	11.88	4090.	-627.	8254.	0.8083	-0.1240	0.1426	-132.	2003.	-5116.
		5			99.94	4090.	-627.	8254.	-0.0262	0.0103	-0.0262	-132.	2003.	-5116.
1137		16	0.	-0.	11.90	3689.	-748.	7547.	0.7279	-0.1476	0.1302	-95.	1217.	-3618.
		5			100.02	3689.	-748.	7547.	-0.0187	0.0062	-0.0185	-95.	1217.	-3618.
1138		17	4.00	-0.	11.95	7937.	2346.	7902.	1.5587	0.4606	0.1357	-308.	3822.	-3348.
		5			100.27	7937.	2346.	7902.	-0.0604	0.0194	-0.0170	-308.	3822.	-3348.
1139		18	8.00	-0.	11.97	9010.	2665.	8159.	1.7665	0.5226	0.1308	-259.	3207.	-2721.
		5			100.35	9010.	2665.	8159.	-0.0507	0.0163	-0.0138	-259.	3207.	-2721.

TABLE A-2 (Continued)

Test Point No.	Run No.	Point of Run	Left N_p RPM	Right N_p RPM	Left β_h Deg.	Left β_b Deg.	Right β_h Deg.	Right β_b Deg.	Tail i_t Deg.	δ_f Deg.	Baro. in. Hg	To °F	Left $N_{.785}$ % RPM	Right $N_{.785}$ % RPM	Average V_p/V_{tip}	q/qc
1140	II-9	19	1655	1770	0	0	0	0	OFF	0	30.03	83	87.4	85.0	0.2205	N/A
1141		20	1655	1725								83		83.0	0.2235	
1142		21	1660	1680								84		80.0	0.2265	
1143		22	1670	1720										79.8	0.2230	
1144		23	1530	1640									85.0	82.0	0.3150	
1145		24	1525	1615										81.7	0.3190	
1146		25	1540	1600	20	20	20	20						81.3	0.3175	
1147		26	1560	1600	35	35	35	35						81.0	0.3160	
1148		27	1575	1600	40	40	40	40						80.5	0.3130	
1149		28	1585	1600	45	45	45	45							0.3135	
1150		29	1520	1570	0	0	0	0				85			0.3225	
1151		30	1530	1575											0.3230	
1152		31	1520	1650										76.5	0.3170	
1153		32	1520	1650										77.0	0.3155	
1154		33	1540	1650										77.0	0.3120	
1155		34	1560	1645								86		82.0	0.3895	
1156		35	1560	1645								87		76.0	0.3930	
1157		36	1565	1645	20	20	20	20						82.0	0.3915	
1158		37	1560	1645	35	35	35	35							0.3895	
1159		38	1570	1660	40	40	40	40							0.3880	
1160		39	1585	1660	45	45	45	45							0.3815	
1161		40	1565	1630	0	0	0	0						76.0	0.3900	
1162		41	1630	1640								88			0.3835	
1163		42	1630	1640											0.3835	
1164		43	1630	1635											0.3840	
1165		44	1745	0									89.0	0	0.3610	
1166		45	1750	0	20	20							89.0	0	0.3600	
1167		46	1770	0	35	35						87	89.0	0	0.3530	

Test Point No.	Run No.	PT AVG	ALPHA	BETA	Q V,NOM	LIFT,U CL*QS	DRAG,U CD*QS	M,U CM*QSC	CL CY	CD CN	CM CROLL	SIDE F,U CY*QS	YAW,U CN*QSB	ROLL,U CL*QSB
1140	II-9	19	12.00	-0.	11.90	9998.	3033.	9287.	1.9735	0.5985	0.1602	-118.	2285.	-2805.
		5			100.02	9998.	3033.	9287.	-0.0232	0.0117	-0.0143	-118.	2285.	-2805.
1141		20	14.00	-0.	12.01	10326.	3347.	9067.	2.0182	0.6542	0.1549	-106.	1595.	-2255.
		5			100.51	10326.	3347.	9067.	-0.0206	0.0081	-0.0114	-106.	1595.	-2255.
1142		21	16.00	-0.	11.97	10612.	3461.	4476.	2.0807	0.6787	0.0767	-62.	-1149.	-180.
		5			100.35	10612.	3461.	4476.	-0.0122	-0.0058	-0.0009	-62.	-1149.	-180.
1143		22	18.00	-0.	12.09	11126.	3708.	-710.	2.1696	0.7200	-0.0120	15.	-2592.	805.
		5			100.83	11126.	3708.	-710.	0.003	-0.0130	0.0040	15.	-2592.	805.
1144		23	-4.00	-0.	20.87	6091.	2562.	7531.	0.6852	0.2881	0.0741	-55.	1798.	-5889.
		5			132.48	6091.	2562.	7531.	-0.0062	0.0052	-0.0172	-55.	1798.	-5889.
1145		24	0.	-0.	21.17	7678.	2573.	8652.	0.8511	0.2852	0.0838	-64.	2214.	-5746.
		5			133.45	7678.	2573.	8652.	-0.0071	0.0064	-0.0165	-64.	2214.	-5746.
1146		25	0.	-0.	20.81	6658.	1451.	7963.	0.7504	0.1637	0.0785	-52.	1432.	-3905.
		5			132.30	6658.	1451.	7963.	-0.0059	0.0042	-0.0114	-52.	1432.	-3905.
1147		26	0.	-0.	21.25	5575.	707.	7983.	0.6158	0.0781	0.0771	-214.	2620.	-4274.
		5			133.69	5575.	707.	7983.	-0.0236	0.0075	-0.0122	-214.	2620.	-4274.
1148		27	0.	-0.	20.72	5122.	461.	7295.	0.5804	0.0522	0.0723	-145.	1832.	-1325.
		5			131.99	5122.	461.	7295.	-0.0164	0.0054	-0.0039	-145.	1832.	-1325.
1149		28	0.	-0.	21.02	4802.	302.	6833.	0.5363	0.0337	0.0667	-60.	1098.	-1913.
		5			132.97	4802.	302.	6833.	-0.0068	0.0032	-0.0055	-60.	1098.	-1913.
1150		29	4.00	-0.	20.85	9274.	2538.	9080.	1.0441	0.2857	0.0894	-36.	1582.	-3063.
		5			132.42	9274.	2538.	9080.	-0.0041	0.0046	-0.0089	-36.	1582.	-3063.
1151		30	8.00	-0.	21.19	11414.	2704.	9156.	1.2642	0.2995	0.0886	-116.	2000.	-132.
		5			133.51	11414.	2704.	9156.	-0.0129	0.0057	-0.0004	-116.	2000.	-132.
1152		31	12.00	-0.	21.14	11819.	2560.	6301.	1.3126	0.2843	0.0612	-306.	-1221.	5355.
		5			133.33	11819.	2560.	6301.	-0.0344	-0.0035	0.0154	-306.	-1221.	5355.
1153		32	14.00	-0.	20.89	12359.	3153.	5562.	1.3890	0.3543	0.0546	-274.	-1584.	7541.
		5			132.54	12359.	3153.	5562.	-0.0308	-0.0046	0.0219	-274.	-1584.	.7541.
1154		33	16.00	-0.	20.70	12926.	3761.	4374.	1.4667	0.4266	0.0434	-179.	-3891.	9509.
		5			131.93	12926.	3761.	4374.	-0.0203	-0.0114	0.0279	-179.	-3891.	9509.
1155		34	-4.00	-0.	32.77	6883.	3287.	6926.	0.4930	0.2355	0.0434	-47.	1956.	-7632.
		5			166.02	6883.	3287.	6926.	-0.0034	0.0036	-0.3142	-47.	1956.	-7632.
1156		35	0.	-0.	32.62	7706.	2378.	1447.	0.5546	0.1711	0.0093	-360.	545.	2572.
		5			165.63	7706.	2378.	1447.	-0.0259	0.0010	0.0048	-360.	545.	2572.
1157		36	0.	-0.	32.70	8549.	2162.	6142.	0.6138	0.1552	0.0385	-113.	1946.	-5452.
		5			165.83	8549.	2162.	6142.	-0.0081	0.0036	-0.0101	-113.	1946.	-5452.
1158		37	0.	-0.	32.91	7411.	1433.	6039.	0.5287	0.1022	0.0377	-159.	2754.	-3739.
		5			166.36	7411.	1433.	6039.	-0.0114	0.0051	-0.0069	-159.	2754.	-3739.
1159		38	0.	-0.	32.89	6866.	1234.	4843.	0.4901	0.0881	0.0302	-91.	1517.	-4267.
		5			166.31	6866.	1234.	4843.	-0.0065	0.0028	-0.0079	-91.	1517.	-4267.
1160		39	0.	-0.	31.78	6110.	974.	4505.	0.4513	0.0719	0.0291	-49.	728.	-2557.
		5			163.49	6110.	974.	4505.	-0.0036	0.0014	-0.0049	-49.	728.	-2557.
1161		40	4.00	-0.	32.85	10258.	2285.	2123.	0.7330	0.1633	0.0133	-386.	1426.	5421.
		5			166.21	10258.	2285.	2123.	-0.0276	0.0026	0.0100	-386.	1426.	5421.
1162		41	6.00	-0.	32.69	11491.	2203.	1862.	0.8202	0.1573	0.0116	-296.	1089.	3641.
		5			166.31	11491.	2203.	1862.	-0.0211	0.0020	0.0067	-296.	1089.	3641.
1163		42	8.00	-0.	32.85	12586.	2480.	1899.	0.8994	0.1773	0.0119	-288.	1237.	4678.
		5			166.21	12586.	2480.	1899.	-0.0206	0.0023	0.0087	-288.	1237.	4678.
1164		43	10.00	-0.	32.66	13888.	2703.	4216.	0.9983	0.1943	0.0265	-233.	318.	7054.
		5			165.73	13888.	2703.	4216.	-0.0168	0.0006	0.0131	-233.	318.	7054.
1165		44	0.	-0.	32.30	5928.	2345.	4800.	0.4309	0.1704	0.0305	-731.	3651.	17519.
		5			164.81	5928.	2345.	4800.	-0.0531	0.0069	0.0330	-731.	3651.	17519.
1166		45	0.	-0.	33.00	5510.	1655.	4283.	0.3920	0.1177	0.0246	-592.	5032.	15706.
		5			166.60	5510.	1655.	4283.	-0.0421	0.0093	0.0289	-592.	5032.	15706.
1167		46	0.	-0.	32.54	4939.	1150.	2725.	0.3565	0.0830	0.0172	-420.	6516.	14017.
		5			165.44	4939.	1150.	2725.	-0.0303	0.0122	0.0262	-420.	6516.	14017.

TABLE A-2 (Continued)

Test Point No.	Run No.	Point of Run	Left N_p RPM	Right N_p RPM	Left β_1 Deg.	Left β_0 Deg.	Right β_1 Deg.	Right β_0 Deg.	Tail i_t Deg.	δ_f Deg.	Baro. in. Hg	To $^\circ_F$	Left $N_{.785}$ % RPM	Right $N_{.785}$ % RPM	Average V_p/V_{tip}	q/qc
1168	II-9	47	1785	0	40	40	0	0	OFF	0	30.03	87	89.0	0	0.3500	N/A
1169		48	1805		45	45						87			0.3460	
1170		49	1735		0	0						85			0.2790	
1171		50	1760		20	20									0.2840	
1172		51	1775		35	35									0.2770	
1173		52	1800		40	40									0.2790	
1174		53	1815		45	45									0.2760	
1175		54	1715		0	0						84			0.2180	
1176		55	1715		20	20						84			0.2190	
1177		56	1775		35	35						83			0.2120	
1178		57	1805		40	40									0.2080	
1179		58	1830		45	45									0.2050	
1180		59	1680		0	0									0.1490	
1181		60	1685		20	20									0.1490	
1182		61	1855		30	30							88.5		0.1410	
1183	II-10	1	0	1150	0	0	0	0	OFF	0	30.09	56	0	68.0	0	N/A
1184		2		1405								69		75.0		
1185		3		1620								70		81.0		
1186		4		1820								72		85.5		
1187		5		2270								74		91.0		
1188		6		2590								74		95.0		
1189	II-II	1	0	1150	0	0	0	0	OFF	0	30.09	56	0	56.6	0	N/A
1190		2		1420								69		Not Recorded		
1191		3		1620								70				
1192		4		1810								72				
1193		5		2270								74				
1194		6		2590								74				
1195		7		2640								74				

Test Point No.	Run No.	PT AVG	ALPHA	BETA	Q V,NOM	LIFT,U CL*QS	DRAG,U CD*QS	M,U CM*QSC	CL CY	CD CN	CM CROLL	SIDE F,U CY*QS	YAW,U CN*QSB	ROLL,U CL*QSB
1168	II-9	47	0.	-0.	32.47	4658.	1028.	2711.	0.3368	0.0743	0.0171	-275.	5943.	11181.
		5			165.25	4658.	1028.	2711.	-0.0199	0.0111	0.0209	-275.	5943.	11181.
1169		48	0.	-0.	32.51	4248.	926.	2464.	0.3068	0.0669	0.0130	-178.	5254.	8468.
		5			165.34	4248.	926.	2464.	-0.0128	0.0098	0.0158	-178.	5254.	8468.
1170		49	0.	-0.	20.22	4618.	1774.	4722.	0.5363	0.2060	0.0479	-645.	815.	16990.
		5			130.40	4618.	1774.	4722.	-0.0748	0.0024	0.0511	-645.	815.	16990.
1171		50	0.	-0.	20.91	4255.	976.	4243.	0.4778	0.1095	0.0416	-537.	4869.	13579.
		5			132.60	4255.	976.	4243.	-0.0603	0.0142	0.0395	-537.	4869.	13579.
1172		51	0.	-0.	20.05	3526.	419.	4195.	0.4129	0.0491	0.0429	-429.	7289.	11740.
		5			129.84	3526.	419.	4195.	-0.0502	0.0221	0.0356	-429.	7289.	11740.
1173		52	0.	-0.	20.81	3240.	397.	3663.	0.3655	0.0448	0.0361	-384.	7647.	9214.
		5			132.30	3240.	397.	3663.	-0.0434	0.0223	0.0269	-384.	7647.	9214.
1174		53	0.	-0.	20.95	3012.	329.	3067.	0.3376	0.0369	0.0300	-286.	7360.	6486.
		5			132.72	3012.	329.	3067.	-0.0321	0.0214	0.0188	-286.	7360.	6486.
1175		54	0.	-0.	11.86	3797.	1281.	3744.	0.7517	0.2536	0.0648	-540.	194.	15027.
		5			99.86	3797.	1281.	3744.	-0.1069	0.0010	0.0770	-540.	194.	15027.
1176		55	0.	-0.	12.13	3456.	374.	3601.	0.6690	0.0724	0.0609	-452.	4515.	14721.
		5			100.99	3456.	374.	3601.	-0.0874	0.0226	0.0738	-452.	4515.	14721.
1177		56	0.	-0.	11.78	2628.	-140.	3428.	0.5237	-0.0278	0.0597	-372.	8224.	9085.
		5			99.54	2628.	-140.	3428.	-0.0742	0.0424	0.0469	-372.	8224.	9085.
1178		57	0.	-0.	11.84	2206.	-204.	3385.	0.4374	-0.0405	0.0587	-428.	9369.	6847.
		5			99.78	2204.	-204.	3385.	-0.0849	0.0481	0.0352	-428.	9369.	6847.
1179		58	0.	-0.	11.86	1954.	-248.	2605.	0.3872	-0.0490	0.0485	-313.	8881.	5550.
		5			99.86	1954.	-248.	2605.	-0.062	0.0455	0.0284	-313.	8881.	5550.
1180		59	0.	-0.	5.14	3214.	756.	1364.	1.4689	0.3458	0.0545	-269.	-1626.	16375.
		5			65.72	3214.	756.	1364.	-0.1231	-0.0192	0.1938	-269.	-1626.	16375.
1181		60	0.	-0.	5.81	2602.	-283.	3396.	1.0504	-0.1143	0.1198	-211.	5067.	11780.
		5			69.93	2602.	-283.	3396.	-0.0851	0.0530	0.1232	-211.	5067.	11780.
1182		61	0.	-0.	5.62	1250.	-448.	2979.	0.5223	-0.1873	0.1088	-274.	8110.	4191.
		5			68.75	1250.	-448.	2979.	-0.1145	0.0853	0.0853	-274.	8110.	4191.
1183	II-10	1	0.	-0.	1.00	1169.	19.	-1208.	2.7437	0.0439	-0.2479	-17.	65.	-12603.
		10			0.	1169.	19.	-1208.	-0.0389	0.0040	-0.7660	-17.	65.	-12603.
1184		2	0.	-0.	1.00	1715.	-86.	490.	4.0254	-0.2028	0.1005	-1.	-264.	-15844.
		10			0.	1715.	-86.	490.	-0.0023	-0.0160	-0.9631	-1.	-264.	-15844.
1185		3	0.	-0.	1.00	2252.	-147.	2090.	5.2873	-0.3448	0.4288	14.	-274.	-19548.
		10			0.	2252.	-147.	2090.	0.0332	-0.0166	-1.1082	14.	-274.	-19548.
1186		4	0.	-0.	1.00	2928.	-78.	-292.	6.8732	-0.1837	-0.0600	6.	94.	-24362.
		10			0.	2928.	-78.	-292.	0.6146	0.0057	-1.4795	6.	94.	-24362.
1187		5	0.	-0.	1.00	4562.	56.	-6406.	10.7099	0.1324	-1.2325	80.	436.	-36456.
		10			0.	4562.	56.	-6406.	0.1870	0.0265	-2.2159	80.	436.	-36456.
1188		6	0.	-0.	1.00	5782.	102.	-7812.	13.5718	0.2406	-1.6031	112.	537.	-45566.
		10			0.	5782.	102.	-7812.	0.2625	0.0326	-2.7696	112.	537.	-45566.
1189	II-II	1	0.	-0.	1.00	1200.	-10.	-1582.	2.8169	-0.0237	-0.3246	3.	-264.	-8437.
		10			0.	1200.	-10.	-1582.	0.0079	-0.0160	-0.5128	3.	-264.	-8437.
1190		2	0.	-0.	1.00	1776.	-0.	-2579.	4.1690	-0.0011	-0.5291	2.	-179.	-12051.
		10			0.	1776.	-0.	-2579.	0.0056	-0.0109	-0.7325	2.	-179.	-12051.
1191		3	0.	-0.	1.00	2336.	19.	-3117.	5.4845	0.0451	-0.6305	26.	-82.	-16089.
		10			0.	2336.	19.	-3117.	0.0414	-0.0050	-0.9779	26.	-82.	-16089.
1192		4	0.	-0.	1.00	2876.	28.	-4260.	6.7521	0.0648	-0.8741	33.	-415.	-20239.
		10			0.	2876.	28.	-4260.	0.0783	-0.0252	-1.2302	33.	-415.	-20239.
1193		5	0.	-0.	1.00	4590.	28.	-6506.	10.7746	0.0654	-1.3350	95.	-40.	-33167.
		10			0.	4590.	28.	-6506.	0.2237	-0.0024	-2.0148	95.	-40.	-33167.
1194		6	0.	-0.	1.00	5870.	83.	-8434.	13.7803	0.1949	-1.7307	140.	292.	-43349.
		10			0.	5870.	83.	-8434.	0.3285	0.0178	-2.6349	140.	292.	-43349.
1195		7	0.	-0.	1.00	5245.	99.	-7503.	12.3127	0.2315	-1.5395	94.	438.	-40789.
		10			0.	5245.	99.	-7503.	0.2197	0.0266	-2.4793	94.	438.	-40789.

TABLE A-2 (Continued)

Test Point No.	Run No.	Point of Run	Left N_p RPM	Right N_p RPM	Left β_1 Deg.	Left β_0 Deg.	Right β_1 Deg.	Right β_0 Deg.	Tail i_t Deg.	δ_f Deg.	Baro. in. Hg	T_0 °F	Left $N_{.785}$ % RPM	Right $N_{.785}$ % RPM	Average V_p/V_{tip}	q/qc
1196	II-12	1	1110	0	0	0	0	0	OFF	30	30.40	56	73.0	0	0	N/A
1197		2	1390									69	62.0			
1198		3	1715									70	88.7			
1199		4	2000									72	93.5		0.0152	
1200		5	2265									74	98.0		0.0190	
1201		6	2330									74	98.5		0.0207	
1202		7	0	1100								78	0	65.0	0	
1203		8		1395								78		74.5		
1204		9		1600								76		80.0		
1205		10		1805								76		85.0	0.0146	
1206		11		2275								80		91.0	0.0116	
1207		12		2420								80		93.0	0.0127	
1208		13		2625								82		95.5	0	
1209		14	1120	1240								78	73.0	69.4	0	
1210		15	1370	1475								92	83.5	77.5	0.0219	
1211		16	1735	1825								96	90.5	86.0	0.0248	
1212		17	1645	1740								68	87.0	84.0	0.1452	
1213		18	1645	1740								70			0.1462	
1214		19	1645	1725								71			0.1463	
1215		20	1640	1725								72	87.2		0.1462	
1216		21	1680	1750								77	87.0	84.5	0.2177	
1217		22	1655	1740								78			0.2191	
1218		23	1655	1740								78			0.2191	
1219		24	1650	1735								78			0.2200	
1220		25	1640	1740								80	86.5		0.2920	
1221		26	1635	1735								81			0.2935	
1222		27	1640	1730								81			0.2934	
1223		28	1290	1420								81	73.0	76.0	0.3660	

Test Point No.	Run No.	PT AVG	ALPHA	BETA	Q V_0NOM	LIFT,U CL*QS	DRAG,U CD*QS	M,U CM*QSC	CL CY	CD CN	CM CROLL	SIDE F,U CY*QS	YAW,U CN*QSB	ROLL,U CL*QSB
1196	II-12	1	0.	-0.	1.00	1277.	-151.	-923.	2.9972	-0.3549	-0.1893	-27.	1421.	9271.
		10			0.	1277.	-151.	-923.	-0.0631	0.6864	0.5635	-27.	1421.	9271.
1197		2	0.	-0.	1.00	1979.	-242.	-2000.	4.6451	-0.5673	-0.4105	-58.	2167.	13899.
		10			0.	1979.	-242.	-2000.	-0.1352	0.1317	0.8448	-58.	2167.	13899.
1198		5	0.	-0.	0.28	2975.	-365.	-3608.	24.850	-3.0454	-2.6348	-92.	3286.	21256.
		10			15.37	2975.	-365.	-3608.	-0.7658	0.7108	4.5977	-92.	3286.	21256.
1199		4	0.	-0.	1.00	4110.	-499.	-4618.	9.6479	-1.1718	-0.9477	-212.	4445.	29344.
		10			0.	4110.	-499.	-4618.	-0.4969	0.2702	1.7836	-212.	4445.	29344.
1200		5	0.	-0.	0.26	5406.	-675.	-5315.	48.5042	-6.0531	-4.1687	-241.	5571.	38457.
		10			14.83	5406.	-675.	-5315.	-2.1641	1.2943	8.9344	-241.	5571.	38457.
1201		6	0.	-0.	0.41	5461.	-658.	-5836.	31.4997	-3.7930	-2.9424	-243.	5448.	38837.
		10			18.50	5461.	-658.	-5836.	-1.4023	0.8137	5.8003	-243.	5448.	38837.
1202		7	0.	-0.	1.00	1210.	-6.	-310.	2.8413	-0.0152	-0.0635	-2.	-119.	-7697.
		10			0.	1210.	-6.	-310.	-0.0039	-0.0072	-0.4679	-2.	-119.	-7697.
1203		8	0.	-0.	1.00	1766.	-38.	-1443.	4.1465	-0.0901	-0.2960	9.	-401.	-12012.
		10			0.	1766.	-38.	-1443.	0.0214	-0.0243	-0.7301	9.	-401.	-12012.
1204		9	0.	-0.	1.00	2249.	5.	-2908.	5.2789	0.0118	-0.5966	24.	-278.	-15862.
		10			0.	2249.	5.	-2908.	0.0569	-0.0169	-0.9641	24.	-278.	-15862.
1205		10	0.	-0.	1.00	2865.	-22.	-3167.	6.7211	-0.0524	-0.6499	27.	-129.	-20092.
		10			0.	2865.	-22.	-3167.	0.0637	-0.0079	-1.2213	27.	-129.	-20092.
1206		11	0.	-0.	1.00	4566.	61.	-6494.	10.7183	0.1431	-1.3326	92.	618.	-33027.
		10			0.	4566.	61.	-6494.	0.2169	0.0376	-2.0075	92.	618.	-33027.
1207		12	0.	-0.	1.00	5137.	25.	-6815.	12.0592	0.0580	-1.3984	106.	144.	-36519.
		10			0.	5137.	25.	-6815.	0.2490	0.0088	-2.2197	106.	144.	-36519.
1208		13	0.	-0.	1.00	5962.	105.	-8186.	13.9944	0.2456	-1.6797	125.	280.	-42581.
		10			0.	5962.	105.	-8186.	0.2941	0.0170	-2.5862	125.	280.	-42581.
1209		14	0.	-0.	1.00	2449.	-73.	-2842.	5.7493	-0.1707	-0.5831	-37.	890.	-12488.
		10			0.	2449.	-73.	-2842.	-0.0871	0.0541	-0.0759	-37.	890.	-12488.
1210		15	0.	-0.	1.00	3629.	-204.	-4261.	8.5183	-0.4783	-0.8743	-40.	1959.	-13362.
		10			0.	3629.	-204.	-4261.	-0.0941	0.1191	-0.0828	-40.	1959.	-13362.
1211		16	0.	-0.	0.28	5723.	-420.	-6849.	47.8055	-3.5105	-5.0012	-122.	3591.	-15537.
		10			15.37	5723.	-420.	-6849.	-1.0225	0.7766	-0.3325	-122.	3591.	-15537.
1212		17	0.	-0.	5.43	7057.	1627.	1476.	3.0529	0.7039	0.0558	-113.	2205.	-923.
		10			67.56	7057.	1627.	1476.	-0.0489	0.0247	-0.0103	-113.	2205.	-923.
1213		18	0.	-4.0	5.43	7046.	1665.	470.	3.0482	0.7202	0.0178	1.	1839.	-351.
		10			67.56	7046.	1665.	470.	0.0005	0.0206	-0.0039	1.	1839.	-351.
1214		19	0.	-8.0	5.33	6998.	1665.	-565.	3.0825	0.7332	-0.0217	156.	1619.	506.
		10			66.95	6998.	1665.	-565.	0.0685	0.0185	0.0058	156.	1619.	506.
1215		20	0.	-12.0	5.33	7027.	1682.	-622.	3.0952	0.7410	-0.0239	148.	2153.	1679.
		10			66.95	7027.	1682.	-622.	0.0651	0.0246	0.0191	148.	2153.	1679.
1216		21	0.	-0.	11.97	8624.	2519.	473.	1.6910	0.4939	0.0081	-87.	3410.	-4149.
		10			100.35	8624.	2519.	473.	-0.0170	0.0173	-0.0211	-87.	3410.	-4149.
1217		22	0.	-4.0	11.97	8599.	2520.	616.	1.6860	0.4981	0.0106	-160.	5023.	-2220.
		10			100.35	8599.	2520.	616.	-0.0313	0.0255	-0.0113	-160.	5023.	-2220.
1218		23	0.	-8.0	12.03	8550.	2474.	722.	1.6684	0.4828	0.0123	-47.	5295.	2054.
		10			100.59	8550.	2474.	722.	-0.0092	0.0268	0.0104	-47.	5295.	2054.
1219		24	0.	-12.0	11.89	8360.	2525.	-396.	1.6511	0.4986	-0.0068	105.	5410.	4704.
		10			99.98	8360.	2525.	-396.	0.0207	0.0277	0.0241	105.	5410.	4704.
1220		25	0.	-0.	20.83	11044.	3291.	-900.	1.2468	0.3708	-0.0089	-45.	3864.	-2259.
		10			152.36	11044.	3291.	-900.	-0.0051	0.0113	-0.0046	-45.	3864.	-2259.
1221		26	0.	-4.0	20.97	11215.	3325.	-2335.	1.2552	0.3721	-0.0228	48.	6175.	1020.
		10			152.82	11215.	3325.	-2335.	0.0053	0.0179	0.0030	48.	6175.	1020.
1222		27	0.	-8.0	20.95	11038.	3324.	-2127.	1.2365	0.3724	-0.0208	278.	6990.	2402.
		10			152.75	11038.	3324.	-2127.	0.0311	0.0203	0.0070	278.	6990.	2402.
1223		28	0.	-0.	20.81	7792.	2443.	-7336.	0.8789	0.2756	-0.0724	374.	1112.	-8877.
		10			152.30	7792.	2443.	-7336.	0.0422	0.0032	-0.0259	374.	1112.	-8877.

TABLE A-2 (Continued)

Test Point No.	Run No.	Point of Run	Left n_p RPM	Right n_p RPM	Left δ_A Deg.	Left δ_R Deg.	Right δ_A Deg.	Right δ_R Deg.	Tail i_t Deg.	δ_f Deg.	Baro. in. Hg	To $^\circ_F$	Left n_{385} % RPM	Right n_{385} % RPM	Average V_p/V_{tip}	q/qc
1224	II-12	29	1310	1420	0	0	0	0	097	30	30.40	81	73.0	76.0	0.3634	N/A
1225	II-12	30	1320	1410	0	0	0	0	097	30	30.40	81	73.0	76.0	0.3637	N/A
1226	II-13	1	1650	1770	0	0	0	0	097	30	30.40	54	87.0	84.0	0.1630	N/A
1227		2	1655	1775	0	0	0	0				56			0.1399	
1228		3	1655	1760	20	20	20	20				58			0.1436	
1225		4	1725	1745	35	35	35	35				59			0.1398	
1320		5	1665	1750	0	0	0	0				60			0.1415	
1231		6	1670	1715								62	87.5		0.1440	
1232		7	1675	1715								63	87.7		0.1427	
1233		8	1670	1725								63	87.5	83.5	0.1433	
1234		9	1675	1725								64			0.1431	
1235		10	1675	1760								66			0.1415	
1236		11	1640	1730								66		84.5	0.1439	
1237		12	1655	1730								67			0.1452	
1238		13	1660	1735								68			0.1432	
1239		14	1670	1750								68			0.1434	
1240		15	1670	1740								69			0.1440	
1241		16	1670	1760								69			0.1428	
1242		17	1675	1795								70			0.1436	
1243		18	1670	1800								70			0.1413	
1244		19	1645	1745								73	87.0	85.0	0.2174	
1245		20	1645	1745								73			0.2174	
1246		21	1650	1765								74			0.2164	
1247		22	1645	1755											0.2170	
1248		23	1650	1760											0.2160	
1249		24	1640	1780											0.2190	
1250		25	1650	1760										82.0	0.2160	
1251		26	1650	1760										82.0	0.2160	

Test Point No.	Run No.	PT AVG	ALPHA	BETA	Q V,NOM	LIFT,U CL*QS	DRAG,U CD*QS	M,U CM*QSC	CL CY	CD CN	CM CROLL	SIDE F,U CY*QS	YAW,U CN*QSB	ROLL,U CL*QSB
1224	II-12	29	0.	-4.0	20.90	7925.	2451.	-7402.	0.8902	0.2753	-0.0727	520.	2967.	-6580.
		10			132.57	7925.	2451.	-7402.	0.0584	0.0086	-0.0191	520.	2967.	-6580.
1225	II-12	30	0.	-8.0	20.94	7909.	2500.	-7571.	0.8868	0.2803	-0.0742	715.	5096.	-5177.
		10			132.69	7909.	2500.	-7571.	0.0802	0.0168	-0.0150	715.	5096.	-5177.
1226	II-13	1	-4.00	-0.	5.48	6943.	1410.	958.	2.9717	0.6033	0.0359	-94.	1105.	-2051.
		5			67.92	6943.	1410.	958.	-0.0401	0.0123	-0.0227	-94.	1105.	-2051.
1227		2	0.	-0.	5.08	7272.	1667.	794.	3.3619	0.7708	0.0321	-66.	1155.	-1337.
		5			65.35	7272.	1667.	794.	-0.0295	0.0138	-0.0160	-66.	1155.	-1337.
1228		3	0.	-0.	5.52	6542.	-225.	2507.	2.7887	-0.0955	0.0931	-82.	1995.	-2511.
		5			68.16	6542.	-225.	2567.	-0.0347	0.0220	-0.0254	-82.	1995.	-2511.
1229		4	0.	-0.	5.33	5383.	-1281.	2836.	2.3711	-0.5642	0.1092	-155.	1928.	-2483.
		5			66.95	5383.	-1281.	2836.	-0.0485	0.0220	-0.0283	-155.	1928.	-2483.
1320		5	4.00	-0.	5.23	7548.	2021.	95.	3.3861	0.9065	0.0037	-91.	1039.	-1446.
		5			66.34	7548.	2021.	95.	-0.0409	0.0121	-0.0168	-91.	1039.	-1446.
1231		6	8.00	-0.	5.10	7975.	2413.	-635.	3.673	1.1112	-0.0256	-38.	1235.	-3902.
		5			65.47	7975.	2413.	-635.	-0.0177	0.0147	-0.0465	-38.	1235.	-3902.
1232		7	10.00	-0.	5.08	8153.	2593.	-201.	3.7491	1.1987	-0.0081	-98.	1819.	183.
		5			65.35	8153.	2593.	-201.	-0.0455	0.0218	0.0022	-98.	1819.	183.
1233		8	12.00	-0.	5.23	8446.	2826.	-357.	3.7886	1.2676	-0.0140	-22.	1282.	-2307.
		5			66.34	8446.	2826.	-387.	-0.0097	0.0149	-0.0268	-22.	1282.	-2307.
1234		9	14.00	-0.	5.33	8664.	3089.	-452.	3.8161	1.3626	-0.0174	3.	1455.	-3389.
		5			66.95	8664.	3089.	-452.	0.0011	0.0166	-0.0386	3.	1455.	-3389.
1235		10	16.00	-0.	5.14	8734.	3307.	-1065.	3.9919	1.5117	-0.0425	-12.	1441.	-1191.
		5			65.72	8734.	3307.	-1065.	-0.0057	0.0171	-0.0141	-12.	1441.	-1191.
1236		11	-4.00	-8.0	5.14	6386.	1374.	-728.	2.9191	0.6278	-0.0291	235.	401.	867.
		5			65.72	6386.	1374.	-728.	0.1075	0.0048	0.0103	235.	401.	867.
1237		12	0.	-8.0	5.33	7003.	1718.	-1057.	3.0846	0.7566	-0.0467	212.	279.	538.
		5			66.95	7003.	1718.	-1057.	0.0934	0.0052	0.0061	212.	279.	538.
1238		13	4.00	-8.0	5.08	7553.	1995.	-1076.	3.4918	0.9222	-0.0435	-9.	1591.	2472.
		5			65.35	7553.	1995.	-1076.	-0.0042	0.0191	0.0296	-9.	1591.	2472.
1239		14	8.00	-8.0	5.14	8030.	2385.	-839.	3.6705	1.0903	-0.0335	-107.	1625.	-9.
		5			65.72	8030.	2385.	-839.	-0.0687	0.0149	-0.0001	-107.	1625.	-9.
1240		15	10.00	-8.0	5.19	8206.	2662.	-1196.	3.7206	1.2531	-0.0433	-63.	1467.	-1161.
		5			66.09	8206.	2662.	-1.96.	-0.0284	0.0172	-0.0136	-63.	1467.	-1161.
1241		16	12.00	-8.0	5.19	8362.	2894.	-1515.	3.7791	1.3681	-0.0598	-75.	1840.	-822.
		5			66.09	8362.	2894.	-1515.	-0.0338	0.0215	-0.0096	-75.	1840.	-822.
1242		17	14.00	-8.0	5.48	8767.	3158.	-1839.	3.7524	1.3517	-0.0688	-77.	2317.	1304.
		5			67.92	8767.	3158.	-1839.	-0.0331	0.0257	0.0145	-77.	2317.	1304.
1243		18	16.00	-8.0	5.19	8681.	3349.	-1250.	3.9234	1.5135	-0.0494	-105.	2078.	-376.
		5			66.09	8681.	3349.	-1250.	-0.0475	0.0243	-0.0084	-105.	2078.	-376.
1244		19	-4.00	-8.0	11.70	7742.	2371.	-3139.	1.5529	0.4755	-0.0550	167.	2275.	733.
		5			99.21	7742.	2371.	-3139.	0.0335	0.0118	0.0038	167.	2275.	733.
1245		20	0.	-8.0	11.68	8539.	2569.	-791.	1.7155	0.5162	-0.0139	-36.	4639.	-501.
		5			99.13	8539.	2569.	-791.	-0.0071	0.0241	-0.0026	-36.	4639.	-501.
1246		21	4.00	-8.0	11.70	9559.	2773.	-743.	1.9173	0.5562	-0.0130	-81.	5042.	86.
		5			99.21	9559.	2773.	-743.	-0.0163	0.0262	0.0004	-81.	5042.	86.
1247		22	8.00	-8.0	11.68	10450.	3127.	715.	2.0788	0.6221	0.0124	-152.	5454.	1111.
		5			99.62	10450.	3127.	715.	-0.0303	0.0281	0.0057	-152.	5454.	1111.
1248		23	10.00	-8.0	11.76	10972.	3347.	-389.	2.1934	0.6690	-0.0048	-188.	5891.	3015.
		5			99.38	10972.	3347.	-389.	-0.0375	0.0305	0.0156	-188.	5891.	3015.
1249		24	12.00	-8.0	11.72	11241.	3617.	-986.	2.2508	0.7243	-0.0166	-253.	6396.	2948.
		5			99.30	11241.	3617.	-986.	-0.0507	0.0332	0.0153	-253.	6396.	2948.
1250		25	14.00	-8.0	11.90	11567.	3806.	-840.	2.2826	0.7511	-0.0145	-287.	5112.	1533.
		5			100.02	11567.	3806.	-840.	-0.0565	0.0261	0.0078	-287.	5112.	1533.
1251		26	16.00	-8.0	11.70	12026.	4039.	-169.	2.4119	0.8101	-0.0030	-266.	3790.	5891.
		5			99.21	12026.	4039.	-169.	-0.0533	0.0197	0.0306	-266.	3790.	5891.

TABLE A-2 (Continued)

Test Point No.	Run No.	Point of Run	Left N_p RPM	Right N_p RPM	Left β_1 Deg.	Left β_0 Deg.	Right β_1 Deg.	Right β_0 Deg.	Tail i_t Deg.	δ_f Deg.	Baro. in. Hg	To $^\circ_F$	Left $N_{.85}$ % RPM	Right $N_{.85}$ % RPM	Average V_p/V_{tip}	q/qc
1252	II-13	27	1630	1760	0	0	0	0	OFF	30	30.40	75	87.0	82.5	0.2184	N/A
1253		28	1630	1765	0	0	0	0					86.5	85.0	0.2176	
1254		29	1635	1765	20	20	20	20							0.2174	
1255		30	1670	1765	35	35	35	35				76			0.2160	
1256		31	1690	1765	40	40	40	40				76			0.2136	
1257		32	1630	1755	0	0	0	0				77			0.2191	
1258		33	1635	1755											0.2178	
1259		34	1630	1780											0.2175	
1260		35	1630	1720										83.5	0.2210	
1261		36	1630	1720										81.5	0.2210	
1262		37	1635	1720										80.0	0.2195	
1263	II-14	1	1620	1720	0	0	0	0	OFF	30	30.40	48	85.0	82.5	0.286	N/A
1264		2	1620	1720	0	0	0	0				51		82.5	0.288	
1265		3	1620	1720	20	20	20	20				52		82.7	0.297	
1266		4	1655	1725	35	35	35	35				53	85.2	85.0	0.285	
1267		5	1675	1735	40	40	40	40				54			0.282	
1268		6	1700	1750	45	45	45	45				56			0.279	
1269		7	1605	1700	0	0	0	0				58	85.5		0.293	
1270		8	1605	1700								59			0.292	
1271		9	1625	1695								60			0.292	
1272		10	1650	1705								61			0.288	
1273		11	1675	1770								62			0.282	
1274		12	1670	1820								63			0.277	
1275		13	1730	1850								63			0.272	
1276		14	1600	1680								66		83.2	0.297	
1277		15	1600	1680								67			0.297	
1278		16	1630	1680								68			0.295	
1279		17	1700	1680								68			0.289	

Test Point No.	Run No.	PT AVG	ALPHA	BETA	Q V,NOM	LIFT,U CL*QS	DRAG,U CD*QS	M,U CM*QSC	CL CY	CD CN	CM CROLL	SIDE F,U CY*QS	YAW,U CN*QSB	ROLL,U CL*QSB
1252	II-13	27	-4.00	-0.	11.86	7702.	2329.	-1807.	1.5247	0.4611	-0.0313	-51.	3107.	-5965.
		5			99.86	7702.	2329.	-1807.	-0.0102	0.0159	-0.0306	-51.	3107.	-5965.
1253		28	0.	-0.	11.70	8455.	2537.	-1430.	1.6958	0.5088	-0.0251	-37.	3389.	-4571.
		5			98.21	8455.	2537.	-1430.	-0.0074	0.0176	-0.0237	-37.	3389.	-4571.
1254		29	0.	-0.	11.88	7778.	1070.	-358.	1.5374	0.2114	-0.0062	3.	906.	-2061.
		5			99.94	7778.	1070.	-358.	0.0006	0.0046	-0.0105	3.	906.	-2061.
1255		30	0.	-0.	12.05	7020.	145.	-1218.	1.3674	0.0282	-0.0207	11.	1203.	-2795.
		5			100.67	7020.	145.	-1218.	0.0022	0.0061	-0.0141	11.	1203.	-2790.
1256		31	0.	-0.	11.72	6480.	-110.	-1383.	1.2975	-0.0221	-0.0242	-115.	1394.	-3109.
		5			99.30	6480.	-110.	-1383.	-0.0230	0.0072	-0.0161	-115.	1394.	-3109.
1257		32	4.00	0.	11.74	9365.	2796.	-1198.	1.8721	0.5589	-0.0209	-40.	4054.	-4051.
		5			99.38	9365.	2796.	-1198.	-0.0080	0.0210	-0.0210	-40.	4054.	-4051.
1258		33	8.00	-0.	11.65	10493.	3086.	-82.	2.1149	0.6219	-0.0014	-40.	4016.	-4276.
		5			98.97	10493.	3086.	-82.	-0.0008	0.0210	-0.0223	-40.	4016.	-4276.
1259		34	10.00	-0.	11.76	11085.	3333.	-677.	2.2124	0.6653	-0.0118	-27.	3987.	-3303.
		5			99.46	11085.	3333.	-677.	-0.0055	0.0206	-0.0171	-27.	3987.	-3303.
1260		35	12.00	-0.	11.93	11334.	3494.	-1090.	2.2295	0.6873	-0.0187	45.	2390.	-2014.
		5			100.18	11334.	3494.	-1090.	0.0089	0.0122	-0.0103	45.	2390.	-2014.
1261		36	14.00	-0.	11.78	11654.	3753.	-1970.	2.3183	0.7478	-0.0343	192.	-587.	-3738.
		5			99.54	11654.	3753.	-1970.	0.0384	-0.0030	-0.0193	192.	-587.	-3738.
1262		37	16.00	-0.	11.72	11798.	3919.	-4144.	2.3623	0.7847	-0.0725	177.	-3534.	2597.
		5			99.30	11798.	3919.	-4144.	0.0354	-0.0183	0.0135	177.	-3534.	2597.
1263	II-14	1	-4.00	-0.	21.06	9653.	3321.	-5203.	1.0759	0.3702	-0.0507	115.	1726.	-4806.
		5			133.09	9653.	3321.	-5203.	0.0128	0.0050	-0.0139	115.	1726.	-4806.
1264		2	0.	-0.	21.10	11142.	3395.	-3553.	1.2397	0.3778	-0.0346	9.	2831.	-2269.
		5			133.21	11142.	3395.	-3553.	0.0016	0.0082	-0.0065	9.	2831.	-2269.
1265		3	0.	-0.	21.16	10720.	2256.	-2380.	1.1895	0.2503	-0.0231	1.	1392.	-2277.
		5			133.39	10720.	2256.	-2380.	0.0002	0.0040	-0.0065	1.	1392.	-2277.
1266		4	0.	-0.	21.14	9374.	1385.	-7573.	1.0411	0.1538	-0.0735	-66.	725.	-253.
		5			133.33	9374.	1385.	-7573.	-0.0074	0.0021	-0.0007	-66.	725.	-253.
1267		5	0.	-0.	21.02	8806.	1128.	-7733.	0.9833	0.1260	-0.0755	-68.	1016.	-2669.
		5			132.97	8806.	1128.	-7733.	-0.0076	0.0029	-0.0077	-68.	1016.	-2669.
1268		6	0.	-0.	20.89	8232.	922.	-8694.	0.9251	0.1036	-0.0854	-6.	495.	-2296.
		5			132.54	8232.	922.	-8694.	-0.0006	0.0014	-0.0067	-6.	495.	-2296.
1269		7	4.00	-0.	21.21	12242.	3577.	-2276.	1.3546	0.3958	-0.0220	94.	2299.	-3025.
		5			133.57	12242.	3577.	-2276.	0.0104	0.0066	-0.0087	94.	2299.	-3025.
1270		8	6.00	-0.	21.06	12971.	3650.	-1801.	1.4458	0.4068	-0.0176	104.	2195.	-3149.
		5			133.09	12971.	3650.	-1801.	0.0116	0.0063	-0.0091	104.	2195.	-3149.
1271		9	8.00	-0.	21.14	13866.	3787.	775.	1.5401	0.4206	0.0075	235.	1877.	-5503.
		5			133.33	13866.	3787.	775.	0.0261	0.0054	-0.0158	235.	1877.	-5503.
1272		10	10.00	-0.	20.95	14810.	3974.	2412.	1.6598	0.4454	0.0236	183.	2375.	-3708.
		5			132.72	14810.	3974.	2412.	0.0205	0.0069	-0.0108	183.	2375.	-3708.
1273		11	12.00	-0.	21.19	15390.	4118.	-355.	1.7046	0.4561	-0.0034	200.	1211.	-3176.
		5			133.51	15390.	4118.	-355.	0.0221	0.0035	-0.0091	200.	1211.	-3176.
1274		12	14.00	-0.	20.70	15491.	4496.	2516.	1.7574	0.5099	0.0249	98.	538.	-980.
		5			131.93	15491.	4496.	2516.	0.0112	0.0016	-0.0029	98.	538.	-980.
1275		13	16.00	-0.	20.93	15458.	5012.	-7316.	1.7340	0.5622	-0.0717	275.	35.	-3387.
		5			132.66	15458.	5012.	-7316.	0.0308	0.0001	-0.0098	275.	35.	-3387.
1276		14	-4.00	-8.0	21.17	9487.	3315.	-6473.	1.0517	0.3675	-0.0627	408.	5513.	-1003.
		5			133.45	9487.	3315.	-6473.	0.0455	0.0158	-0.0029	408.	5513.	-1003.
1277		15	0.	-8.0	21.12	10632.	3423.	-5592.	1.1819	0.3805	-0.0545	352.	6039.	1056.
		5			133.27	10632.	3423.	-5592.	0.0392	0.0174	0.0030	352.	6039.	1056.
1278		16	4.00	-8.0	21.17	12018.	3500.	758.	1.3323	0.3880	0.0073	266.	6874.	3229.
		5			133.45	12018.	3500.	758.	0.0295	0.0197	0.0093	266.	6874.	3229.
1279		17	6.00	-8.0	21.21	12754.	3519.	2012.	1.4113	0.3894	0.0195	387.	6315.	648.
		10			133.57	12754.	3519.	2012.	0.0428	0.0181	0.0019	387.	6315.	648.

TABLE A-2 (Continued)

Test Point No.	Run No.	Point of Run	Left N_p RPM	Right N_p RPM	Left δ_h Deg.	Left δ_e Deg.	Right δ_h Deg.	Right δ_e Deg.	Tail i_t Deg.	δ_f Deg.	Baro. in. Hg	To °F	Left N_{305} % RPM	Right N_{305} % RPM	Average V_p/V_{tip}	q/qc
1280	II-14	18	1730	1680	0	0	0	0	OFF	30	30.40	69	85.5	83.2	0.287	N/A
1281		19	1750	1685								69		83.3	0.284	
1282		20	1750	1710								70		83.3	0.282	
1283		21	1650	1760								73	87.8	85.4	0.142	
1284		22	1655	1760								74			0.145	
1285		23	1650	1760								75			0.144	
1286		24	1655	1760								76	87.9		0.142	
1287		25	1630	1750								78	87.5	85.2	0.144	
1288		26	1630	1730								79			0.146	
1289		27	1620	1730								80				
1290		28	1645	1735								81	87.7			
1291		29	1640	1740								81				
1292		30	1645	1740								81				
1293		31	1640	1740								82			0.147	
1294		32	1640	1730								82	87.4		0.147	
1295		33	1625	1730								83			0.148	
1296		34	1640	1725								83			0.147	
1297		35	1633	1740								70	86.0	83.7	0.222	
1298		36	1655	1735								72		84.0	0.217	
1299		37	1650	1735								73			0.217	
1300		38	1650	1735								74	86.2		0.219	
1301		39	1630	1735								78	86.6	84.4	0.219	
1302		40	1630	1730								78	86.5	84.6	0.220	
1303		41	1625	1725								79	86.4	84.6	0.221	
1304		42	1630	1735								81		84.7	0.219	
1305		43	1630	1735								81		84.8	0.221	
1306		44	1630	1735								82		84.8	0.221	
1307		45	1640	1740								83		84.9	0.220	

Test Point No.	Run No.	PT AVG	ALPHA	BETA	Q V,NOM	LIFT,U CL*QS	DRAG,U CD*QS	M,U CM*QSC	CL CY	CD CN	CM CROLL	SIDE F,U CY*QS	YAW,U CN*QSB	ROLL,U CL*QSB
1280	II-14	18	8.00	-8.0	21.18	13487.	3697.	2512.	1.4945	0.4097	0.0243	415.	6051.	2870.
		10			153.48	13487.	3697.	2512.	0.0461	0.0174	0.0082	415.	6051.	2870.
1281		19	10.00	-8.0	20.98	13870.	3872.	1368.	1.5516	0.4332	0.0134	446.	6007.	535.
		10			152.85	13870.	3872.	1368.	0.0499	0.0174	0.0010	446.	6007.	535.
1282		20	12.00	-8.0	20.94	14343.	3934.	906.	1.6082	0.4411	0.0089	370.	5345.	3713.
		10			152.69	14343.	3934.	906.	0.0415	0.0155	0.0108	370.	5345.	3713.
1283		21	0.	-0.	5.14	7063.	1739.	800.	3.2284	0.7947	0.0320	-66.	1170.	-2325.
		10			65.72	7063.	1739.	800.	-0.0299	0.0138	-0.0275	-66.	1170.	-2325.
1284		22	0.	4.0	5.33	7092.	1773.	-175.	3.1237	0.7811	-0.0047	-121.	1257.	-4834.
		10			66.95	7092.	1773.	-175.	-0.0533	0.0143	-0.0551	-121.	1257.	-4834.
1285		23	0.	8.0	5.19	7036.	1763.	-33.	3.1798	0.7968	-0.0013	-114.	814.	-7121.
		10			66.09	7036.	1763.	-33.	-0.0513	0.0048	-0.0835	-114.	814.	-7121.
1286		24	0.	12.0	5.13	6857.	1737.	1063.	3.1420	0.7953	0.0425	-94.	-810.	-7427.
		10			65.66	6857.	1737.	1063.	-0.0431	-0.0096	-0.0881	-94.	-810.	-7427.
1287		25	0.	-4.0	5.04	6935.	1730.	178.	3.2307	0.8062	0.0072	46.	1181.	-1605.
		10			65.10	6935.	1730.	178.	0.0216	0.0143	-0.0194	46.	1181.	-1605.
1288		24	0.	-8.0	5.14	6917.	1744.	-560.	3.1615	0.7970	-0.0224	179.	1223.	-63.
		10			65.72	6917.	1744.	-560.	0.0818	0.0145	-0.0008	179.	1223.	-63.
1289		27	0.	-12.0	5.14	6902.	1806.	-2209.	3.1549	0.8256	-0.0882	246.	1263.	69.
		10			65.72	6902.	1806.	-2209.	0.1122	0.0149	0.0008	246.	1263.	69.
1290		28	8.00	-0.	5.14	7021.	2443.	-344.	3.6206	1.1166	-0.0137	-25.	1616.	-4004.
		10			65.72	7021.	2443.	-344.	-0.0115	0.0191	-0.0474	-25.	1616.	-4004.
1291		29	8.00	4.0	5.24	7090.	2488.	-698.	3.5335	1.1143	-0.0273	59.	1633.	-8562.
		10			66.40	7090.	2488.	-698.	0.0263	0.0166	-0.0529	59.	1633.	-8562.
1292		30	8.00	8.0	5.27	7901.	2474.	-1008.	3.5183	1.1018	-0.0393	103.	167.	-4689.
		10			66.58	7901.	2474.	-1008.	0.0457	0.0019	-0.0541	103.	167.	-4689.
1293		31	8.00	12.0	5.26	7897.	2435.	298.	3.5232	1.0864	0.0116	144.	-514.	-5220.
		10			66.52	7897.	2435.	298.	0.0646	-0.0059	-0.0603	144.	-514.	-5220.
1294		32	8.00	-4.0	5.33	7780.	2479.	-853.	3.4266	1.0920	-0.0328	-88.	2082.	-2452.
		10			66.95	7780.	2479.	-853.	-0.0307	0.0237	-0.0280	-88.	2082.	-2452.
1295		33	8.00	-8.0	5.24	7854.	2478.	-1764.	3.5169	1.1096	-0.0491	-92.	2078.	-413.
		10			66.40	7854.	2478.	-1764.	-0.0414	0.0241	-0.0048	-92.	2078.	-413.
1296		34	8.00	-12.0	5.23	7741.	2504.	-2419.	3.4728	1.1233	-0.0948	-83.	2650.	2989.
		10			66.36	7741.	2504.	-2419.	-0.0376	0.0308	0.0347	-83.	2650.	2989.
1297		35	0.	-0.	11.66	8597.	2637.	-1588.	1.7342	0.5320	-0.0280	19.	2643.	-5516.
		10			98.93	8597.	2637.	-1588.	0.0039	0.0138	-0.0288	19.	2643.	-5516.
1298		36	0.	4.0	11.70	8578.	2603.	-68.	1.7204	0.5221	-0.0012	-88.	1705.	-5034.
		10			99.21	8578.	2603.	-68.	-0.0177	0.0089	-0.0261	-88.	1705.	-5034.
1299		37	0.	8.0	11.75	8342.	2609.	-507.	1.6664	0.5212	-0.0089	-114.	796.	-8748.
		10			99.42	8342.	2609.	-507.	-0.0227	0.0041	-0.0452	-114.	796.	-8748.
1300		38	0.	12.0	11.79	8100.	2633.	199.	1.6127	0.5265	0.0035	-167.	-175.	-11732.
		10			99.58	8100.	2633.	199.	-0.0292	-0.0009	-0.0605	-167.	-175.	-11732.
1301		39	0.	-4.0	11.77	8522.	2614.	-1246.	1.6996	0.5212	-0.0217	-160.	4759.	-1865.
		10			99.50	8522.	2614.	-1246.	-0.0318	0.0246	-0.0096	-160.	4759.	-1865.
1302		40	0.	-8.0	11.79	8478.	2604.	-1933.	1.6880	0.5189	-0.0336	-22.	5216.	596.
		10			99.58	8478.	2604.	-1933.	-0.0043	0.0269	0.0020	-22.	5216.	596.
1303		41	0.	-12.0	11.77	8309.	2640.	-1975.	1.6570	0.5265	-0.0346	157.	4885.	615.
		10			99.50	8309.	2640.	-1975.	0.0314	0.0252	0.0032	157.	4885.	615.
1304		42	8.00	-0.	11.43	10251.	3087.	-780.	2.1864	0.6342	-0.0141	-44.	3670.	-4875.
		10			98.03	10241.	3087.	-780.	-0.0091	0.0195	-0.0259	-44.	3670.	-4875.
1305		43	8.00	4.0	11.83	10547.	3147.	-812.	2.0930	0.6265	-0.0141	55.	2527.	-6444.
		10			99.76	10547.	3147.	-812.	0.0109	0.0130	-0.0331	55.	2527.	-6444.
1306		44	8.00	8.0	11.77	10410.	3100.	-1320.	2.0760	0.6181	-0.0238	152.	745.	-10003.
		10			99.50	10410.	3100.	-1320.	0.0303	0.0038	-0.0550	152.	745.	-10003.
1307		45	8.00	12.0	11.79	10253.	3128.	-49.	2.0413	0.6228	-0.0008	144.	-209.	-11018.
		10			99.58	10253.	3128.	-49.	0.0326	-0.0011	-0.0568	144.	-209.	-11018.

TABLE A-2 (Continued)

Test Point No.	Run No.	Point of Run	Left N_p RPM	Right N_p RPM	Left β_1 Deg.	Left β_0 Deg.	Right β_1 Deg.	Right β_0 Deg.	Tail i_t Deg.	δ_f Deg.	Baro. in. Hg	To $^\circ$F	Left $N_{.85}$ % RPM	Right $N_{.85}$ % RPM	Average V_p/V_{tip}	q/qc
1308	II-14	46	2350	2350	0	0	0	0	OFF	30	30.40	84	98.7	93.5	0.142	N/A
1309	II-14	47	1640	1760	0	0	0	0	OFF	30	30.40	87	86.5	85.4	0.222	N/A
1310	II-15	1	1660	1750	0	0	0	0	OFF	30	30.25	67	86.5	84.0	0.215	N/A
1311		2	1660	1750								69	86.5		0.215	
1312		3	1660	1750								70	86.5		0.220	
1313		4	1670	1765								72	87.0		0.288	
1314		5	1700	1750								72	87.0		0.284	
1315	II-16	1	1660	1745	0	0	0	0	OFF	30	30.40	45	88.0	83.0	0.1055	N/A
1316		2	1660	1745	0	0	0	0				47		83.3	0.1035	
1317		3	1660	1745	0	0	0	0				49		83.3	0.1065	
1318		4	1670	1745	20	20	20	20				52		83.6	0.1035	
1319		5	1735	1755	35	35	35	35				53		83.7	0.1095	
1320		6	1660	1730	0	0	0	0				56		84.0	0.1085	
1321		7	1660	1730								58			0.1070	
1322		8	1665	1725								59			0.1070	
1323		9		1725								60			0.1080	
1324		10		1725								61			0.1080	
1325		11		1720								62			0.1075	
1326		12		1720								63	88.2	84.2	0.1100	
1327		13	1640	1740								66	88.0	85.0	0.1505	
1328		14	1645	1740								67			0.1430	
1329		15	1645	1740	20	20	20	20				68			0.1440	
1330		16	1710	1760	35	35	35	35				69			0.1420	
1331		17	1650	1740	0	0	0	0				70			0.1450	
1332		18	1650	1740								71			0.1430	
1333		19	1660	1740								72		85.2	0.1465	
1334		20	1660	1755								72		85.2	0.1435	

Test Point No.	Run No.	PT AVG	ALPHA	BETA	Q V,NOM	LIFT,U CL*QS	DRAG,U CD*QS	M,U CM*QSC	CL CY	CD CN	CM CROLL	SIDE F,U CY*QS	YAW,U CN*QSB	ROLL,U CL*QSB
1308	II-14	46	8.00	8.0	9.43	14974.	4477.	683.	3.7281	1.1146	0.0149	95.	42.	-8440.
		10			89.05	14974.	4477.	683.	0.0237	0.0003	-0.0557	95.	42.	-8440.
1309	II-14	47	8.00	-4.0	11.81	10436.	3101.	-29.	2.0745	0.6165	-0.0005	-70.	4448.	-2619.
		10			99.66	10436.	3101.	-29.	-0.0139	0.0229	-0.0135	-70.	4448.	-2619.
1310	II-15	1	0.	-0.	11.72	8450.	2608.	-1528.	1.7320	0.5222	-0.0267	-52.	3388.	-9233.
		5			99.30	8450.	2608.	-1528.	-0.0104	0.0176	-0.0479	-52.	3388.	-9233.
1311		2	4.00	-0.	11.67	9506.	2868.	-1722.	1.9129	0.5772	-0.0303	-75.	4082.	-5855.
		5			99.05	9506.	2868.	-1722.	-0.0151	0.0213	-0.0305	-75.	4082.	-5855.
1312		3	8.00	-0.	11.68	10558.	3175.	-400.	2.1211	0.6379	-0.0070	-77.	3752.	-4178.
		5			99.13	10558.	3175.	-400.	-0.0155	0.0195	-0.0217	-77.	3752.	-4178.
1313		4	0.	-0.	20.81	10846.	3359.	-3525.	1.2233	0.3789	-0.0348	24.	3032.	-5867.
		5			132.30	10846.	3359.	-3525.	0.0027	0.0089	-0.0171	24.	3032.	-5867.
1314		5	4.00	-0.	20.87	12069.	3440.	-939.	1.3576	0.3870	-0.0092	125.	2074.	-5287.
		5			132.48	12069.	3440.	-939.	0.014	0.0060	-0.0154	125.	2074.	-5287.
1315	II-16	1	-4.00	-0.	3.00	6487.	875.	-550.	5.0695	0.6834	-0.0376	-67.	1324.	-260.
		5			50.26	6487.	875.	-550.	-0.0525	0.0268	-0.0053	-67.	1324.	-260.
1316		2	-2.00	-0.	2.91	6622.	1055.	-522.	5.3471	0.8522	-0.0368	-29.	1172.	-743.
		5			49.45	6622.	1055.	-522.	-0.0236	0.0245	-0.0155	-29.	1172.	-743.
1317		3	0.	-0.	2.85	6780.	1230.	-839.	5.5866	1.0132	-0.0604	-24.	1129.	-1648.
		5			48.95	6780.	1230.	-839.	-0.0194	0.0241	-0.0352	-24.	1129.	-1648.
1318		4	0.	-0.	3.04	6014.	-834.	1258.	4.6401	-0.6436	0.0848	-39.	2082.	-1146.
		5			50.59	6014.	-834.	1258.	-0.0304	0.0416	-0.0229	-39.	2082.	-1146.
1319		5	0.	-0.	3.28	4682.	-1955.	1788.	3.3560	-1.4011	0.1120	-116.	2191.	-2786.
		5			52.48	4682.	-1955.	1788.	-0.0833	0.0407	-0.0517	-116.	2191.	-2786.
1320		6	2.00	-0.	3.10	6826.	1481.	-486.	5.1672	1.1213	-0.0295	-17.	1067.	-2186.
		5			51.07	6826.	1481.	-486.	-0.0127	0.0209	-0.0428	-17.	1067.	-2186.
1321		7	4.00	-0.	3.00	7003.	1673.	-1027.	5.4727	1.3071	-0.0702	3.	974.	-1314.
		5			50.26	7003.	1673.	-1027.	0.0023	0.0197	-0.0246	3.	974.	-1314.
1322		8	6.00	-0.	3.00	7104.	1919.	-1145.	5.5515	1.4999	-0.0782	-37.	1626.	-2799.
		5			50.26	7104.	1919.	-1145.	-0.0293	0.0329	-0.0566	-37.	1626.	-2799.
1323		9	8.00	-0.	3.00	7178.	2139.	-314.	5.6096	1.6717	-0.0215	-30.	1401.	-422.
		5			50.26	7178.	2139.	-314.	-0.0233	0.0284	-0.0085	-30.	1401.	-422.
1324		10	10.00	-0.	3.02	7370.	2376.	-45.	5.7227	1.8447	-0.0031	-58.	1986.	67.
		5			50.43	7370.	2376.	-45.	-0.0447	0.0399	0.0013	-58.	1986.	67.
1325		11	12.00	-0.	2.97	7344.	2574.	144.	5.8146	2.0374	0.0100	-100.	1869.	950.
		5			49.94	7344.	2574.	144.	-0.0790	0.0383	0.0195	-100.	1869.	950.
1326		12	14.00	-0.	3.28	7723.	2881.	57.	5.5554	2.0651	0.0036	-60.	1751.	-1476.
		5			52.48	7723.	2881.	57.	-0.0463	0.0325	-0.0274	-60.	1751.	-1476.
1327		13	-4.00	-0.	5.62	6715.	1400.	828.	2.8038	0.5845	0.0302	-42.	1256.	-3540.
		5			88.75	6715.	1400.	828.	-0.0176	0.0136	-0.0303	-42.	1256.	-3540.
1328		14	0.	-0.	5.14	7145.	1664.	1493.	3.2657	0.7608	0.0596	-5.	500.	-2681.
		5			65.72	7145.	1664.	1493.	-0.0022	0.0059	-0.0317	-5.	500.	-2681.
1329		15	0.	-0.	5.33	6372.	-308.	3043.	2.8066	-0.1355	0.1171	-71.	1989.	-3206.
		5			66.95	6372.	-308.	3043.	-0.0311	0.0227	-0.0366	-71.	1989.	-3206.
1330		16	0.	-0.	5.56	5338.	-1309.	2368.	2.2527	-0.5526	0.0873	-128.	1889.	-3034.
		5			68.40	5338.	-1309.	2368.	-0.0539	0.0206	-0.0332	-128.	1889.	-3034.
1331		17	4.00	-0.	5.33	7596.	2048.	639.	3.3657	0.9021	0.0246	24.	1037.	-3366.
		5			66.95	7596.	2048.	639.	0.0108	0.0118	-0.0368	24.	1037.	-3366.
1332		18	8.00	-0.	5.17	8177.	2400.	773.	3.7094	1.0889	0.0306	10.	1751.	-1968.
		5			65.97	8177.	2400.	773.	0.0046	0.0206	-0.0231	10.	1751.	-1968.
1333		19	10.00	-0.	5.43	8534.	2691.	642.	3.6919	1.1640	0.0243	18.	2151.	-3067.
		5			67.56	8534.	2691.	642.	0.0077	0.0241	-0.0344	18.	2151.	-3067.
1334		20	12.00	-0.	5.27	8784.	2855.	1033.	3.9117	1.2715	0.0402	-3.	2075.	-1737.
		5			66.58	8784.	2855.	1033.	-0.0013	0.0239	-0.0200	-3.	2075.	-1737.

TABLE A-2 (Continued)

Test Point No.	Run No.	Point of Run	Left N_p RPM	Right N_p RPM	Left β_1 Deg.	Left β_0 Deg.	Right β_1 Deg.	Right β_0 Deg.	Tail i_t Deg.	δ_f Deg.	Baro. in. Hg	To °F	Left $N_{.385}$ % RPM	Right $N_{.385}$ % RPM	Average V_p/V_{tip}	q/qc
1335	II-16	21	1660	1745	0	0	0	0	OFF	30	30.40	73	88.0	85.2	0.1450	N/A
1336		22	1660	1785								73		85.0	0.1435	
1337		23	1640	1750								75	87.5	85.0	0.2190	
1338		24	1640	1750								76		85.2	0.2190	
1339		25	1645	1750	20	20	20	20							0.2160	
1340		26	1680	1760	35	35	35	35							0.2150	
1341		27	1705	1780	40	40	40	40					87.4		0.2095	
1342		28	1735	1800	45	45	45	45				77	87.3		0.2165	
1343		29	1650	1750	0	0	0	0				78	87.5		0.2175	
1344		30	1640	1750								78			0.2185	
1345		31	1640	1760								78			0.2180	
1346		32	1640	1795								79			0.2185	
1347		33	1640	1860								79			0.2110	
1348		34	1650	1880								79			0.2120	
1349		35	1655	1745								81	88.0	85.4	0.2910	
1350		36	1655	1745								81	87.9		0.2910	
1351		37	1655	1745	20	20	20	20				81	87.9		0.2895	
1352		38	1680	1760	35	35	35	35				81	87.8		0.2875	
1353		39	1710	1775	40	40	40	40				82	87.7		0.2830	
1354		40	1740	1790	45	45	45	45				82	87.6	85.3	0.2810	
1355		41	1650	1740	0	0	0	0				82	87.8		0.2925	
1356		42	1645	1745								83	88.0		0.2910	
1357		43	1650	1750								84		84.7	0.2940	
1358		44	1650	1750								84		82.0	0.2905	
1359		45	1660	1780								84		81.0	0.2890	
1360	II-17	1	1660	1740	0	0	0	0	OFF	30	30.30	58	87.0	83.0	0.2135	N/A
1361		2	1670	1740	0	0	0	0	OFF	30	30.30	60	87.0	83.0	0.2133	N/A
1362		3	1675	1745	0	0	0	0	OFF	30	30.30	61	87.0	83.5	0.2129	N/A

Test Point No.	Run No.	PT AVG	ALPHA	BETA	Q V,NOM	LIFT,U CL*QS	DRAG,U CD*QS	M,U CM*QSC	CL CY	CD CN	CM CROLL	SIDE F,U CY*QS	YAW,U CN*QSB	ROLL,U CL*QSB
1335	II-16	21	14.00	-0.	5.33	8923.	3096.	1534.	3.9503	1.3635	0.0591	-16.	2711.	-2045.
		5			66.95	8923.	3098.	1534.	-0.0072	0.0309	-0.0233	-16.	2711.	-2045.
1336		22	16.00	-0.	5.45	9264.	3382.	1062.	3.9933	1.4579	0.0400	17.	2221.	-452.
		5			67.68	9264.	3382.	1062.	0.0072	0.0248	-0.0050	17.	2221.	-452.
1337		23	-4.00	-0.	11.95	7548.	2245.	143.	1.4823	0.4409	0.0025	-51.	2529.	-4252.
		5			100.27	7548.	2245.	143.	-0.0101	0.0129	-0.0216	-51.	2529.	-4252.
1338		24	0.	-0.	12.01	8566.	2497.	560.	1.6741	0.4881	0.0095	3.	2686.	-5541.
		5			100.51	8566.	2497.	560.	0.0007	0.0136	-0.0280	3.	2686.	-5541.
1339		25	0.	-0.	11.80	7642.	872.	2738.	1.5202	0.1736	0.0476	52.	1240.	-2207.
		5			99.62	7642.	872.	2738.	0.0104	0.0064	-0.0114	52.	1240.	-2207.
1340		26	0.	-0.	12.09	6710.	-141.	1393.	1.3032	-0.0273	0.0236	18.	842.	-2984.
		5			100.83	6710.	-141.	1393.	0.0035	0.0042	-0.0150	18.	842.	-2984.
1341		27	0.	-0.	11.70	6163.	-402.	1251.	1.2361	-0.0806	0.0219	-97.	2299.	-3118.
		5			99.21	6165.	-402.	1251.	-0.0195	0.0119	-0.0162	-97.	2299.	-3118.
1342		28	0.	-0.	11.72	5791.	-487.	-1162.	1.1594	-0.0976	-0.0203	14.	1681.	-4136.
		5			99.30	5791.	-487.	-1162.	0.0029	0.0087	-0.0214	14.	1681.	-4136.
1343		29	4.00	-0.	11.80	9590.	2694.	925.	1.9079	0.5360	0.0161	2.	3068.	-5714.
		5			99.62	9590.	2694.	925.	0.0004	0.0158	-0.0294	2.	3068.	-5714.
1344		30	8.00	-0.	11.78	8362.	3128.	-27500.	1.6661	0.6235	-0.4790	42.	2988.	-5674.
		5			99.54	8362.	3128.	-27500.	0.0084	0.0154	-0.0293	42.	2988.	-5674.
1345		31	10.00	-0.	11.90	11195.	3383.	1023.	2.2087	0.6676	0.0177	-5.	3765.	-3815.
		5			100.02	11195.	3383.	1023.	-0.0010	0.0192	-0.0195	-5.	3765.	-3815.
1346		32	12.00	-0.	12.20	11819.	3642.	1709.	2.2737	0.7007	0.0287	79.	3604.	-3535.
		5			101.31	11819.	3642.	1709.	0.0151	0.0180	-0.0176	79.	3604.	-3535.
1347		33	14.00	-0.	11.76	11927.	3952.	914.	2.3805	0.7888	0.0159	259.	1810.	-5107.
		5			99.46	11927.	3952.	914.	0.0517	0.0094	-0.0264	259.	1810.	-5107.
1348		34	16.00	-0.	12.09	12671.	4209.	-327.	2.4608	0.8175	-0.0055	213.	7.	-1689.
		5			100.83	12671.	4209.	-327.	0.0413	0.0000	-0.0085	213.	7.	-1689.
1349		35	-4.00	-0.	21.10	8844.	3150.	581.	0.984.	0.3505	0.0037	168.	2330.	-5522.
		5			133.21	8844.	3150.	581.	0.0188	0.0067	-0.0159	168.	2330.	-5522.
1350		36	0.	-0.	21.14	10653.	3301.	1339.	1.1831	0.3666	0.0130	198.	2733.	-3522.
		5			133.33	10653.	3301.	1339.	0.0220	0.0079	-0.0101	198.	2733.	-3522.
1351		37	0.	-0.	20.91	10046.	1981.	-771.	1.128	0.2226	-0.0076	157.	1235.	-2237.
		5			132.60	10046.	1981.	-771.	0.0176	0.0036	-0.0065	157.	1235.	-2237.
1352		38	0.	-0.	21.21	9235.	1028.	-2899.	1.0220	0.1138	-0.0280	86.	817.	-1705.
		5			133.57	9235.	1028.	-2899.	0.0095	0.0023	-0.0049	86.	817.	-1705.
1353		39	0.	-0.	20.87	8534.	787.	-3279.	0.960	0.0885	-0.0322	13.	1598.	-3597.
		5			132.48	8534.	787.	-3279.	0.0015	0.0047	-0.0105	13.	1598.	-3597.
1354		40	0.	-0.	21.08	8254.	624.	-4865.	0.9191	0.0695	-0.0474	34.	1187.	-3954.
		5			133.15	8254.	624.	-4865.	0.0037	0.0036	-0.0114	34.	1187.	-3954.
1355		41	4.00	-0.	21.14	12510.	3437.	2863.	1.3894	0.3818	0.0278	178.	2865.	-3805.
		5			133.33	12510.	3437.	2863.	0.0198	0.0082	-0.0109	178.	2865.	-3805.
1356		42	8.00	-0.	21.00	14426.	3767.	5330.	1.6123	0.4211	0.0521	100.	3420.	-2544.
		5			132.91	14426.	3767.	5330.	0.0112	0.0099	-0.0074	100.	3420.	-2544.
1357		43	10.00	-0.	21.19	15357.	4016.	3966.	1.7009	0.4448	0.0384	140.	2204.	-2033.
		5			133.51	15357.	4016.	3966.	0.0178	0.0063	-0.0058	140.	2204.	-2033.
1358		44	12.00	-0.	21.10	15568.	4026.	2452.	1.7321	0.4479	0.0238	77.	-1593.	4161.
		5			133.21	15568.	4026.	2452.	0.0085	-0.0046	0.0120	77.	-1593.	4161.
1359		45	14.00	-0.	21.21	15909.	4469.	4609.	1.7604	0.4946	0.0446	51.	-1217.	5036.
		5			133.57	15909.	4469.	4609.	0.0057	-0.0035	0.0167	51.	-1217.	5036.
1360	II-17	1	-4.00	-0.	11.61	7896.	2240.	1365.	1.5968	0.4529	0.0241	-144.	2188.	-5095.
		5			98.81	7896.	2240.	1365.	-0.0331	0.0115	-0.0247	-144.	2188.	-5095.
1361		2	0.	-0.	11.59	8978.	2513.	2512.	1.8187	0.5091	0.0445	-225.	3256.	-2137.
		5			98.73	8978.	2513.	2512.	-0.0455	0.0171	-0.0112	-225.	3256.	-2137.
1362		3	4.00	-0.	11.61	10106.	2852.	3453.	2.0438	0.5768	0.0610	-148.	2439.	-5314.
		5			98.81	10106.	2852.	3453.	-0.0300	0.0128	-0.0278	-148.	2439.	-5314.

TABLE A-2 (Continued)

Test Point No.	Run No.	Point of Run	Left N_p RPM	Right N_p RPM	Left β_L Deg.	Left β_R Deg.	Right β_L Deg.	Right β_R Deg.	Tail i_t Deg.	δ_f Deg.	Baro. in. Hg	T_0 °F	Left $N_{.385}$ % RPM	Right $N_{.385}$ % RPM	Average V_p/V_{tip}	q/qc
1363	IX-17	4	1675	1740	0	0	0	0	OFF	30	30.30	62	87.0	83.5	0.2161	N/A
1364		5	1675	1735								63			0.2139	
1365		6	1675	1735								64			0.2142	
1366		7	1675	1745								65			0.2163	
1367		8	Not Recorded										Not Recorded			
1368		9	0	1610								53	0	81.5	-	
1369		10	1660	1770								59	86.5	83.5	0.2119	
1370		11	1660	1790								61	87.0	84.0	0.2138	
1371		12	1660	1790								62	87.0	84.0	0.2114	
1372		13	1200	1220								63	74.0	69.0	0.3013	
1373		14		1210								64	75.0		0.3029	
1374		15		1210								65	75.0		0.3032	
1375		16										65	75.0		0.3032	
1376		17										65	74.0		0.3032	
1377		18	1190									66			0.3043	
1378		19													0.3043	
1379		20		1215									75.0		0.3027	
1380		21		1250									75.0		0.3015	
1381		22		1220								67	74.0		0.3531	
1382		23	1200	1380								67	75.0		0.3795	
1383		24		1220								68	75.0		0.3529	
1384		25		1230	20	20	20	20					74.0		0.3517	
1385		26		1230	35	35	35	35					74.0		0.3509	
1386		27	1210	1230	40	40	40	40					75.0		0.3500	
1387		28	1260	1250	45	45	45	45					74.0		0.3609	
1388		29	0	1110	0	0	0	0				72	0	66.0	0.0335	
1389		30	0	1420	0	0	0	0				77	0	76.0	0.0216	
1390		31	0	1740	0	0	0	0				83	0	84.5	0	

Test Point No.	Run No.	PT AVG	ALPHA	BETA	Q V,NOM	LIFT,U CL*QS	DRAG,U CD*QS	M,U CM*QSC	CL CY	CD CN	CM CROLL	SIDE F,U CY*QS	YAW,U CN*QSB	ROLL,U CL*QSB
1363	IX-17	4	8.00	-0.	11.97	11071.	3281.	593.	2.1767	0.6434	0.0102	-181.	2677.	-3069.
		5			100.35	11071.	3281.	593.	-0.0355	0.0136	-0.0156	-181.	2677.	-3069.
1364		5	10.00	-0.	11.67	11682.	3555.	4304.	2.3508	0.7154	0.0757	-169.	3121.	-3687.
		5			99.05	11682.	3555.	4304.	-0.034	0.0163	-0.0192	-169.	3121.	-3687.
1365		6	12.00	-0.	11.61	12141.	3961.	3296.	2.4552	0.8010	0.0583	-276.	4169.	-1652.
		5			98.81	12141.	3961.	3296.	-0.0557	0.0218	-0.0086	-276.	4169.	-1652.
1366		7	14.00	-0.	11.68	12378.	4314.	4916.	2.4868	0.8667	0.0863	-91.	2954.	-5624.
		5			99.13	12378.	4314.	4916.	-0.0182	0.0154	-0.0293	-91.	2954.	-5624.
1367		8	16.00	-0.	11.44	12796.	4658.	3523.	2.6267	0.9561	0.0632	-15.	1598.	-5199.
		5			98.07	12796.	4658.	3523.	-0.0031	0.0085	-0.0276	-15.	1598.	-5199.
1368		9	0.	-0.	1.00	2441.	5.	-3120.	5.7296	0.0124	-0.6402	45.	-56.	-17120.
		5			0.	2441.	5.	-3120.	0.1059	-0.0035	-1.0406	45.	-58.	-17120.
1369		10	14.00	-0.	11.65	12525.	4379.	3487.	2.5245	0.8827	0.0614	-164.	3705.	-5689.
		5			98.97	12525.	4379.	3487.	-0.033	0.0193	-0.0297	-164.	3705.	-5689.
1370		11	16.00	-0.	11.74	12873.	4756.	3512.	2.5734	0.9508	0.0614	25.	1991.	-8003.
		5			99.38	12873.	4756.	3512.	0.0051	0.0103	-0.0414	25.	1991.	-8003.
1371		12	18.00	-0.	11.67	13346.	5132.	2116.	2.6855	1.0527	0.0372	59.	1199.	-8514.
		5			99.05	13346.	5132.	2116.	0.0118	0.0062	-0.0444	59.	1199.	-8514.
1372		13	-4.00	-0.	11.70	4908.	1651.	-567.	0.9844	0.3311	-0.0089	23.	747.	-1894.
		5			99.21	4908.	1651.	-567.	0.0046	0.0039	-0.0098	23.	747.	-1894.
1373		14	0.	-0.	11.70	6070.	1714.	802.	1.2174	0.3438	0.0141	16.	656.	-1602.
		5			99.21	6070.	1714.	802.	0.0032	0.0034	-0.0083	16.	656.	-1602.
1374		15	4.00	-0.	11.61	6948.	1868.	1430.	1.4051	0.3779	0.0253	21.	543.	-940.
		5			98.81	6948.	1868.	1430.	0.0043	0.0028	-0.0049	21.	543.	-940.
1375		16	8.00	-0.	11.61	8083.	2093.	2531.	1.6346	0.4233	0.0447	13.	458.	-686.
		5			98.81	8083.	2093.	2531.	0.0026	0.0024	-0.0036	13.	458.	-686.
1376		17	10.00	-0.	11.70	8587.	2190.	3237.	1.7223	0.4393	0.0567	58.	153.	-581.
		5			99.21	8587.	2190.	3237.	0.0116	0.0008	-0.0030	58.	153.	-581.
1377		18	12.00	-0.	11.42	8830.	2480.	2906.	1.8156	0.5098	0.0522	-79.	1314.	3608.
		5			97.99	8830.	2480.	2906.	-0.0162	0.0070	0.0192	-79.	1314.	3608.
1378		19	14.00	-0.	11.55	9322.	2732.	3864.	1.8944	0.5551	0.0686	-25.	349.	1595.
		5			98.56	9322.	2732.	3864.	-0.0052	0.0018	0.0084	-25.	349.	1595.
1379		20	16.00	-0.	11.45	9298.	3089.	4675.	1.9054	0.6330	0.0838	34.	-490.	404.
		5			98.15	9298.	3089.	4675.	0.0070	-0.0026	0.0021	34.	-490.	404.
1380		21	18.00	-0.	11.76	9479.	3332.	5516.	1.8919	0.6651	0.0962	49.	-1852.	1219.
		5			99.46	9479.	3332.	5516.	0.0099	-0.0096	0.0063	49.	-1852.	1219.
1381		22	0.	-0.	15.73	6821.	1946.	-1622.	1.0178	0.2904	-0.0212	16.	652.	-520.
		5			115.03	6821.	1946.	-1622.	0.0024	0.0025	-0.0020	16.	652.	-520.
1382		23	0.	-0.	21.04	6862.	1797.	-9067.	0.7655	0.2005	-0.0884	-137.	-801.	5128.
		5			133.03	6862.	1797.	-9067.	-0.0153	-0.0023	0.0148	-137.	-801.	5128.
1383		24	0.	-0.	16.02	6890.	1949.	-1434.	1.0097	0.2855	-0.0184	5.	408.	81.
		5			116.07	6890.	1949.	-1434.	0.0008	0.0015	0.0003	5.	408.	81.
1384		25	0.	-0.	15.94	6432.	1332.	-2519.	0.9471	0.1962	-0.0324	3.	654.	-1438.
		5			115.79	6432.	1332.	-2519.	0.0005	0.0025	-0.0055	3.	654.	-1438.
1385		26	0.	-0.	15.79	6002.	880.	-4884.	0.8924	0.1308	-0.0435	-62.	862.	-1240.
		5			115.24	6002.	880.	-4884.	-0.0092	0.0033	-0.0048	-62.	862.	-1240.
1386		27	0.	-0.	15.90	5623.	736.	-4899.	0.8300	0.1090	-0.0432	-35.	477.	-1438.
		5			115.46	5623.	736.	-4899.	-0.0052	0.0018	-0.0055	-35.	477.	-1438.
1387		28	0.	-0.	15.96	5213.	618.	-5962.	0.7666	0.0909	-0.0766	29.	329.	-1092.
		5			115.86	5213.	618.	-5962.	0.0042	0.0013	-0.0042	29.	329.	-1092.
1388		29	0.	-0.	1.00	1044.	68.	-1405.	2.4507	0.1589	-0.2882	-7.	508.	-7556.
		5			0.	1044.	68.	-1405.	-0.0169	0.0309	-0.4592	-7.	508.	-7556.
1389		30	0.	-0.	1.00	1766.	14.	-2265.	4.1465	0.0327	-0.4648	-6.	-92.	-12616.
		10			0.	1766.	14.	-2265.	-0.0141	-0.0056	-0.7668	-6.	-92.	-12616.
1390		31	0.	-0.	1.00	2592.	57.	-3258.	6.0845	0.1341	-0.4686	-4.	123.	-19420.
		10			0.	2592.	57.	-3258.	-0.0085	0.0075	-1.1804	-4.	123.	-19420.

TABLE A-2 (Continued)

Test Point No.	Run No.	Point of Run	Left N_p RPM	Right N_p RPM	Left β_L Deg.	Left β_0 Deg.	Right β_L Deg.	Right β_0 Deg.	Tail i_t Deg.	δ_f Deg.	Baro. in. Hg	T_0 °F	Left N_{J85} % RPM	Right N_{J85} % RPM	Average V_p/V_{tip}	q/qc
1391	II-17	32	0	2240	0	0	0	0	OFF	30	30.30	80	0	92.0	0.0153	N/A
1392	II-18	1	0	1700	0	0	0	0	OFF	30	30.39	46	0	82.5	0	N/A
1393		2		2250										90.0		
1394		3		2410										92.0		
1395		4		2630										94.5		
1396		5		2255										90.0		
1397	II-19	1	1100	0	0	0	0	0	OFF	30	30.24	50	73.0	0	0	N/A
1398		2	1395									63	82.5			
1399		3	1535									64	87.0			
1400		4	1775									66	90.0			
1401		5	1995									68	93.3			
1402		6	2200									72	96.5			
1403		7	2310									72	98.0			
1404		8	0	1120								70	0	65.7		
1405		9		1390								70		74.9		
1406		10		1625								76		81.0		
1407		11		1795								74		85.0		
1408		12		2260								74		91.0		
1409		13		2390								76		93.0		
1410		14		2615								76		95.5		
1411		15	1660	1740								63	87.0	84.0		
1412		16	1660									64	87.0	84.0	0.2175	
1413		17	1670									66	87.2	84.3	0.2158	
1414		18	1660									67	87.2	84.3	0.2146	
1415		19										68	87.5	84.3	0.2182	
1416		20		1765								68		84.5	0.2152	
1417		21		1765								70			0.2173	
1418		22		1780								71			0.2144	

Test Point No.	Run No.	PT AVG	ALPHA	BETA	Q V,NOM	LIFT,U CL*QS	DRAG,U CD*QS	M,U CM*QSC	CL CY	CD CN	CM CROLL	SIDE F,U CY*QS	YAW,U CN*QSB	ROLL,U CL*QSB
1391	II-17	32	0.	-0.	1.00	4366.	110.	-5980.	10.2479	0.2575	-1.2271	59.	348.	-31981.
		10			0.	4366.	110.	-5980.	0.1386	0.0211	-1.9439	59.	348.	-31981.
1392	II-18	1	0.	-0.	1.00	2626.	9.	-3492.	6.1634	0.0214	-0.7165	21.	-227.	-20180.
		5			0.	2626.	9.	-3492.	0.0485	-0.0138	-1.2266	21.	-227.	-20180.
1393		2	0.	-0.	0.25	4622.	82.	-6425.	43.0686	0.7603	-5.2325	70.	491.	-35207.
		5			14.56	4622.	82.	-6425.	0.6485	0.1184	-8.4940	70.	491.	-35207.
1394		3	0.	-0.	1.00	5148.	144.	-7197.	12.0845	0.3369	-1.4562	82.	239.	-37509.
		5			0.	5148.	144.	-7197.	0.1927	0.0145	-2.2799	82.	239.	-37509.
1395		4	0.	-0.	1.00	6214.	152.	-8752.	14.5859	0.3572	-1.7958	109.	232.	-44378.
		5			0.	6214.	152.	-8752.	0.2569	0.0181	-2.6974	109.	232.	-44378.
1396		5	0.	-0.	1.00	4531.	95.	-6277.	10.6366	0.2220	-1.2879	84.	247.	-32427.
		5			0.	4531.	95.	-6277.	0.1972	0.0150	-1.9710	84.	247.	-32427.
1397	II-19	1	0.	-0.	1.00	1310.	-118.	-1721.	3.0761	-0.2761	-0.3531	-26.	1124.	9167.
		5			0.	1310.	-118.	-1721.	-0.062	0.0683	0.5572	-26.	1124.	9167.
1398		2	0.	-0.	1.00	2044.	-197.	-2645.	4.7972	-0.4620	-0.5427	-56.	1834.	14604.
		10			0.	2044.	-197.	-2645.	-0.1307	0.1115	0.8877	-56.	1834.	14604.
1399		3	0.	-0.	1.00	2752.	-267.	-3696.	6.4592	-0.6259	-0.7585	-98.	2315.	19900.
		10			0.	2752.	-267.	-3696.	-0.231	0.1407	1.2096	-98.	2315.	19900.
1400		4	0.	-0.	0.25	3340.	-323.	-4449.	31.1165	-3.0099	-3.6231	-119.	2715.	24208.
		10			14.56	3340.	-323.	-4449.	-1.1091	0.6551	5.8405	-119.	2715.	24208.
1401		5	0.	-0.	1.00	4146.	-366.	-5122.	9.7324	-0.8580	-1.0510	-199.	3639.	30098.
		10			0.	4146.	-366.	-5122.	-0.467	0.2212	1.8296	-199.	3639.	30098.
1402		6	0.	-0.	0.46	5029.	-407.	-6676.	25.922	-2.0968	-3.0078	-246.	4109.	35287.
		10			19.57	5029.	-407.	-6676.	-1.2655	0.5484	4.7094	-246.	4109.	35287.
1403		7	0.	-0.	0.30	5387.	-493.	-6449.	42.0955	-3.8523	-4.4052	-248.	4492.	39722.
		10			15.89	5387.	-493.	-6449.	-1.9303	0.9089	8.0375	-248.	4492.	39722.
1404		8	0.	-0.	1.00	1181.	26.	-1430.	2.7718	0.0620	-0.2934	-1.	261.	-7872.
		10			0.	1181.	26.	-1430.	-0.0017	0.0159	-0.4785	-1.	261.	-7872.
1405		9	0.	-0.	1.00	1769.	21.	-2613.	4.1521	0.0490	-0.5361	2.	123.	-12353.
		10			0.	1769.	21.	-2613.	0.0039	0.0075	-0.7509	2.	123.	-12353.
1406		10	0.	-0.	1.00	2356.	47.	-3252.	5.5296	0.1110	-0.6673	20.	-117.	-16352.
		10			0.	2356.	47.	-3252.	0.0473	-0.0071	-0.9959	20.	-117.	-16352.
1407		11	0.	-0.	1.00	2936.	52.	-3895.	6.8935	0.1228	-0.7992	12.	240.	-21050.
		10			0.	2936.	52.	-3895.	0.0293	0.0146	-1.2795	12.	240.	-21050.
1408		12	0.	-0.	1.00	4638.	130.	-6507.	10.8873	0.3042	-1.5552	95.	328.	-32864.
		10			0.	4638.	130.	-6507.	0.2225	0.0199	-1.9976	95.	328.	-32864.
1409		13	0.	-0.	1.00	5107.	117.	-7341.	11.9887	0.2749	-1.5065	84.	465.	-37183.
		10			0.	5107.	117.	-7341.	0.1983	0.0283	-2.2601	84.	465.	-37183.
1410		14	0.	-0.	1.00	6128.	189.	-8409.	14.3859	0.4434	-1.7254	140.	584.	-43508.
		10			0.	6128.	189.	-8409.	0.3290	0.0355	-2.6445	140.	584.	-43508.
1411		15	-4.00	-0.	11.99	8088.	2313.	145.	1.5833	0.4528	0.0025	-235.	2555.	-4154.
		5			100.43	8088.	2313.	145.	-0.0459	0.0129	-0.0211	-235.	2555.	-4154.
1412		16	0.	-0.	11.78	9031.	2583.	1349.	1.7996	0.5147	0.0235	-241.	3098.	-2510.
		5			99.54	9031.	2583.	1349.	-0.0481	0.0160	-0.0150	-241.	3098.	-2510.
1413		17	4.00	-0.	11.61	10178.	2907.	2720.	2.0582	0.5879	0.0482	-184.	2324.	-3543.
		5			98.81	10178.	2907.	2720.	-0.0373	0.0121	-0.0186	-184.	2320.	-3543.
1414		18	8.00	-0.	11.59	11274.	3349.	3735.	2.2837	0.6784	0.0661	-197.	2863.	-2259.
		5			98.73	11274.	3349.	3735.	-0.0409	0.0150	-0.0118	-197.	2863.	-2259.
1415		19	10.00	-0.	11.95	12006.	3647.	4085.	2.3579	0.7162	0.0701	-225.	3279.	-2724.
		5			100.27	12006.	3647.	4085.	-0.0441	0.0167	-0.0138	-225.	3279.	-2724.
1416		20	12.00	-0.	11.67	12290.	4008.	3562.	2.4730	0.8065	0.0627	-243.	3647.	-4701.
		5			99.05	12290.	4008.	3562.	-0.0490	0.0190	-0.0245	-243.	3647.	-4701.
1417		21	14.00	-0.	11.99	12750.	4440.	4274.	2.4966	0.8691	0.0731	-201.	3513.	-4091.
		5			100.43	12750.	4440.	4274.	-0.0393	0.0178	-0.0207	-201.	3513.	-4091.
1418		22	16.00	-0.	11.74	12947.	4844.	3330.	2.5883	0.9603	0.0582	25.	2252.	-8179.
		5			99.38	12947.	4844.	3330.	0.0051	0.0117	-0.0423	25.	2252.	-8179.

TABLE A-2 (Continued)

Test Point No.	Run No.	Point of Run	Left N_p RPM	Right N_p RPM	Left β_t Deg.	Left β_0 Deg.	Right β_t Deg.	Right β_0 Deg.	Tail i_t Deg.	δ_f Deg.	Bare. in. Hg	To $^\circ_F$	Left N_{J85} % RPM	Right N_{J85} % RPM	Average V_p/V_{tip}	q/qc
1419	II-19	23	1665	1800	0	0	0	0	OFF	30	30.24	72	87.5	84.5	0.2152	N/A
1420		24	1200	1245								73	75.0	70.3	0.3028	
1421		25	1200	1245									75.5		0.3028	
1422		26													0.3040	
1423		27													0.3031	
1424		28												70.2	0.3031	
1425		29													0.3026	
1426		30		1250								74	76.2		0.3016	
1427		31		1260									75.5		0.3034	
1428		32		1300											0.2977	
1429		33		1260											0.3543	
1430		34	1240	1430											0.3771	
-	II-20	No aerodynamic data taken														
-	II-21	"	"	"	"											
1431	II-22	1	0	0	90	90	90	90	OFF	30	30.16	78	0	0	N/A	N/A
1432		2														
1433		3														
1434		4														
1435		5														
1436		6														
1437		7														
1438		8														
1439		9														

Test Point No.	Run No.	Pt AVG	ALPHA	BETA	Q V,NOM	LIFT,U CL*QS	DRAG,U CD*QS	M,U CM*QSC	CL CY	CD CN	CM CMDLL	SIDE F,U CY*QS	YAW,U CN*QSB	ROLL,U CL*QSB
1419	II-19	23	18.00	-0.	11.99	13422.	5257.	2397.	2.6275	1.0292	0.0410	130.	1609.	-8480.
		5			100.43	13422.	5257.	2397.	0.0255	0.0082	-0.0430	130.	1609.	-8480.
1420		24	-4.00	-0.	11.80	4997.	1704.	-508.	0.994	0.3390	-0.0088	30.	566.	-2422.
		5			99.62	4997.	1704.	-508.	0.006	0.0029	-0.0125	30.	566.	-2422.
1421		25	0.	-0.	11.80	6146.	1782.	453.	1.2227	0.3544	0.0079	-1.	1252.	-1278.
		5			99.62	6146.	1782.	453.	-0.0031	0.0044	-0.0066	-1.	1252.	-1278.
1422		26	4.00	-0.	11.90	7234.	1966.	1357.	1.4274	0.3880	0.0234	27.	772.	-469.
		5			100.02	7234.	1966.	1357.	0.0053	0.0039	-0.0024	27.	772.	-469.
1423		27	8.00	-0.	11.82	8340.	2182.	2445.	1.6564	0.4334	0.0424	75.	355.	-2576.
		5			99.70	8340.	2182.	2445.	0.0144	0.0018	-0.0132	75.	355.	-2576.
1424		28	10.00	-0.	11.82	8902.	2340.	2402.	1.768	0.4648	0.0417	41.	372.	-1859.
		5			99.70	8902.	2340.	2402.	0.0082	0.0019	-0.0096	41.	372.	-1859.
1425		29	12.00	-0.	11.78	9379.	2572.	2980.	1.8689	0.5124	0.0519	-46.	1125.	1232.
		5			99.54	9379.	2572.	2980.	-0.0091	0.0058	0.0064	-46.	1125.	1232.
1426		30	14.00	-0.	11.72	9588.	2891.	3167.	1.9199	0.5789	0.0589	-24.	-146.	1085.
		5			99.30	9588.	2891.	3167.	-0.0049	-0.0008	0.0056	-24.	-146.	1085.
1427		31	16.00	-0.	11.95	9887.	3217.	2758.	1.9417	0.6317	0.0473	69.	-899.	-147.
		5			100.27	9887.	3217.	2758.	0.0136	-0.0046	-0.0007	69.	-899.	-147.
1428		32	18.00	-0.	11.90	9926.	3495.	5247.	1.9587	0.6897	0.0905	99.	-726.	-159.
		5			100.02	9926.	3495.	5247.	0.0195	-0.0037	-0.0008	99.	-726.	-159.
1429		33	0.	-0.	16.31	7080.	2042.	-1000.	1.0192	0.2946	-0.0126	94.	-116.	-3427.
		5			117.11	7080.	2042.	-1000.	0.0135	-0.0004	-0.0128	94.	-116.	-3427.
1430		34	0.	-0.	21.77	7202.	1861.	-8338.	0.7767	0.2007	-0.0786	-122.	-1081.	3770.
		5			135.31	7202.	1861.	-8338.	-0.0132	-0.0030	0.0105	-122.	-1081.	3770.
-	II-20													
-	II-21													
1431	II-22	1	-3.82	-0.	11.80	1001.	557.	-9613.	0.1991	0.1114	-0.1672	9.	-446.	516.
		5			99.62	1001.	560.	-9613.	0.0017	-0.0023	0.0027	9.	-446.	516.
1432		2	0.48	-0.	11.99	2366.	564.	-9570.	0.4632	0.1139	-0.1638	0.	-207.	1663.
		5			100.43	2366.	582.	-9570.	0.0001	-0.0010	0.0084	0.	-207.	1663.
1433		3	4.69	-0.	12.09	3842.	654.	-8583.	0.7462	0.1359	-0.1457	4.	-161.	1700.
		5			100.83	3842.	700.	-8583.	0.0007	-0.0018	0.0085	4.	-161.	1700.
1434		4	8.94	-0.	11.70	5059.	833.	-7012.	1.0147	0.1836	-0.1229	-4.	-163.	2569.
		5			99.21	5059.	915.	-7012.	-0.0008	-0.0008	0.0133	-4.	-163.	2569.
1435		5	11.07	-0.	11.80	5844.	959.	-6674.	1.1626	0.2126	-0.1056	3.	-276.	2141.
		5			99.62	5844.	1069.	-6674.	0.0006	-0.0014	0.0110	3.	-276.	2141.
1436		6	13.17	-0.	11.90	6439.	1102.	-5165.	1.2707	0.2434	-0.0891	6.	-291.	2574.
		5			100.02	6439.	1234.	-5165.	0.0012	-0.0015	0.0132	6.	-291.	2574.
1437		7	15.27	-0.	11.80	6914.	1244.	-4058.	1.3755	0.2779	-0.0706	-0.	-279.	3130.
		5			99.62	6914.	1397.	-4058.	-0.	-0.0014	0.0161	-0.	-279.	3130.
1438		8	17.35	-0.	11.70	7267.	1565.	-3686.	1.4576	0.3480	-0.0646	-3.	-291.	868.
		5			99.21	7267.	1735.	-3686.	-0.0007	-0.0015	0.0045	-3.	-291.	868.
1439		9	19.41	-0.	11.80	7668.	1916.	-3468.	1.5254	0.4187	-0.0603	-21.	-179.	2168.
		5			99.62	7668.	2105.	-3468.	-0.0042	-0.0009	0.0112	-21.	-179.	2168.

TABLE A-2 (Continued)

TABLE A-3. GROUND EFFECTS TEST RESULTS

Run No.	Reading No.	Fan	Configuration	h/d_p	Wind Velocity Knots	Wind Direction	N_p RPM	F lbs.	$N_p/\sqrt{\theta}$ RPM	F/δ lbs.	HP	HP/δ/θ
1	7	Left	No Doors	1.82	-	Calm -	1910	6190	1930	6155	-	-
	8						2130	5100	2135	5060	-	-
	9						1900	6080	1920	6045	-	-
	17						1910	6070	1930	6035	-	-
2	5	Left	Paired	1.82	-	Calm -	2120	5040	2125	5000	-	-
	6						2310	5930	2310	5890	3155	3130
	7						2480	6730	2435	6680	4015	3990
	8						2300	5840	2290	5800	3100	3055
	9						2315	5870	2315	5830	3160	3130
	10						2310	5810	2310	5770	3150	3120
	11						2300	5860	2300	5820	3190	3160
	12						2320	5830	2320	5790	3200	3170
	31						2330	-	2340	-	3130	3120
	31	Right	No Doors				2340	-	2345	-	2880	2860
	31	Both	Right - No Doors Left - Paired				-	11250	-	11150	6010	5980
4	4	Left	Paired	0.98	-	Calm -	1900	6025	1905	6020	-	-
	5						2100	4810	2105	4805	-	-
	6						2320	5840	2325	5835	3030	3030
	7						2060	4720	2065	4715	2125	2125
5	4	Left	No Doors	0.98	7 - 8	SE	1900	6100	1905	6105	-	-
	5						2120	5180	2120	5175	2410	2410
	6						2300	6070	2300	6060	3050	3050
	7						2310	6090	2310	6080	3050	3050
	8						1900	4110	1895	4105	-	-
	16						1920	4130	1910	4125	-	-
6	4	Left	No Doors	1.30	5	NW to SE	1960	3730	1935	3730	-	-
	5						2120	4445	2105	4445	2315	2300
	6						2280	4970	2255	4970	2915	2885
	7						2290	5000	2260	5000	2980	2940
7	4	Left	Vane Up No Doors	1.82	8	SSE	1930	4050	1925	4050	-	-
	5						2140	5000	2135	5000	-	-
	6						2350	5920	2345	5920	3280	3270
	7						2360	5980	2355	5980	3370	3360
	8						2370	6060	2365	6060	3400	3390
	9						2100	4705	2095	4705	-	-
	10						1890	3630	1885	3830	-	-
8	2	Left	Vane Normal No Doors	1.82	8	SSE	1940	3870	1935	3870	-	-
	3						2160	4955	2155	4955	-	-
	4						2310	5625	2305	5625	3165	3155
	5						2340	5710	2335	5710	3190	3180
	6						2340	5720	2335	5720	3200	3190
9	4	Left	Straight Door	0.98	15 - 20	SSE	1890	4030	1880	4045	-	-
	5						2140	5030	2130	5050	2280	2280
	6						2310	5870	2300	5890	2860	2860
	7						2315	5940	2305	5960	-	-
	8						2320	5890	2310	5910	-	-
10	2	Left	No Doors	0.98	15 - 20	SSE	1915	-	-	-	-	-
	3						2120	-	-	-	-	-
	4						2260	5560	2240	5580	2630	2620
	5						2265	5670	2260	5690	2675	2650
	6						2260	5520	2235	5540	2675	2650
11	2	Right	No Doors	1.82	5 - 10	SE	2340	4635	2320	4655	2820	2815
	3						2345	4520	2325	4540	2755	2750
	4						2340	4570	2320	4590	2800	2795

Notes:
1. The nose of the aircraft pointed South.
2. The flaps were at 30° and the left wing tip was removed.
3. The left fan had the fixed vanes removed and had nine six-inch vane stubs welded to the circular vane pointing radially towards the hub. The right fan inlet was unchanged from tunnel tests (circular vane plus fixed side vane inlet).

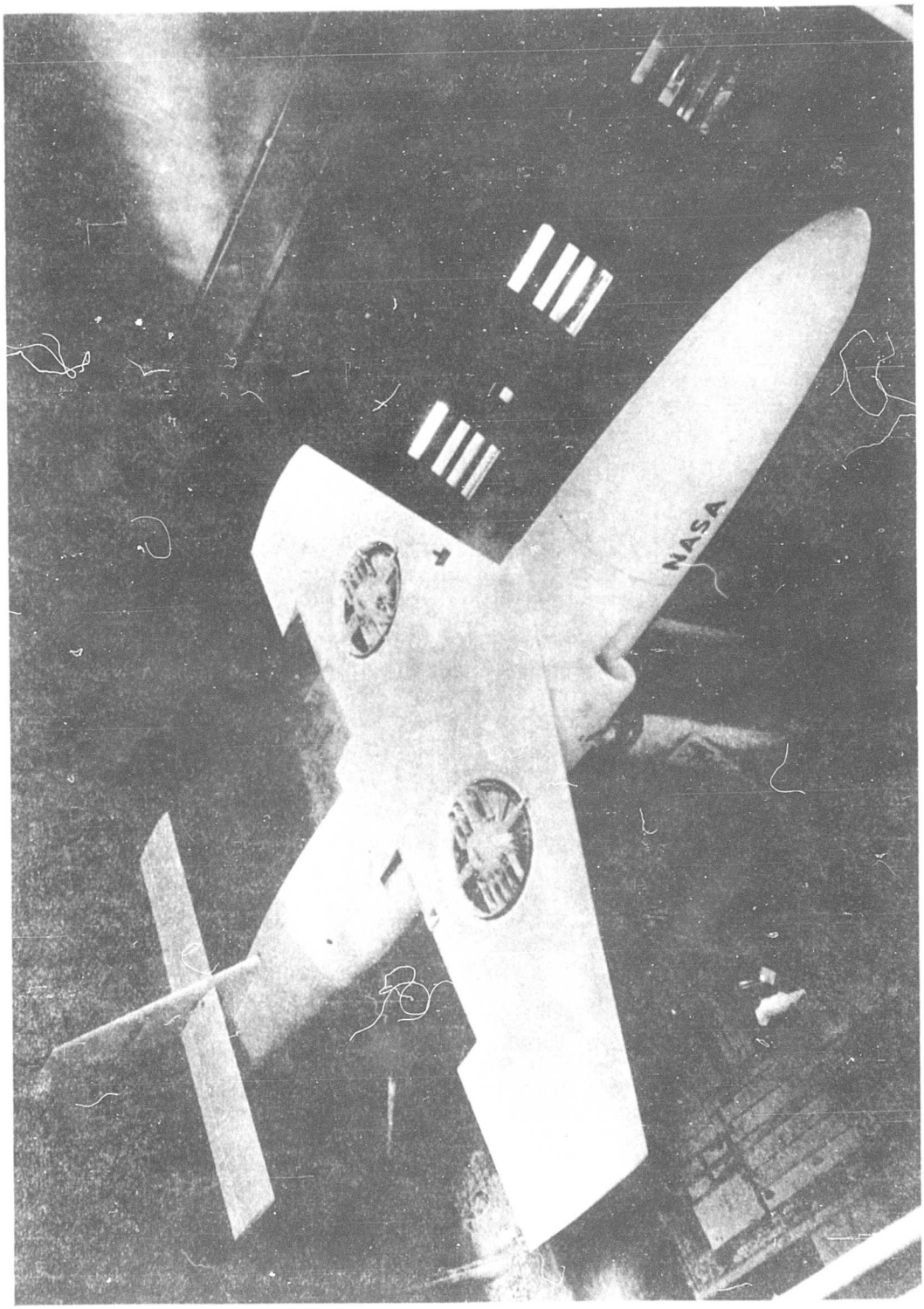


FIGURE 1. NASA FAN-IN-WING, FULL SCALE WIND TUNNEL MODEL

WING CONFIGURATION #1

Area	426 Square Feet
Aspect Ratio	5
Taper Ratio	0.5
Mean Aerodynamic Chord	11.44
Airfoil Section	65-210

WING CONFIGURATION # 2

Area	305.9 Square Feet
Aspect Ratio	2.0
Taper Ratio	0.68
Mean Aerodynamic Chord	12.50
Airfoil Section	65-210

HORIZONTAL TAIL

Area	100 Square Feet
Aspect Ratio	4.97
Taper Ratio	1.0
Airfoil Section	63-009

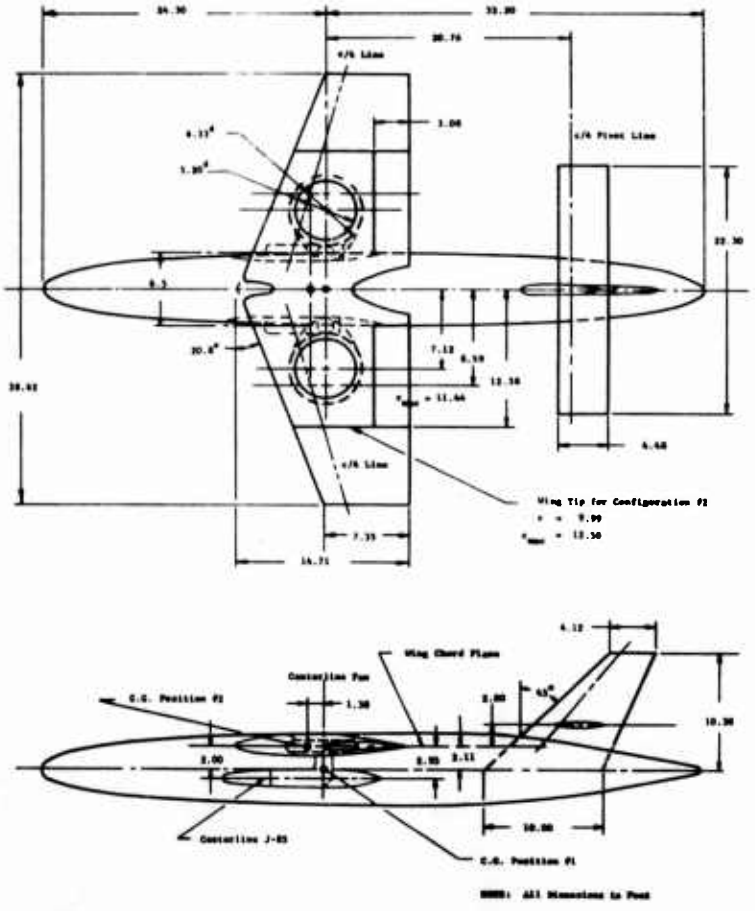


FIGURE 2. SKETCH OF NASA FULL-SCALE AIRCRAFT MODEL

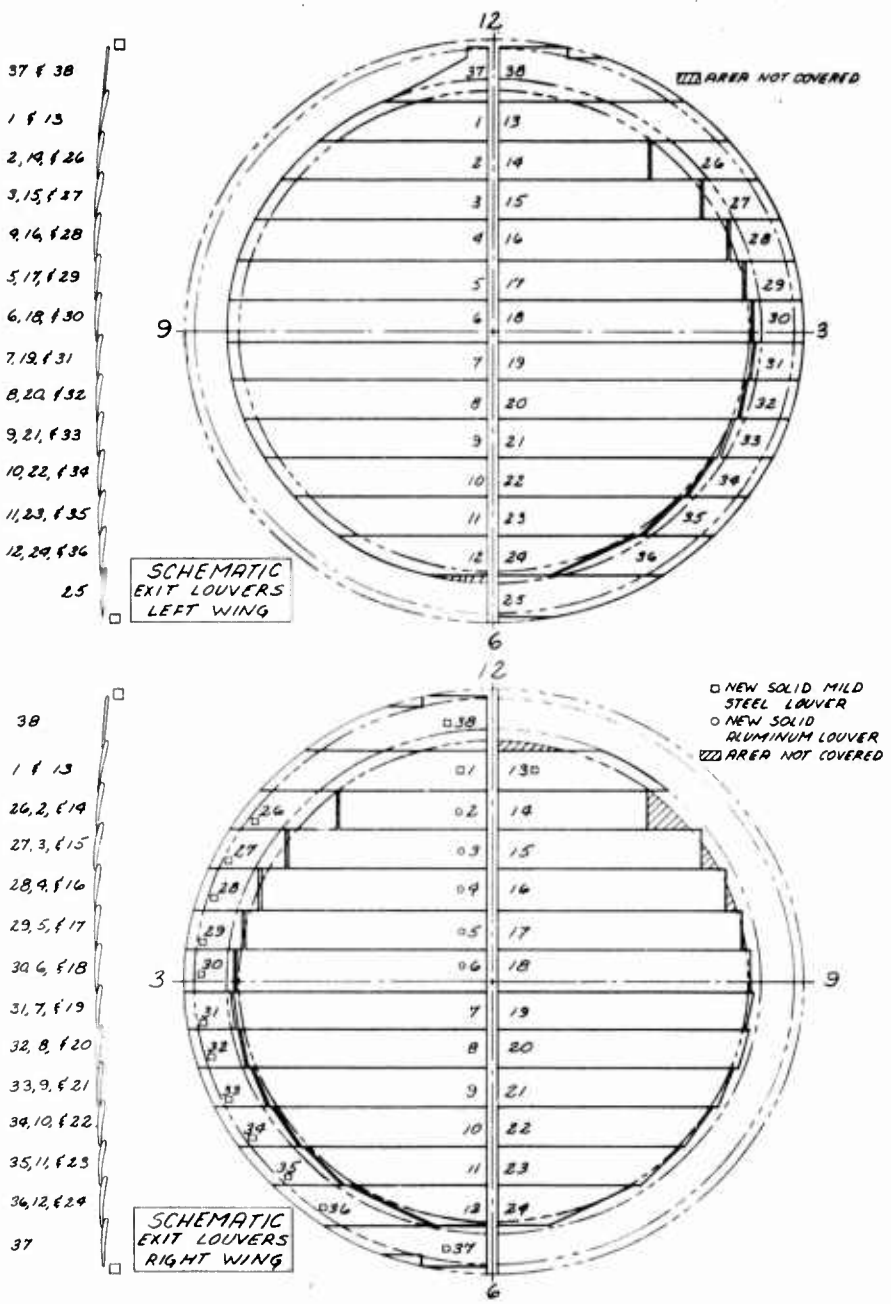


FIGURE 3. SCHEMATIC OF LEFT AND RIGHT WING FAN EXIT LOUVER INSTALLATION

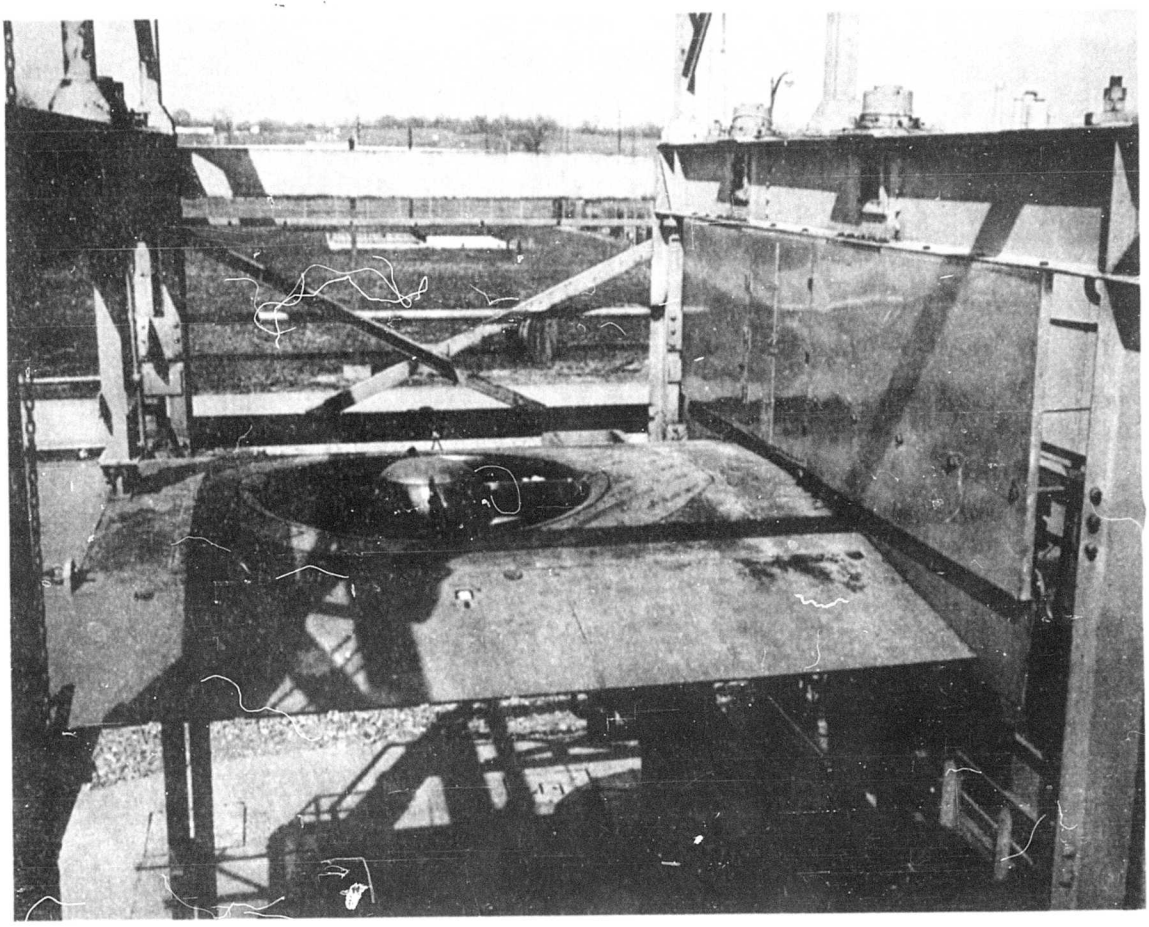


FIGURE 4. VIEW OF FAN INSTALLED IN WING SHOWING THE CIRCULAR VANE INLET

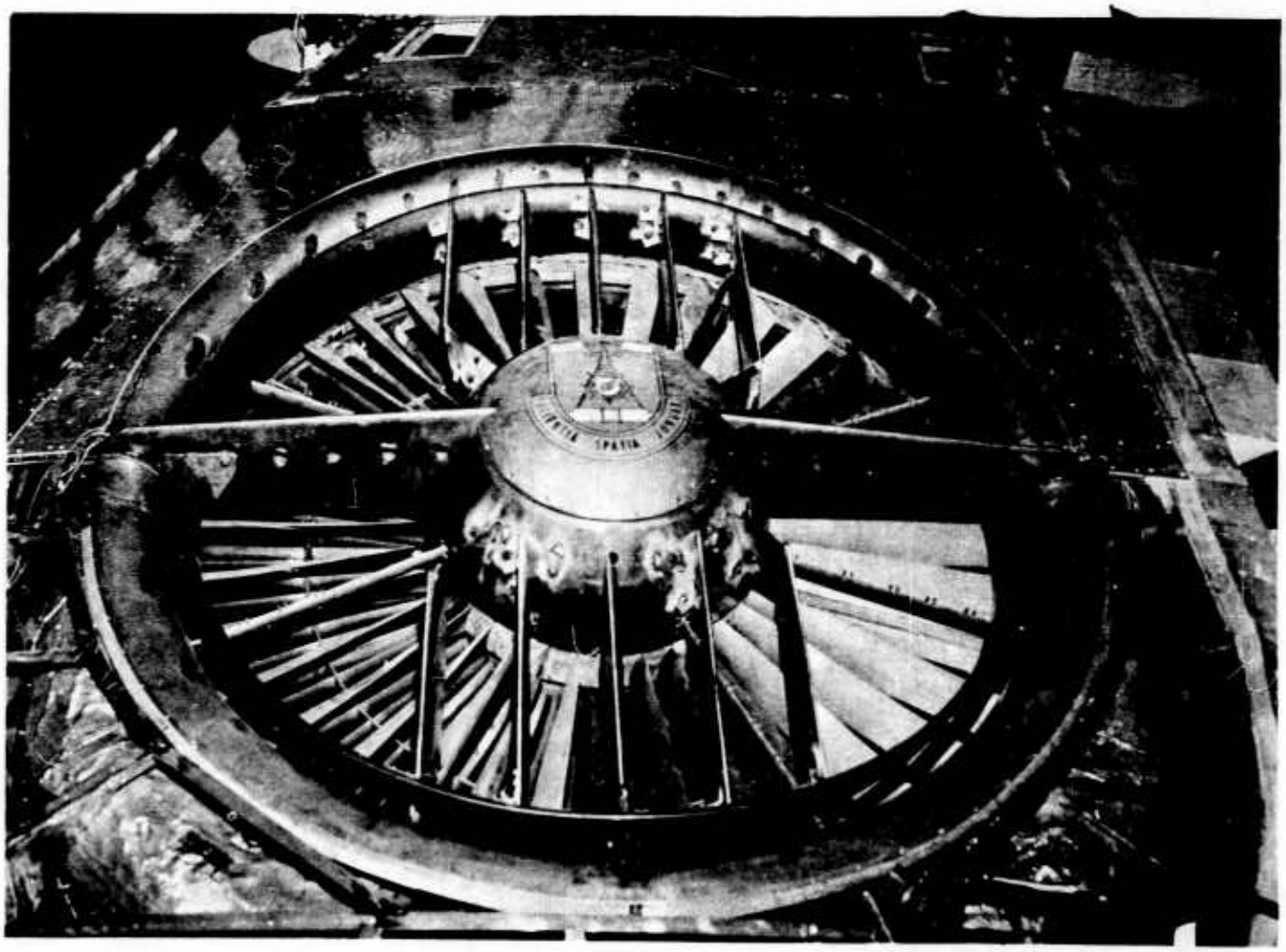


FIGURE 5. CIRCULAR VANE WITH FIXED SIDE VANES INLET CONFIGURATION



FIGURE 6. ARTICULATED INLET LOUVER SYSTEM, CLOSED POSITION

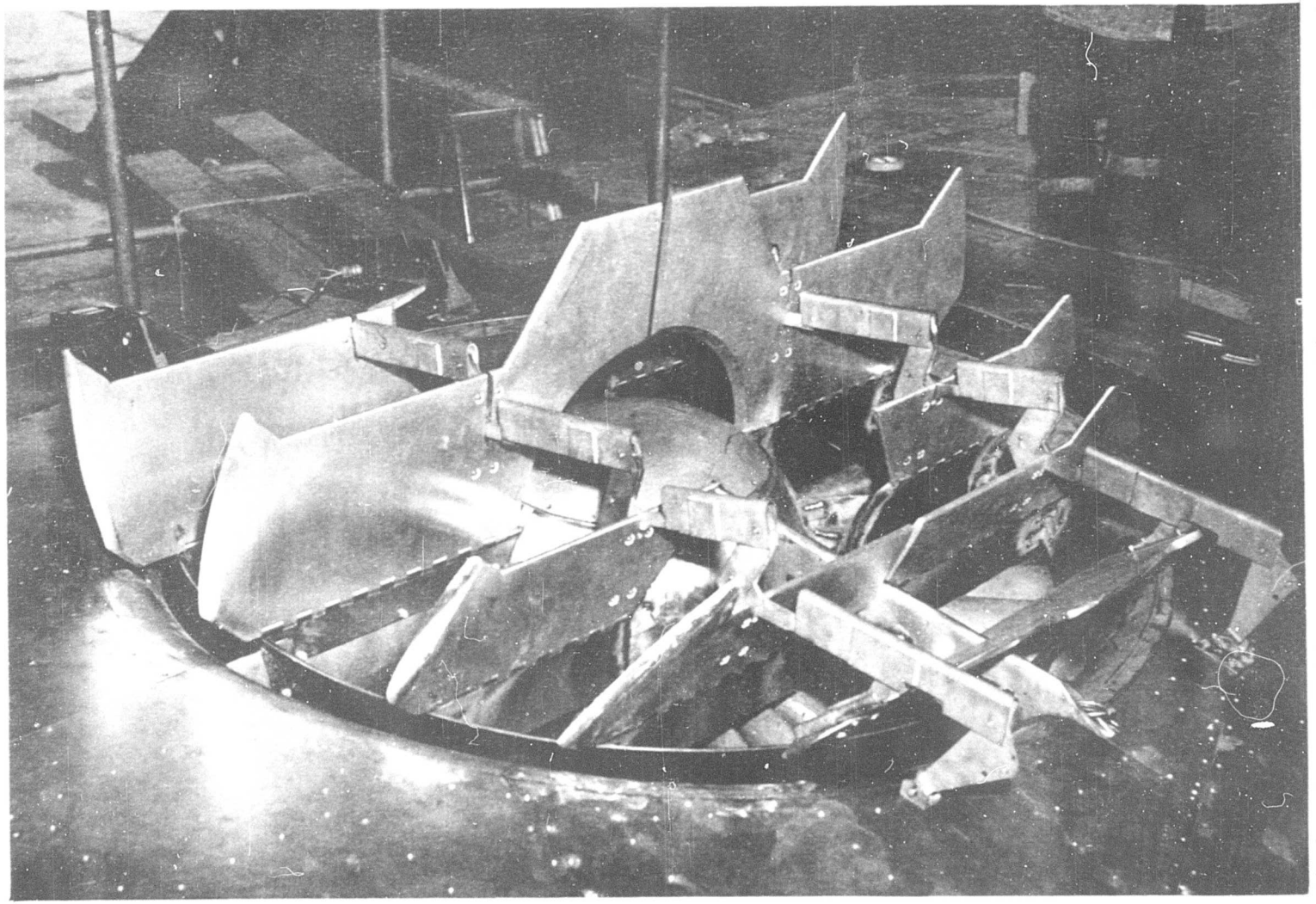
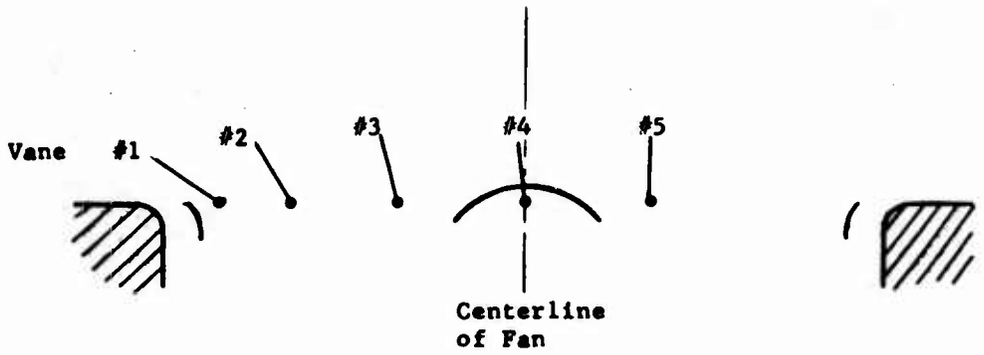


FIGURE 7. ARTICULATED INLET LOUVER SYSTEM, OPEN POSITION



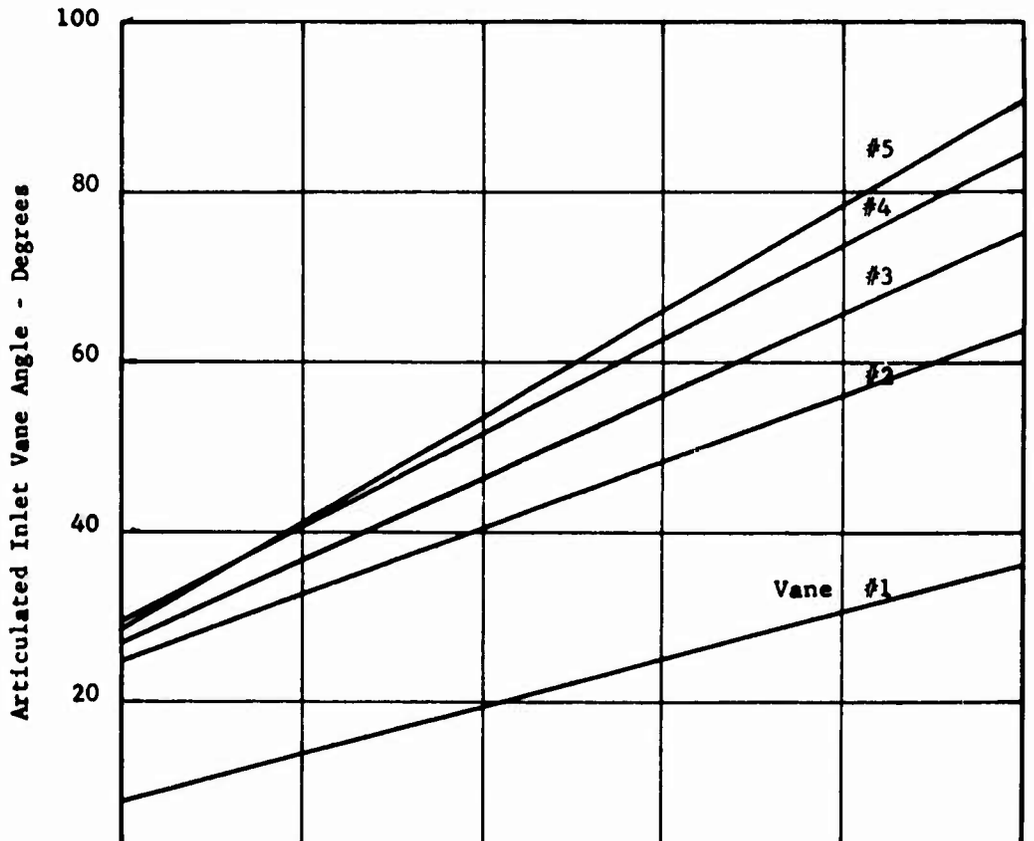


FIGURE 8 - ARTICULATED INLET VANE ANGLE VERSUS INDICATOR READING

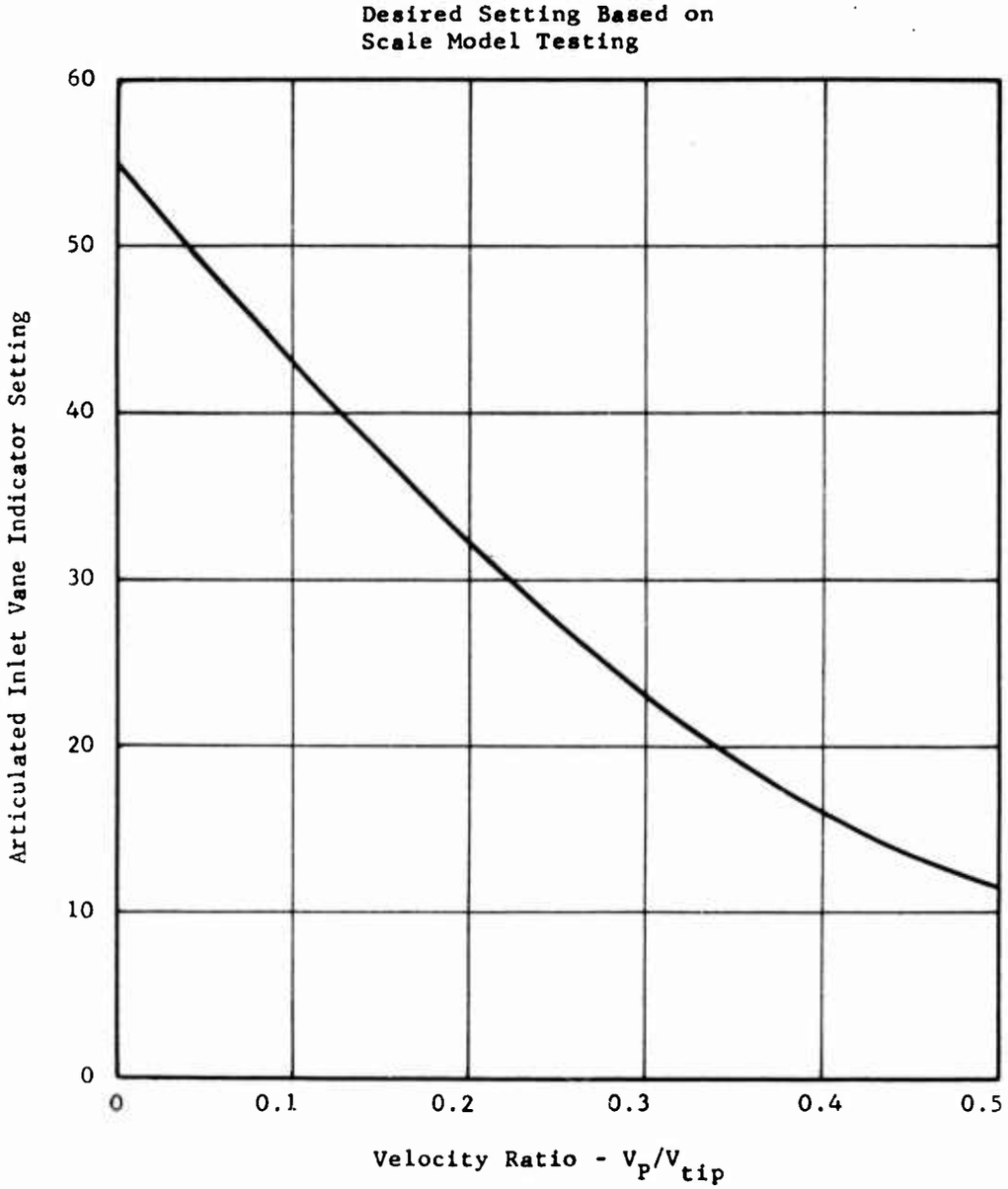


FIGURE 9 - ARTICULATED INLET VANE INDICATOR SETTING VERSUS VELOCITY RATIO

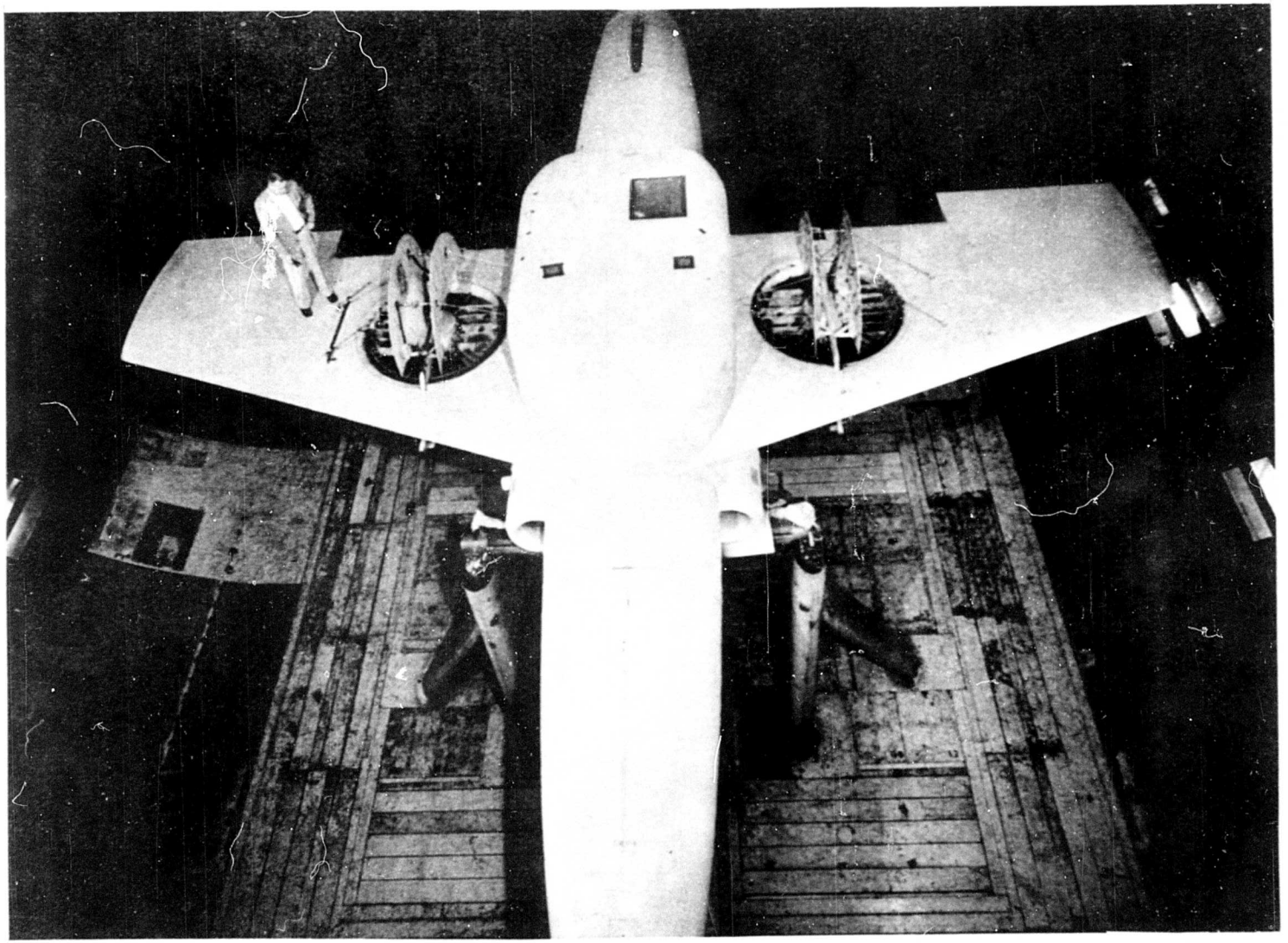


FIGURE 10. FAN-IN-WING TEST MODEL WITH FUSELAGE ADDITION FOR MID-WING VZ-11 SIMULATION AND FAIRED INLET CLOSURE DOORS

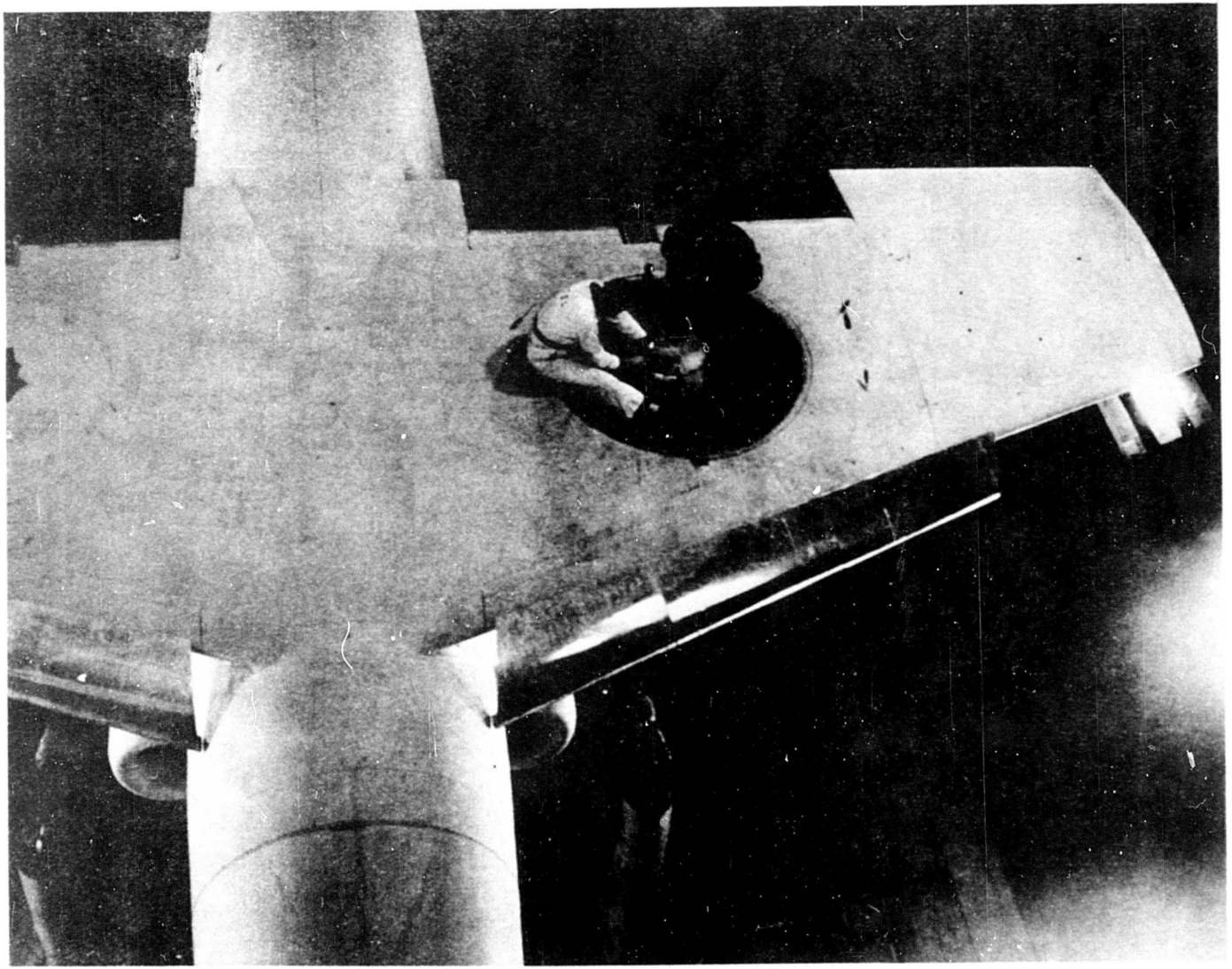


FIGURE 11. LEADING EDGE (KRUGER) FLAP INSTALLATION

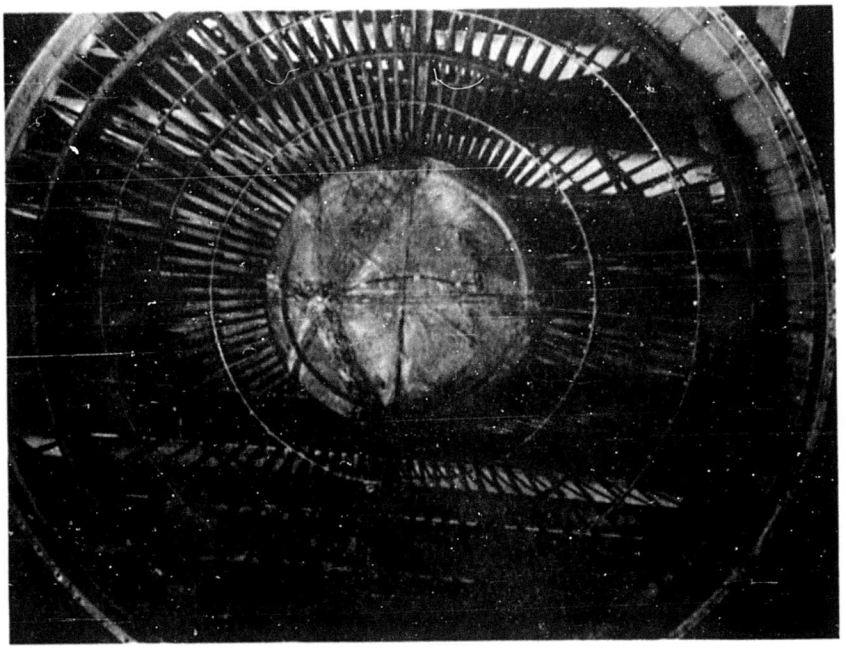


FIGURE 12a. EXTRA STATOR STIFFNER RINGS (FAN 001)

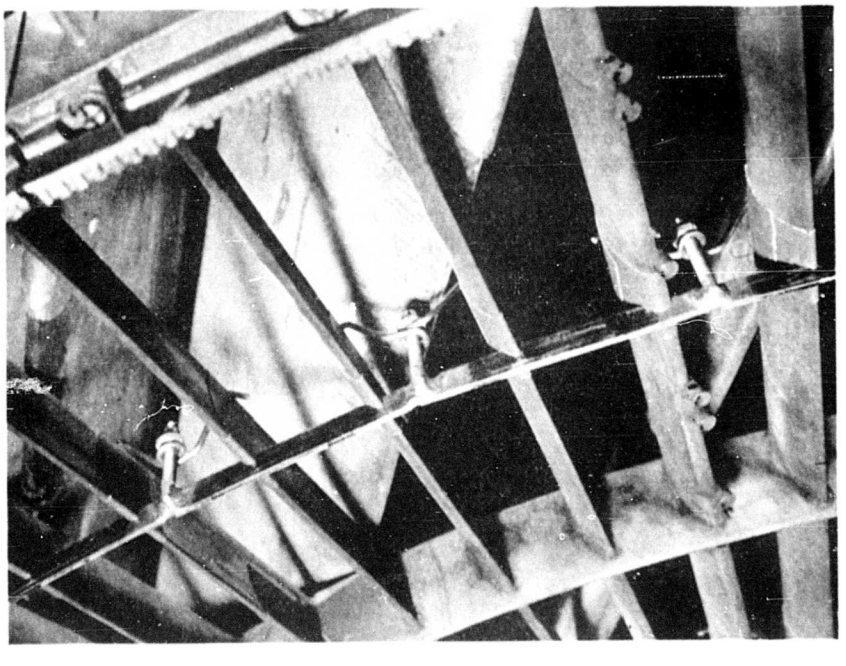


FIGURE 12b. DETAIL, STATOR STIFFNER RINGS

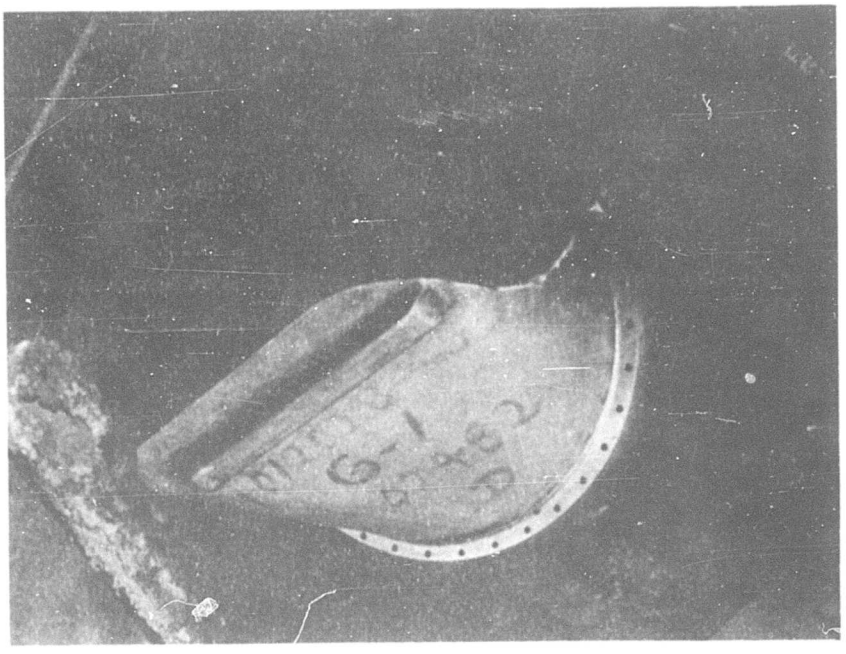


FIGURE 13. SCROLL BLOCKER

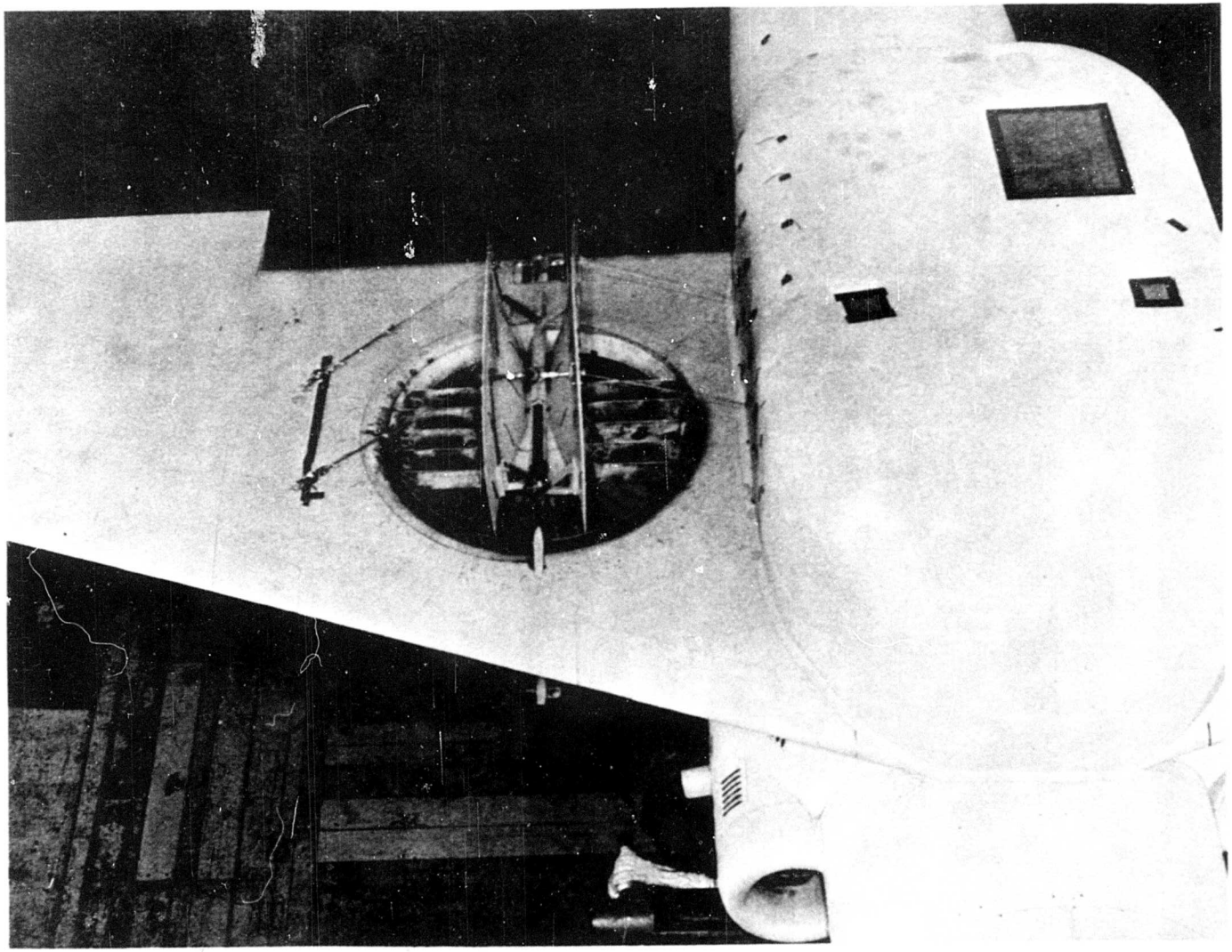


FIGURE 14. FAIRED INLET DOOR INSTALLATION

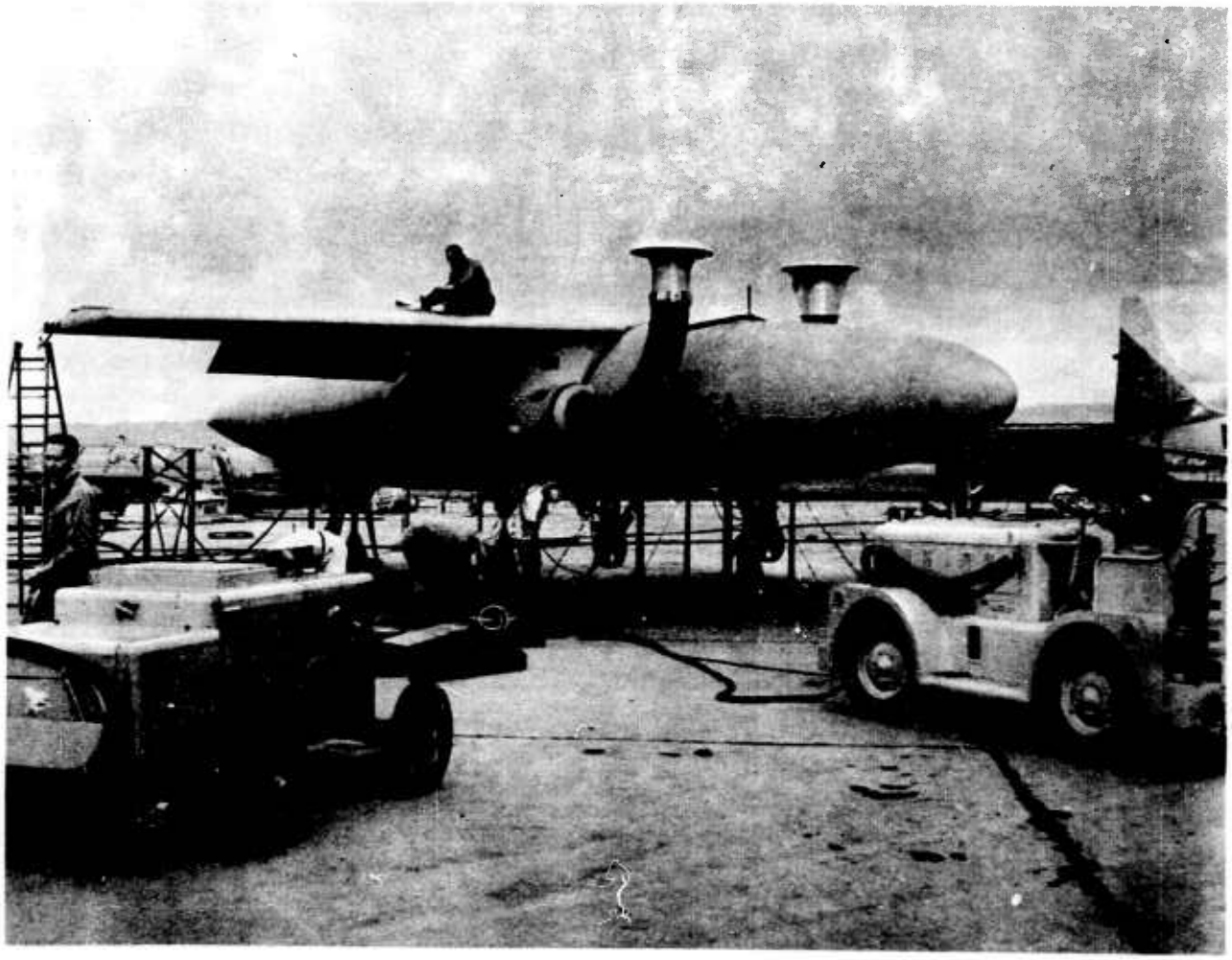


FIGURE 15. GENERAL ARRANGEMENT FOR FLIGHT LINE TESTING "OUT OF GROUND EFFECT"; RIGHT FAN h/d_F = 1.82

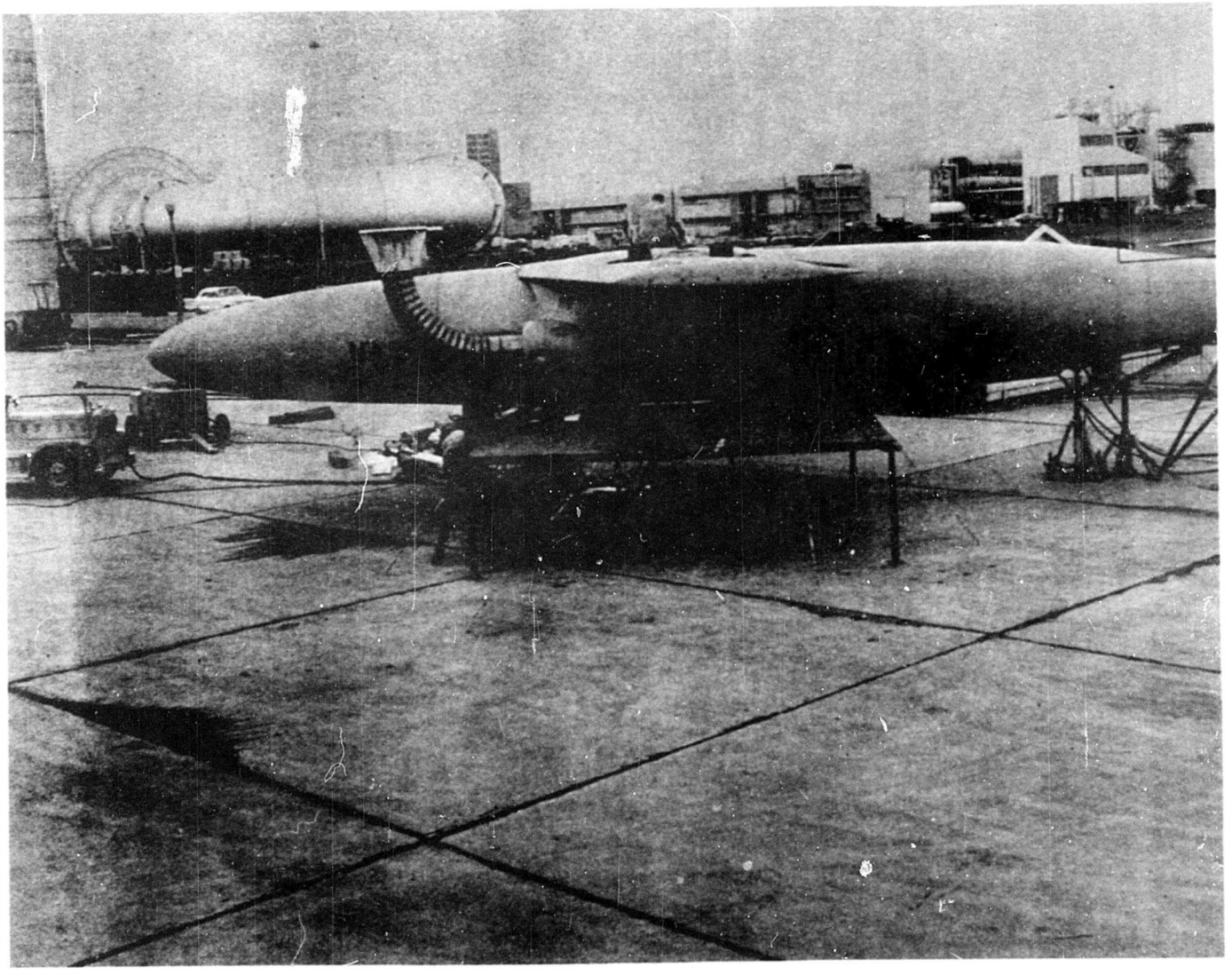


FIGURE 16. GENERAL ARRANGEMENT FOR FLIGHT LINE TESTING "IN GROUND EFFECT"; LEFT FAN $h/d_F = 0.98$

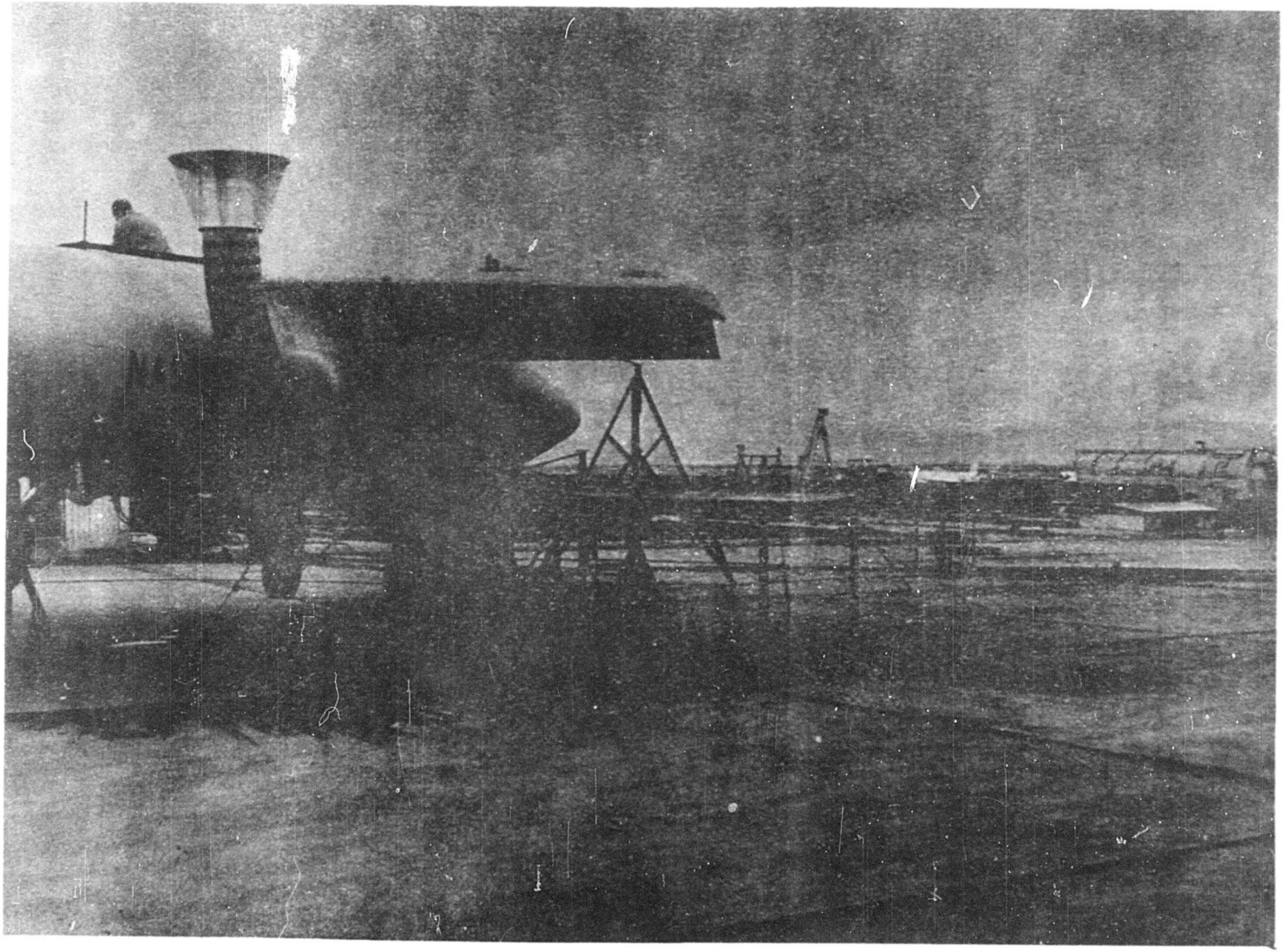


FIGURE 17a. DETAILS OF GROUND EFFECT TEST SETUP FOR LEFT WING

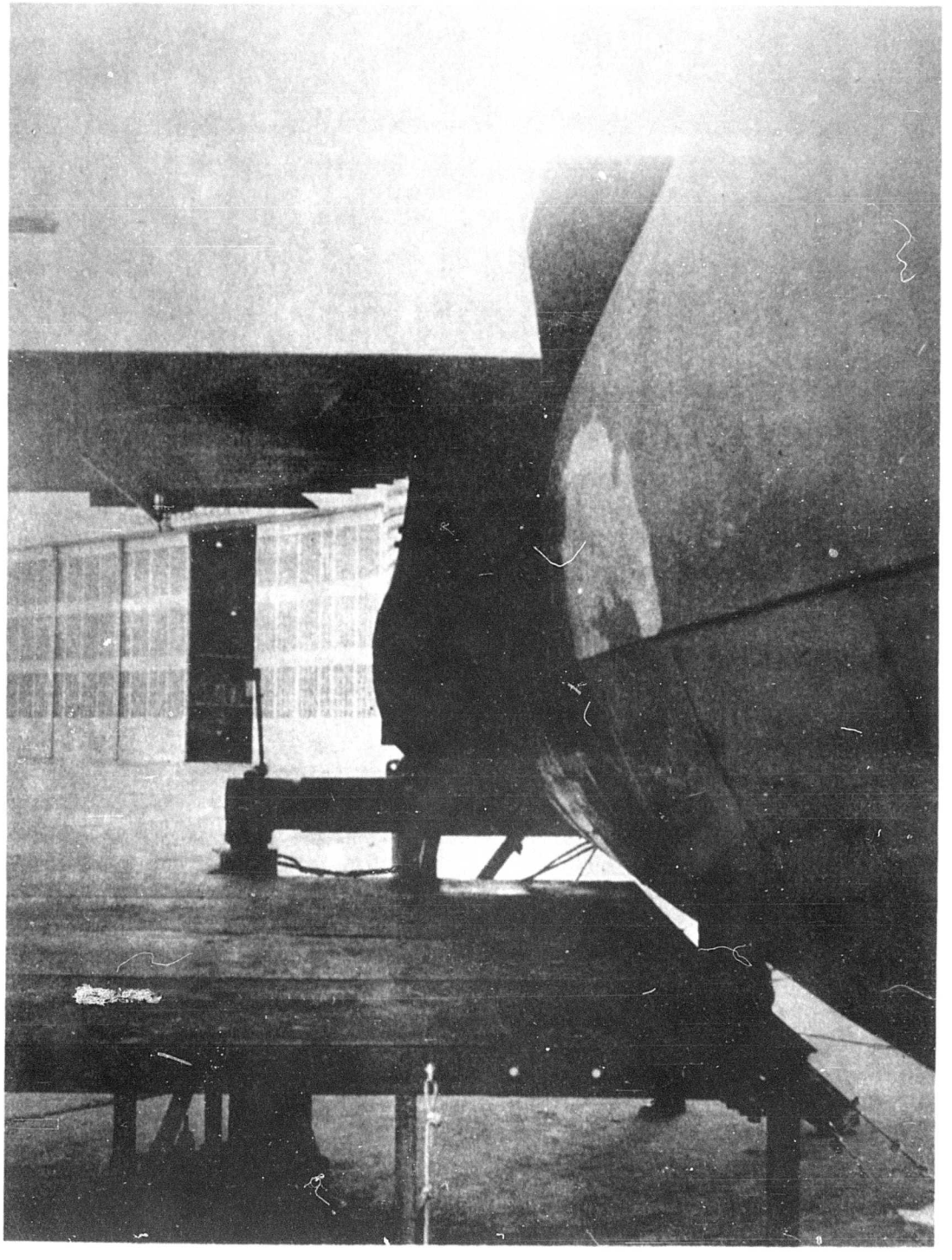


FIGURE 17b. DETAILS OF GROUND EFFECT TEST SETUP FOR LEFT WING

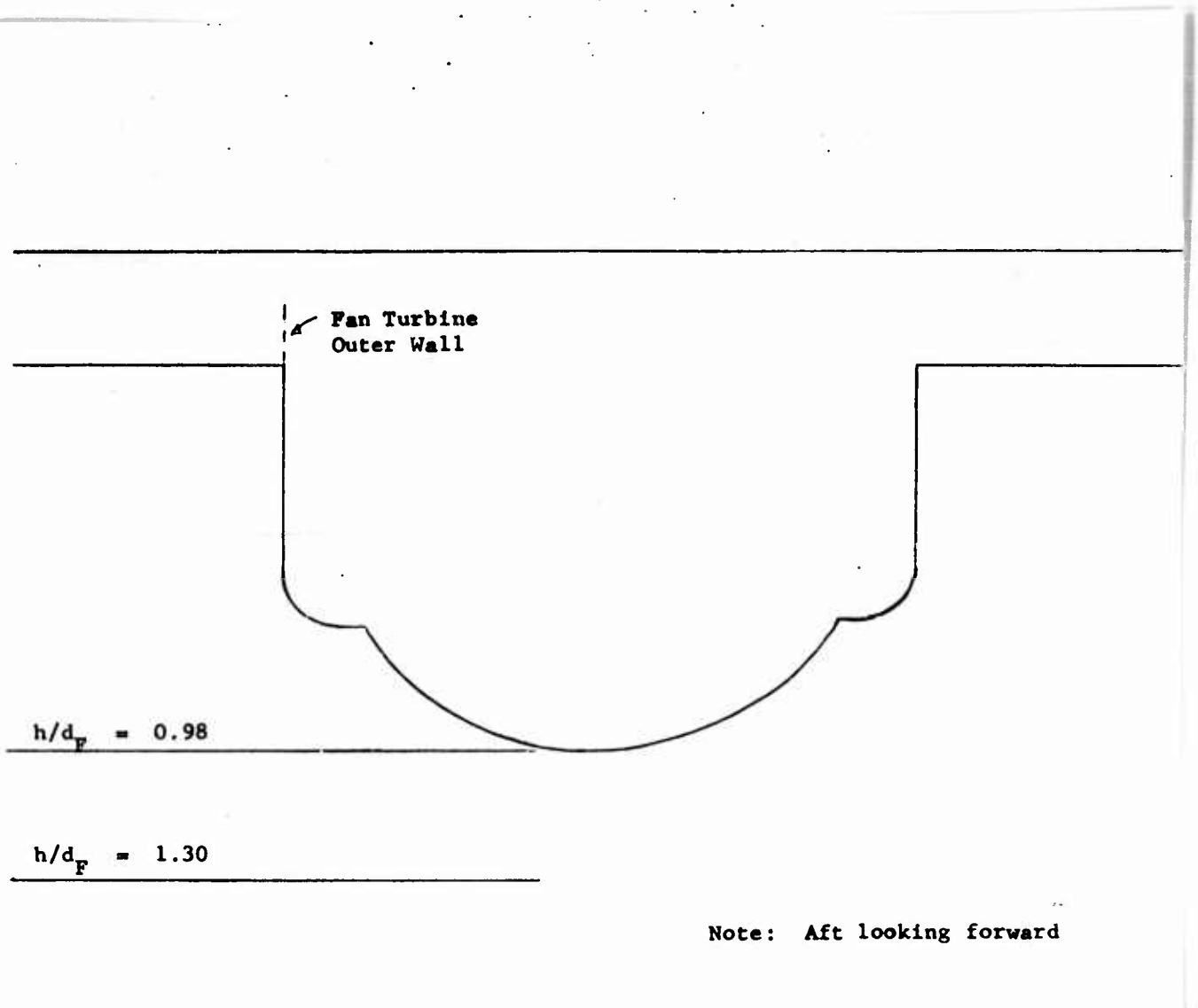


FIGURE 18 - GROUND EFFECT SIMULATION

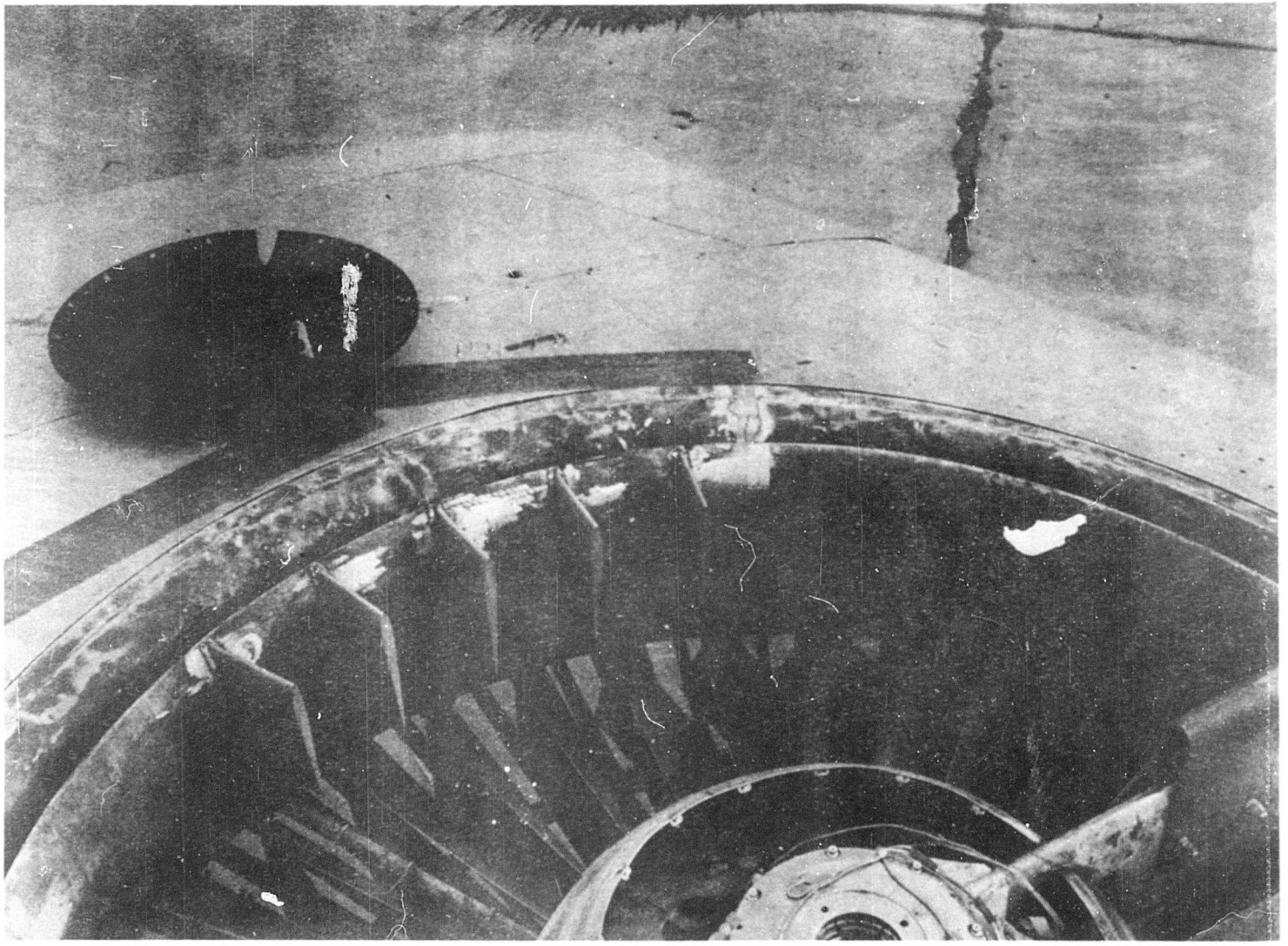


FIGURE 19. INLET VANE CONFIGURATION (LEFT FAN ONLY) FOR GROUND EFFECT TESTS

PLANE NO.	J-85
0.0	Ambient
1.0	Inlet
2.0	Compressor Inlet
3.0	Compressor Discharge
4.0	Turbine Inlet
5.1	Turbine Discharge
	FAN (TURBINE)
5.3	Scroll Inlet
5.4	Turbine Nozzle Inlet
5.45	Turbine Nozzle Discharge
5.5	Turbine Rotor Discharge
5.6	Turbine Stator Discharge
5.8	Exit Louver Discharge

PLANE NO.	FAN
10.0	Fan Louver Inlet
10.3	Fan Rotor Inlet
10.6	Fan Rotor Discharge
11.0	Fan Stator Discharge
13.0	Exit Louver Discharge

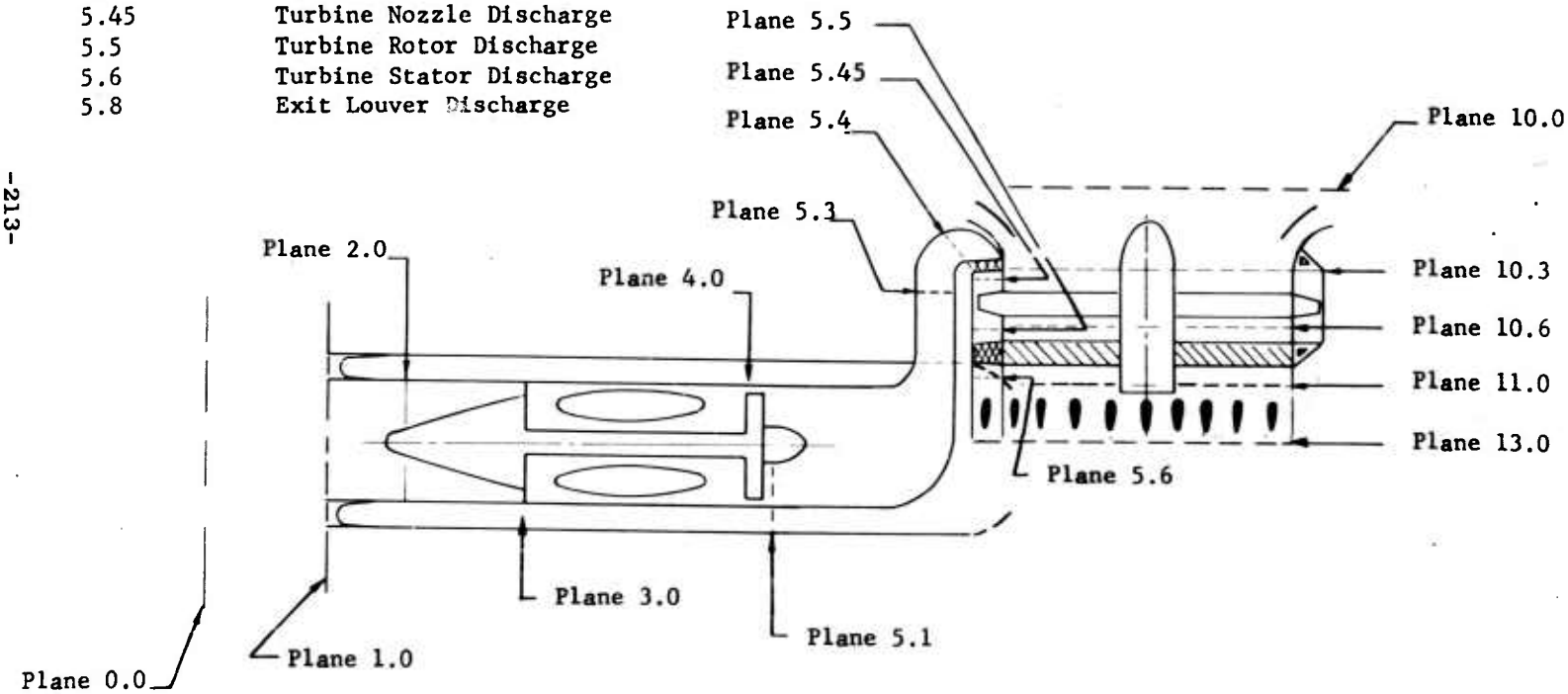


FIGURE 20 - SCHEMATIC OF INSTRUMENTATION PLANES

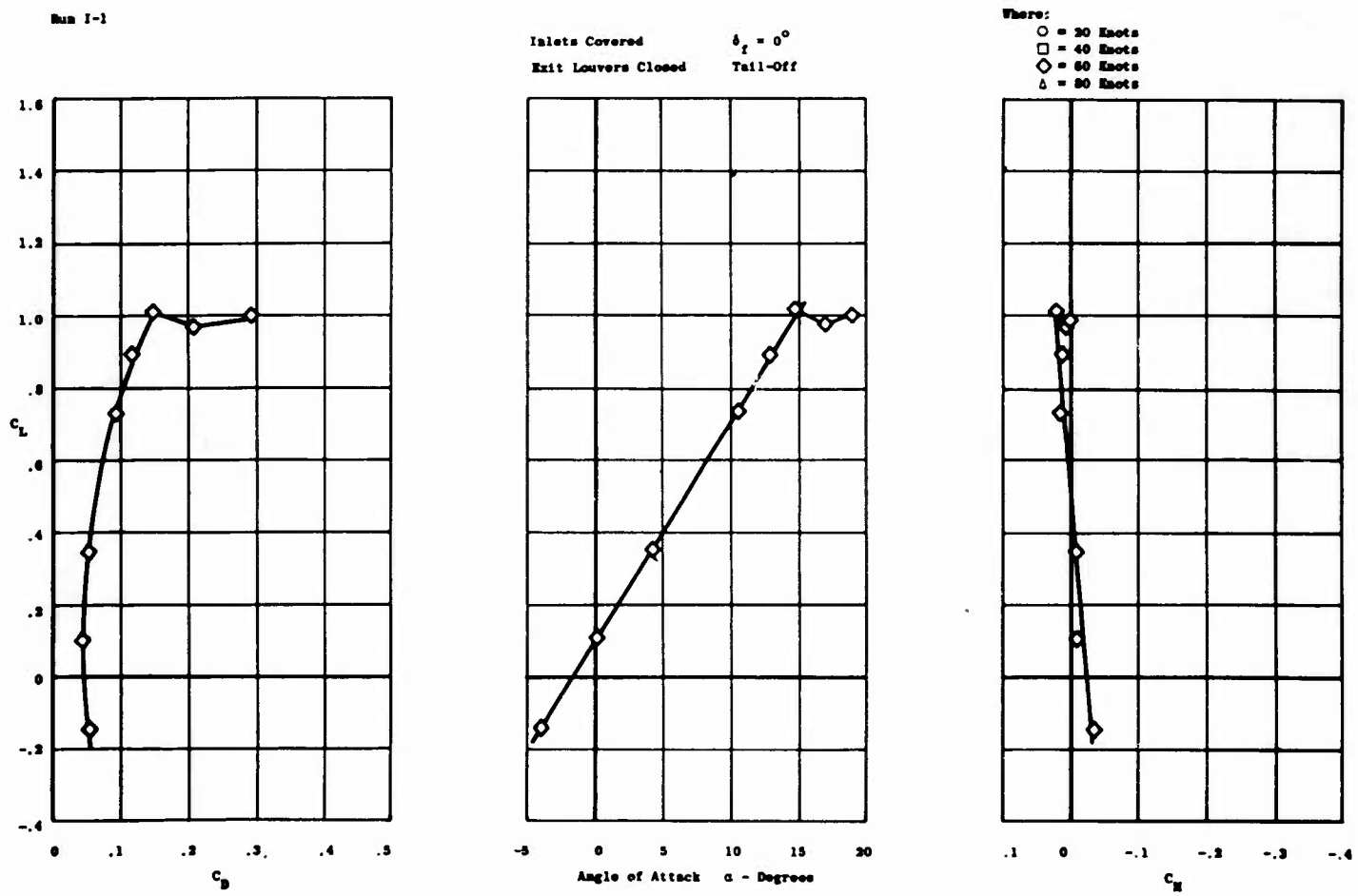


FIGURE 21 - UNPOWERED AIRCRAFT PERFORMANCE

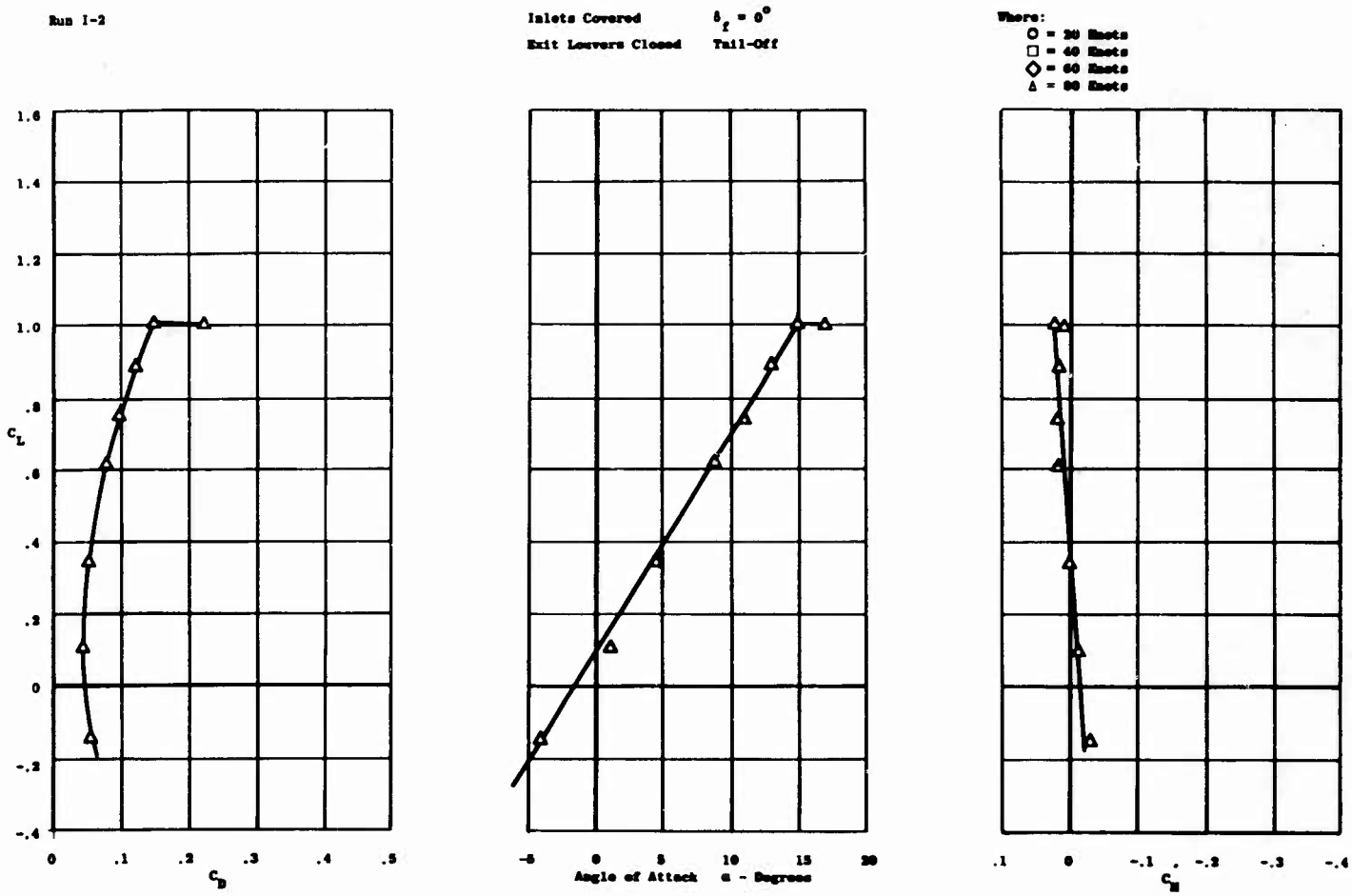


FIGURE 22 - UNPOWERED AIRCRAFT PERFORMANCE

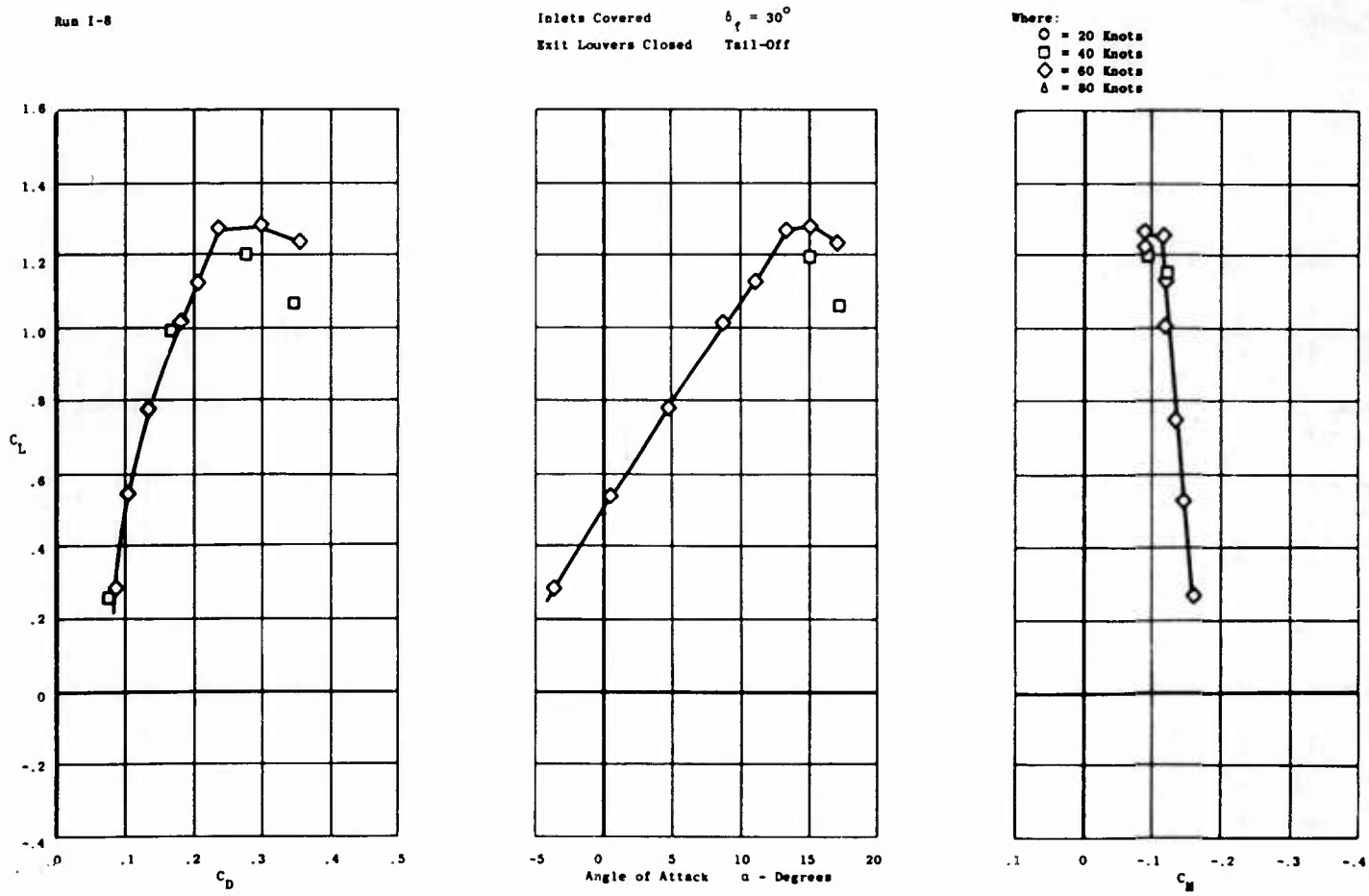


FIGURE 23 - UNPOWERED AIRCRAFT PERFORMANCE

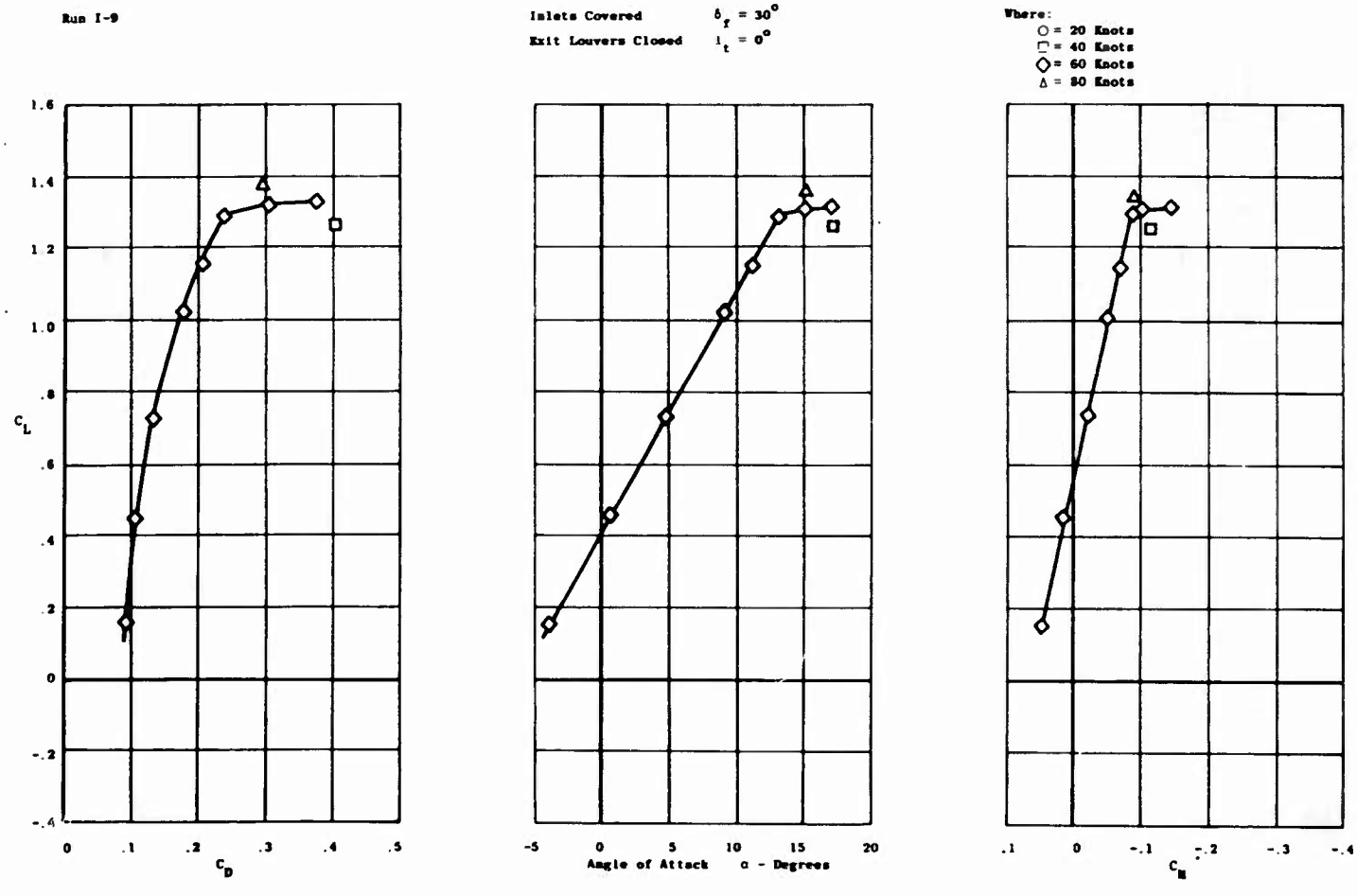


FIGURE 24 - UNPOWERED AIRCRAFT PERFORMANCE

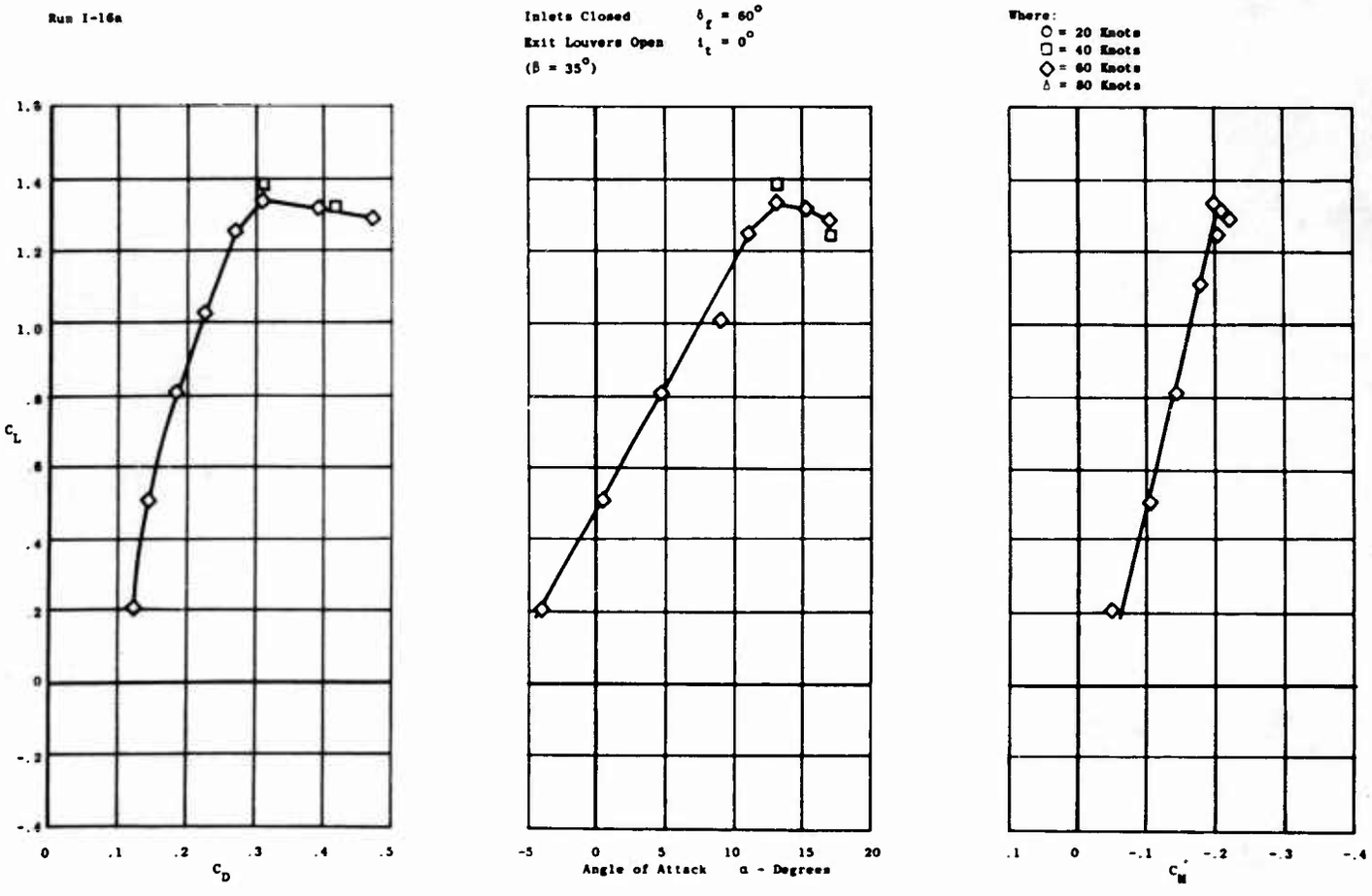


FIGURE 25 - UNPOWERED AIRCRAFT PERFORMANCE

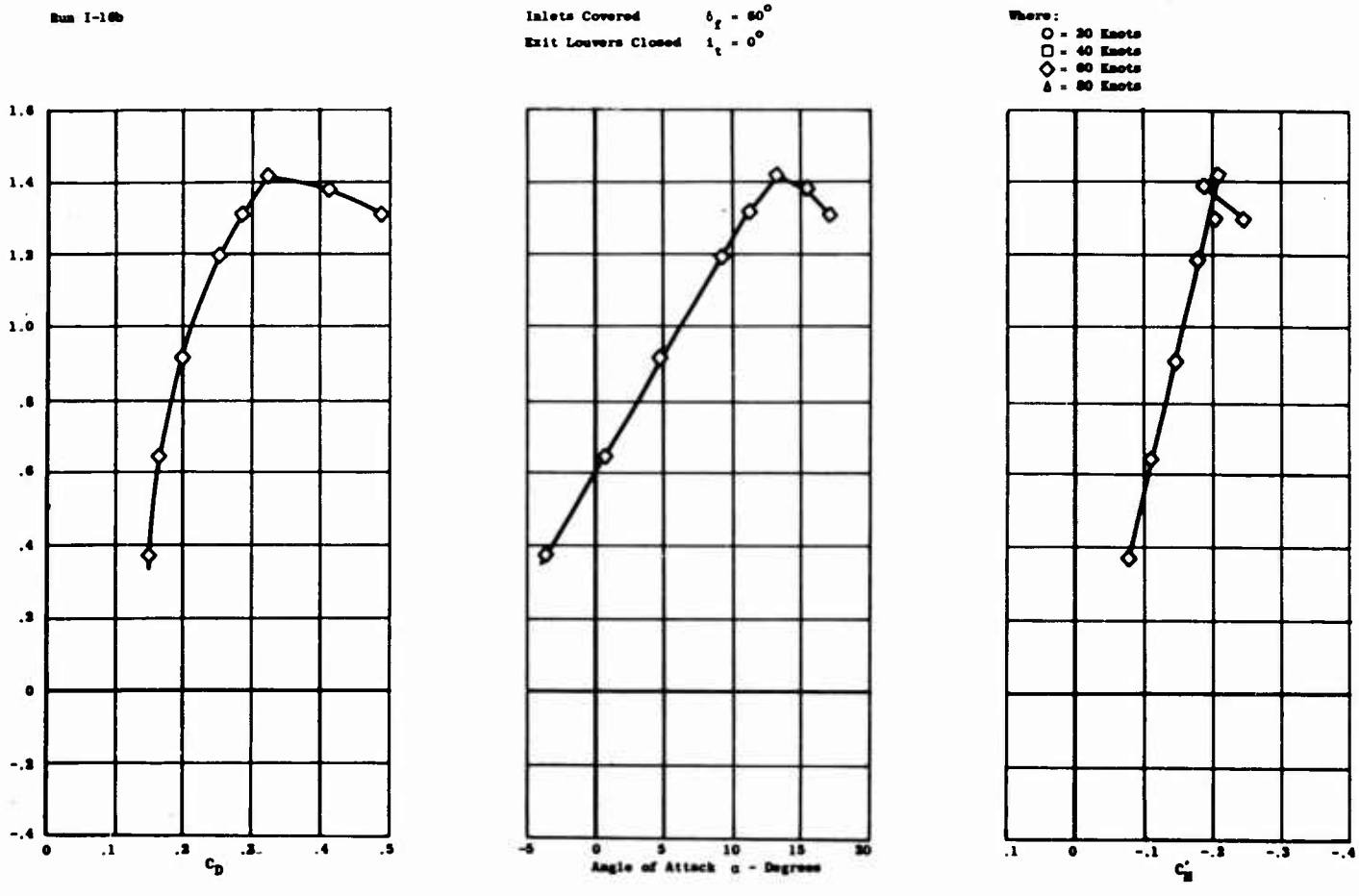


FIGURE 26 - UNPOWERED AIRCRAFT PERFORMANCE

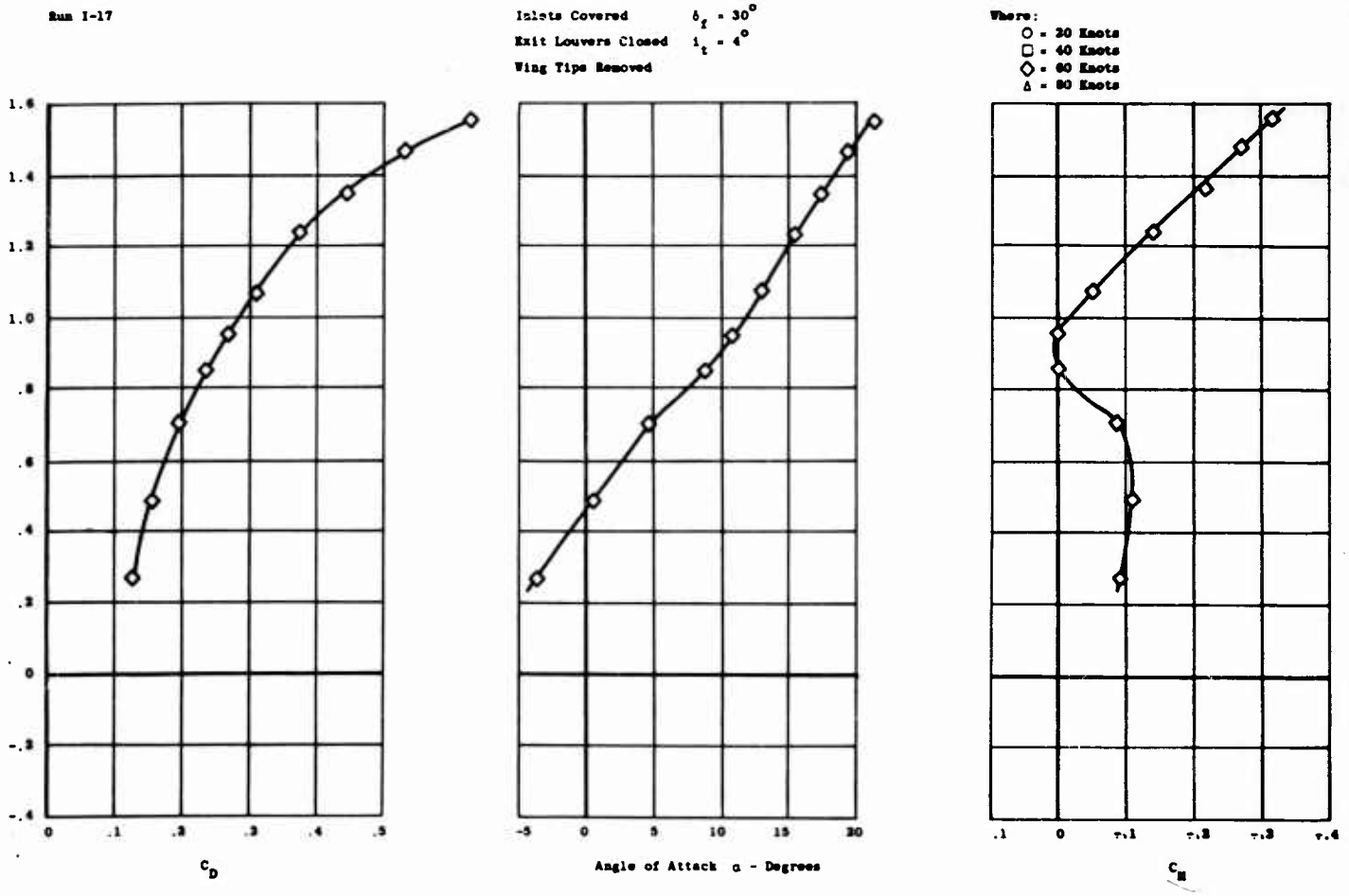


FIGURE 27 - UNPOWERED AIRCRAFT PERFORMANCE

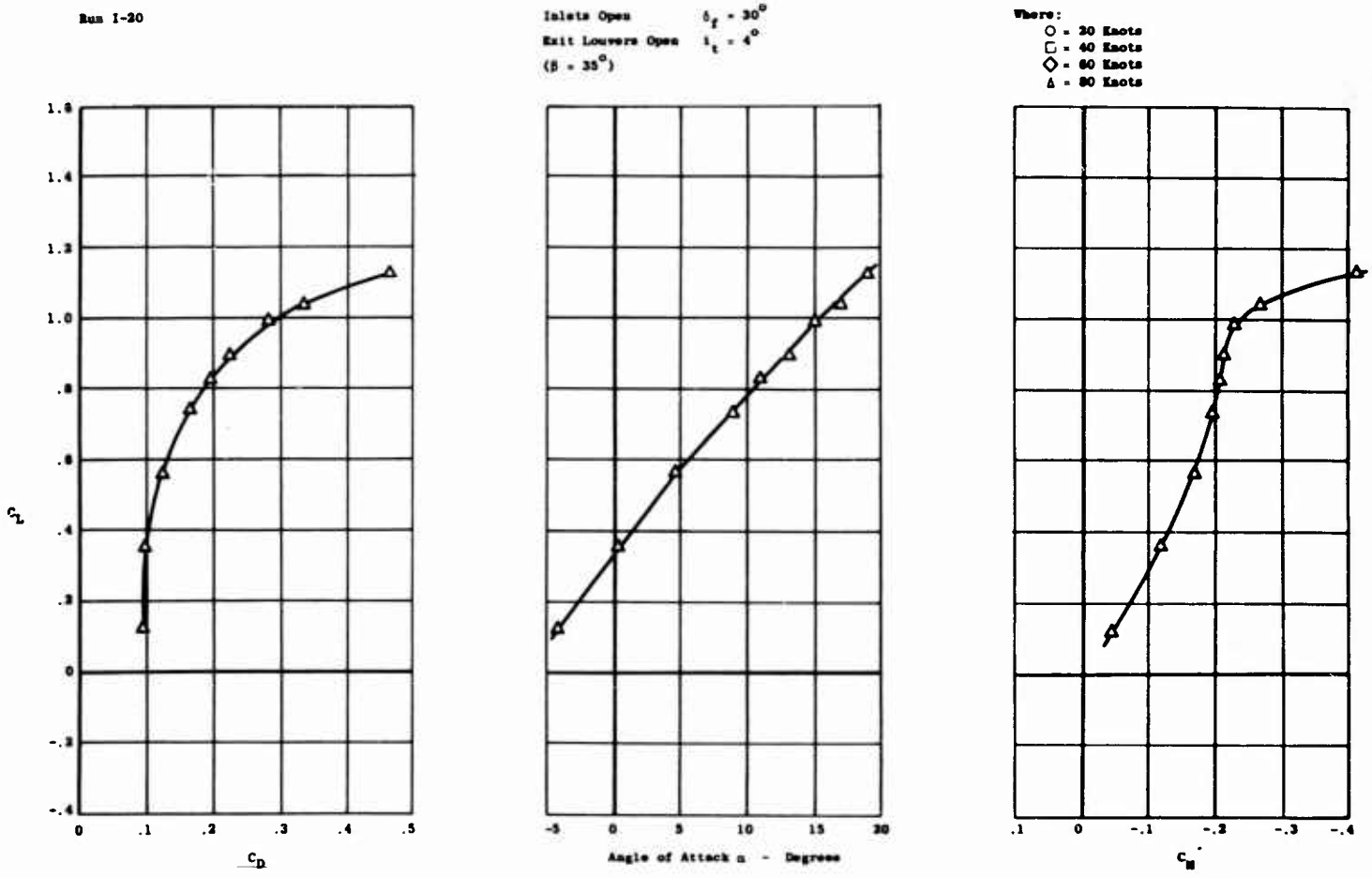


FIGURE 28 - UNPOWERED AIRCRAFT PERFORMANCE

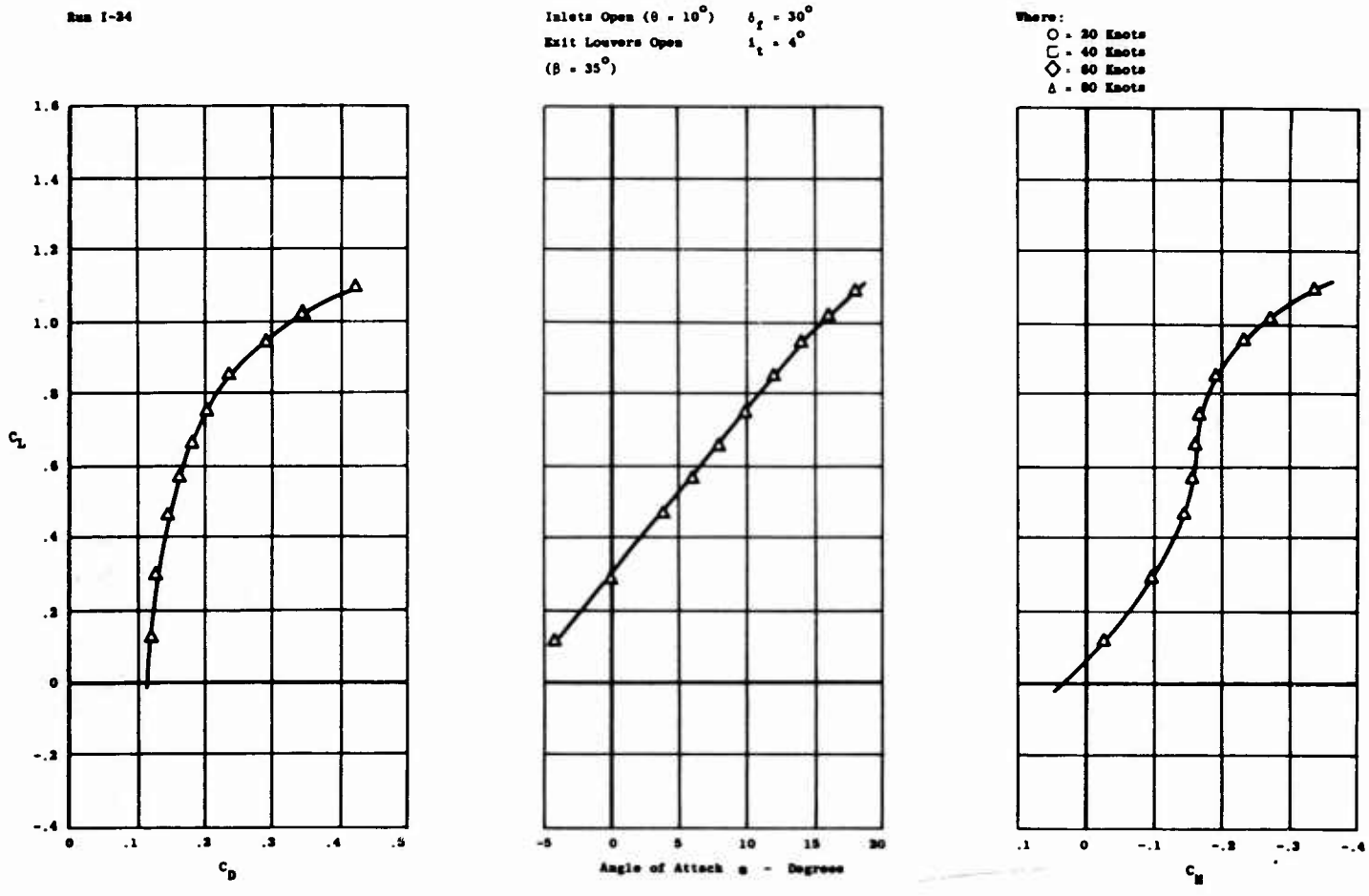


FIGURE 29 - UNPOWERED AIRCRAFT PERFORMANCE

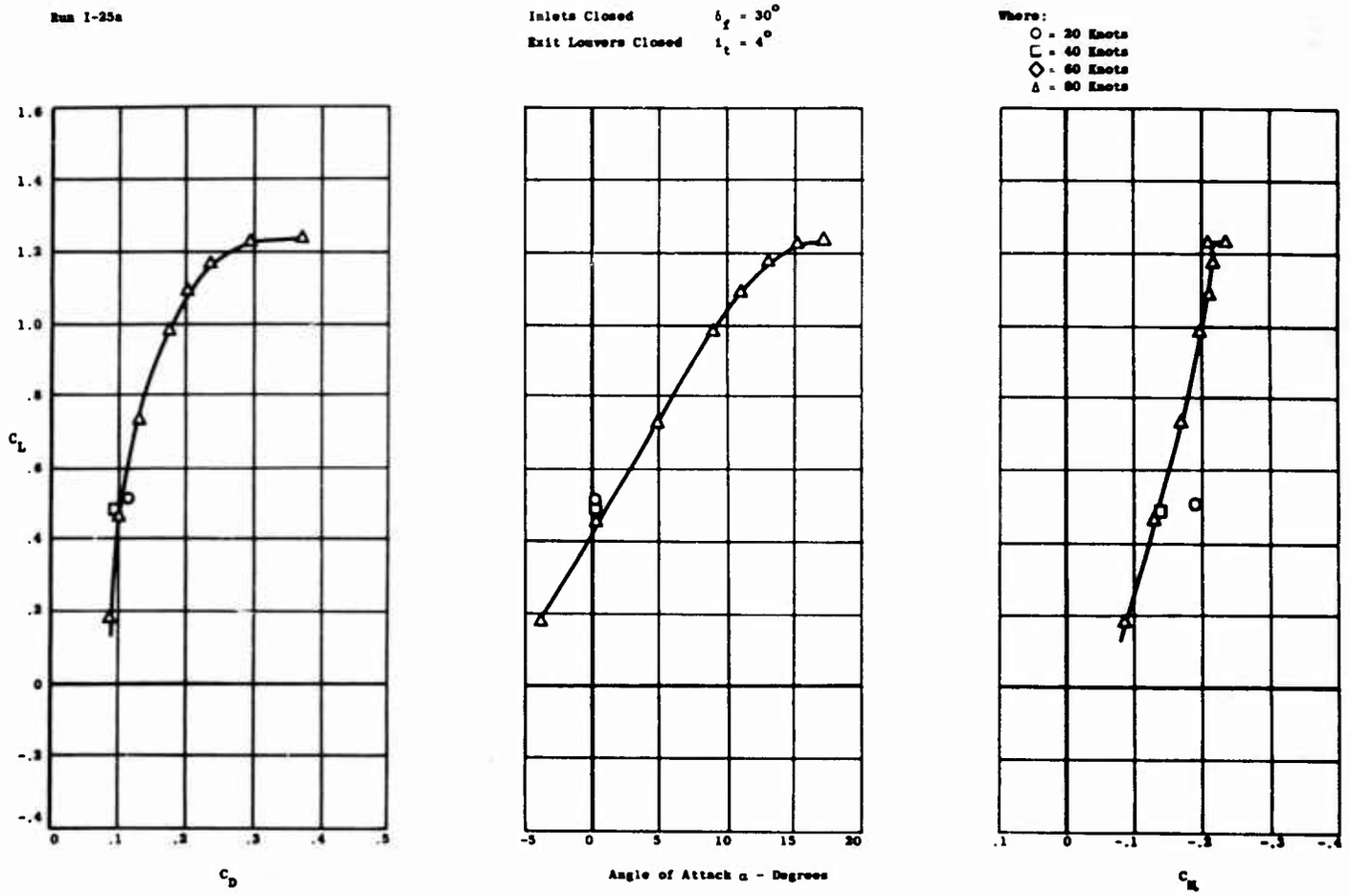


FIGURE 30 - UNPOWERED AIRCRAFT PERFORMANCE

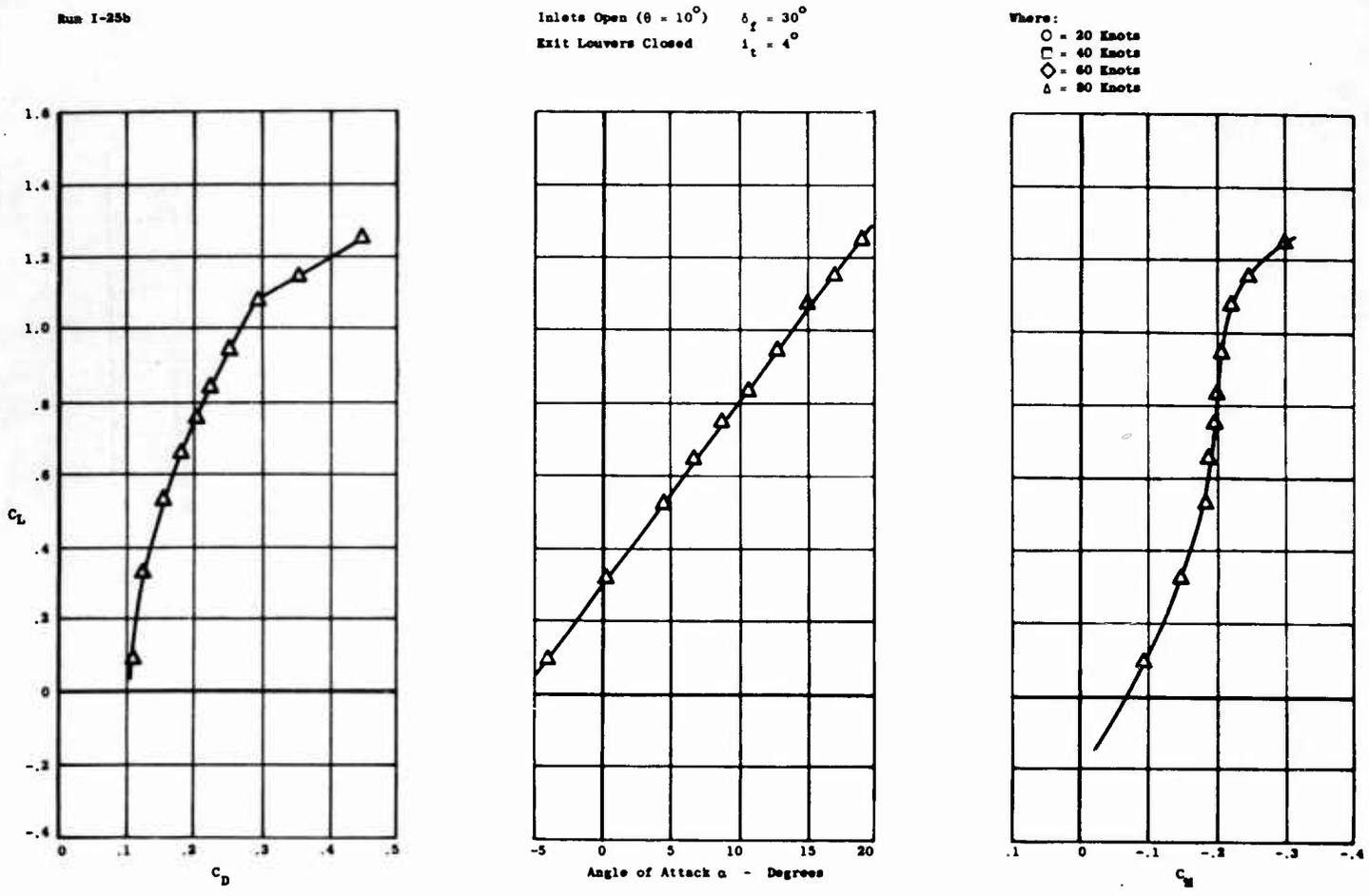


FIGURE 31 - UNPOWERED AIRCRAFT PERFORMANCE

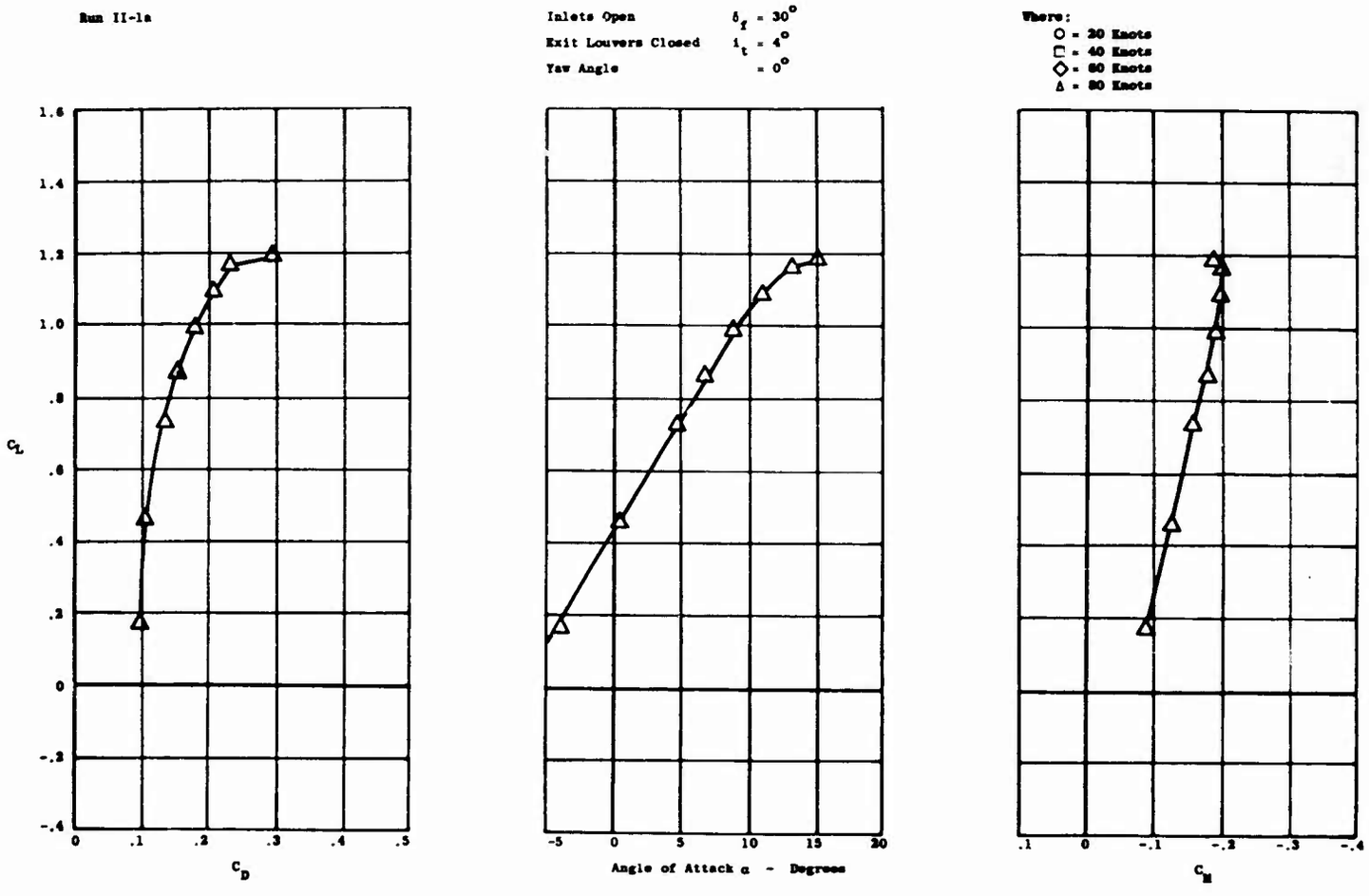


FIGURE 32 - UNPOWERED AIRCRAFT PERFORMANCE

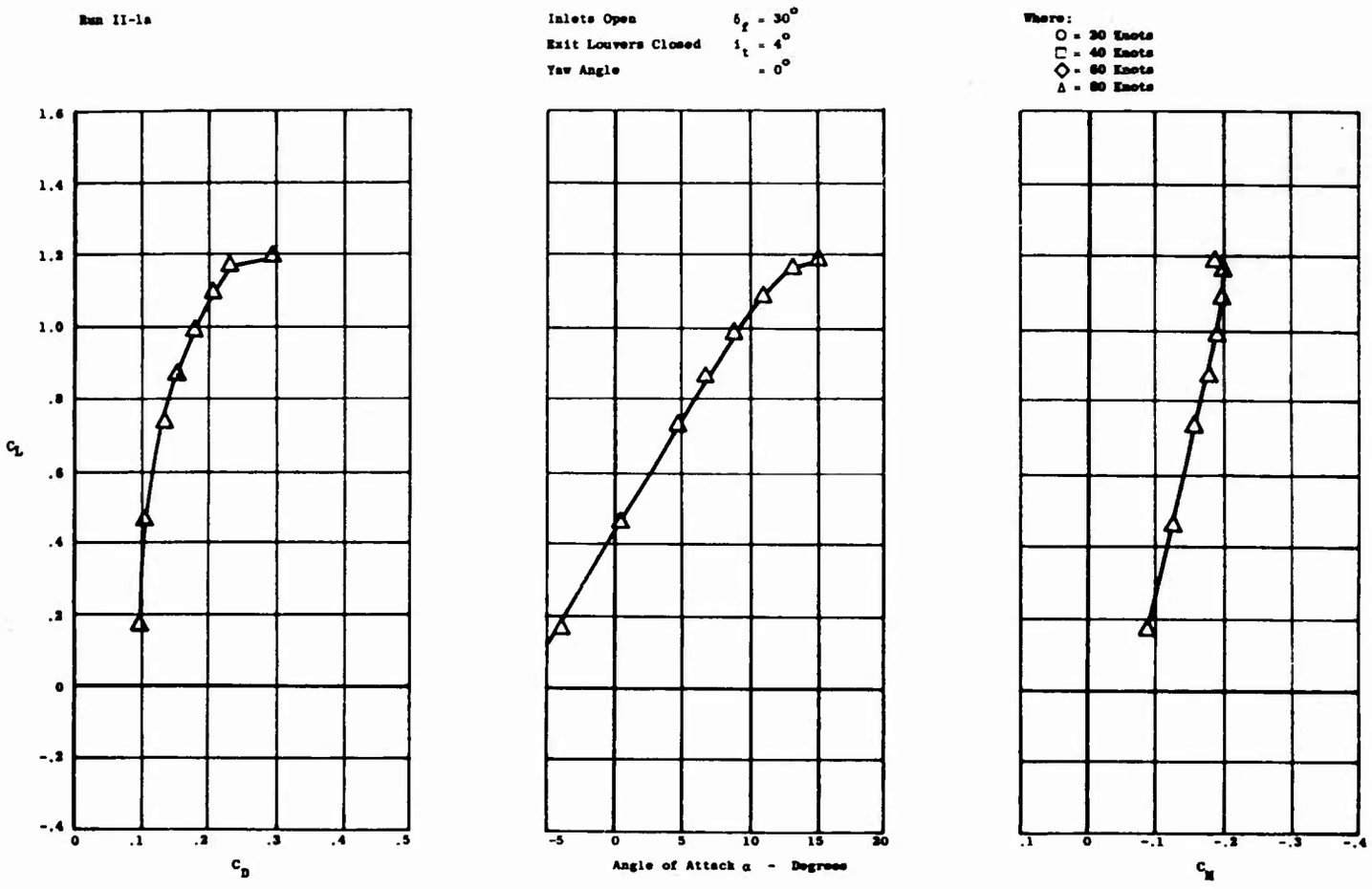


FIGURE 32 - UNPOWERED AIRCRAFT PERFORMANCE

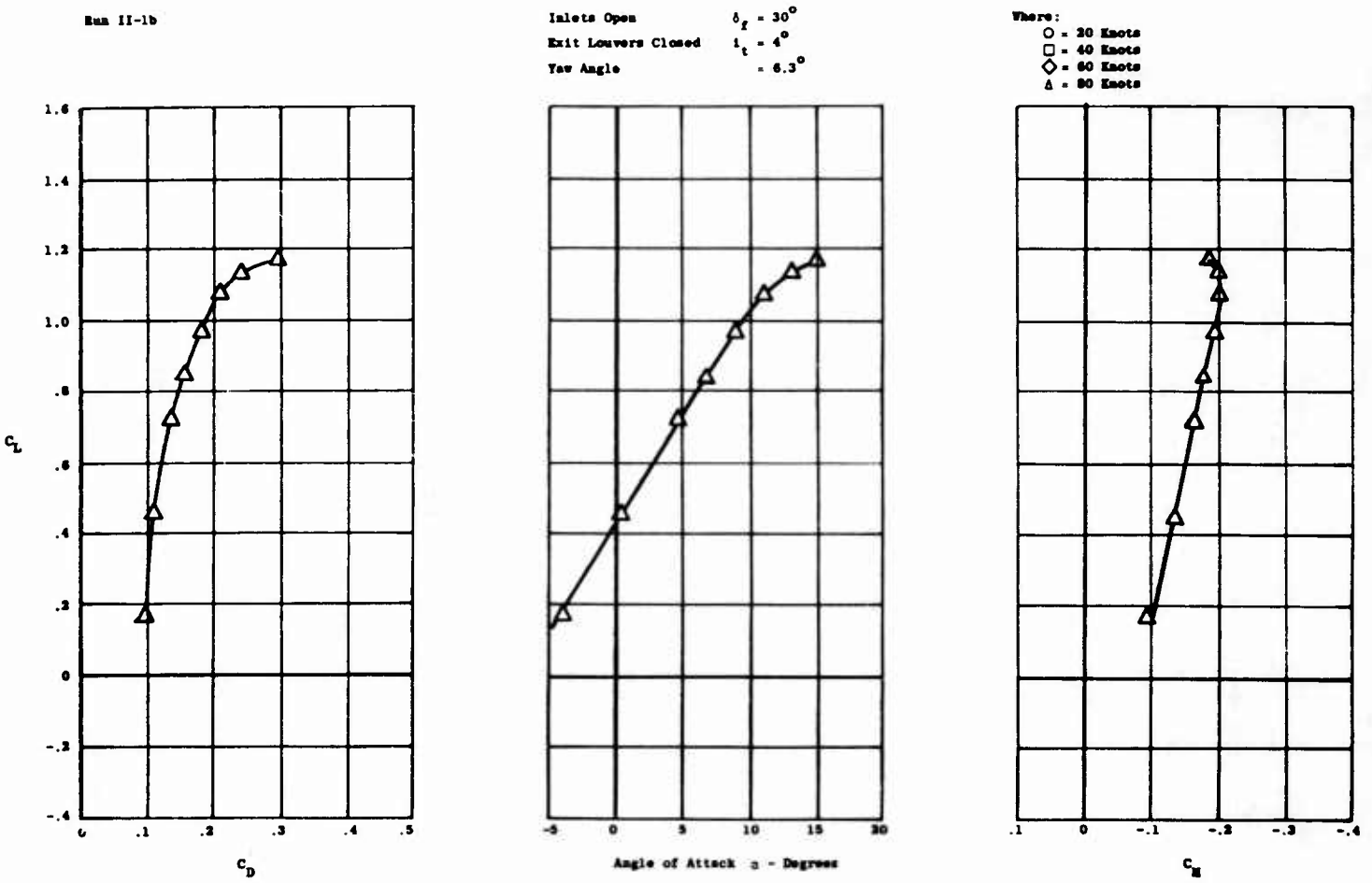


FIGURE 33 - UNPOWERED AIRCRAFT PERFORMANCE

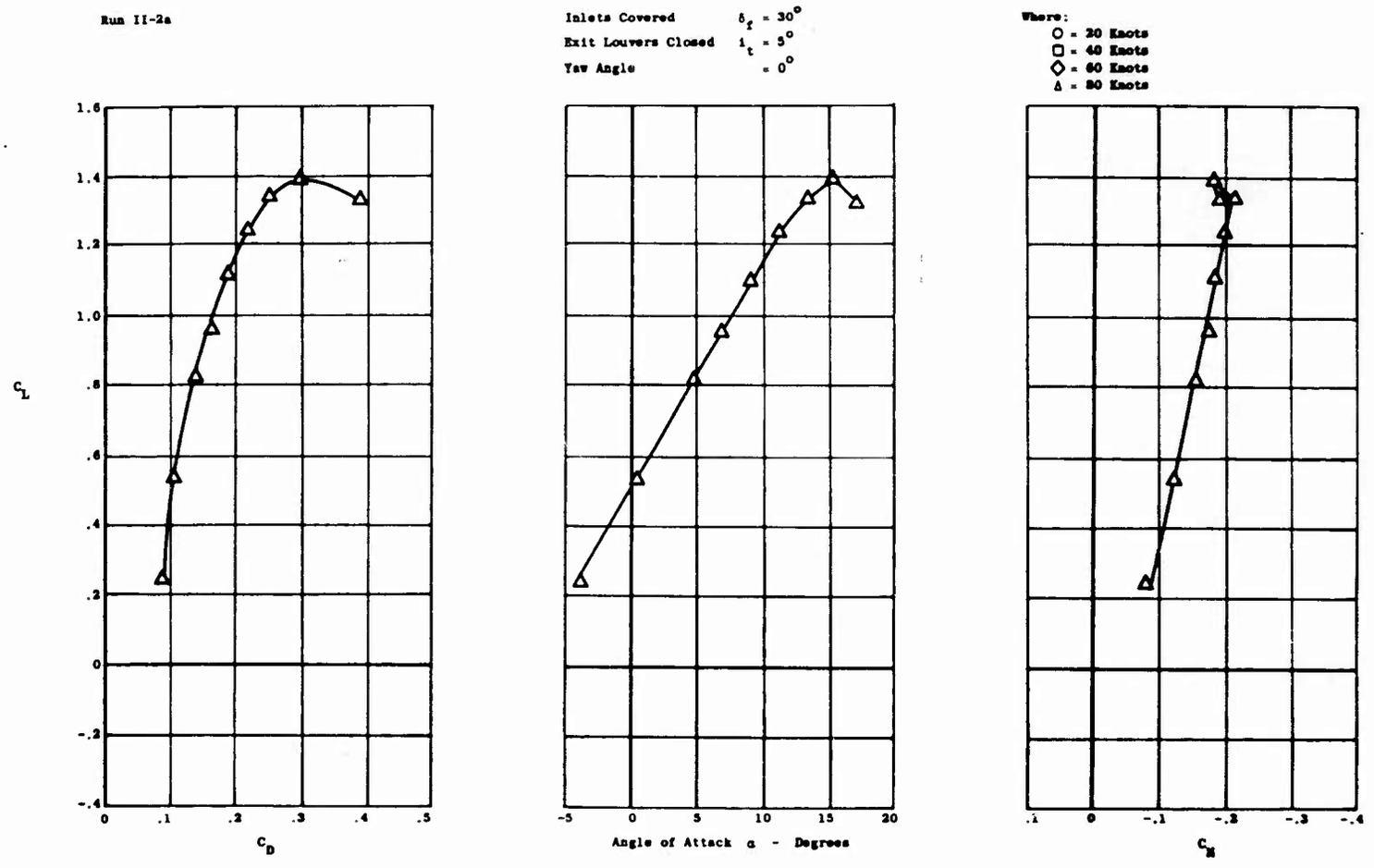


FIGURE 34 - UNPOWERED AIRCRAFT PERFORMANCE

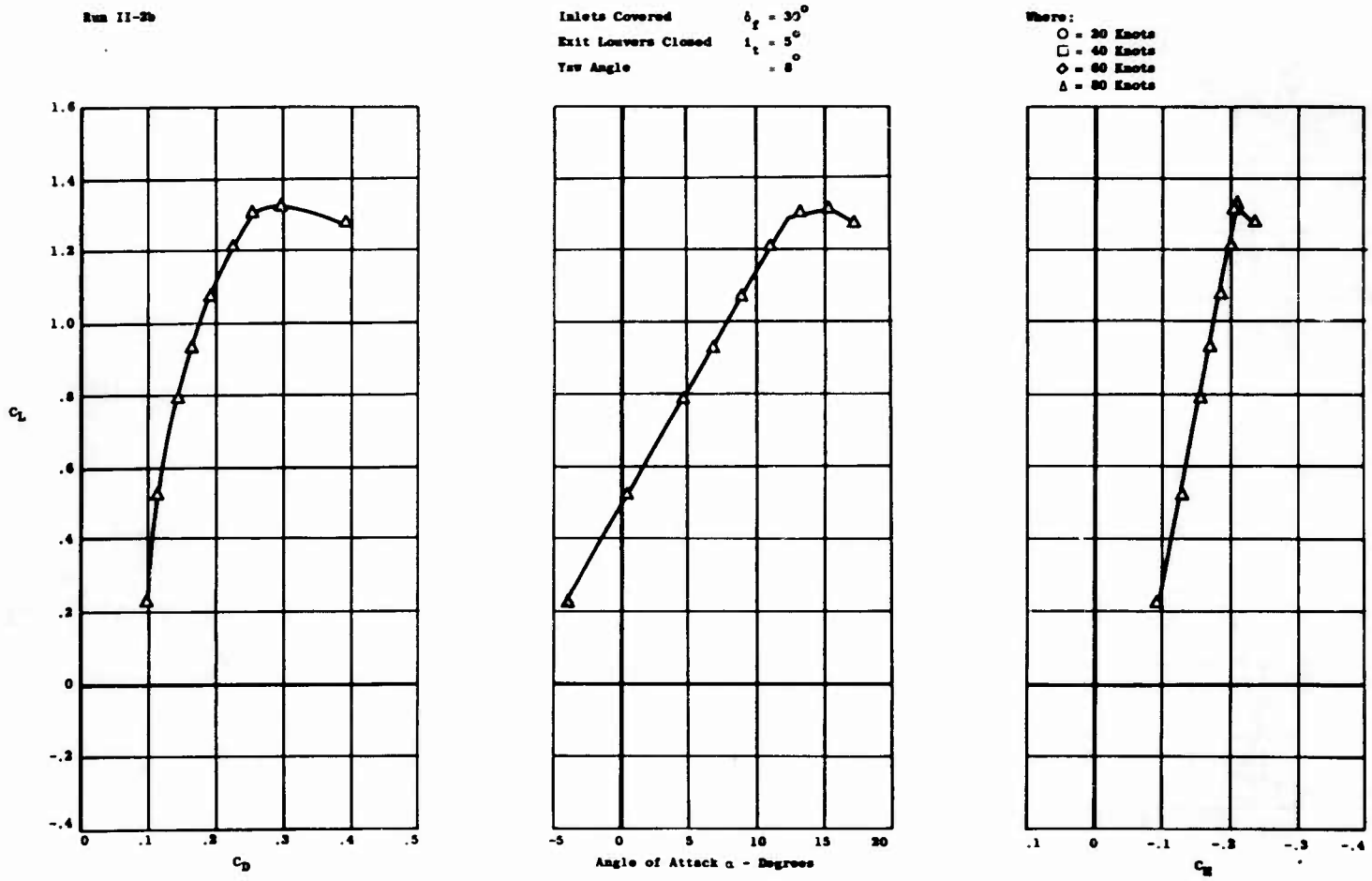


FIGURE 35 UNPOWERED AIRCRAFT PERFORMANCE

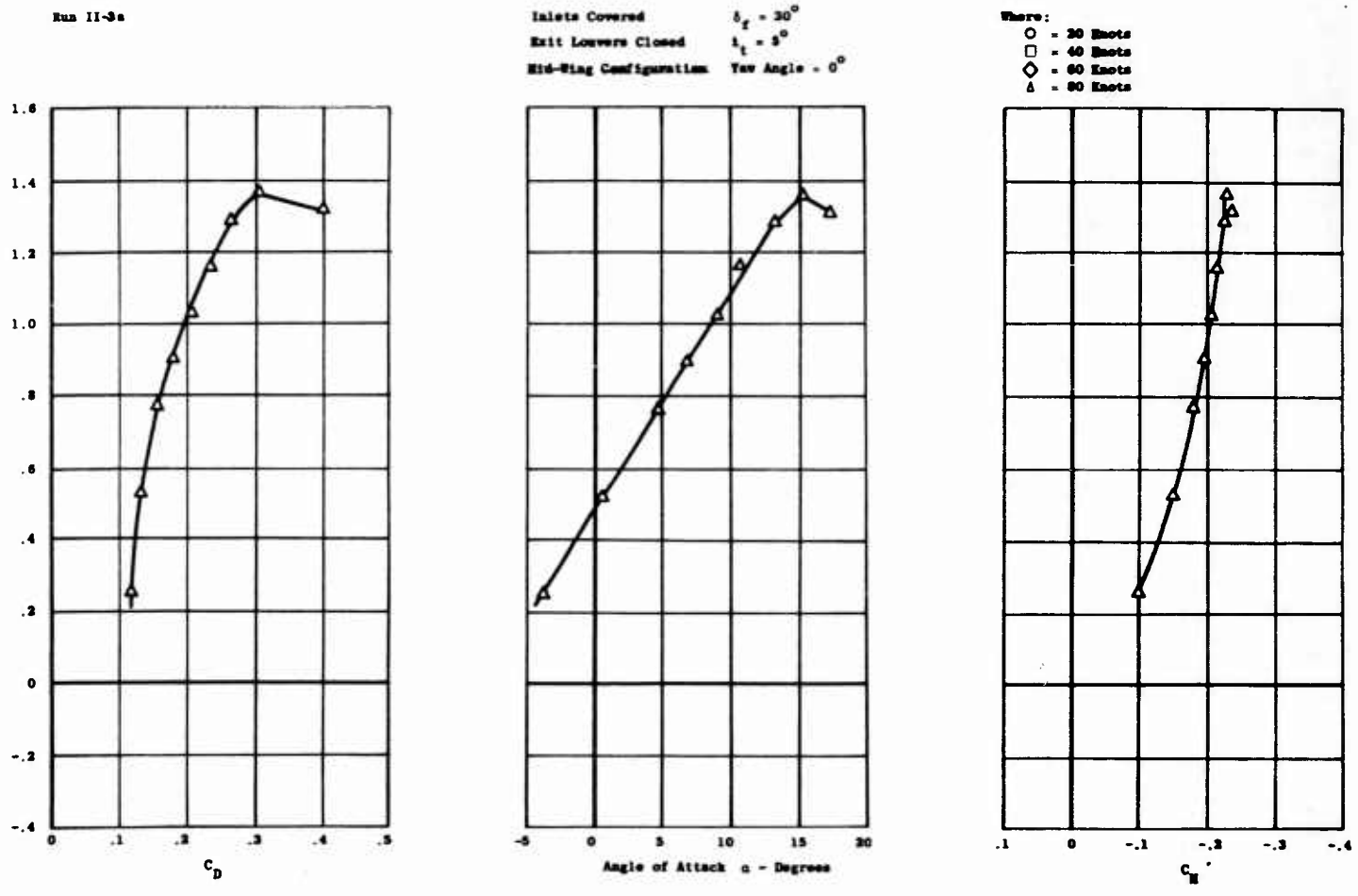


FIGURE 36 - UNPOWERED AIRCRAFT PERFORMANCE

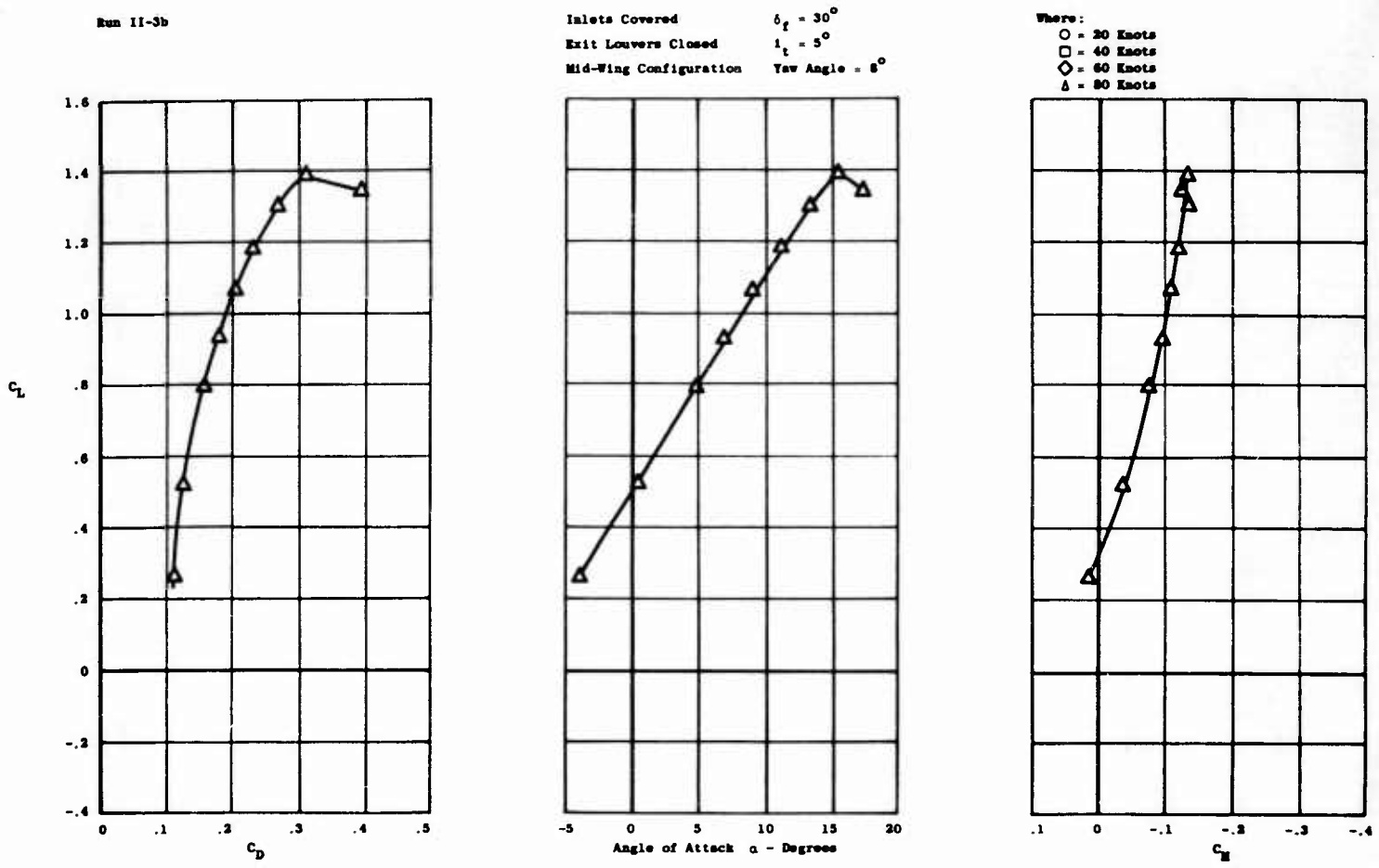


FIGURE 37 - UNPOWERED AIRCRAFT PERFORMANCE

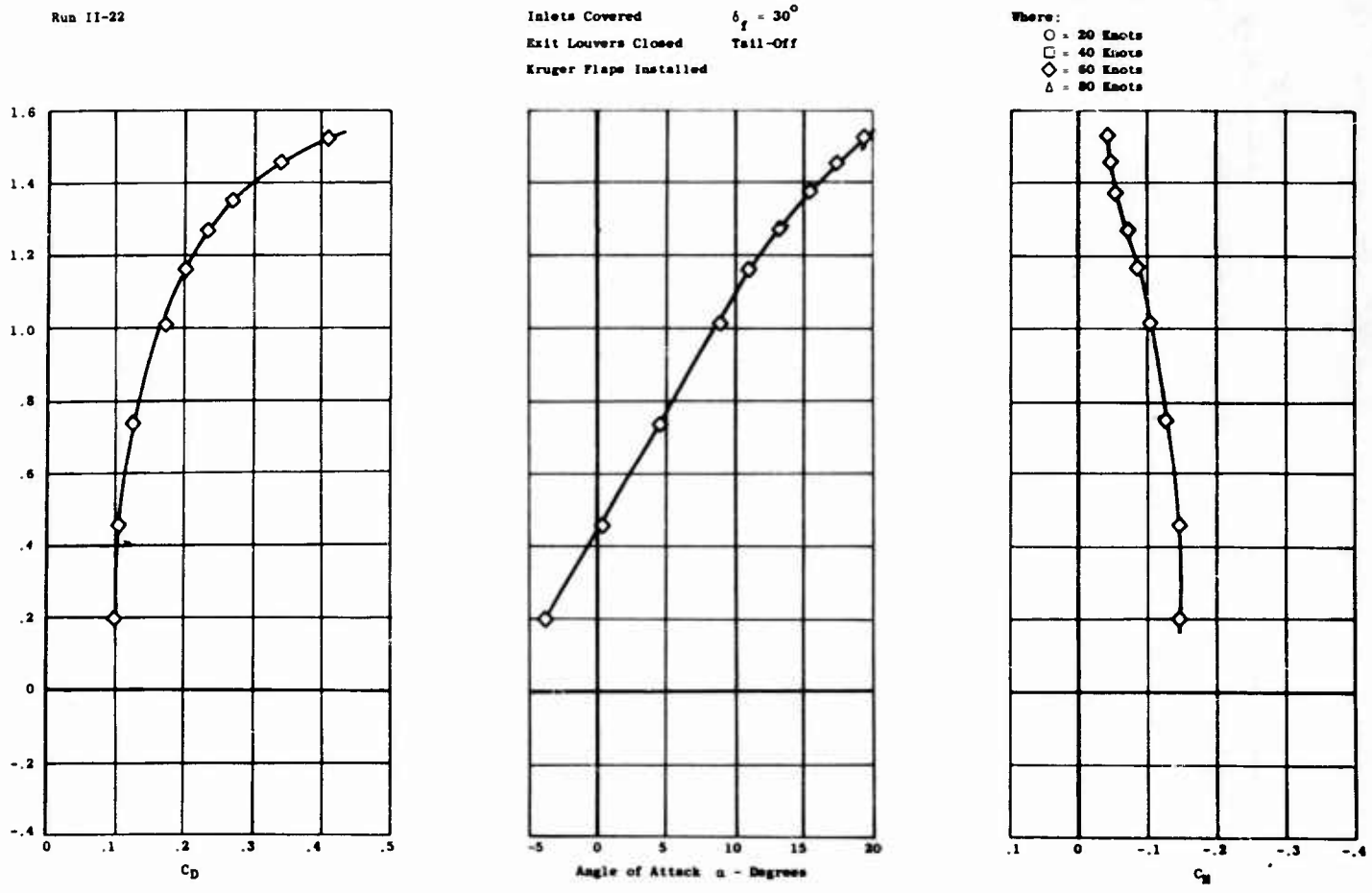


FIGURE 38 - UNPOWERED AIRCRAFT PERFORMANCE

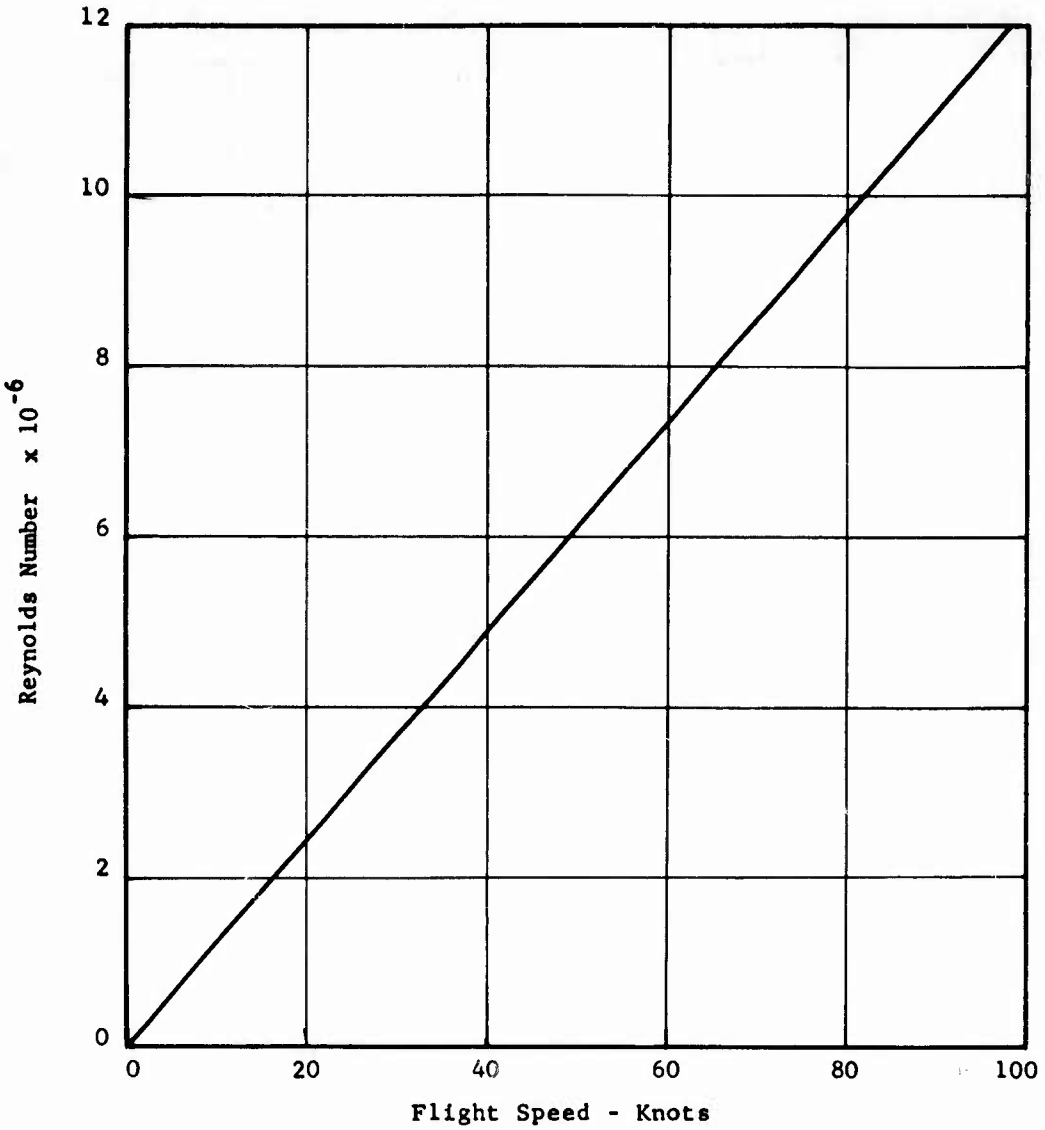


FIGURE 39 - REYNOLDS NUMBER BASED ON WING MEAN AERODYNAMIC CHORD VERSUS FLIGHT SPEED

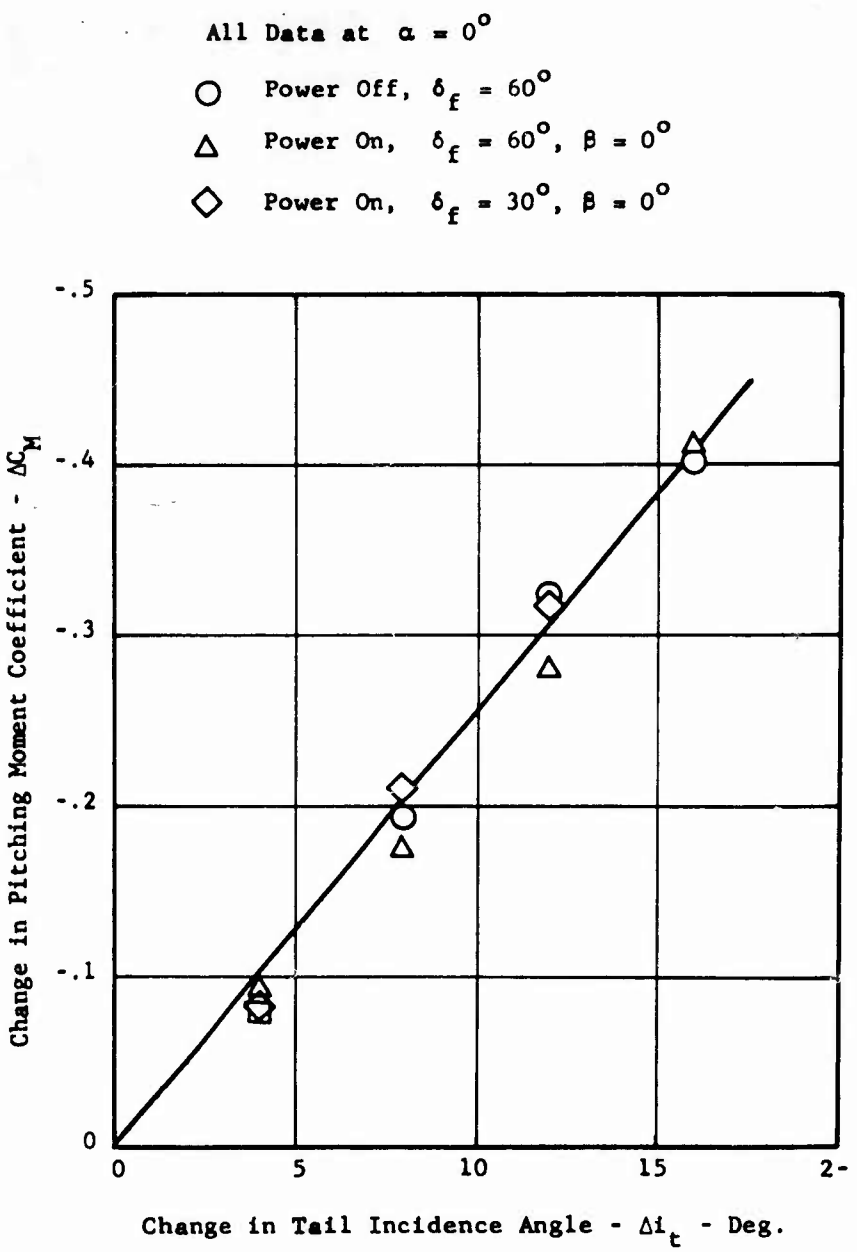


FIGURE 40 - CHANGE IN PITCHING MOMENT COEFFICIENT WITH CHANGE IN TAIL INCIDENCE ANGLE ($\alpha = 0^\circ$)

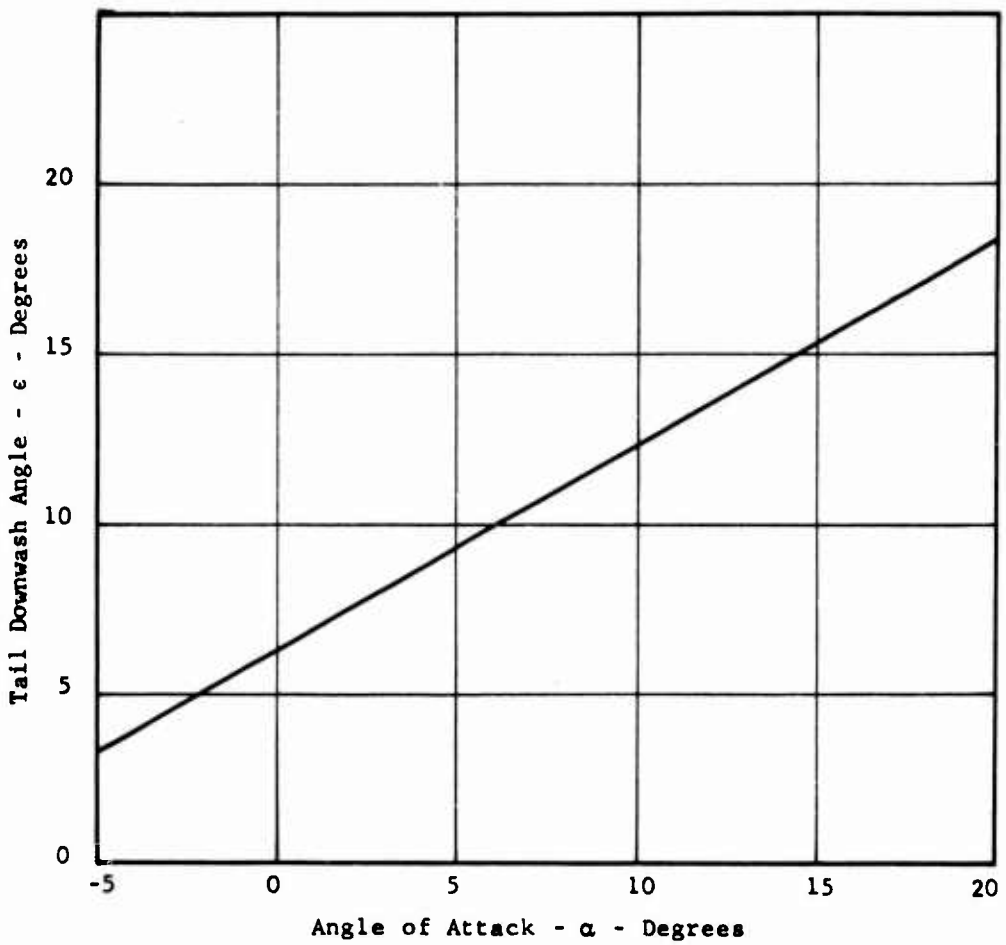


FIGURE 41 - TAIL DOWNWASH ANGLE VERSUS ANGLE OF ATTACK

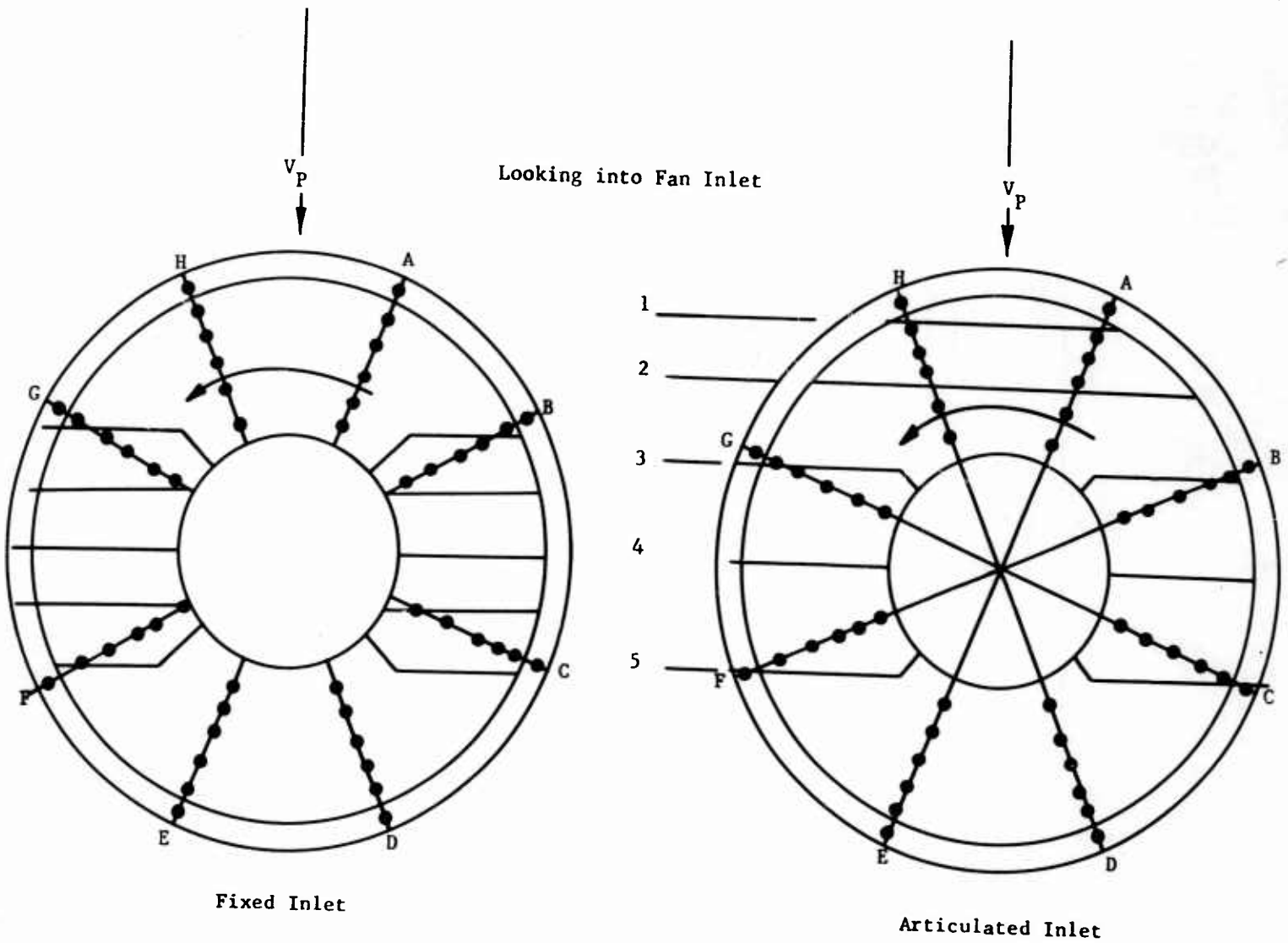
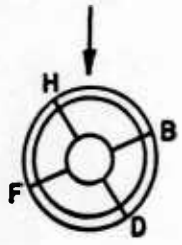


FIGURE 42 - LOCATION OF FAN ROTOR INLET (10.3) AND EXIT (10.6) PRESSURE MEASURING INSTRUMENTATION



Circular Vane Inlet

Left Fan - X353-5 Rotor

α = 0°

β = 0°

δ_f = 30°

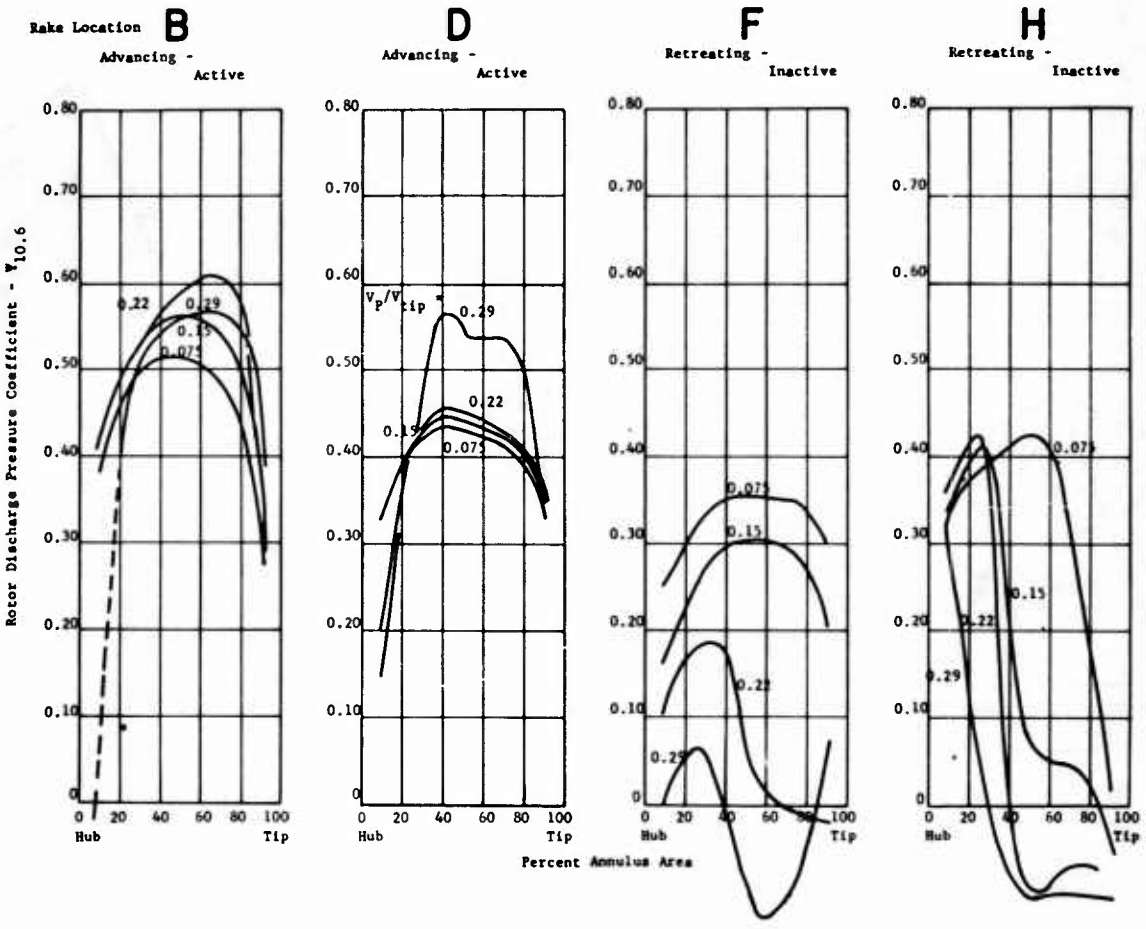


FIGURE 43 - PRESSURE COEFFICIENT VERSUS PERCENT ANNULUS AREA

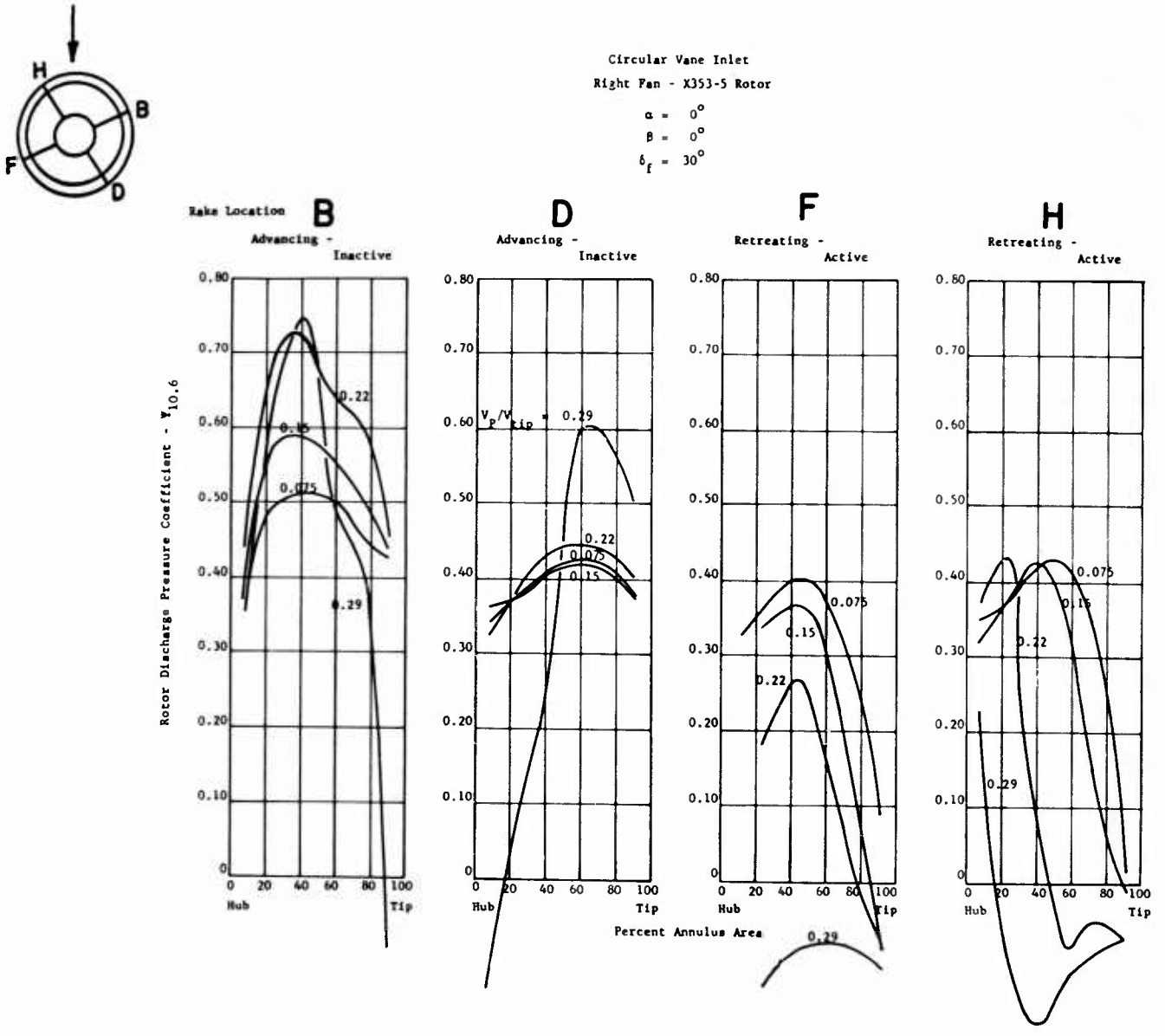


FIGURE 44a. PRESSURE COEFFICIENT VERSUS PERCENT ANNULUS AREA

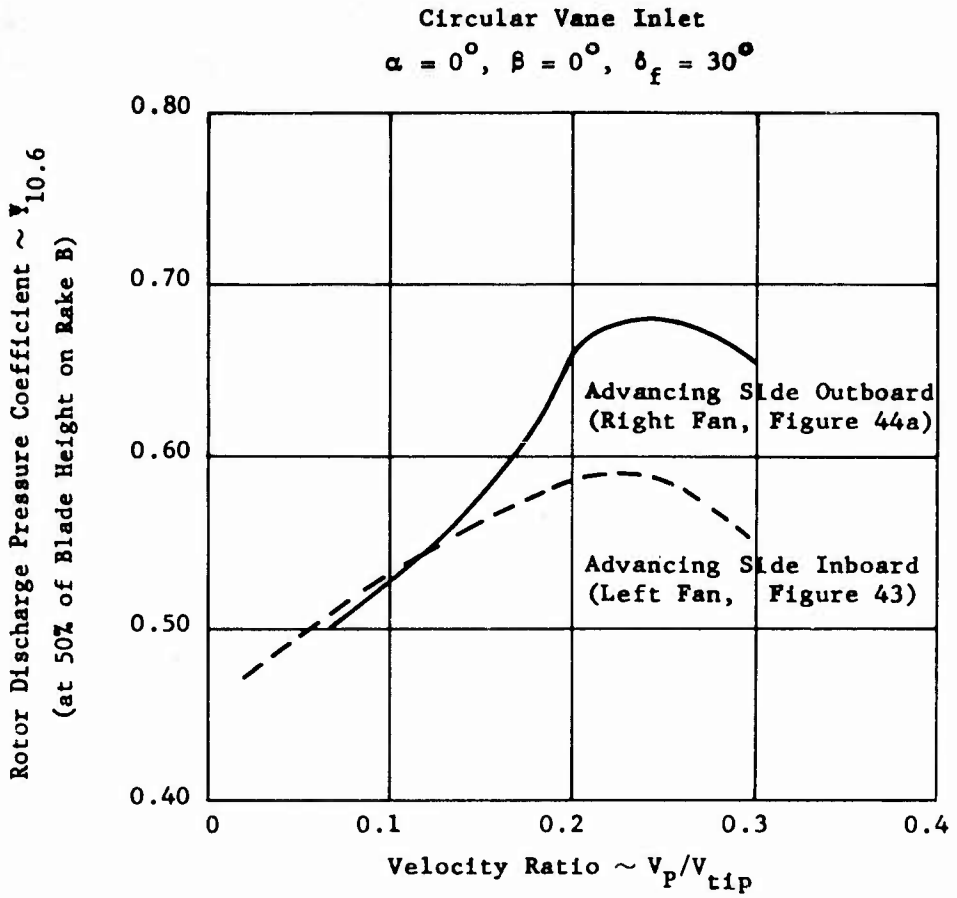


FIGURE 44b - ROTOR DISCHARGE PRESSURE COEFFICIENT VERSUS VELOCITY RATIO

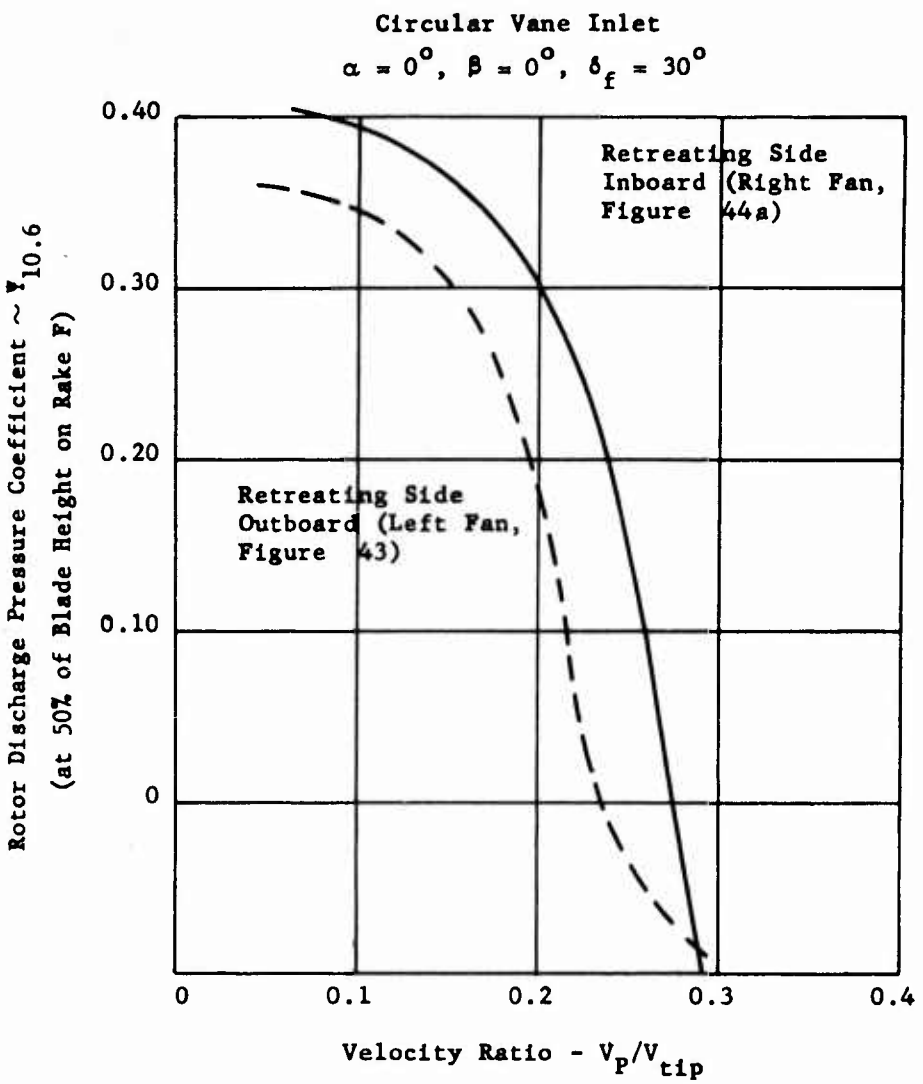
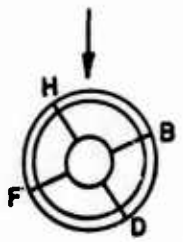


FIGURE 44c - ROTOR DISCHARGE PRESSURE COEFFICIENT VERSUS VELOCITY RATIO



Circular Vane Inlet

Left Fan - X353-5 Rotor

α = 0°

β = 35°

δ_f = 30°

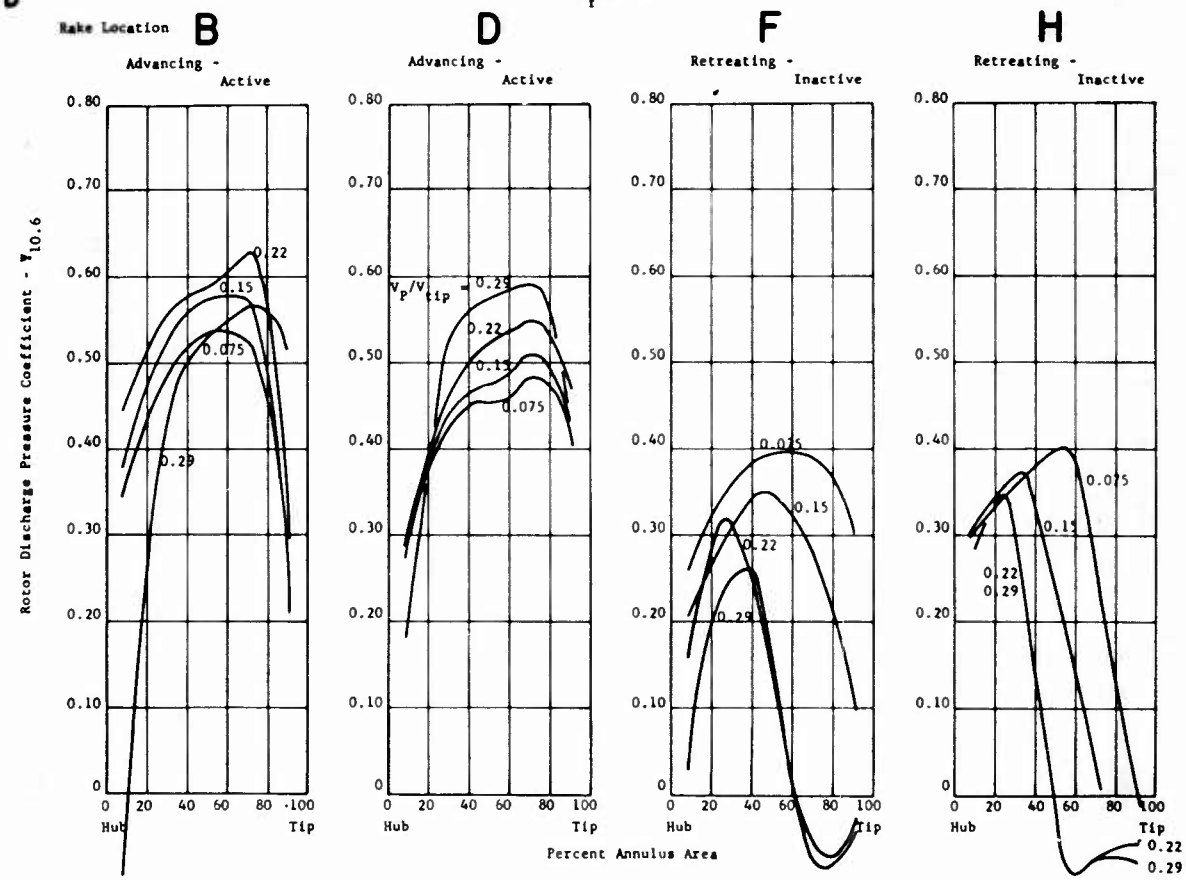


FIGURE 45 - PRESSURE COEFFICIENT VERSUS PERCENT ANNULUS AREA

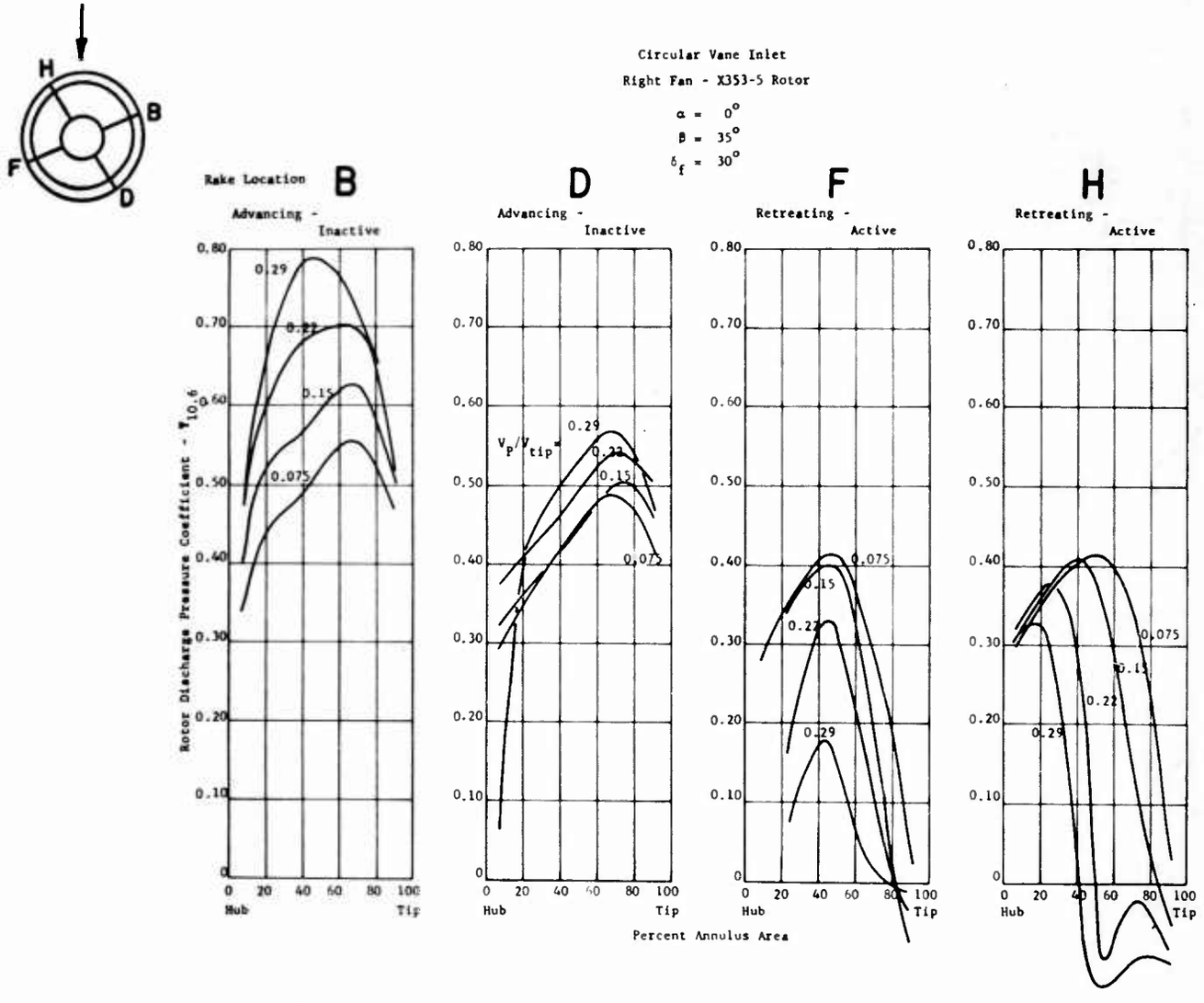


FIGURE 46 - PRESSURE COEFFICIENT VERSUS PERCENT ANNULUS AREA

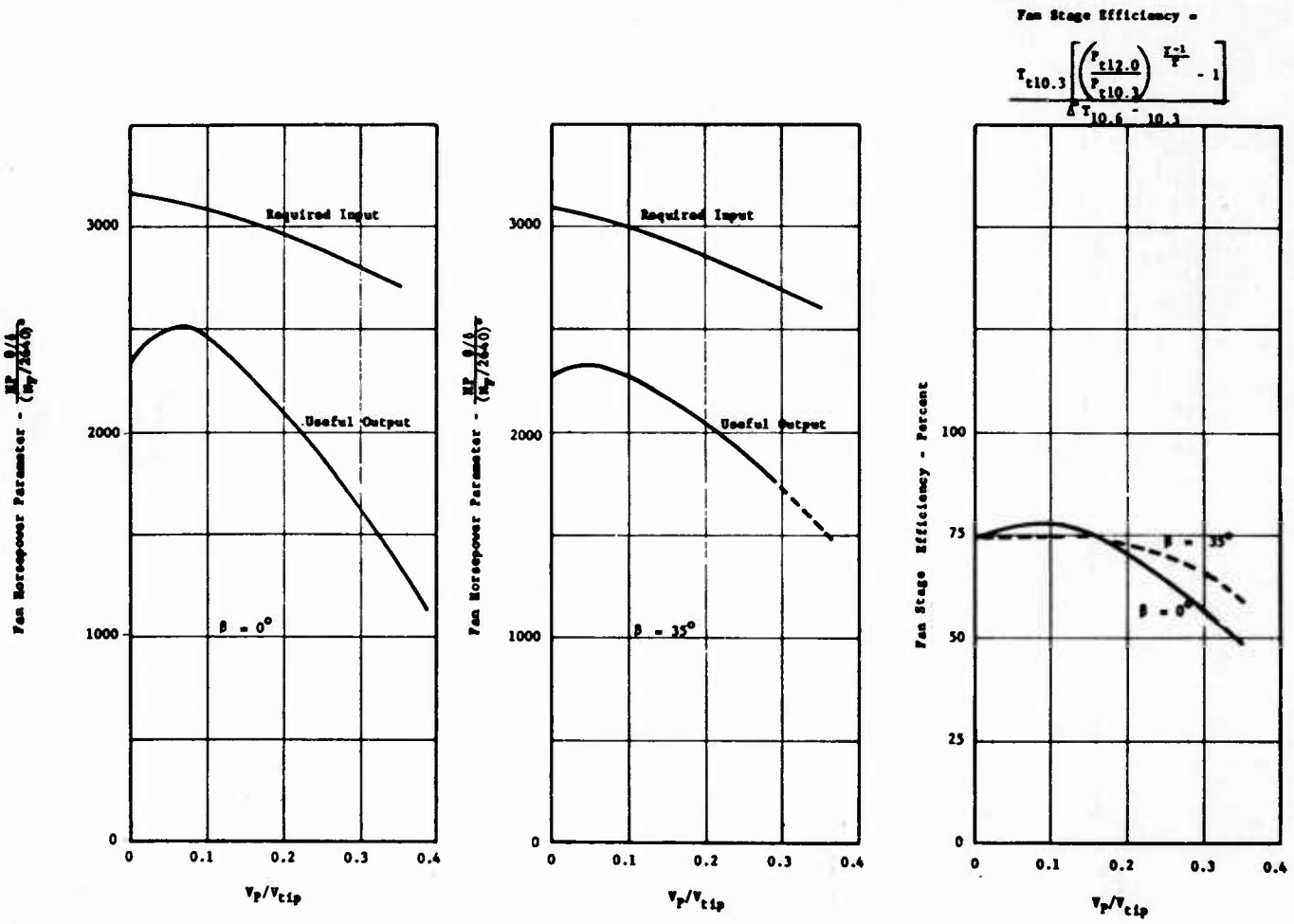


FIGURE 47 - FAN HORSEPOWER PARAMETER AND EFFICIENCY VERSUS VELOCITY RATIO

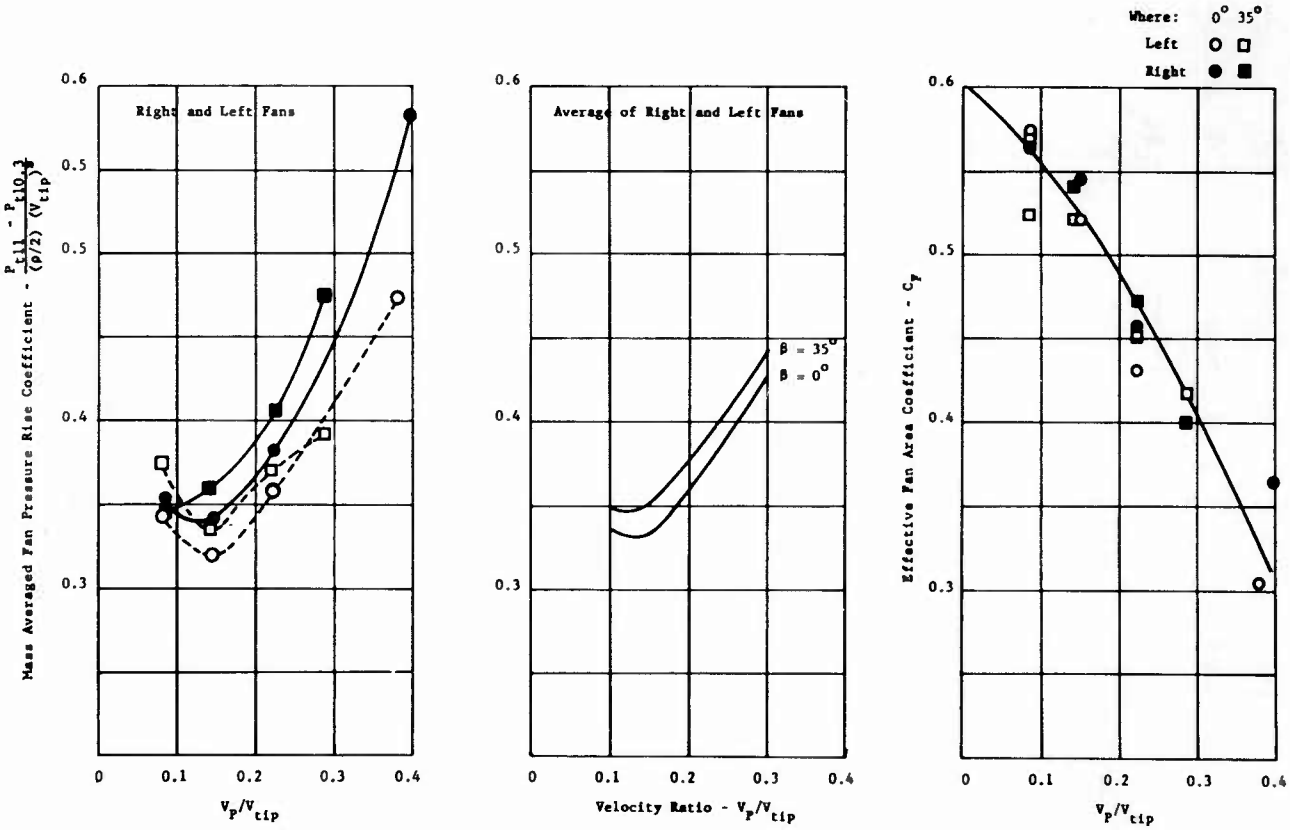


FIGURE 48. FAN PRESSURE RISE COEFFICIENT AND EFFECTIVE AREA COEFFICIENT VERSUS VELOCITY RATIO (CIRCULAR VANE INLET)

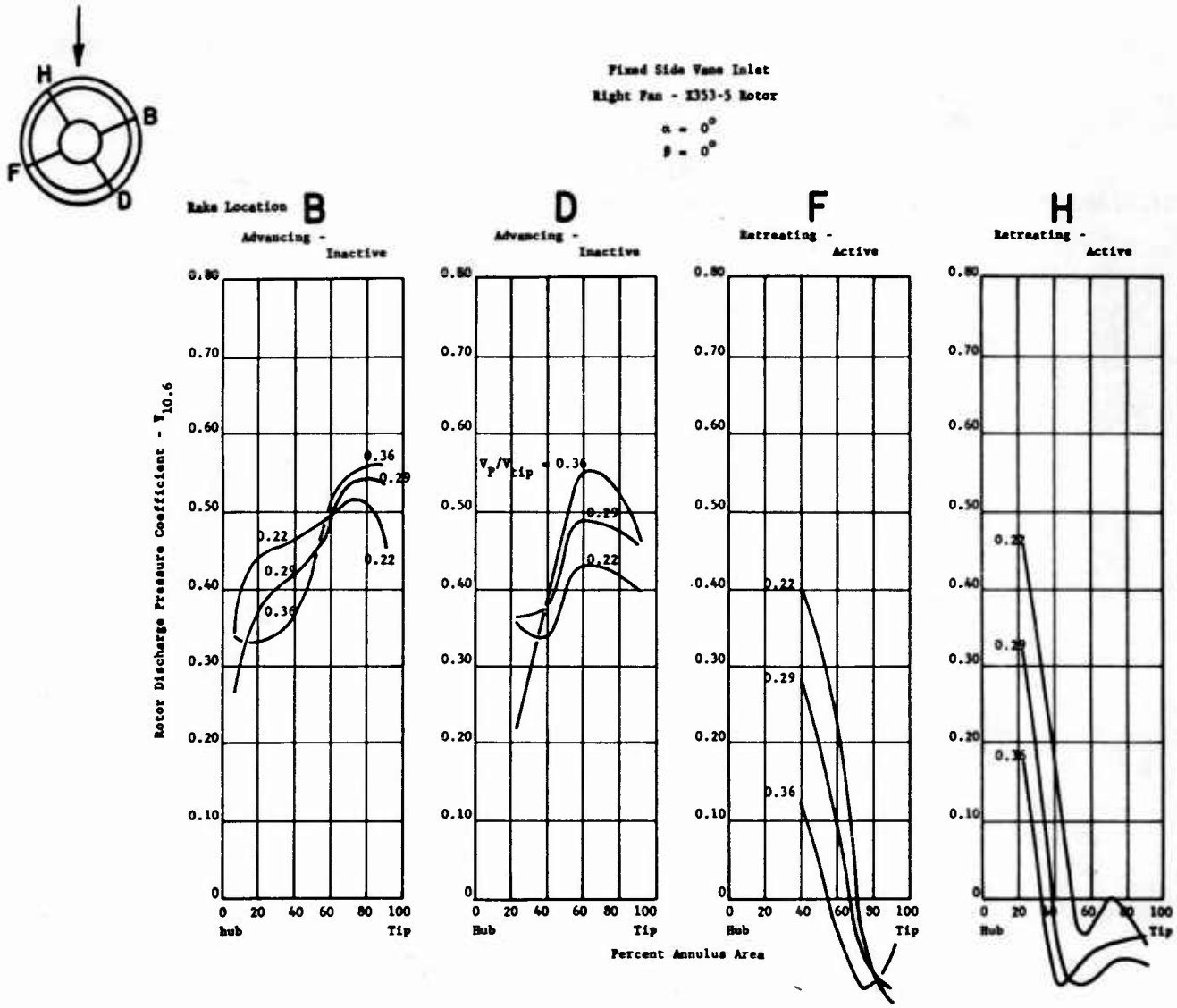


FIGURE 49a. PRESSURE COEFFICIENT VERSUS PERCENT ANNULUS AREA

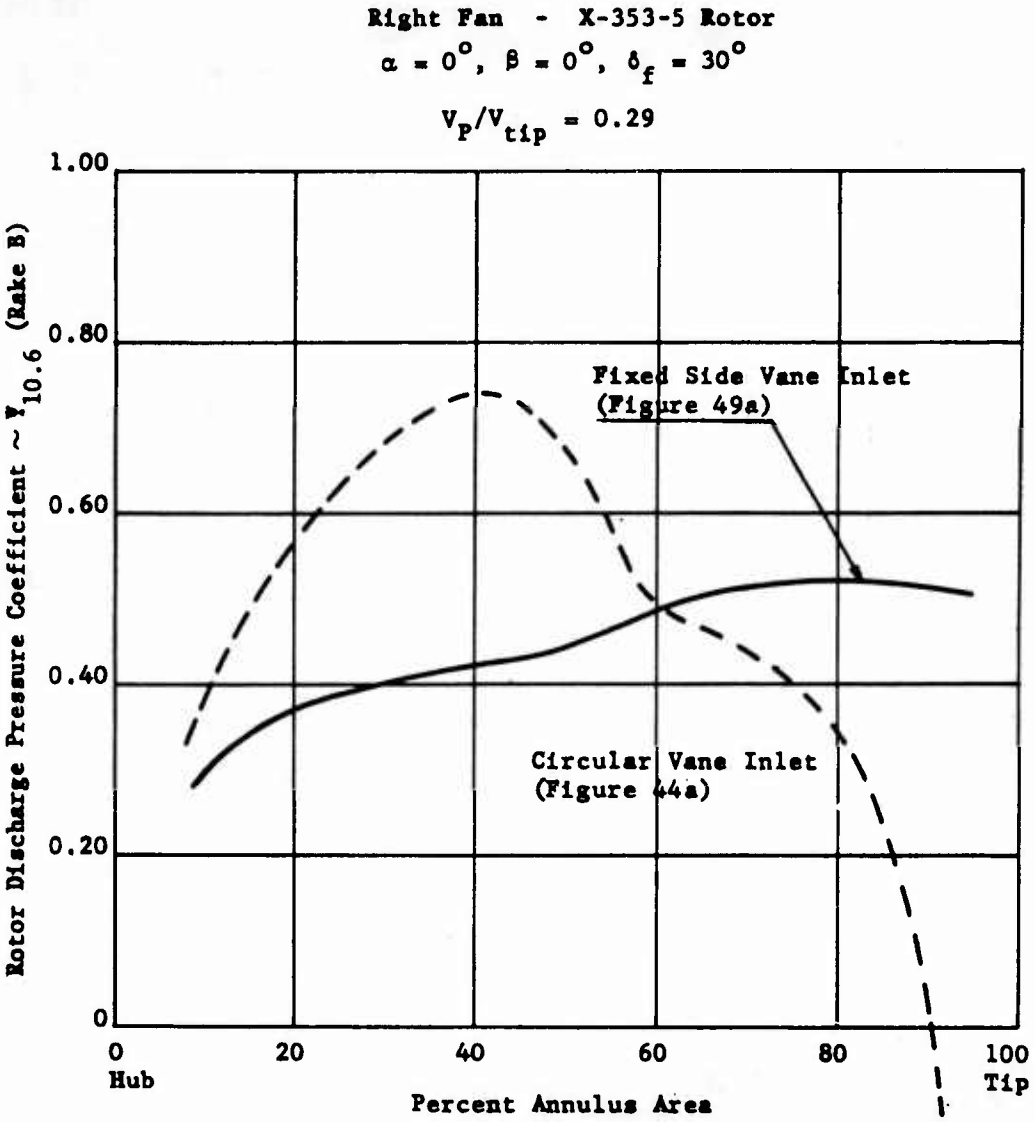


FIGURE 49b - PRESSURE COEFFICIENT VERSUS PERCENT ANNULUS AREA

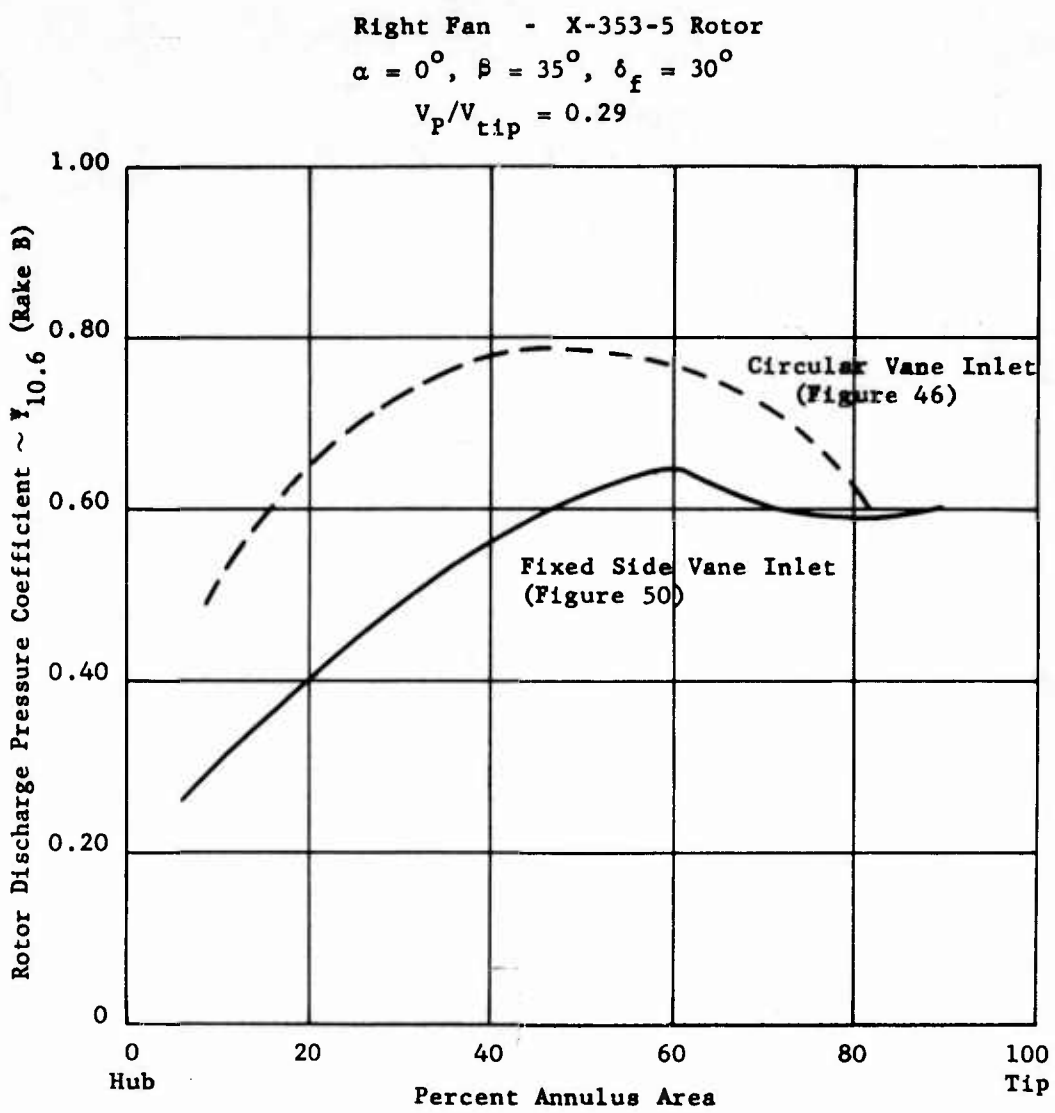
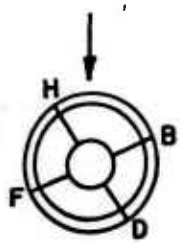


FIGURE 49c - ROTOR DISCHARGE PRESSURE COEFFICIENT VERSUS PERCENT ANNULUS AREA



Fixed Side Vane Inlet
Right Fan - X353-5 Rotor
α = 0°
β = 35°

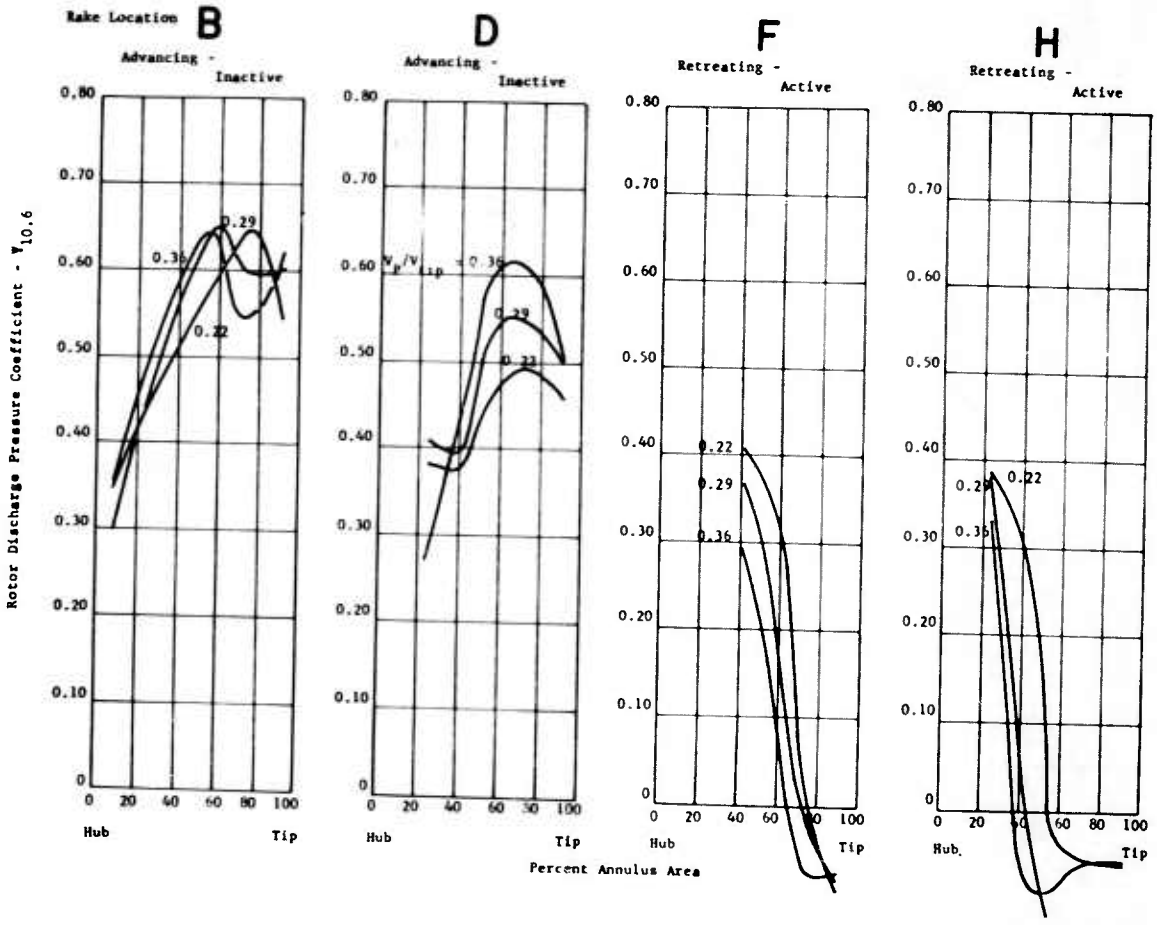


FIGURE 50 - PRESSURE COEFFICIENT VERSUS PERCENT ANNULUS AREA

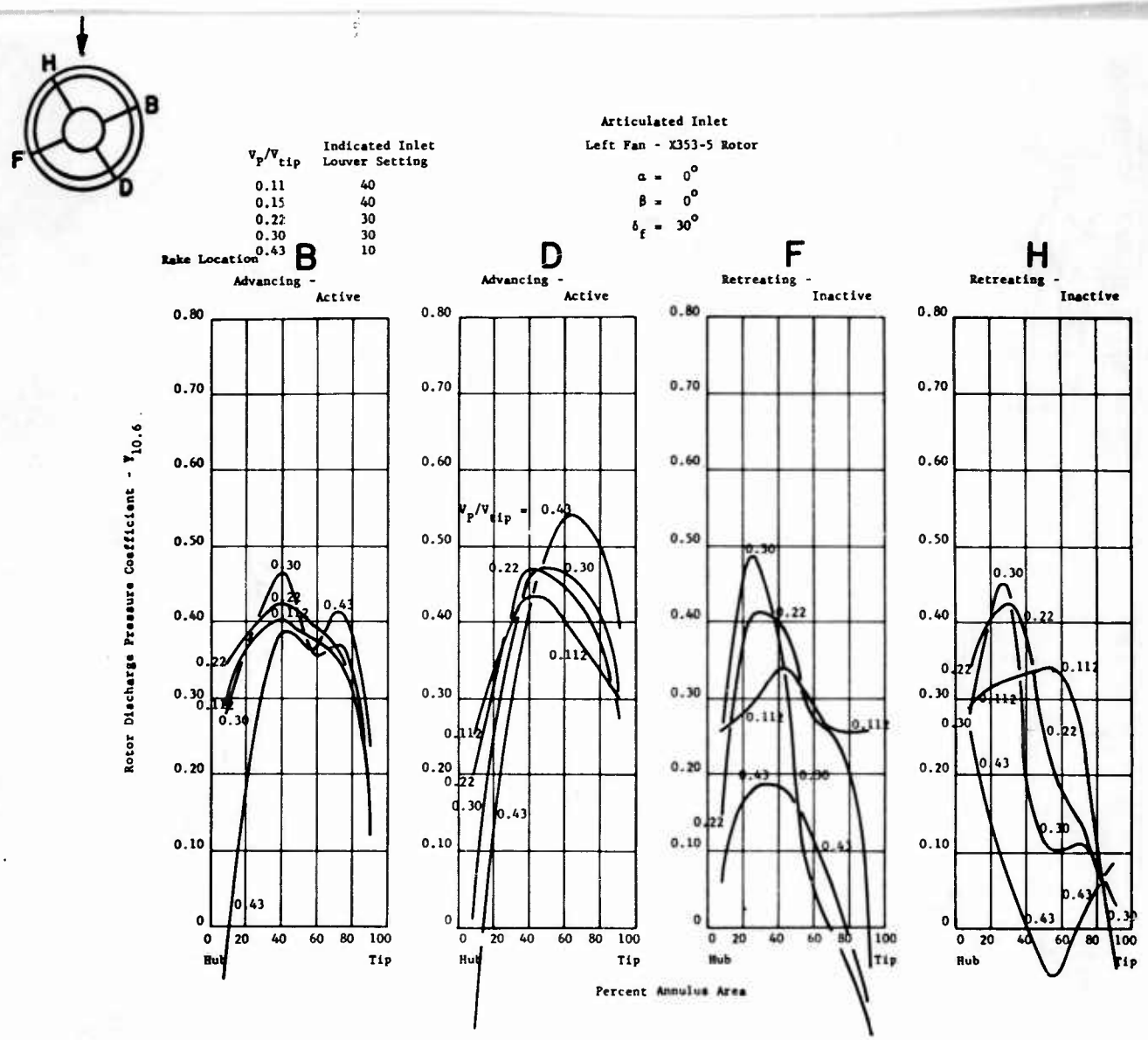


FIGURE 51 - PRESSURE COEFFICIENT VERSUS PERCENT ANNULUS AREA

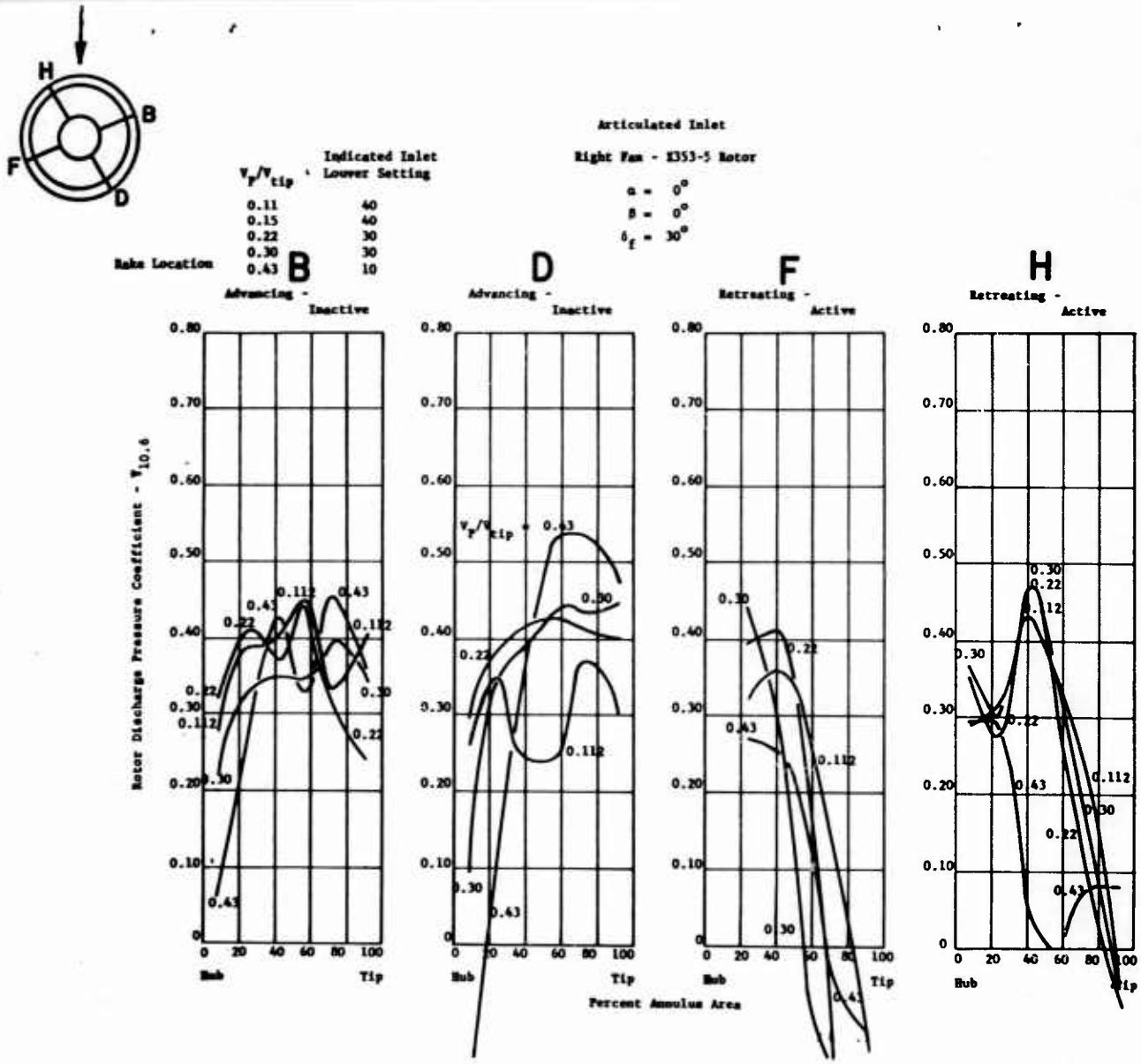
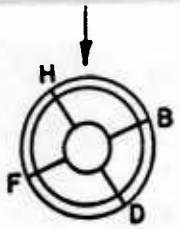


FIGURE 52 - PRESSURE COEFFICIENT VERSUS PERCENT ANNULUS AREA



V_p/V_{tip}	Indicated Inlet Louver Setting
0.11	40
0.15	40
0.22	30
0.30	30
0.45	10

Articulated Inlet

Left Fan - X353-5 Rotor

$\alpha = 0^{\circ}$

$\beta = 35^{\circ}$

$\delta_f = 30^{\circ}$

Rake Location

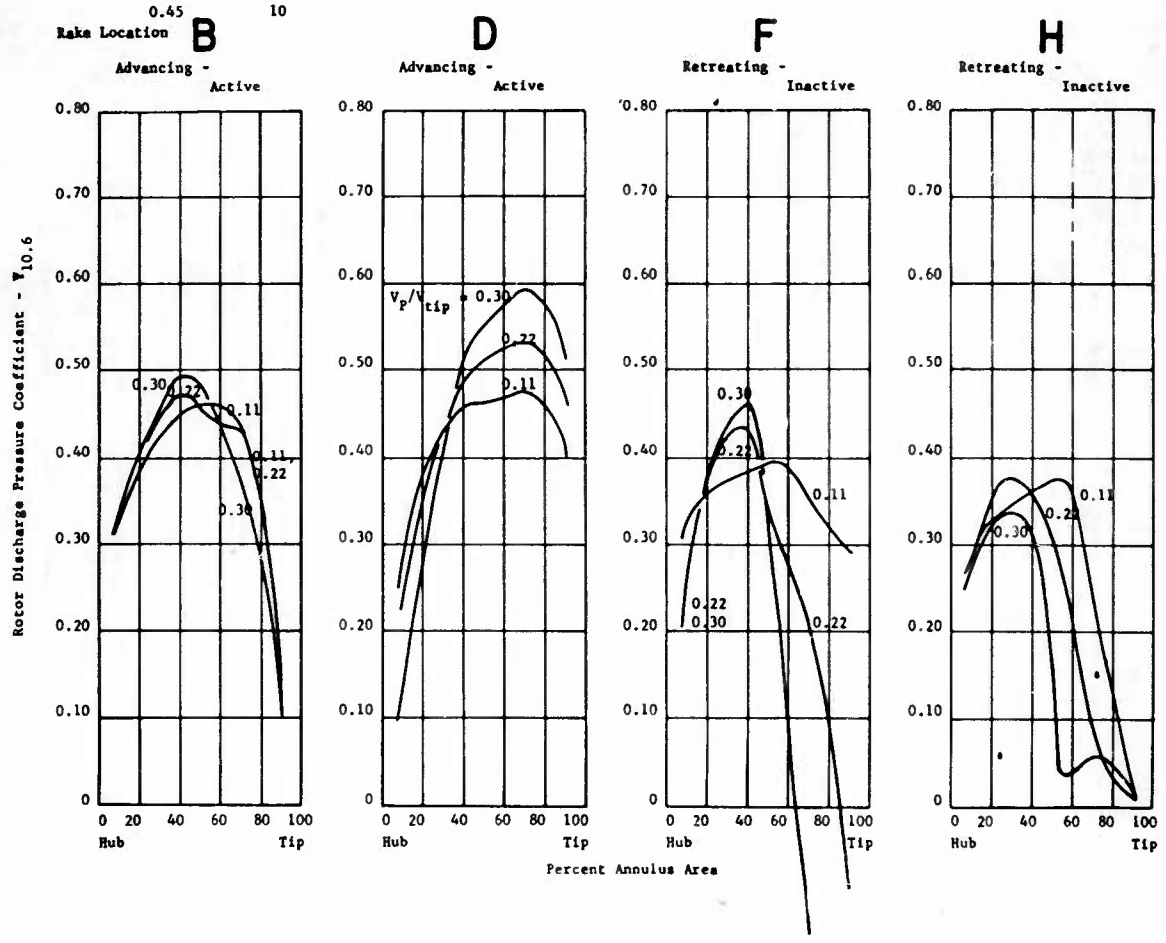
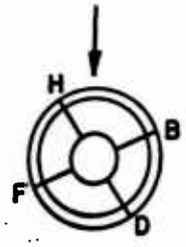


FIGURE 53 - PRESSURE COEFFICIENT VERSUS PERCENT ANNULUS AREA



V_p/V_{tip}	Indicated Inlet Louver Setting
0.11	40
0.22	30
0.30	10

Articulated Inlet

Right Fan - X353-5 Rotor

$\alpha = 0^o$

$\beta = 35^o$

$\delta_f = 30^o$

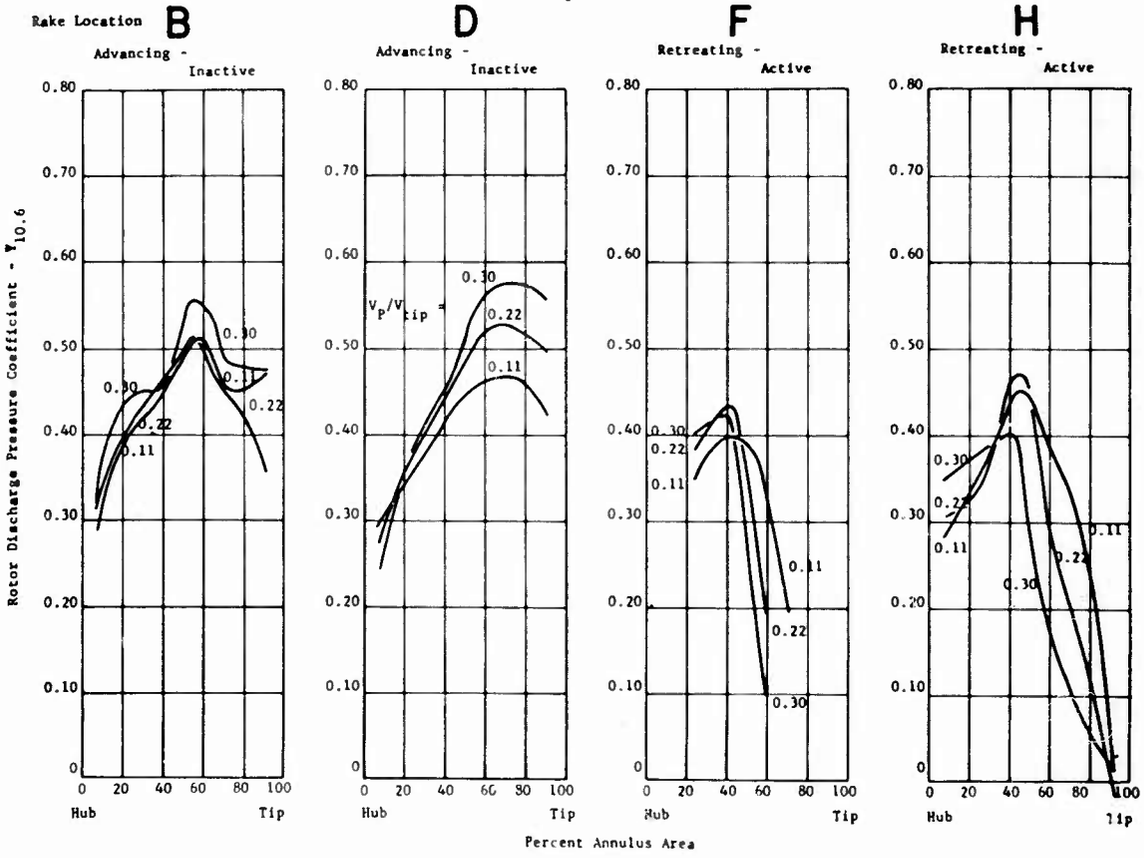


FIGURE 54 - PRESSURE COEFFICIENT VERSUS PERCENT ANNULUS AREA

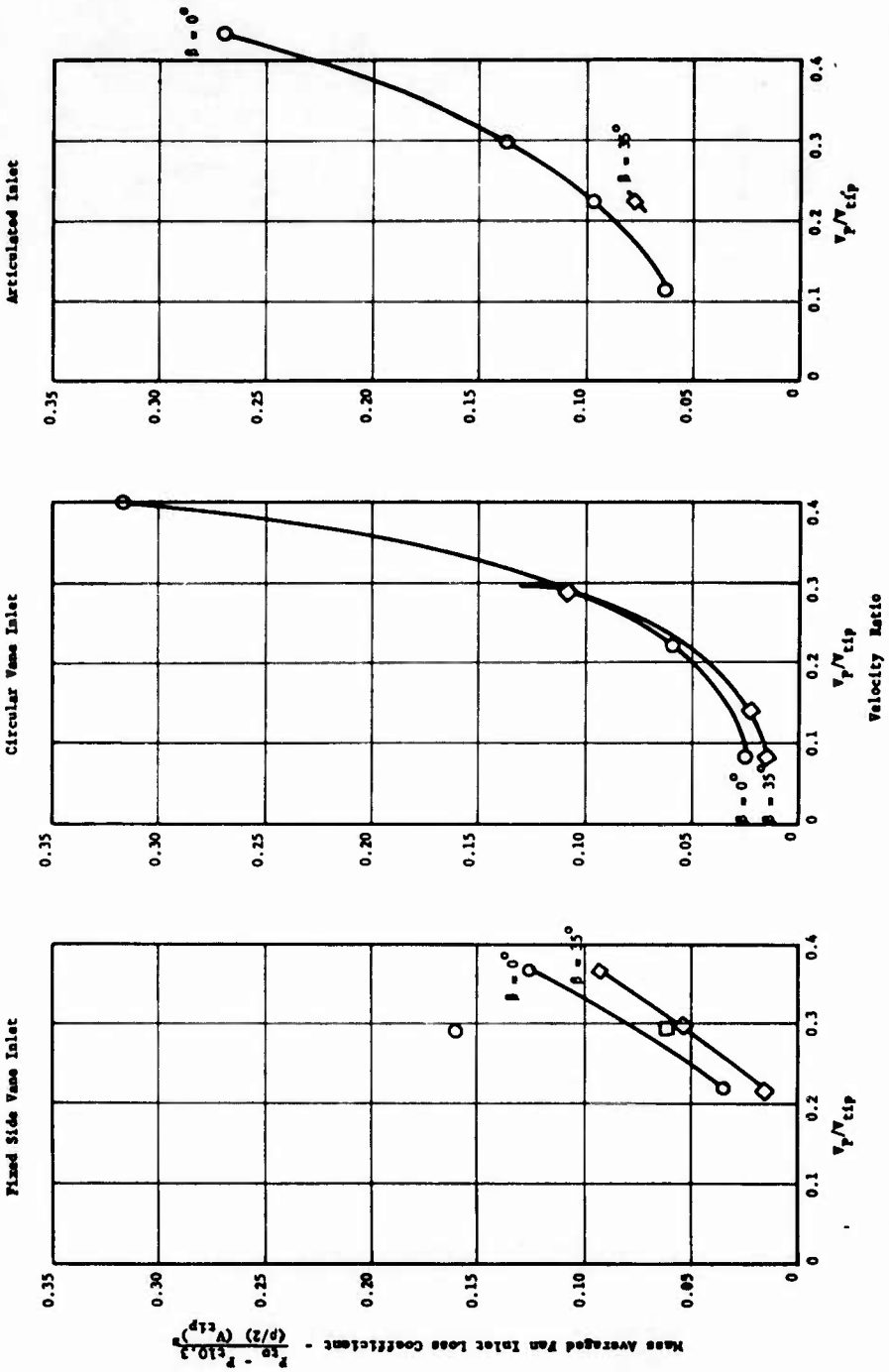


FIGURE 55 a - MASS AVERAGED FAN INLET LOSS COEFFICIENT VERSUS VELOCITY RATIO

$\beta = 0^{o}$

$\alpha = 0^{o}$

$\Psi = 0^{o}$

$N_F = 100\%$

Sea Level Standard

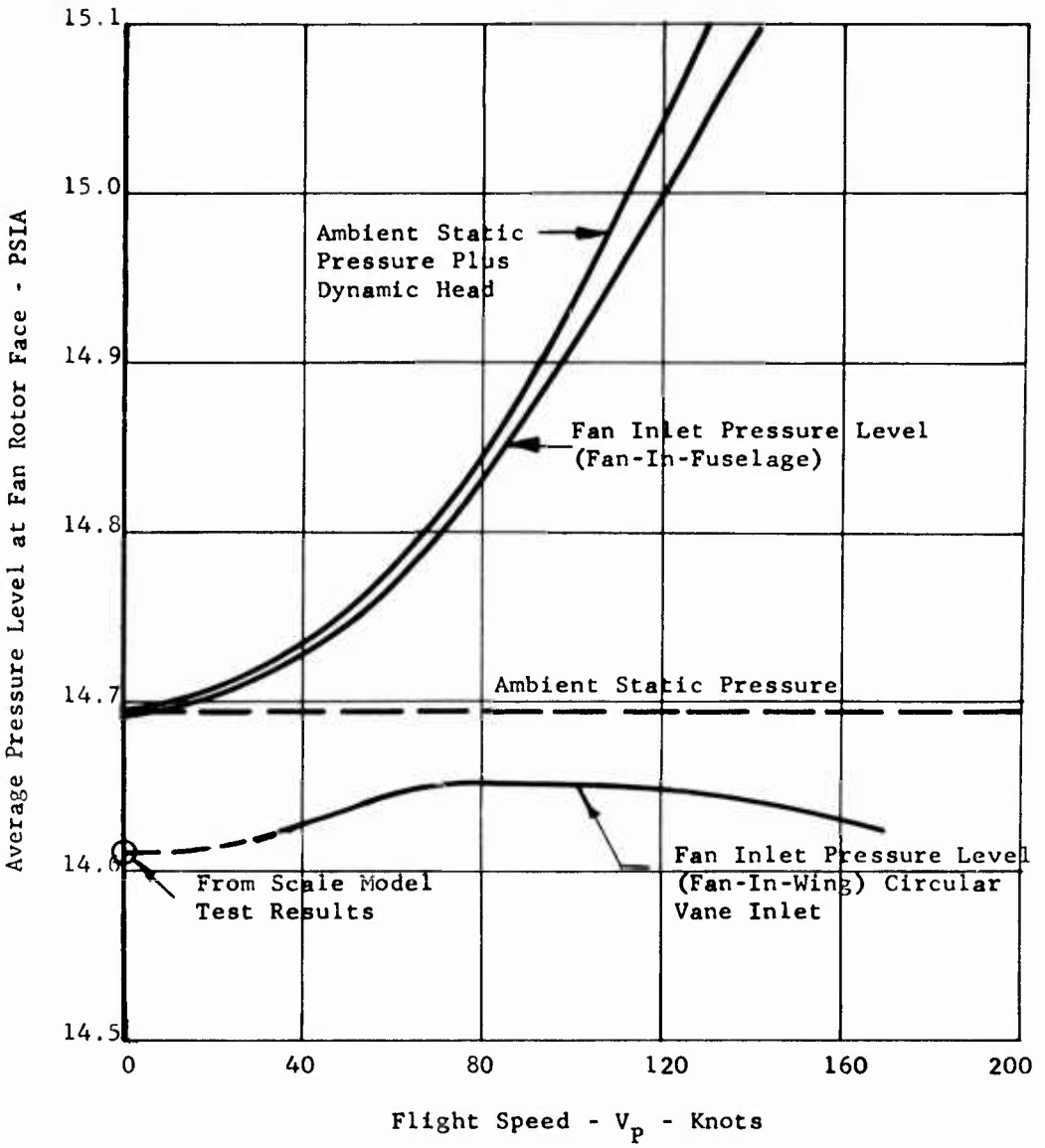


FIGURE 55b - FAN INLET PRESSURE VERSUS FLIGHT SPEED

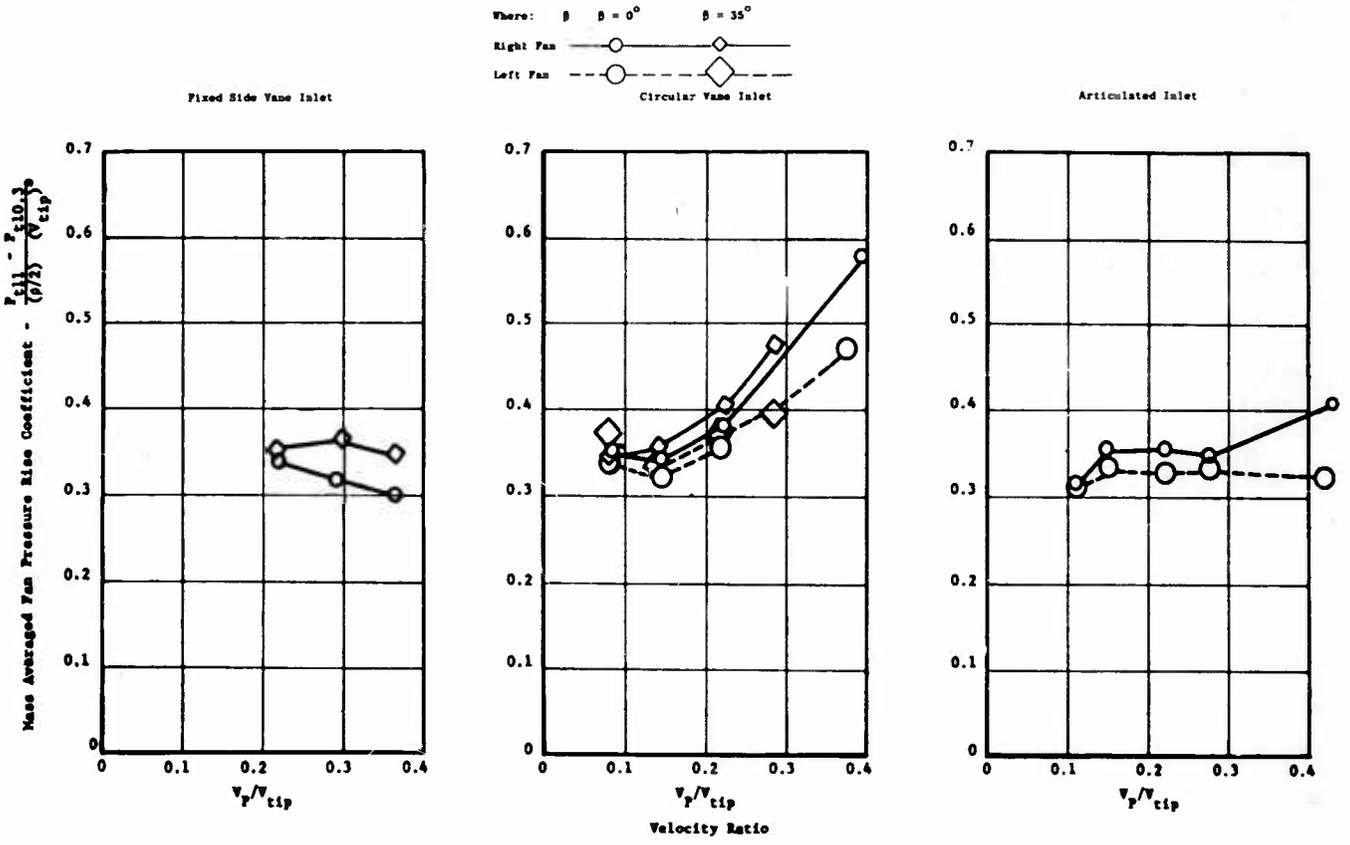


FIGURE 56 - MASS AVERAGED FAN PRESSURE RISE COEFFICIENT VERSUS VELOCITY RATIO

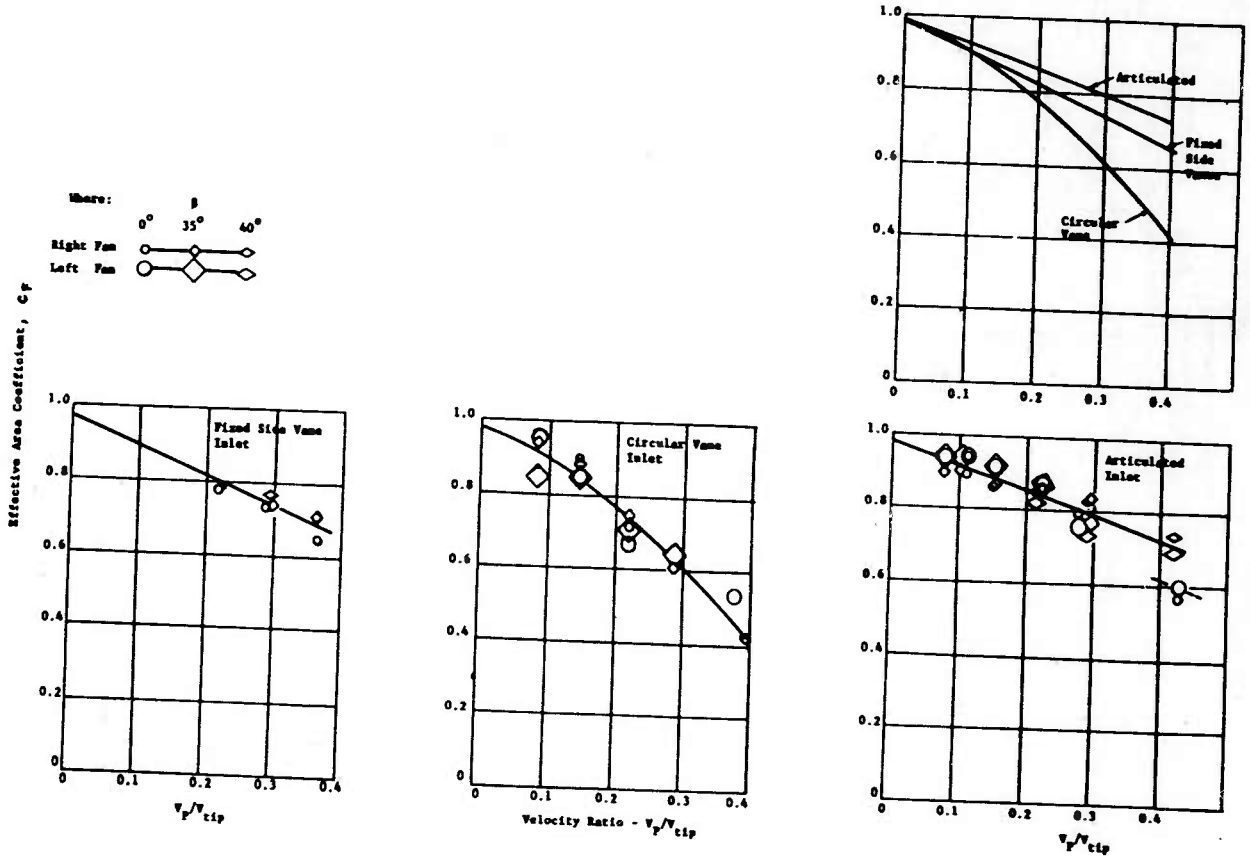


FIGURE 57 - EFFECTIVE AREA COEFFICIENT VERSUS VELOCITY RATIO

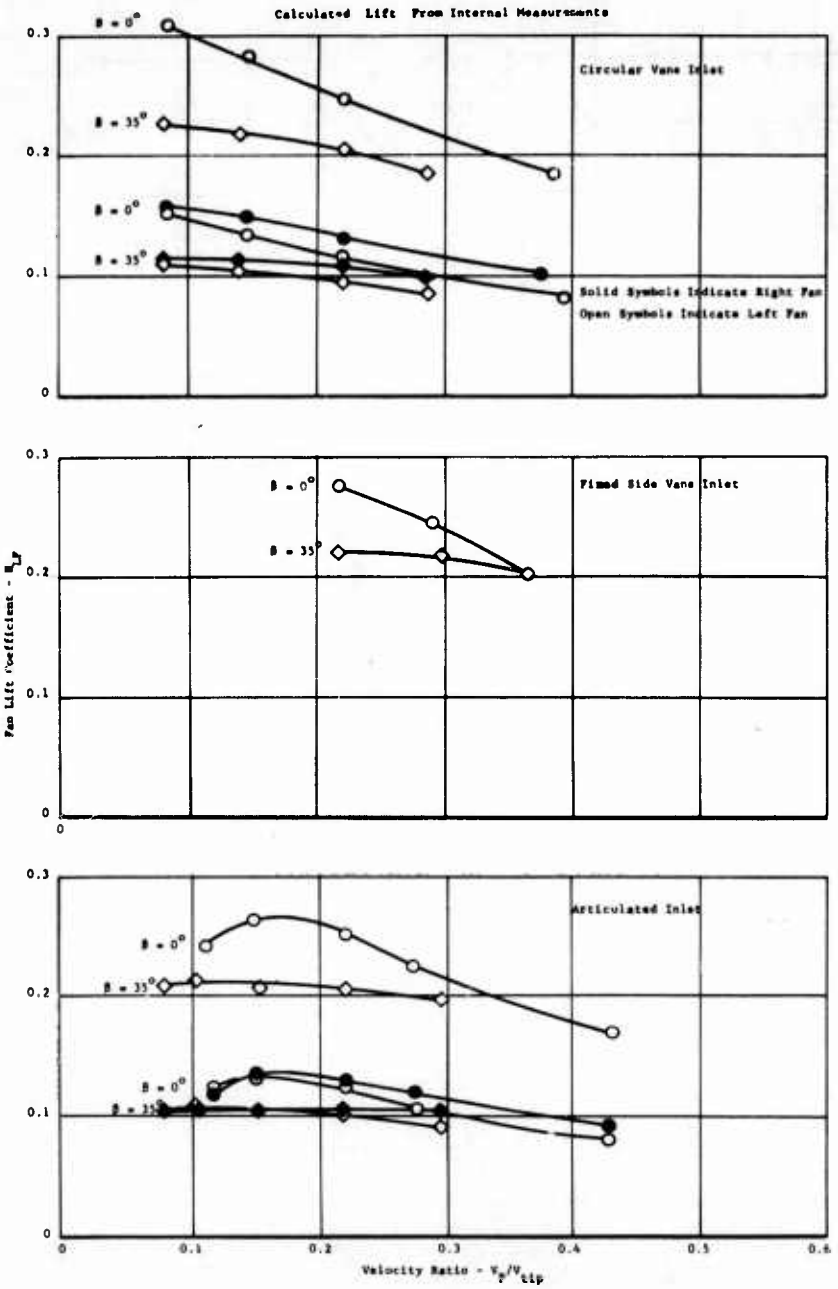


FIGURE 58 - FAN LIFT COEFFICIENT VERSUS VELOCITY RATIO

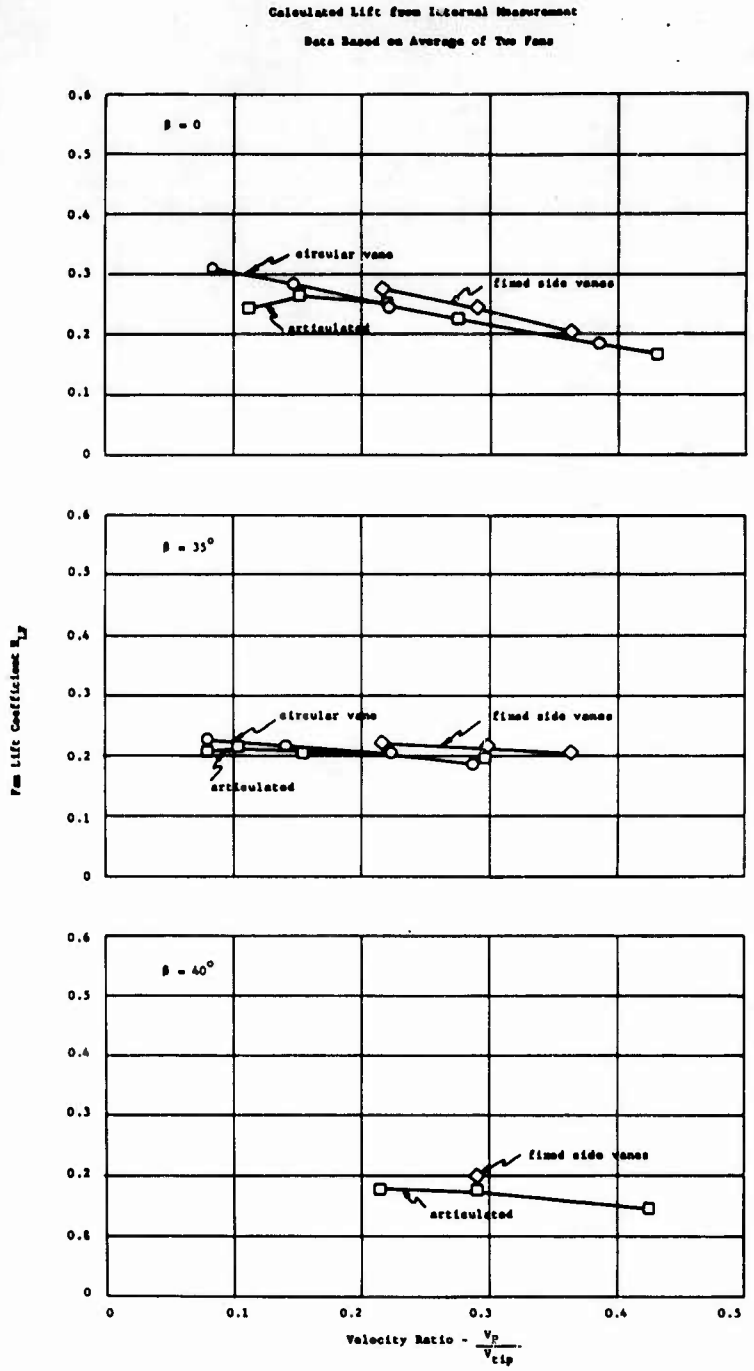


FIGURE 59 - FAN LIFT COEFFICIENT VERSUS VELOCITY RATIO

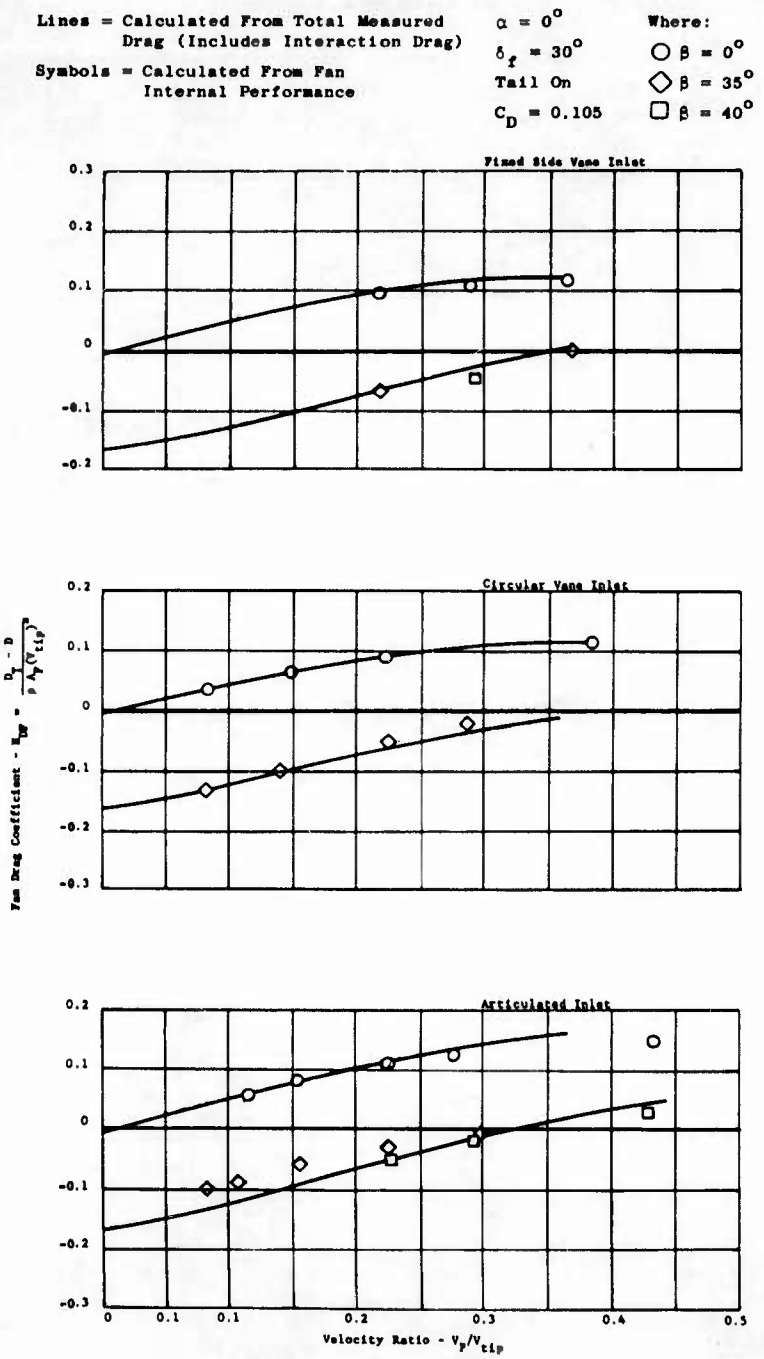


FIGURE 60 - FAN DRAG COEFFICIENT VERSUS VELOCITY RATIO

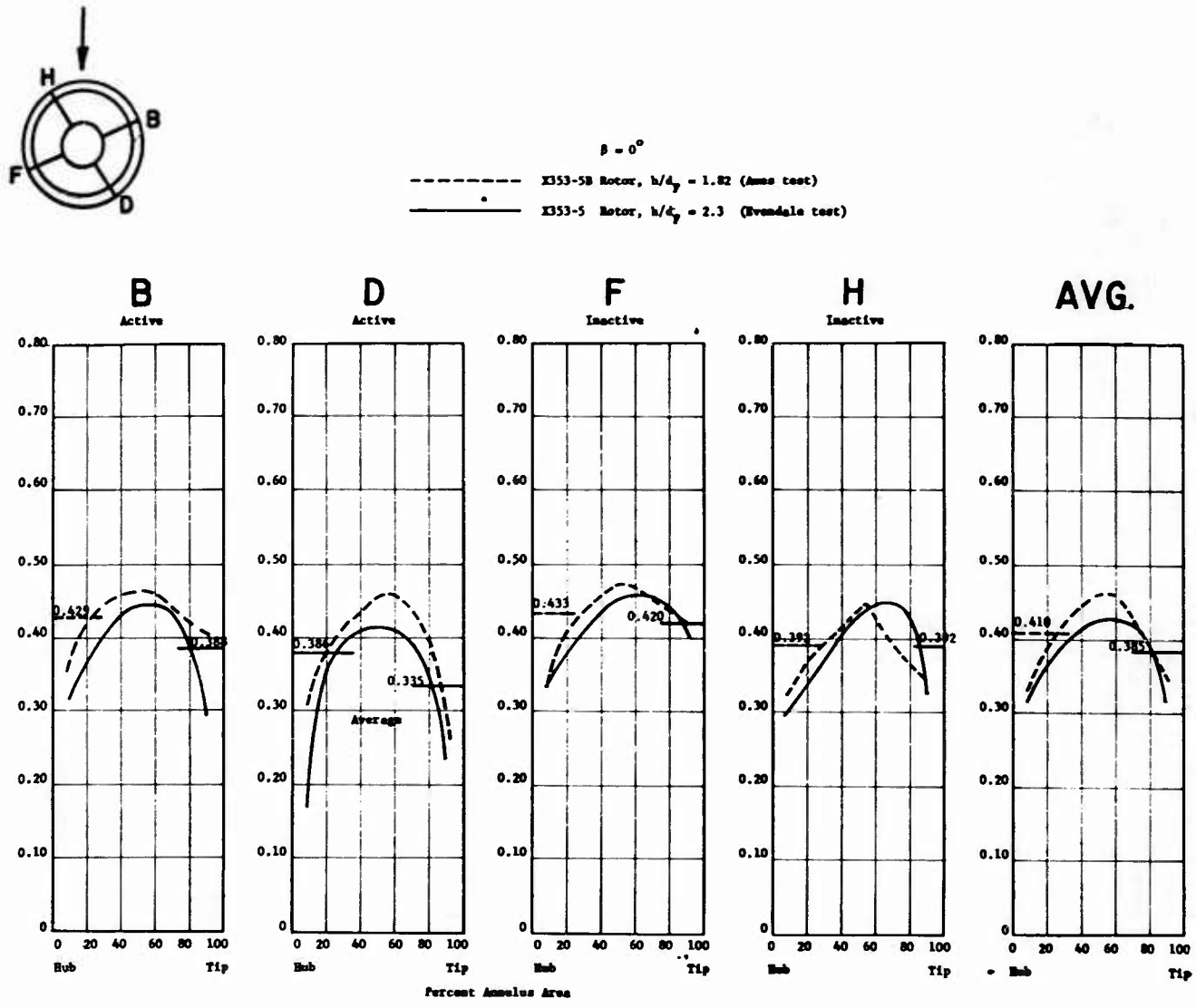


FIGURE 61 - PRESSURE COEFFICIENT VERSUS PERCENT ANNULUS AREA

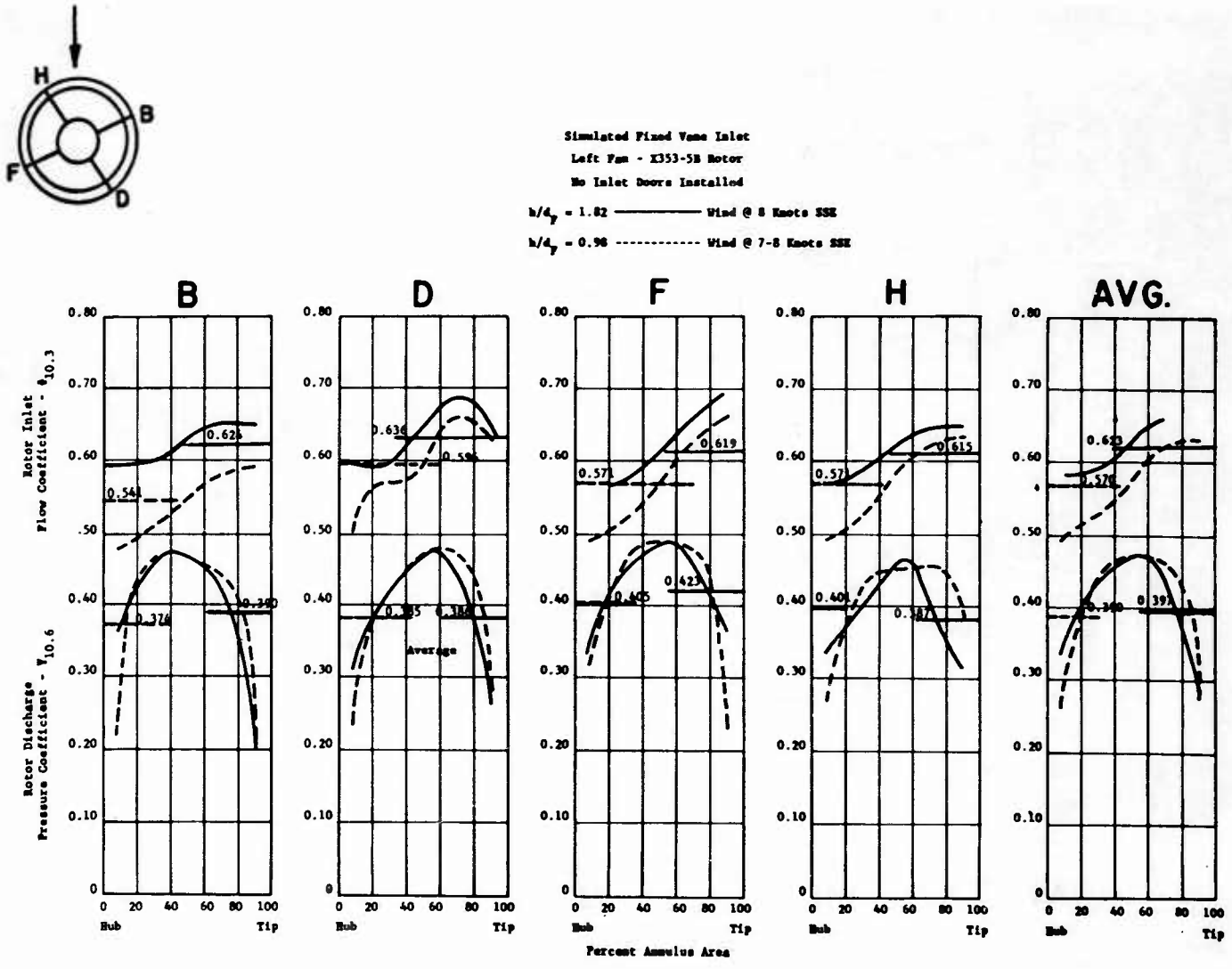


FIGURE 62 - PRESSURE AND FLOW COEFFICIENTS VERSUS PERCENT ANNULUS AREA

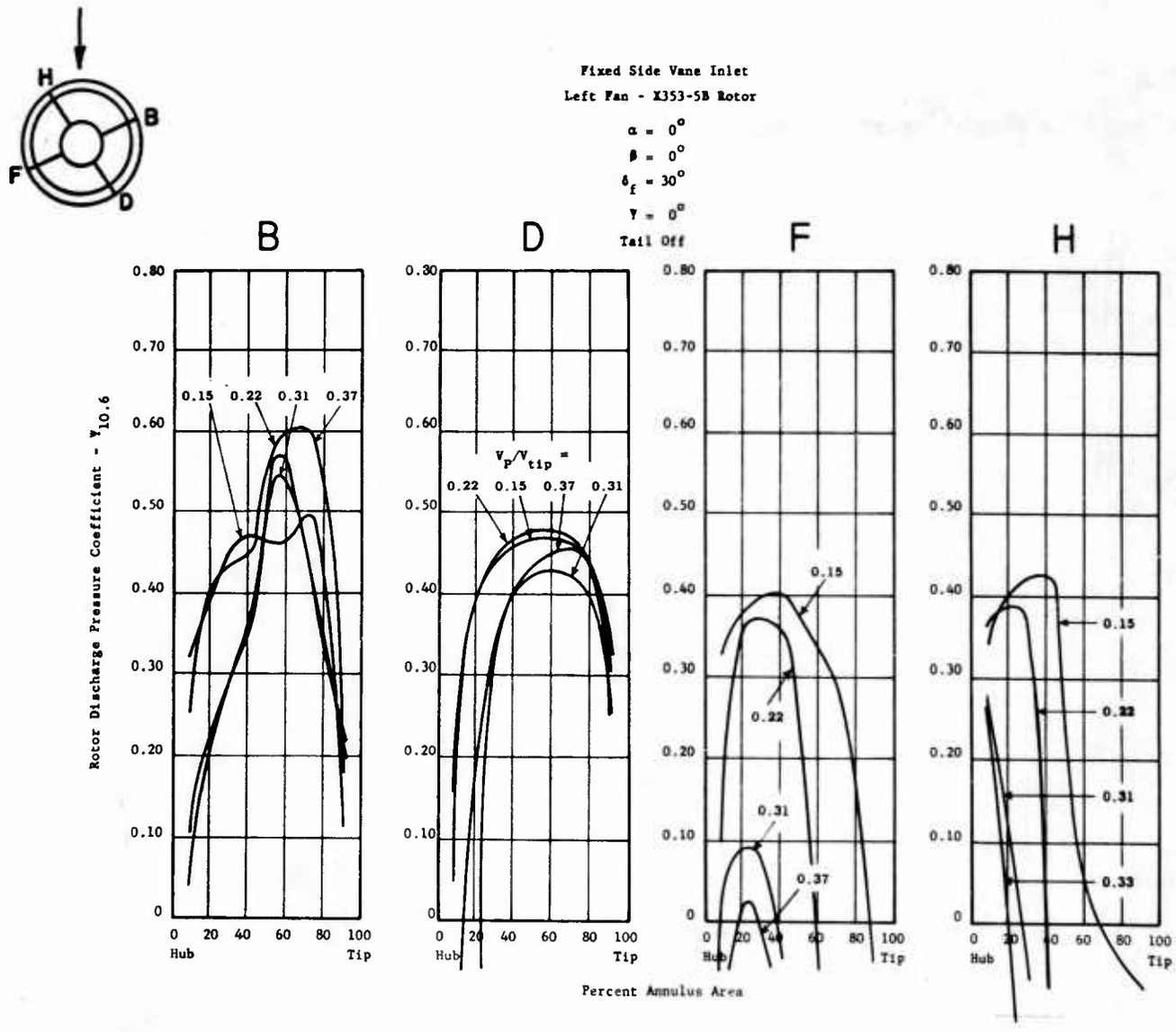


FIGURE 63. PRESSURE COEFFICIENT VERSUS PERCENT ANNULUS AREA

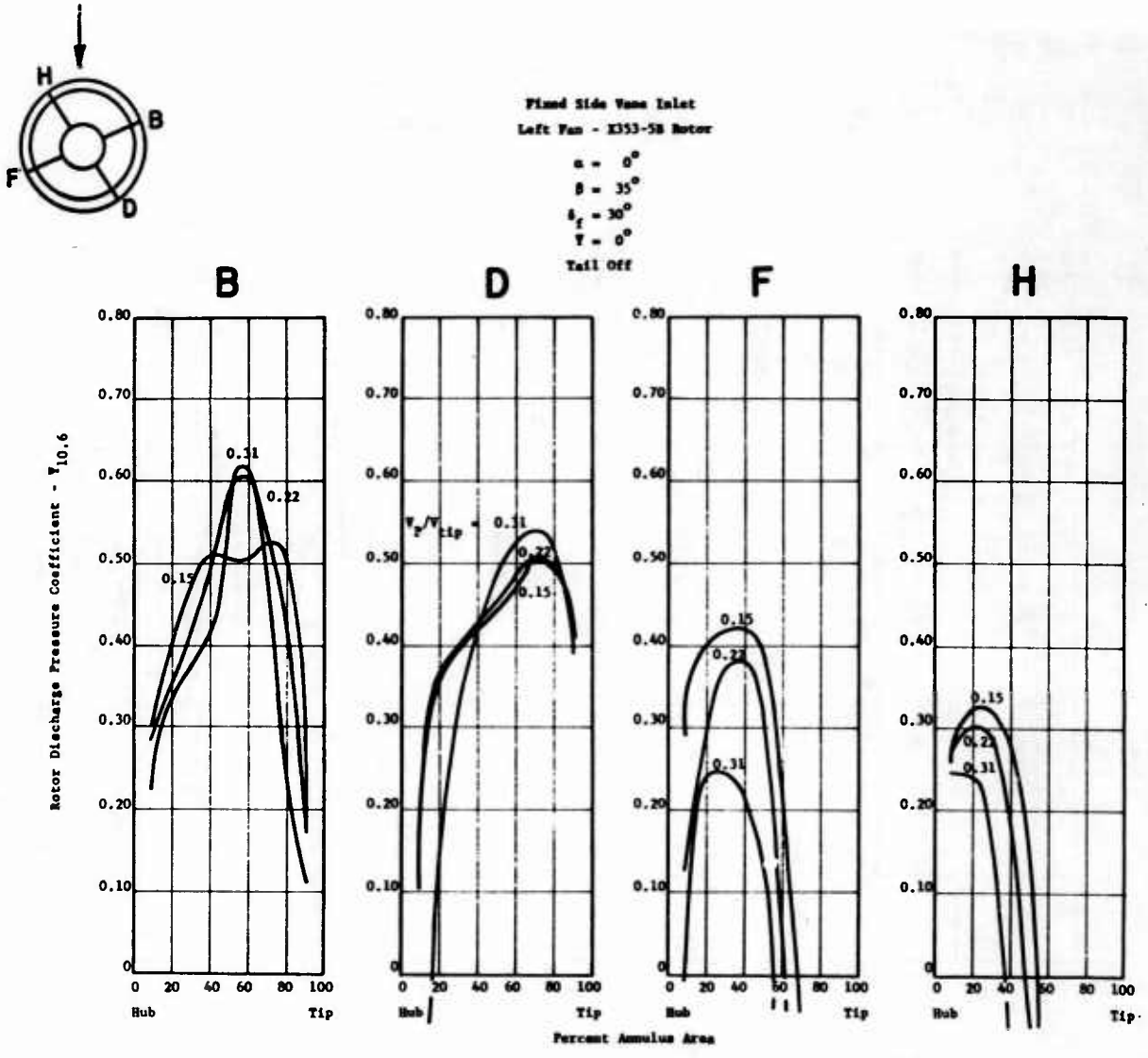


FIGURE 64 - PRESSURE COEFFICIENT VERSUS PERCENT ANNULUS AREA

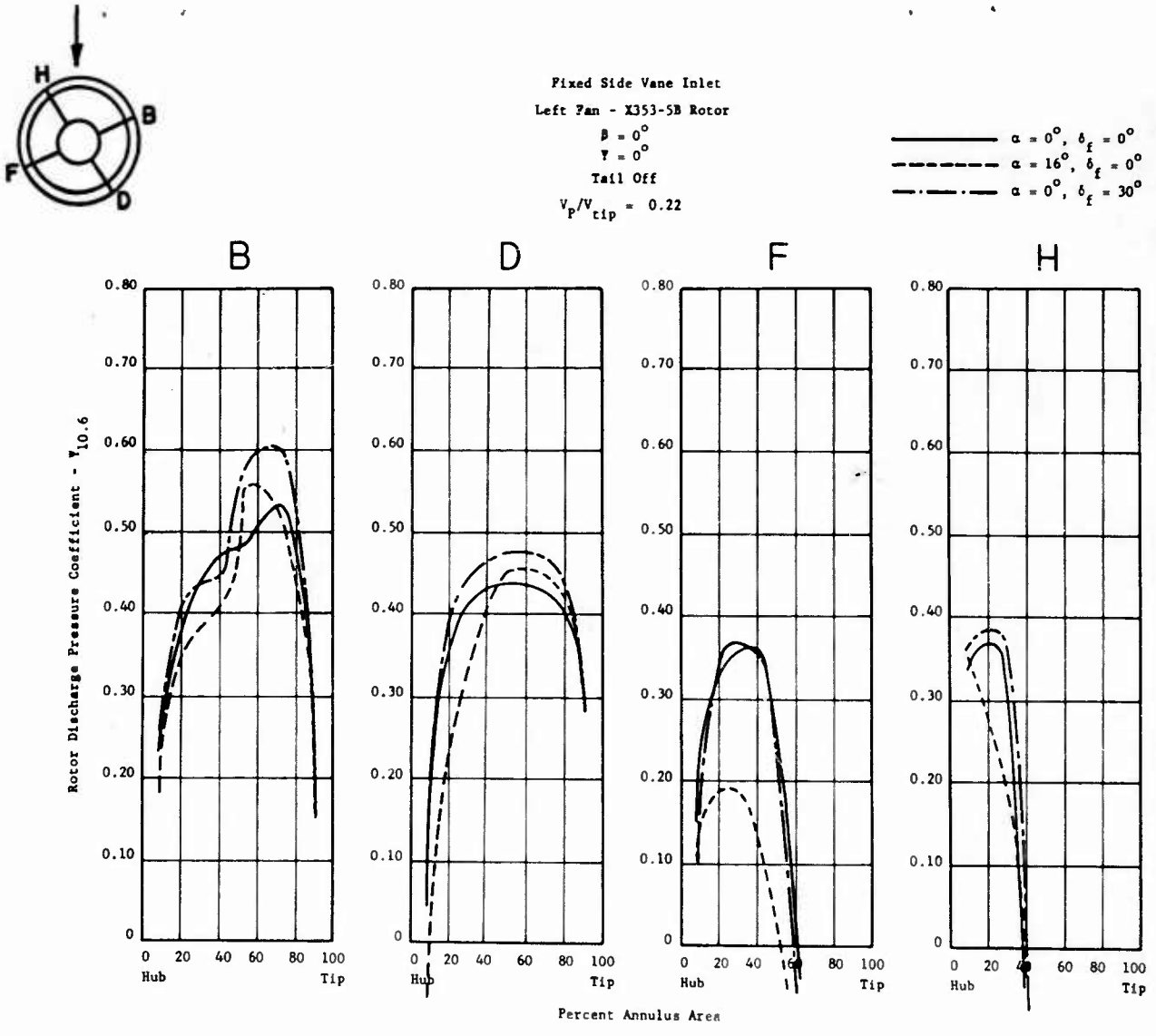


FIGURE 65a. PRESSURE COEFFICIENT VERSUS PERCENT ANNULUS AREA

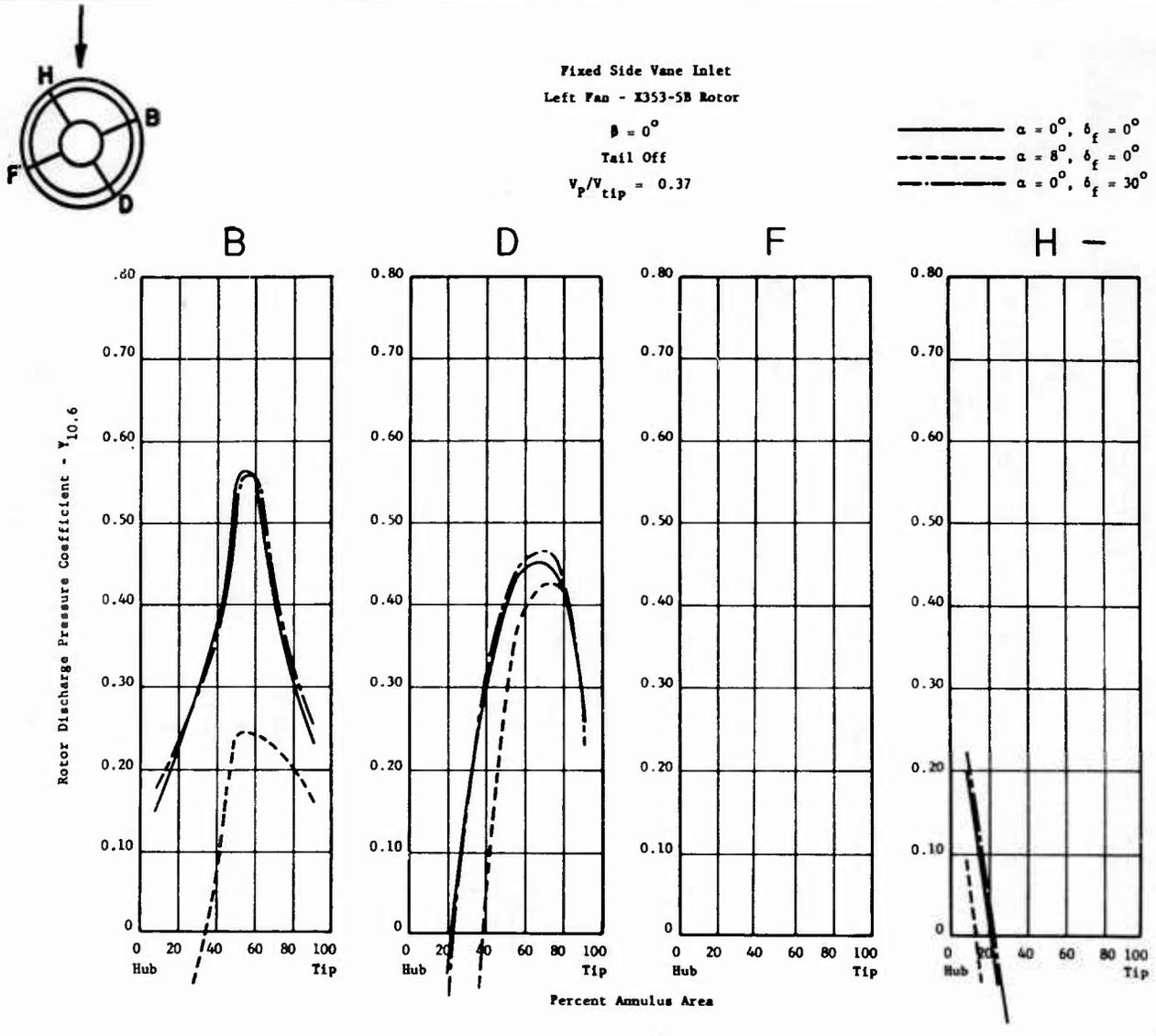
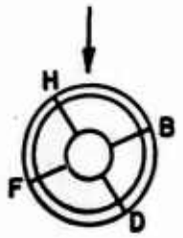


FIGURE 65b. PRESSURE COEFFICIENT VERSUS PERCENT ANNULUS AREA



Fixed Side Vane Inlet
Left Fan - X353-5B Rotor
$\alpha = 0^\circ$
$\beta = 0^\circ$
$\delta_f = 30^\circ$
Tail Off
$V_p/V_{tip} = 0.22$

$\Psi = 0^\circ$
$\Psi = -12^\circ$
$\Psi = +12^\circ$

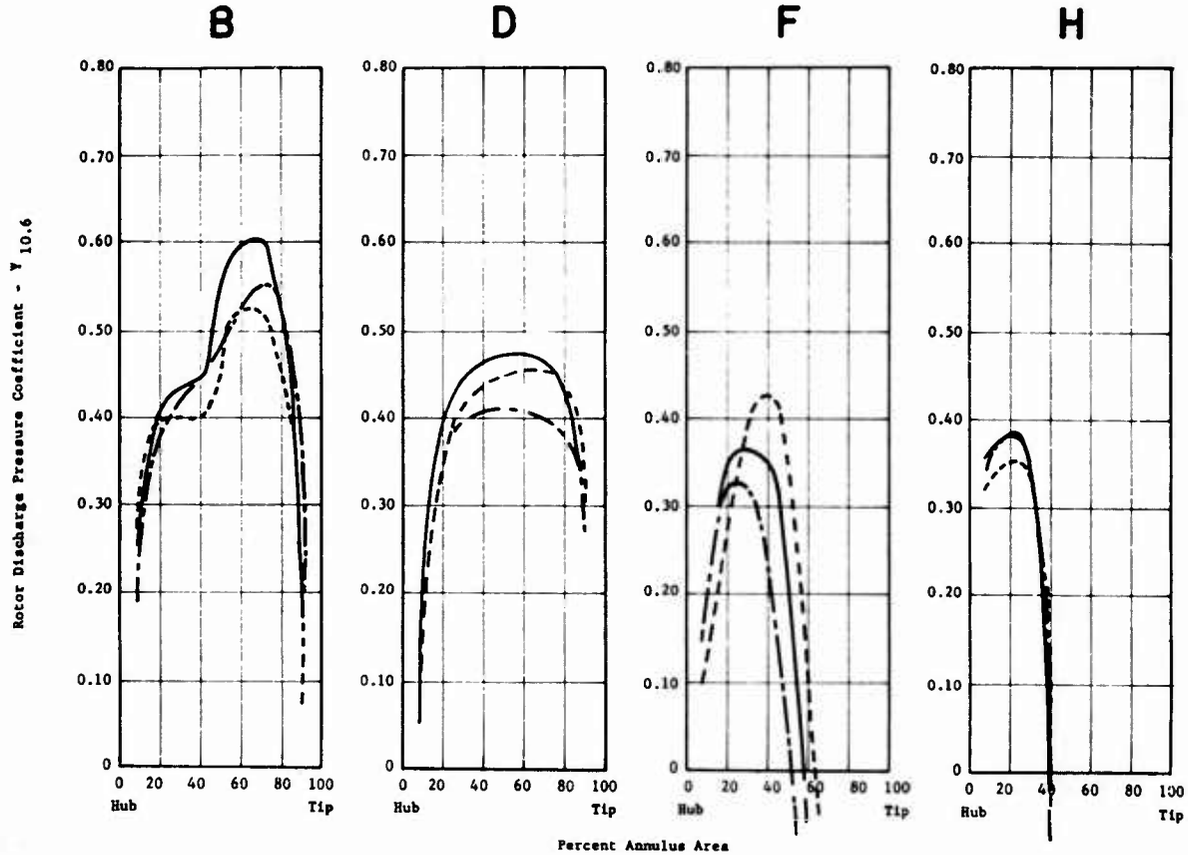
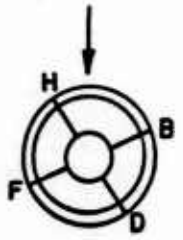


FIGURE 66 - PRESSURE COEFFICIENT VERSUS PERCENT ANNULUS AREA



Simulated Fixed Vane Inlet
Left Fan - X353-5B Rotor
Paired Doors Installed

h/d_T = 1.82 ——
h/d_T = 0.98 - - - -

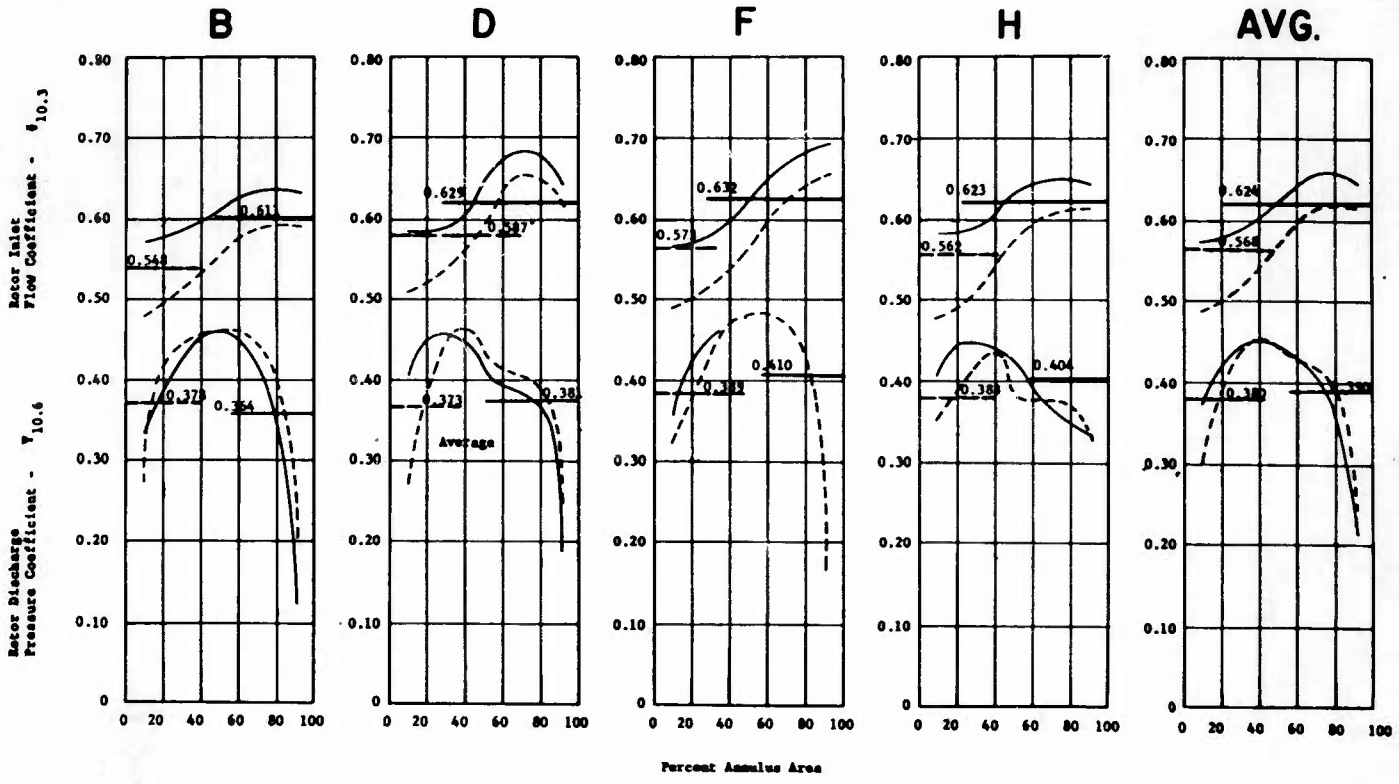


FIGURE 67 - PRESSURE AND FLOW COEFFICIENT VERSUS PERCENT ANNULUS AREA

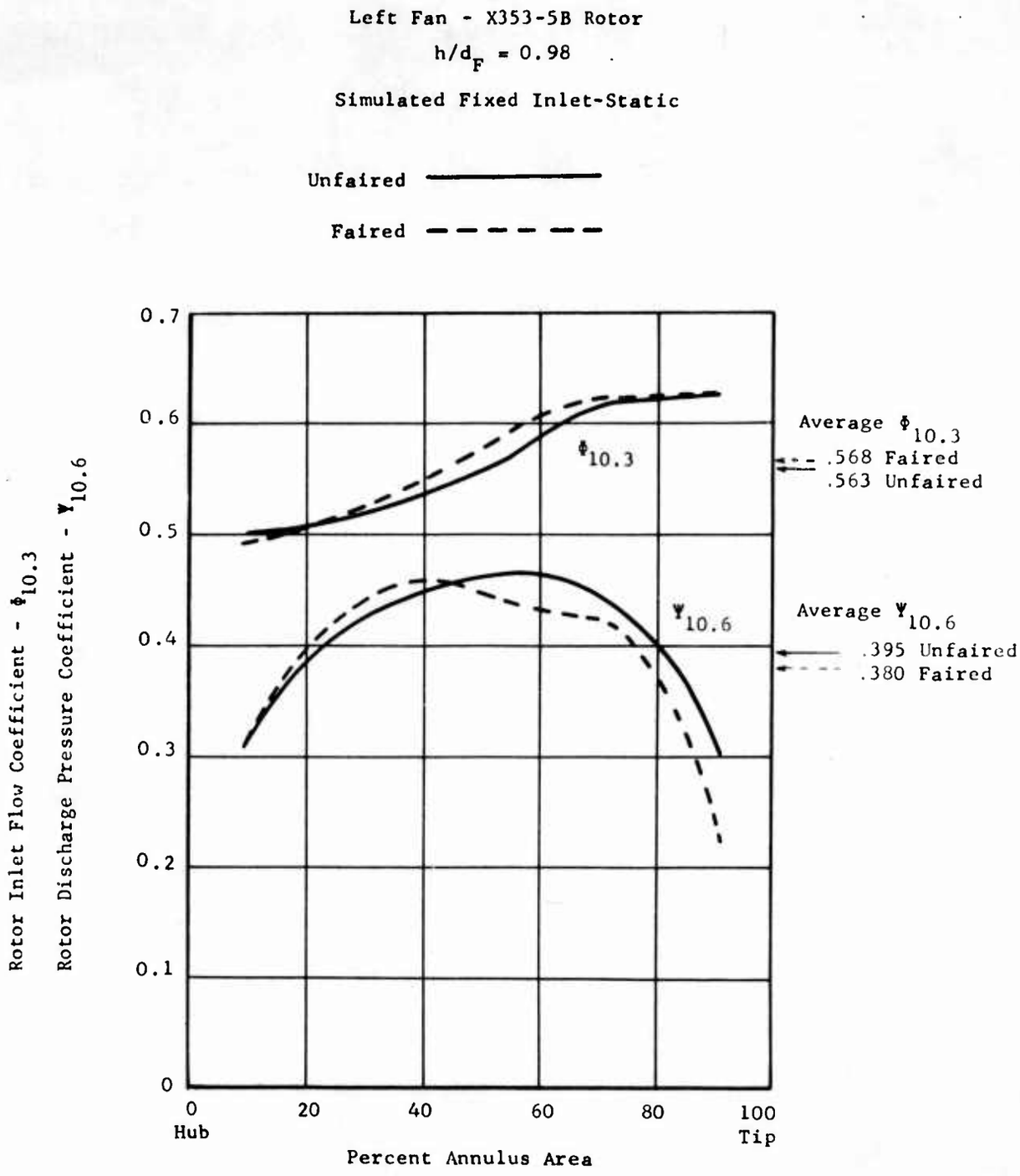


FIGURE 68 - PRESSURE AND FLOW COEFFICIENTS VERSUS ANNULUS AREA FOR FAIRED AND UNFAIRED CLOSURE DOORS.

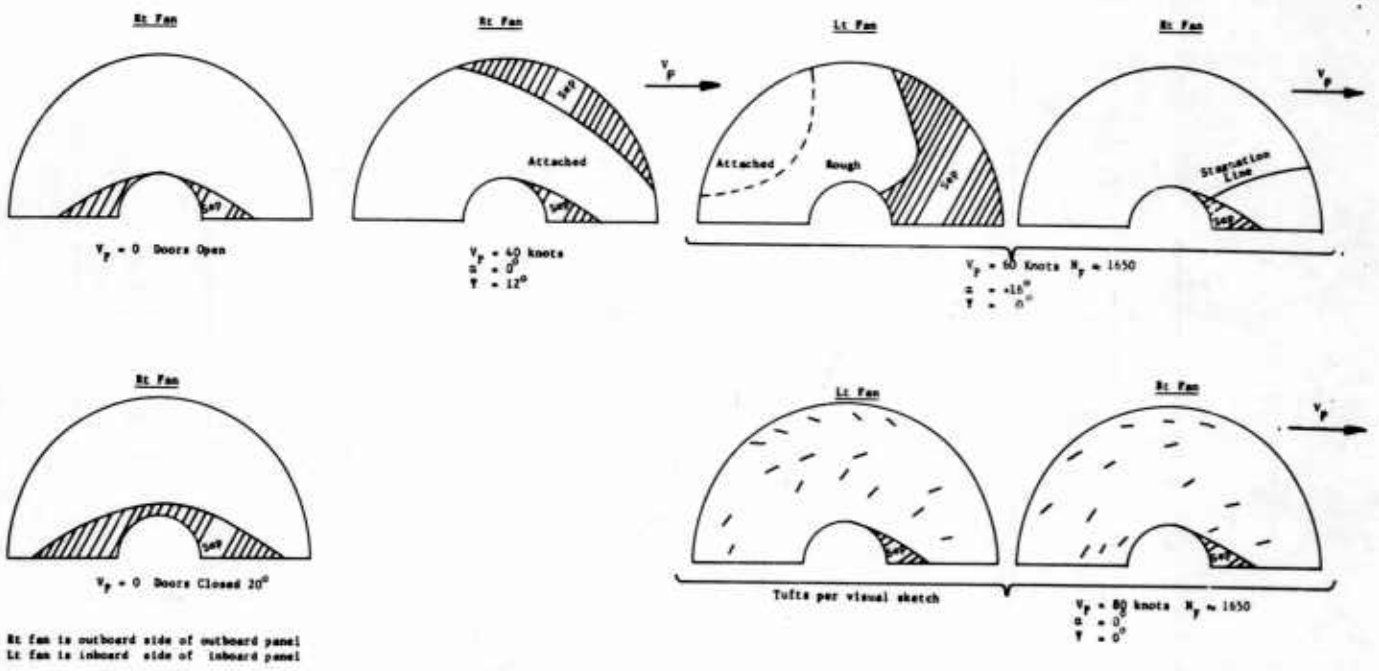


FIGURE 69 - FLOW AT FAIRED DOORS FROM TUFT OBSERVATIONS

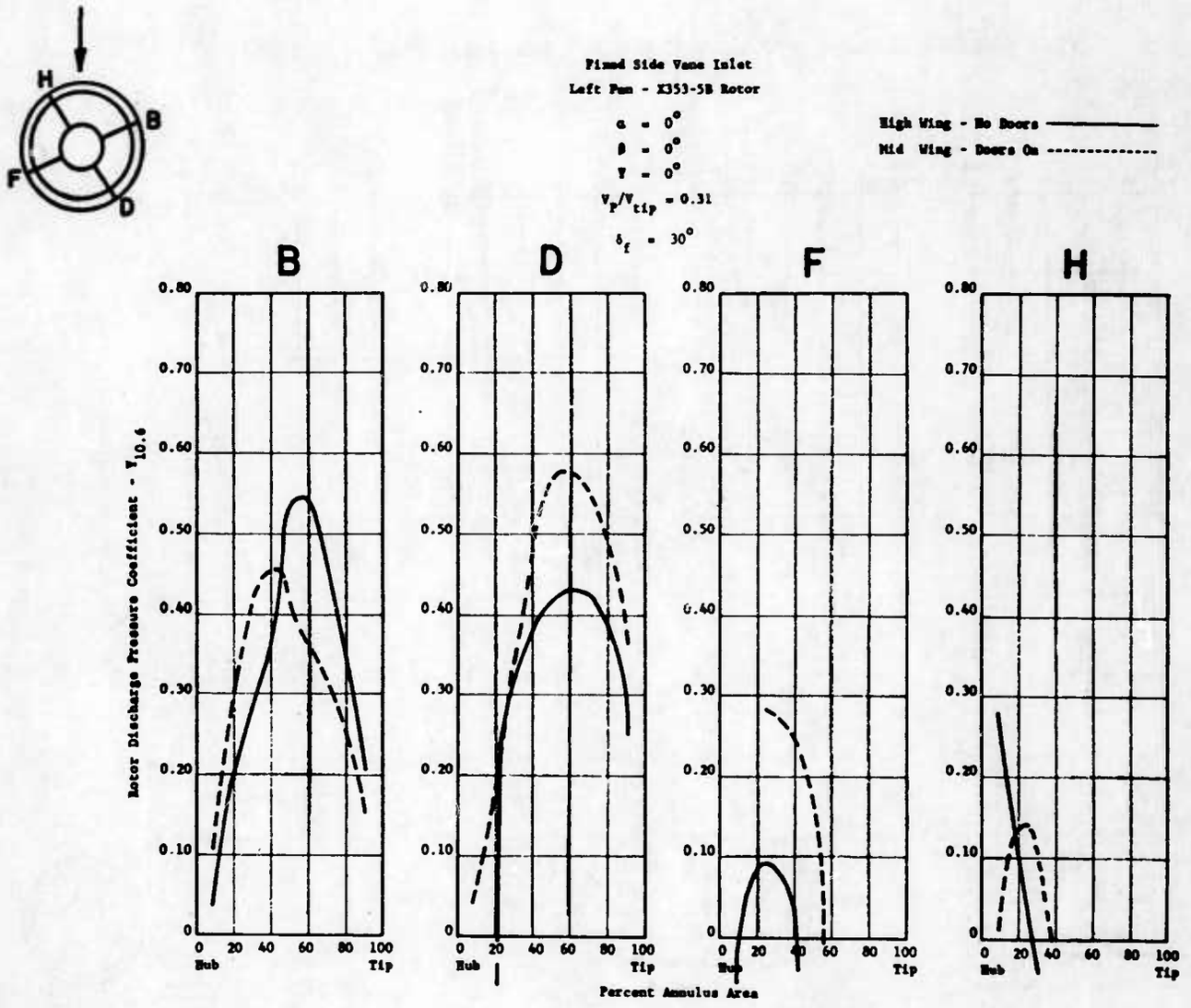


FIGURE 70 - PRESSURE COEFFICIENT VERSUS PERCENT ANNULUS AREA

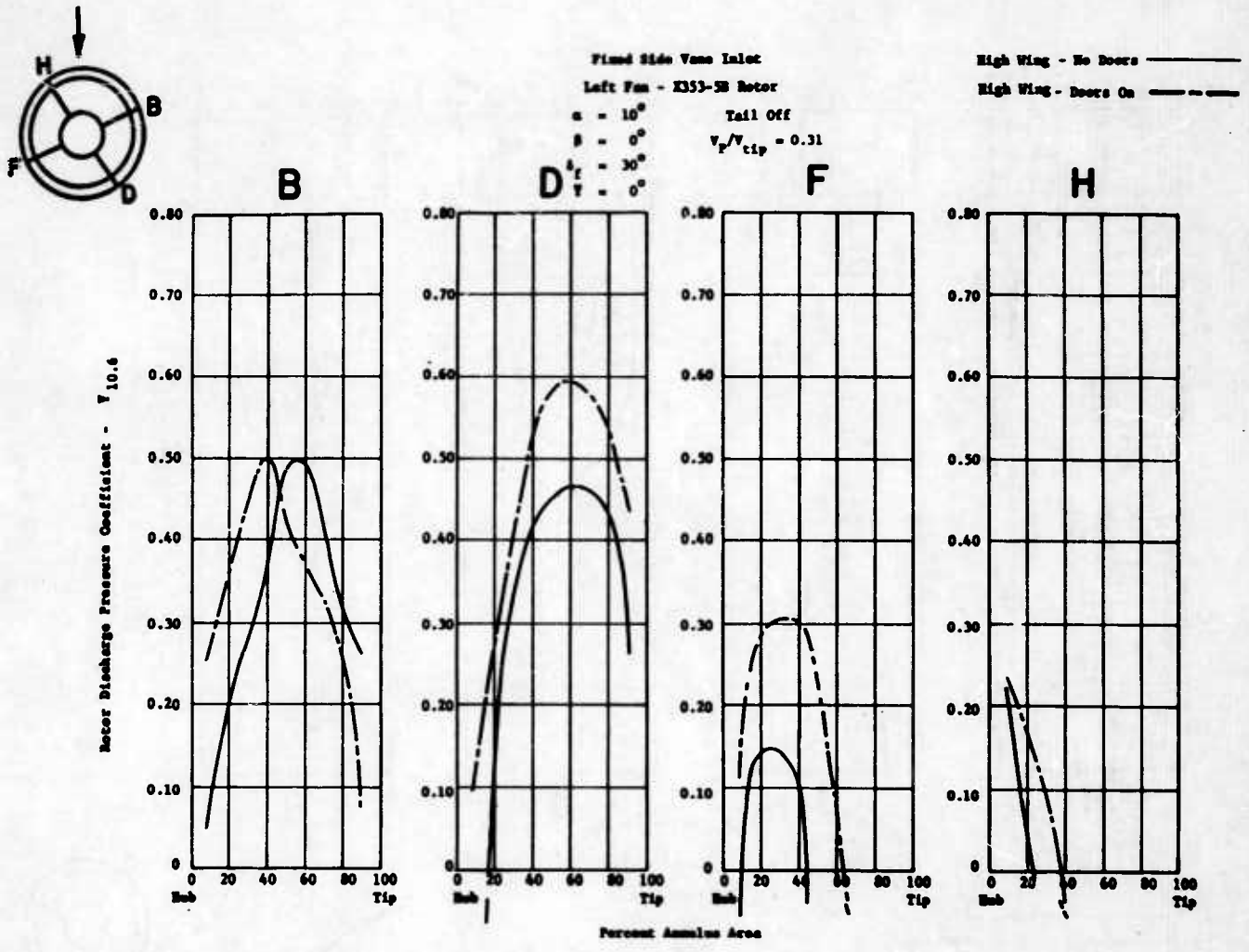


FIGURE 71 - PRESSURE COEFFICIENT VERSUS PERCENT ANNULUS AREA

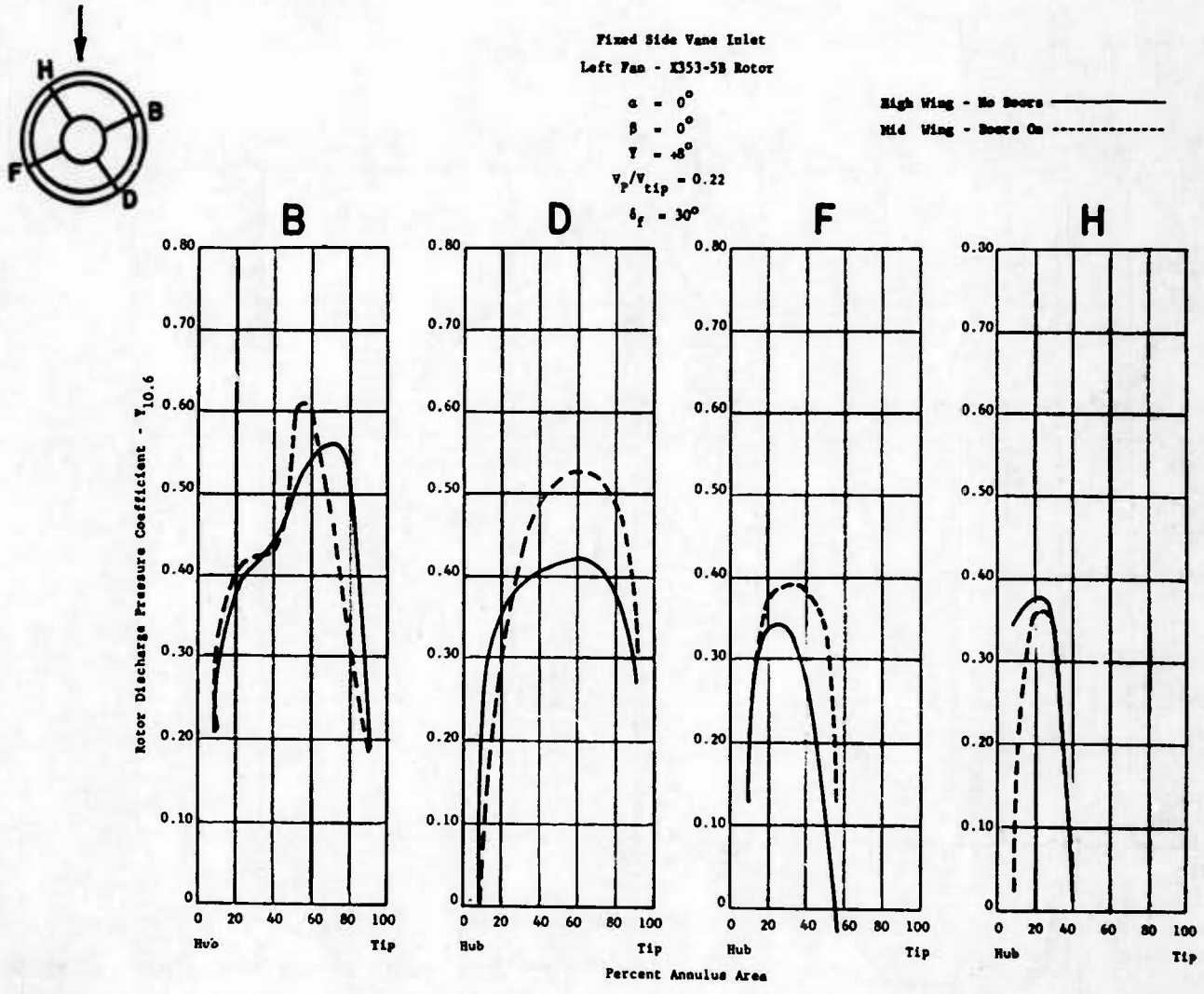


FIGURE 72 - PRESSURE COEFFICIENT VERSUS PERCENT ANNULUS AREA

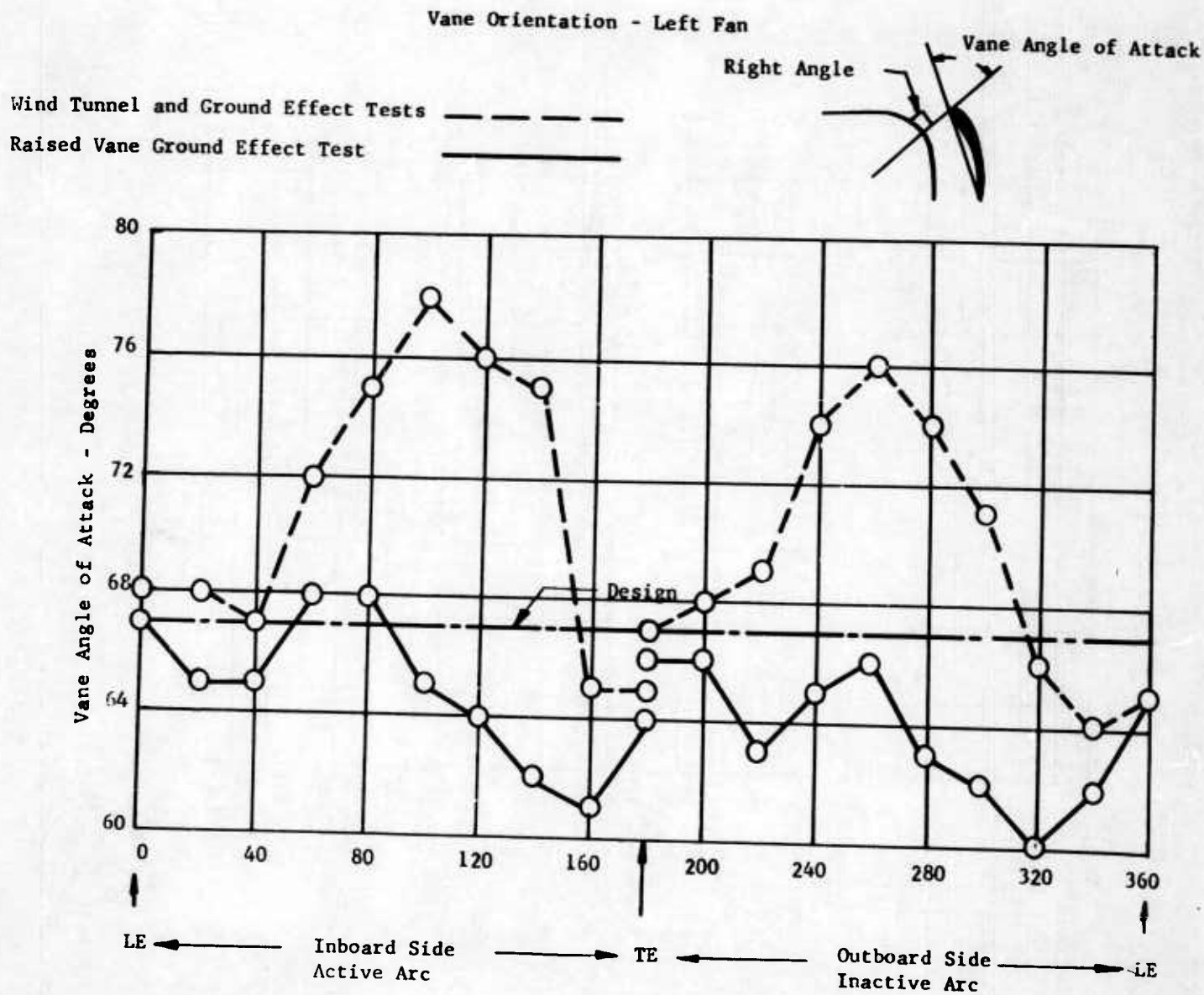
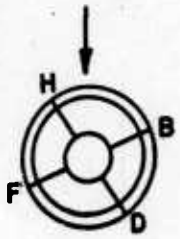


FIGURE 73 - INLET VANE ANGLE OF ATTACK



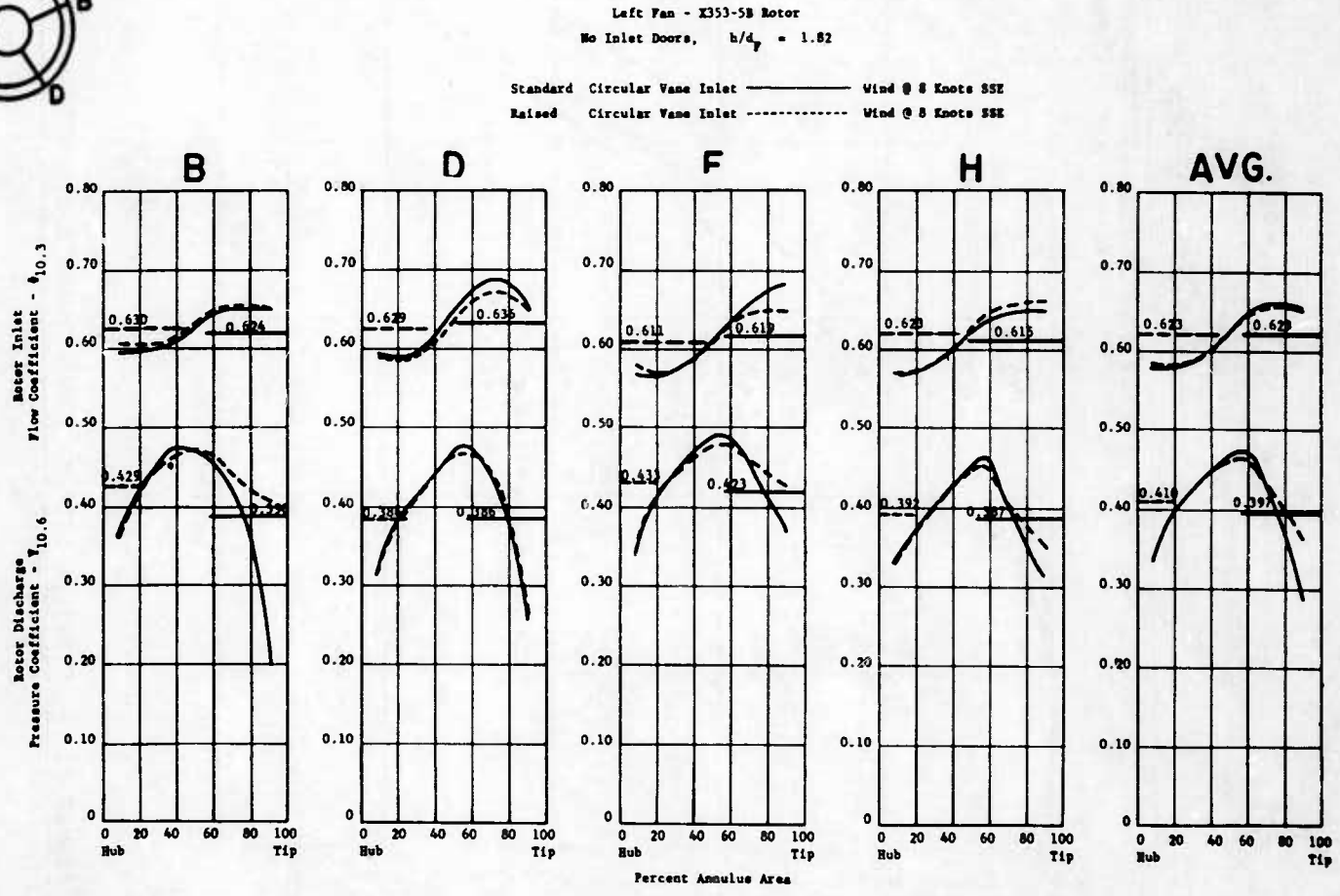


FIGURE 74 - PRESSURE AND FLOW COEFFICIENT VERSUS PERCENT ANNULUS AREA

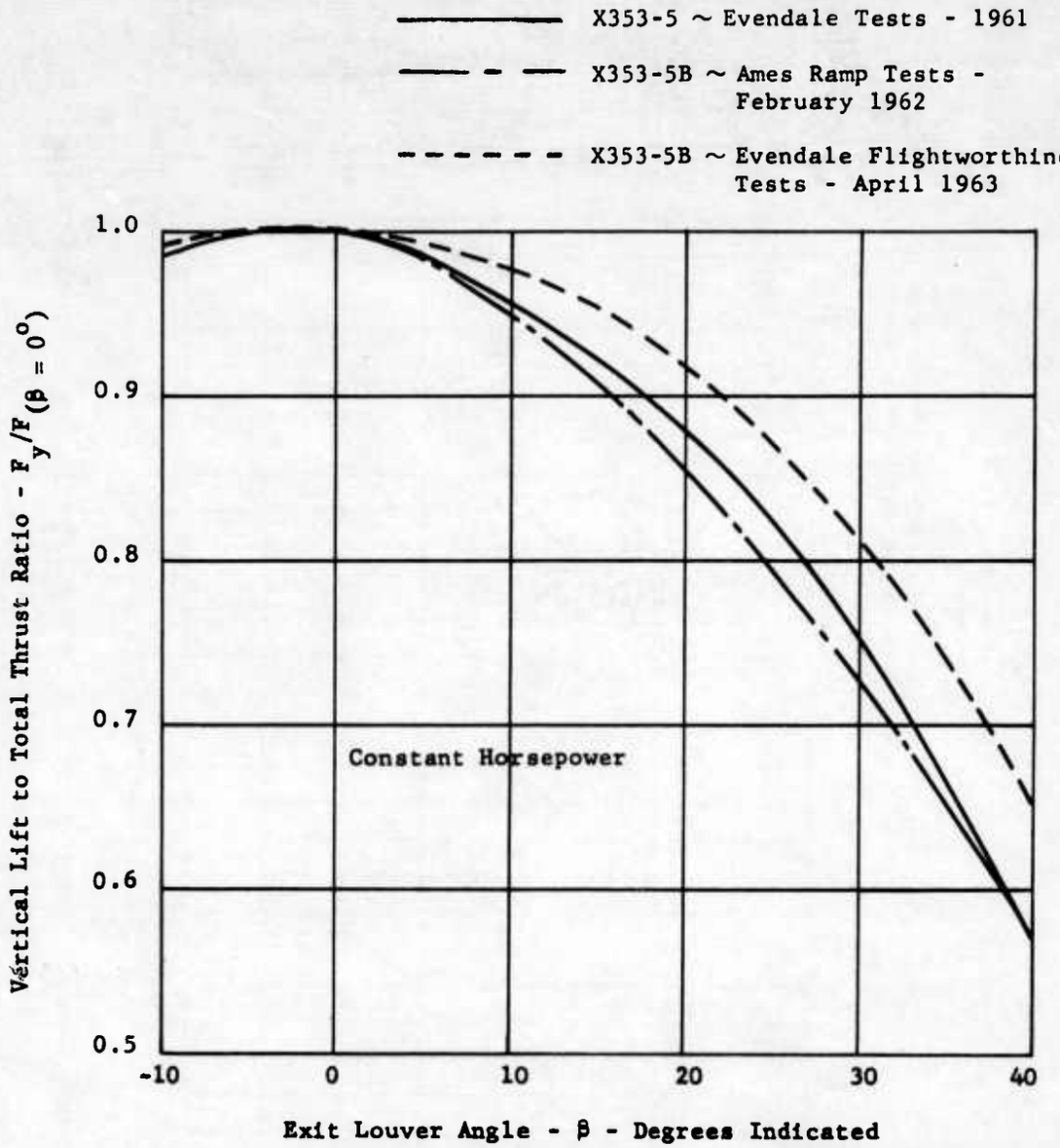


FIGURE 75 - VERTICAL LIFT TO TOTAL THRUST RATIO VERSUS EXIT LOUVER ANGLE (STATIC)

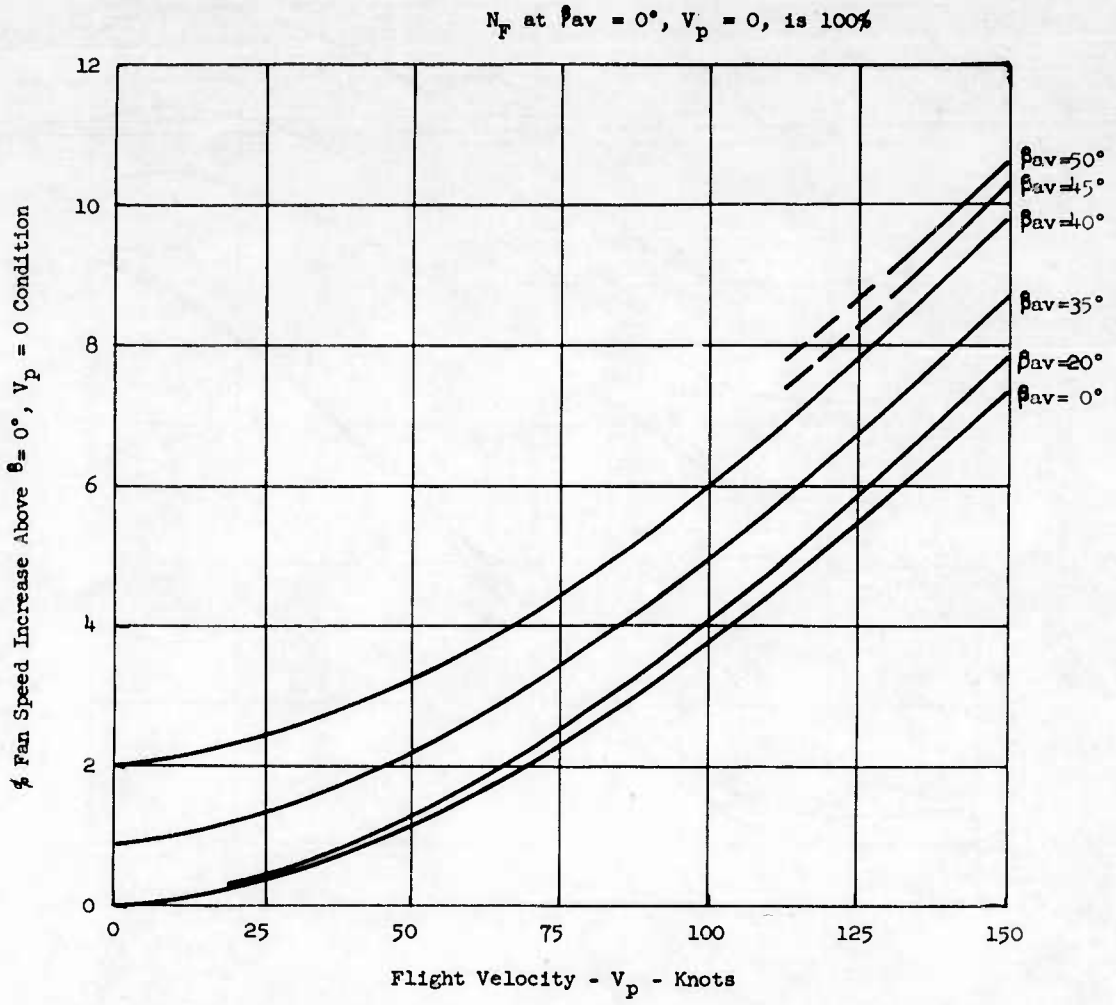


FIGURE 76. FAN SPEED CHANGE AT CONSTANT THROTTLE VERSUS FLIGHT VELOCITY AND EXIT LOUVER ANGLE FOR THE X353-5 FAN IN THE LEFT WING

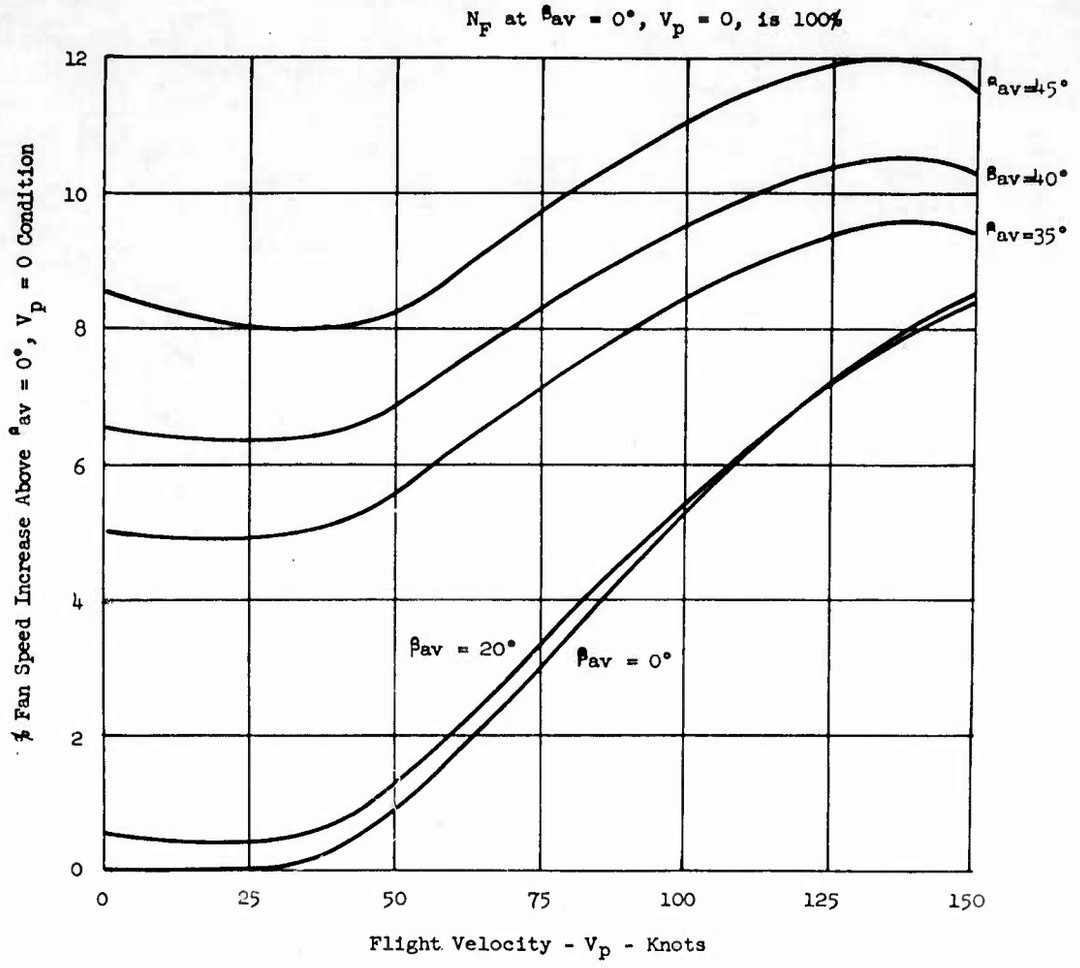


FIGURE 77a. FAN SPEED CHANGE AT CONSTANT THROTTLE VERSUS FLIGHT VELOCITY AND EXIT LOUVER ANGLE FOR THE X353-5B FAN IN THE LEFT WING

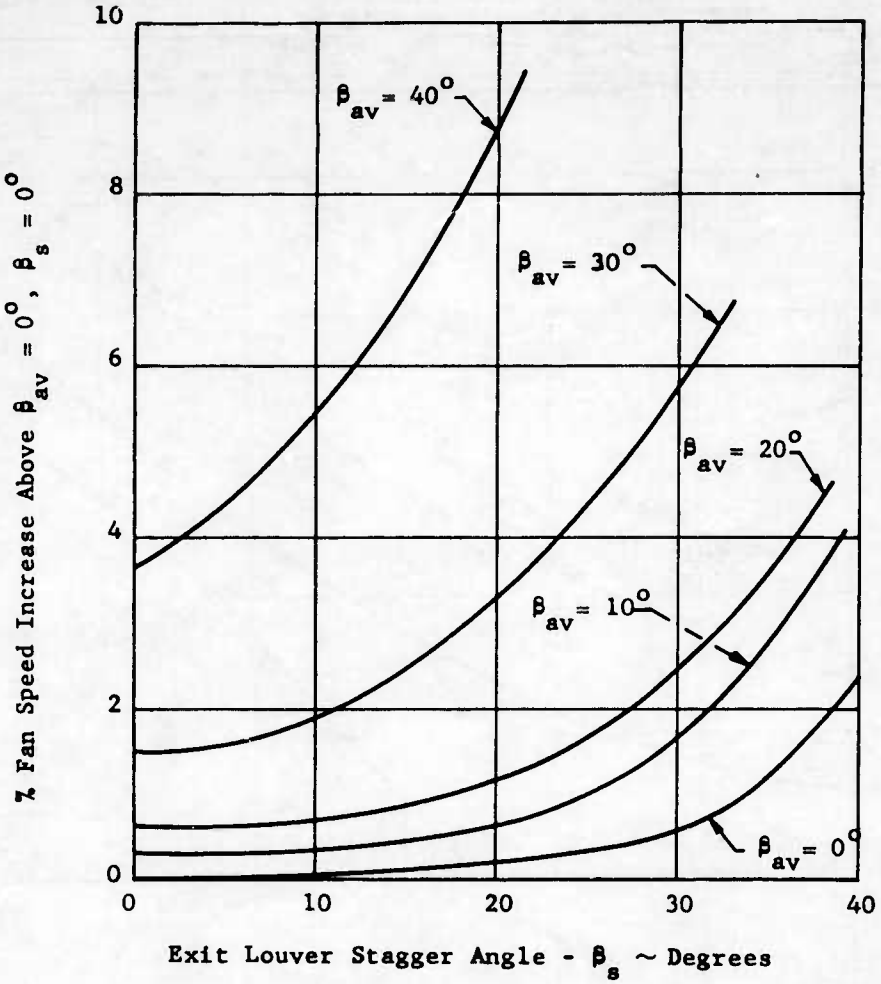


FIGURE 77b - HOVER FAN SPEED CHANGE AT CONSTANT THROTTLE VERSUS EXIT LOUVER VECTOR AND STAGGER ANGLES FOR THE X353-5B FAN (EVENDALE FLIGHTWORTHINESS TESTS)

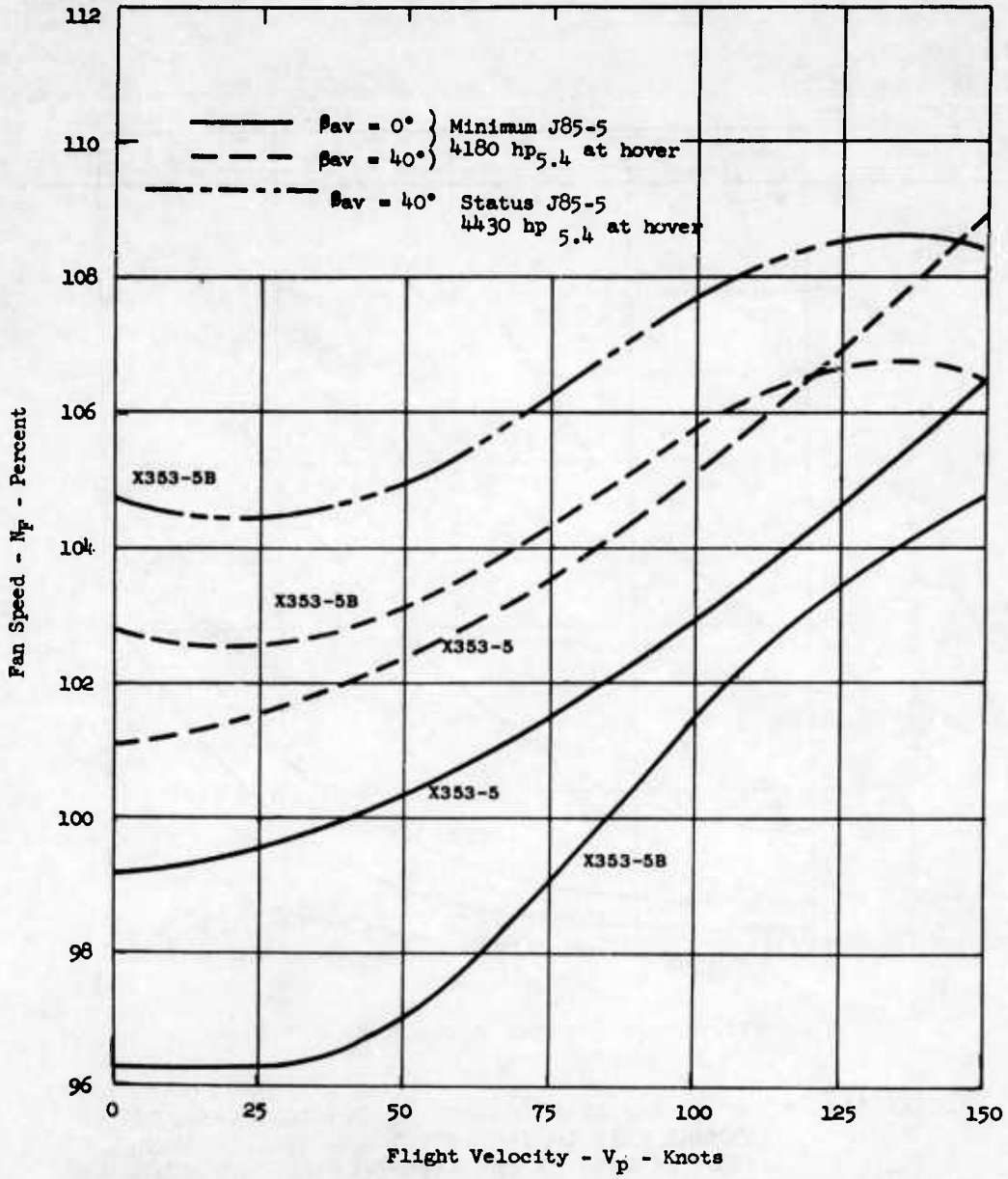


FIGURE 78. COMPARISON OF X353-5 AND X353-5B ROTOR FAN SPEED AS A FUNCTION OF FLIGHT SPEED AND EXIT LOUVER ANGLE

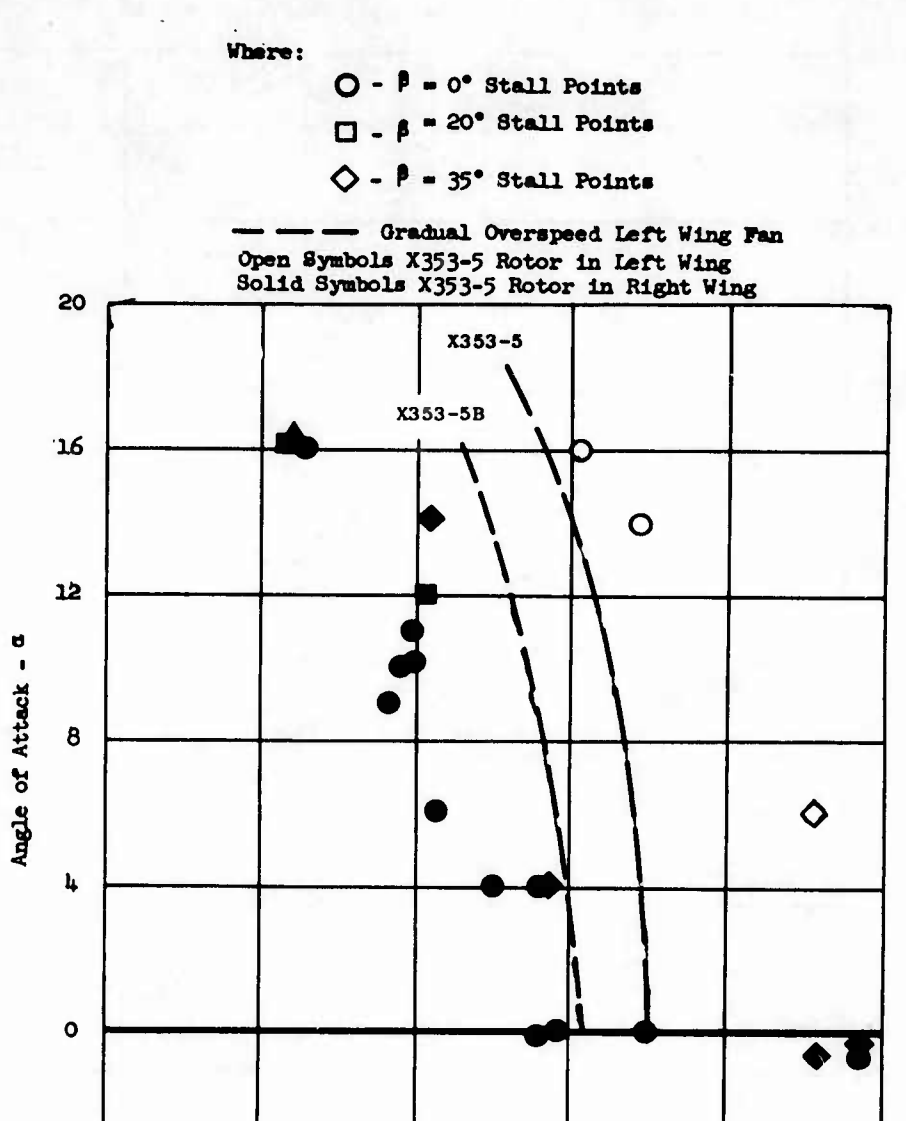


FIGURE 79. FAN STALL CHARACTERISTICS AS A FUNCTION OF VELOCITY RATIO AND ANGLE OF ATTACK

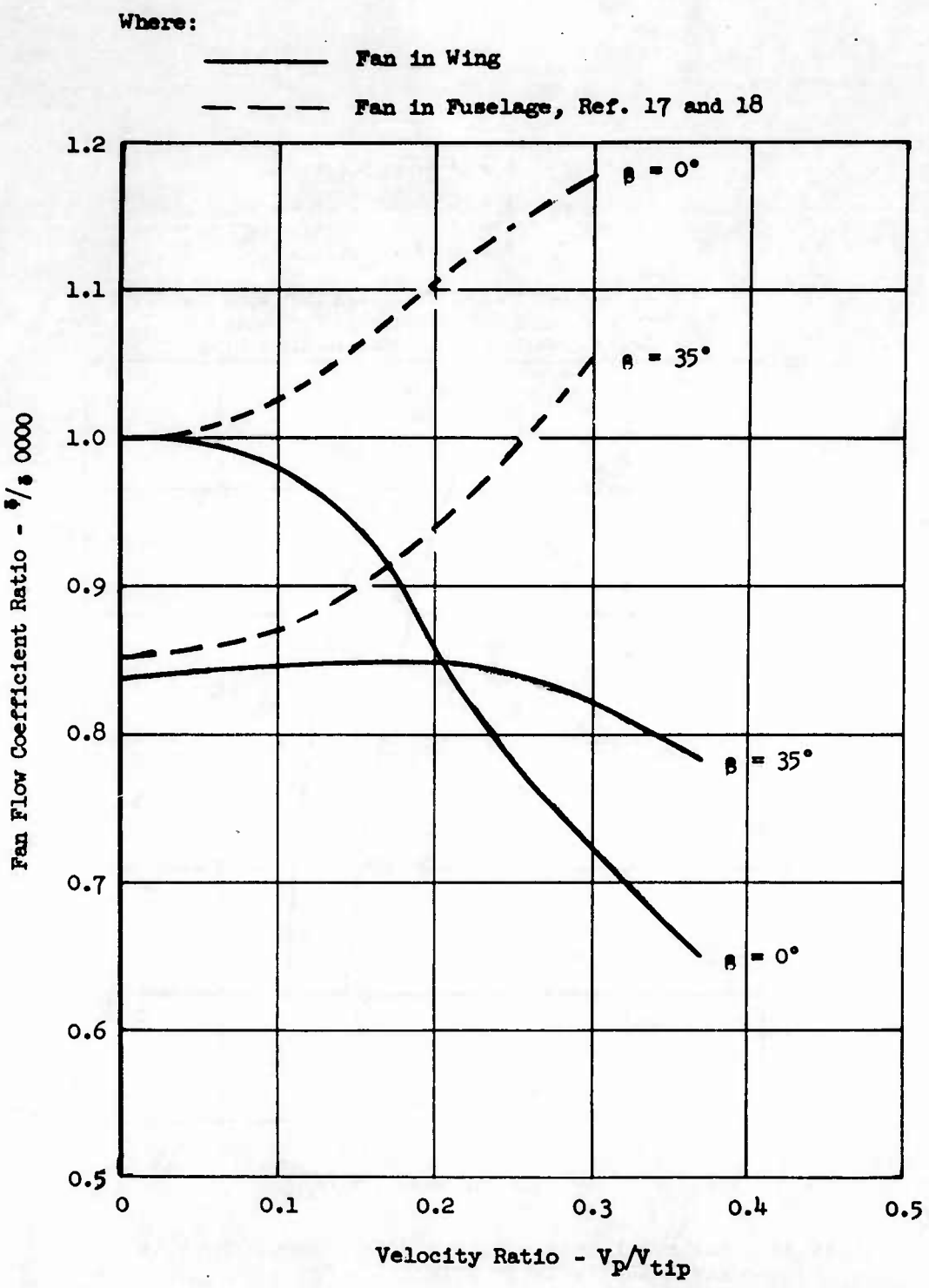


FIGURE 80. FAN FLOW COEFFICIENT RATIO VERSUS VELOCITY RATIO

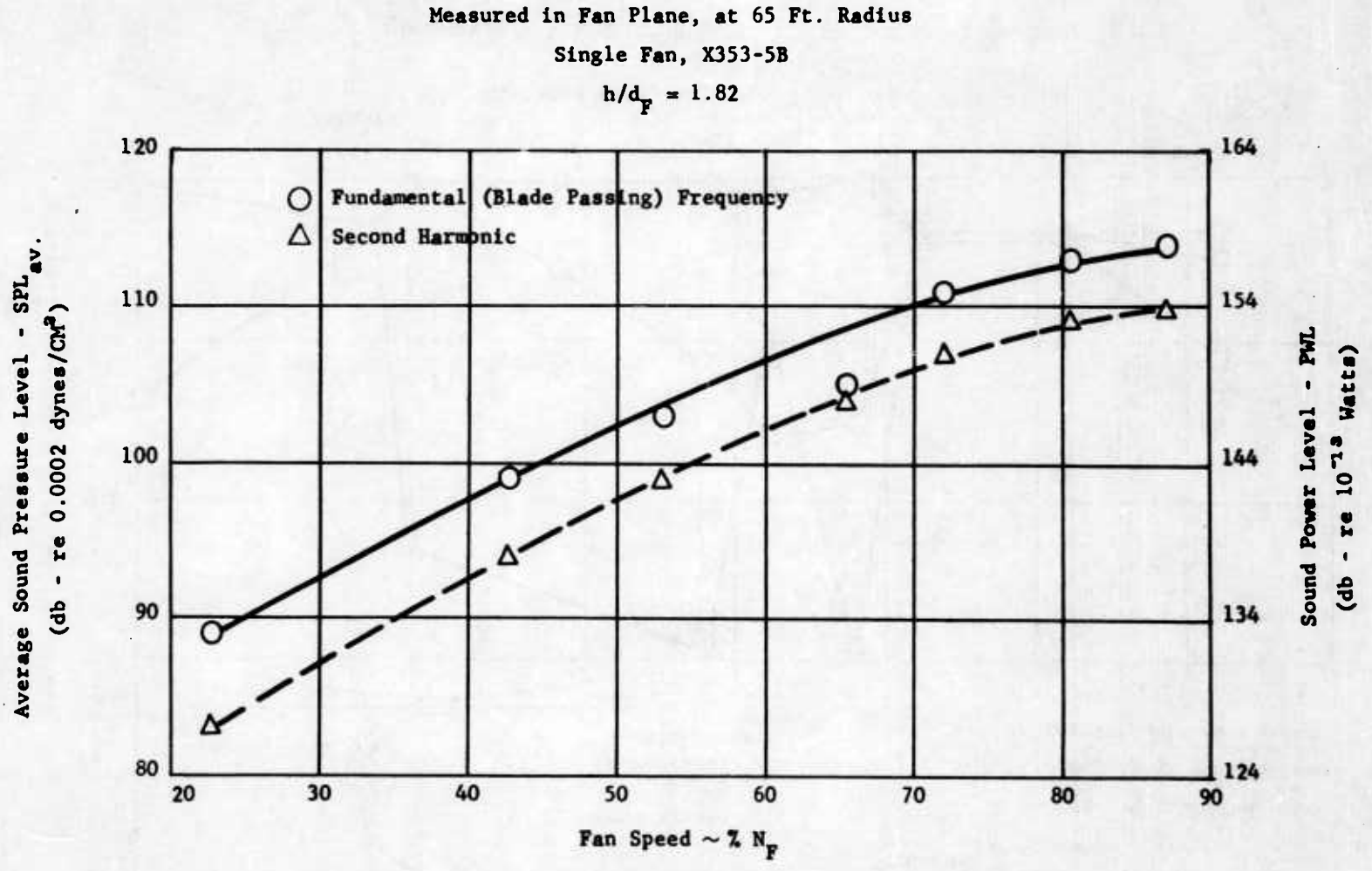


FIGURE 81 - SOUND LEVEL SURVEY DATA (RAMP TEST)

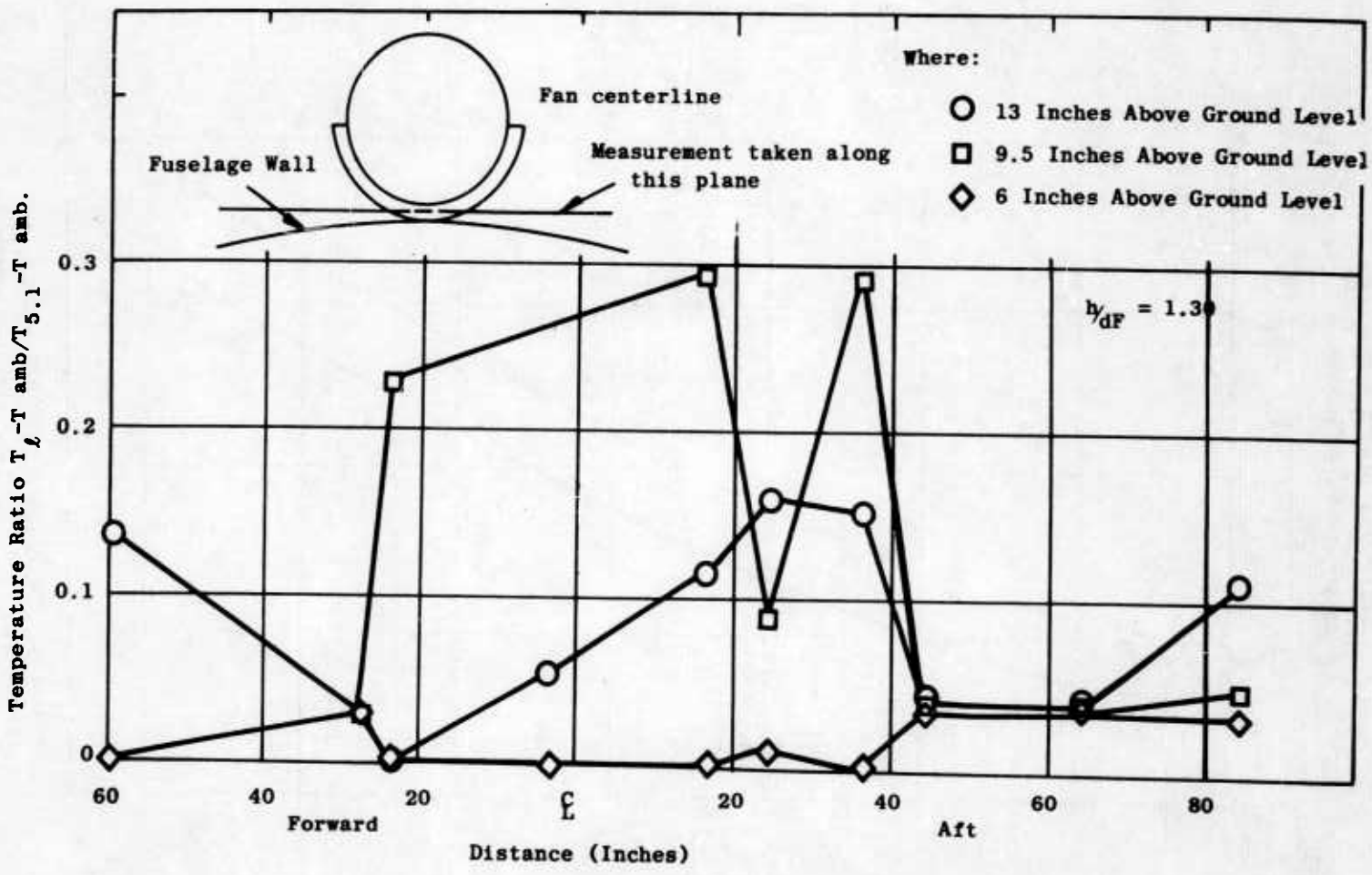


FIGURE 82a. TEMPERATURE RATIO VS. HEIGHT ABOVE GROUND

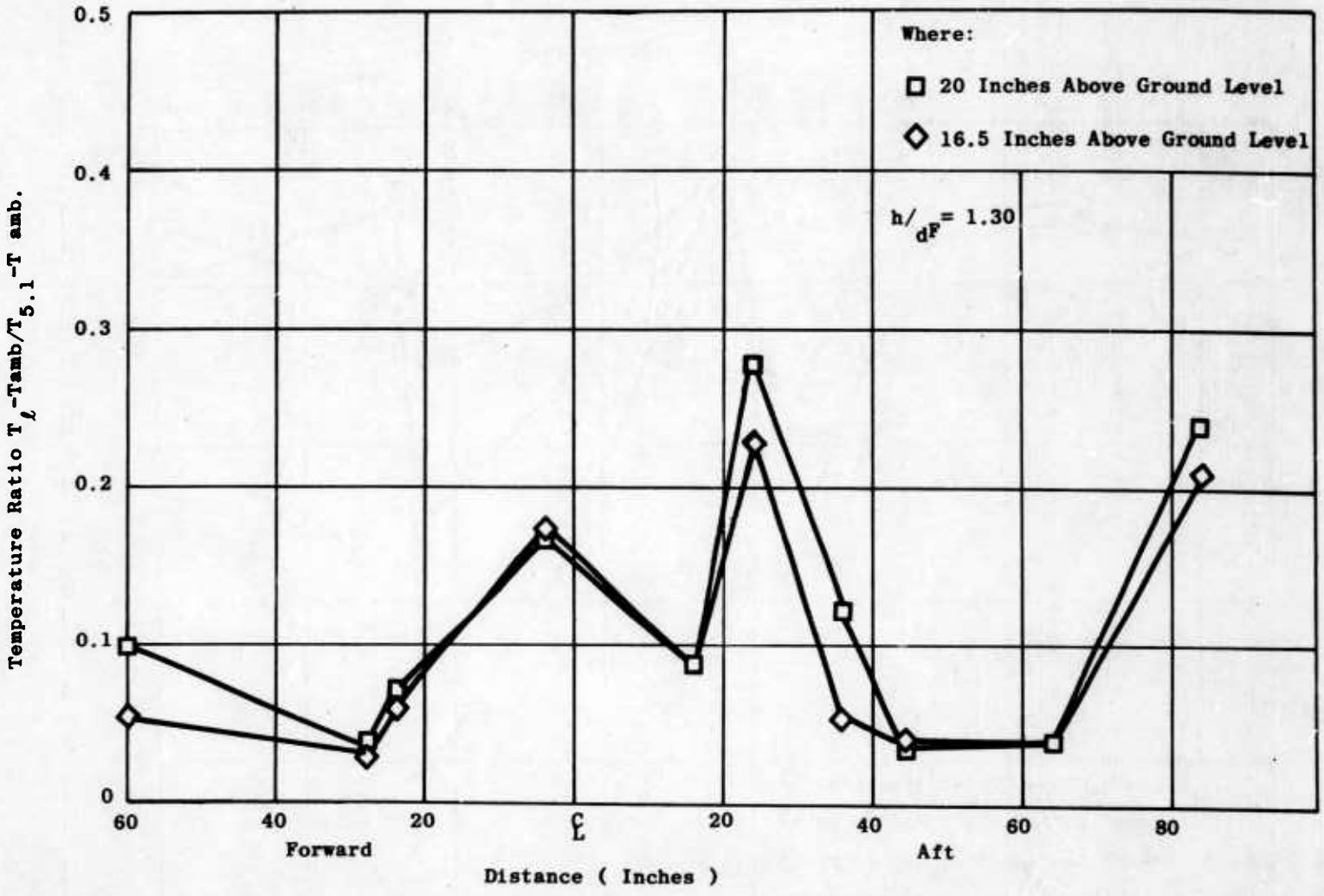


FIGURE 82b. TEMPERATURE RATIO VS. HEIGHT ABOVE GROUND

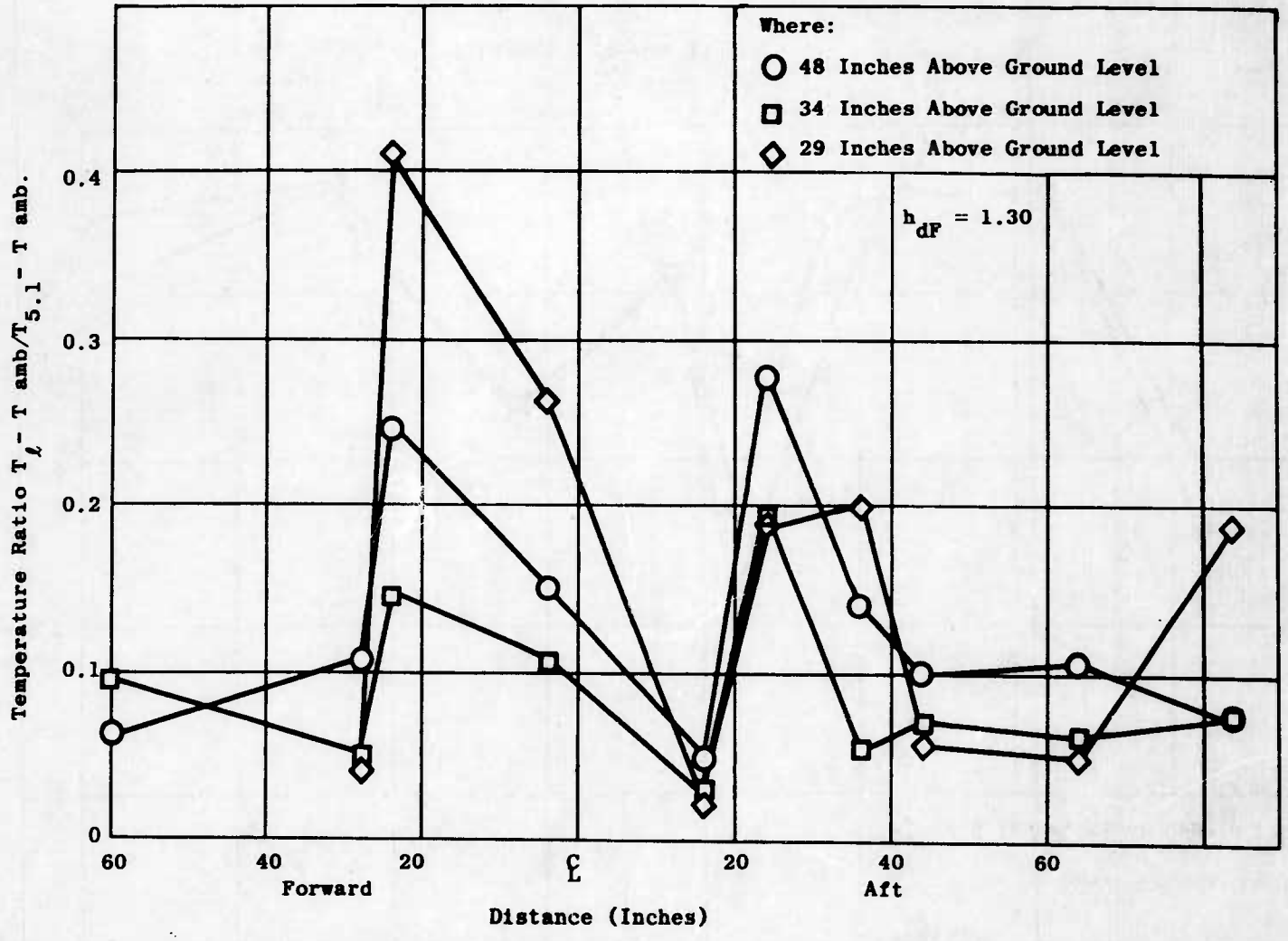


FIGURE 82c. TEMPERATURE RATIO VS. HEIGHT ABOVE GROUND

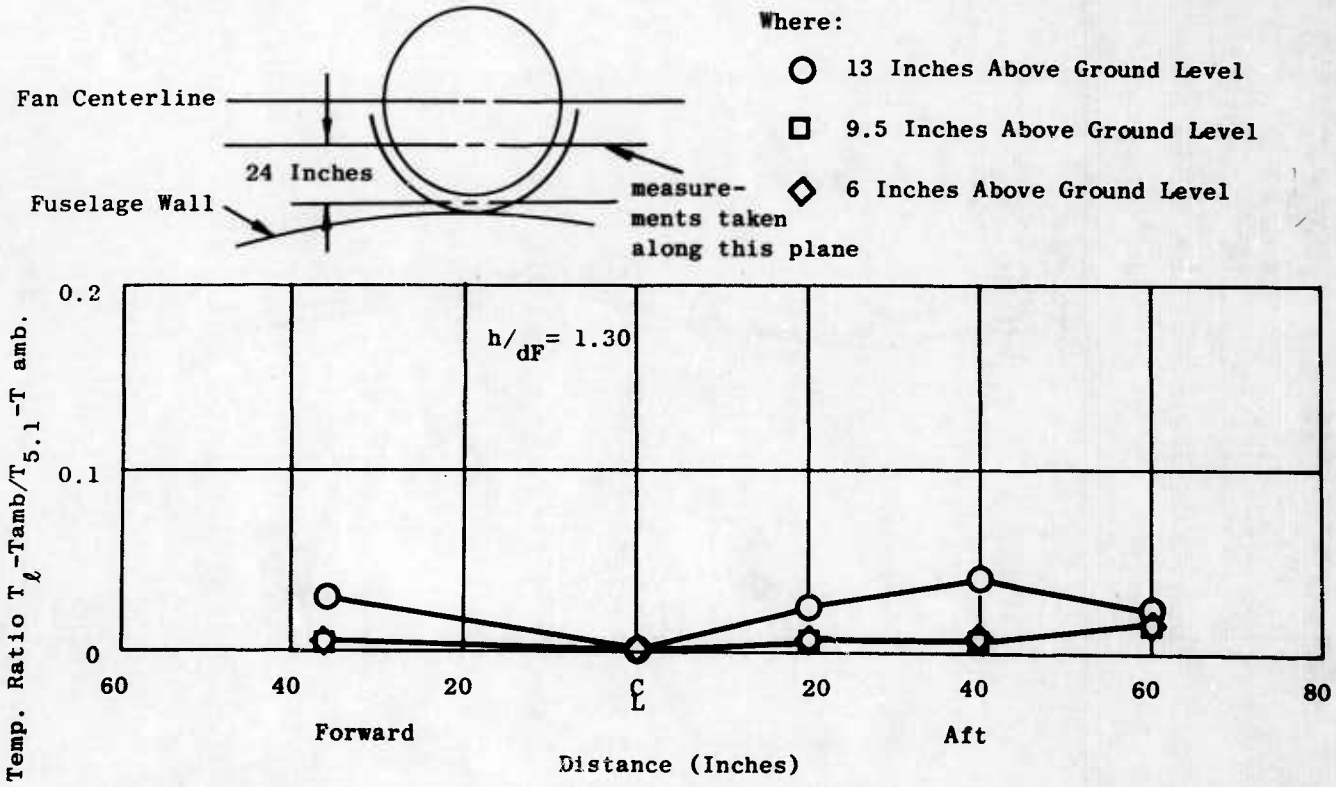


FIGURE 83a. TEMPERATURE RATIO VS. HEIGHT ABOVE GROUND

Where:

○ 24 Inches Above Ground Level

□ 20 Inches Above Ground Level

◇ 16.5 Inches Above Ground Level

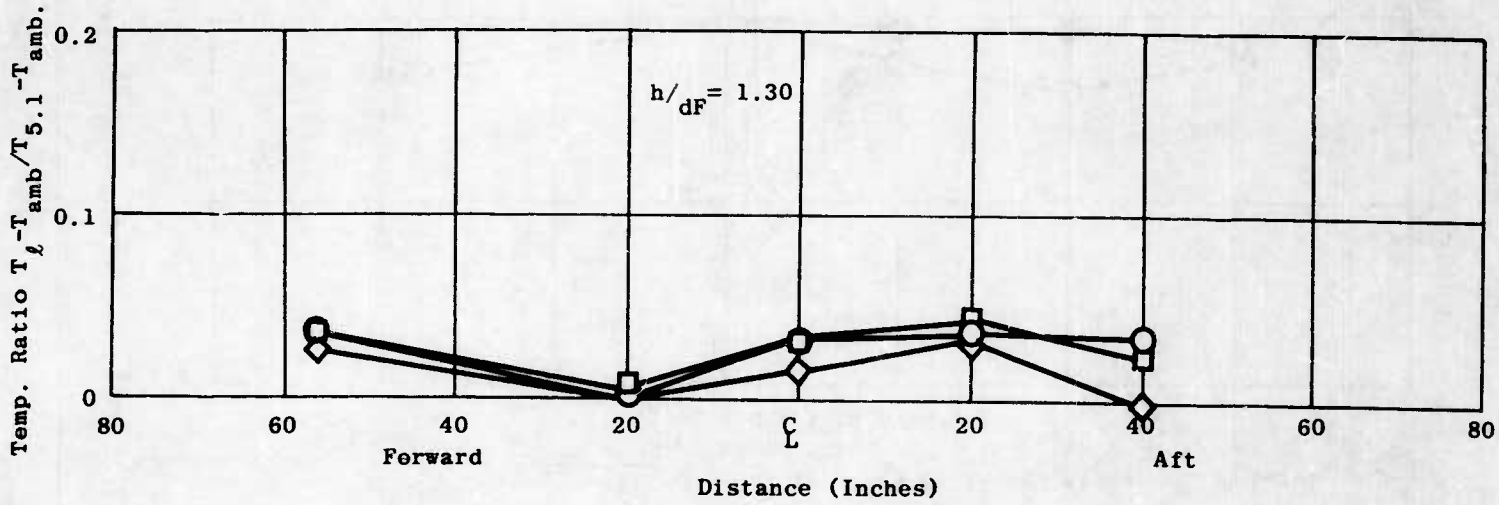


FIGURE 83b. TEMPERATURE RATIO VS. HEIGHT ABOVE GROUND

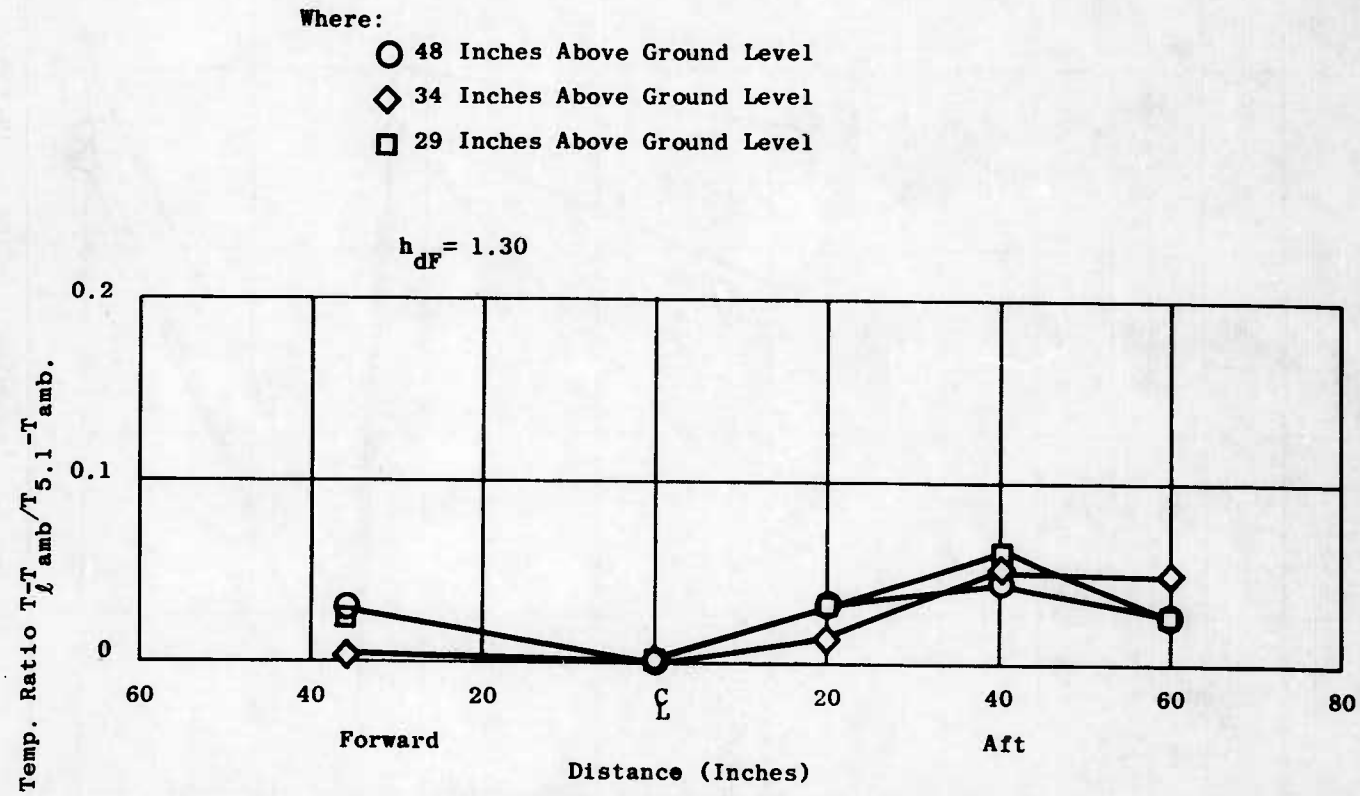


FIGURE 83c. TEMPERATURE RATIO VS. HEIGHT ABOVE GROUND

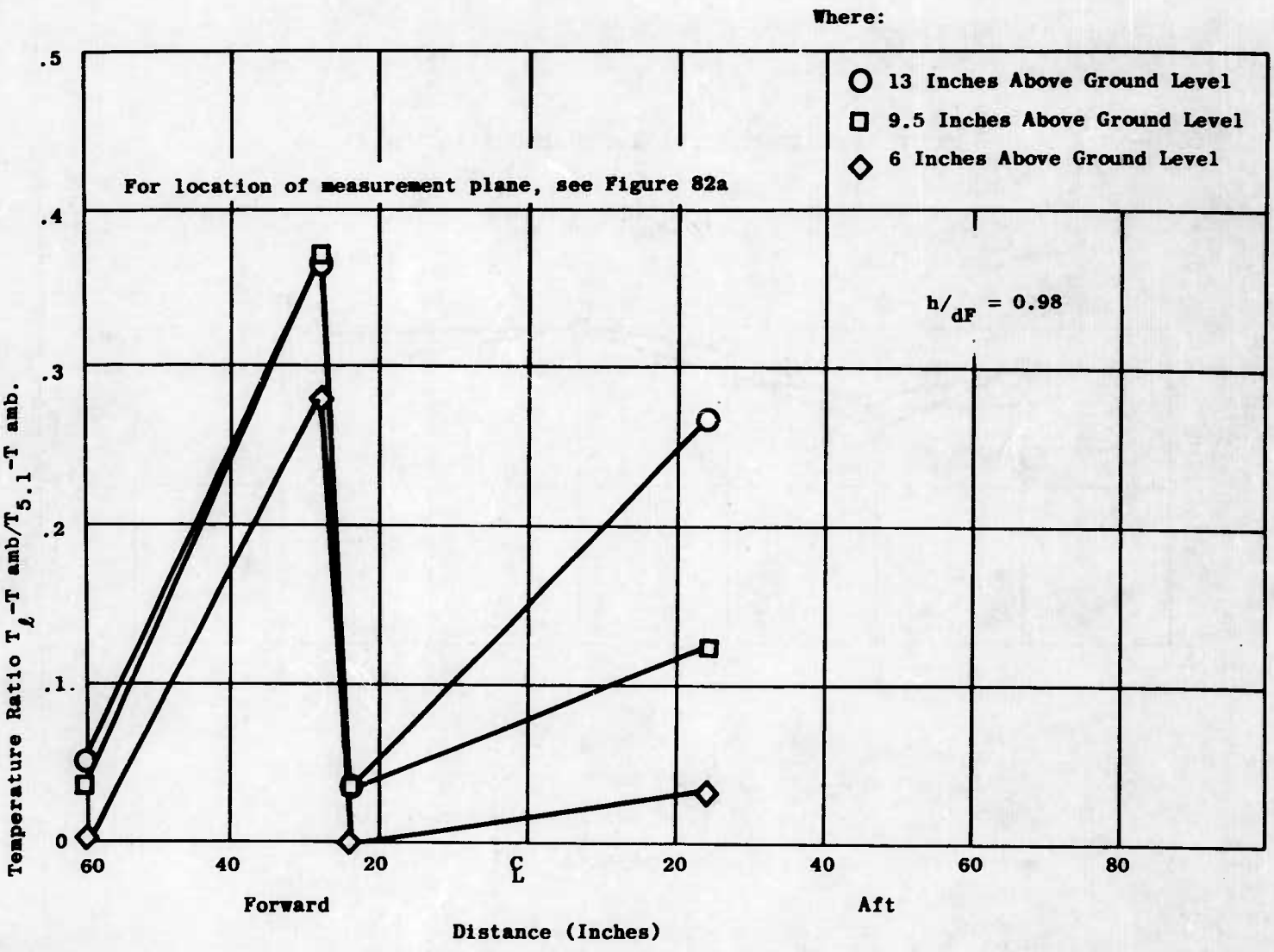


FIGURE 84a. TEMPERATURE RATIO VS. HEIGHT ABOVE GROUND

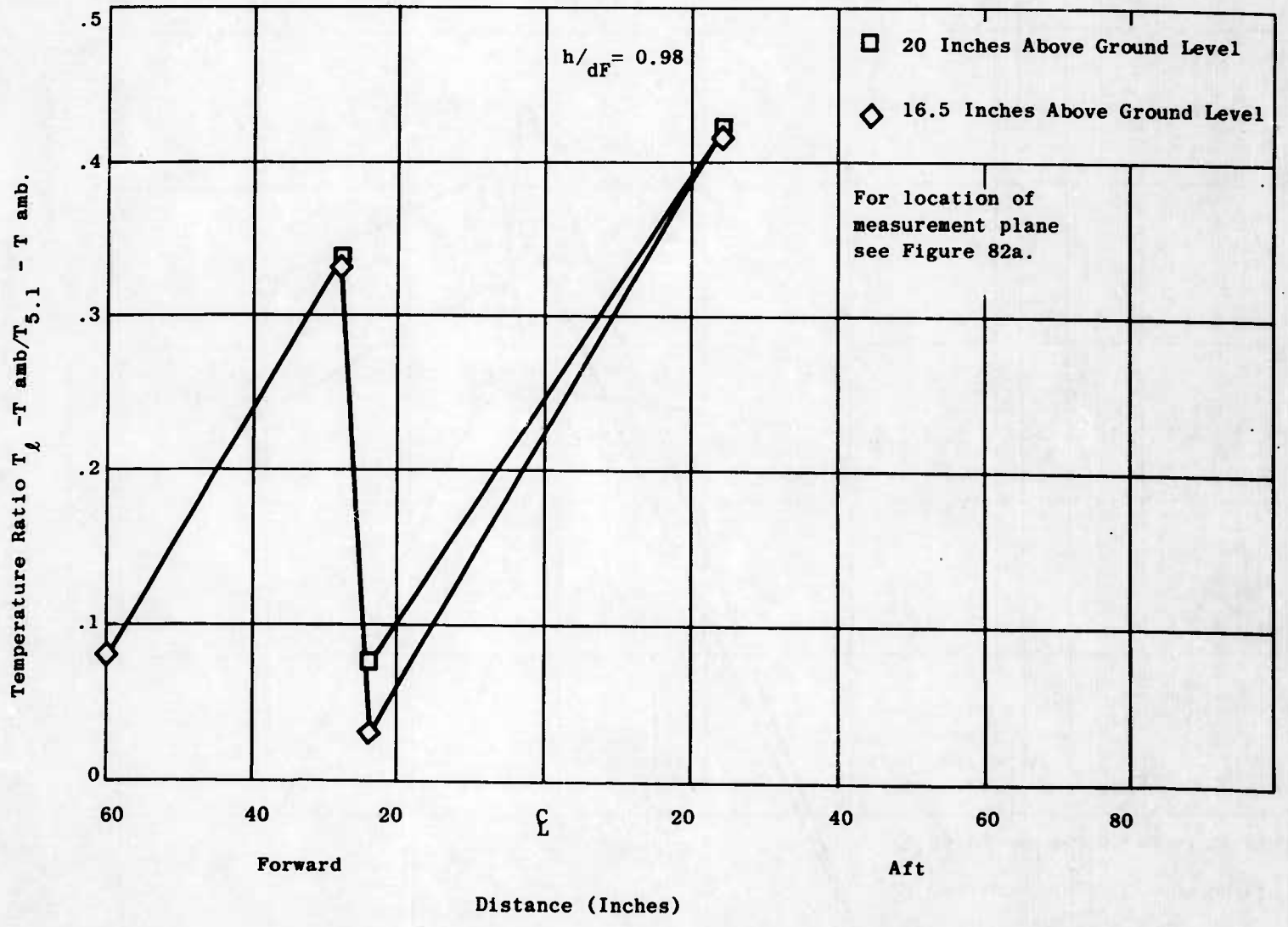


FIGURE 84b. TEMPERATURE RATIO VS. HEIGHT ABOVE GROUND

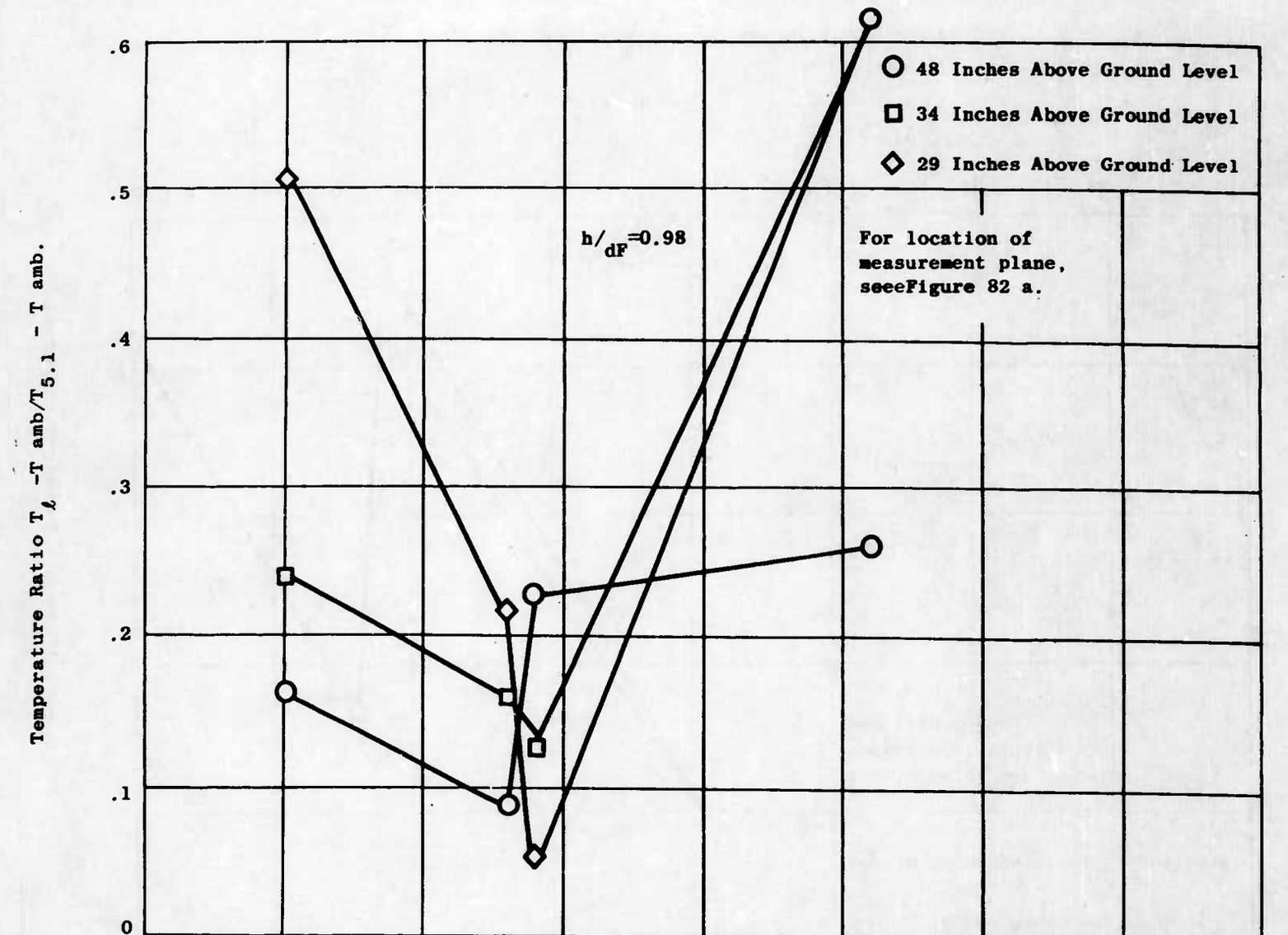


FIGURE 84c. TEMPERATURE RATIO VS. HEIGHT ABOVE GROUND

Where:

O - Skin Thermocouple Locations

Thermocouple Locations	$\frac{T_{\ell} - T_{amb}}{T_{5.1} - T_{amb}}$ $h/d_F = 1.30$	$h/d_F = 0.98$
1	0.11	0.48
2	0.19	0.57
3	0.24	0.61
4	0.69	0.77
5	0.63	0.66
6	0.57	0.56
7	0.07	0.47
8	0.09	0.60
9	0.30	0.56

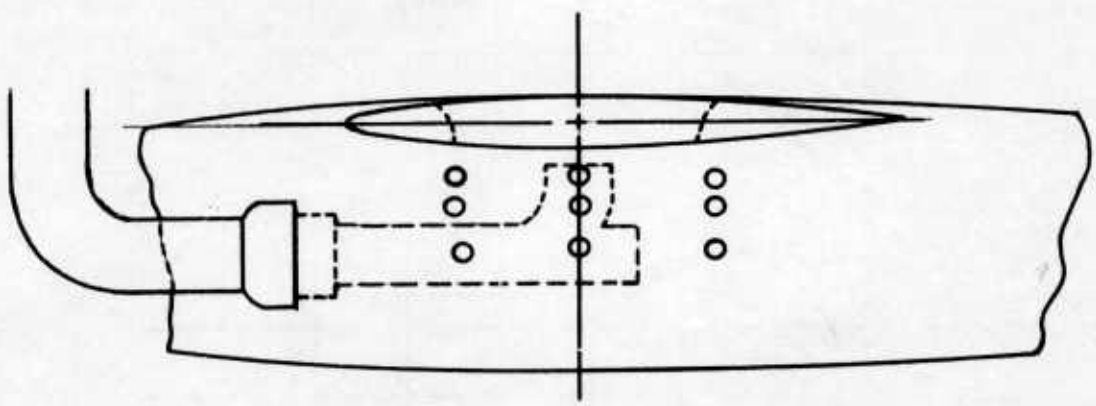


FIGURE 85. FUSELAGE SKIN TEMPERATURE RATIO IN GROUND EFFECT

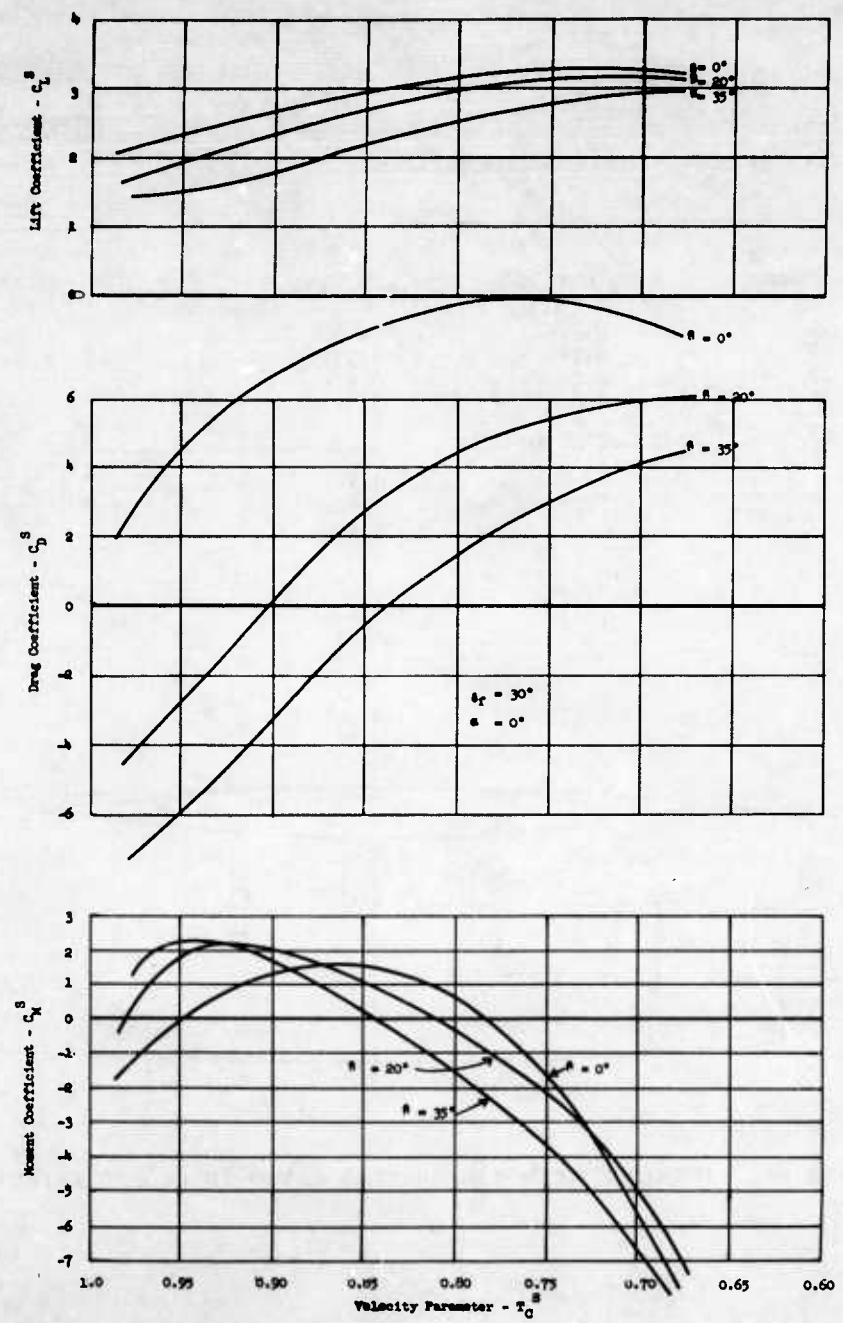


FIGURE 86. LIFT, DRAG AND MOMENT COEFFICIENT (SLIP STREAM NOTATION) VERSUS VELOCITY PARAMETER

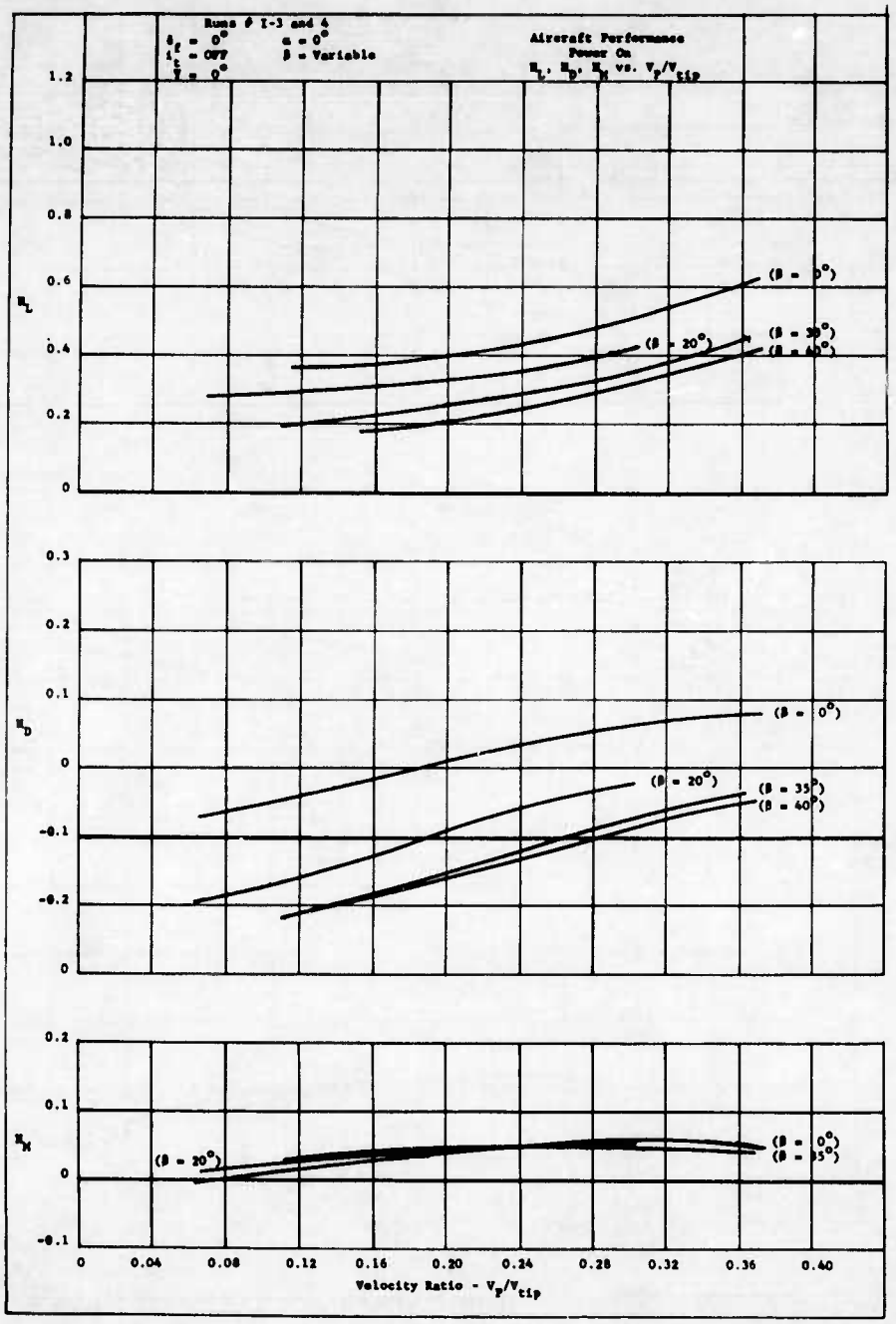


FIGURE 87 - FAN POWERED AIRCRAFT PERFORMANCE

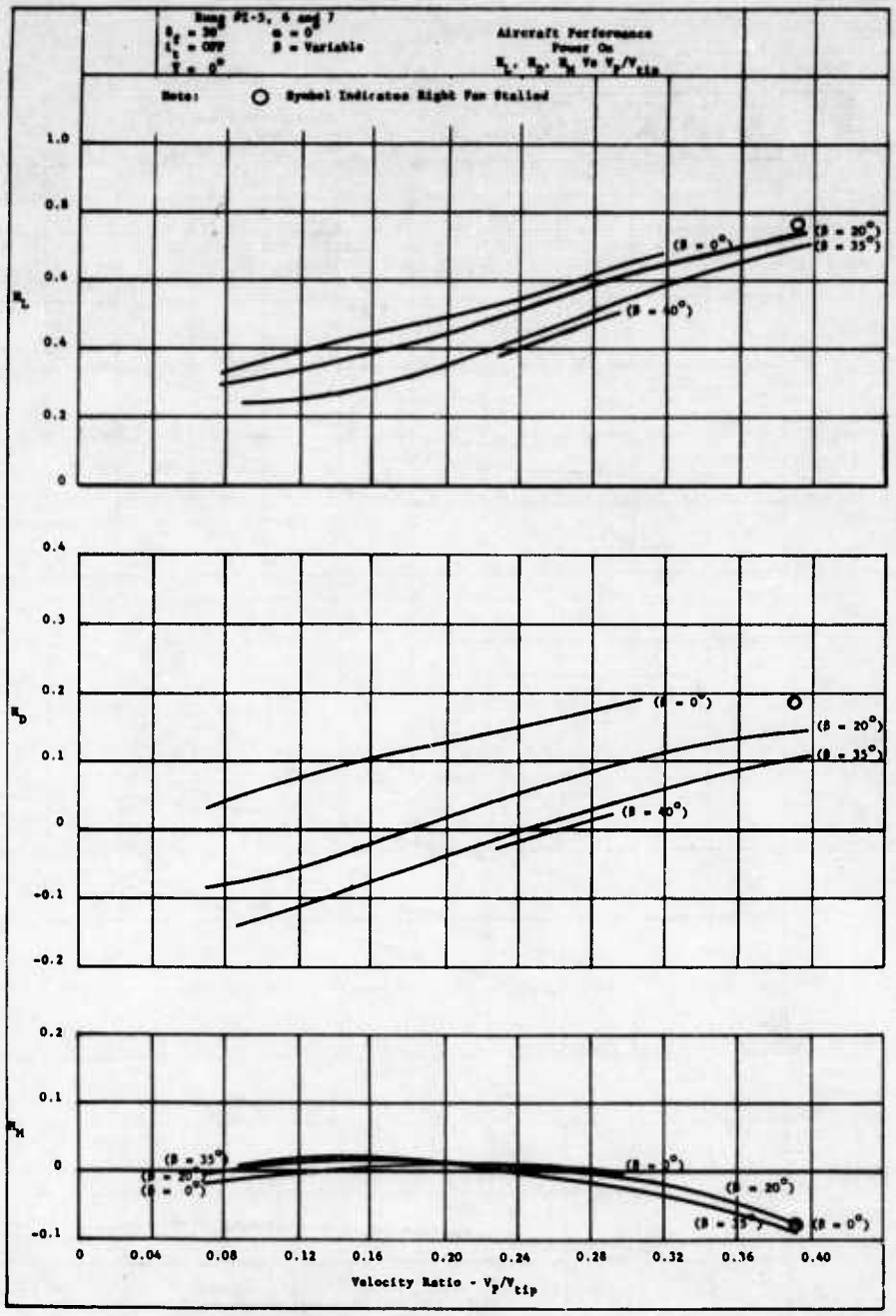


FIGURE 88a - FAN POWERED AIRCRAFT PERFORMANCE

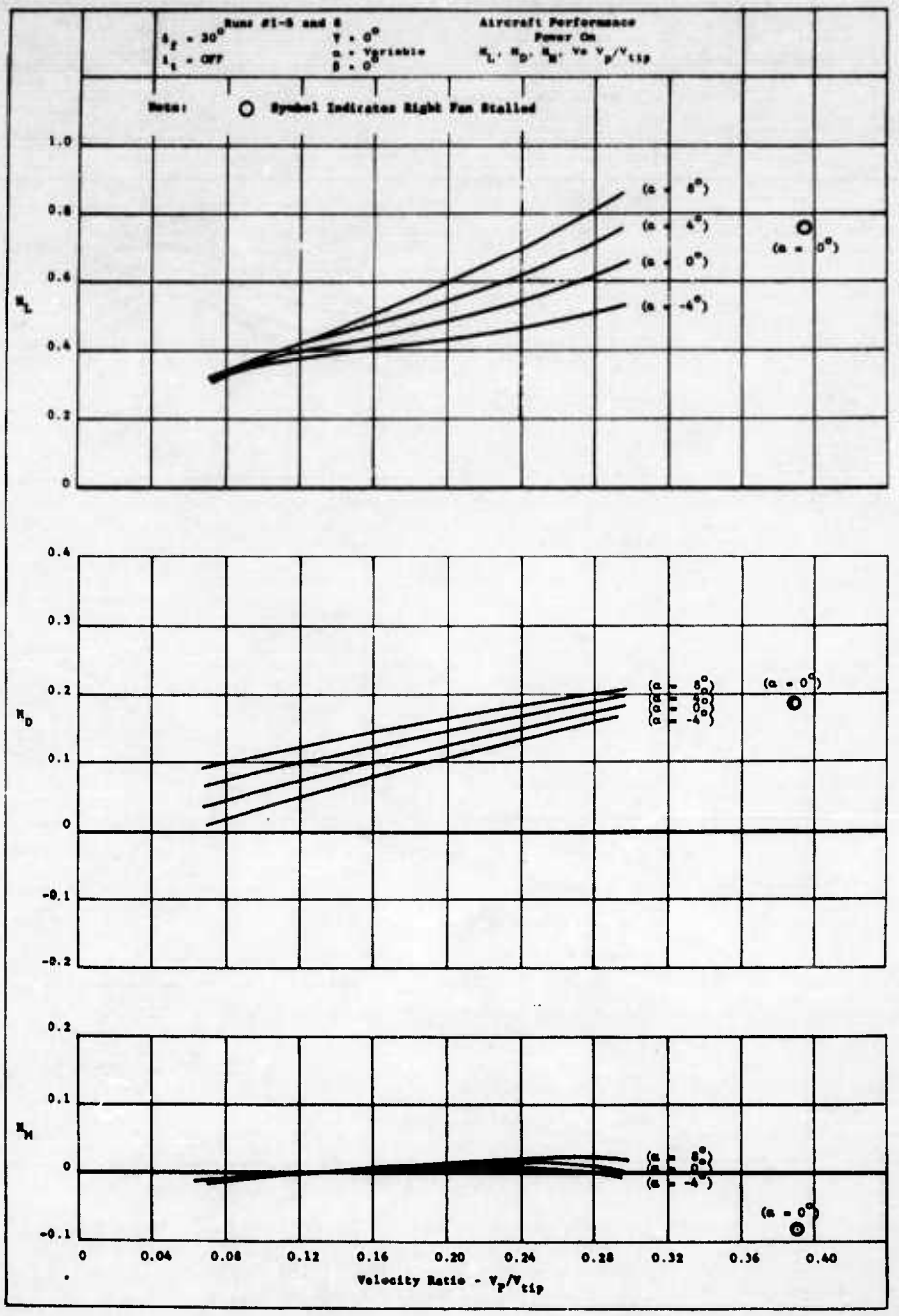


FIGURE 88b - FAN POWERED AIRCRAFT PERFORMANCE

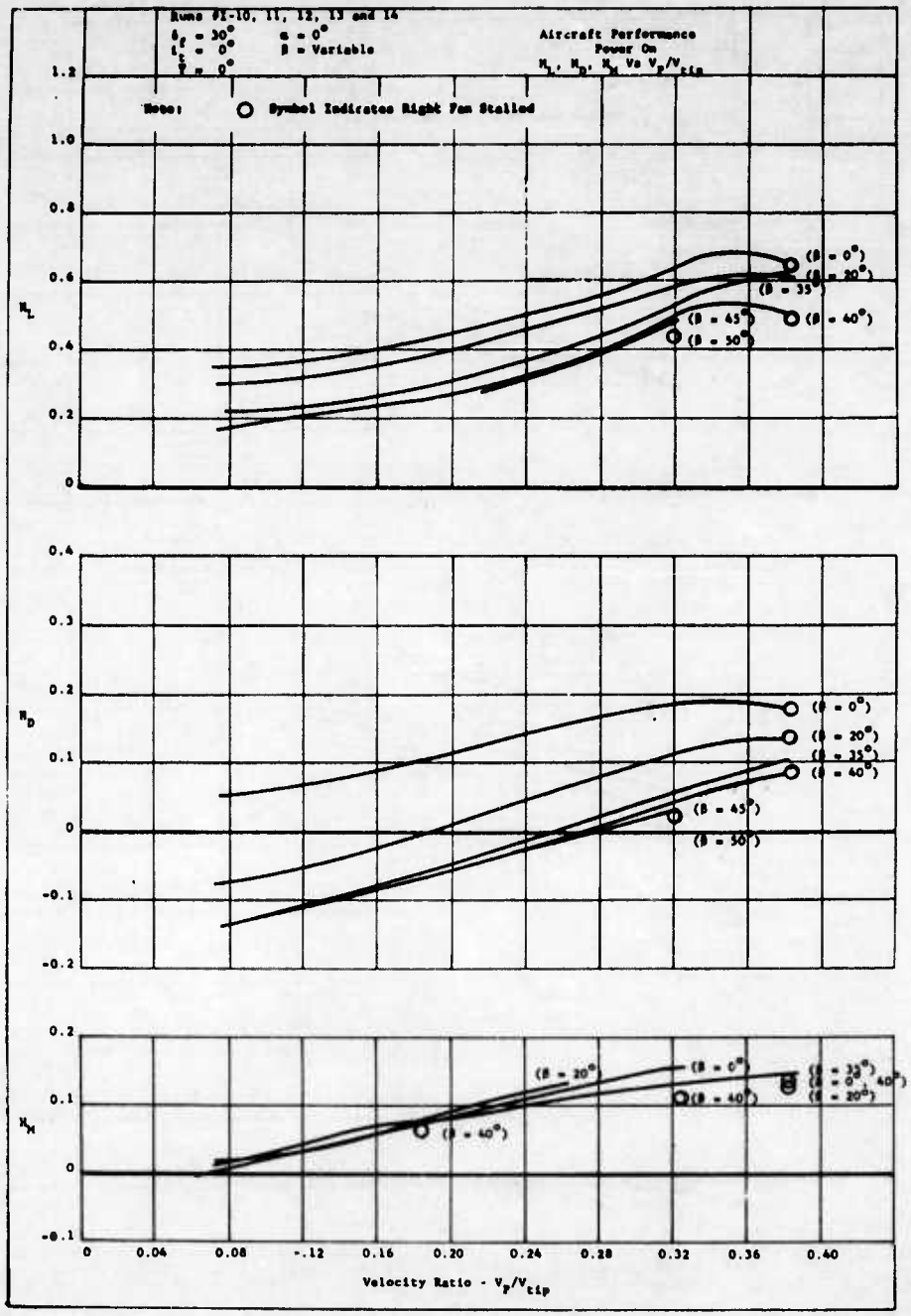


FIGURE 89a - FAN POWERED AIRCRAFT PERFORMANCE

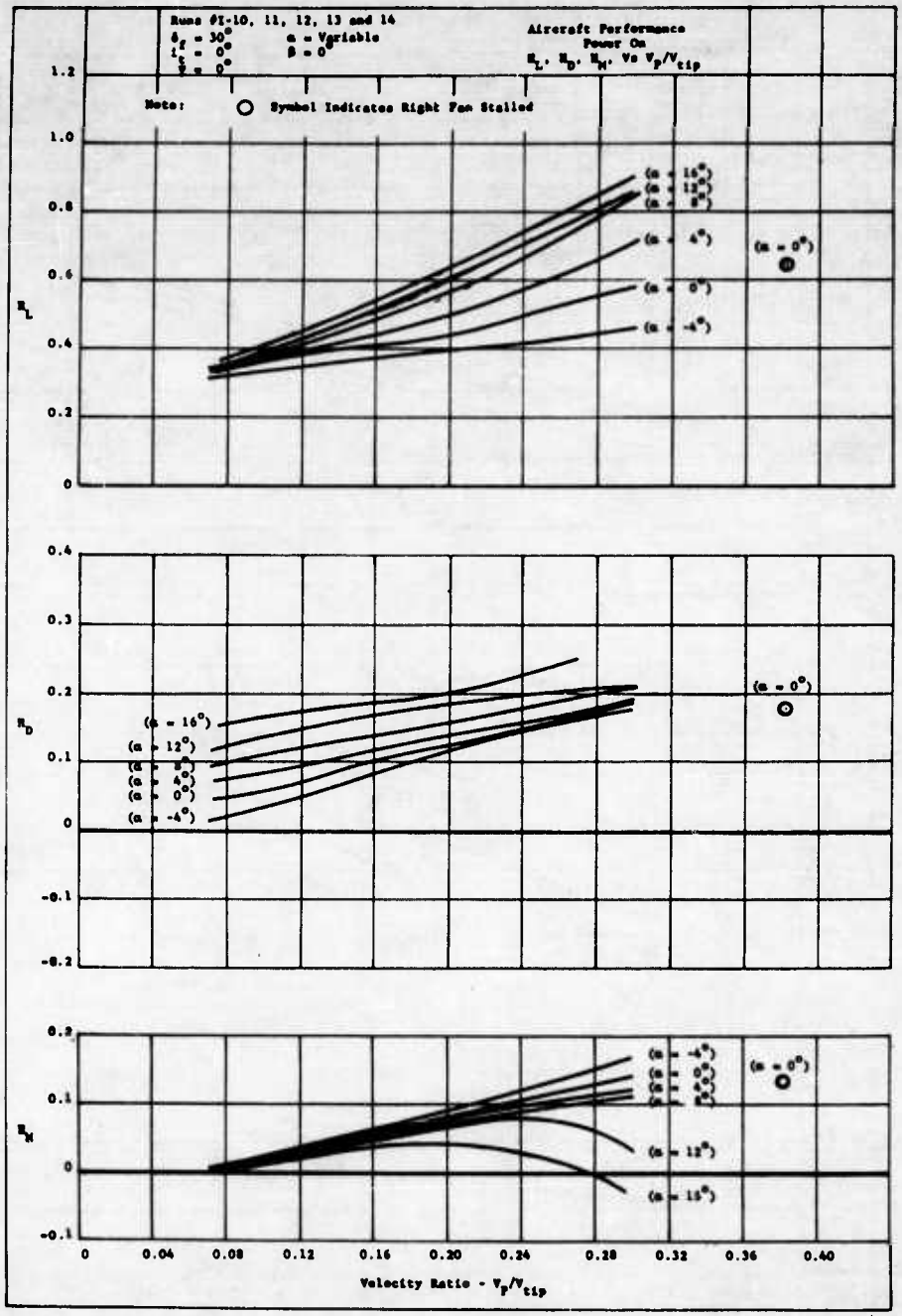


FIGURE 89b - FAN POWERED AIRCRAFT PERFORMANCE

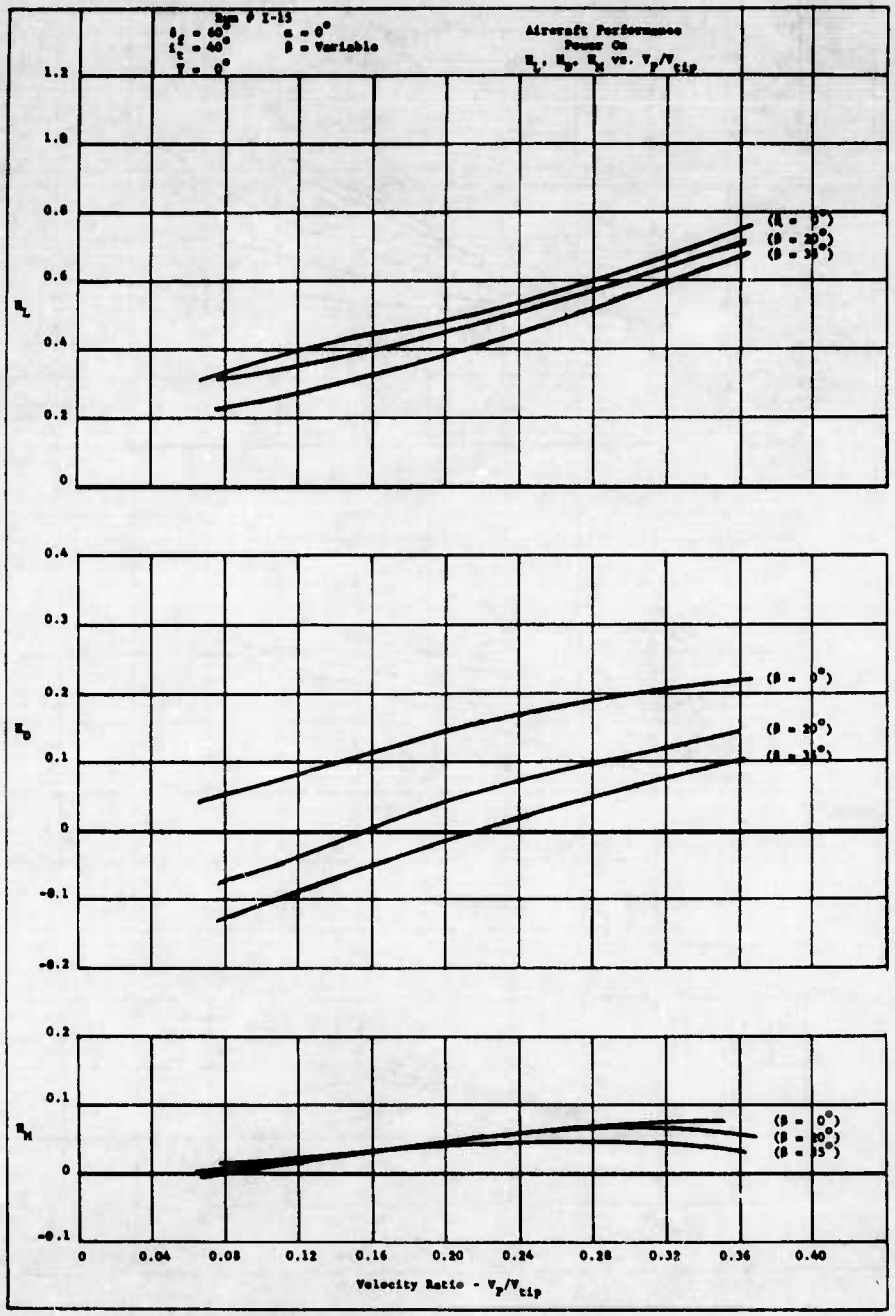


FIGURE 90a - FAN POWERED AIRCRAFT PERFORMANCE

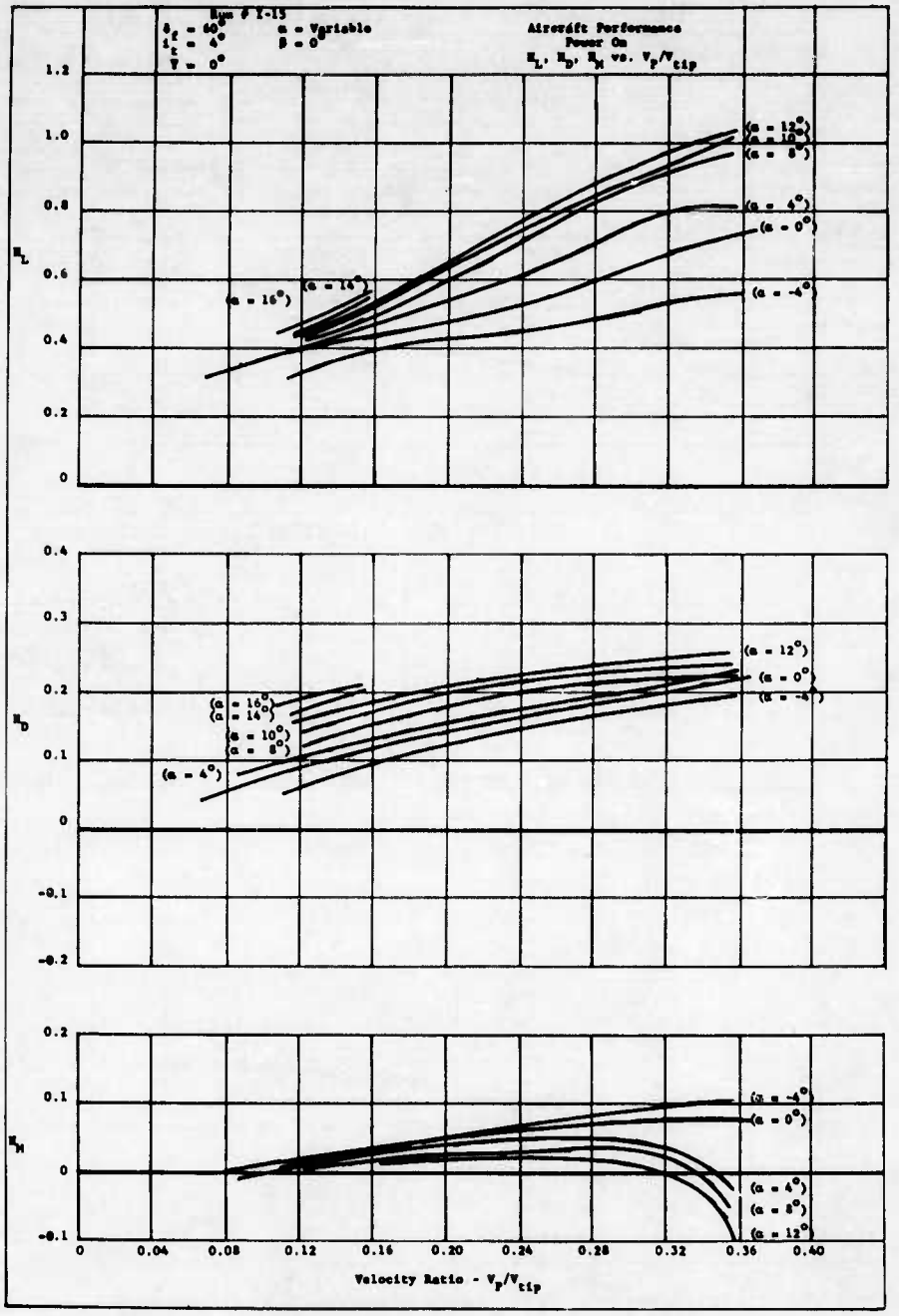


FIGURE 90b - FAN POWERED AIRCRAFT PERFORMANCE

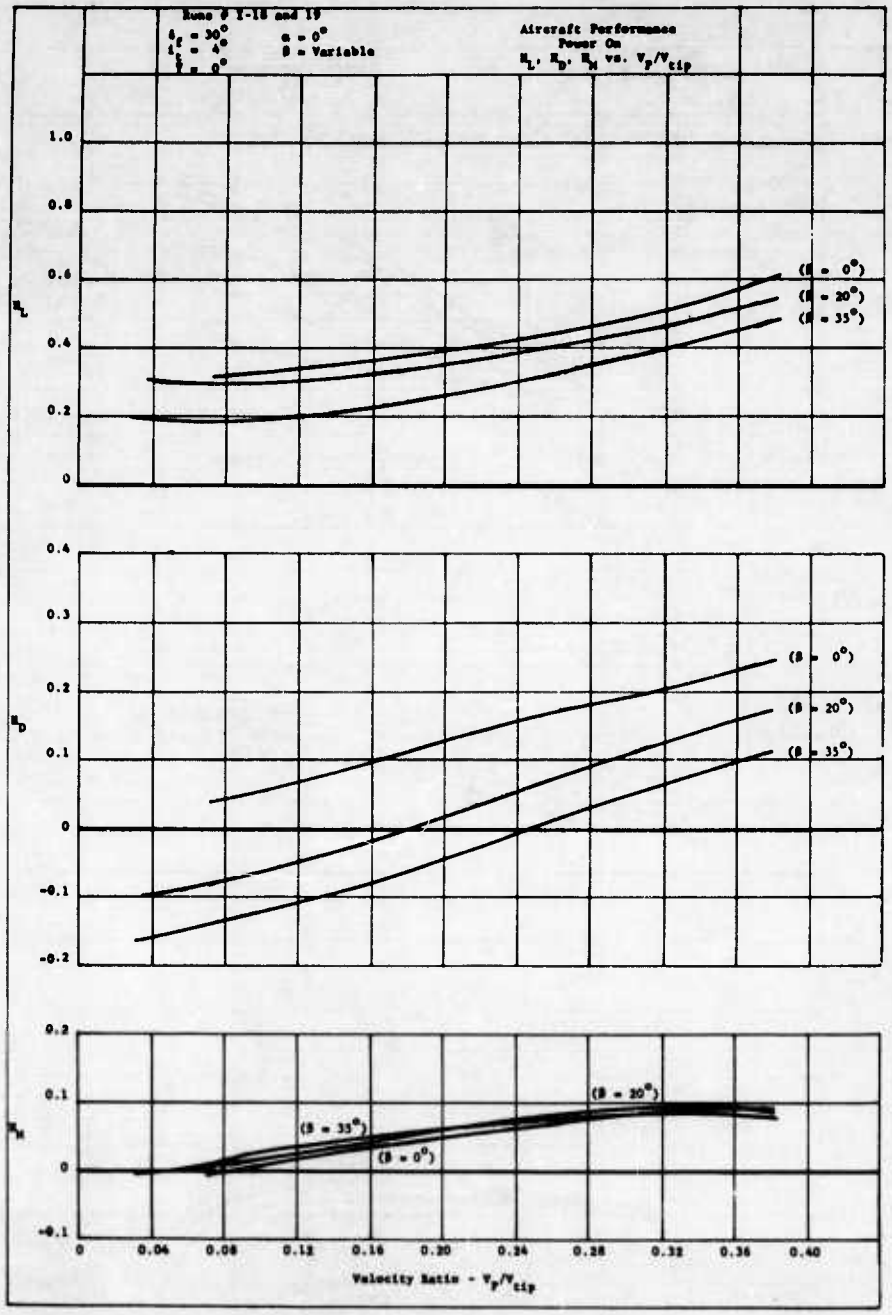


FIGURE 91a - FAN POWERED AIRCRAFT PERFORMANCE

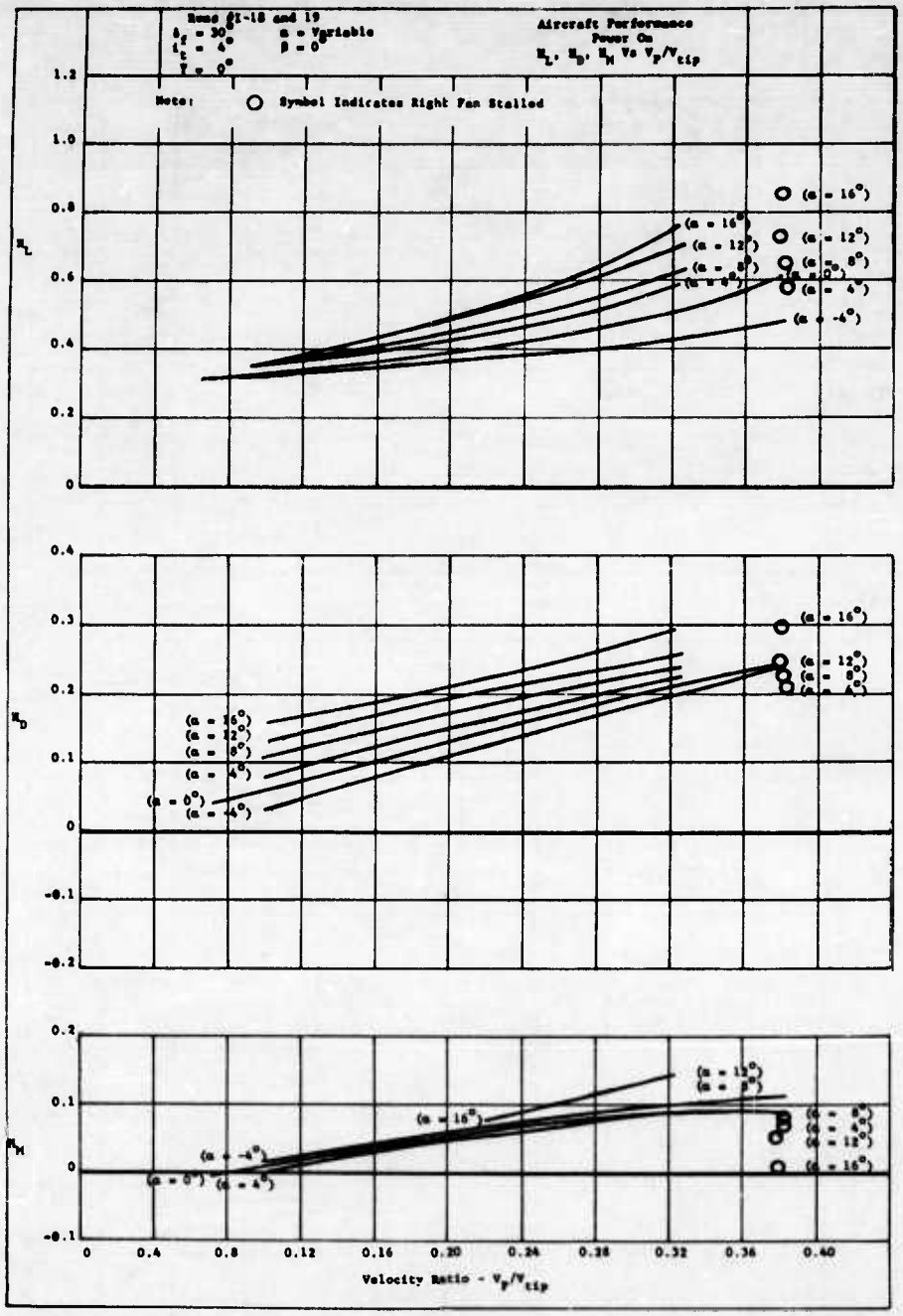


FIGURE 91b - FAN POWERED AIRCRAFT PERFORMANCE

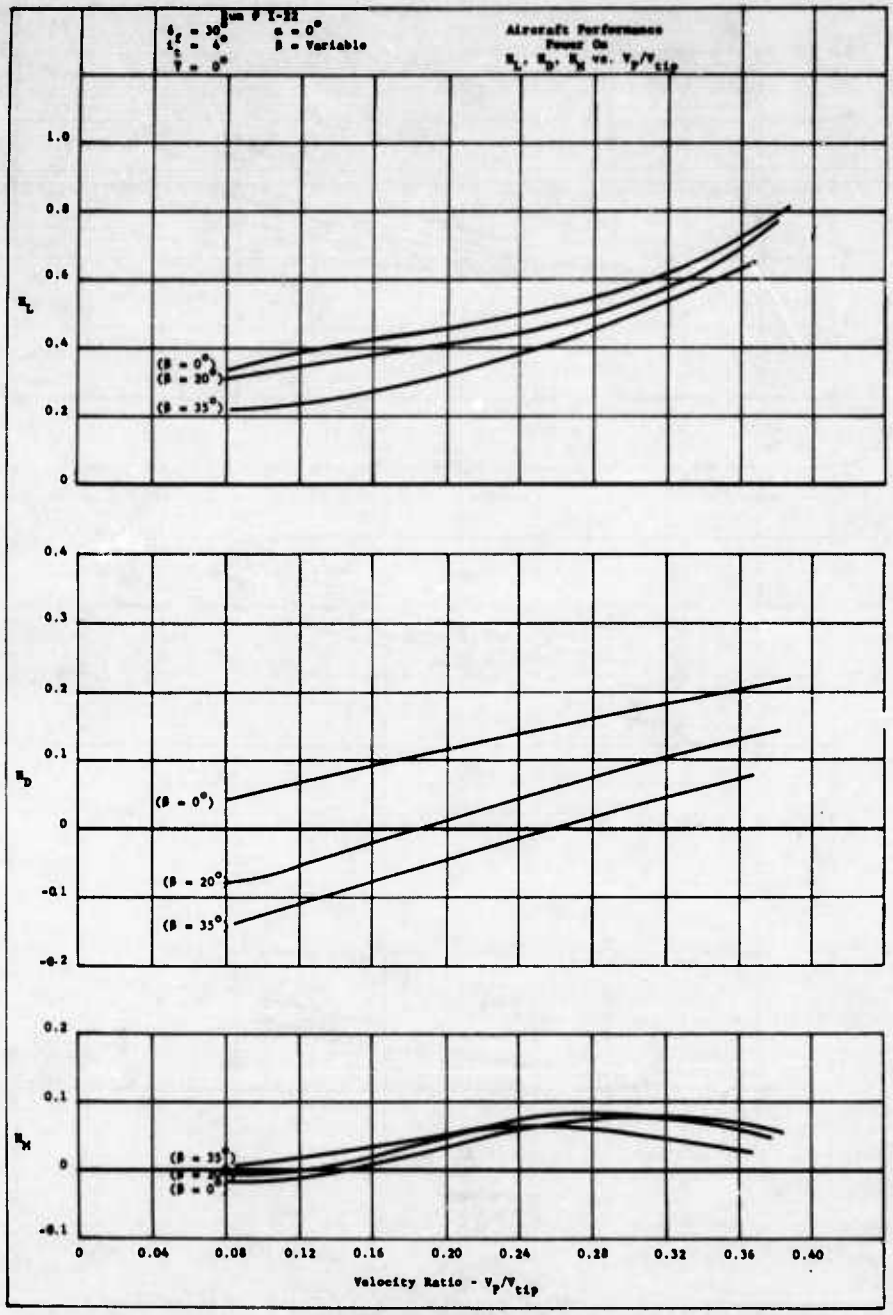


FIGURE 92a - FAN POWERED AIRCRAFT PERFORMANCE

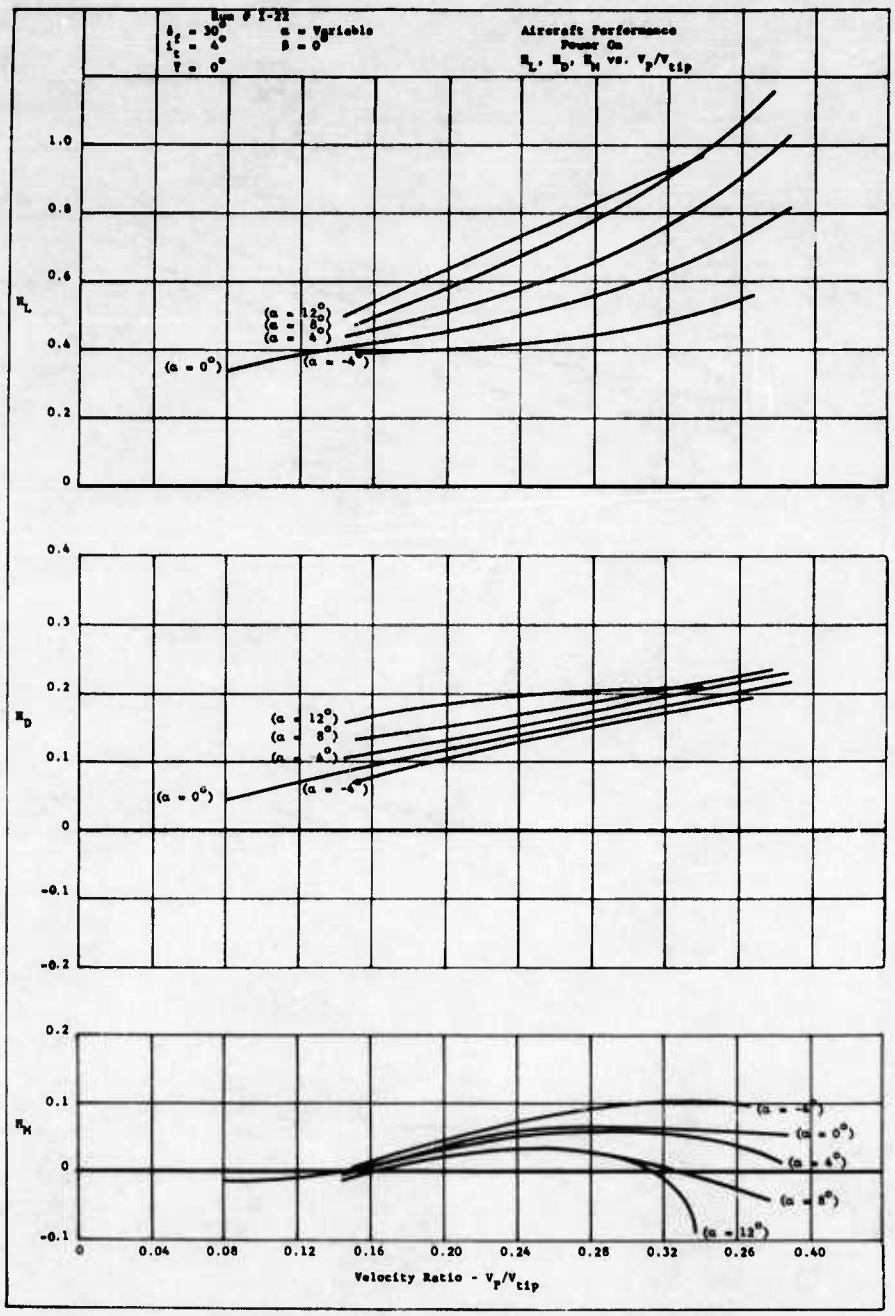


FIGURE 92b - FAN POWERED AIRCRAFT PERFORMANCE

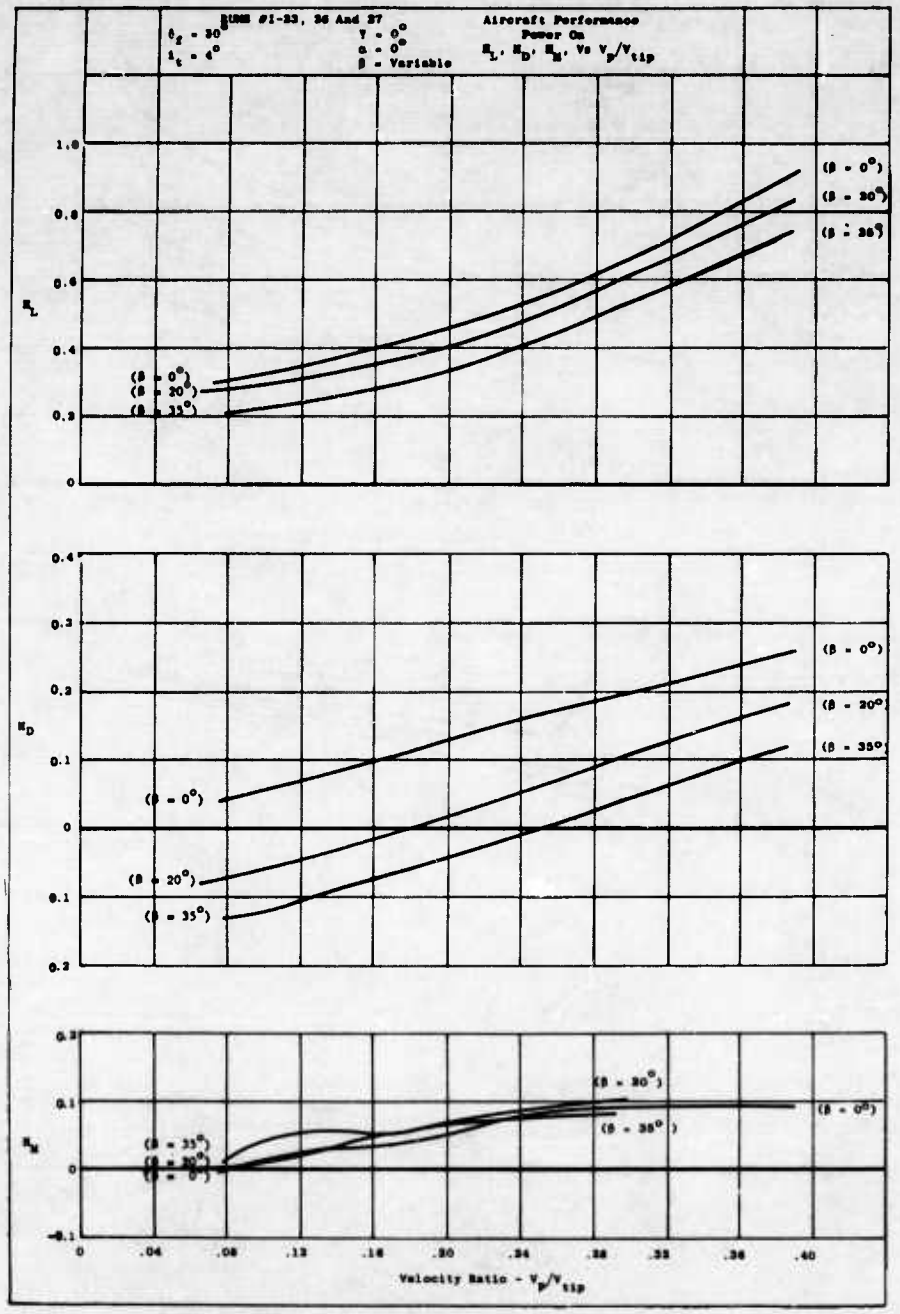


FIGURE 93a - FAN POWERED AIRCRAFT PERFORMANCE

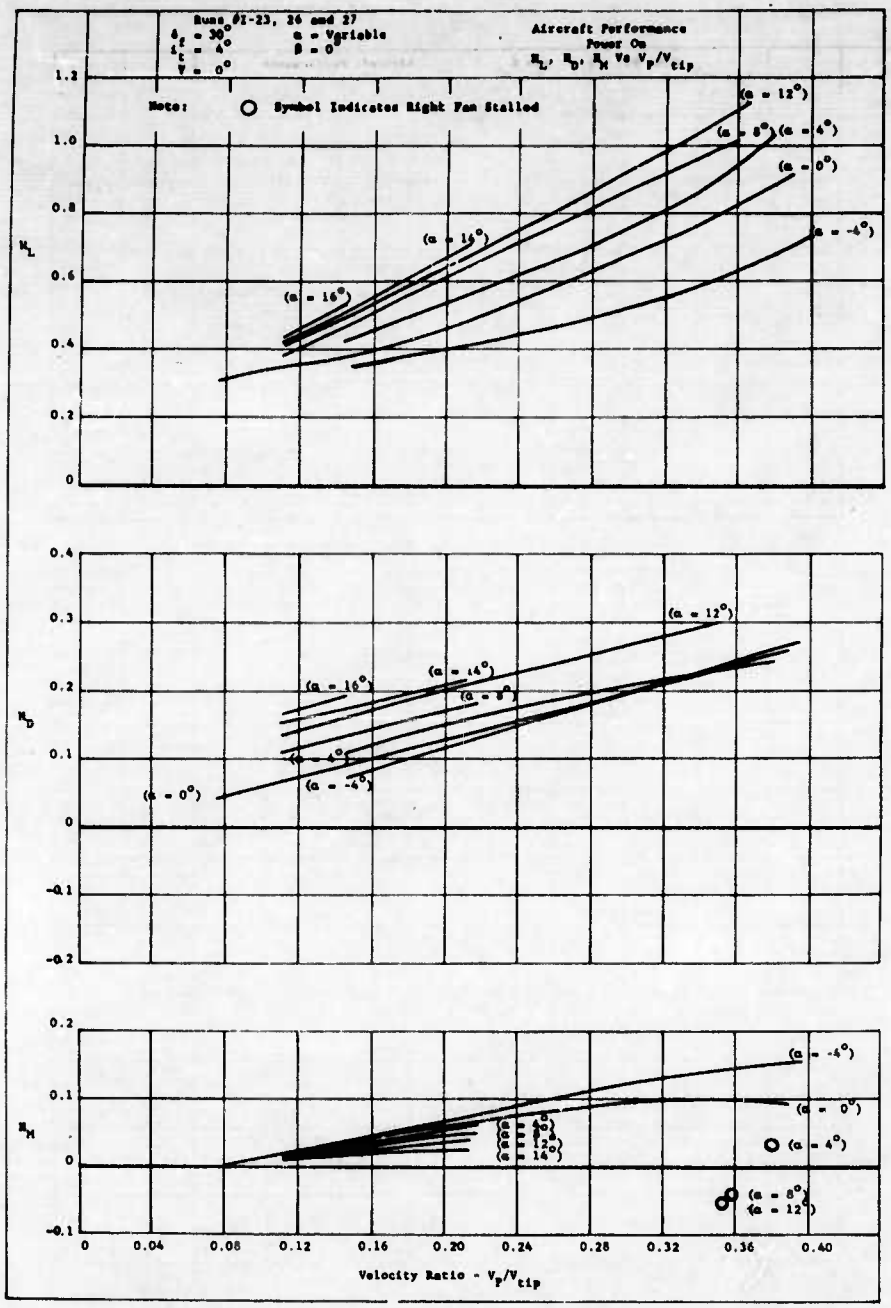


FIGURE 93b - FAN POWERED AIRCRAFT PERFORMANCE

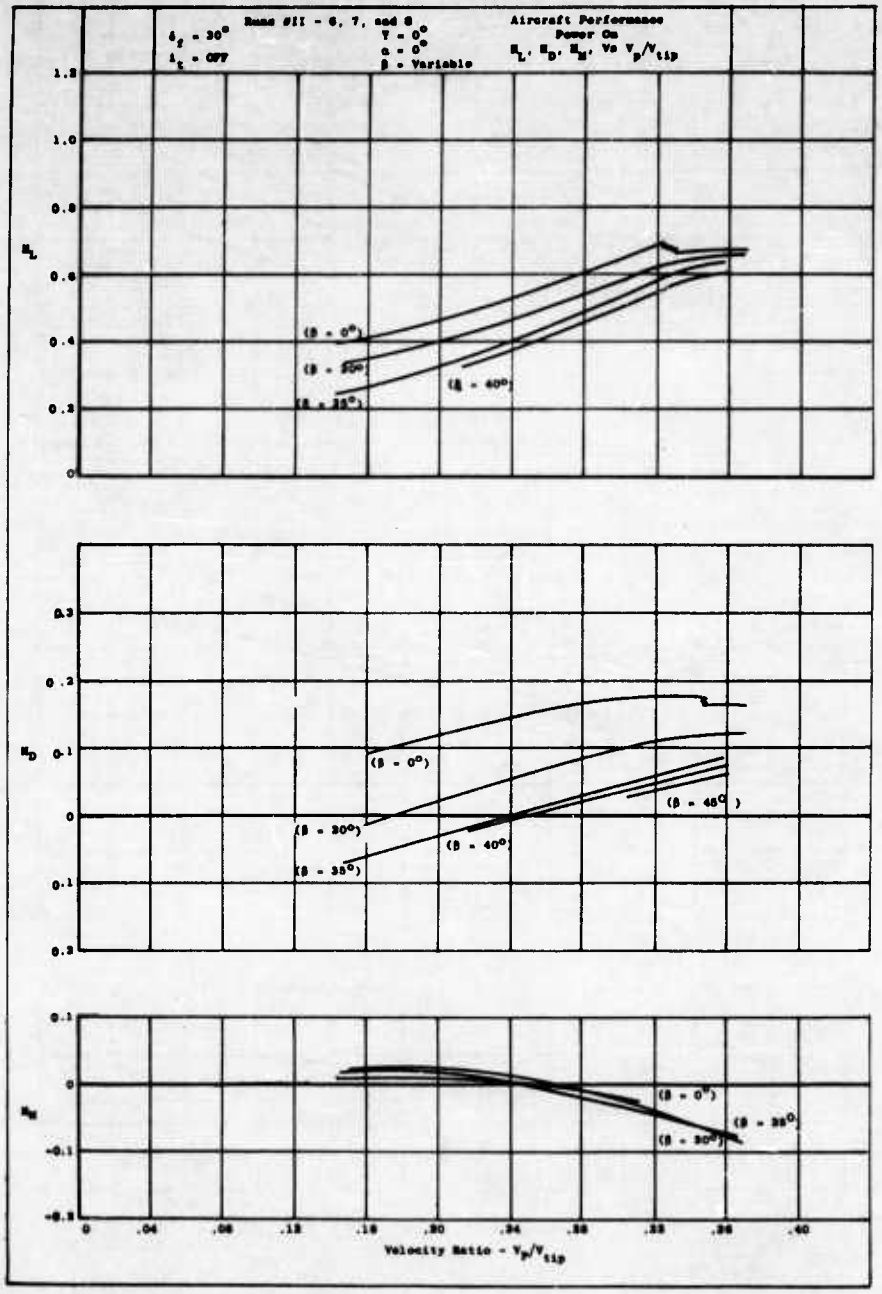


FIGURE 94a - FAN POWERED AIRCRAFT PERFORMANCE

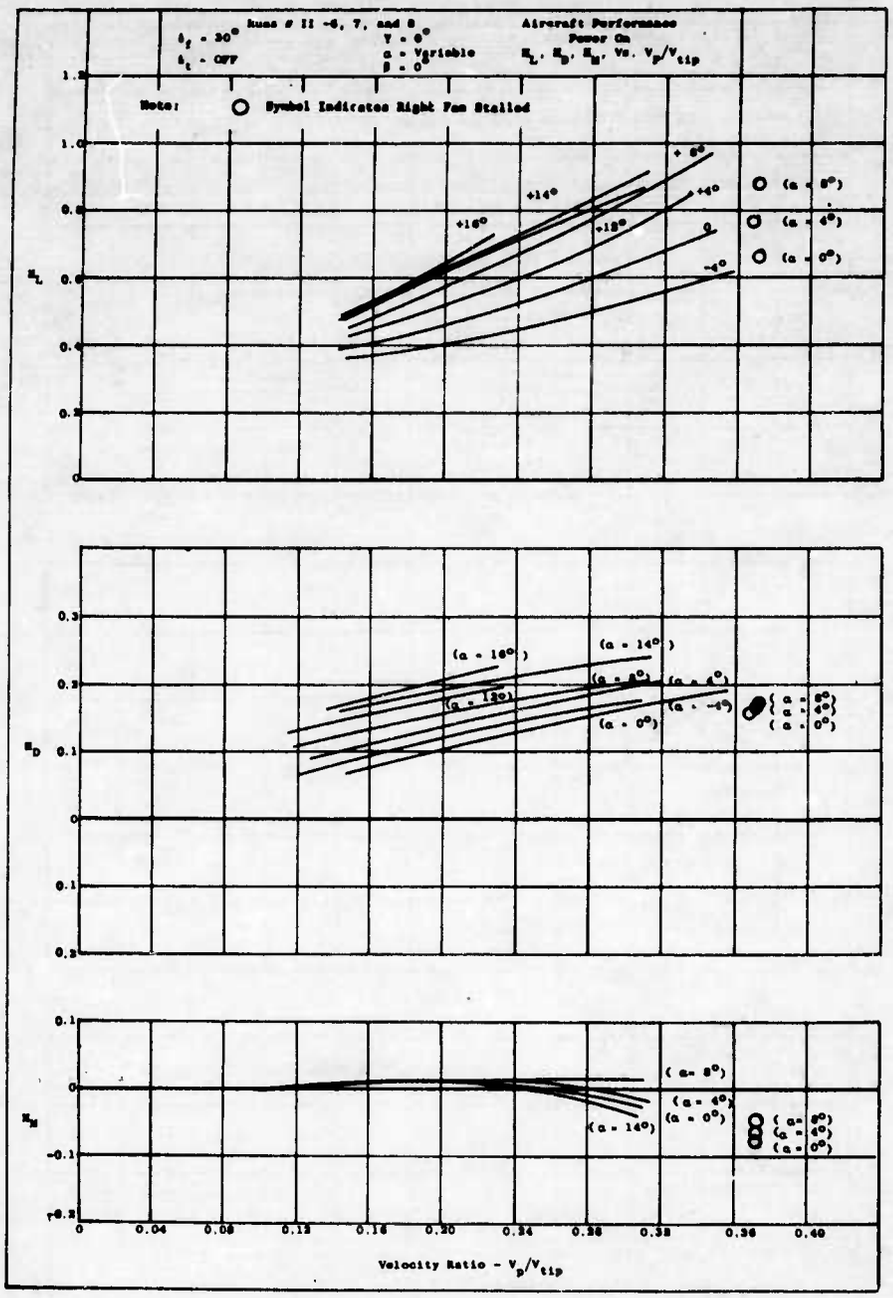


FIGURE 94b - FAN POWERED AIRCRAFT PERFORMANCE

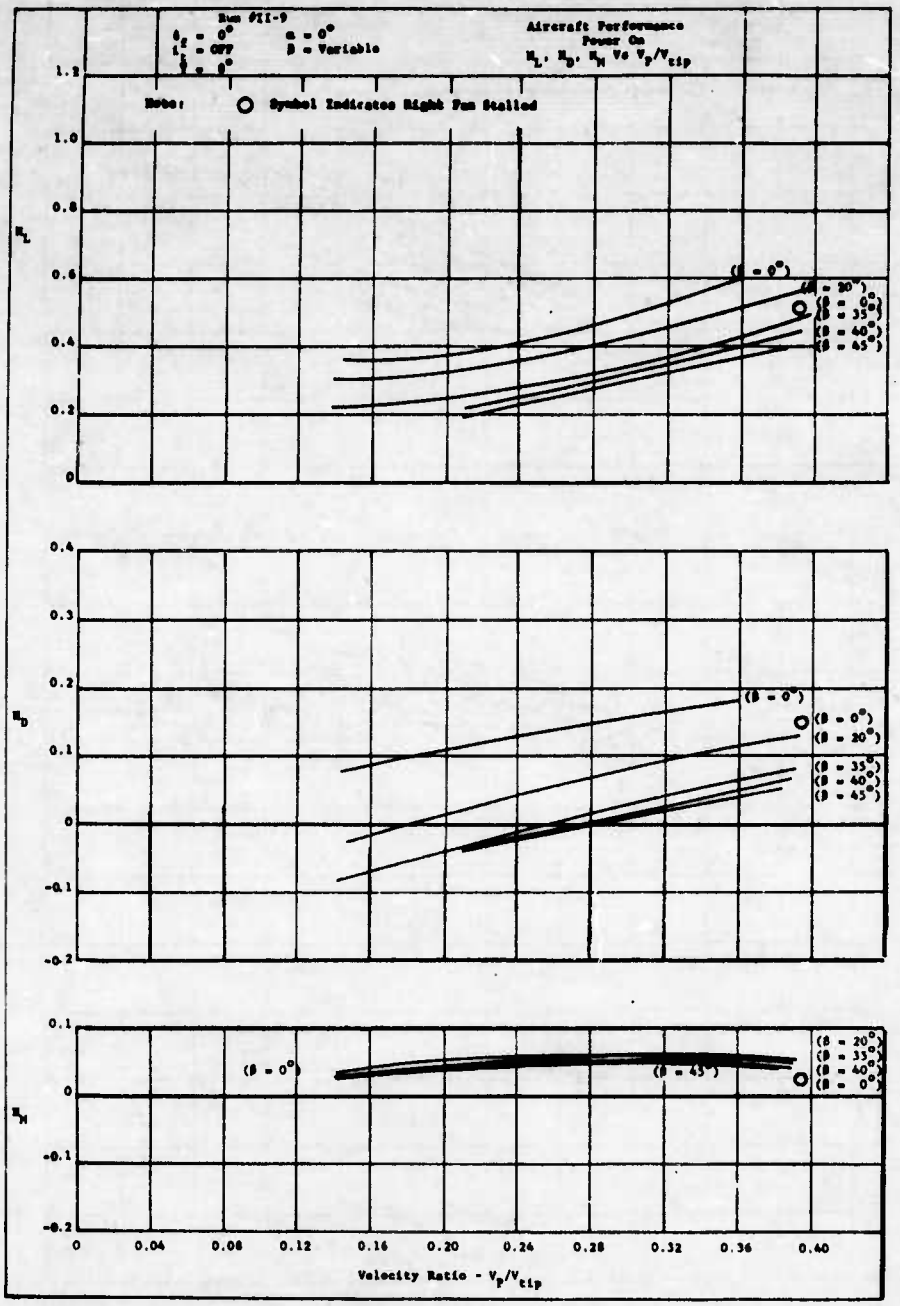


FIGURE 95a - FAN POWERED AIRCRAFT PERFORMANCE

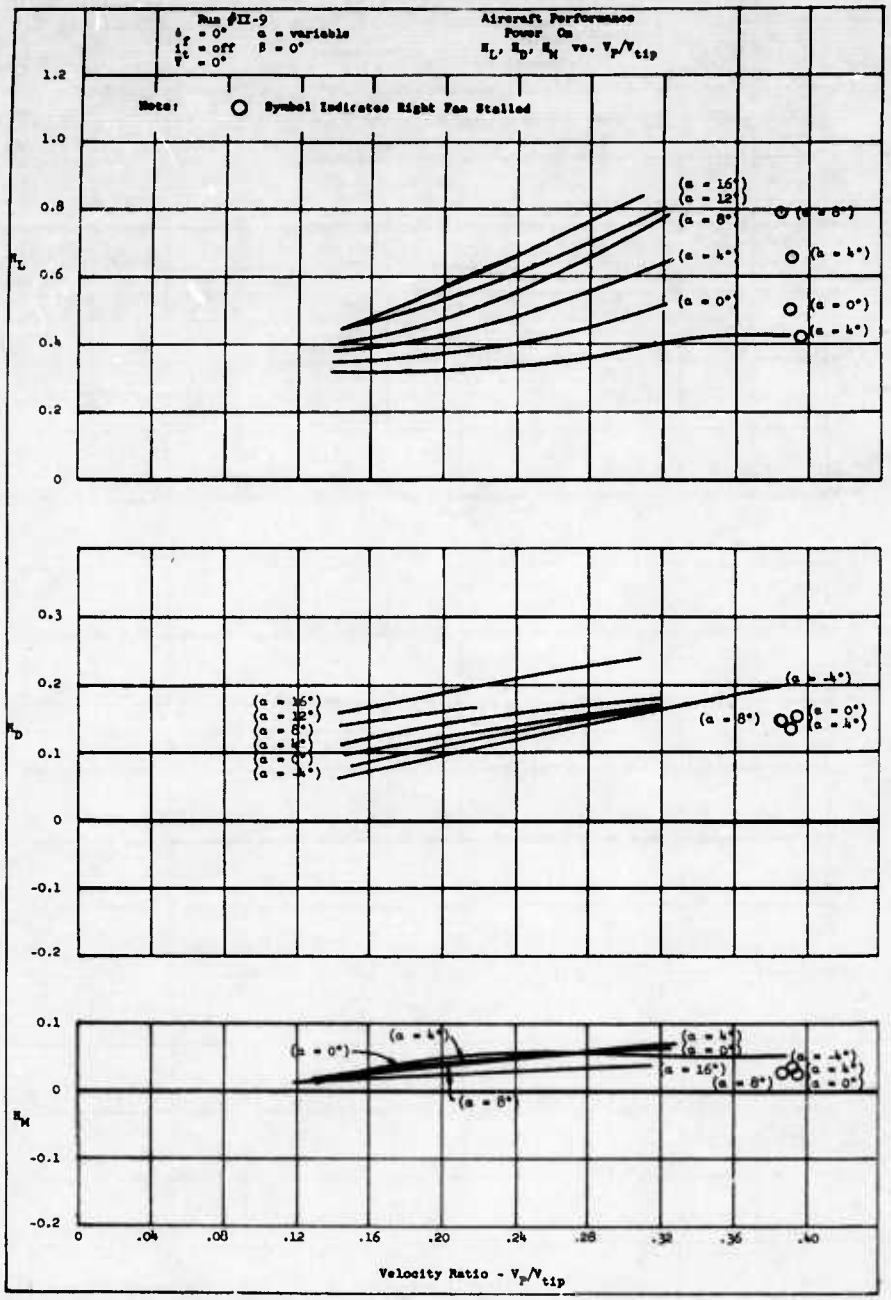


FIGURE 95b - FAN POWERED AIRCRAFT PERFORMANCE

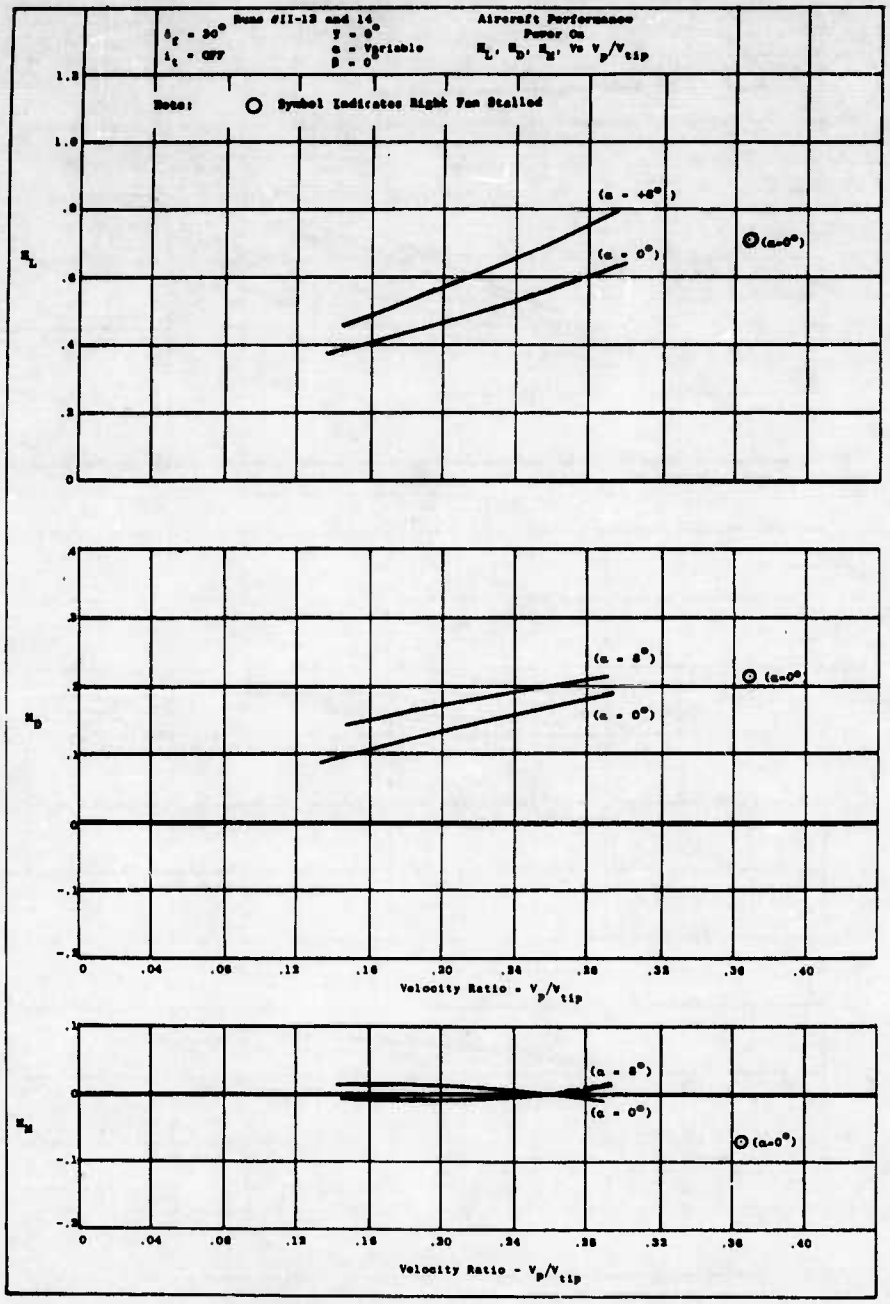


FIGURE 96 - FAN POWERED AIRCRAFT PERFORMANCE

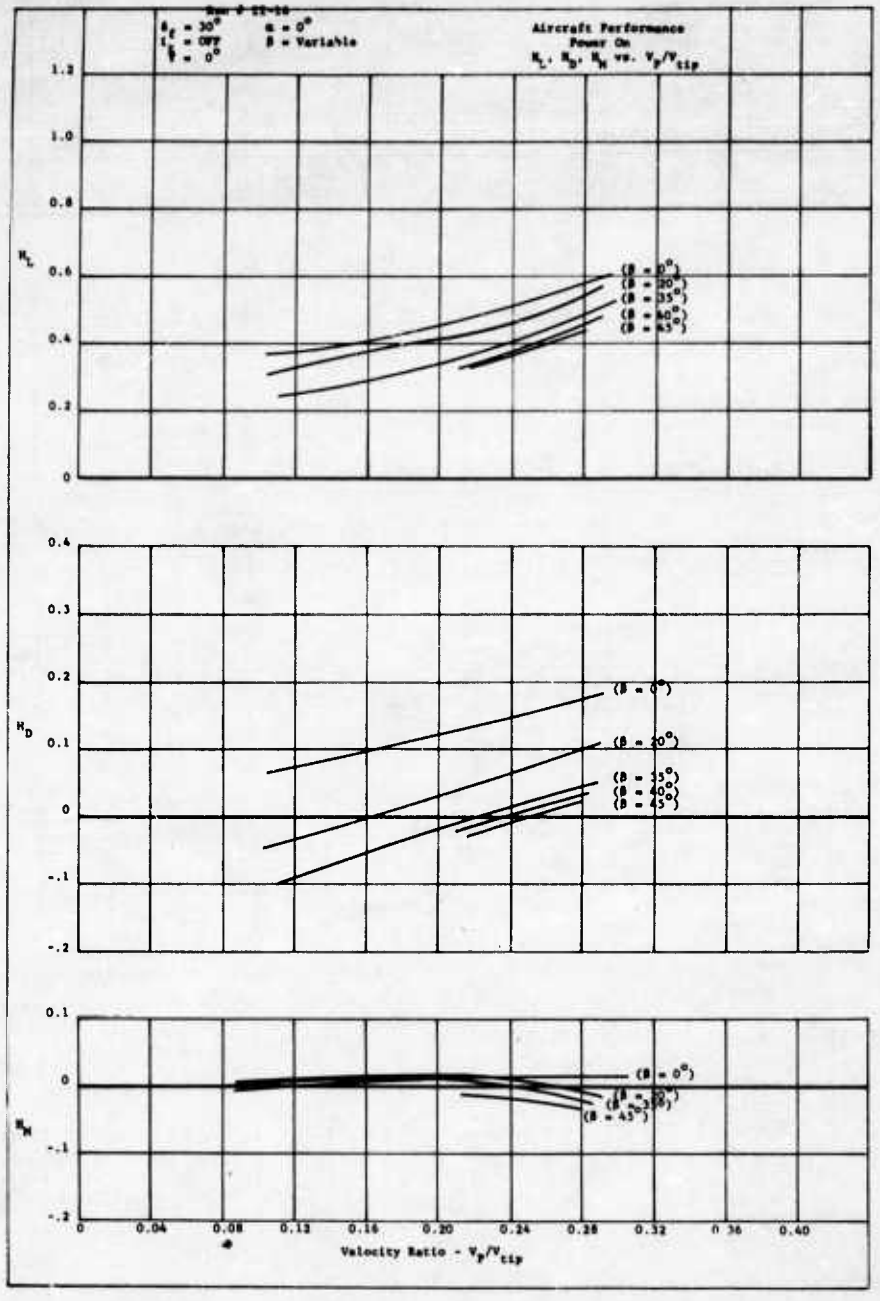


FIGURE 97a - FAN POWERED AIRCRAFT PERFORMANCE

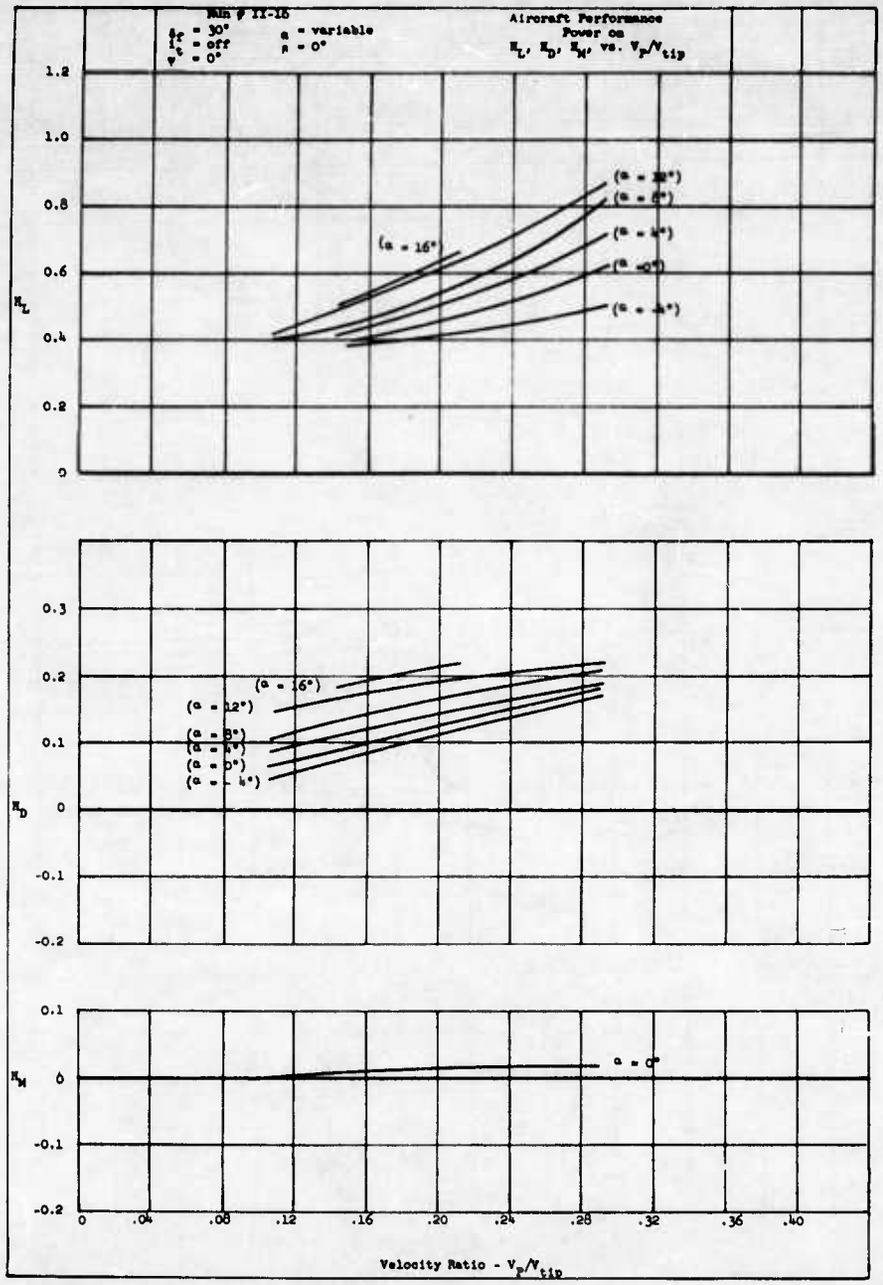


FIGURE 97b - FAN POWERED AIRCRAFT PERFORMANCE

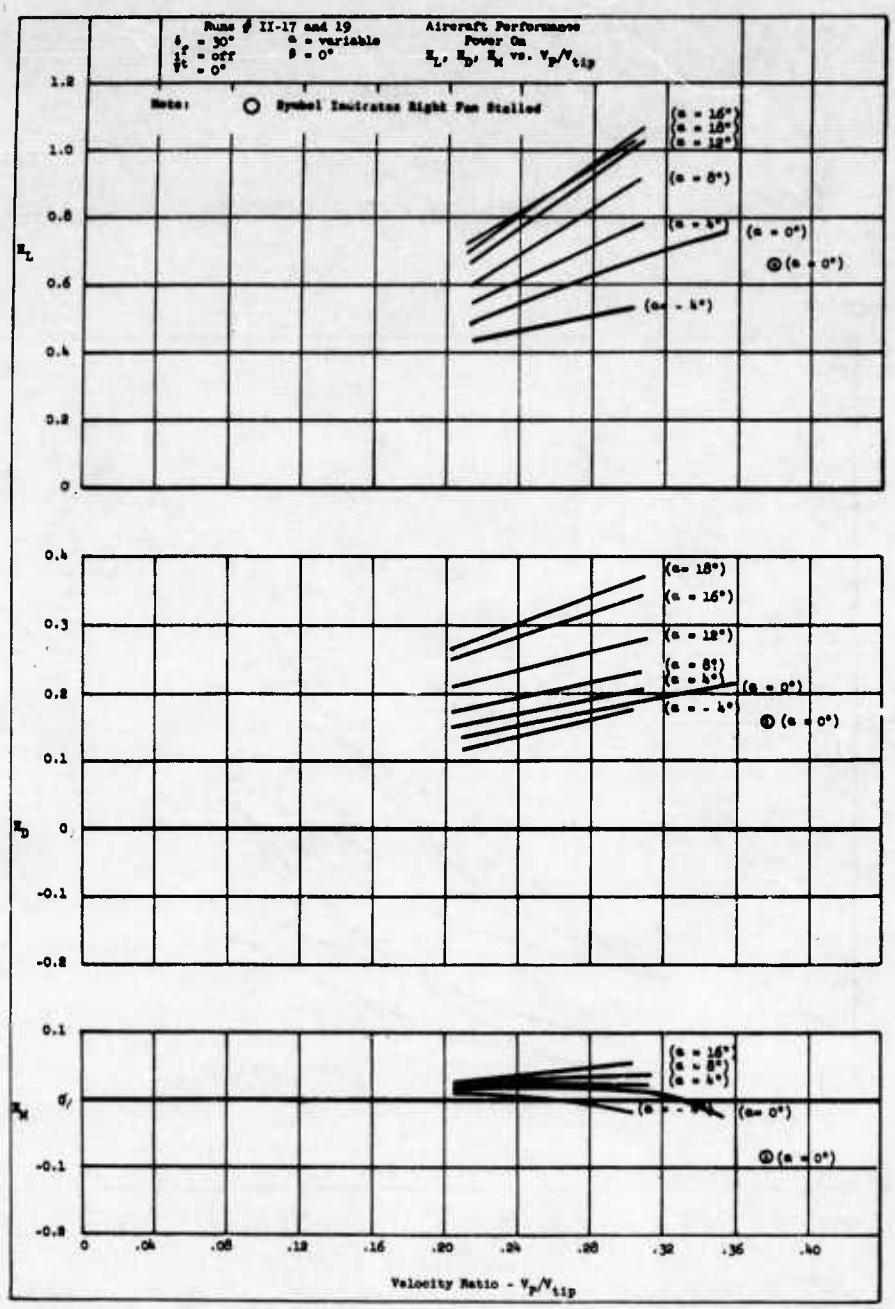


FIGURE 98 - FAN POWERED AIRCRAFT PERFORMANCE

Where:

1. $\beta = 0^o$, $\delta_f = 0^o$
2. $\beta = 0^o$, $\delta_f = 30^o$
3. $\beta = 0^o$, $\delta_f = 30^o$ Short Span Wing
4. $\beta = 35^o$, $\delta_f = 0^o$
5. $\beta = 35^o$, $\delta_f = 30^o$
6. $\beta = 35^o$, $\delta_f = 30^o$ Short Span Wing

– – – – Fan in Fuselage, Ref. 17, $\beta = 0^o$, $\delta_f = 0^o$

$\alpha = 0^o$

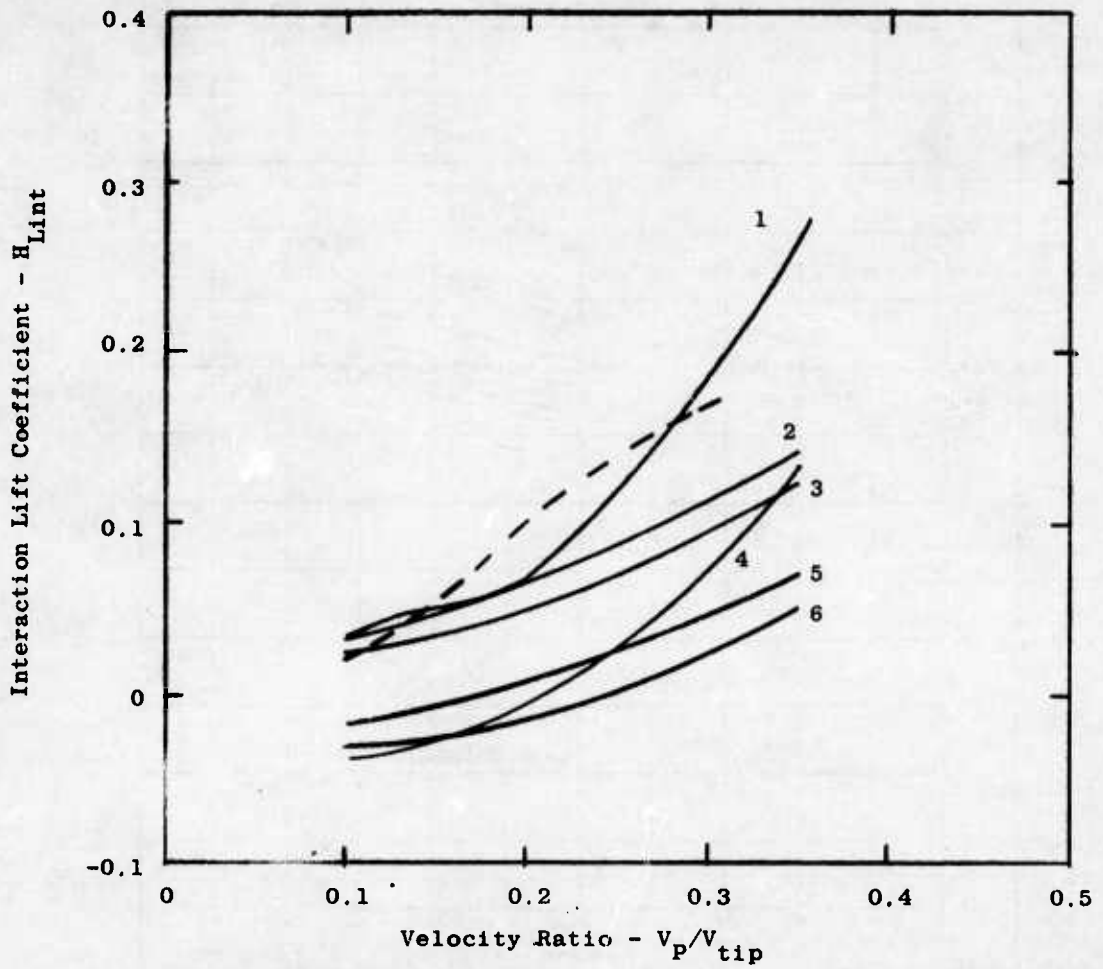


FIGURE 99. INTERACTION LIFT COEFFICIENT VERSUS VELOCITY RATIO

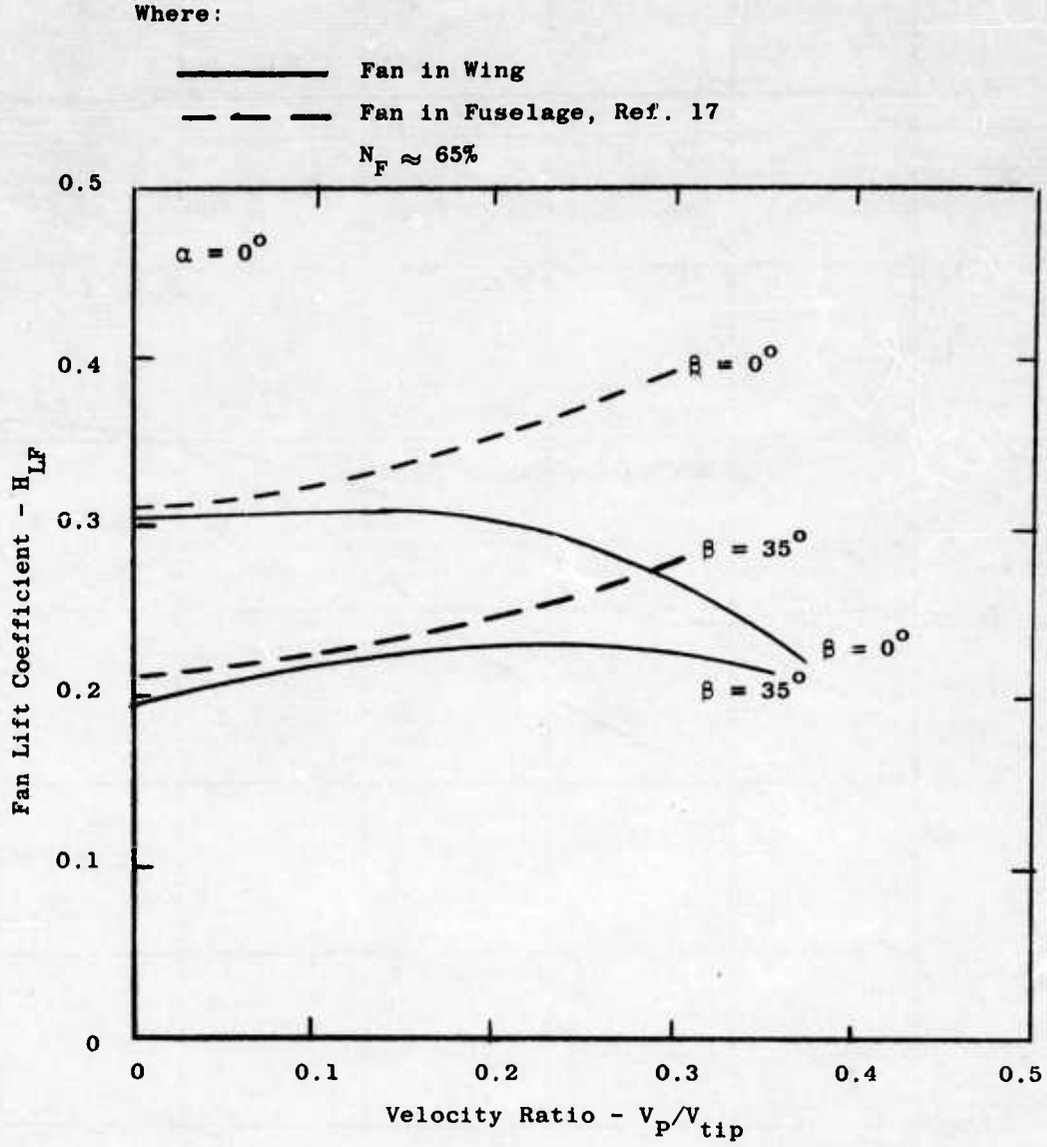


FIGURE 100. FAN LIFT COEFFICIENT VERSUS VELOCITY RATIO

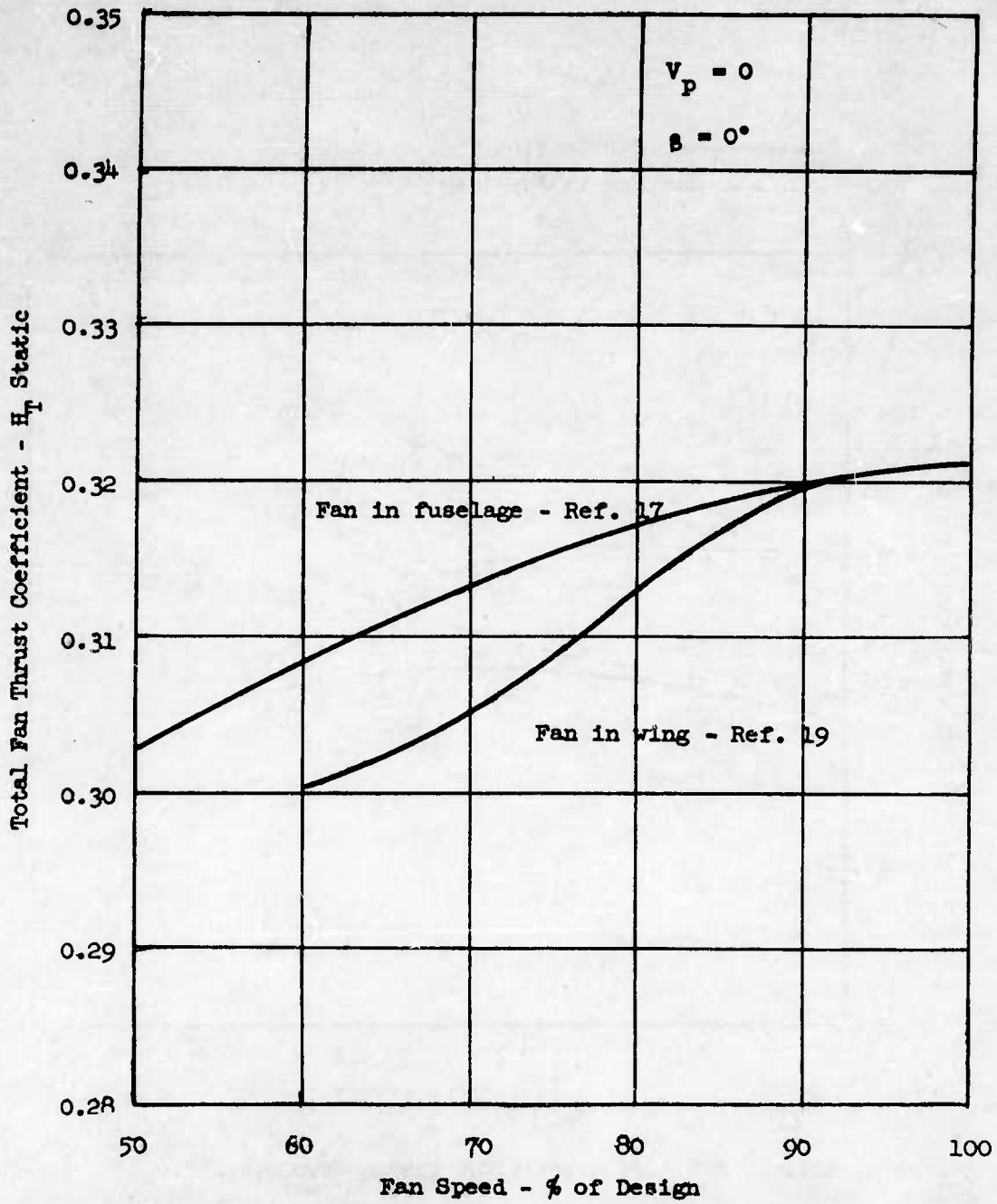


FIGURE 101. TOTAL FAN THRUST COEFFICIENT VERSUS FAN SPEED

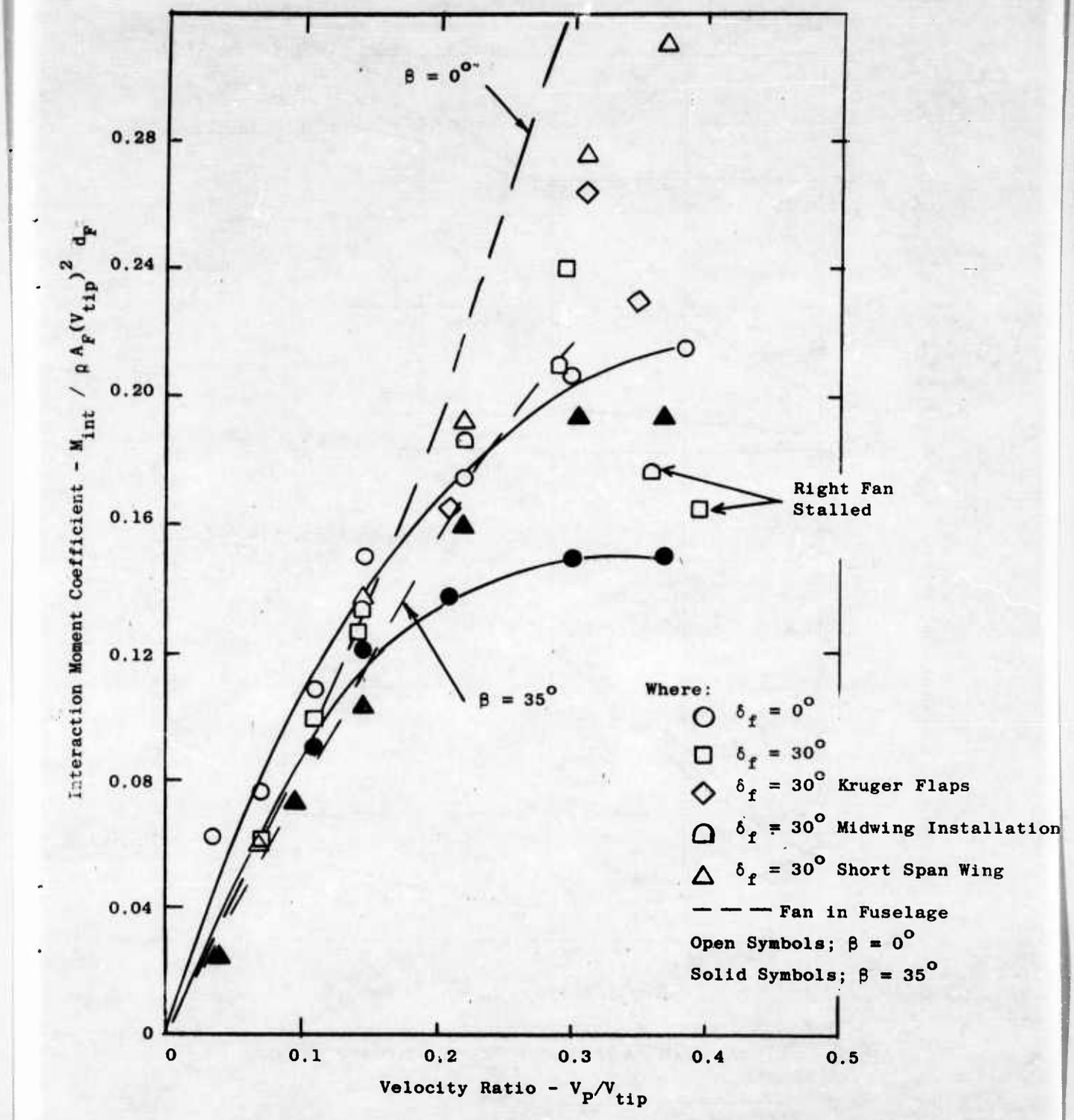


FIGURE 102. INTERACTION MOMENT COEFFICIENT VERSUS VELOCITY RATIO

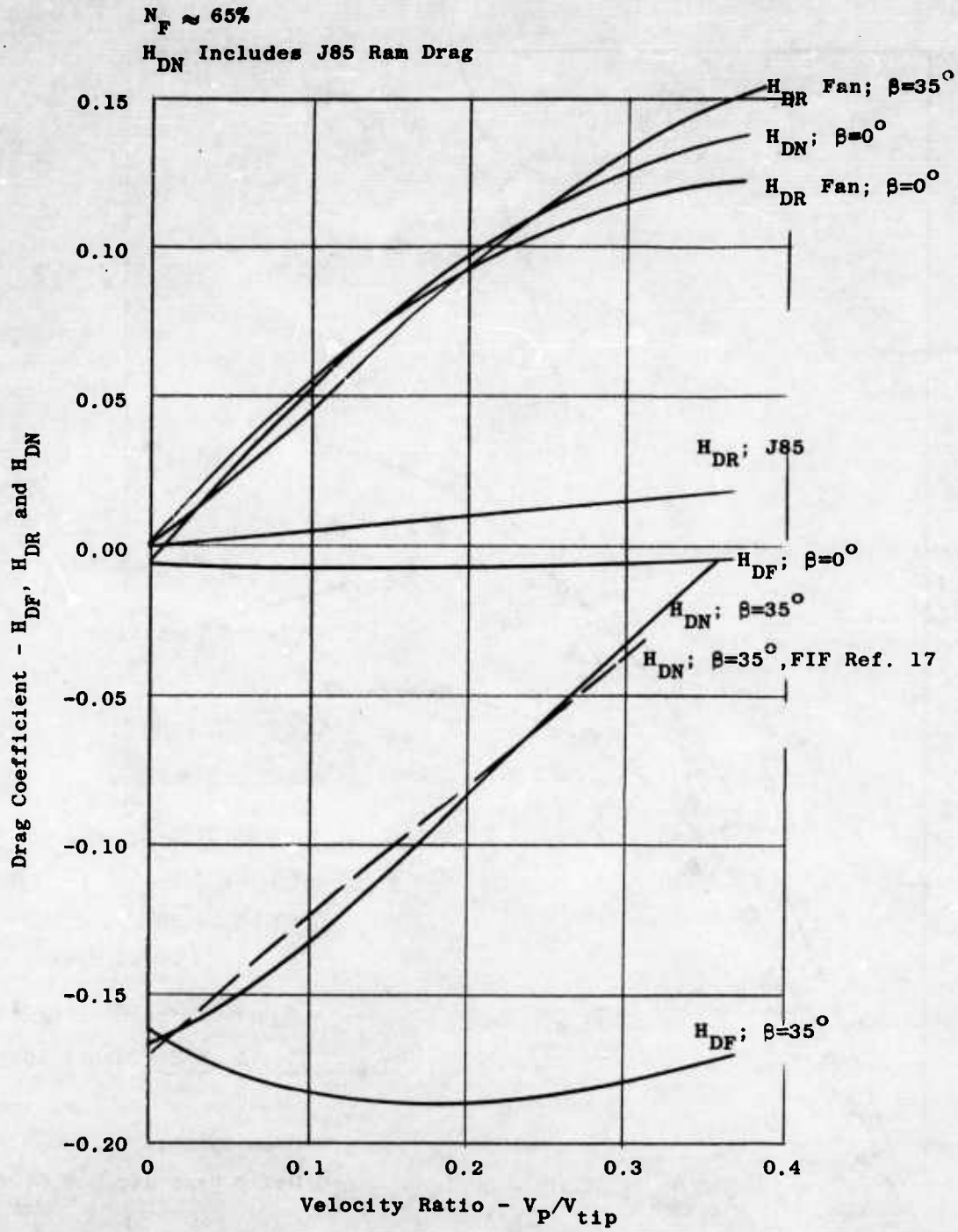


FIGURE 103. FAN DRAG COEFFICIENTS VERSUS VELOCITY RATIO

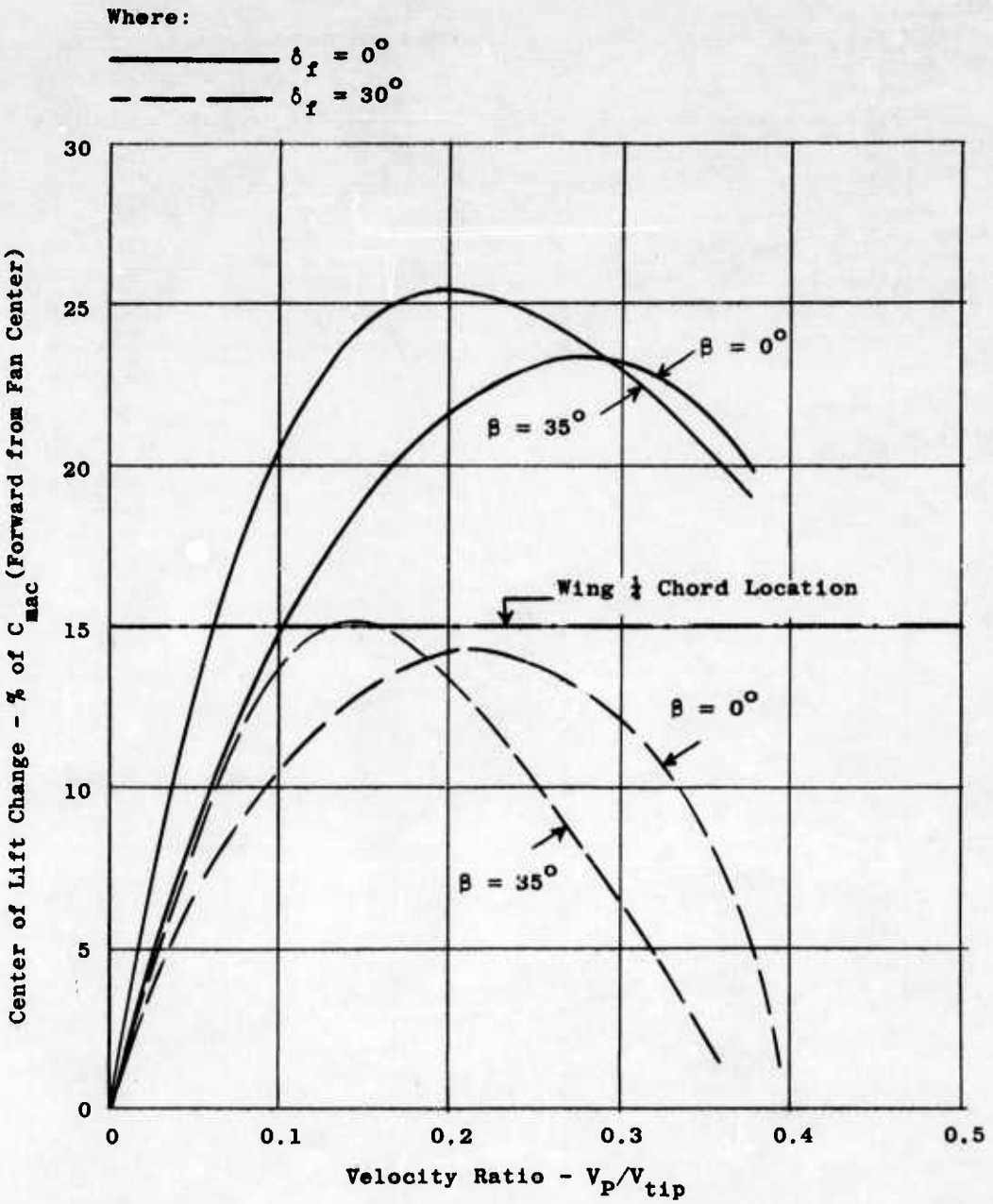


FIGURE 104. LIFT CENTER CHANGE VERSUS VELOCITY RATIO

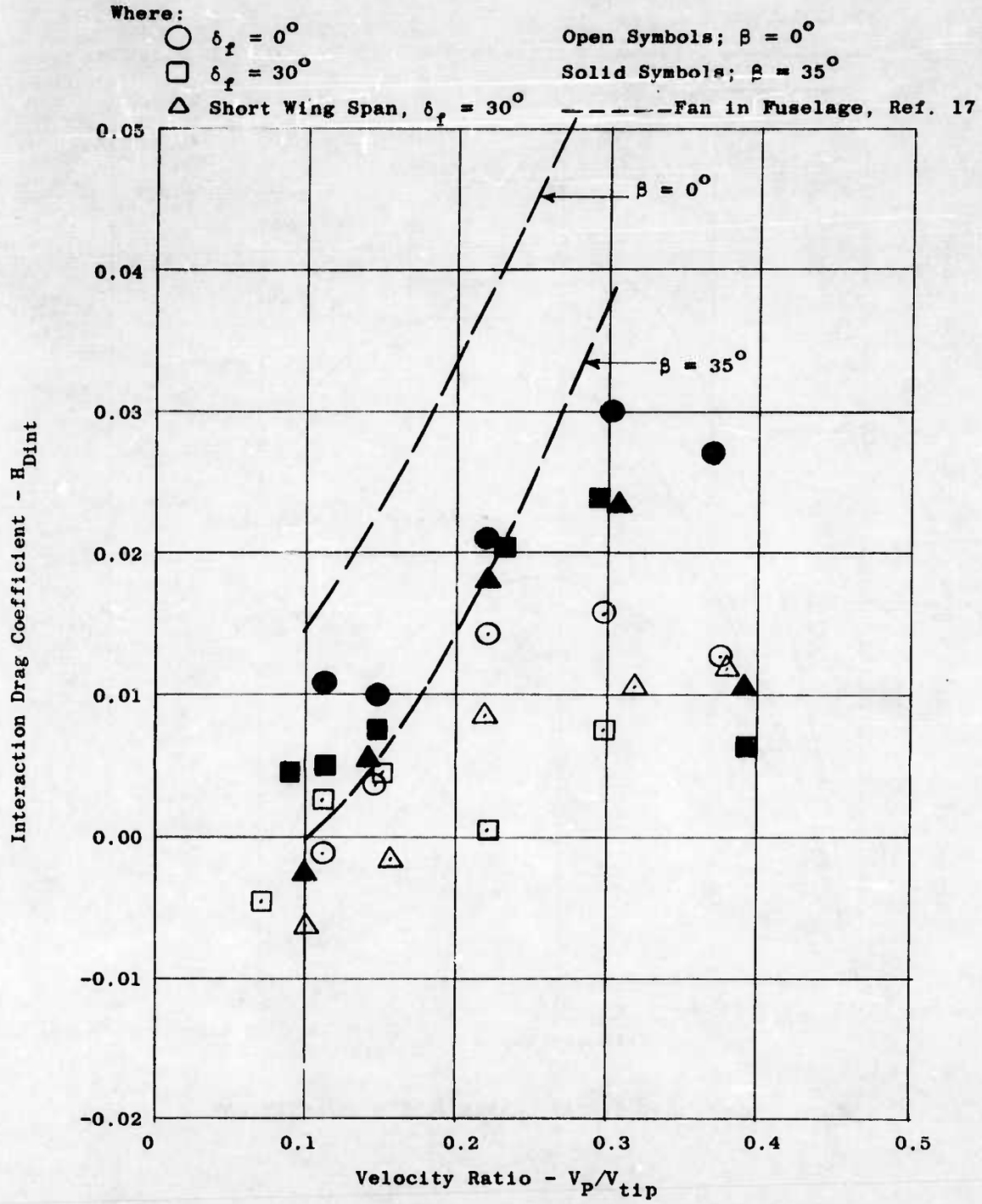


FIGURE 105. INTERACTION DRAG COEFFICIENT VERSUS VELOCITY RATIO

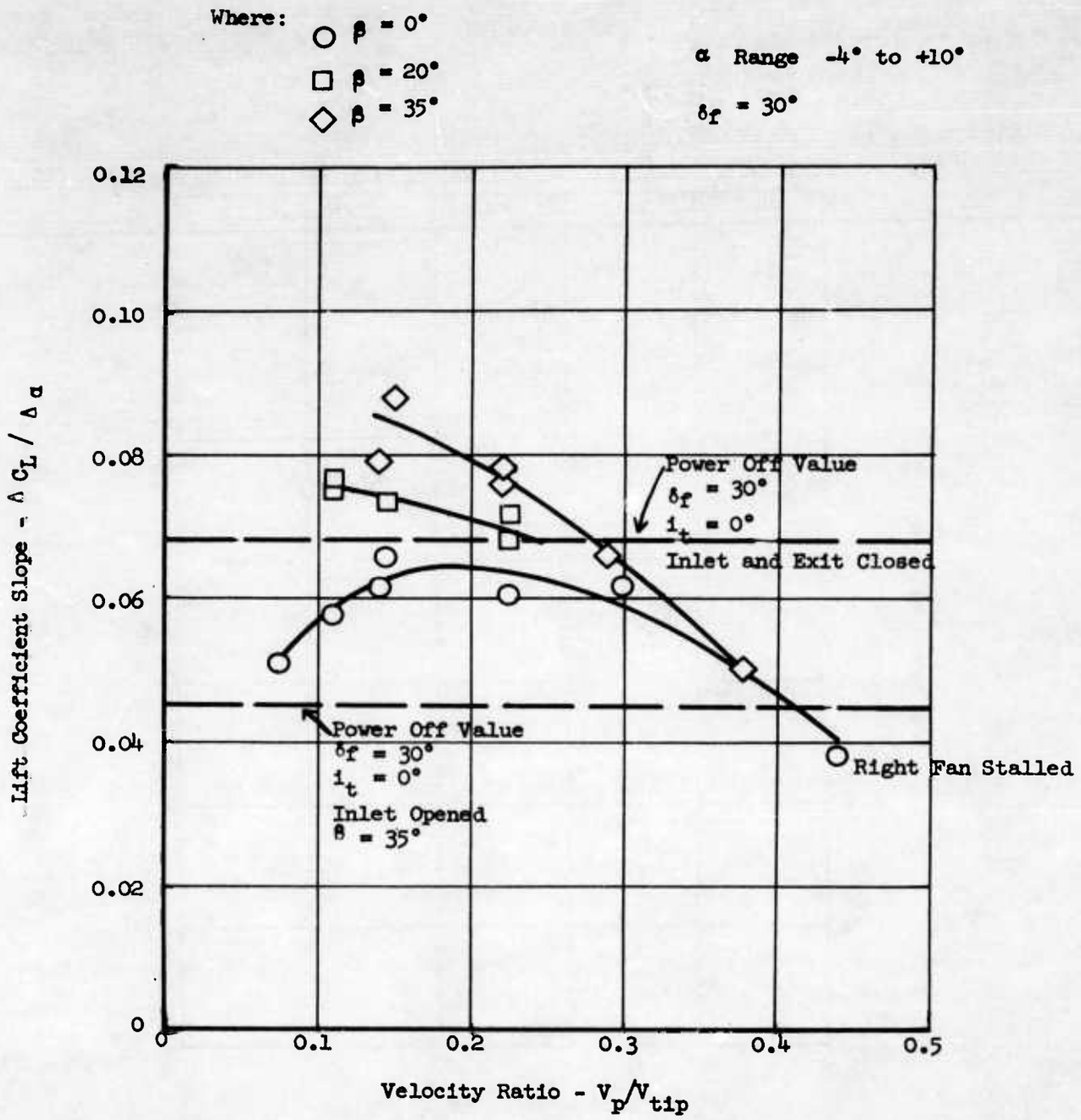


FIGURE 106. LIFT COEFFICIENT SLOPE VERSUS VELOCITY RATIO

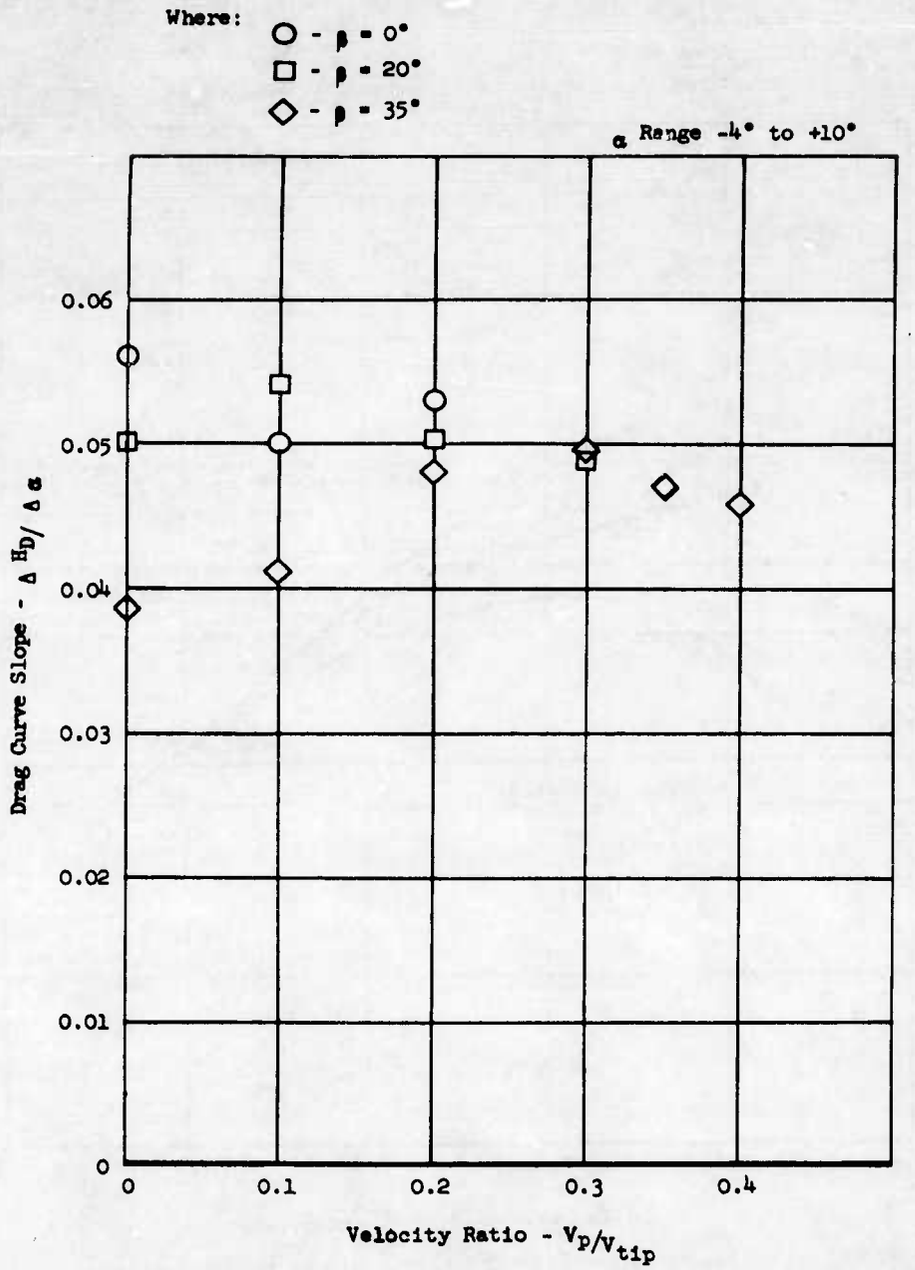


FIGURE 107. DRAG CURVE SLOPE VERSUS VELOCITY RATIO

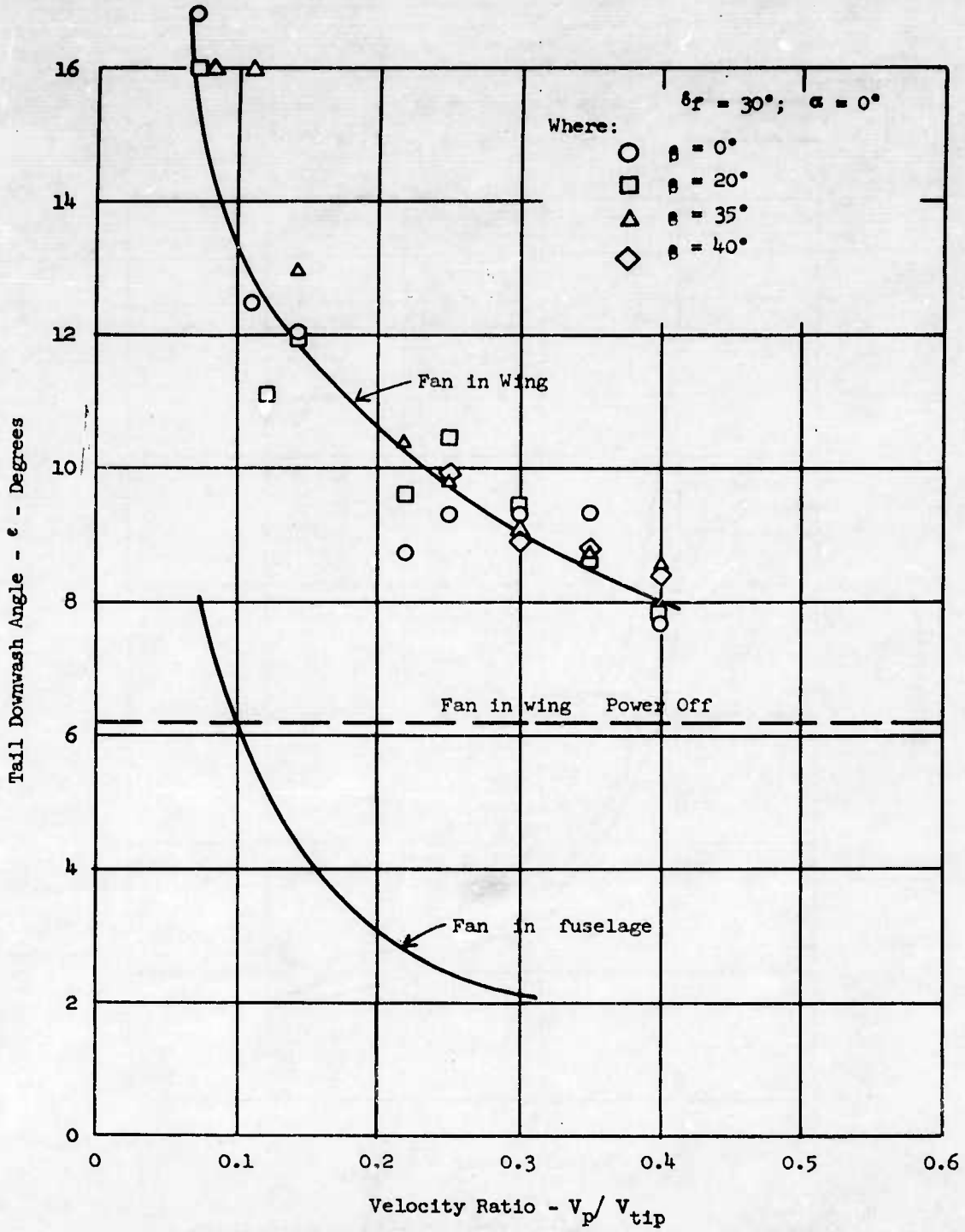


FIGURE 108. TAIL DOWNWASH ANGLE VERSUS VELOCITY RATIO

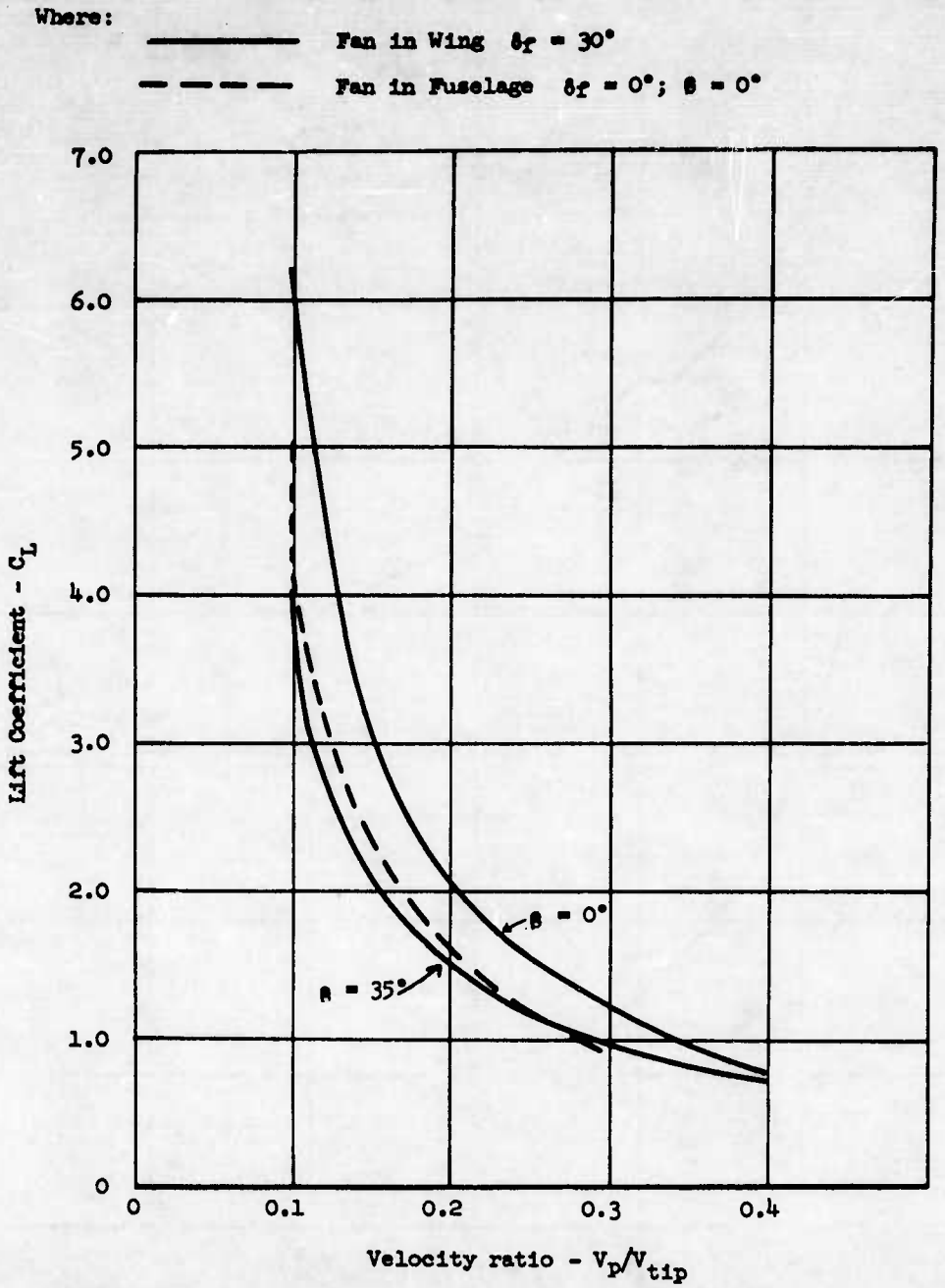


FIGURE 109. LIFT COEFFICIENT VERSUS VELOCITY RATIO

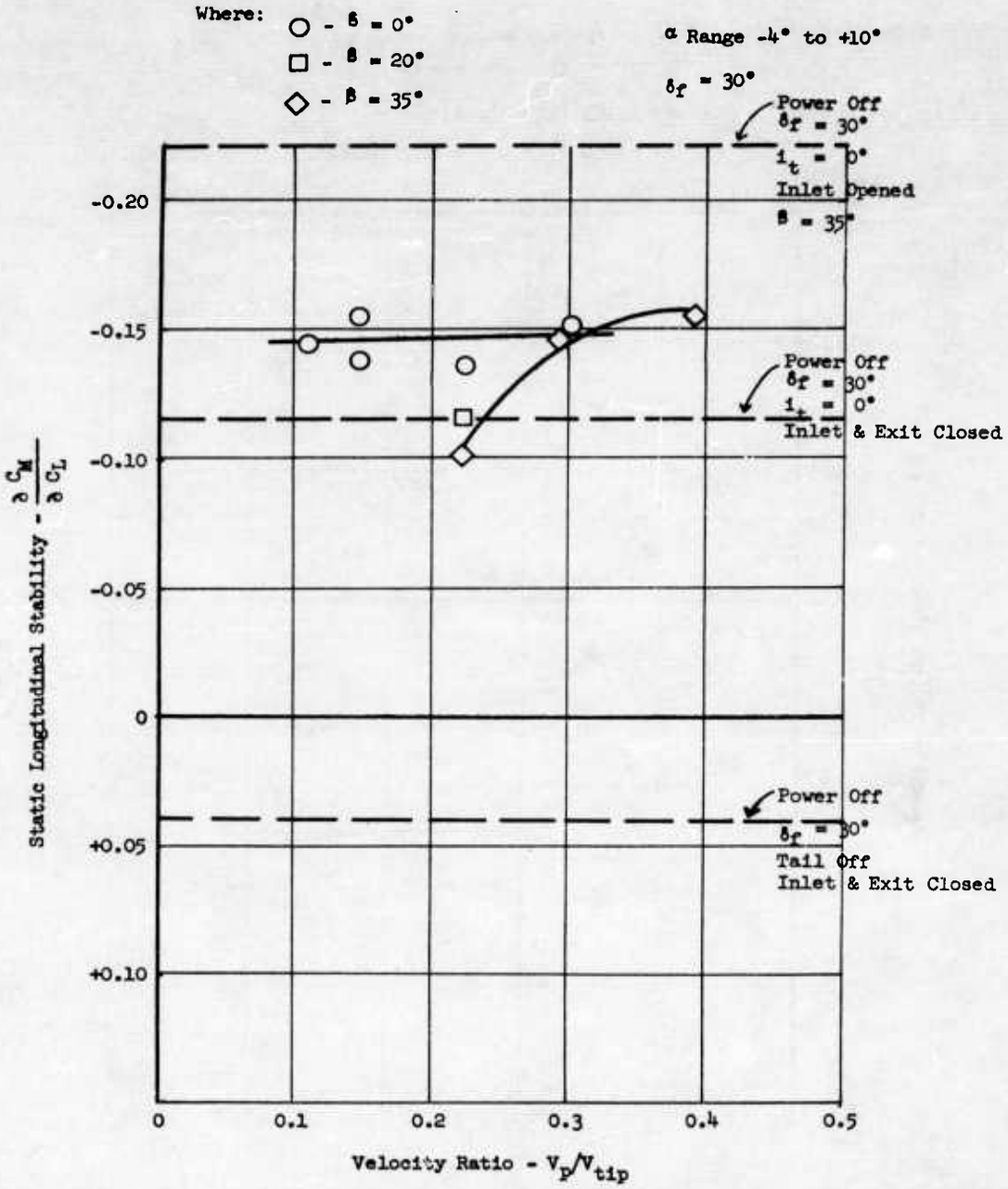


FIGURE 110. STATIC LONGITUDINAL STABILITY VERSUS VELOCITY RATIO POWER ON AND OFF

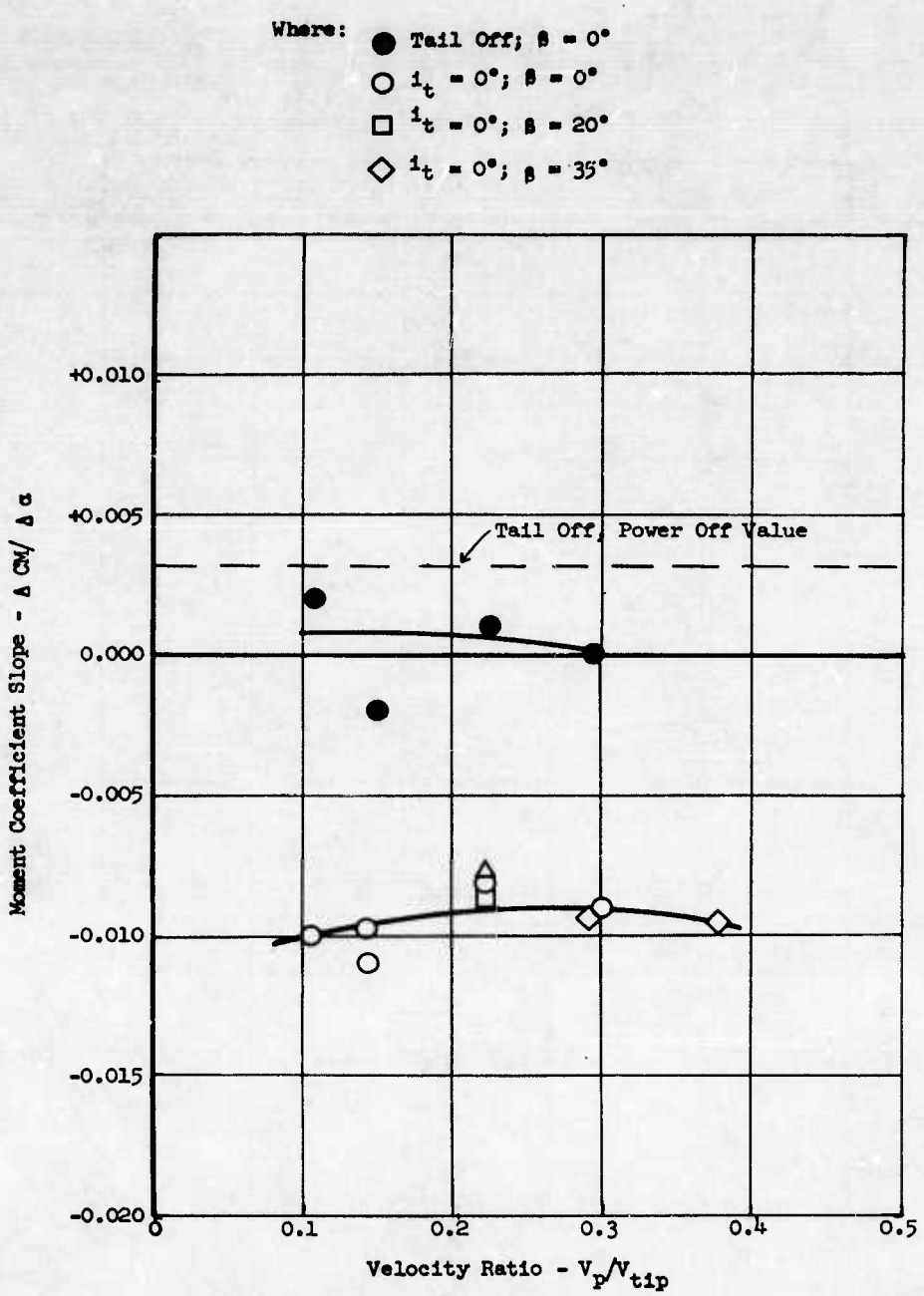


FIGURE 111. MOMENT COEFFICIENT SLOPE VERSUS VELOCITY RATIO

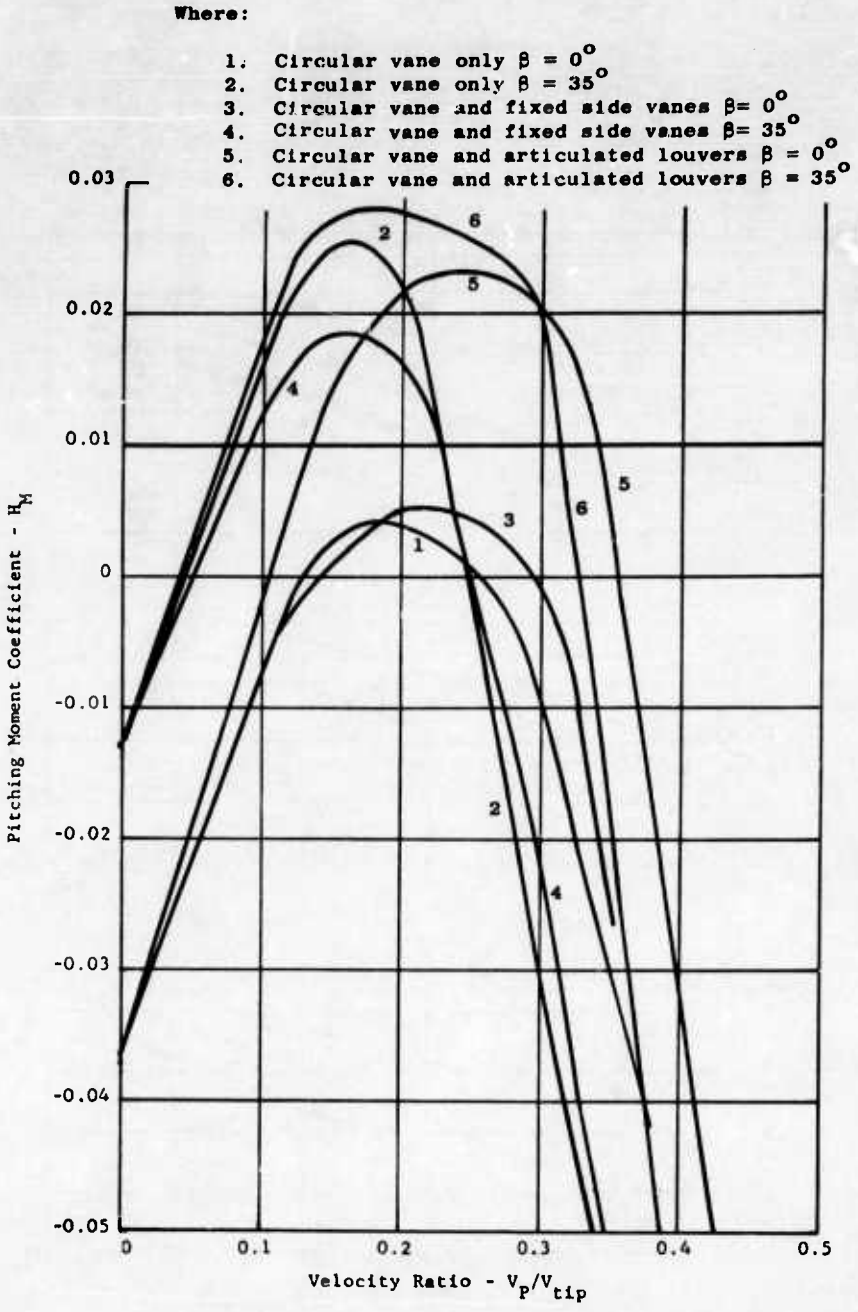


FIGURE 112. PITCHING MOMENT COEFFICIENT VERSUS VELOCITY RATIO

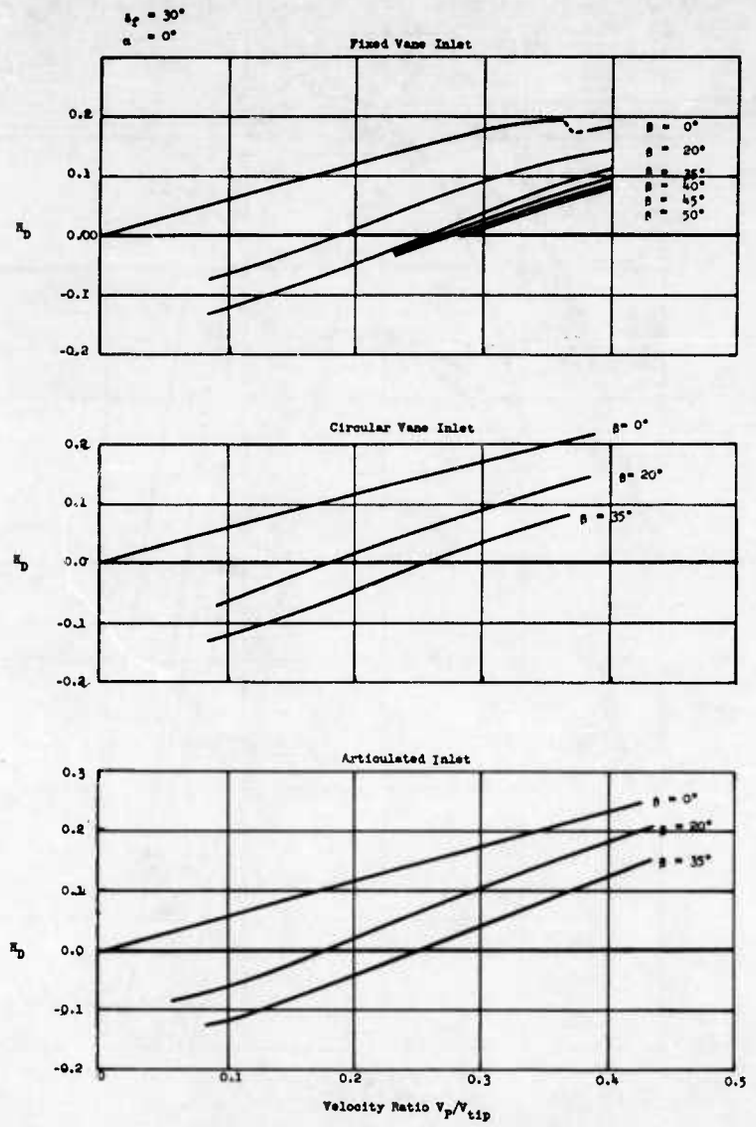


FIGURE 113 - DRAG COEFFICIENT VERSUS VELOCITY RATIO

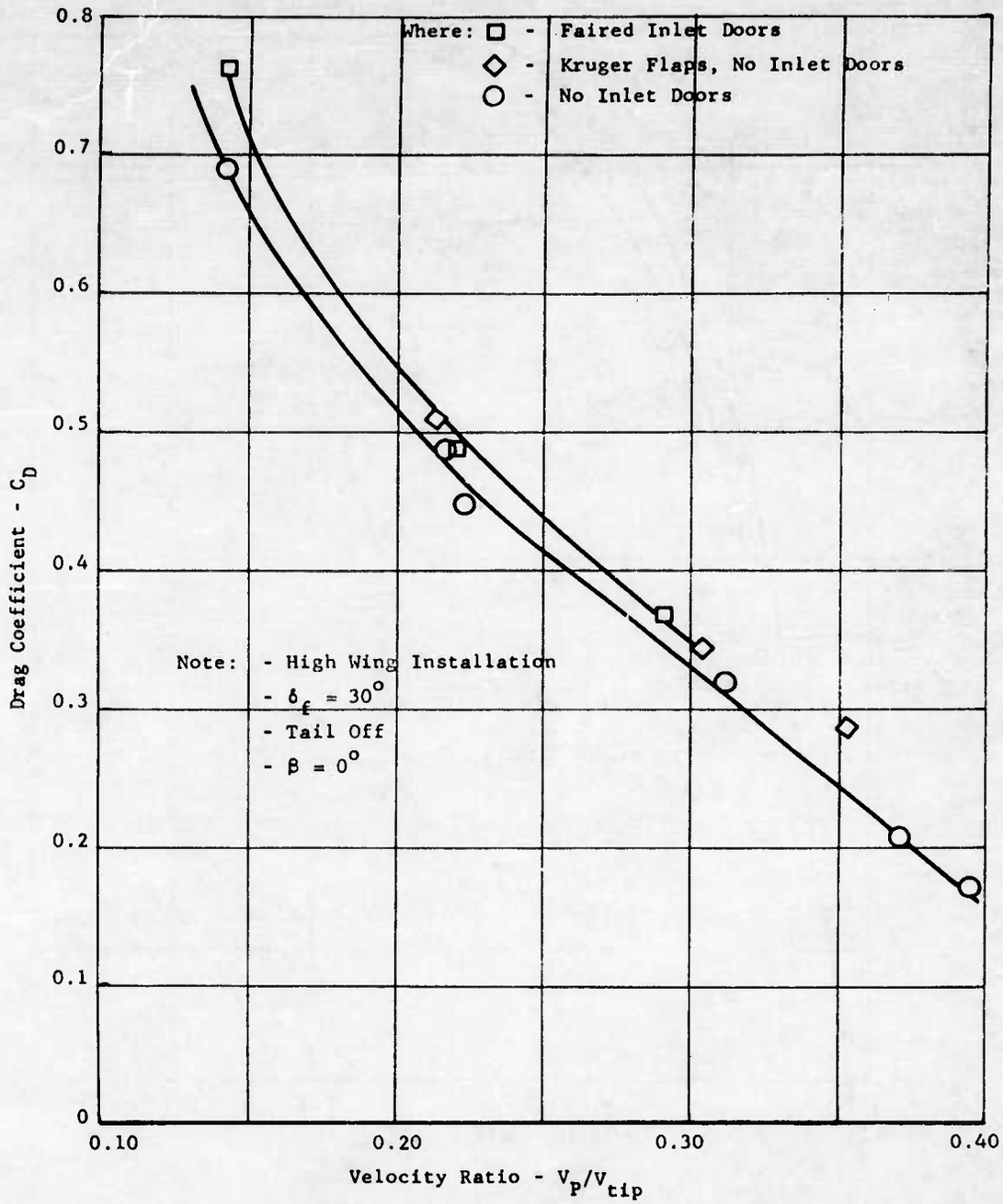


FIGURE 114a. DRAG COEFFICIENT VERSUS VELOCITY RATIO

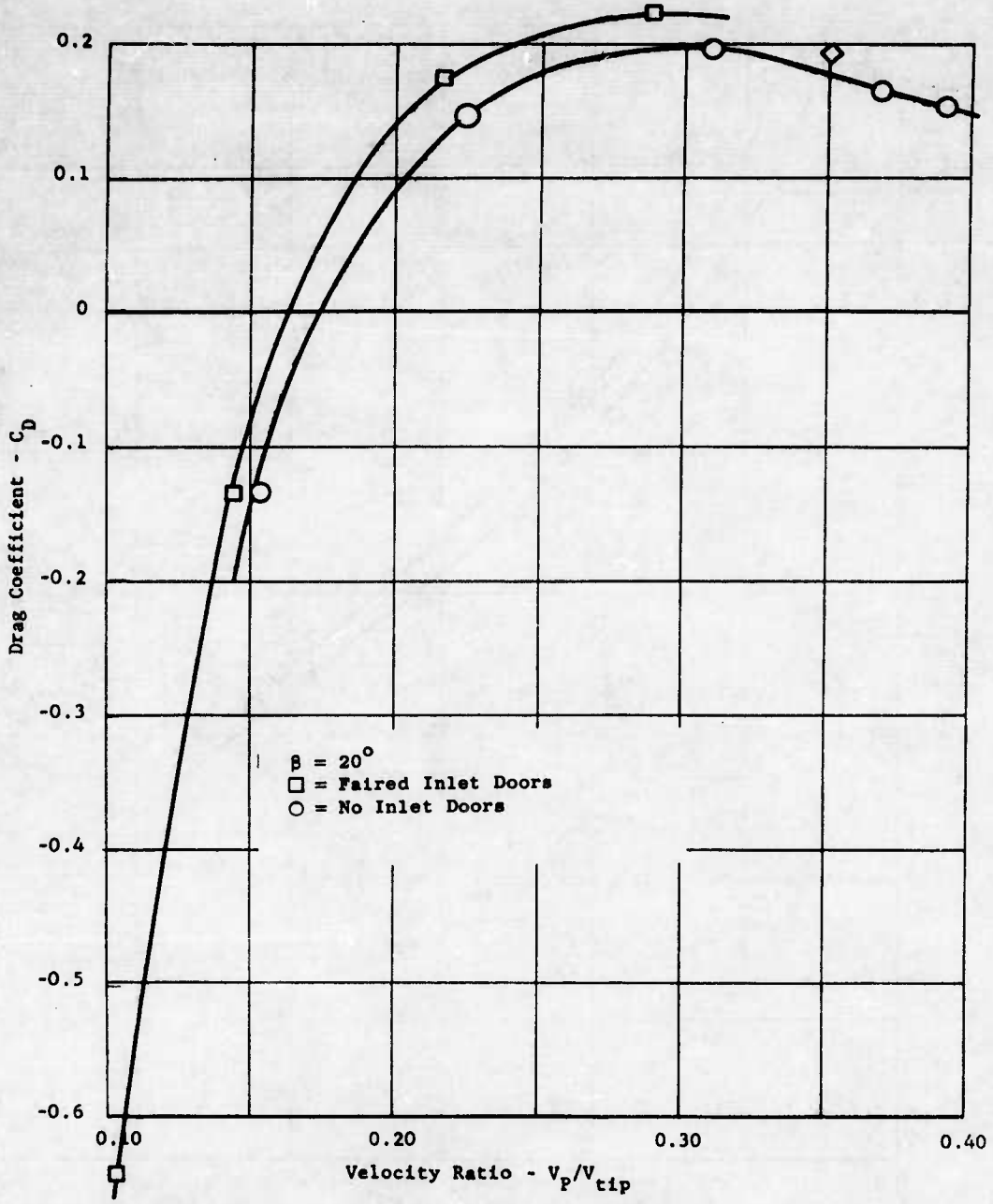


FIGURE 114b. DRAG COEFFICIENT VERSUS VELOCITY RATIO

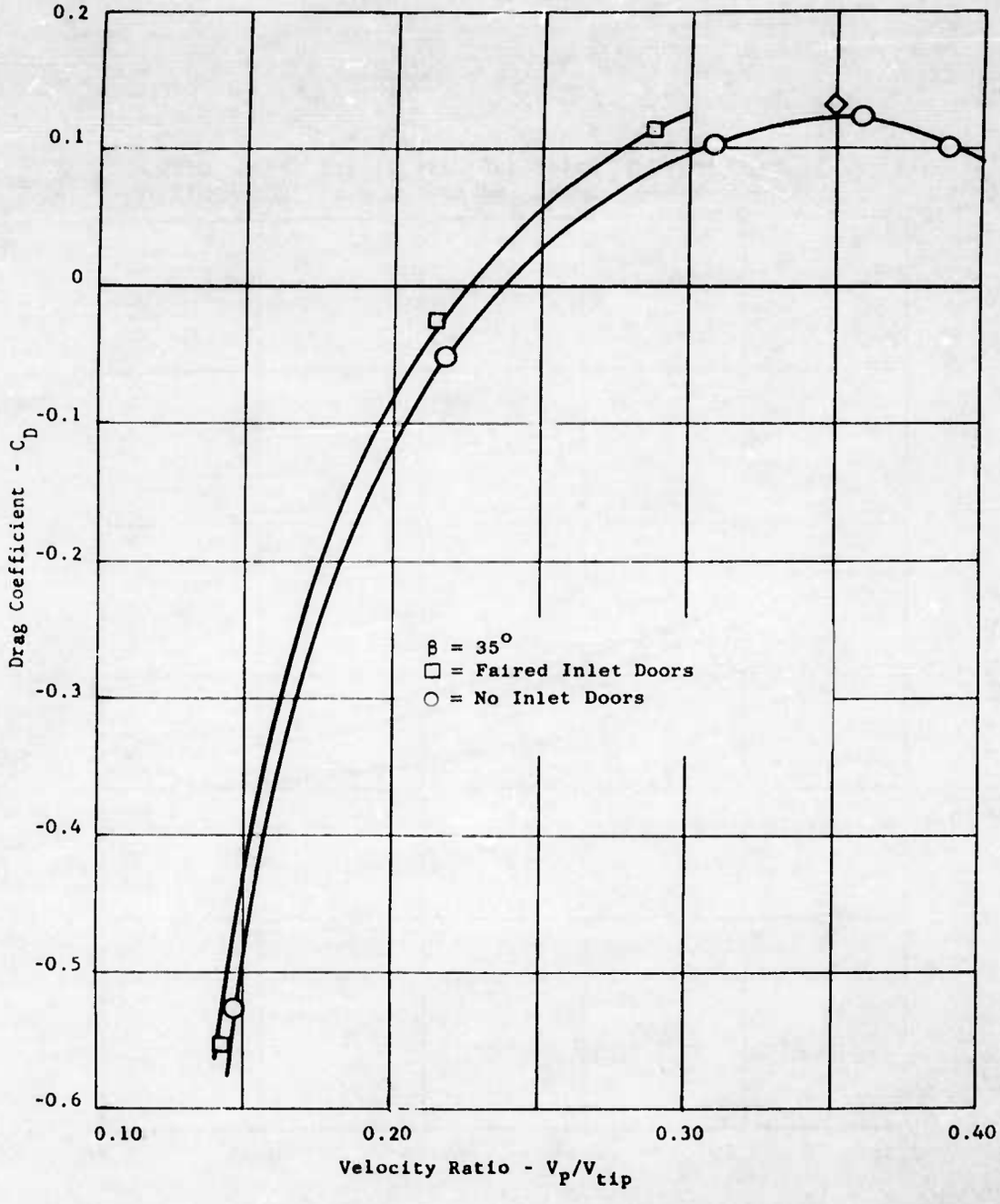


FIGURE 114c. DRAG COEFFICIENT VERSUS VELOCITY RATIO

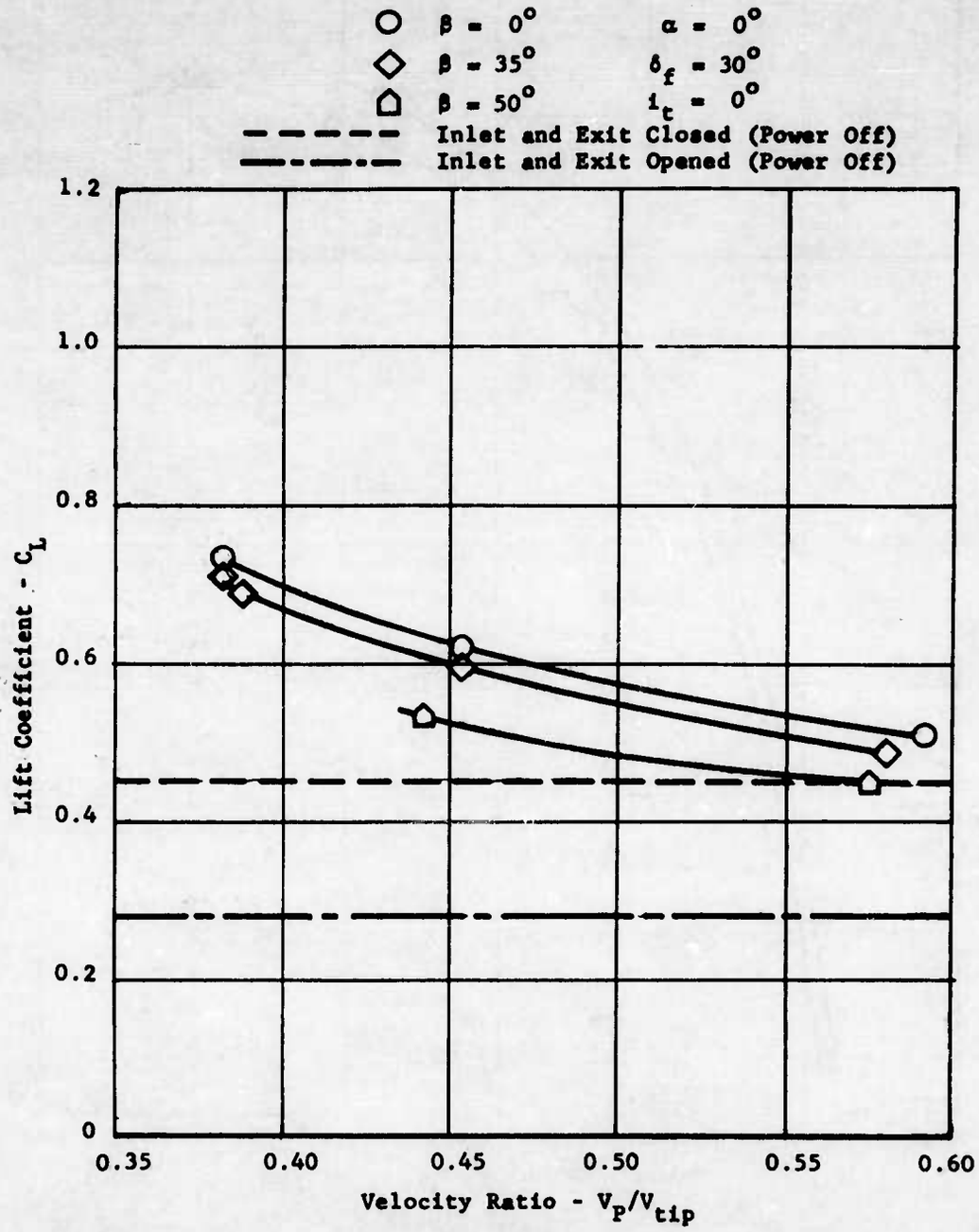


FIGURE 115a - LIFT COEFFICIENT VERSUS VELOCITY RATIO

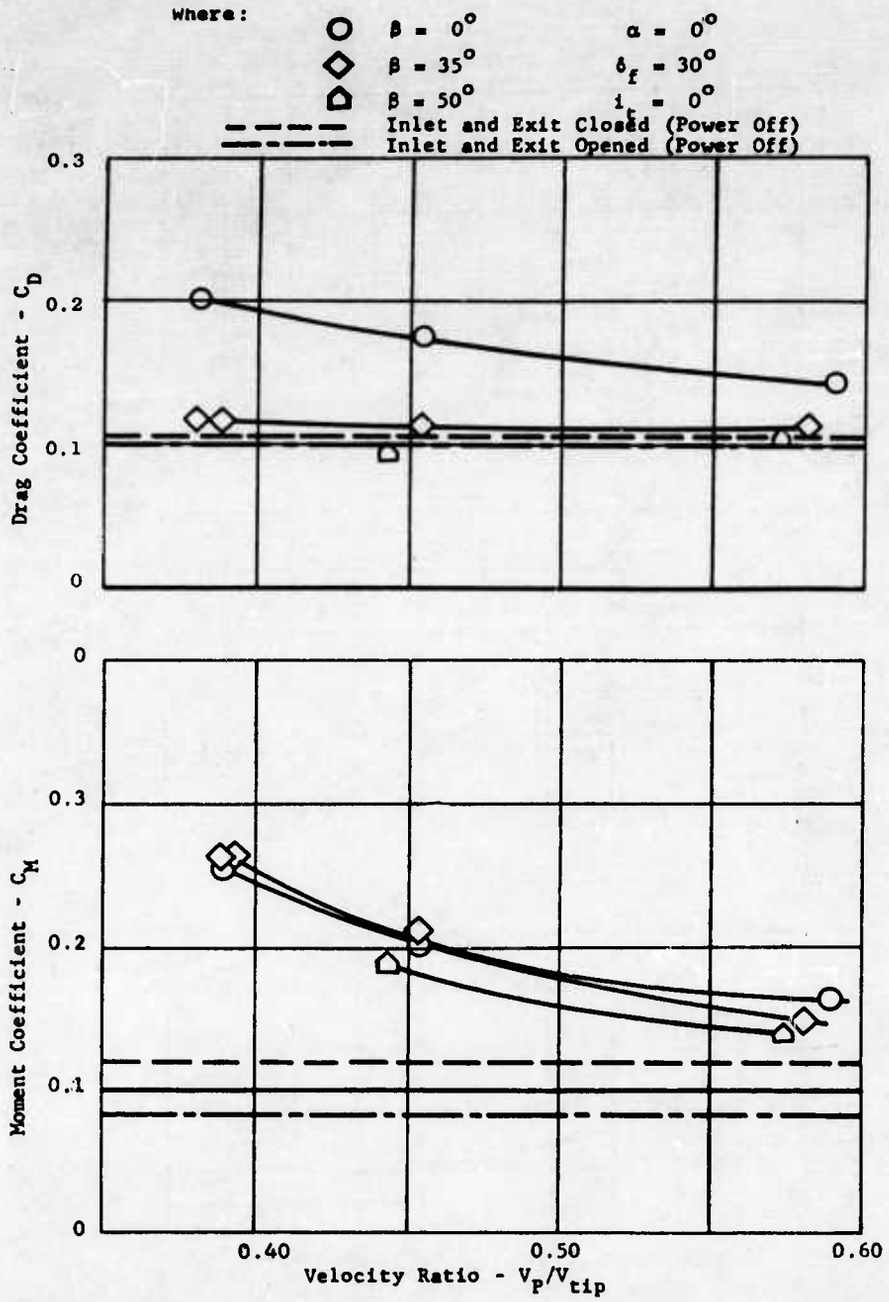


FIGURE 115b. MOMENT AND DRAG COEFFICIENTS VERSUS VELOCITY RATIO

1. Exit and Inlet Closed (Power Off)

2. $\beta = 45^{\circ}$ $V_p/V_{tip} = 0.57$

3. Exit and Inlet Open (Power Off)

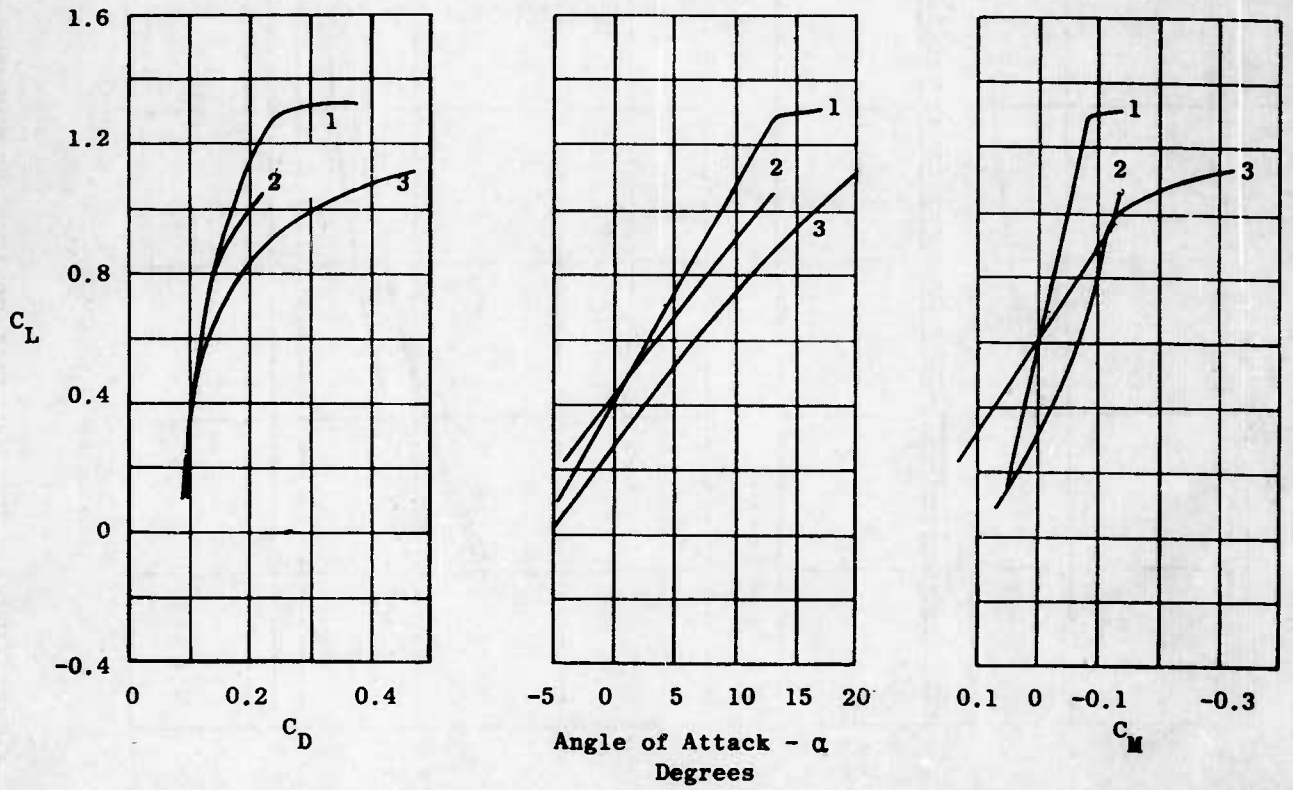


FIGURE 116 - COMPARISON OF POWER-OFF AND HIGH VELOCITY RATIO POLARS

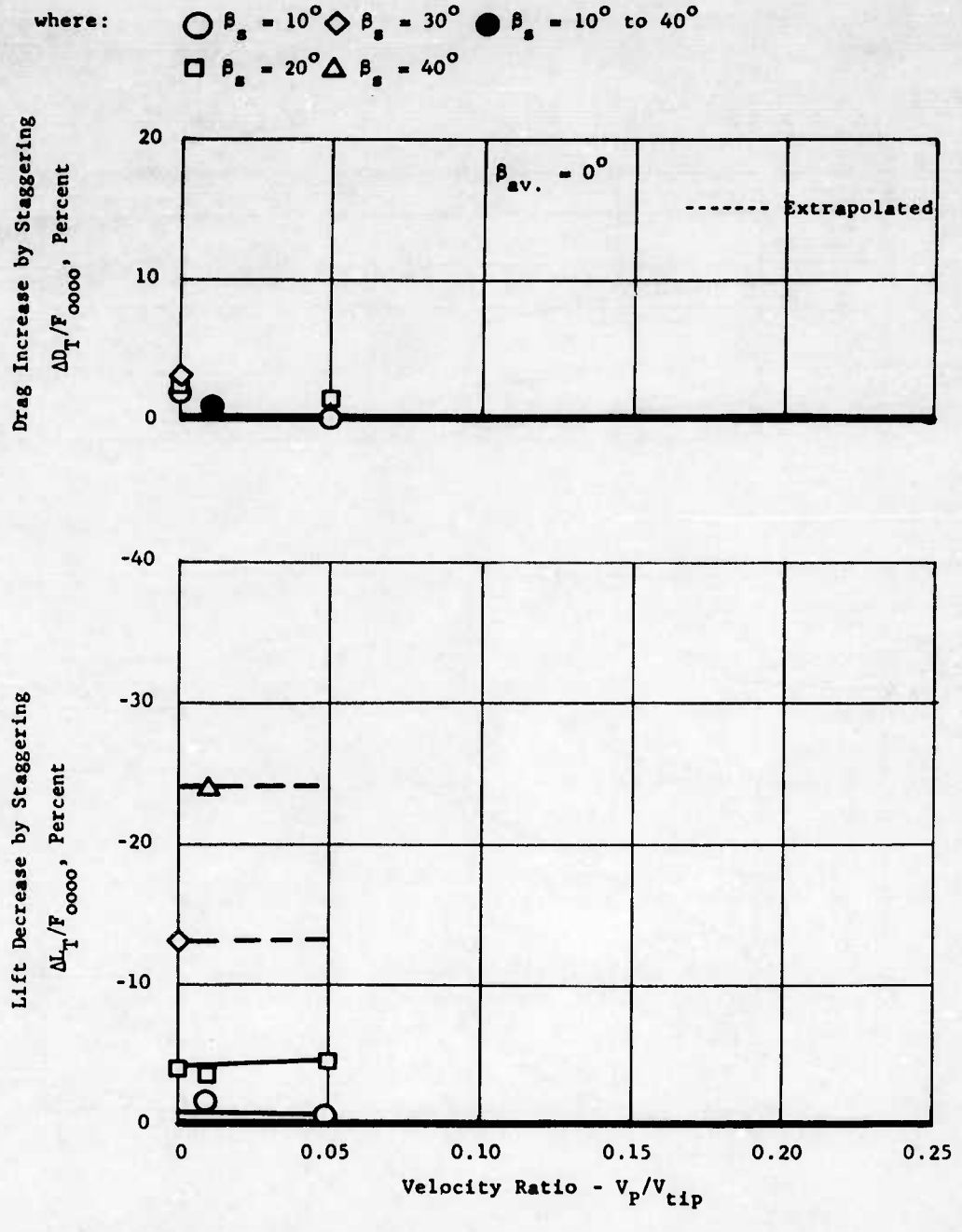


FIGURE 117a. TOTAL LIFT AND DRAG VARIATION VERSUS β_s AND V_p/V_{tip} AT CONSTANT J85 ENGINE POWER

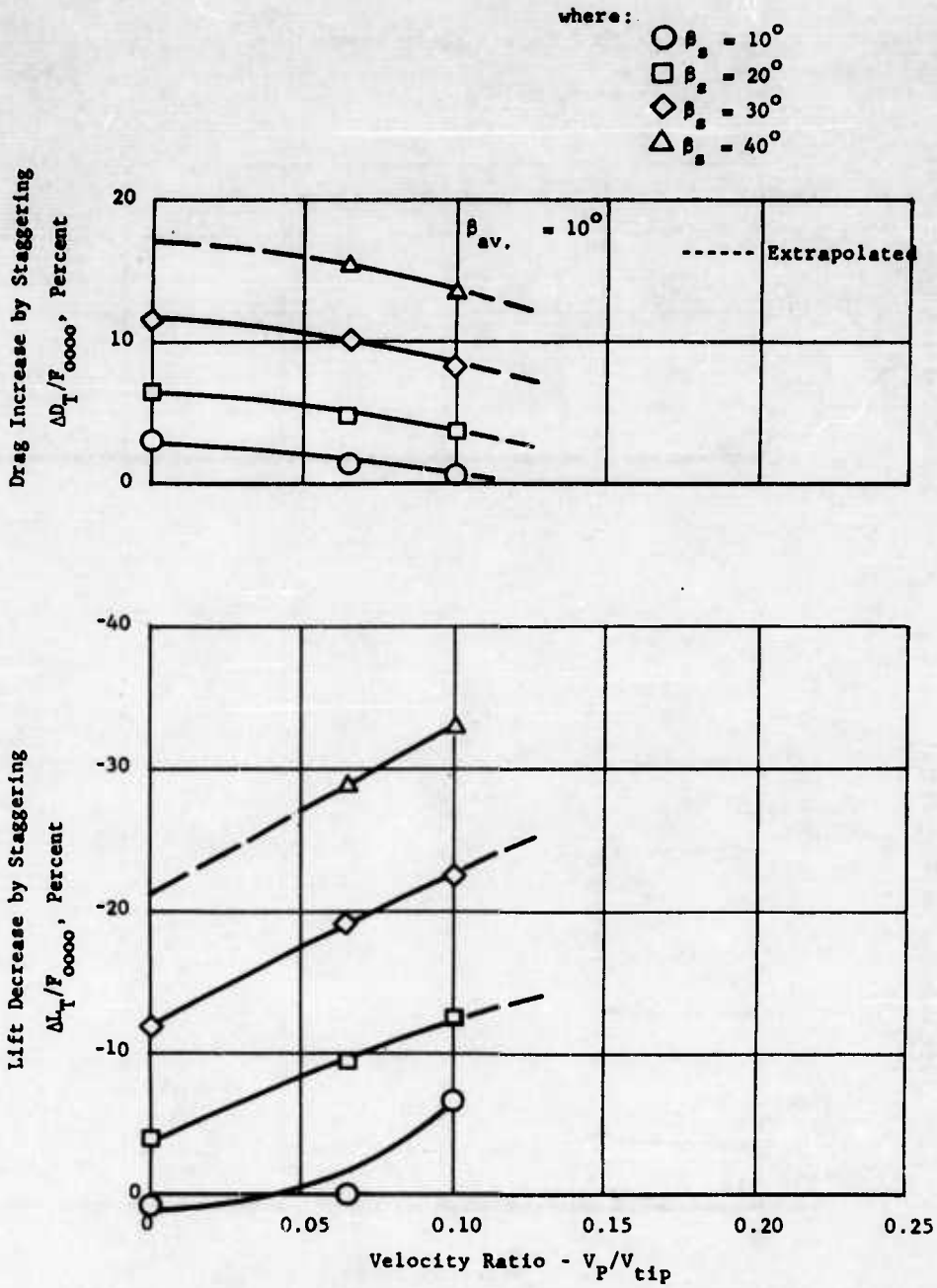


FIGURE 117b. TOTAL LIFT AND DRAG VARIATION VERSUS β_s AND V_p/V_{tip} AT CONSTANT J85 ENGINE POWER

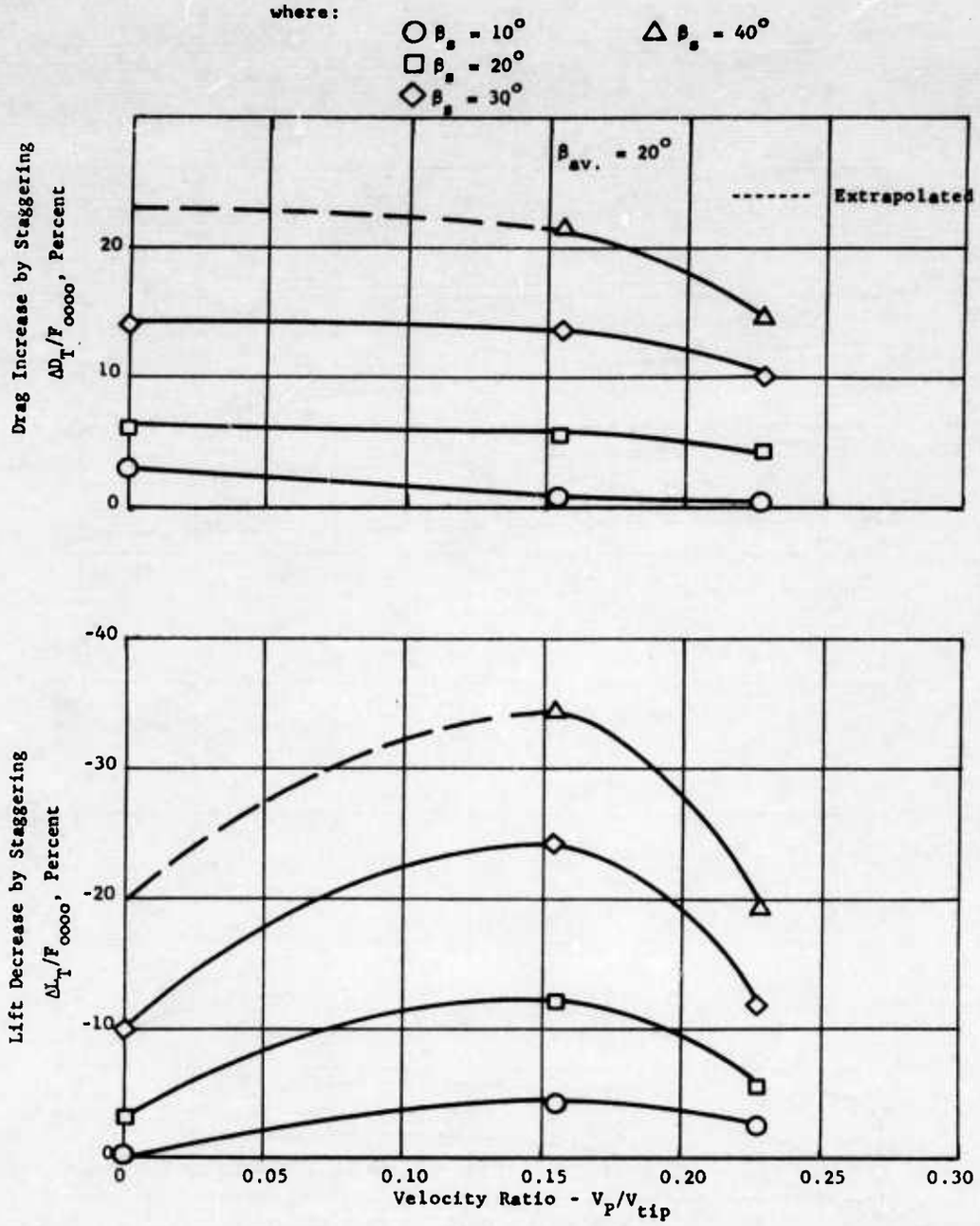


FIGURE 117c. TOTAL LIFT AND DRAG VARIATION VERSUS β_s AND V_p/V_{tip} AT CONSTANT J85 ENGINE POWER

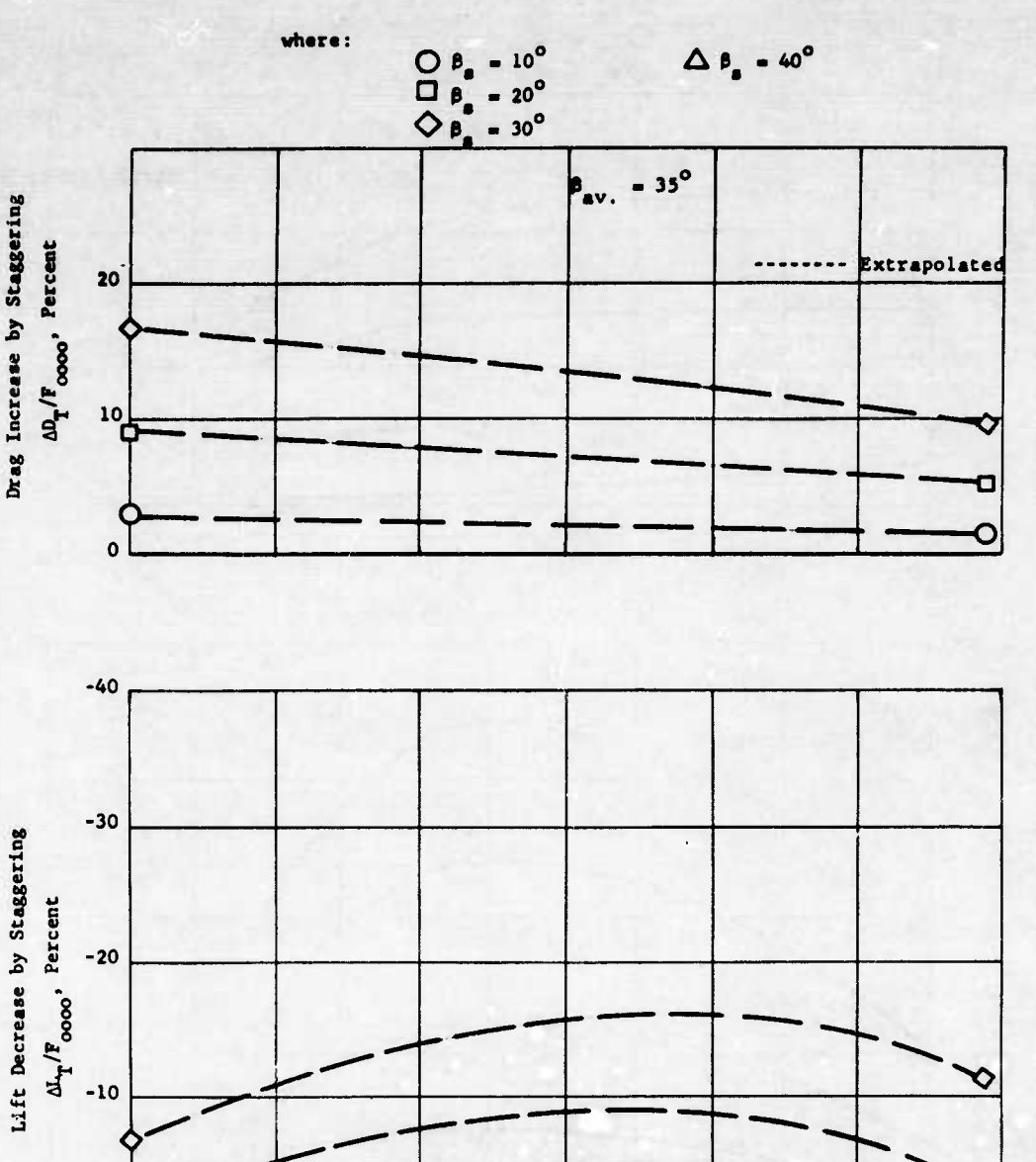


FIGURE 117d. TOTAL LIFT AND DRAG VARIATION VERSUS β_s AND V_p/V_{tip} AT CONSTANT J85 ENGINE POWER

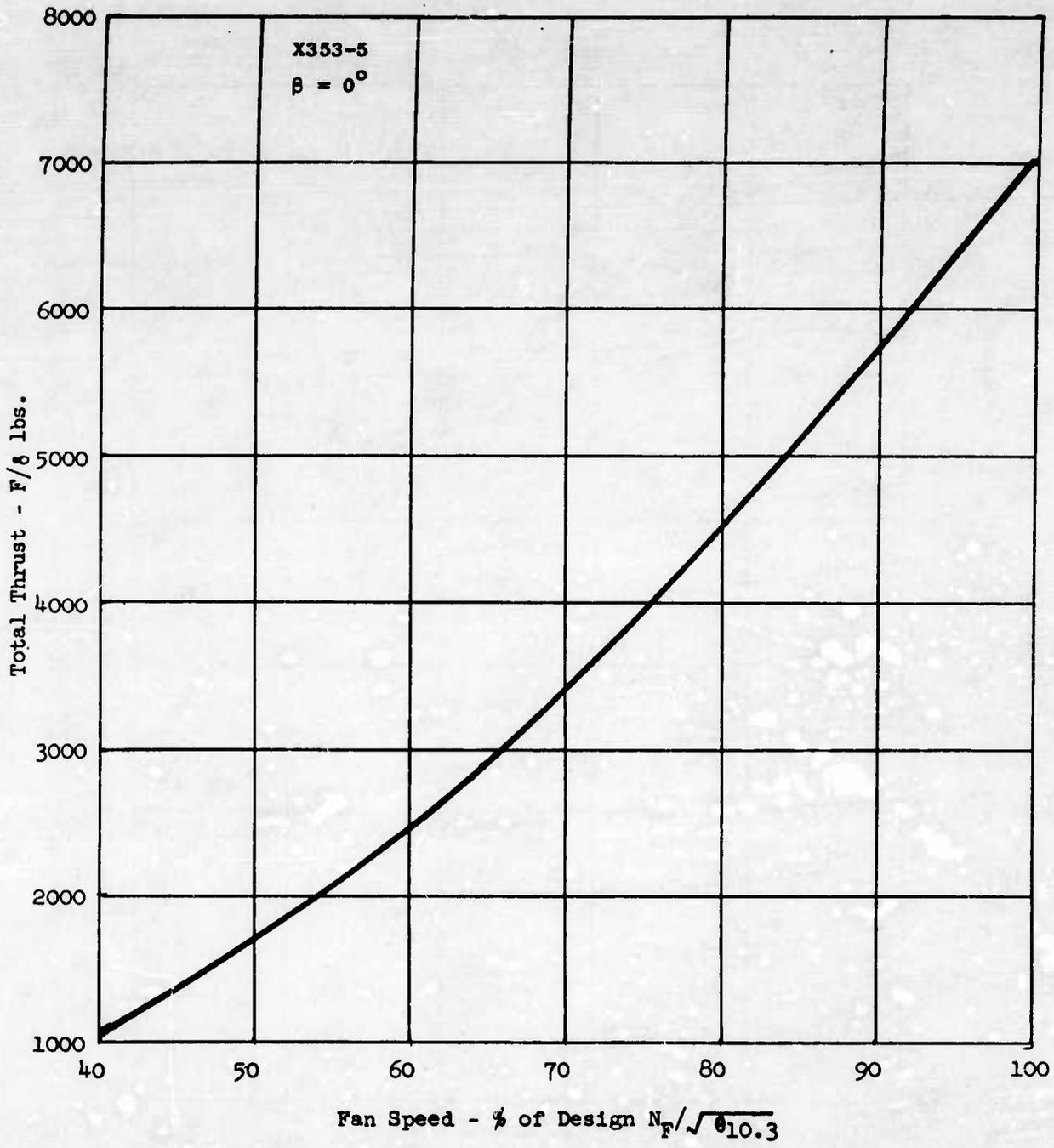


FIGURE 118. TOTAL FAN THRUST VERSUS FAN SPEED (REF. 19)

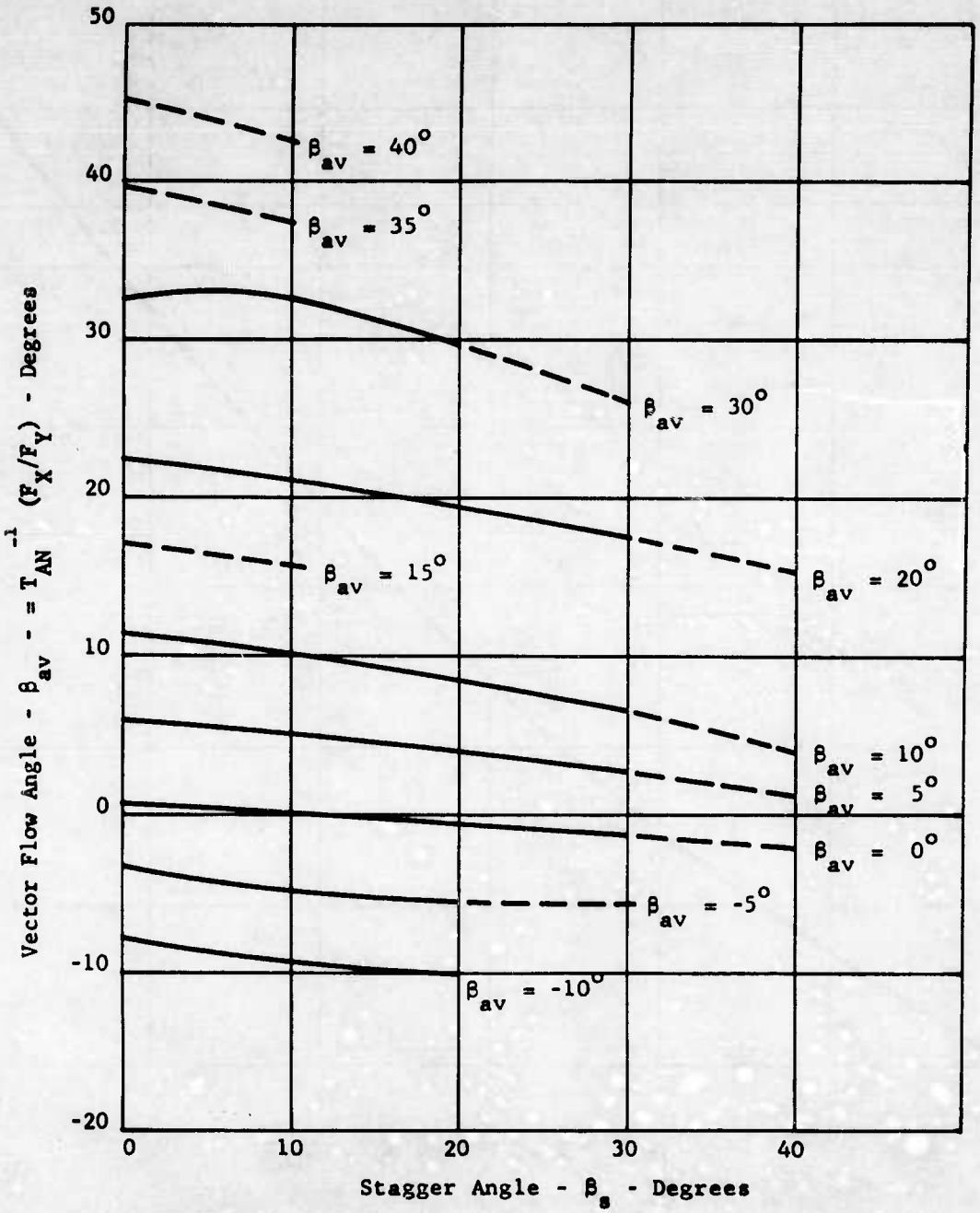


FIGURE 119 - VECTOR FLOW ANGLE VERSUS β_s AND β_{av} STATIC RESULTS, REFERENCE 19

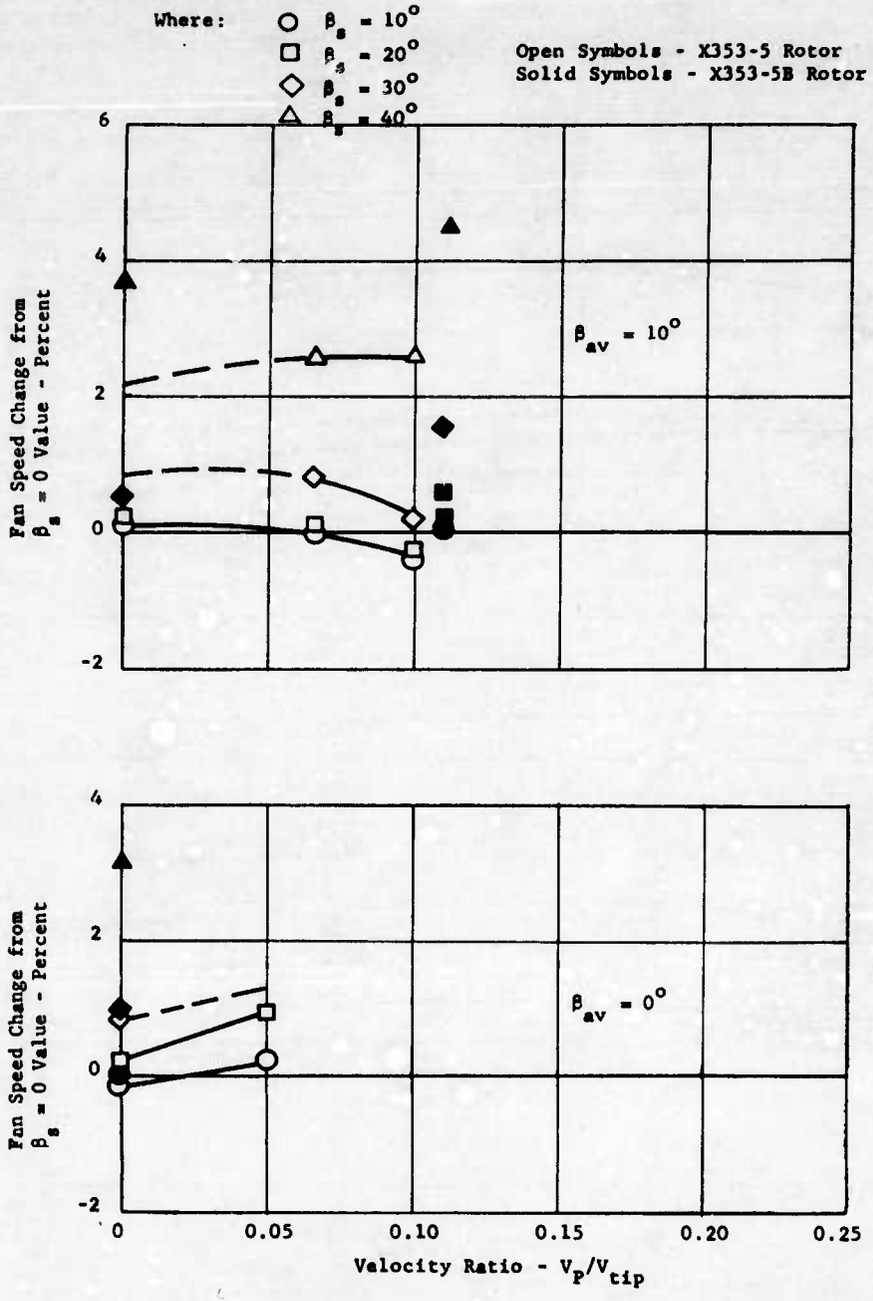


FIGURE 120a. FAN SPEED CHANGE VERSUS VELOCITY RATIO AND β_s, AT CONSTANT J85 ENGINE POWER

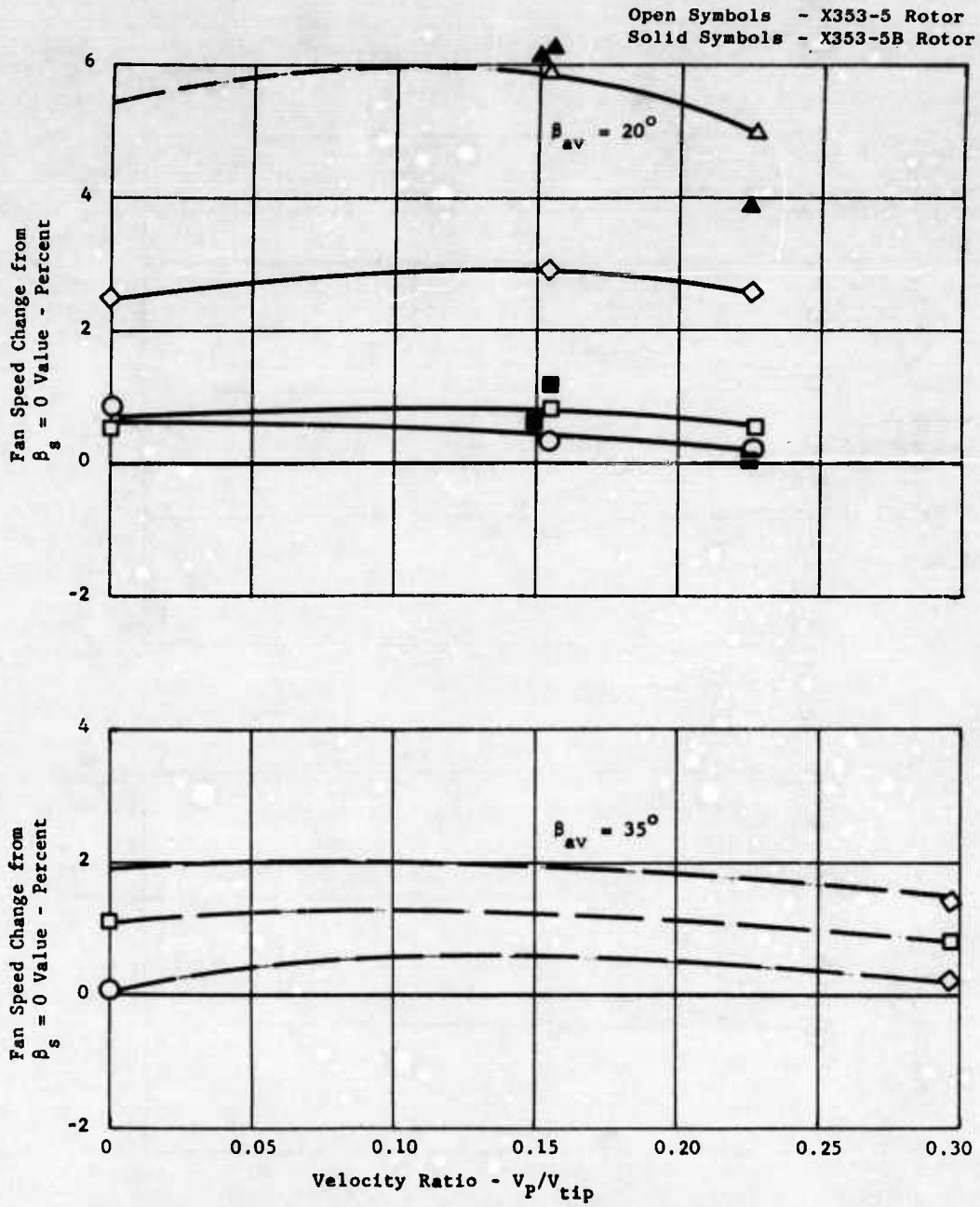


FIGURE 120b. FAN SPEED CHANGE VERSUS VELOCITY RATIO AND β_s, AT CONSTANT J85 ENGINE POWER

Where:

○ $\beta_s = 10^\circ$

□ $\beta_s = 20^\circ$

◇ $\beta_s = 30^\circ$

△ $\beta_s = 40^\circ$

$h/d_F = 1.82$ X353-5B Rotor

——— ——— Reference 19, X353-5 Rotor at 2.3 h/d_F

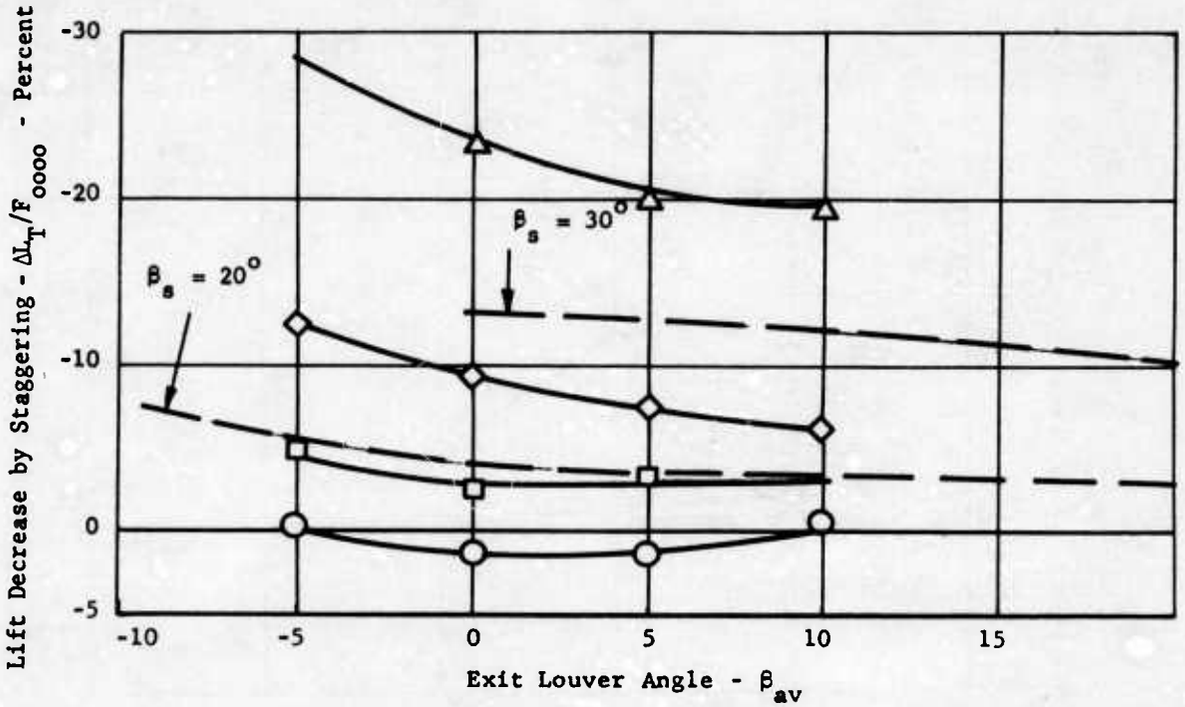


FIGURE 121a - TOTAL LIFT VARIATION VERSUS β_{av} AND β_s AT 1.82 h/d_F AND CONSTANT J85 ENGINE POWER

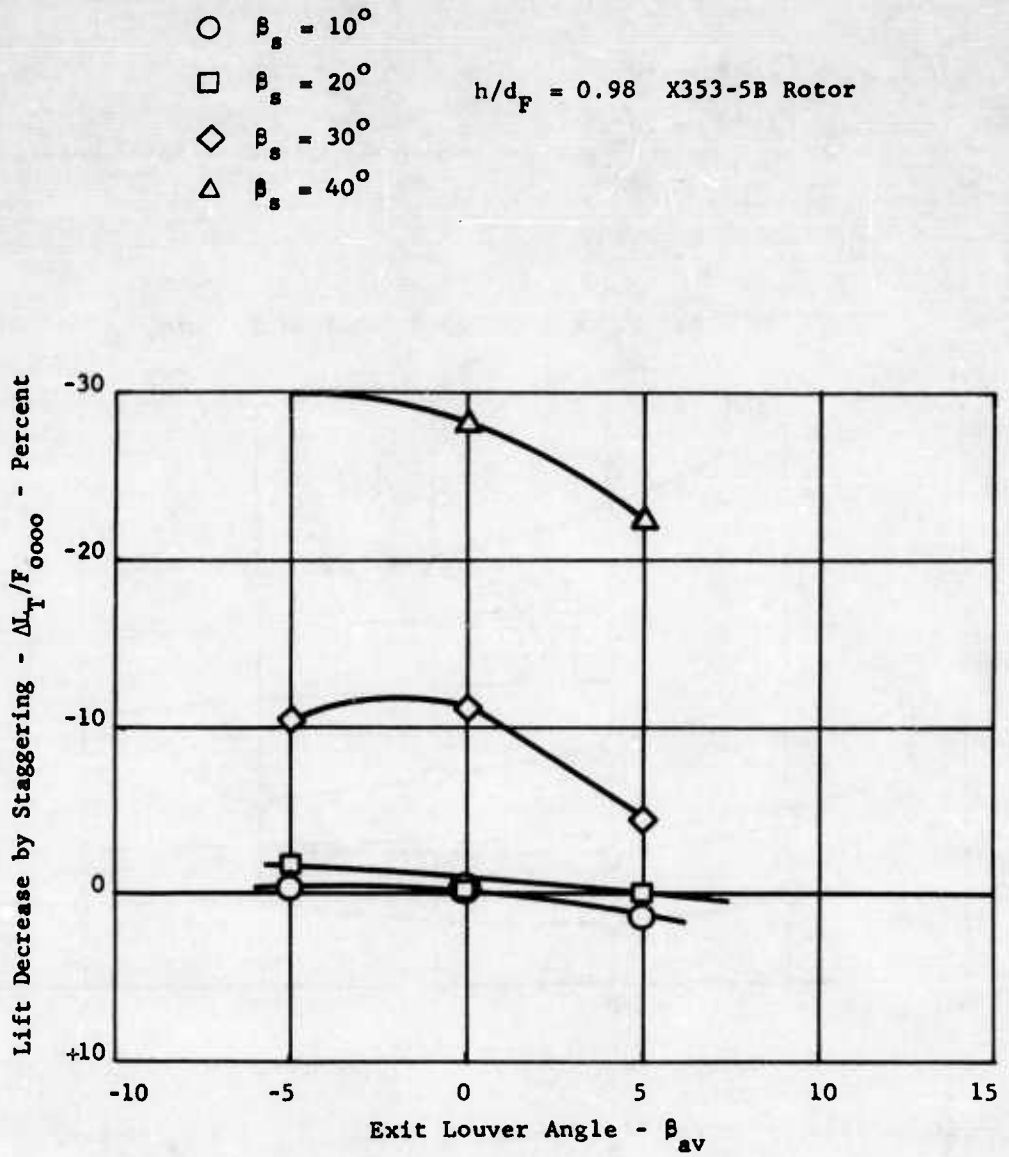


FIGURE 121b - TOTAL LIFT VARIATION VERSUS β_{av} AND β_s AT 0.98 h/d_F AND CONSTANT J85 ENGINE POWER

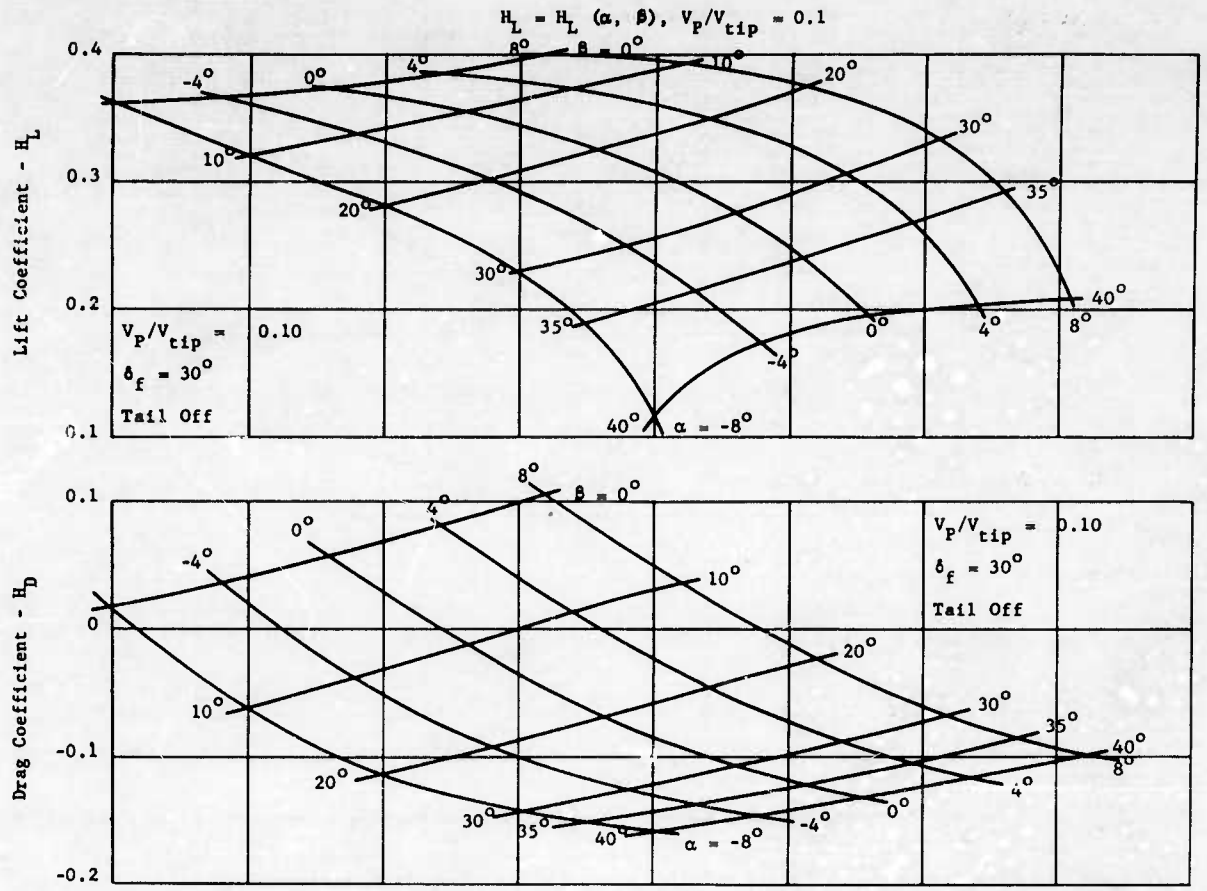


FIGURE 122a. LIFT AND DRAG COEFFICIENTS VERSUS ANGLE OF ATTACK AND EXIT LOUVER ANGLE

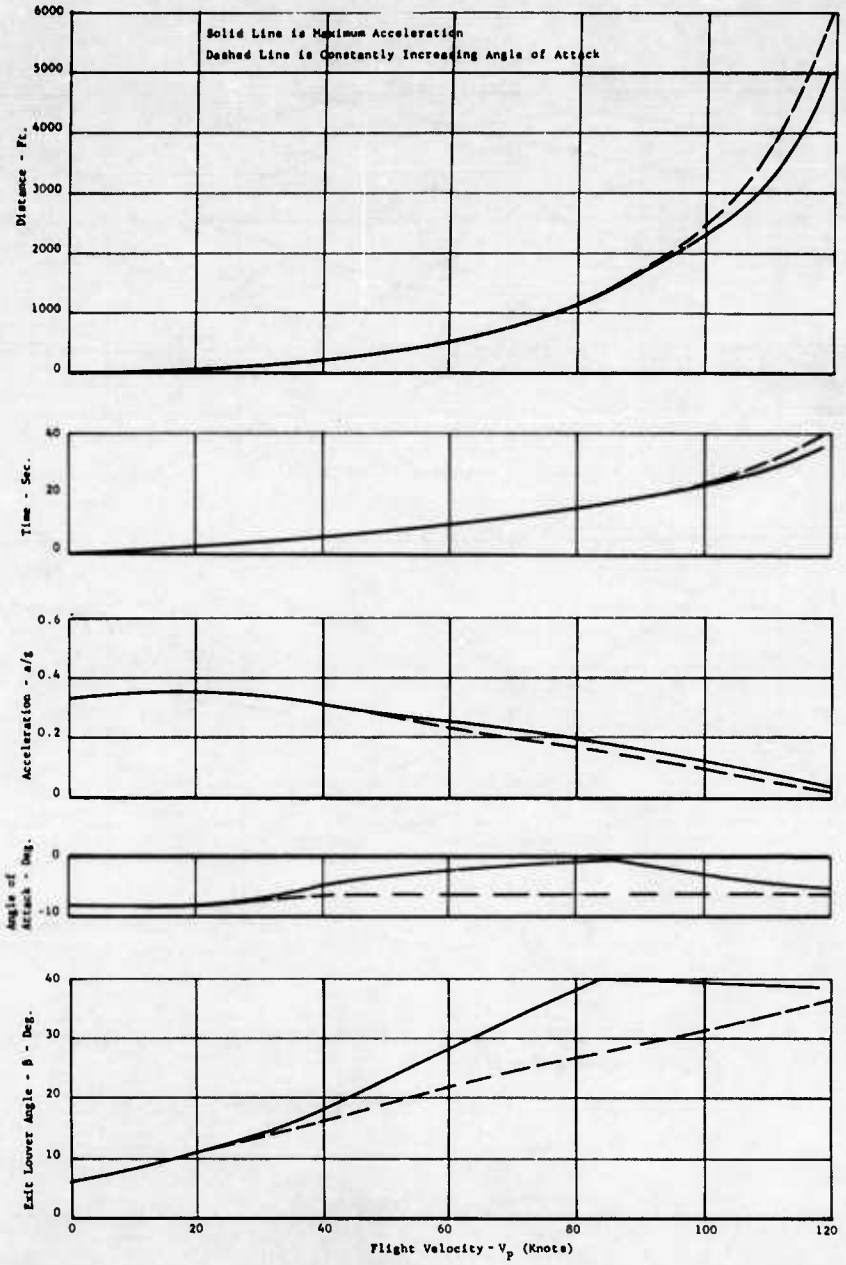


FIGURE 122b. TRANSITION CHARACTERISTICS - MAXIMUM LEVEL ACCELERATION L/GW = 1.05, N_F = 100%, X353-5 ROTOR, $\delta_f = 30^\circ$, W/S = 31.5

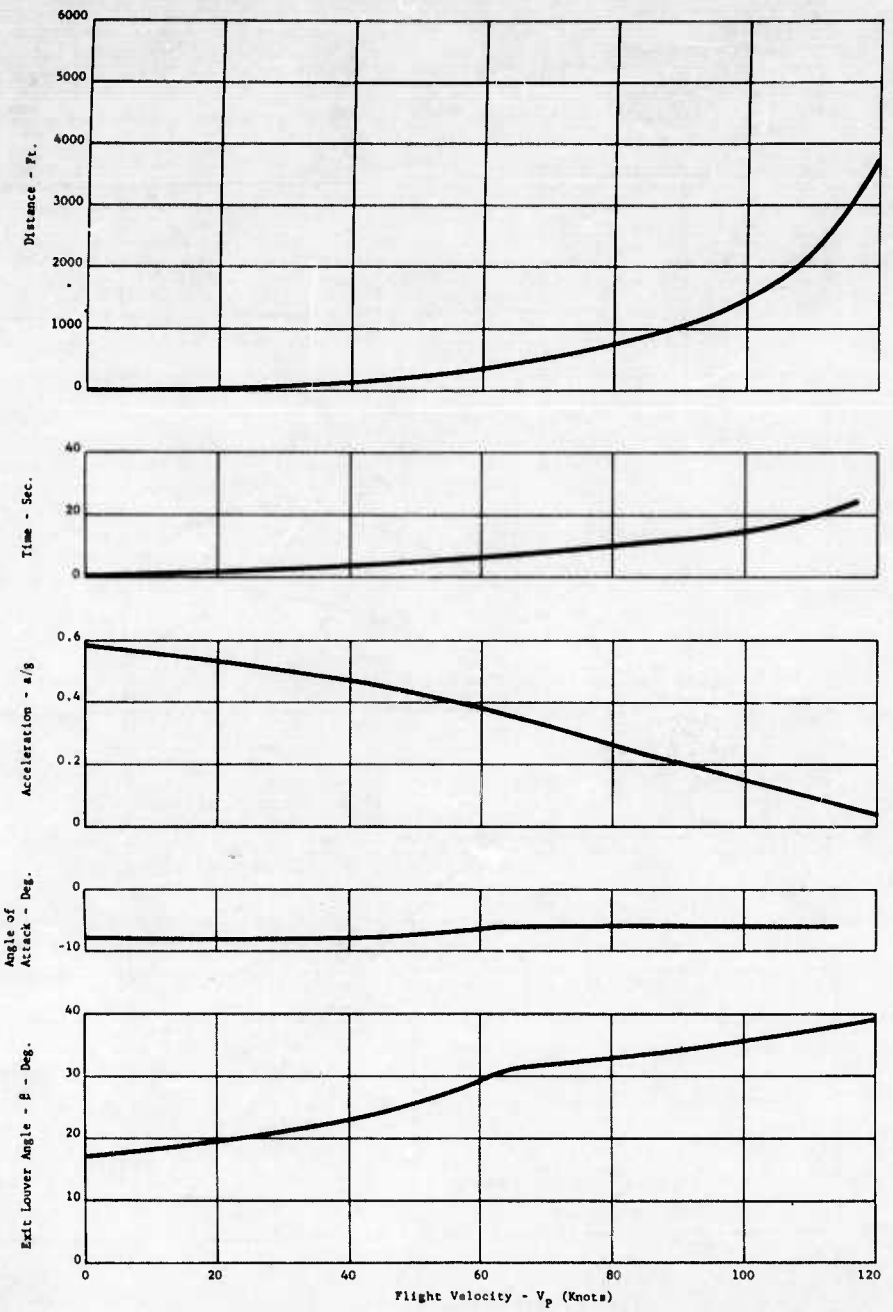


FIGURE 122c. TRANSITION CHARACTERISTICS - MAXIMUM LEVEL ACCELERATION L/GW = 1.20, N_F = 100%, X353-5 ROTOR, $\delta_f = 30^o$, W/S = 27.6

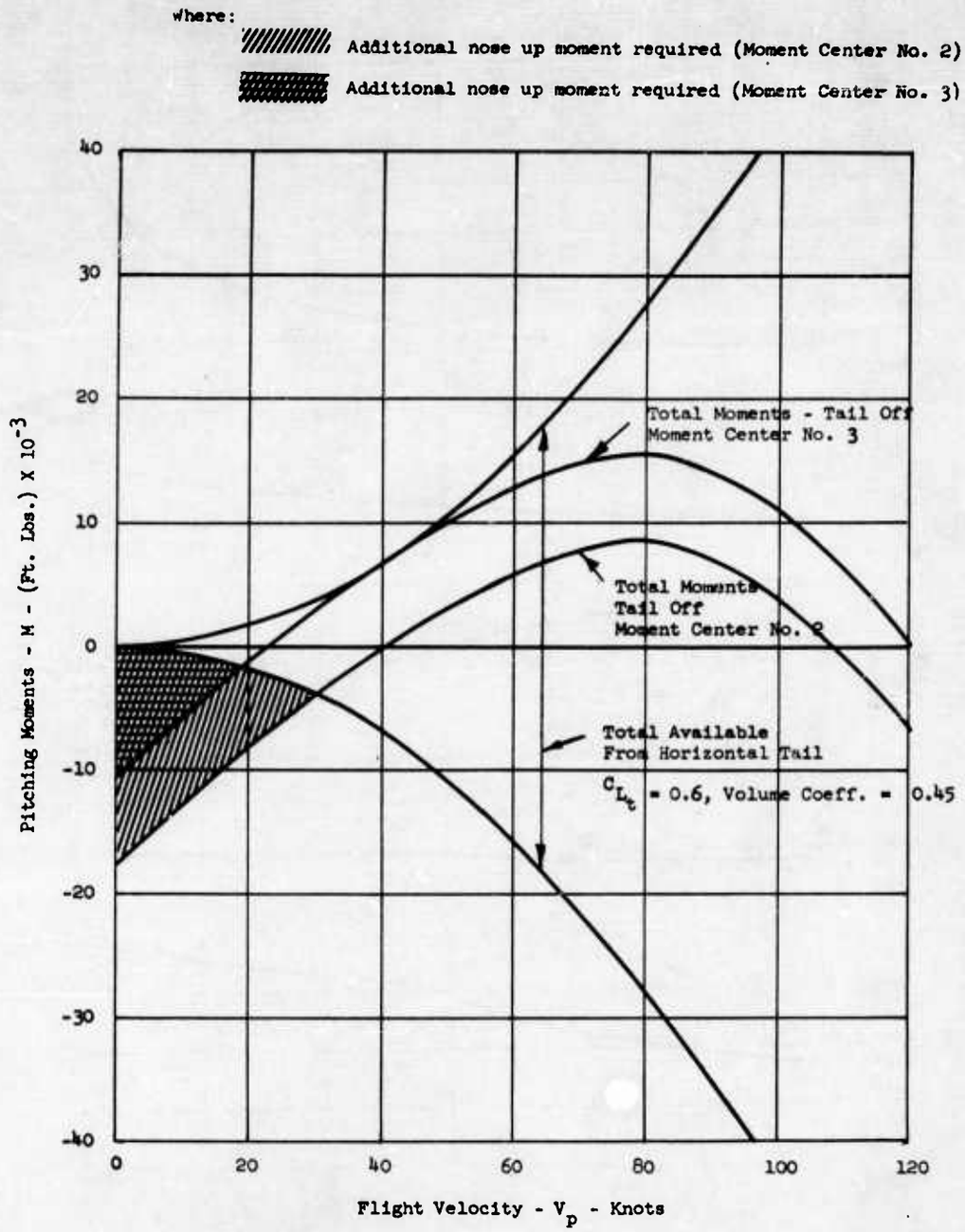


FIGURE 123a. PITCHING MOMENTS FOR MAXIMUM LEVEL ACCELERATION TRANSITION L/GW = 1.05, N_F = 100%, $\delta_f = 30^\circ$

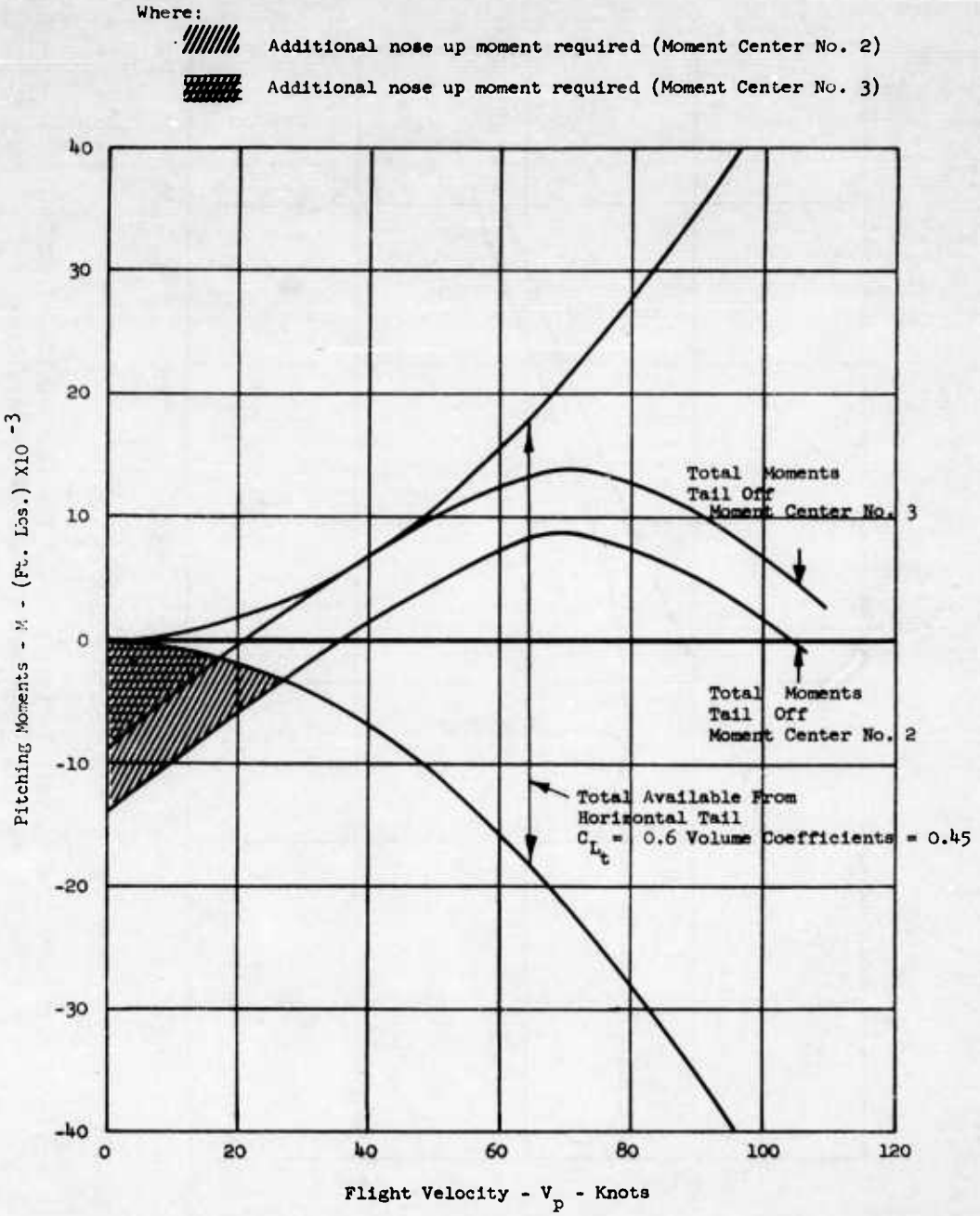


FIGURE 123b. PITCHING MOMENTS FOR MAXIMUM LEVEL ACCELERATION TRANSITION L/GW = 1.20, N_F = 100%, $\delta_f = 30^\circ$

Where:

○ Tail incidence for trimmed flight - conventional flight (inlet and exit closed)

● Tail incidence for trimmed flight - conventional flight (inlet and exit opened)

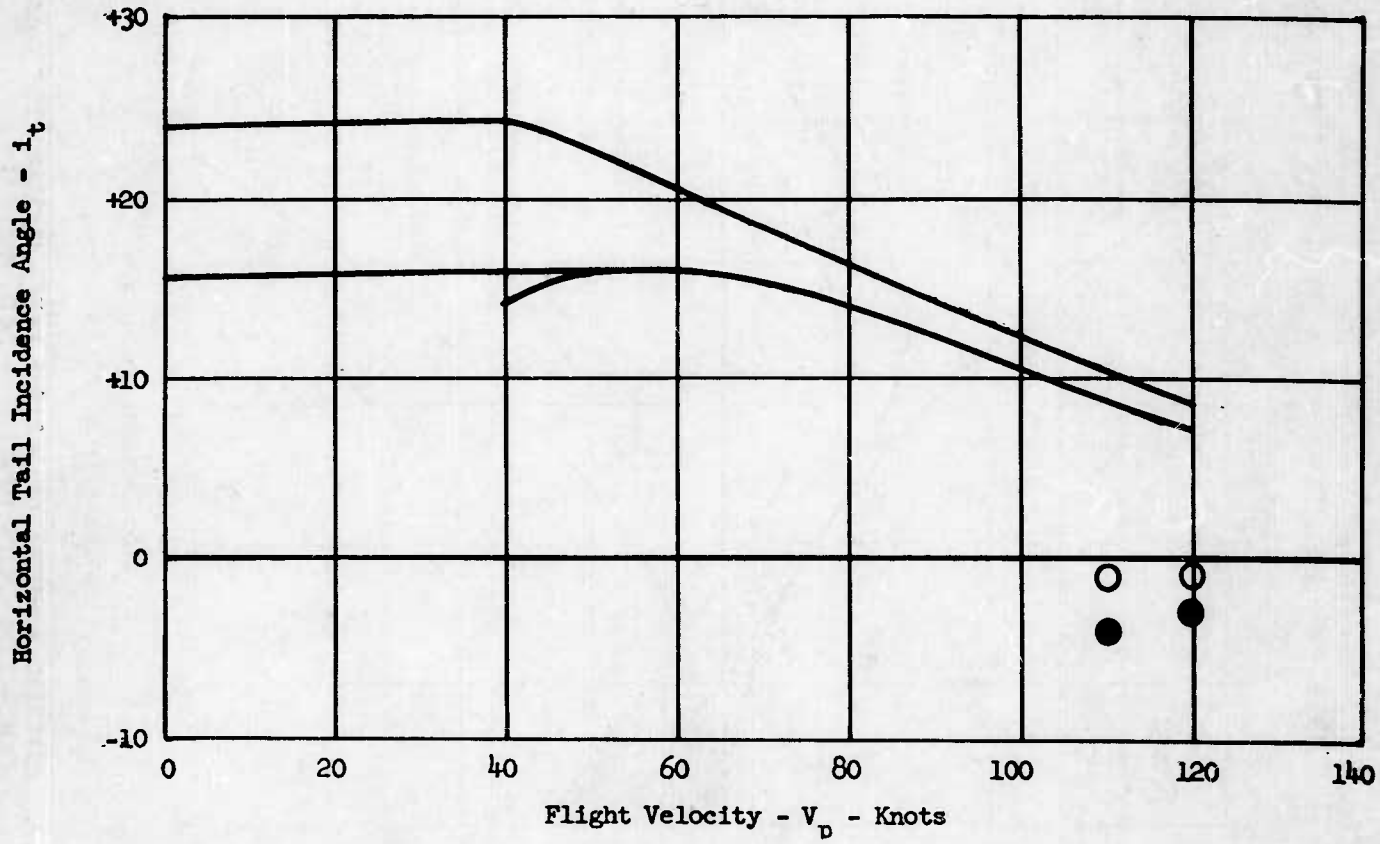


FIGURE 124a. HORIZONTAL TAIL INCIDENCE ANGLE FOR TRIMMED FLIGHT VERSUS FLIGHT VELOCITY - MAXIMUM ACCELERATION TRANSITION
L/GW = 1.05, N_F = 100%, $\delta_f = 30^o$

Where:

○ Tail incidence for trimmed flight - conventional flight (inlet and exit closed)

● Tail incidence for trimmed flight - conventional flight (inlet and exit opened)

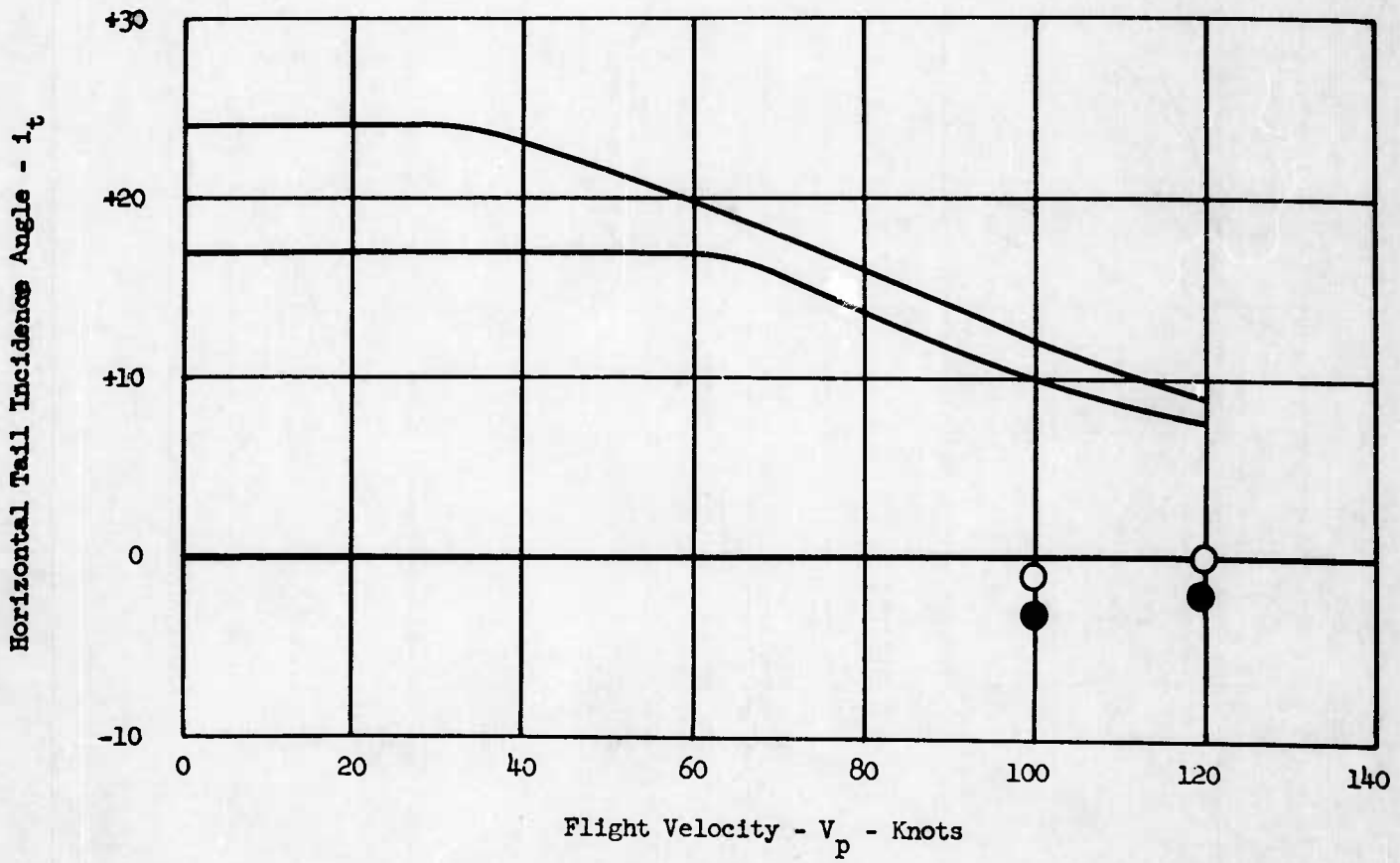


FIGURE 124b. HORIZONTAL TAIL INCIDENCE ANGLE FOR TRIMMED FLIGHT VERSUS FLIGHT VELOCITY - MAXIMUM ACCELERATION TRANSITION
L/GW = 1.20, N_F =100%, δ_f = 30°

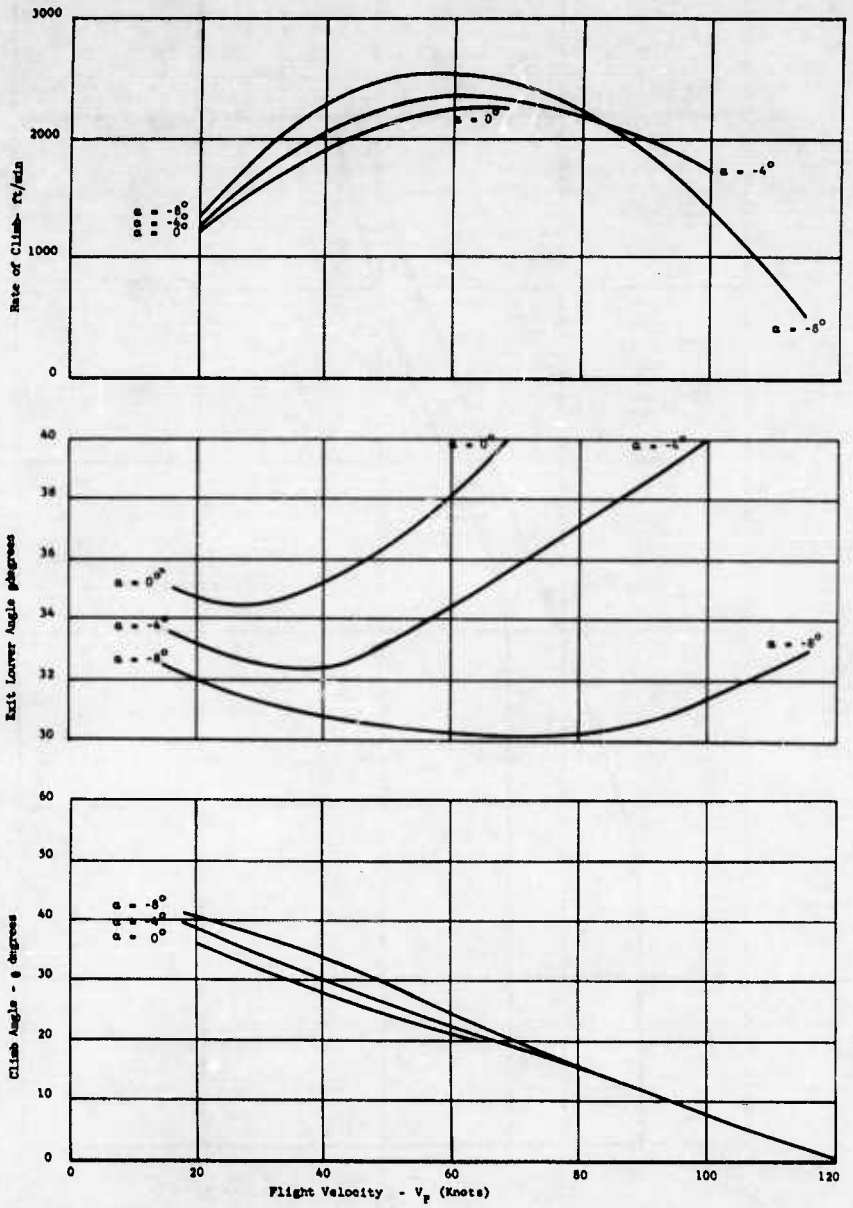


FIGURE 125 - MAXIMUM RATE OF CLIMB VERSUS FLIGHT VELOCITY
L/GW = 1.20, N_F = 100%, δ_f = 30°, X353-5 Rotor

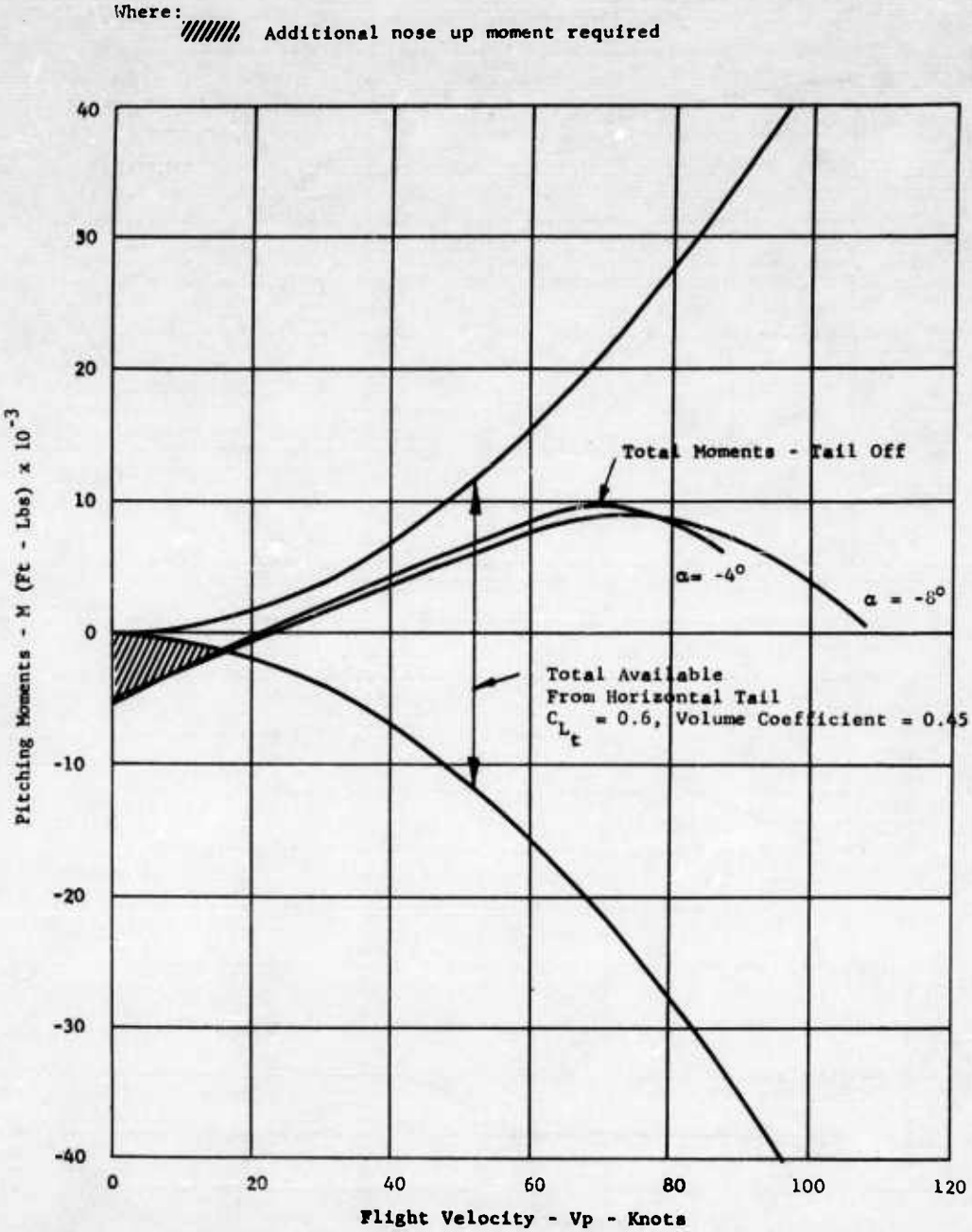


FIGURE 126. PITCHING MOMENTS FOR MAXIMUM RATE OF CLIMB, L/GW = 1.20, MOMENT CENTER NO. 2, N_F = 100%, δ_f = 30°

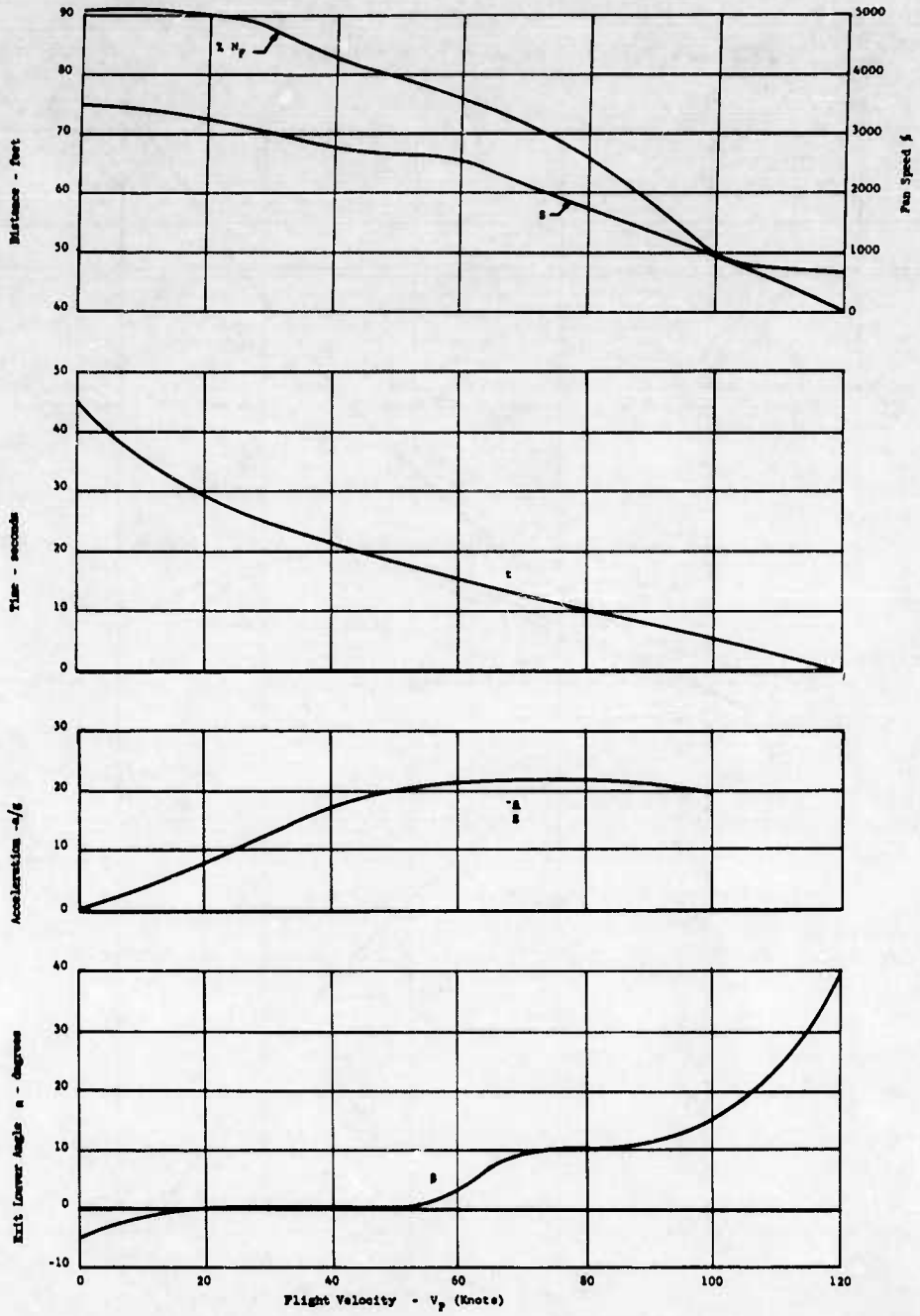


FIGURE 127 - TRANSITION CHARACTERISTICS - LEVEL DECELERATION
L/GW = 1.20, $\delta_f = 30^\circ$, $\alpha = 0^\circ$

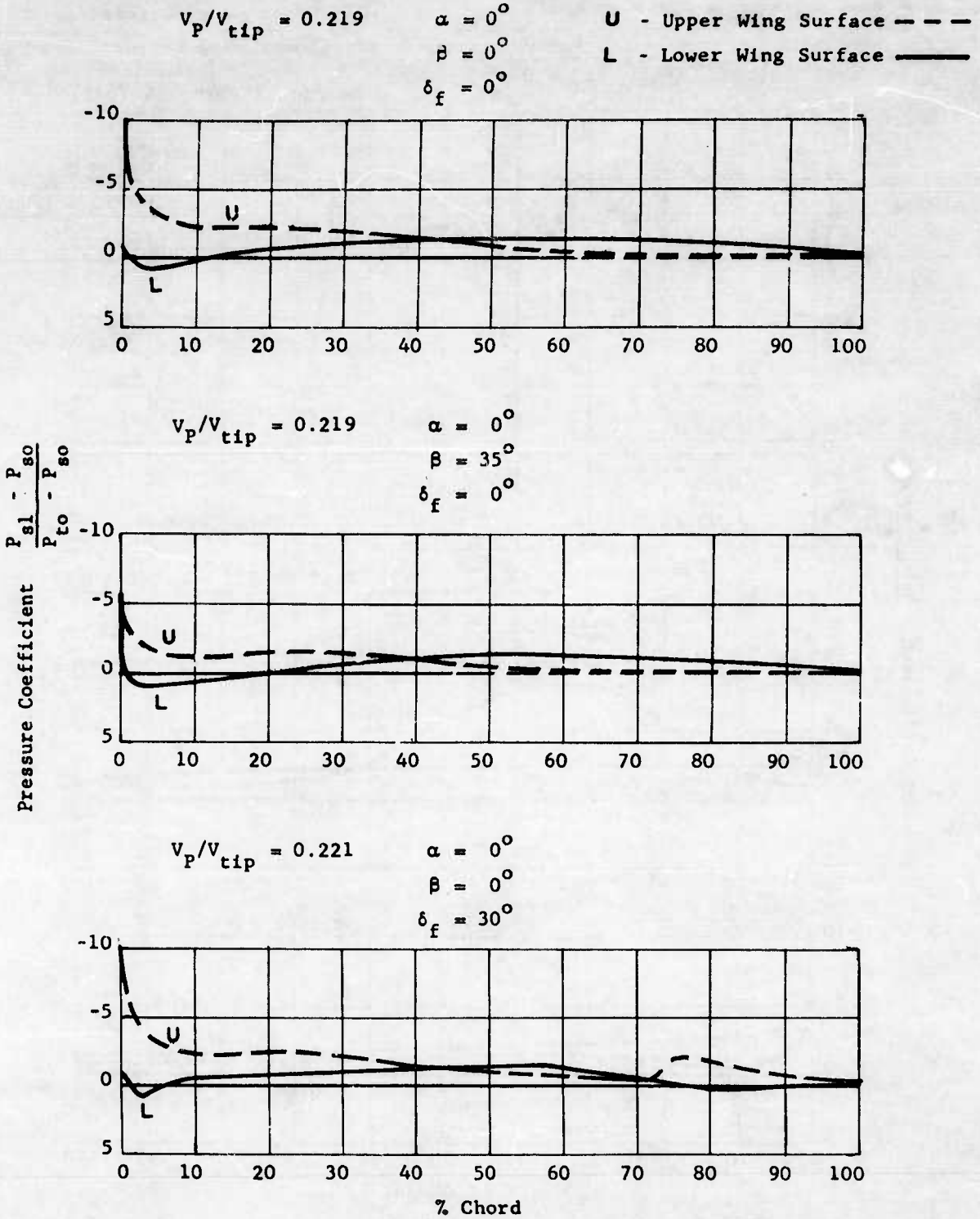


FIGURE 128a - CHORDWISE PRESSURE DISTRIBUTION AT STATION III (V_p/V_{tip} = 0.219)

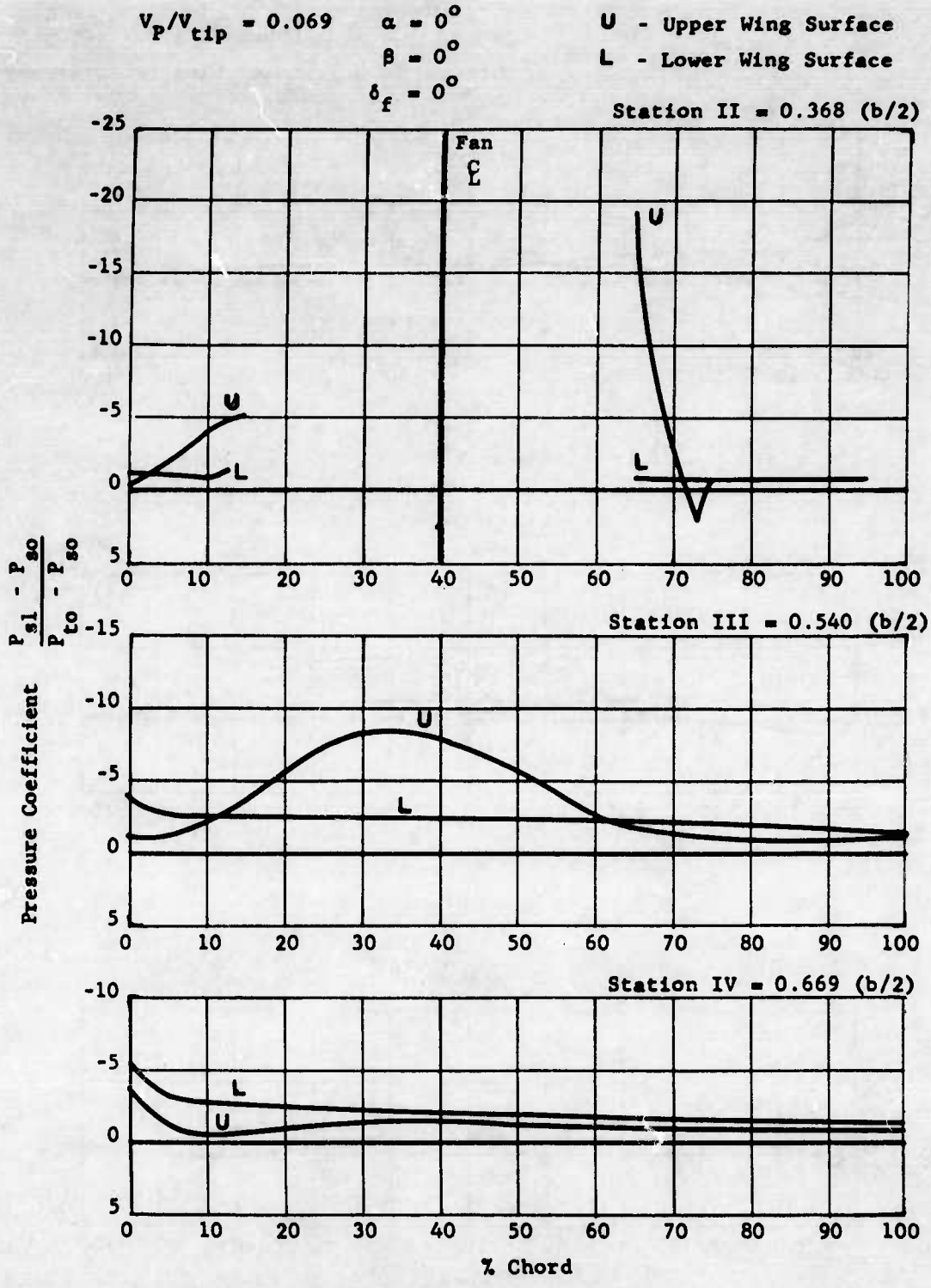


FIGURE 128b - CHORDWISE PRESSURE COEFFICIENT DISTRIBUTION (V_p/V_{tip} = 0.069)

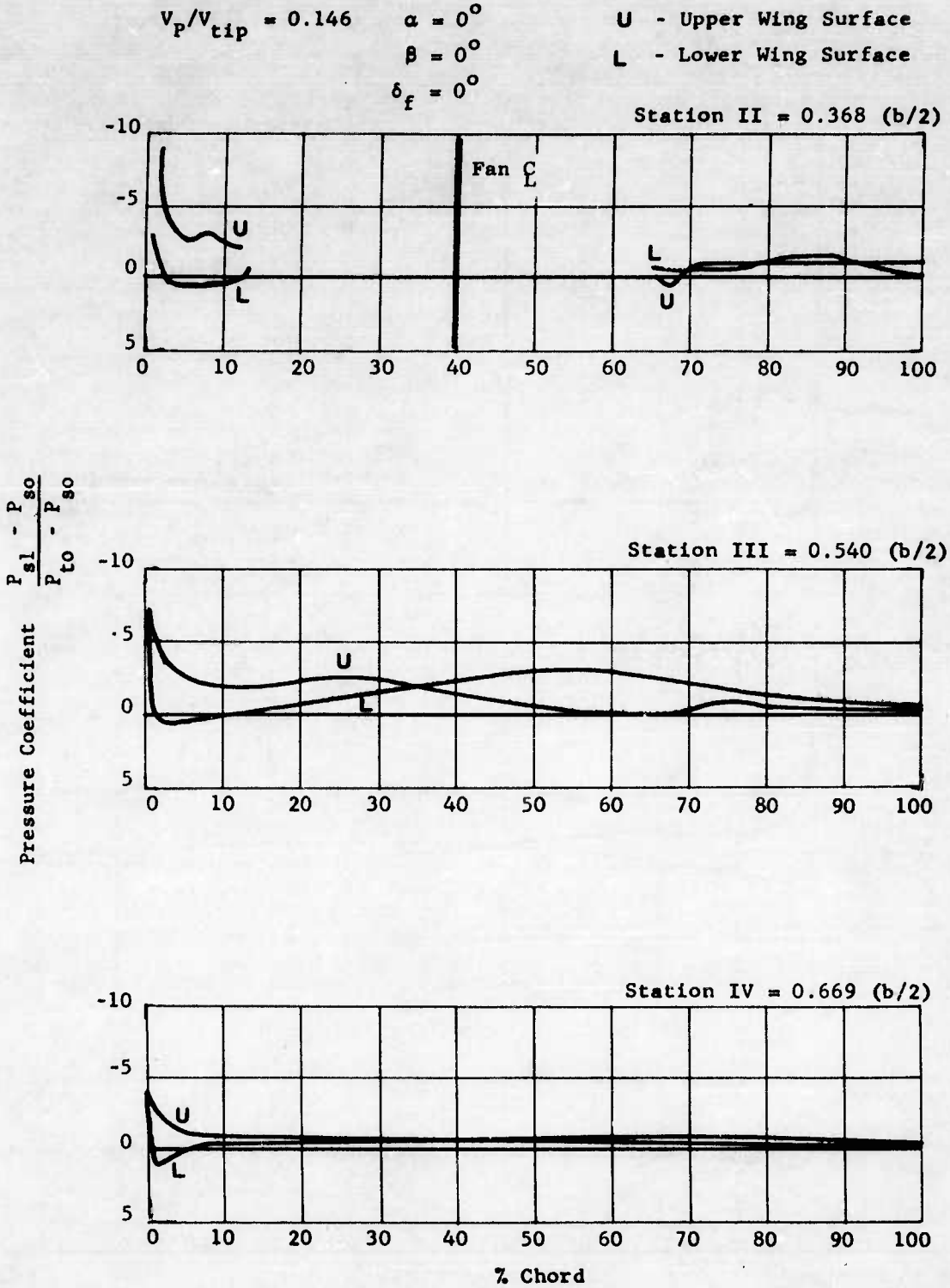


FIGURE 128c- CHORDWISE PRESSURE COEFFICIENT DISTRIBUTION (V_p/V_{tip} = 0.146)

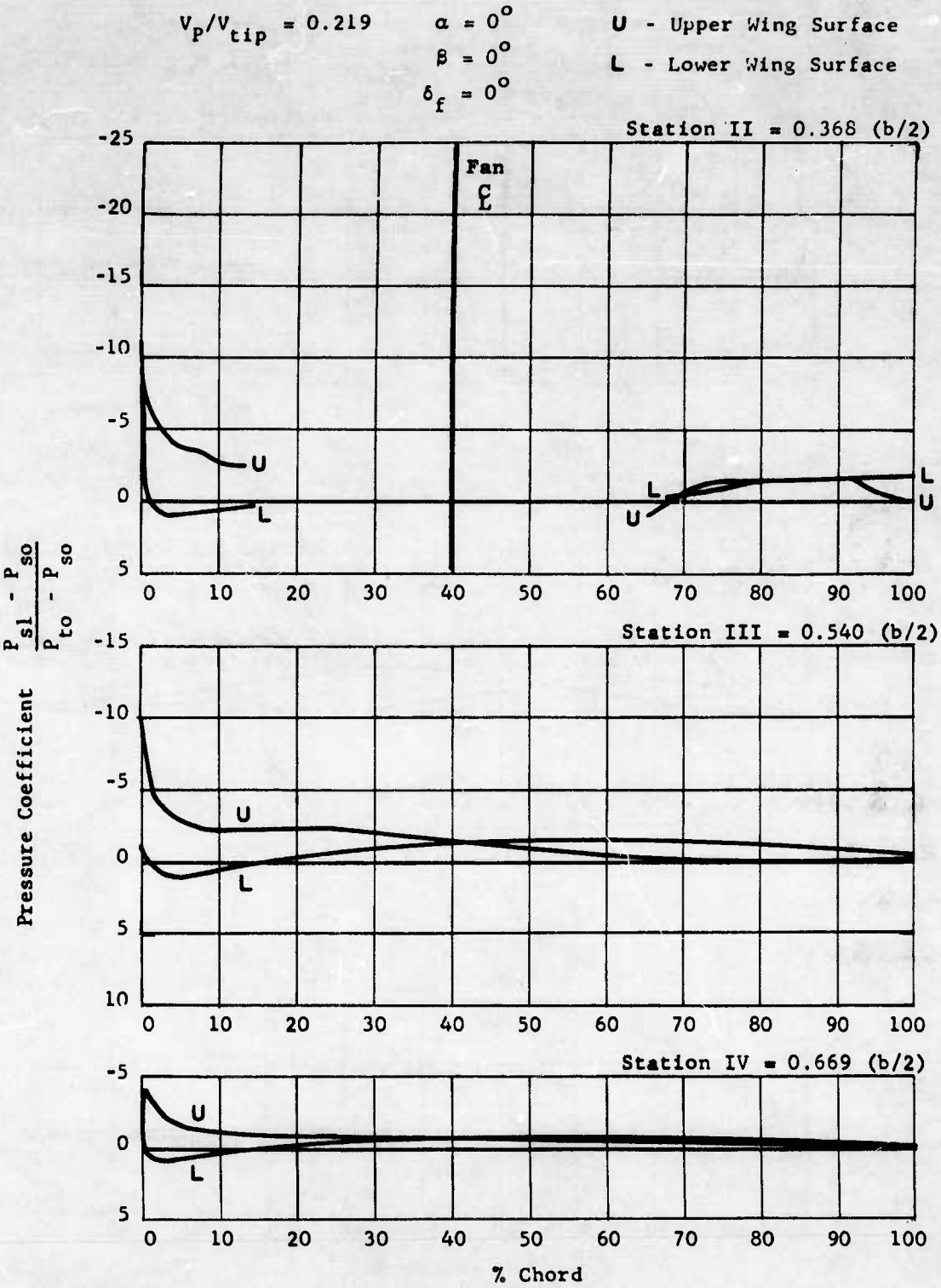


FIGURE 128d - CHORDWISE PRESSURE COEFFICIENT DISTRIBUTION (V_p/V_{tip} = 0.219)

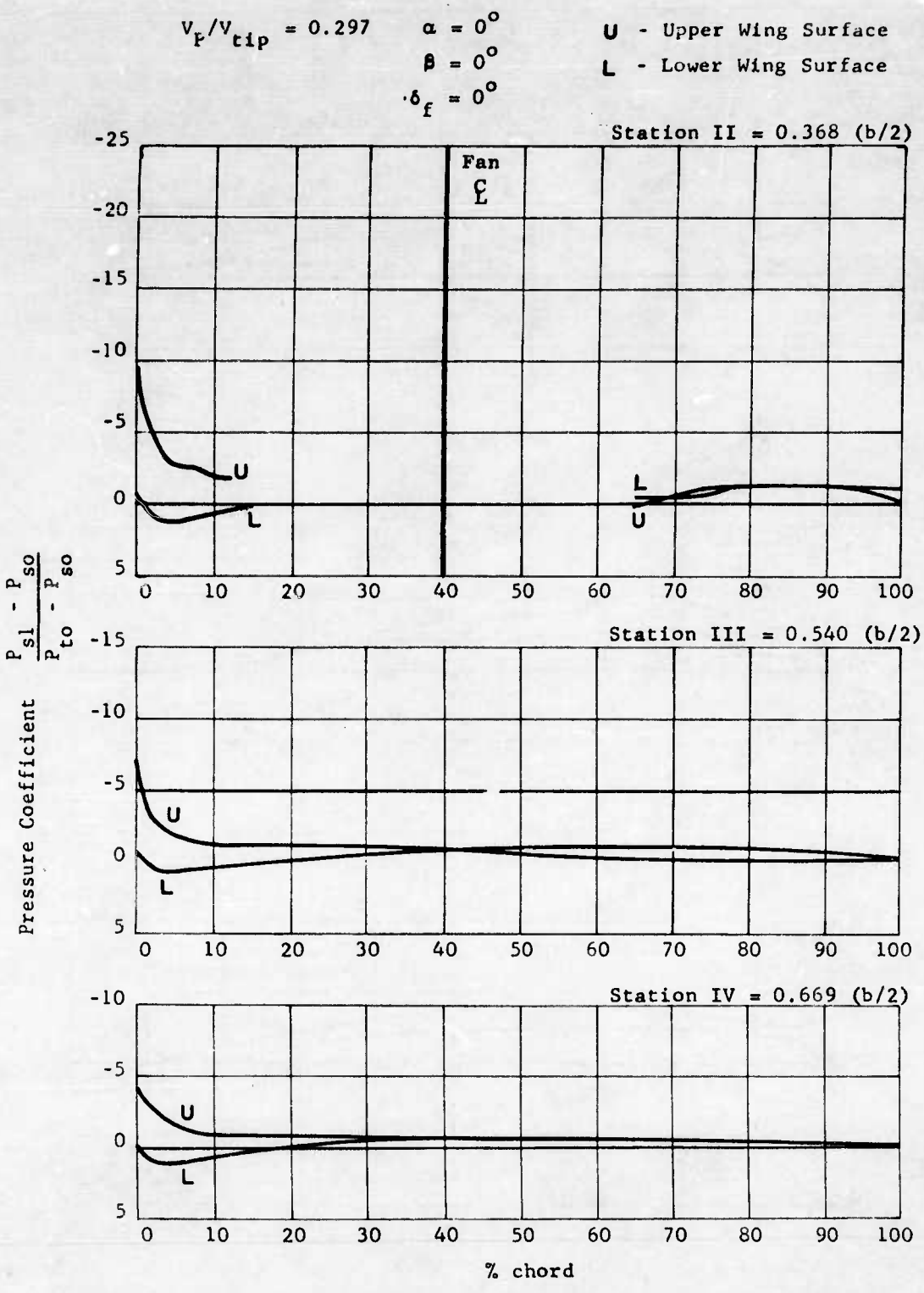


FIGURE 128e - CHORDWISE PRESSURE COEFFICIENT DISTRIBUTION (V_p/V_{tip} = 0.297)

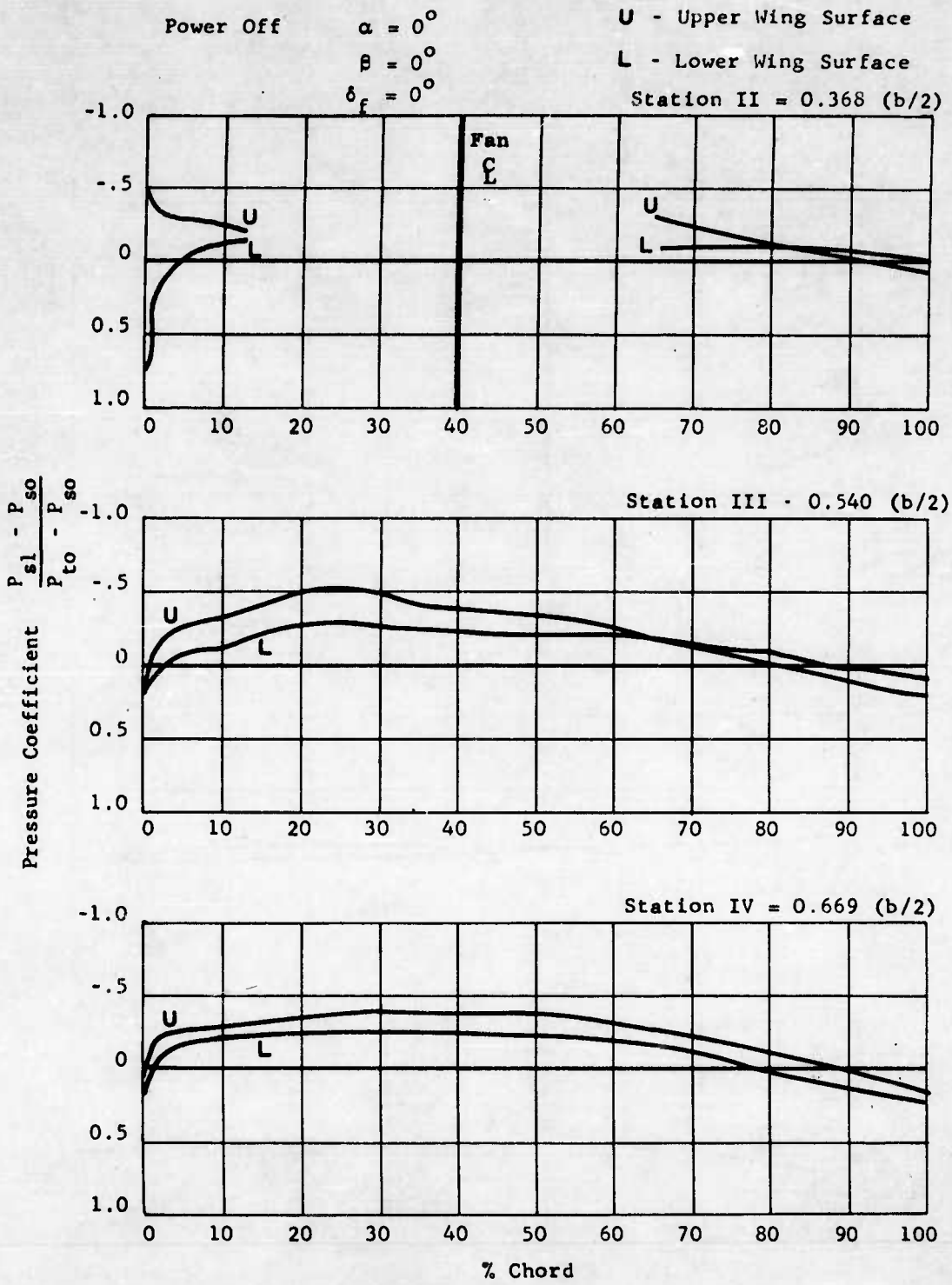


FIGURE 128f - CHORDWISE PRESSURE COEFFICIENT DISTRIBUTION (POWER-OFF)

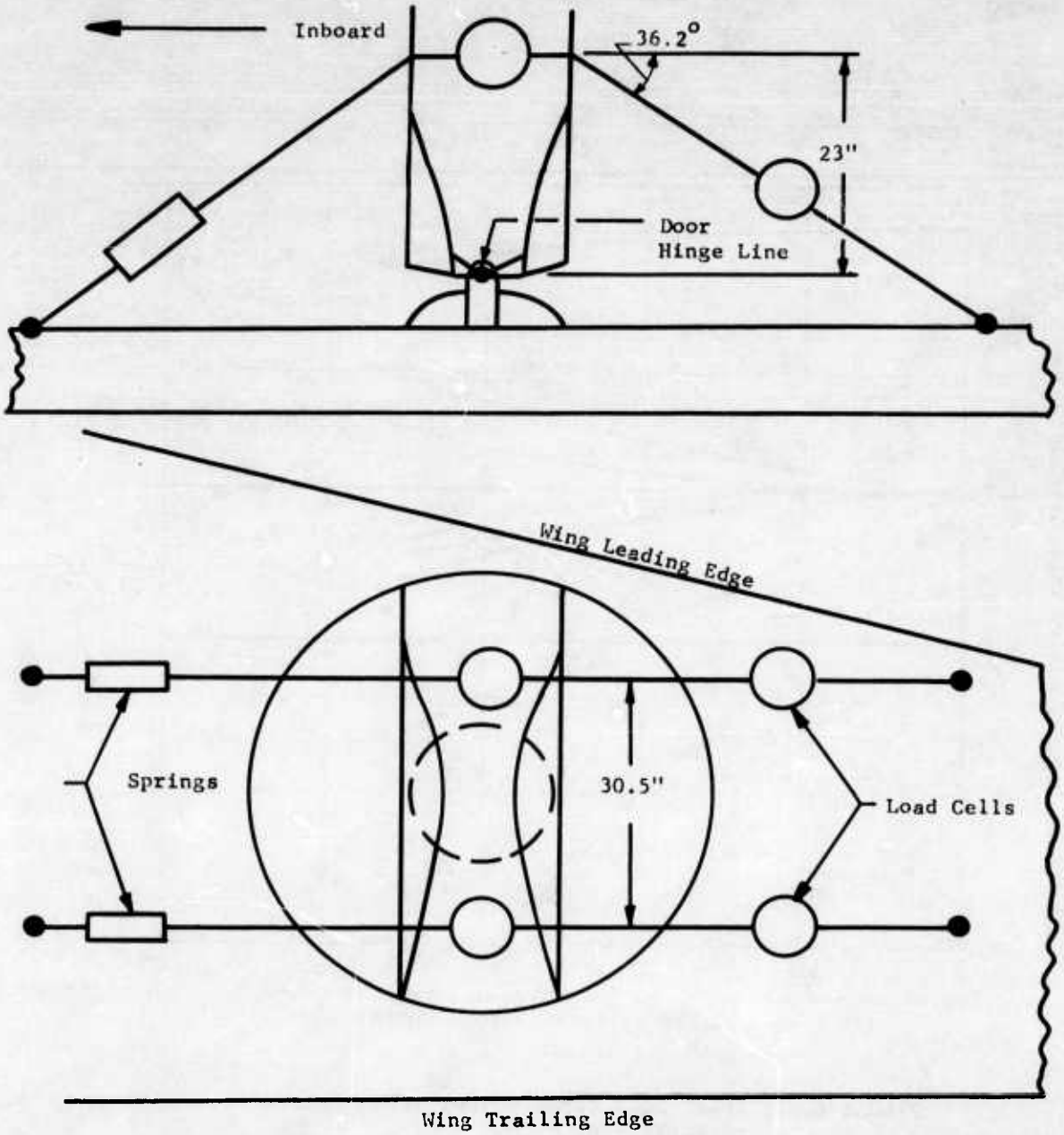


FIGURE 129 - DIAGRAM OF TEST SET-UP FOR MEASUREMENT OF FAN CLOSURE DOOR HINGE MOMENTS

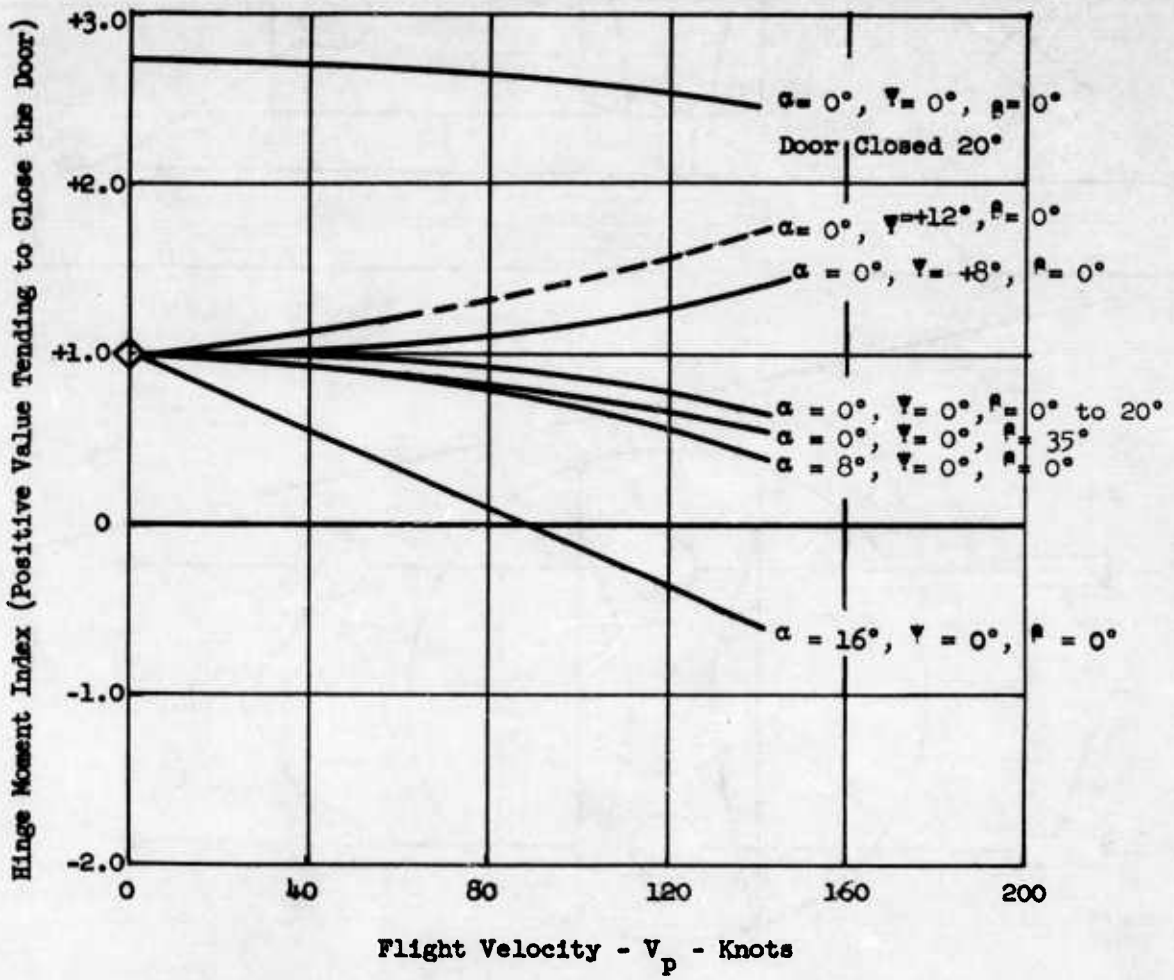


FIGURE 130. INLET DOOR HINGE MOMENT INDEX VERSUS FLIGHT VELOCITY - N_F = 100%

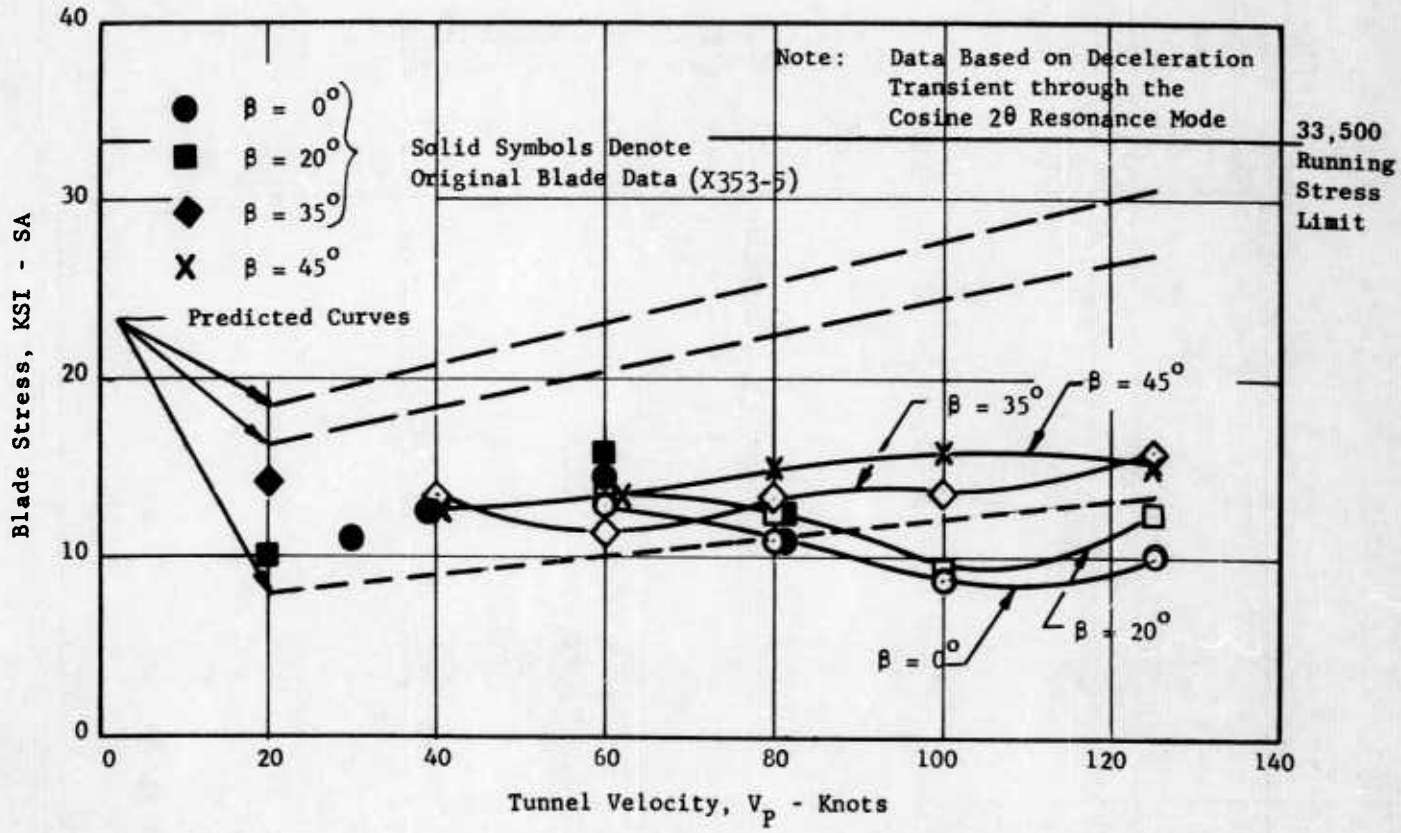


FIGURE 131a - COSINE 2θ MODE STRESS AS A FUNCTION OF FLIGHT SPEED AND EXIT LOUVER SETTING (FIVE SECOND DECELERATION)

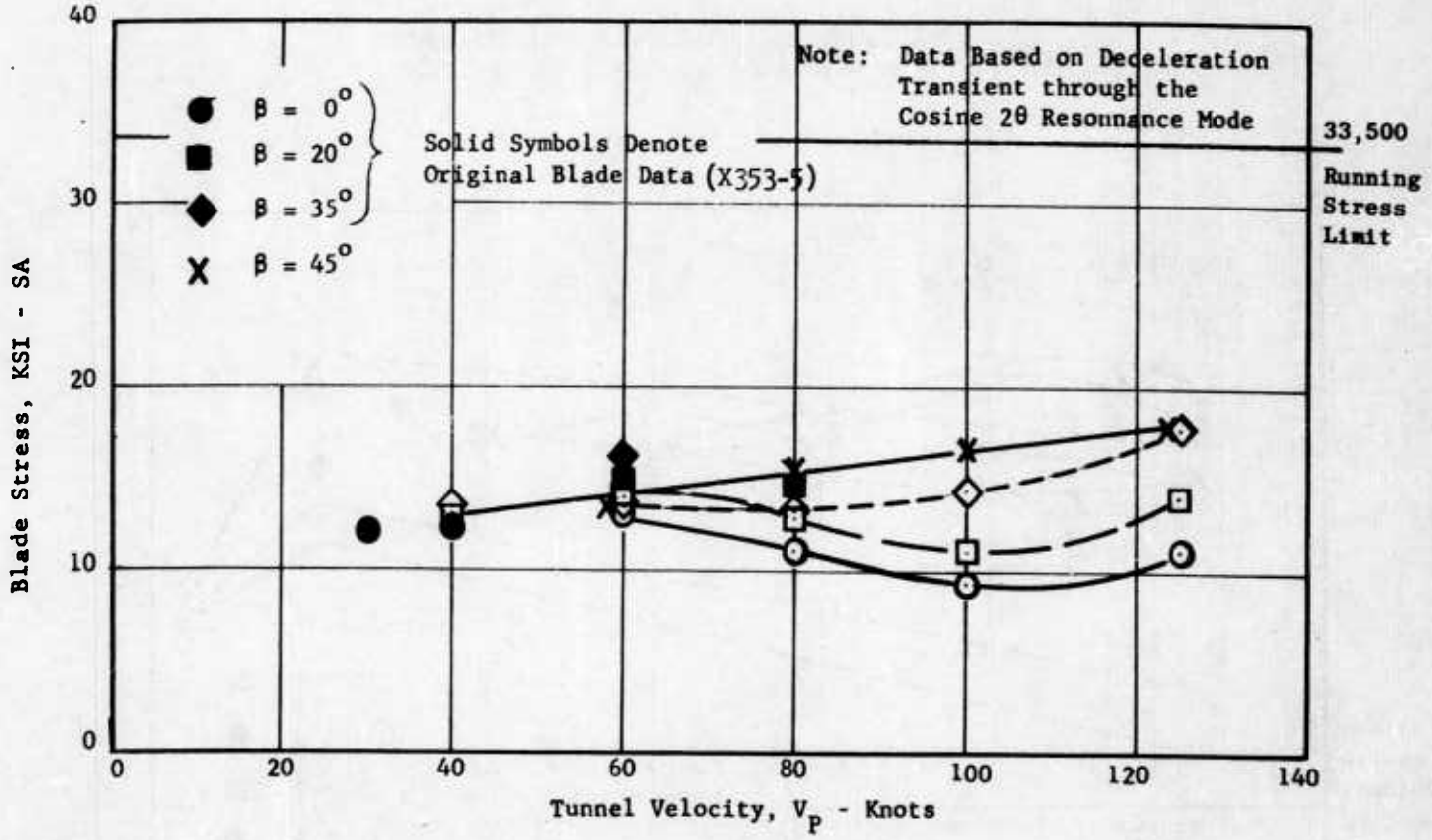


FIGURE 131b - COSINE 2θ MODE STRESS AS A FUNCTION OF FLIGHT SPEED AND EXIT LOUVER SETTING (ONE SECOND DECELERATION)

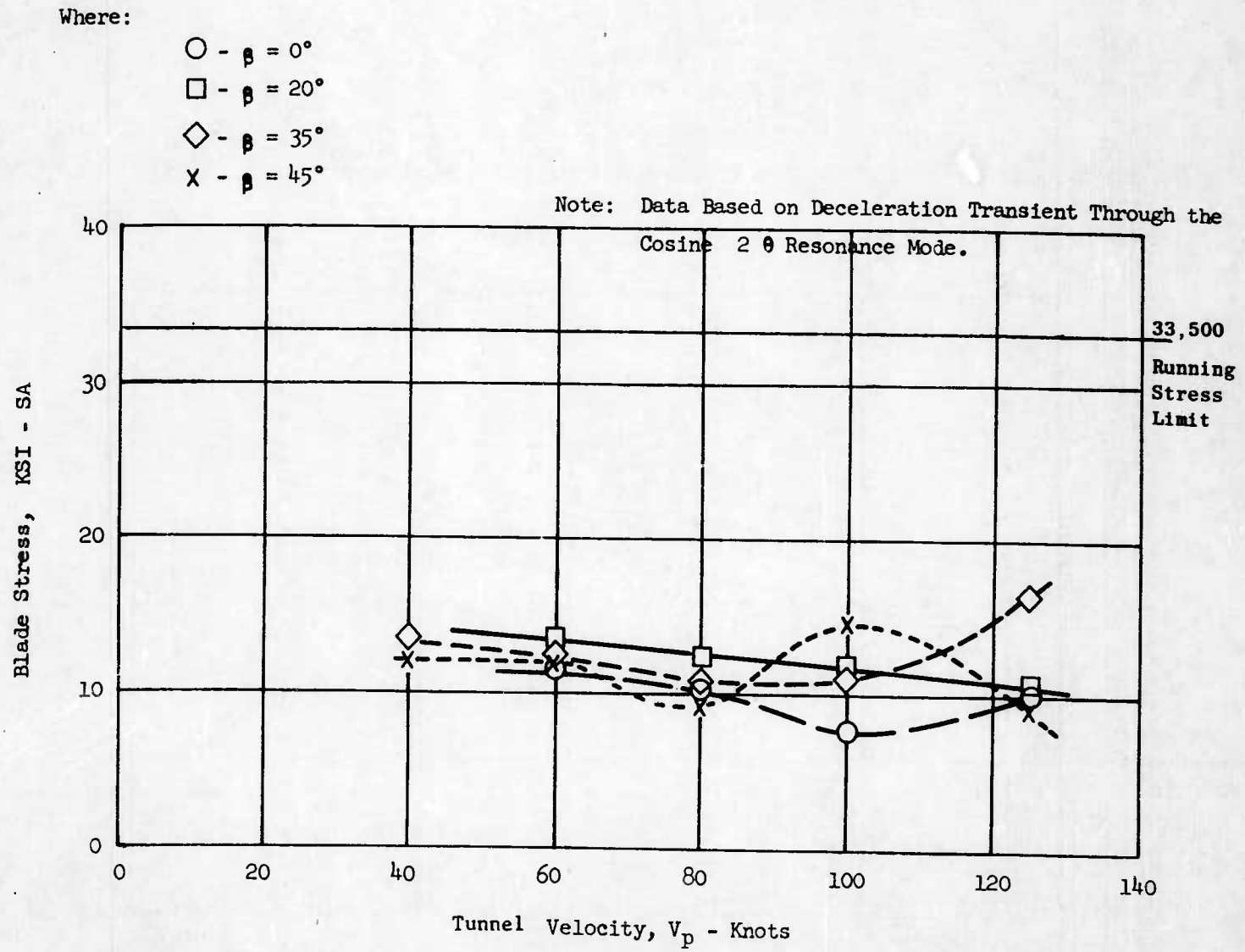


FIGURE 131c - COSINE 2θ MODE STRESS AS A FUNCTION OF FLIGHT SPEED AND EXIT LOUVER SETTING (DIVERTER VALVE DECELERATION)

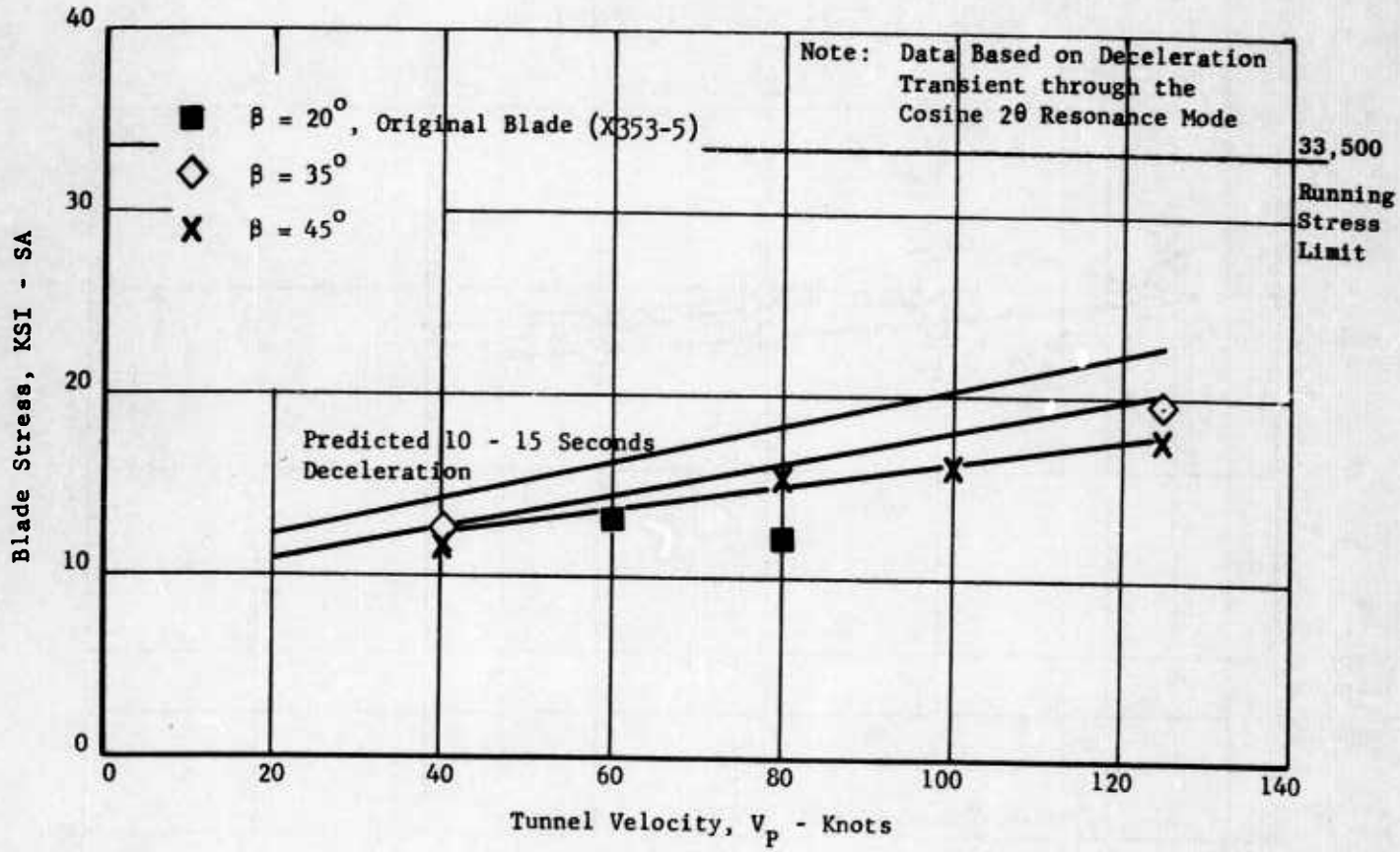


FIGURE 131d - COSINE 2θ MODE STRESS AS A FUNCTION OF FLIGHT SPEED AND EXIT LOUVER SETTING

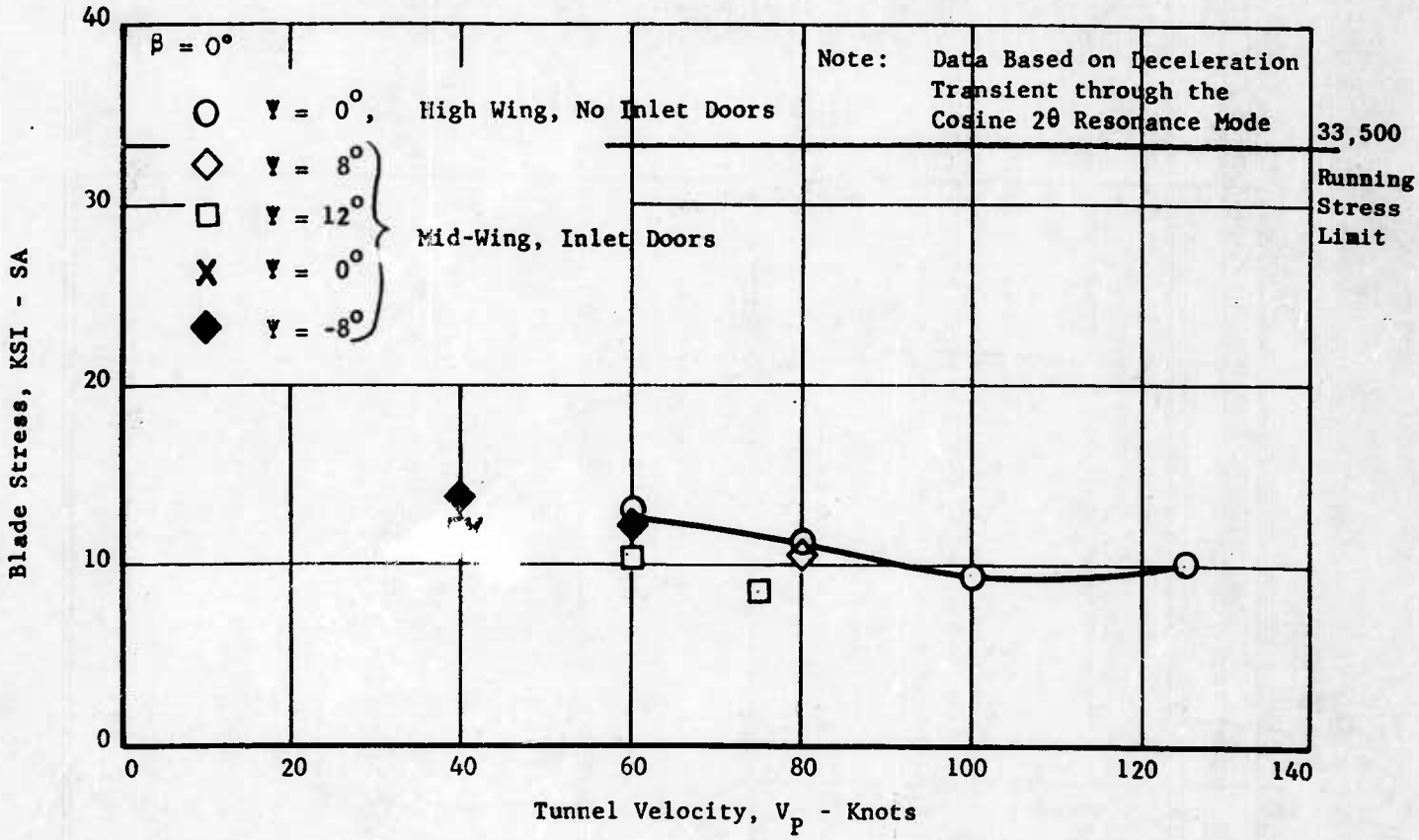


FIGURE 131e - COSINE 2θ MODE STRESS AS A FUNCTION OF FLIGHT SPEED AND YAW ANGLE (FIVE SECOND DECELERATION)

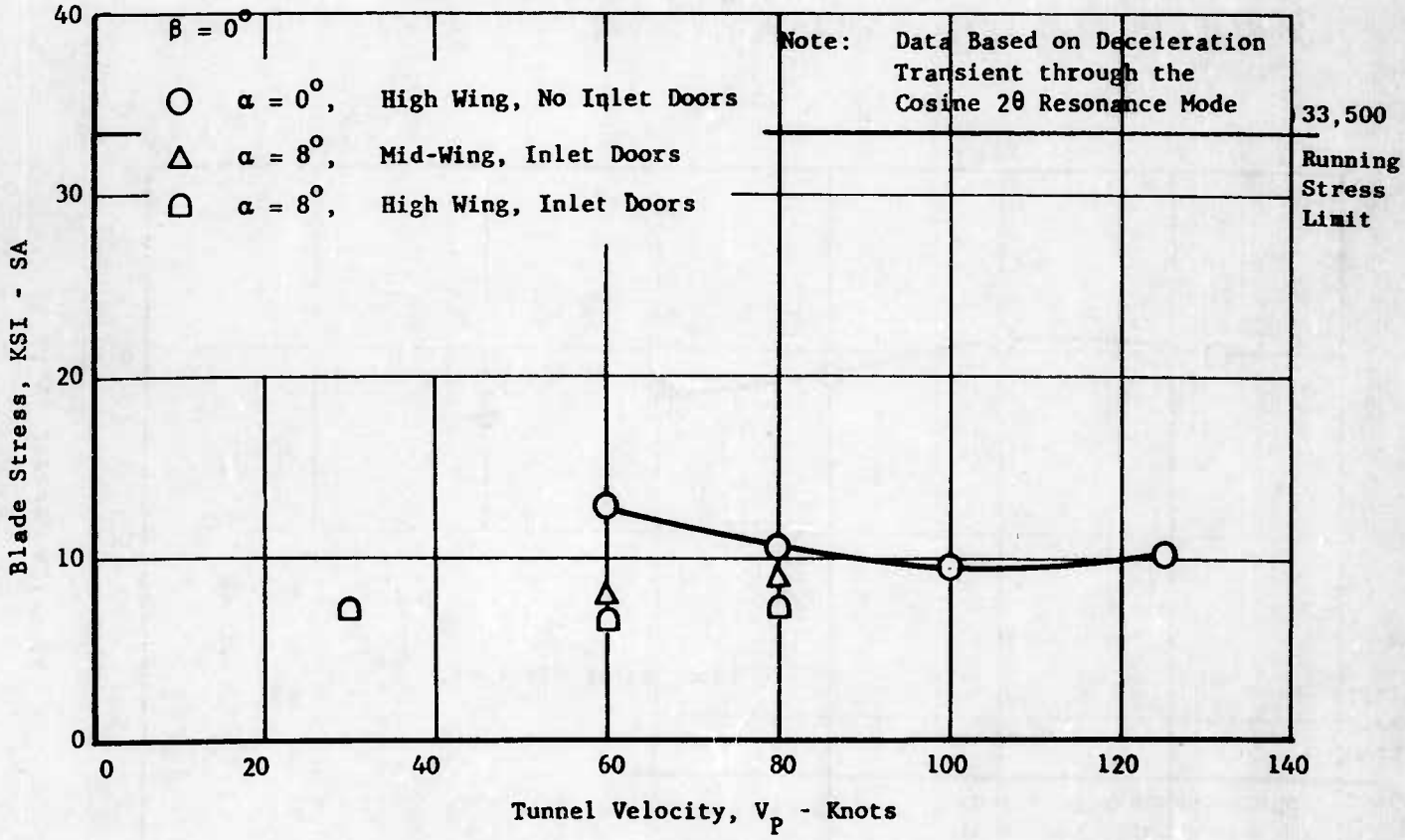


FIGURE 131f - COSINE 2θ MODE STRESS AS A FUNCTION OF FLIGHT SPEED, AIRPLANE CONFIGURATION AND ANGLE OF ATTACK (FIVE SECOND DECELERATION)

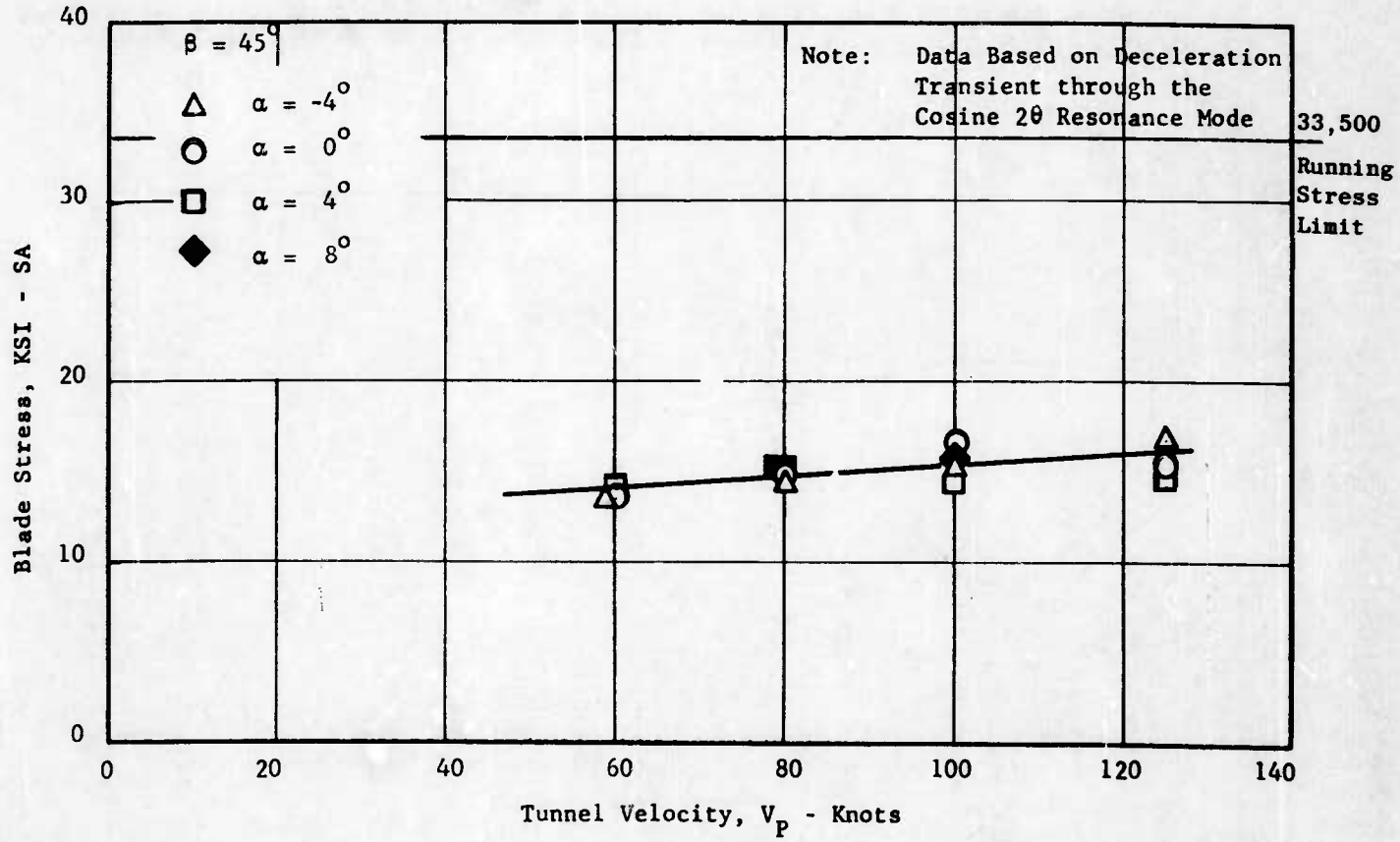


FIGURE 131g - COSINE 2θ MODE STRESS AS A FUNCTION OF FLIGHT SPEED AND ANGLE OF ATTACK (FIVE SECOND DECELERATION)

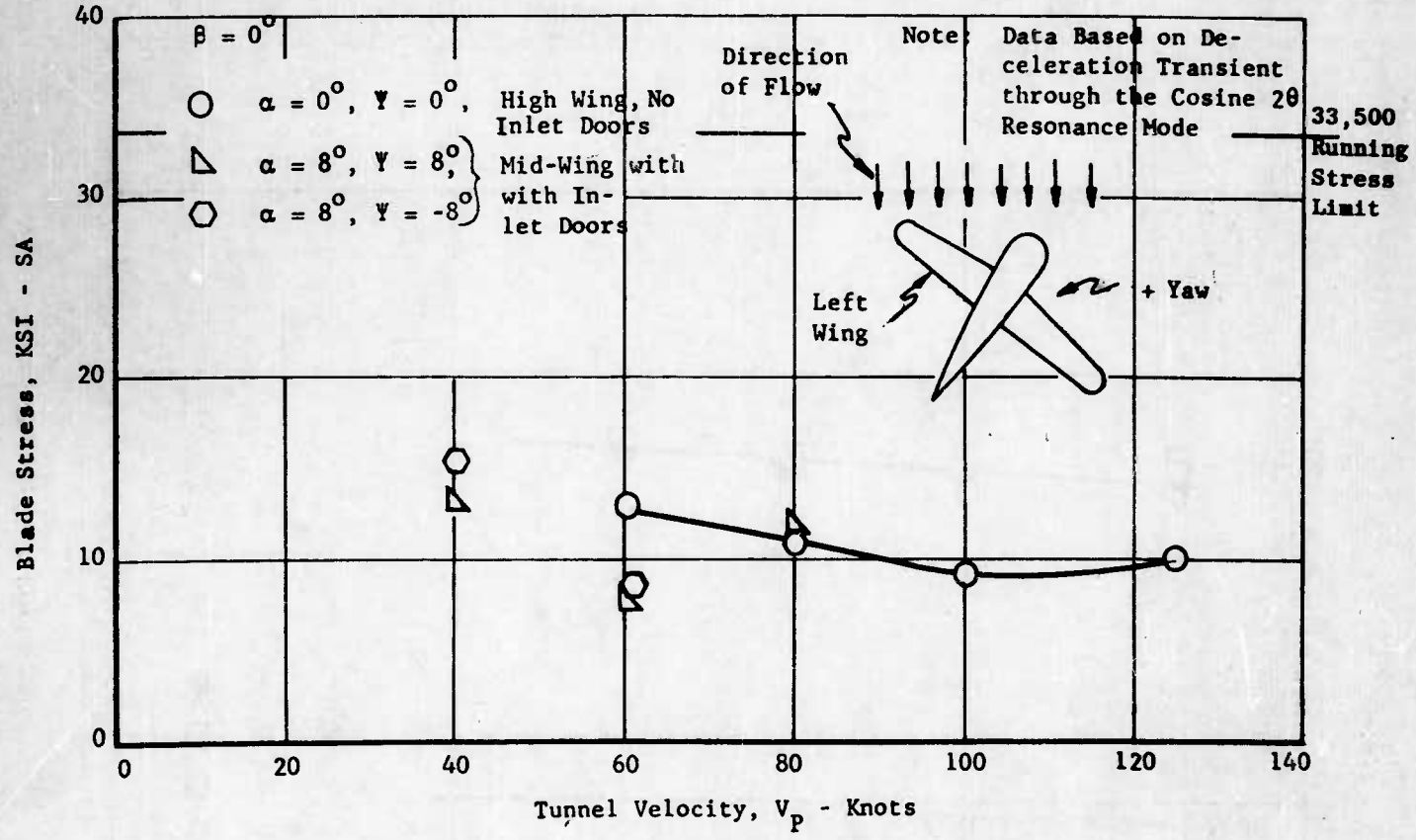


FIGURE 131h - COSINE 2θ MODE STRESS AS A FUNCTION OF FLIGHT SPEED, AIRPLANE CONFIGURATION, YAW ANGLE AND ANGLE OF ATTACK (FIVE SECOND DECELERATION)

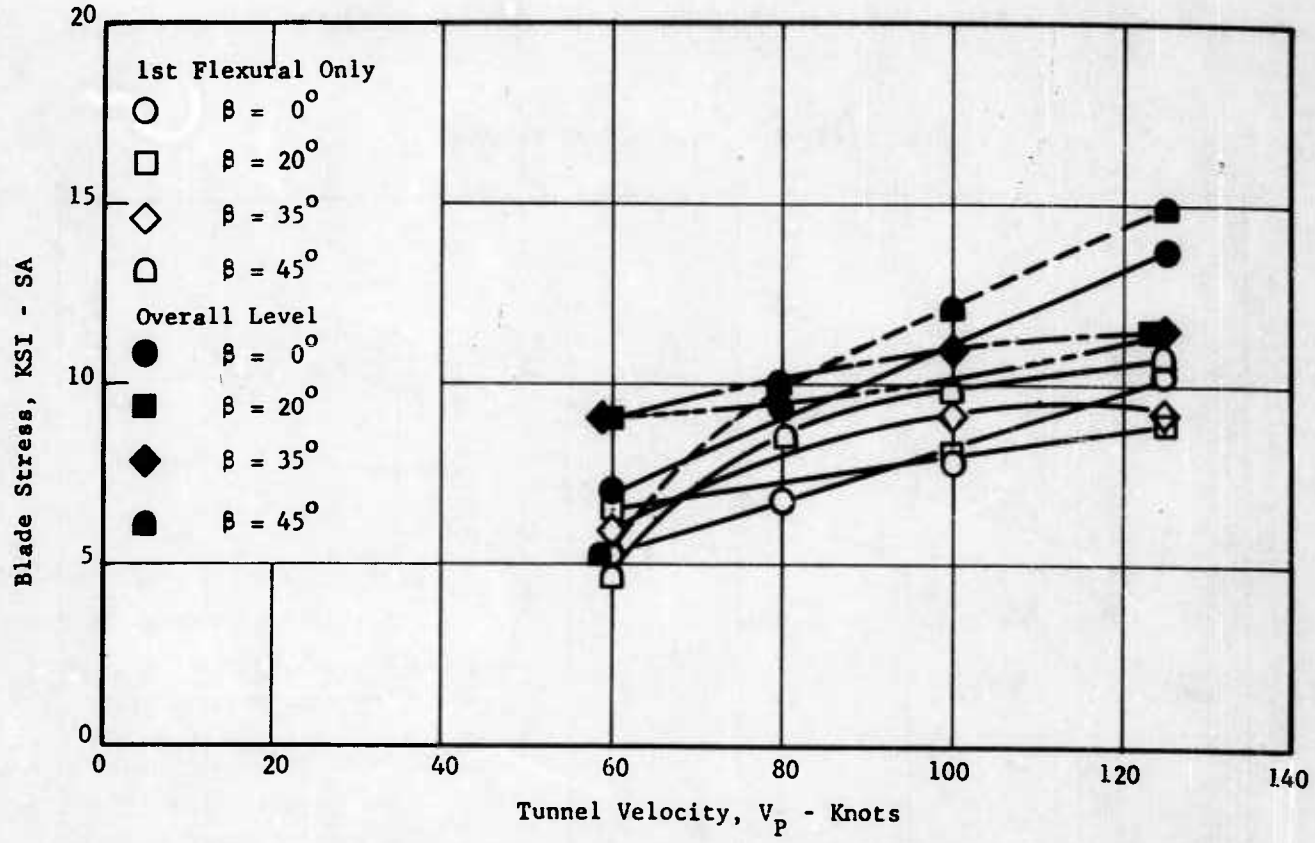


FIGURE 132a - OVERALL AND FIRST FLEXURAL RESONANCE STRESS AT 1850 RPM VERSUS FLIGHT SPEED

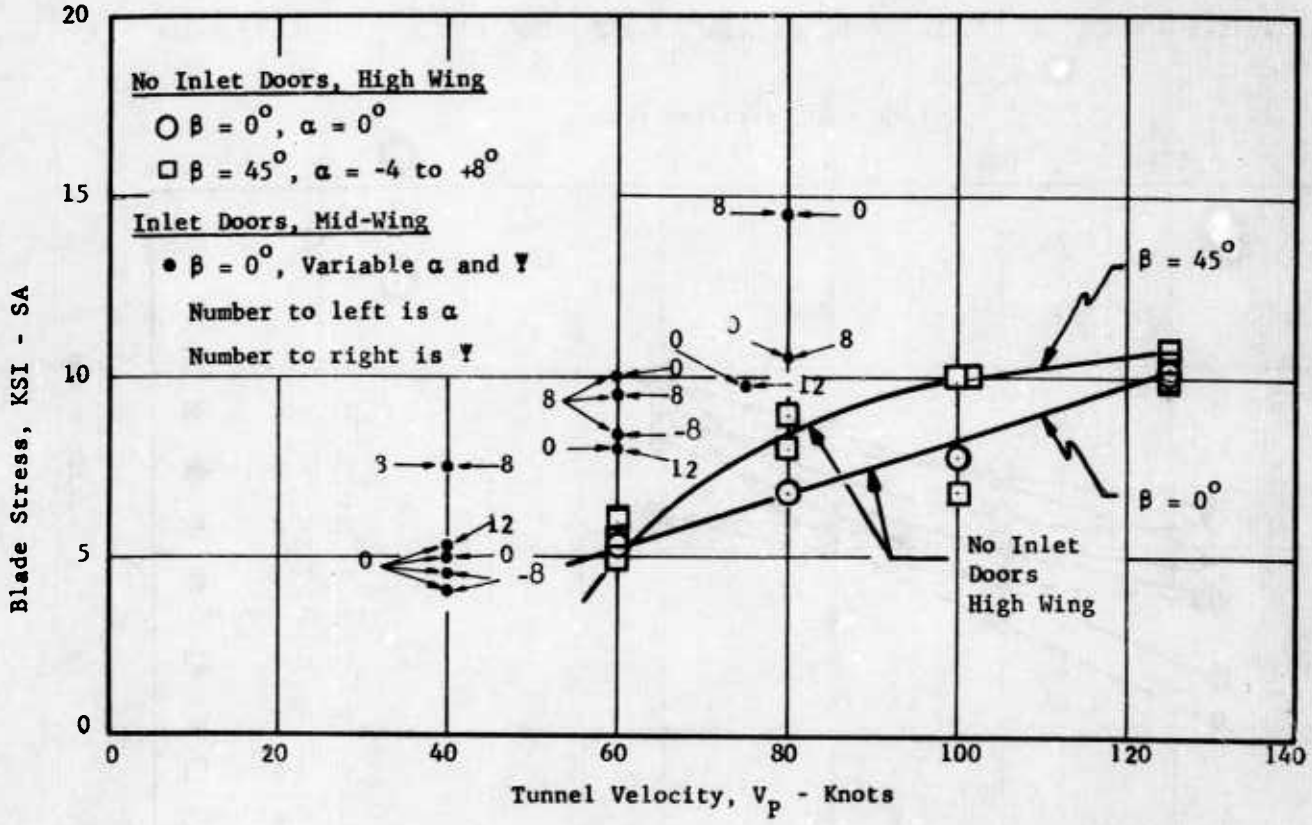


FIGURE 132b - FIRST FLEXURAL RESONANCE STRESS AT 1850 RPM VERSUS FLIGHT SPEED

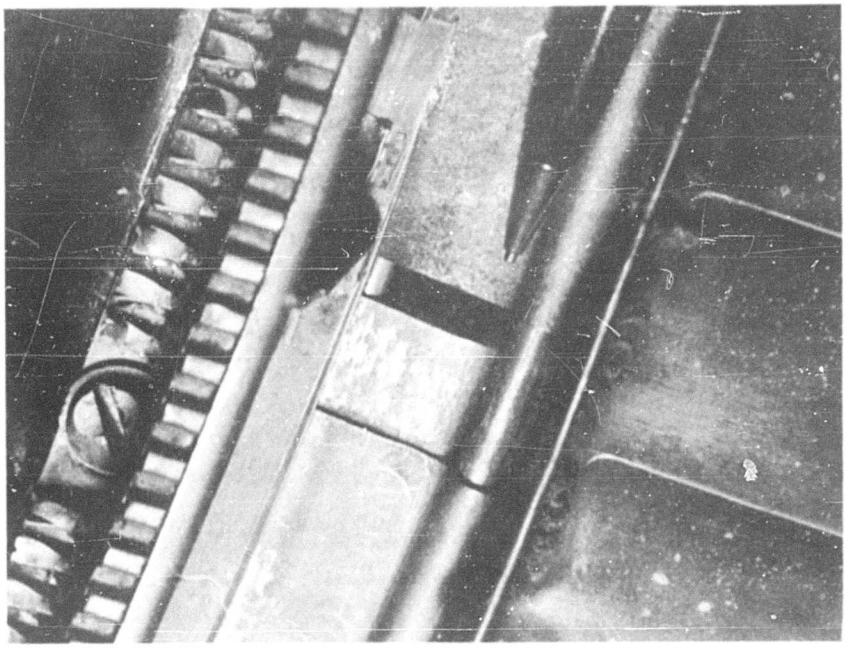


FIGURE 133a. SCROLL AIR SEAL LEAK (FAN 001)

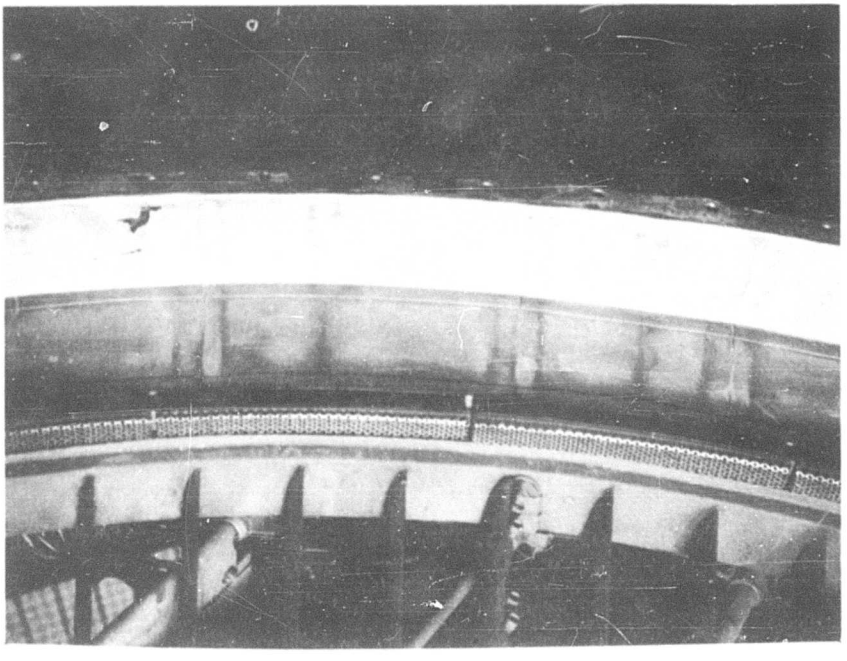


FIGURE 133b TURBINE RUB, REAR FRAME INSULATION BLANKET (FAN 002)

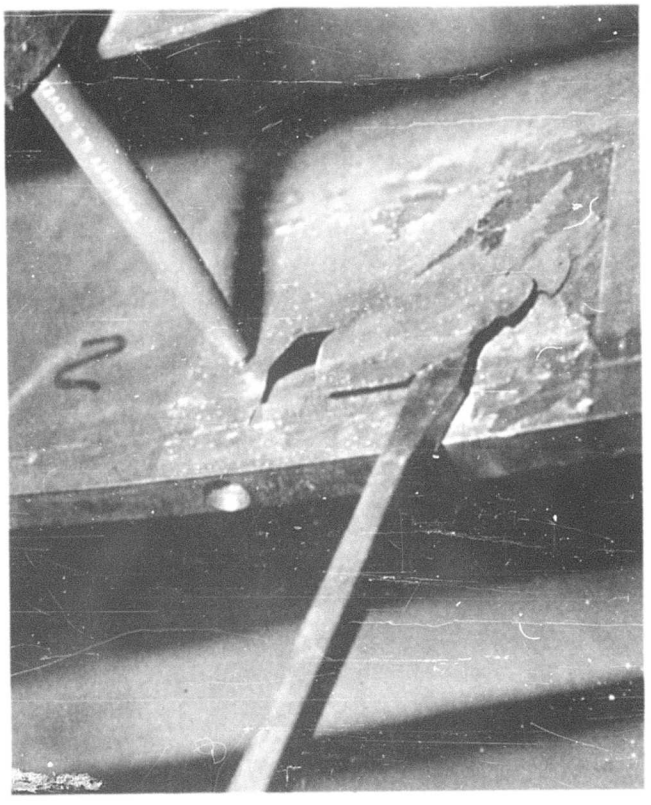


FIGURE 134. FRONT FRAME SKIN FAILURE (S/N002)

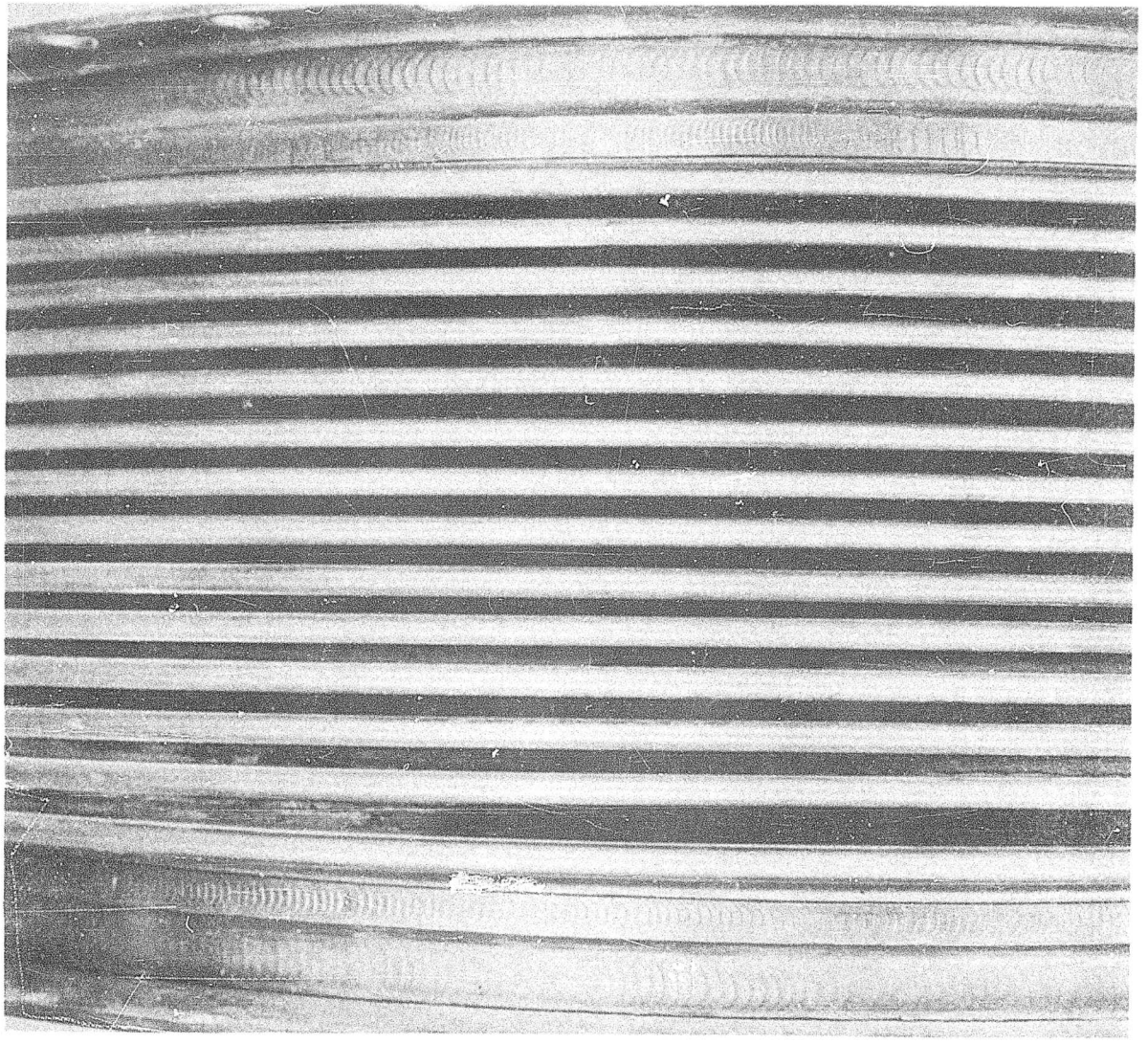


FIGURE 135. YIELDED CONVOLUTION IN BELLOWS S/N001 (1st & 2nd CONVOLUTIONS FROM BOTTOM)

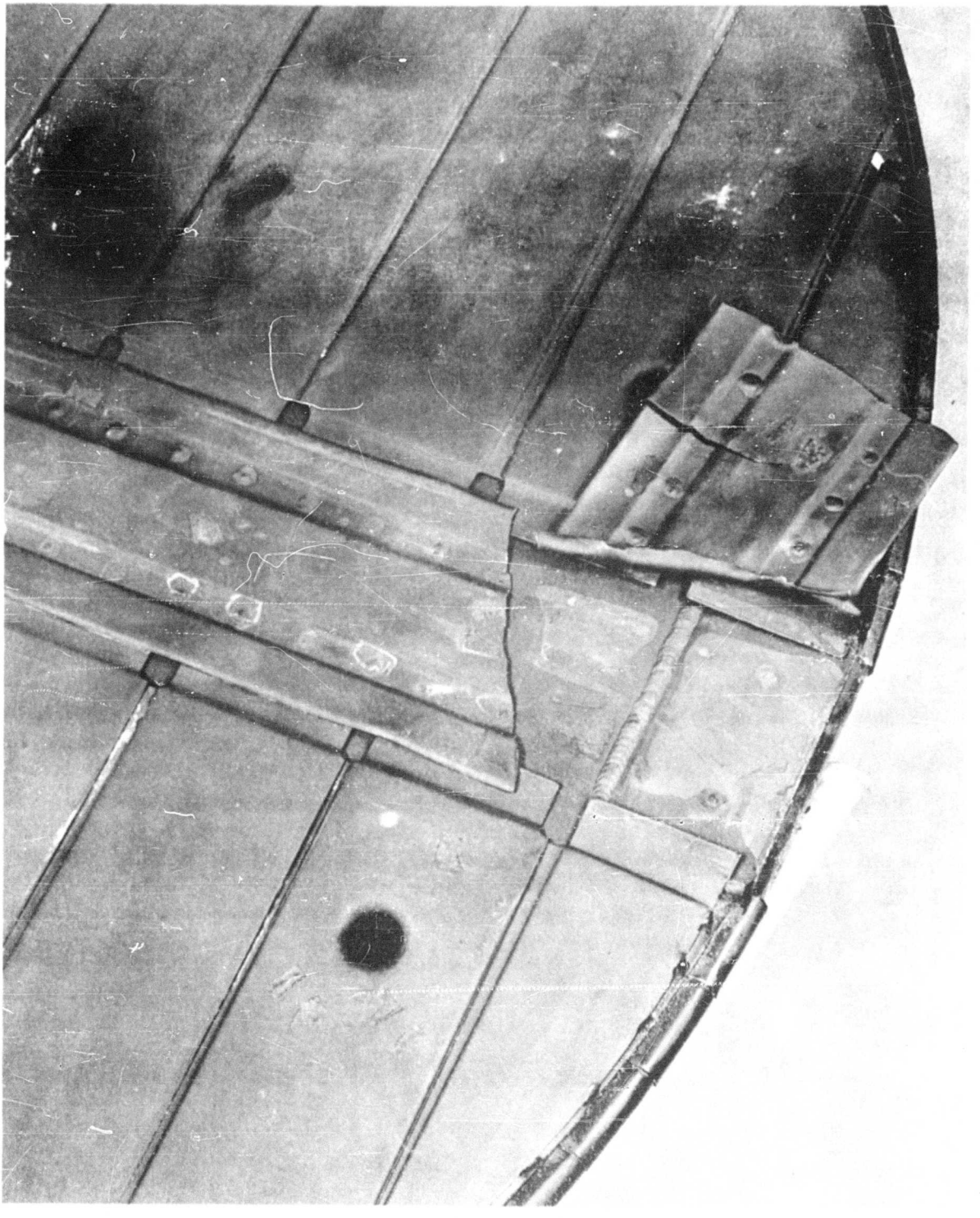


FIGURE 136a. "STRAIGHT" DIVERTER VALVE DOOR, S/N001, SHOWING FAILED PIECE OF HEAT SHIELD

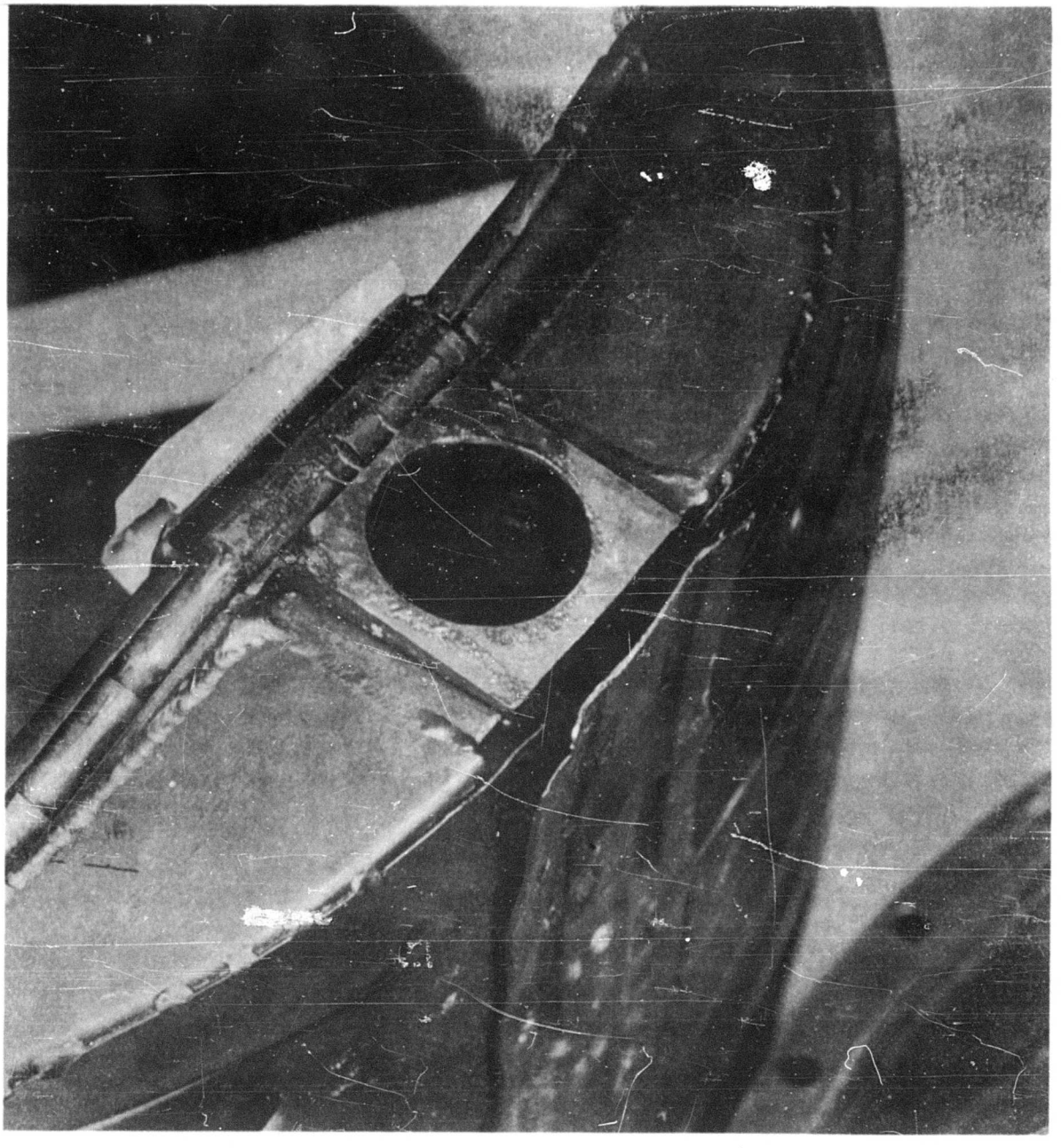


FIGURE 136b. "CURVED" DIVERTER VALVE DOOR, S/N001 SHOWING SEPARATED HEAT SHIELD

DISTRIBUTION

U. S. Army Command and General Staff College	1
U. S. Army Aviation Test Board	1
Aviation Test Office, Edwards AFB	1
Army Research Office, Durham	2
Office of Chief of R&D, D/A	1
Naval Air Test Center	1
U. S. Army Aviation School	1
U. S. Army Aviation and Surface Materiel Command	1
U. S. Army Transportation Research Command	21
U. S. Army Research and Development Group (Europe)	1
U. S. Army Aviation School	1
Air University Library, Maxwell AFB	1
Air Force Systems Command, Wright-Patterson AFB	3
Bureau of Naval Weapons	1
U. S. Naval Postgraduate School	1
U. S. Army Standardization Group, Canada	1
Canadian Army Liaison Officer, U. S. Army Transportation School	3
British Army Staff, British Embassy	4
U. S. Army Standardization Group, U. K.	1
NASA-LRC, Langley Station	2
George C. Marshall Space Flight Center, NASA	1
Manned Spacecraft Center, NASA	1
Ames Research Center, NASA	2
Lewis Research Center, NASA	1
NASA Representative, Scientific and Technical Information Facility	1
Defense Documentation Center	10
U. S. Army Mobility Command	2
U. S. Army Materiel Command	2

AP_____ Accession No._____

General Electric Company, Cincinnati, Ohio

RESULTS OF WIND TUNNEL TESTS OF A FULL-SCALE, WING-MOUNTED, TIP-TURBINE-DRIVEN LIFT FAN.

October, 1963, 377 pages - illustrations - tables (Contract DA 44-177-TC-584) USA TRECOM Project 1D121401D14402 (formerly 9X38-01-020-02), TRECOM 63-21. Unclassified Report.

This report covers 107 hours of testing in the NASA-Ames, 40' x 80' Wind Tunnel and 6 hours of outdoor ground effect testing at Ames.

Propulsion and aircraft performance and interactions are discussed.

UNCLASSIFIED

1. VTOL Propulsion System

2. Contract DA 44-177-TC-584

AP_____ Accession No._____

General Electric Company, Cincinnati, Ohio

RESULTS OF WIND TUNNEL TESTS OF A FULL-SCALE, WING MOUNTED, TIP-TURBINE-DRIVEN LIFT FAN.

October, 1963, 377 pages - illustrations - tables (Contract DA 44-177-TC-584) USA TRECOM Project 1D121401D14402 (formerly 9X38-01-020-02) TRECOM 63-21. Unclassified Report.

This report covers 107 hours of testing in the NASA-Ames, 40' x 80' Wind Tunnel and 6 hours of outdoor ground effect testing at Ames.

Propulsion and aircraft performance and interactions are discussed.

UNCLASSIFIED

1. VTOL Propulsion System

2. Contract DA 44-177-TC-584

AP_____ Accession No._____

General Electric Company, Cincinnati, Ohio

RESULTS OF WIND TUNNEL TESTS OF A FULL-SCALE, WING-MOUNTED, TIP-TURBINE-DRIVEN LIFT FAN.

October, 1963, 377 pages - illustrations - tables (Contract DA 44-177-TC-584) USA TRECOM Project 1D121401D14402 (formerly 9X38-01-020-02), TRECOM 63-21. Unclassified Report.

This report covers 107 hours of testing in the NASA-Ames, 40' x 80' Wind Tunnel and 6 hours of outdoor ground effect testing at Ames.

Propulsion and aircraft performance and interactions are discussed.

UNCLASSIFIED

1. VTOL Propulsion System

2. Contract DA 44-177-TC-584

AP_____ Accession No._____

General Electric Company, Cincinnati, Ohio

RESULTS OF WIND TUNNEL TESTS OF A FULL-SCALE, WING MOUNTED, TIP-TURBINE-DRIVEN LIFT FAN.

October, 1963, 377 pages - illustrations - tables (Contract DA 44-177-TC-584) USA TRECOM Project 1D121401D14402 (formerly 9X38-01-020-02) TRECOM 63-21. Unclassified Report.

This report covers 107 hours of testing in the NASA-Ames, 40' x 80' Wind Tunnel and 6 hours of outdoor ground effect testing at Ames.

Propulsion and aircraft performance and interactions are discussed.

UNCLASSIFIED

1. VTOL Propulsion System

2. Contract DA 44-177-TC-584

AP_____ Accession No._____

General Electric Company, Cincinnati, Ohio

RESULTS OF WIND TUNNEL TESTS OF A FULL-SCALE, WING-MOUNTED, TIP-TURBINE-DRIVEN LIFT FAN.

October, 1963, 377 pages - illustrations - tables (Contract DA 44-177-TC-584) USA TRECOM Project 1D121401D14402 (formerly 9X38-01-020-02), TRECOM 63-21. Unclassified Report.

This report covers 107 hours of testing in the NASA-Ames, 40' x 80' Wind Tunnel and 6 hours of outdoor ground effect testing at Ames.

Propulsion and aircraft performance and interactions are discussed.

UNCLASSIFIED

1. VTOL Propulsion System
2. Contract DA 44-177-TC-584

AP_____ Accession No._____

General Electric Company, Cincinnati, Ohio

RESULTS OF WIND TUNNEL TESTS OF A FULL-SCALE, WING MOUNTED, TIP-TURBINE-DRIVEN LIFT FAN.

October, 1963, 377 pages - illustrations - tables (Contract DA 44-177-TC-584) USA TRECOM Project 1D121401D14402 (formerly 9X38-01-020-02) TRECOM 63-21. Unclassified Report.

This report covers 107 hours of testing in the NASA-Ames, 40' x 80' Wind Tunnel and 6 hours of outdoor ground effect testing at Ames.

Propulsion and aircraft performance and interactions are discussed.

UNCLASSIFIED

1. VTOL Propulsion System
2. Contract DA 44-177-TC-584

AP_____ Accession No._____

General Electric Company, Cincinnati, Ohio

RESULTS OF WIND TUNNEL TESTS OF A FULL-SCALE, WING-MOUNTED, TIP-TURBINE-DRIVEN LIFT FAN.

October, 1963, 377 pages - illustrations - tables (Contract DA 44-177-TC-584) USA TRECOM Project 1D121401D14402 (formerly 9X38-01-020-02), TRECOM 63-21. Unclassified Report.

This report covers 107 hours of testing in the NASA-Ames, 40' x 80' Wind Tunnel and 6 hours of outdoor ground effect testing at Ames.

Propulsion and aircraft performance and interactions are discussed.

UNCLASSIFIED

1. VTOL Propulsion System
2. Contract DA 44-177-TC-584

AP_____ Accession No._____

General Electric Company, Cincinnati, Ohio

RESULTS OF WIND TUNNEL TESTS OF A FULL-SCALE, WING MOUNTED, TIP-TURBINE-DRIVEN LIFT FAN.

October, 1963, 377 pages - illustrations - tables (Contract DA 44-177-TC-584) USA TRECOM Project 1D121401D14402 (formerly 9X38-01-020-02) TRECOM 63-21. Unclassified Report.

This report covers 107 hours of testing in the NASA-Ames, 40' x 80' Wind Tunnel and 6 hours of outdoor ground effect testing at Ames.

Propulsion and aircraft performance and interactions are discussed.

UNCLASSIFIED

1. VTOL Propulsion System
2. Contract DA 44-177-TC-584

UNCLASSIFIED

UNCLASSIFIED